

# NISTIR 8271 DRAFT SUPPLEMENT

## Face Recognition Vendor Test (FRVT) Part 2: Identification

Patrick Grother  
Mei Ngan  
Kayee Hanaoka  
*Information Access Division  
Information Technology Laboratory*

This document is a draft supplement of [NIST Interagency Report 8271](#)

2022/04/28



# NISTIR 8271 DRAFT SUPPLEMENT

## Face Recognition Vendor Test (FRVT) Part 2: Identification

Patrick Grother  
Mei Ngan  
Kayee Hanaoka  
*Information Access Division  
Information Technology Laboratory*

This document is a draft supplement of [NIST Interagency Report 8271](#)

February 2022



U.S. Department of Commerce  
*Gina M. Raimondo, Secretary*

National Institute of Standards and Technology  
*Laurie E. Locascio, NIST Director and Undersecretary of Commerce for Standards and Technology*

## RELEASE NOTES

**2022-04-28:** The 1:N track of the FRVT remains open.

- ▷ This document is the sixteenth draft update to [NIST Interagency Report 8271](#). It includes results for algorithms submitted by one first-time participants: Hangzhou Allu Network Information Technology.
- ▷ The document also includes results for algorithms from three returning developers: HyperVerge Inc, Qnap Security, and Realnetworks Inc.
- ▷ The [1:N results page](#) has been updated.

**2022-03-30:** The 1:N track of the FRVT remains open.

- ▷ This document is the sixteenth draft update to [NIST Interagency Report 8271](#). It includes results for algorithms submitted by two first-time participants: Intellivision, and Pangiam.
- ▷ The document also includes results for algorithms from three returning developers: Fujitsu Research and Development Center, Idemia, and Gorilla Technology.
- ▷ The [1:N results page](#) has been updated.

**2022-02-23:** The 1:N track of the FRVT remains open.

- ▷ This document is the fifteenth draft update to [NIST Interagency Report 8271](#). It includes results for algorithms submitted by four first-time participants: Cloudwalk - Moontime Smart Technology, Decatur Industries Inc, NotionTag Technologies Private Limited, and Reveal Media Ltd.
- ▷ The document also includes results for algorithms from three returning developers: Cognitec Systems GmbH, Sensetime Group, and Viettel Group
- ▷ The [1:N results page](#) has been updated.

**2022-01-20:** The 1:N track of the FRVT remains open.

- ▷ This document is the fourteenth draft update to [NIST Interagency Report 8271](#). It includes results for algorithms recently submitted by two first-time participants: Daon and SQIsoft.
- ▷ The document also includes results for algorithms from five returning developers: Cyberlink Corp, NEC, Neurotechnology, Paravision, and Rank One Computing.
- ▷ The [1:N results page](#) has been updated.

**2021-12-16:** The 1:N track of the FRVT remains open.

- ▷ This document is the thirteenth draft update to [NIST Interagency Report 8271](#). It includes results for algorithms from six returning developers: Dahua Technology, Imagus Technology, Line Corporation, N-Tech Lab, Qnap Security, and Realnetworks Inc.
- ▷ The [1:N results page](#) has been updated.

**2021-11-22:** The 1:N track of the FRVT remains open.

- ▷ This document is the twelfth draft update to [NIST Interagency Report 8271](#). It includes results for algorithms recently submitted by three first-time participants Clearview AI, Griaule, and Mantra Softech India.
- ▷ This document and the [1:N results page](#) also include results for algorithms from six returning developers: Acer Incorporated, Canon, Dermalog, Samsung S1, VisionLabs, and Veridas Digital Authentication.

**2021-10-28:** The 1:N track of the FRVT remains open.

- ▷ This document is the eleventh draft update to [NIST Interagency Report 8271](#). It includes results for algorithms recently submitted by three first-time participants (20Face, Fujitsu Research and Development Center, and Vision-Box), and five returning participants (Alchera, Gorilla Technology, Tevian, Thales-Cogent, and Visidon). Visidon
- ▷ Both the main [1:N results page](#) and the small-gallery [paperless travel page](#) have been updated.

**2021-09-21:** The 1:N track of the FRVT remains open. Three news items:

- ▷ This document is the tenth draft update to [NIST Interagency Report 8271](#). It includes results for algorithms recently submitted by six first-time developers: Cubox, Fincore, HyperVerge, Qnap Security, Staqu Technologies, and Tripleize (Aize, 3-ize).
- ▷ It includes results also for four returning developers: Cognitec Systems, Incode Technologies, Innovatrics, Neurotechnology, and Rank One Computing.

**2021-08-02:** The 1:N track of the FRVT remains open. Three news items:

- ▷ This document is the ninth draft update to [NIST Interagency Report 8271](#). It includes results for algorithms recently submitted by eight participants: Cyberlink Corp, NEC Corp, N-Tech Lab, Realnetworks Inc., Sensetime Group, Veridas Digital, Viettel Group, and Vigilant Solutions.
- ▷ Algorithms submitted since July 24 will be included in the next update scheduled for September 9, 2021.
- ▷ A new report, NIST Interagency Report 8381 - FRVT Part 7: Identification for Paperless Travel and Immigration, has been released [[PDF](#), [webpage](#)]. It documents the use of FRVT 1:N algorithms in positive access control and immigration status update travel applications where the enrolled population size is as low as 420 people for aircraft boarding, and 42 000 for an airport security line. These population sizes are much smaller than those used in the main [1:N evaluation](#). Going forward, we will update the report and webpage with results for new algorithms.

**2021-07-07:** The 1:N track of the FRVT remains open. One update:

- ▷ This document is the eighth draft update to [NIST Interagency Report 8271](#). It include results for an algorithm from one participant: Kakao Enterprises.

**2021-06-22:** The 1:N track of the FRVT remains open. Three updates:

- ▷ This is the seventh draft of the update to [NIST Interagency Report 8271](#). It includes results for algorithms from three new participants: Line Corporation, Rendip, and Samsung S1 Corp.
- ▷ We have also added results for algorithms from five returning developers: Imagus Technology, Kneron, Tevian, Visidon, and Xforward AI Technology.
- ▷ The algorithm-specific report cards (examples: [1](#), [2](#), and [3](#)) now include figures showing how low threshold values can be used to reduce candidate list lengths for human review, while (usually) elevating miss rates (FNIR) only modestly. The reports also feature some minor additions and clarifications.

**2021-03-26:** The 1:N track of the FRVT remains open. Three updates:

- ▷ This is the sixth draft of the update to [NIST Interagency Report 8271](#). It includes results for algorithms from three returning developers: Neurotechnology, Guangzhou Pixel Solutions, and Tech5 SA.
- ▷ We have added results on the webpage and in the report for a new ageing dataset in which border crossing photos are searched against a gallery of border crossing photos collected between 10 and 15 years prior to the mated search photos. See section [2](#) for a description of the images. Table [1](#) has a new entry describing the experiment.
- ▷ We will mostly discontinue running the mugshot ageing test, reserving it for algorithms that show high accuracy on the new border-crossing set.

**2021-03-26:** Regarding the fifth draft of the update to [NIST Interagency Report 8271](#):

- ▷ In addition have added results for first algorithms from two new participants: Viettel Group and Veridas Digital Authentication Solutions.
- ▷ We have added results for algorithms from two returning developers: Idemia and Cognitec Systems.
- ▷ In addition to the report, the [results page](#) and its hyperlinked [report cards](#) have been updated.

**2021-02-08:** Regarding the fourth draft of the update to [NIST Interagency Report 8271](#):

- ▷ We have added results for eight algorithms submitted by eight developers: Cyberlink, Dermalog, Imagus, Paravision, Sensetime, Trueface, Vigilant Solutions, and X-Forward AI. With the exception of Trueface, all of these developers have participated previously.
- ▷ We anticipate updating this report again in the first week of March 2021.
- ▷ The main [results page](#) has been revised with tabs for the investigative and lights-out identification tables, and a new tab dedicated to speed and resource consumption.
- ▷ The report cards (example [here](#)) hyperlinked from the [results page](#) have been revised to improve content and format.

**2020-12-14:** Regarding third draft of the update to [NIST Interagency Report 8271](#):

- ▷ We have added results for fifteen algorithms submitted by thirteen developers. The four first-time participants are: Acer, Akurat Satu Indonesia, Canon, and Xforward AI Technology. The ten returning developers are: AllGoVision, Cyberlink Corp, Dahua Technology, Deepglint, Guangzhou Pixel Solutions, IIT Vision, Innovatrics, Rank One Computing, Scanovate, Sensetime Group, Synesis, and VisionLabs.
- ▷ We have added two new datasets to the evaluation: First a set of “visa-border” photos, representing search of an airport immigration lane photo against a database of closely ISO standard portraits; second a “visa-kiosk” set representing search of a photo collected in a registered traveller kiosk against the same ISO portrait gallery. The images are described in section [2.1](#).
- ▷ As in previous reports, we include results for searching mugshots against a mugshot gallery containing a single image of each of 12 million people. However we have suspending running searches against a gallery in which multiple lifetime photos per person are present, because this is computationally expensive. We retain a  $N = 3$  million search test dedicated to ageing in which mugshots taken up to 18 years after the first photograph are searched - see Table [7](#).
- ▷ Tables containing computational resource information, Table [2](#) . . . , now include duration of the finalization step, in which search algorithms can, at their option, build fast-search data structures.
- ▷ We have linked revised per-algorithm PDF report cards from the main [results page](#).
- ▷ We have regenerated all figures and tables to drop algorithms submitted before June 2018. Results for prior algorithms appear in [archived editions](#) of this report.
- ▷ Going forward, we anticipate producing more frequent updates to this report. Developers may submit one algorithm to this evaluation every four calendar months.

**2020-03-24:** Regarding the second draft of the update to [NIST Interagency Report 8271](#):

- ▷ Adds results for three algorithms from three developers, Dermalog, Innovatrics, and Synesis.
- ▷ Adds Table [7](#) on ageing showing the increase in false negative rates with time elapsed between two photos. Some of the results were contained in graphs in prior editions of this report, but the table adds results for some newly submitted algorithms.

- ▷ Adjusts frontal mugshot results (for recent and lifetime consolidated galleries) to include the effect of removing some images that should not have been included in image test sets. These images were mostly profile views, images of tattoos containing faces, images of faces on tee shirts, and images of photographs on walls behind the intended subject. This affects many tables and reduces false negative identification rates for all algorithms. The reduction is larger for “recent” enrollments than for “lifetime consolidated” ones with the consequence that accuracy on recent images is now superior.

**2020-02-26:** Regarding the first draft of the update to [NIST Interagency Report 8271](#):

- ▷ Adds results for 38 algorithms from 31 different developers, eleven of whom are entirely new to the 1:N track of FRVT. These are Allgovision, Cyberlink, Deepsea Tencent, Farbar F8, Imperial College London, Intsys MSU, Kedacom, Kneron, Pixelall, and Scanovate.

## DISCLAIMER

Specific hardware and software products identified in this report were used in order to perform the evaluations described in this document. In no case does identification of any commercial product, trade name, or vendor, imply recommendation or endorsement by the National Institute of Standards and Technology, nor does it imply that the products and equipment identified are necessarily the best available for the purpose.

## INSTITUTIONAL REVIEW BOARD

The National Institute of Standards and Technology's Research Protections Office reviewed the protocol for this project and determined it is not human subjects research as defined in Department of Commerce Regulations, 15 CFR 27, also known as the Common Rule for the Protection of Human Subjects (45 CFR 46, Subpart A).

## ACKNOWLEDGMENTS

The authors are grateful for the support and collaboration of the the Department of Homeland Security's Science & Technology Directorate (S&T), Office of Biometric Identity Management (OBIM), and Customs and Border Protection (CBP).

Additionally, the authors are grateful to staff in the NIST Biometrics Research Laboratory for infrastructure supporting rapid evaluation of algorithms.

## Executive Summary

This document is a draft revision of the September 2019 report [NIST Interagency Report 8271](#). That report gave extensive documentation of face recognition applied to mugshots. This report extends that by adding more two more challenging datasets containing images with serious departures from canonical frontal image standards. The report also adds results for algorithms submitted to NIST since in 2019 and 2020. The algorithms, which implement one-to-many identification of faces appearing in two-dimensional images, are prototypes from the research and development laboratories of mostly commercial suppliers, and are submitted to NIST as compiled black-box libraries implementing a NIST-specified C++ test interface. The report therefore does not describe how algorithms operate. The report lists accuracy results alongside developer names and will therefore be useful for comparison of face recognition algorithms and assessment of absolute capability. The report is accompanied by a [webpage](#) with sortable results.

The evaluation uses six datasets: frontal mugshots, profile view mugshots, desktop webcam photos, visa-like immigration application photos, immigration lane photos, and registered traveler kiosk photos. These datasets are sequestered at NIST, meaning that developers do not have access to them for training or testing. This aspect is important because face recognition algorithms are very often deployed without the developer having access to the customers image data. A possible exception to this would be in a cloud-based application where the operational image data is uploaded to a cloud operated by a face recognition developer.

The major result in NIST IR 8271 was that massive gains in accuracy have been achieved in the years 2013 to 2018 and these far exceed improvements made in the prior period, 2010 to 2013. While the industry gains were broad - at least 30 developers' algorithms outperformed the most accurate algorithm from late 2013, there remains a wide range of capability. While this report shows accuracy gains only over the period 2018-2020, the most accurate algorithm reported here is substantially more accurate than anything reported in NIST IR 8271. This is evidence that face recognition development continues apace, and that FRVT reports are but a snapshot of contemporary capability.

From discussion with developers, the accuracy gains stem from the adoption of deep convolutional neural networks. As such, face recognition has undergone an industrial revolution, with algorithms increasingly tolerant of poorly illuminated and other low quality images, and poorly posed subjects. One related result is that a few algorithms correctly match side-view photographs to galleries of frontal photos, with search accuracy approaching that of the best c. 2010 algorithms operating on purely frontal images. The capability to recognize under a 90-degree change in viewpoint - pose invariance - has been a long-sought milestone in face recognition research.

With good quality portrait photos, the most accurate algorithms will find matching entries, when present, in galleries containing 12 million individuals, with rank one miss rates of approaching 0.1%. The remaining errors are in large part attributable to long-run ageing, facial injury and poor image quality. Given this impressive achievement - close to perfect recognition - an advocate might claim that cooperative face recognition is a solved problem, a statement that can be refuted with the following context and caveats:

- ▷ **Mugshots vs. less constrained captures:** The low error rates reported here are attained using mostly excellent cooperative live-capture mugshot images collected with an attendant present. Recognition in other circumstances, particularly those without a dedicated photographic environment and human or automated quality control checks, will lead to declines in accuracy. This is documented here for side-view images, poorer quality webcam images, and, particularly, for newly introduced ATM-style kiosk photos that were not originally intended for automated face recognition. In this case, recognition error rates are much higher, often in excess of 20% even with the more accurate algorithms which variously remain intolerant of face cropping (at image edge) and of large downward head pitch.
- ▷ **Algorithm accuracy spectrum:** Recognition accuracy is very strongly dependent on the algorithm and, more

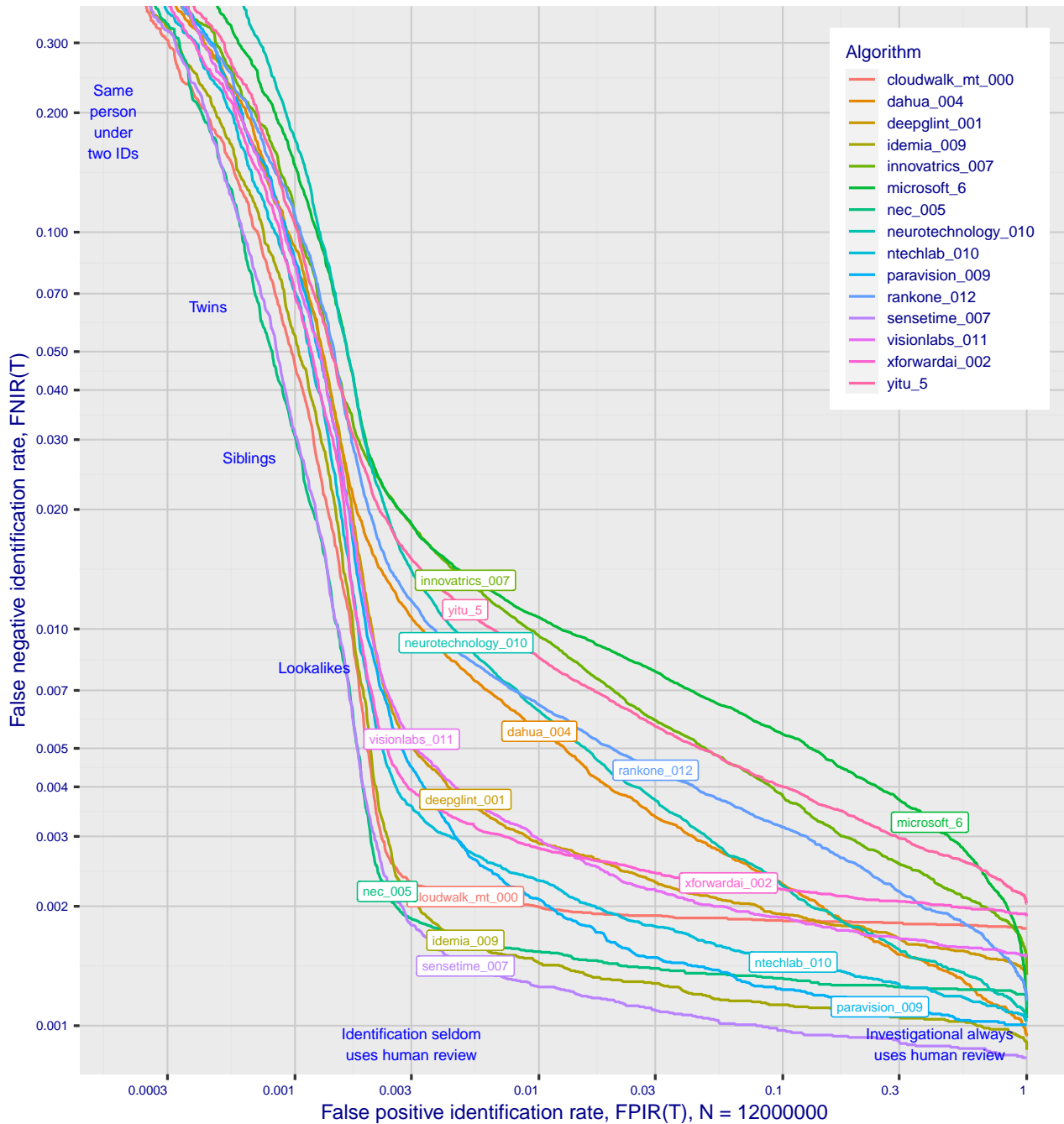


Figure 1: Identification miss rates across the false positive range.  $N = 12$  million individuals are enrolled with one recent image.

generally, on the developer of the algorithm. False negative error rates in a particular scenario range from a few tenths of one percent to beyond fifty percent. This is tabulated exhaustively later: For example Table 10 shows accuracy across datasets. Figure 1 here compares algorithms on mugshot searches in a consolidated gallery of 12 million subjects and 12 million photos. Many algorithms do not achieve the low error rates noted above, and while many of those may still be useful and valuable to end-users, only the most accurate excel on poor quality images and those collected long after the initial enrollment sample.

▷ **Versioning:** While results for up to ten algorithms from each developer are reported here, the intra-provider

accuracy variations are usually smaller than the inter-provider variations. That said different versions give an order of magnitude fewer misses. Some developers demonstrate speed-accuracy tradeoffs<sup>1</sup>. See Figs. 18, 19.

- ▷ **Low similarity scores:** In thousands of mugshot cases the correct gallery image is returned at rank 1 but its similarity score is nevertheless low, below some operationally required score threshold. This is not so important when face recognition is used for “lead generation” in investigational applications because human reviewers are specifically required to review potentially long candidate lists and the threshold is effectively 0. In applications where search volumes are higher and labor is not available to review the results from searches, a higher threshold must be applied. This reduces the length of candidate lists and false positive identification rates at the expense of increased false negative miss rates. The tradeoff between the two error rates is reported extensively later.
- ▷ **Population size:** As the number of enrolled subjects grows, some mates are displaced from rank one, decreasing accuracy. As tabulated later for N up to 12 million, false negative rates generally rise slowly with population size. This enables use of face recognition in very large populations. However in most positive and negative identification applications<sup>2</sup>, a score threshold is set to limit the rate at which non-mate searches produce false positives. This has the consequence that some mated searches will report the mate below threshold, i.e. a miss, even if it is at rank 1. The utility of this is that many non-mated searches will return no candidate identities at all. As the error-tradeoff characteristic shows, investigational miss rates on the right side are very low but then rise steadily (in the center region) as threshold is increased to support “lights-out” applications, and ultimately rise quickly (left side) as discussed below. Thus, if we demand that just one in one thousand non-mate searches produce any false positives, the most accurate algorithms there (Senetime-004 and NEC-3) would fail on between 3 and 5% of mated searches. Even though the graph shows results for the most accurate algorithms, all but two would fail to find the mate in more than 8% of mated searches. While the two most accurate algorithms produce a relatively flat error tradeoff until the threshold is raised to limit false positives to about 1 in 400 non-mated searches<sup>3</sup>.

Thereafter, as the threshold is raised to further reduce false positives, miss rates rise rapidly. This means that low false positive identification rates are inaccessible with these algorithms, a result that does not apply for ten-finger identification algorithms. The rapid rise occurs because the lower mate scores are mixed with very high non-mate scores, the low scores from poor image quality and ageing, the high non-mates from the presence of lookalikes persons (doppelgangers), twins (discussed next) and, ultimately, the presence of a few unconsolidated subjects i.e. persons present under multiple IDs.

- ▷ **False negatives from ageing:** A large source of error in long-run applications where subjects are not re-enrolled on a set schedule is ageing. Changes in facial appearance increase with the time elapsed between photographs. These will depress similarity scores and eventually cause false negatives. All faces age and while this usually proceeds in a graceful and progressive manner, drug use can accelerate this [28]. Elective surgery may be effective in delaying it although this has not been formally quantified with face recognition. As ageing is essentially unavoidable, it can only be mitigated by scheduled re-capture, as in passport re-issuance. To quantify ageing effects, we used the more accurate algorithms to enroll the earliest image of 3.1 million adults and then search

<sup>1</sup>For example, NEC-0 prepares templates much faster than NEC-2 but gives twenty times more misses. Dermalog-5 executes a template search much more quickly than Dermalog-6 but is also much less accurate.

<sup>2</sup>In a positive identification application such as a registered traveler system, a user is making an implicit claim to be enrolled in the system - most users will be. In a negative application, such as with deportees, the implicit claim is that the subject is not enrolled - most will not be.

<sup>3</sup>The gallery size here is 12 million people, one image per person. Given 331 201 non-mated searches, an exhaustive implementation of one-too-many search would execute almost 4 trillion comparisons. At a false positive identification rate of 0.0025 the number of false positives is, to first order, 828 corresponding to single-comparison false match rate of  $828 / 4 \text{ trillion} = 2.1 \times 10^{-10}$  i.e. about 1 in 5 billion. Strictly this FMR computation is meaningful only for algorithms that implement 1:N search using N 1:1 comparisons, which is not always the case.

with 10.3 million newer photos taken up to 18 years after the initial enrollment photo. Figure 2 puts ageing into context by contrasting it with the increase in false negatives that occurs when the number of individuals in an enrollment database becomes larger and the chance of a false positive increases such that higher thresholds may become necessary<sup>4</sup>.

The Figure shows, from top to bottom, increases in false negative identification rates (FNIR) with the algorithm being tested. This applies to increases due to  $N$  on the left side, and increases due to ageing on the right side. The relative spacing of the dots shows that for all algorithms the dependency of FNIR on  $N$  (up to 12 million) is considerably less than on  $\Delta T$  (up to 18 years).

In the inset table, accuracy is seen to degrade progressively with time, as mate scores decline and non-mates displace mates from rank 1 position. More accurate algorithms tend to be less sensitive to ageing. The more accurate algorithms give fewer errors after 18 years of ageing than middle tier algorithms give after four. Note also we do not quantify an ageing rate - more formal methods [2] borrowed from the longitudinal analysis literature have been published for doing so (given suitable repeated measures data). See Figures 60, 83 and 95.

---

<sup>4</sup>Some algorithms implement strategies to automatically adjust scores to account for increased population size. This relieves the system owner of having to increase thresholds as  $N$  increases.

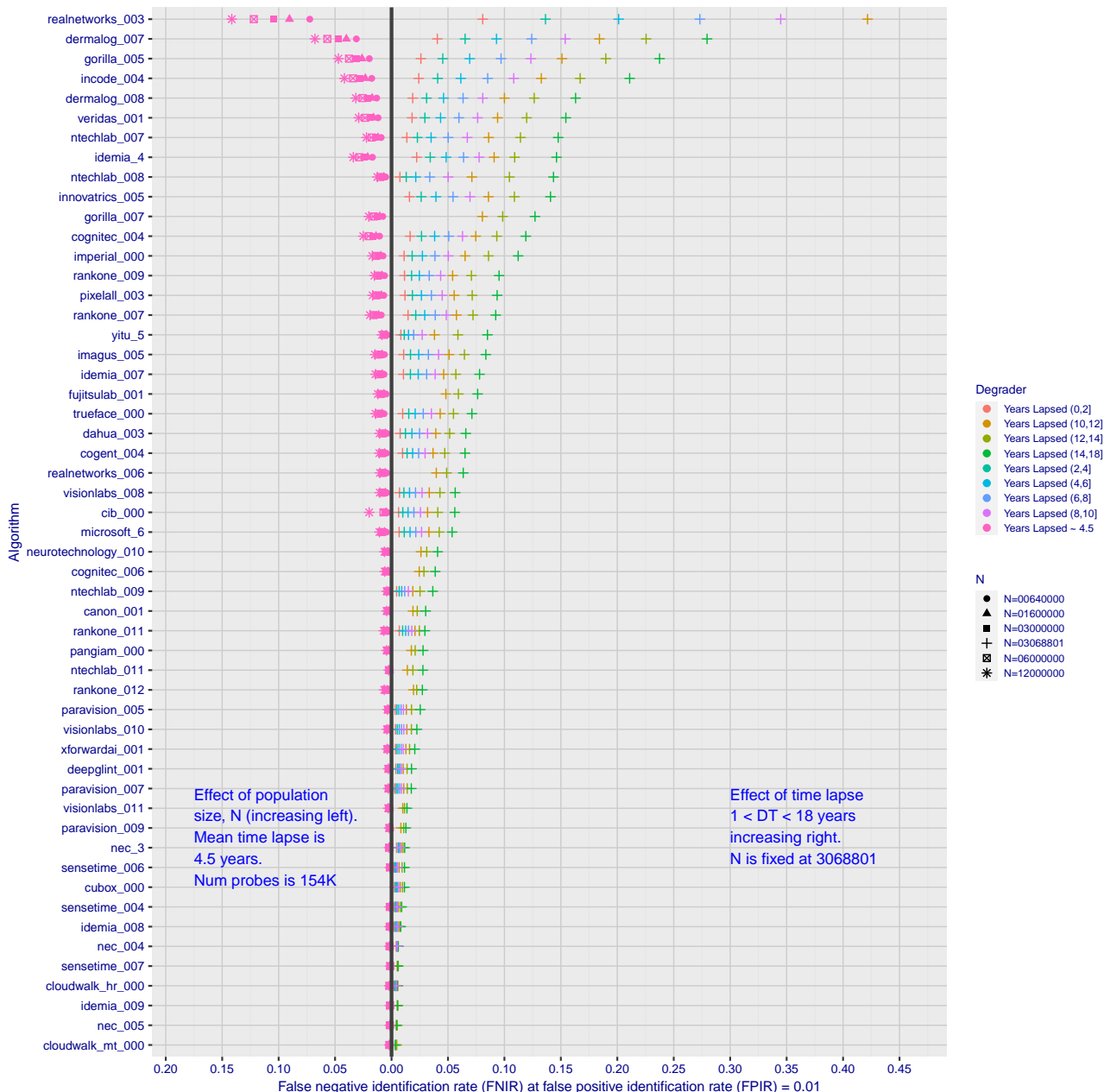


Figure 2: Identification miss rates as a function of enrolled population size,  $N$ , and time-lapse,  $\Delta T$ .

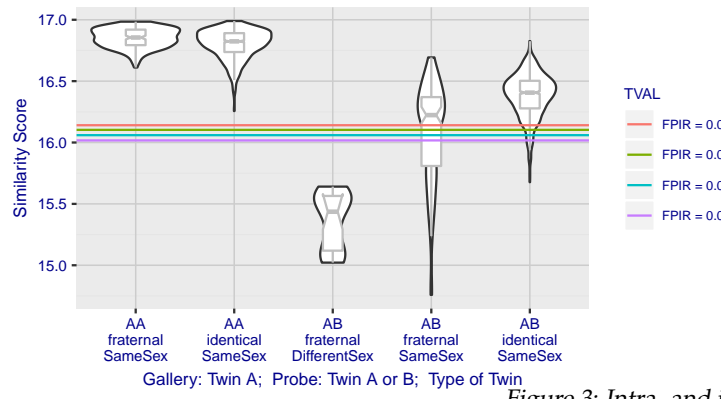


Figure 3: Intra- and inter-twin scores

▷ **False positives from twins:** By enrolling 640 000 mugshots, adding photos of one twin, and then searching photos of those subjects and their twin the inset figure shows, for one typical algorithm, the similarity is generally greater when searching twins against themselves (A) than when searching twins against their sibling (B) but very often still above even stringent thresholds i.e. those corresponding to one in one thousand searches producing a false positive. Thus twins will very often produce a high-scoring non-match on a candidate list and a false alarm in an online identification system. The plot of Fig. 3 shows that fraternal twins are sometimes correctly rejected at those thresholds - including most different sex twins (at center). Figure ?? shows substantially similar behavior for all algorithms tested. In an investigative search, a twin would typically appear at rank 1, or rank 2 if their sibling happened to also be the gallery. Twins (and triplets etc.) constituted 3.3% of all live births [17] in recent years<sup>5</sup>, and because that number is higher today than when the individuals in current adult databases were born, the false positives that arise from twins are now, and will increasingly be, an operational problem. Relative to the United States, twins are born with considerable regional variation. For example they are much less common in East Asia, and much more common in Sub-Saharan Africa [21].

The presence of twins in the mugshot database is inevitable given its size, around 12.3 million people. As this is not an insignificant sample of the domestic United States population, people with other familial ties will be present also. The data was collected over an extended period and because location information is not available, we are unable to estimate the proportion of the domestic population that is present in the dataset. However, if we assume twins are neither more or less disposed to arrest than the general population, we can estimate that hundreds of thousands of individuals in the dataset are twins. This will affect false positive rates because we randomly set aside 331 201 individuals for nonmate searches, and some proportion of those will be twins with siblings in the gallery.

▷ **Database integrity:** An operational error rate should be added to all false negative rates in this report reflecting the proportion of images in a real database that are un-matchable. Such anomalies arise from images that: do not contain a face; include multiple persons; cannot be decoded; are rotated by 90° or 180°; depict a face on clothing; and others introduced by a long tail of various clerical errors. While the mugshot trials in this report have been constructed to minimize such effects, they are a real problem in actual operations.

This report is being updated continuously as new algorithms are submitted to FRVT, and run on new datasets. Participation in the [one-to-many identification track](#) is independent of participation in the [one-to-one verification track](#) of FRVT.

<sup>5</sup>See the CDC's National Vital Statistics Report for 2017: [https://www.cdc.gov/nchs/data/nvsr/nvsr67/nvsr67\\_08-508.pdf](https://www.cdc.gov/nchs/data/nvsr/nvsr67/nvsr67_08-508.pdf)

## Scope and Context

**Audience:** This report is intended for developers, integrators, end users, policy makers and others who have some familiarity with biometrics applications. The methods and metrics documented here will be of interest to organizations engaged in tests of face recognition algorithms. Some of these have been incorporated in the ISO/IEC 19795 Part 1 Biometric Testing and Reporting Framework standard, now nearing publication.

**Prior benchmarks:** Automated face recognition accuracy has improved massively in the two decades since initial commercialization of the various technologies. NIST has tracked that improvement through its conduct of regular independent, free, open, and public evaluations. These have fostered improvements in the state of the art. This report serves as an update to the [NIST Interagency Report 8271](#) on performance of face identification algorithms, published in September 2019.

**Demographics:** In December 2019, NIST published a first report on demographic dependencies in face recognition, [NIST Interagency Report 8280](#) that documented age, sex and race differentials in one-to-one and one-to-many false positive and false negative rates.

**Scope:** NIST IR 8271 documented recognition results for four databases containing in excess of 30.2 million still photographs of 14.4 million individuals. That constituted the largest public and independent evaluation of face recognition ever conducted. It includes results for accuracy, speed, investigative vs. identification applications, scalability to large populations, use of multiple images per person, images of cooperative and non-cooperative subjects.

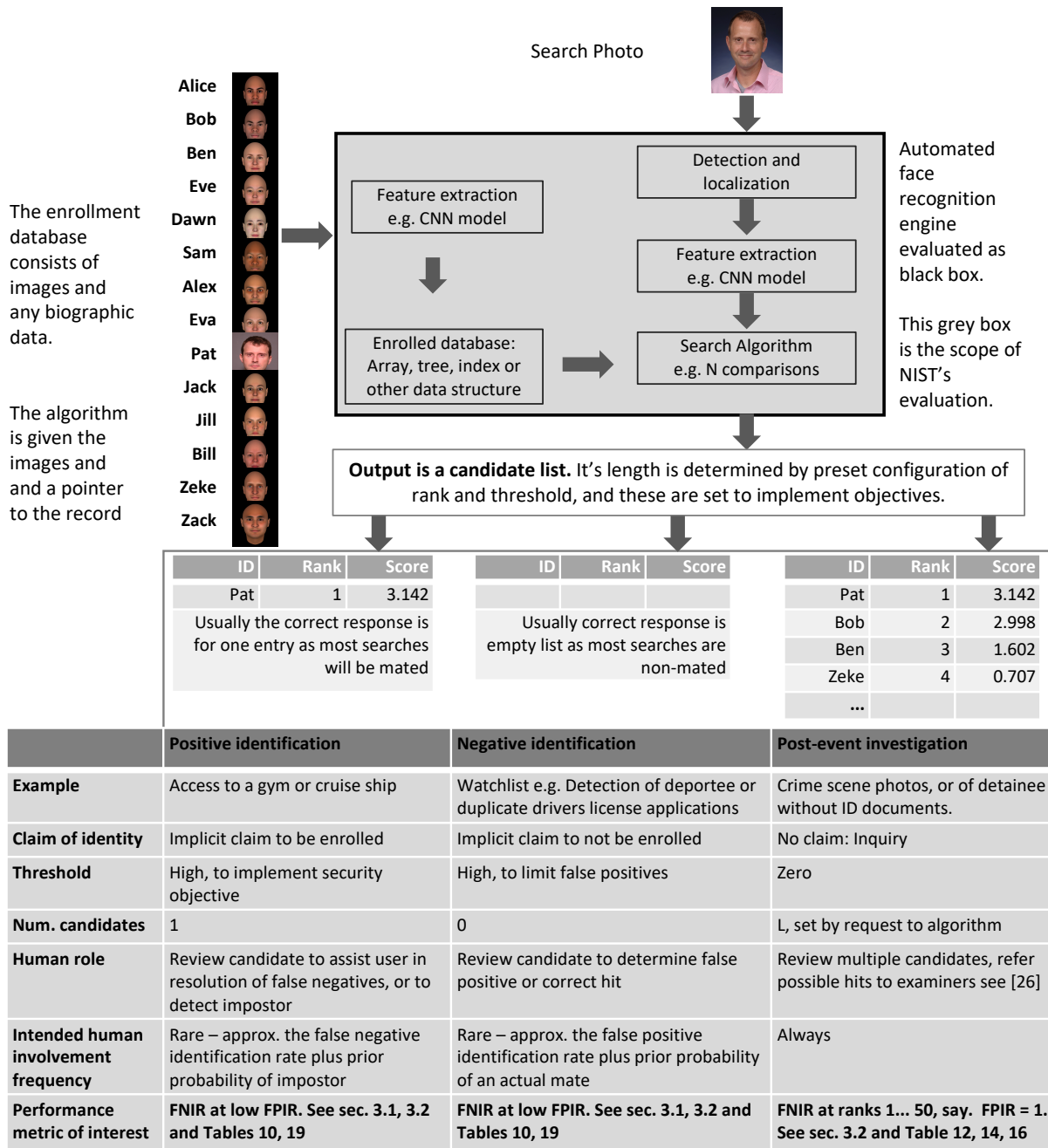
The report also includes results for ageing, recognition of twins, and recognition of profile-view images against frontal galleries. It otherwise does not address causes of recognition failure, neither image-specific problems nor subject-specific factors including demographics. Separate reports on demographic dependencies in face recognition will be published in the future. Additionally out of scope are: performance of live [human-in-the-loop transactional systems](#) like automated border control gates; human recognition accuracy as used in forensic applications; and recognition of persons in video sequences (which NIST evaluated separately [9]). Some of those applications share core matching technologies that *are* tested in this report.

**Images:** Five kinds of images are employed; these are either compared with images of the same kind, or against others from different capture environments as follows. The primary dataset is a set of law enforcement mugshot images (Fig. 5) which are enrolled and then searched with three kinds of images: other mugshots (i.e. within-domain); profile-view photographs (90 degree cross-view); and lower quality webcam images (Fig. 6) collected in similar detention operations (cross-domain). Additionally we compare high quality visa-like photos collected in immigration offices, with: medium quality border crossing images collected in primary immigration lanes; poor quality images collected in ATM-like registered traveller kiosks.

**Participation and industry coverage:** The report includes performance figures for prototype algorithms from the research laboratories of commercial developers and a few universities. This represents a substantial majority of the face recognition industry, but only a tiny minority of the academic community. Participation was open worldwide. While there is no charge for participation, developers incur some software engineering expense in implementing their algorithms behind the NIST application programming interface (API). The test is a black-box test where the function of the algorithm, and the intellectual property associated with it, is hidden inside pre-compiled libraries.

**Recent technology development:** Most face recognition research with deep convolutional neural networks (CNNs) has been aimed at achieving invariance to pose, illumination and expression variations that characterize photojournalism and social media images. The initial research [18, 22] employed large numbers of images of relatively few ( $\sim 10^4$ ) individuals to learn invariance. Inevitably much larger populations ( $\sim 10^7$ ) were employed for training [11, 20] but the benchmark, Labeled Faces in the Wild with (essentially) an equal error rate metric [12], represents an easy task,

one-to-one verification at very high false match rates. While a larger scale identification benchmark duly followed, Megaface [15], its primary metric, rank one hit rate, contrasts with the high threshold discrimination task required in most large-population applications of face recognition, namely credential de-duplication, and background checks. There, identification in galleries containing up to  $10^8$  individuals must be performed using a) very few images per individual and b) stringent thresholds to afford very low false positive identification rates. This track of FRVT was launched to measure the capability of the new technologies, including in these two cases. FRVT has included open-set identification tests since 2002, reporting both false negative and positive identification rates [7].



**Performance metrics for applications:** This report documents the performance of one-to-many face recognition algorithms. The word "performance" here refers to recognition accuracy and computational resource usage, as measured

by executing those algorithms on massive sequestered datasets.

This report includes extensive tabulation of recognition error rates germane to the main use-cases for face search technology. The Figure below, inspired by the Figure 1 in [23] differentiates different applications of the technolgy. The last row directs readers to the main tables relevant to those applications, respectively threshold-based and rank-based metrics that are special cases of the metrics given in section 3. The terms negative identification and positive identification are taken from the ISO/IEC 2382-37:2017 standardized biometrics vocabulary.

The algorithms are specifically configured for these applications by setting thresholds and candidate list lengths. Both rank-based metrics and threshold-based metrics include tradeoffs. In investigation, overall accuracy will be reduced if labor is only available to review a few candidates from the automated system. Note that when a fixed number of candidates are returned, the false positive identification rate of the automated face recognition engine will be 100%, because a probe image of anyone not enrolled will still return candidates. In identification applications where false positives must be limited to satisfy reviewer labor availability or a security objective, higher false negative rates are implied. This report includes extensive quantification of this threshold-based tradeoff.

See Sec. 3

**Template diversity:** The FRVT is designed to evaluate black-box technologies with the consequence that the templates that hold features extracted from face images are entirely proprietary opaque binary data that embed considerable intellectual property of the developer. Despite migration to CNN-based technologies there is no consensus on the optimal feature vector dimension. This is evidenced by template sizes ranging from below 100 bytes to more than four kilobytes. This diversity of approaches, suggests there is no prospect of a standard template something that would require a common feature set to be extracted from faces. Interoperability in automated face recognition remains solidly based on images and documentary standards for those, in particular the ICAO portrait [27] specification deriving from the ISO/IEC 19794-5 Token frontal [24] standard, which are similar to certain ANSI/NIST Type 10 [26] formats.

**Training:** The algorithms submitted to NIST have been developed using image datasets that developers do not disclose. The development will often include application of machine learning techniques and will additionally involve iterative training and testing cycles. NIST itself does not perform any training and does not refine or alter the algorithm in any way. Thus the model, data files, and libraries that define an algorithm are fixed for the duration of the tests. This reflects typical operational reality where recognition software, once installed, is fixed and constant until upgraded. This situation persists because on-site training of algorithms on customer data is atypical essentially because training is not a turnkey process.

**Automated search and human review:** Virtually all applications using automated face search require human review of the outputs at some frequency: Always for investigational applications; rarely in positive identification applications, after rejection (false or otherwise); and rarely in negative identification applications, after an alarm (false or otherwise). The human role is usually to compare a reference image with the query image or the live-subject if present, to render either a definitive decision on “exclusion” (different subjects), or “identification” (same subject), or a declaration that one or both images have “no value” and that no decision can be made. Note that automated face recognition algorithms are not built to do exclusion - low scores from a face comparison arise from different faces *and* poor quality images of the same face.

Human reviewers make recognition errors [5, 19, 25] and are sensitive to image acquisition and quality. Accurate human review is supported by high resolution - as specified in the Type 50, 51 acquisition profiles of the ANSI/NIST Type 10 record [26], and by multiple non-frontal views as specified in the same standard. These often afford views of the ear. Organizations involved in image collection should consider supporting human adjudication by collecting high-resolution frontal and non-frontal views, preparing low resolution versions for automated face recognition [24], and retaining both for any subsequent resolution of candidate matches. Along these lines, the ISO/IEC Joint Technical

Committee 1 subcommittee 37 on biometrics has just initiated projects on image quality assessment and face-aware capture.

## Release Notes

**FRVT Activities:** Since February 2017, NIST has been evaluating one-to-one verification algorithms on an ongoing basis. NIST then restarted FRVT's one-to-many track in February 2018, inviting participants to send up to prototype algorithms. Both tracks allows developers to submit updated algorithms to NIST at any time but no more frequently than four calendar months. This more closely aligns development and evaluation schedules. Results are posted to the web within a few weeks of submission. Details and full report are linked from the [Ongoing FRVT site](#).

**FRVT Reports:** The results of the FRVT appear in the series NIST Interagency Reports tabulated below. The reports were developed separately and released on different schedules. In prior years NIST has mostly reported FRVT results as a single report; this had the disadvantage that results from completed sub-studies were not published until all other studies were complete.

Date	Link	Title	No.
2014-03-20	<a href="#">PDF</a>	FRVT Performance of Automated Age Estimation Algorithms	7995
2015-04-20	<a href="#">PDF</a>	Face Recognition Vendor Test (FRVT) Performance of Automated Gender Classification Algorithms	8052
2014-05-21	<a href="#">PDF</a>	FRVT Performance of face identification algorithms	8009
2017-03-07	<a href="#">PDF</a>	Face In Video Evaluation (FIVE) Face Recognition of Non-Cooperative Subjects	8173
2017-11-23	<a href="#">PDF</a>	The 2017 IARPA Face Recognition Prize Challenge (FRPC)	8197
2018-11-27	<a href="#">PDF</a>	Face Recognition Vendor Test - Part 2: Identification	8271
2019-09-11	<a href="#">PDF</a>	Face Recognition Vendor Test - Part 2: Identification	8271
2019-12-11	<a href="#">PDF</a>	Face Recognition Vendor Test - Part 3: Demographic Effects	8280
2020-01-03	<a href="#">WWW</a>	Face Recognition Vendor Test (FRVT) - Part 1 Verification	Draft

Details appear on pages linked from <https://www.nist.gov/programs-projects/face-projects>.

**Appendices:** This report is accompanied by appendices which present exhaustive results on a per-algorithm basis. These are machine-generated and are included because the authors believe that visualization of such data is broadly informative and vital to understanding the context of the report.

**Typesetting:** Virtually all of the tabulated content in this report was produced automatically. This involved the use of scripting tools to generate directly type-settable L<sup>A</sup>T<sub>E</sub>X content. This improves timeliness, flexibility, maintainability, and reduces transcription errors.

**Graphics:** Many of the Figures in this report were produced using the **ggplot2** package running under **R**, the capabilities of which extend beyond those evident in this document.

# Contents

<b>Release Notes</b>	<b>1</b>
<b>Disclaimer</b>	<b>5</b>
<b>Institutional Review Board</b>	<b>5</b>
<b>Acknowledgments</b>	<b>5</b>
<b>Executive Summary</b>	<b>6</b>
<b>Scope and Context</b>	<b>12</b>
<b>Release Notes</b>	<b>16</b>
<b>1 Introduction</b>	<b>18</b>
<b>2 Evaluation datasets</b>	<b>19</b>
<b>3 Performance metrics</b>	<b>25</b>
<b>4 Results</b>	<b>41</b>
<b>Appendices</b>	<b>78</b>
<b>A Accuracy on large-population FRVT 2018 mugshots</b>	<b>78</b>
<b>B Effect of time-lapse: Accuracy after face ageing</b>	<b>123</b>
<b>C Effect of enrolling multiple images</b>	<b>184</b>
<b>D Accuracy with poor quality webcam images</b>	<b>191</b>
<b>E Accuracy for profile-view to frontal recognition</b>	<b>201</b>
<b>F Search duration</b>	<b>205</b>
<b>G Gallery Insertion Timing</b>	<b>212</b>

# 1 Introduction

One-to-many identification represents the largest market for face recognition technology. Algorithms are used across the world in a diverse range of biometric applications: detection of duplicates in databases, detection of fraudulent applications for credentials such as passports and driving licenses, token-less access control, surveillance, social media tagging, lookalike discovery, criminal investigation, and forensic clustering.

This report contains a breadth of performance measurements relevant to many applications. Performance here refers to accuracy and resource consumption. In most applications, the core accuracy of a facial recognition algorithm is the most important performance variable. Resource consumption will be important also as it drives the amount of hardware, power, and cooling necessary to accommodate high volume workflows. Algorithms consume processing time, they require computer memory, and their static template data requires storage space. This report documents these variables.

## 1.1 Open-set searches

FRVT tested open-set identification algorithms. Real-world applications are almost always “open-set”, meaning that some searches have an enrolled mate, but some do not. For example, some subjects have truly not been issued a visa or drivers license before; some law enforcement searches are from first-time arrestees<sup>6</sup>. In an “open-set” application, algorithms make no prior assumption about whether or not to return a high-scoring result, and for a mated search, the ideal behaviour is that the search produces the correct mate at high score and first rank. For a non-mate search, the ideal behavior is that the search produces zero high-scoring candidates.

Many academic benchmarks execute only closed-set searches. The proportion of mates found in the rank one position is the default accuracy metric. This hit rate metric ignores the score with which a mate is found; weak hits count as much as strong hits. This ignores the real-world imperative that in many applications it is necessary to elevate a threshold to reduce the number of false positives.

---

<sup>6</sup>Operationally closed-set applications are rare because it is usually not the case that all searches have an enrolled mate. One counter-example, however, is a cruise ship in which all passengers are enrolled and all searches should produce exactly one identity. Another example is forensic identification of dental records from an aircraft crash.

## 2 Evaluation datasets

This report documents accuracy for four kinds of images - mugshots, webcam, profiles and wild - as described in the following sections.

### 2.1 Immigration-related images

This report includes benchmark tests sharing a common enrollment of high quality frontal portrait images collected while subject make applications for various immigration benefits. We then search that with two kinds of images, webcam images collected during in-bound immigration and also images collected from registered travelers using a ATM-style kiosk. These are described below and depicted in Figure 4.



Figure 4: Example photos.

- ▷ **Application reference photos:** The images are collected in an attended interview setting using dedicated capture equipment and lighting. The images, at size 300x300 pixels, are smaller than normally indicated by ISO. The images are all high-quality frontal portraits collected in immigration offices and with a white background. As such, potential quality related drivers of high false match rates (such as blur) can be expected to be absent. The images are encoded as ISO/IEC 10918-1 i.e. JPEG. Older images had a compression ration of about 16:1, while newer images, since 2010, are more lightly compressed at 4:1. When these images are provided as input into the algorithm, they are labeled with the type "iso". This report enrols 1 600 000 application images, one per person.
- ▷ **Border crossing photos:** Most images are have width 320 and height 240 pixels. They are JPEG compressed at 16:1 i.e. filesize just below 15KB. The images present challenges for face recognition in that subjects often exhibit non-zero yaw and pitch (associated with the rotational degrees of freedom of the camera mount), low contrast (due to varying and intense background lights), and poor spatial resolution (due to inexpensive cameras). There are often subjects standing in the background, usually at very low resolution (see Figure 4b). In such cases, algorithms should detect all faces and determine which is the largest and most centered. When these images are provided as input into the algorithm, they are labeled with the type "wild".
- ▷ **Kiosk photos:** These photos were collected from subjects whose attention was focused on interaction with an immigration kiosk. They images were not intended for use with automated face recognition. The camera is situated above a display which the user touches, and is triggered either without directing the subject to look at it, or without waiting for the subject to comply. The images are therefore characterized by pitch-down pose, sometimes exceeding 45 degrees, as in Figure 4c. Yaw-angle variation is mild, with most images close to frontal. The images

have width 320 pixels and height 240 pixels and therefore tall individuals are sometimes cropped. This is often just above the eyes and can occur at the nose or mouth. Conversely, short individuals are sometimes cropped such that only the top part of the face is visible. In a quite small number of cases, there other subjects standing just behind the primary subject such that algorithms should detect all faces and determine which is the largest and most centered. Background ceiling lighting is often visible and this sometimes leads to under-exposure of the face. When these images are provided as input into the algorithm, they are labeled with the type "wild".

## 2.2 Law enforcement images

The main mugshot dataset used is referred to as the FRVT 2018 set. This set was collected over the period 2002 to 2017 in routine United States law enforcement operations. This set yields three subsets

- ▷ **Mugshots:** Mugshots comprise about 86% of the database. They have reasonable compliance with the ANSI/NIST ITL1-2011 Type 10 standard's subject acquisition profiles levels 10-20 for frontal images [26]. The most common departure from the standard's requirements is the presence of mild pose variations around frontal - the images of Figure 5 are typical. The images vary in size, with many being 480x600 pixels with JPEG compression applied to produce filesizes of between 18 and 36KB with many images outside this range, implying that about 0.5 bits are being encoded per pixel. When these images are provided as input into the algorithm, they are labeled with the type "mugshot".

Example images appear in Fig. 5

[NIST Interagency Report 8238](#) includes a comparison of this set of mugshots with the smaller and easier sets of mugshots used in tests run in 2010 and 2014.

- ▷ **Profile images:** Profile-view images have been collected in law enforcement for more than 100 years, as human capability is improved with orthogonal information. The profile images used in this report were collected during the same session as the frontal mugshot photograph, in the same standardized photographic setup. These would not therefore be used with automated face recognition. A small subset, 200 000 images, were set aside for testing. When these images are provided as input into the algorithm, they are labeled with the type "wild".

Example images appear in Fig. 7

- ▷ **Webcam images:** The remaining 14% of the images were collected using an inexpensive webcam attached to a flexible operator-directed mount. These images are all of size 240x240 pixels, that are in considerable violation of most quality-related clauses of all face recognition standards. As evident in the figure, the most common defects are non-frontal pose (associated with the rotational degrees of freedom of the camera mount), low contrast (due to varying and intense background lights), and poor spatial resolution (due to inexpensive camera optics) - see examples in Fig 6. The images are overly JPEG compressed, to between 4 and 7KB, implying that only 0.5 to 1 bits are being encoded per color pixel. When these images are provided as input into the algorithm, they are labeled with the type "wild".

Example images appear in Fig. 6

These are drawn from NIST Special Database 32 which may be downloaded [here](#).

These images were partitioned in galleries and probesets for the various experiment listed in Table 1.

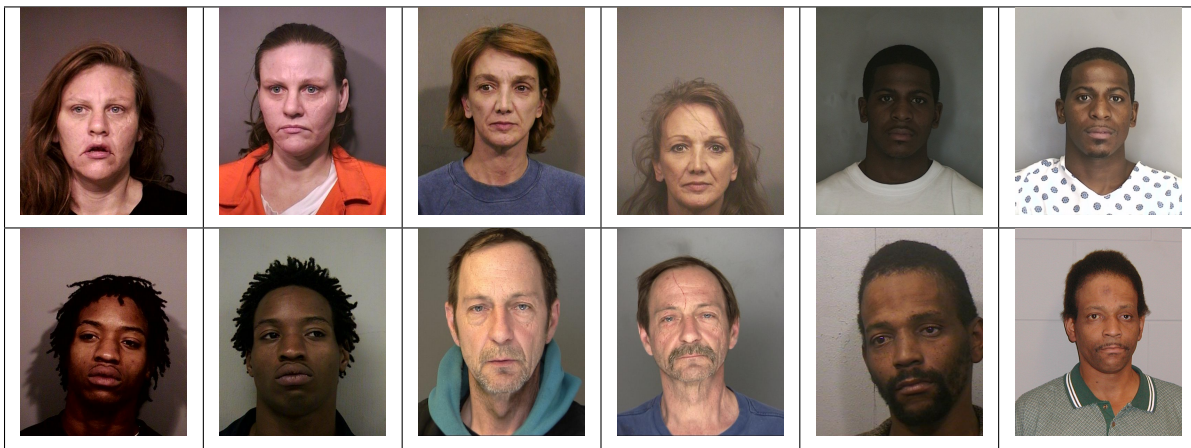


Figure 5: Six mated mugshot pairs representative of the FRVT-2014 (LEO) and FRVT-2018 datasets. The images are collected live, i.e. not scanned from paper. Image source: NIST Special Database 32 the Multiple Encounter Deceased Subjects dataset.



Figure 6: Twelve webcam images representative of probes against the FRVT-2018 mugshot gallery. The first eight images are four mated pairs. Such images present challenges to recognition including pose, non-uniform illumination, low contrast, compression, cropping, and low spatial sampling rate. Image source: NIST Special Database 32 the Multiple Encounter Deceased Subjects dataset.



Figure 7: **[Profile views]** The three images are a frontal enrollment, subsequent frontal probe, and same-session ninety degree profile view. While collection of both frontal and profile views has been typical in law enforcement for more than a century, the recognition of profile to frontal views has essentially been impossible. However, reasonably high accuracy results is now possible - see section E.

Image				
Encounter	1	...	$K_i - 1$	$K_i$
Capture Time	$T_1$	...	$T_{K_i - 1}$	$T_{K_i}$
Role RECENT	Not used	Not used	Enrolled	Search
Role LIFETIME	Enrolled	Enrolled	Enrolled	Search

Figure 8: Depiction of the “recent” and “lifetime” enrollment types. Image source: NIST Special Database 32

## 2.3 Enrollment strategies

Many operational applications include collection and enrollment of biometric data from subjects on more than one occasion. This might be done on a regular basis, as might occur in credential (re-)issuance, or irregularly, as might happen in a criminal recidivist situation [4]. The number of images per person will depend on the application area. In civil identity credentialing (e.g. passports, driver’s licenses), the images will be acquired approximately uniformly over time (e.g. ten years for a passport). While the distribution of dates for such images of a person might be assumed uniform, a number of factors might undermine this assumption<sup>7</sup>. In criminal applications, the number of images would depend on the number of arrests. The distribution of dates for arrest records for a person (i.e. the recidivism distribution) has been modeled using the exponential distribution but is recognized to be more complicated<sup>8</sup>.

In any case, the 2010 NIST evaluation of face recognition showed that considerable accuracy benefits accrue with retention and use of *all* historical images [6].

To this end, the FRVT API document provides  $K \geq 1$  images of an individual to the enrollment software. The software is tasked with producing a single proprietary undocumented “black-box” template<sup>9</sup> from the  $K$  images. This affords the algorithm an ability to generate a *model* of the individual, rather than to simply extract features from each image on a sequential basis.

As depicted in Figure 8, the  $i$ -th individual in the FRVT 2018 dataset has  $K_i$  images. These are labelled as  $x_k$  for  $k = 1 \dots K_i$  in chronological order of capture date. To measure the utility of having multiple enrollment images, this report evaluates three kinds of enrollment:

- ▷ **Recent:** Only the second most recent image,  $x_{K_i - 1}$  is enrolled. This strategy of enrollment mimics the operational policy of retaining the imagery from the most recent encounter. This might be done operationally to ameliorate the effects of face ageing. Obviously retaining only the most recent image should only be done if the identity of the person is trusted to be correct. For example, in an access control situation retention of the most recent successful *authentication* image would be hazardous if it could be a false positive.
- ▷ **Lifetime-consolidated:** All but the most recent image are enrolled,  $x_1 \dots x_{K_i - 1}$ . This subject-centric strategy might be adopted if quality variations exist where an older image might be more suitable for matching, despite the ageing effect.

<sup>7</sup>For example, a person might skip applying for a passport for one cycle, letting it expire. In addition, a person might submit identical images (from the same photography session) to consecutive passport applications at five year intervals.

<sup>8</sup>A number of distributions have been considered to model recidivism, see for example [3].

<sup>9</sup>There are no formal face template standards. Template standards only exist for fingerprint minutiae - see ISO/IEC 19794-2:2011.

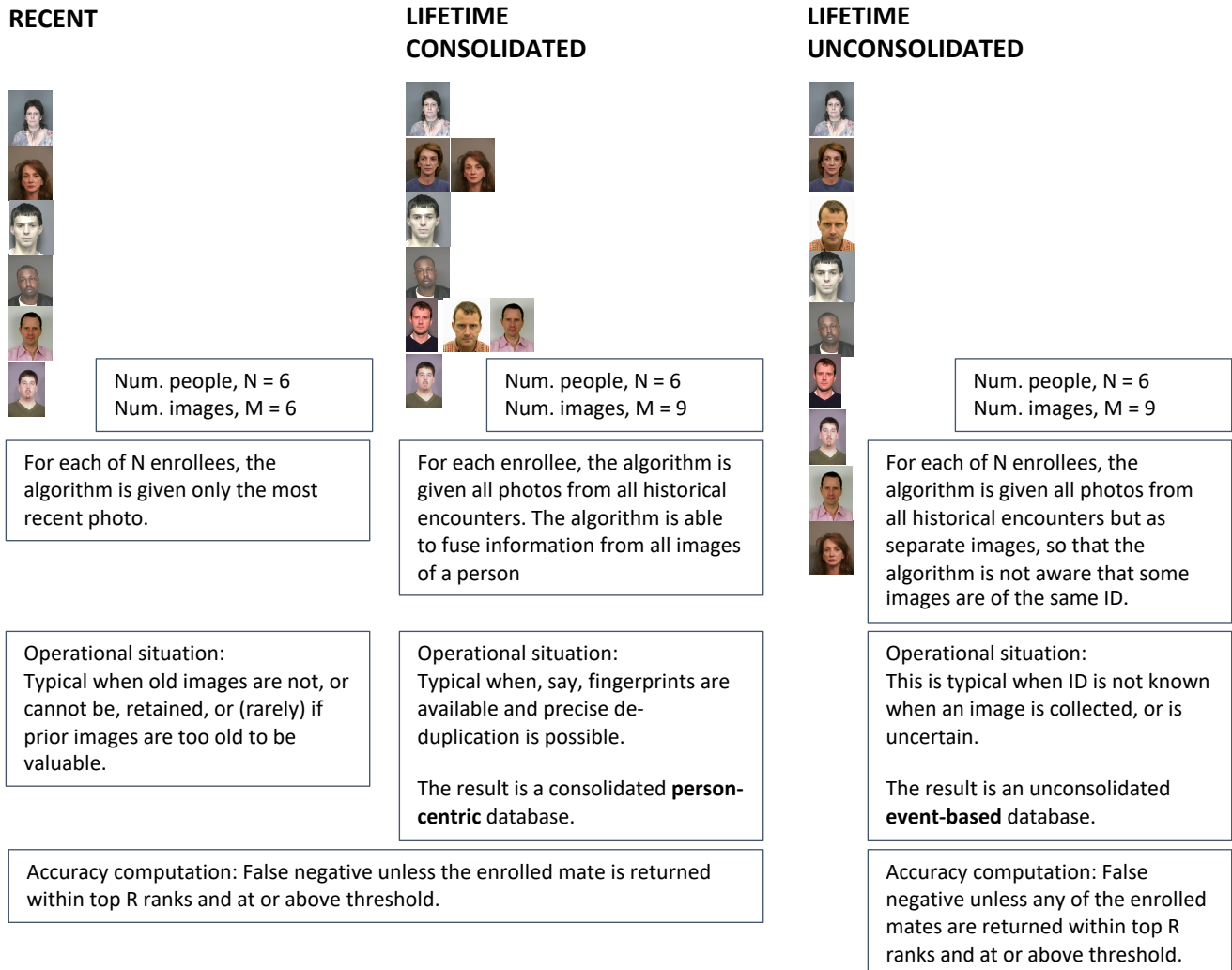


**Figure 9: Enrollment strategies.** The figure shows the three kinds of enrollment databases examined in this report. Image source: NIST Special Database 32

	ENROLLMENT				SEARCH			
	TYPE SEE SECTION 2.3	POPULATION FILTER	N-SUBJECTS	N-IMAGES	MATE N-SUBJECTS	NON-MATE N-IMAGES	N-SUBJECTS	N-IMAGES
<b>Mugshot trials from enrollment of single images</b>								
1	RECENT	NATURAL	640 000	640 000	154 549	154 549	331 254	331 254
2	RECENT	NATURAL	1 600 000	1 600 000				
3	RECENT	NATURAL	3 000 000	3 000 000				
4	RECENT	NATURAL	6 000 000	6 000 000				
5	RECENT	NATURAL	12 000 000	12 000 000				
<b>Cross-domain</b>								
13	MUGSHOTS AS ON ROW 2				82 106 WEBCAM	82 106 WEBCAM	331 254 WEBCAM	331 254 WEBCAM
<b>Cross-view</b>								
14	MUGSHOTS AS ON ROW 2				100 000 PROFILE	100 000 PROFILE	100 000 PROFILE	100 000 PROFILE
<b>Mugshot ageing</b>								
17	OLDEST	NATURAL	3 068 801	3 068 801	2 853 221	10 951 064	0	0
<b>Border crossing ageing</b>								
17	OLDEST	NATURAL	1 600 000	1 600 000	903 655	1 922 393	1 393 076	1 680 000
<b>Visa-border</b>								
19	PRIOR	NATURAL	1 600 000 VISA	1 600 000 VISA	80 000 BORDER	80 000 BORDER	80 000 BORDER	80 000 BORDER
20	VISA AS ON ROW 18				21 016 BORDER	21 016 BORDER	21 016 BORDER	21 016 BORDER

**Table 1: Enrollment and search sets.** Each row summarizes one identification trial. Unless stated otherwise, all entries refer to mugshot images. The term “natural” means that subjects were selected without heed to demographics, i.e. in the distribution native to this dataset. The probe images were collected in a different calendar year to the enrollment image. Missing values in rows 2-12 are the same as in row 1.

▷ **Lifetime-unconsolidated:** Again all but the most recent image are enrolled  $x_1 \dots x_{K_i-1}$  but now separately, with different identifiers, such that the algorithm is not aware that the images are from the same face. This kind of event- or encounter-centric enrollment is very common when operational constraints preclude reliable consolidation of the historical encounters into a single identity. This aspect also prevents the recognition algorithm from a) building a holistic model of identity (as is common in speaker recognition systems) and b) implementing fusion, for example template-level fusion of feature vectors, or post-search score-level fusion. The result is that searches will typically yield more than one image of a person in the top ranks. This has consequences for appropriate metrics, as detailed in section 3.2.1

NIST first evaluated this kind of enrollment in mid 2018, and the results tables include some comparison of accuracy available from all three enrollment styles.

In all cases, the most recent image,  $x_{K_i}$ , is reserved as the search image. For the 1.6 million subject enrollment partition of the FRVT 2018 data,  $1 \leq K_i \leq 33$  with  $K_i = 1$  in 80.1% of the individuals,  $K_i = 2$  in 13.4%,  $K_i = 3$  in 3.7%,  $K_i = 4$  in 1.4%,  $K_i = 5$  in 0.6%,  $K_i = 6$  in 0.3%, and  $K_i > 6$  is 0.2% for everyone else. This distribution is substantially dependent on United States recidivism rates.

We did not evaluate the case of retaining only the highest quality image, since automated quality assessment is out of scope for this report. We do not anticipate that such strategies will prove beneficial when the quality assessment apparatus is imperfect and unvalidated.

### 3 Performance metrics

This section gives specific definitions for accuracy and timing metrics. Tests of open-set biometric algorithms must quantify frequency of two error conditions:

- ▷ **False positives:** Type I errors occur when search data from a person who has never been seen before is incorrectly associated with one or more enrollees' data.
- ▷ **Misses:** Type II errors arise when a search of an enrolled person's biometric does not return the correct identity.

Many practitioners prefer to talk about "hit rates" instead of "miss rates" - the first is simply one minus the other as detailed below. Sections 3.1 and 3.2 define metrics for the Type I and Type II performance variables.

Additionally, because recognition algorithms sometimes fail to produce a template from an image, or fail to execute a one-to-many search, the occurrence of such events must be recorded. Further because algorithms might elect to not produce a template from, for example, a poor quality image, these failure rates must be combined with the recognition error rates to support algorithm comparison. This is addressed in section 3.5.

Finally, section 3.7 discusses measurement of computation duration, and section 3.8 addresses the uncertainty associated with various measurements. Template size measurement is included with the results.

#### 3.1 Quantifying false positives

It is typical for a search to be conducted into an enrolled population of  $N$  identities, and for the algorithm to be configured to return the closest  $L$  candidate identities. These candidates are ranked by their score, in descending order, with all scores required to be greater than or equal to zero. A human analyst might examine either all  $L$  candidates, or just the top  $R \leq L$  identities, or only those with score greater than threshold,  $T$ . The workload associated with such examination is discussed later, in 3.6.

False alarm performance is quantified in two related ways. These express how many searches produces false positives, and then, how many false positives are produced in a search.

**False positive identification rate:** The first quantity, FPIR, is the proportion of non-mate searches that produce an adverse outcome:

$$\text{FPIR}(N, T) = \frac{\text{Num. non-mate searches where one or more enrolled candidates are returned with score at or above threshold}}{\text{Num. non-mate searches attempted.}} \quad (1)$$

Under this definition, FPIR can be computed from the highest non-mate candidate produced in a search - it is not necessary to consider candidates at rank 2 and above. FPIR is the primary measure of Type I errors in this report.

**Selectivity:** However, note that in any given search, several non-mate may be returned above threshold. In order to quantify such events, a second quantity, selectivity (SEL), is defined as the *number* of non-mates returned on a candidate list, averaged over all searches.

$$\text{SEL}(N, T) = \frac{\text{Num. non-mate enrolled candidates returned with score at or above threshold}}{\text{Num. non-mate searches attempted.}} \quad (2)$$

where  $0 \leq \text{SEL}(N, T) \leq L$ . Both of these metrics are useful operationally. FPIR is useful for targeting how often an

adverse false positive outcome can occur, while SEL as a number is related to workload associated with adjudicating candidate lists. The relationship between the two quantities is complicated - it depends on whether an algorithm concentrates the false alarms in the results of a few searches or whether it disburses them across many. This was detailed in FRVT 2014, NISTIR 8009. It has not yet been detailed in FRVT 2018.

### 3.2 Quantifying hits and misses

If  $L$  candidates are returned in a search, a shorter candidate list can be prepared by taking the top  $R \leq L$  candidates for which the score is above some threshold,  $T \geq 0$ . This reduction of the candidate list is done because thresholds may be applied, and only short lists might be reviewed (according to policy or labor availability, for example). It is useful then to state accuracy in terms of  $R$  and  $T$ , so we define a “miss rate” with the general name **false negative identification rate** (FNIR), as follows:

$$\text{FNIR}(N, R, T) = \frac{\text{Num. mate searches with enrolled mate found outside top } R \text{ ranks or score below threshold}}{\text{Num. mate searches attempted.}} \quad (3)$$

This formulation is simple for evaluation in that it does not distinguish between causes of misses. Thus a mate that is not reported on a candidate list is treated the same as a miss arising from face finding failure, algorithm intolerance of poor quality, or software crashes. Thus if the algorithm fails to produce a candidate list, either because the search failed, or because a search template was not made, the result is regarded as a miss, adding to FNIR.

*Hit rates, and true positive identification rates:* While FNIR states the “miss rate” as how often the correct candidate is either not above threshold or not at good rank, many communities prefer to talk of “hit rates”. This is simply the **true positive identification rate**(TPIR) which is the complement of FNIR giving a positive statement of how often mated searches are successful:

$$\text{TPIR}(N, R, T) = 1 - \text{FNIR}(N, R, T) \quad (4)$$

This report does not report true positive “hit” rates, preferring false negative miss rates for two reasons. First, costs rise linearly with error rates. For example, if we double FNIR in an access control system, then we double user inconvenience and delay. If we express that as decrease of TPIR from, say 98.5% to 97%, then we mentally have to invert the scale to see a doubling in costs. More subtly, readers don’t perceive differences in numbers near 100% well, becoming inured to the “high nineties” effect where numbers close to 100 are perceived indifferently.

**Reliability** is a corresponding term, typically being identical to TPIR, and often cited in automated (fingerprint) identification system (AFIS) evaluations.

An important special case is the **cumulative match characteristic**(CMC) which summarizes accuracy of mated-searches only. It ignores similarity scores by relaxing the threshold requirement, and just reports the fraction of mated searches returning the mate at rank  $R$  or better.

$$\text{CMC}(N, R) = 1 - \text{FNIR}(N, R, 0) \quad (5)$$

We primarily cite the complement of this quantity,  $\text{FNIR}(N, R, 0)$ , the fraction of mates *not* in the top  $R$  ranks.

The **rank one hit rate** is the fraction of mated searches yielding the correct candidate at best rank, i.e.  $\text{CMC}(N, 1)$ . While this quantity is the most common summary indicator of an algorithm’s efficacy, it is not dependent on similarity scores, so it does not distinguish between strong (high scoring) and weak hits. It also ignores that an adjudicating reviewer is often willing to look at many candidates.

### 3.2.1 False negative rates for unconsolidated galleries

As detailed in section 2.3 a common type of gallery, here referred to as the lifetime unconsolidate type, is populated with all images of an individual without any association between them. That is, the gallery construction algorithm is not provided with any ID labels that would support processing of a person's images jointly. This contrasts with the lifetime consolidate type where an algorithm may explicitly fuse features from multiple images of a person, or select a best image. In such cases, where the number of enrolled images is a random variable, we define two false negative rates as follows.

The first demands that the algorithm place any of the  $K_i$  mates in the top  $R \geq 1$  ranks. The proportion of searches for which this does not occur forms a false negative identification rate:

$$\text{FNIR}_{\text{any}}(N, R, T) = 1 - \frac{\text{Num. mate searches where any enrolled mate is found in the top } R \text{ ranks and at-or-above threshold}}{\text{Num. mate searches attempted.}} \quad (6)$$

The second demands that the algorithm place all  $K_i$  mates in the top  $R \geq K_i$  ranks. The proportion of searches for which this does not occur forms a false negative identification rate:

$$\text{FNIR}_{\text{all}}(N, R, T) = 1 - \frac{\text{Num. mate searches where all enrolled mates are found in the top } R \text{ ranks and at-or-above threshold}}{\text{Num. mate searches attempted.}} \quad (7)$$

Placing all mates in the top ranks is a more difficult task than correctly retrieving any image, so it holds that:  $\text{FNIR}_{\text{all}} \geq \text{FNIR}_{\text{any}}$ . This is evident in the results presented for November 2018 algorithms in Tables starting at ??.

The information retrieval community might prefer to compute and plot *precision* and *recall*; this is a valid approach, but we advance the two metrics above because they relate to our normal definition of consolidated FNIR, and they cover the two extreme use-cases of wanting any hit vs. all hits.

## 3.3 DET interpretation

In biometrics, a false negative occurs when an algorithm fails to match two samples of one person – a Type II error. Correspondingly, a false positive occurs when samples from two persons are improperly associated – a Type I error.

Matches are declared by a biometric system when the native comparison score from the recognition algorithm meets some threshold. Comparison scores can be either similarity scores, in which case higher values indicate that the samples are more likely to come from the same person, or dissimilarity scores, in which case higher values indicate different people. Similarity scores are traditionally computed by fingerprint and face recognition algorithms, while dissimilarities are used in iris recognition. In some cases, the dissimilarity score is a distance possessing metric properties. In any case, scores can be either mate scores, coming from a comparison of one person's samples, or nonmate scores, coming from comparison of different persons' samples.

The words "genuine" or "authentic" are synonyms for mate, and the word "impostor" is used as a synonym for non-mate. The words "mate" and "nonmate" are traditionally used in identification applications (such as law enforcement search, or background checks) while genuine and impostor are used in verification applications (such as access control).

An error tradeoff characteristic represents the tradeoff between Type II and Type I classification errors. For identification this plots false negative vs. false positive identification rates i.e. FNIR vs. FPIR parametrically with T. Such plots

are often called detection error tradeoff (DET) characteristics or receiver operating characteristic (ROC). These serve the same function – to show error tradeoff – but differ, for example, in plotting the complement of an error rate (e.g.  $TPIR = 1 - FNIR$ ) and in transforming the axes, most commonly using logarithms, to show multiple decades of FPIR. More rarely, the function might be the inverse of the Gaussian cumulative distribution function.

The slides of Figures 10 through 15 discuss presentation and interpretation of DETs used in this document for reporting face identification accuracy. Further detail is provided in formal biometrics testing standards, see the various parts of ISO/IEC 19795 Biometrics Testing and Reporting. More terms, including and beyond those to do with accuracy, appear in ISO/IEC 2382-37 Information technology – Vocabulary – Part 37: Harmonized biometric vocabulary.

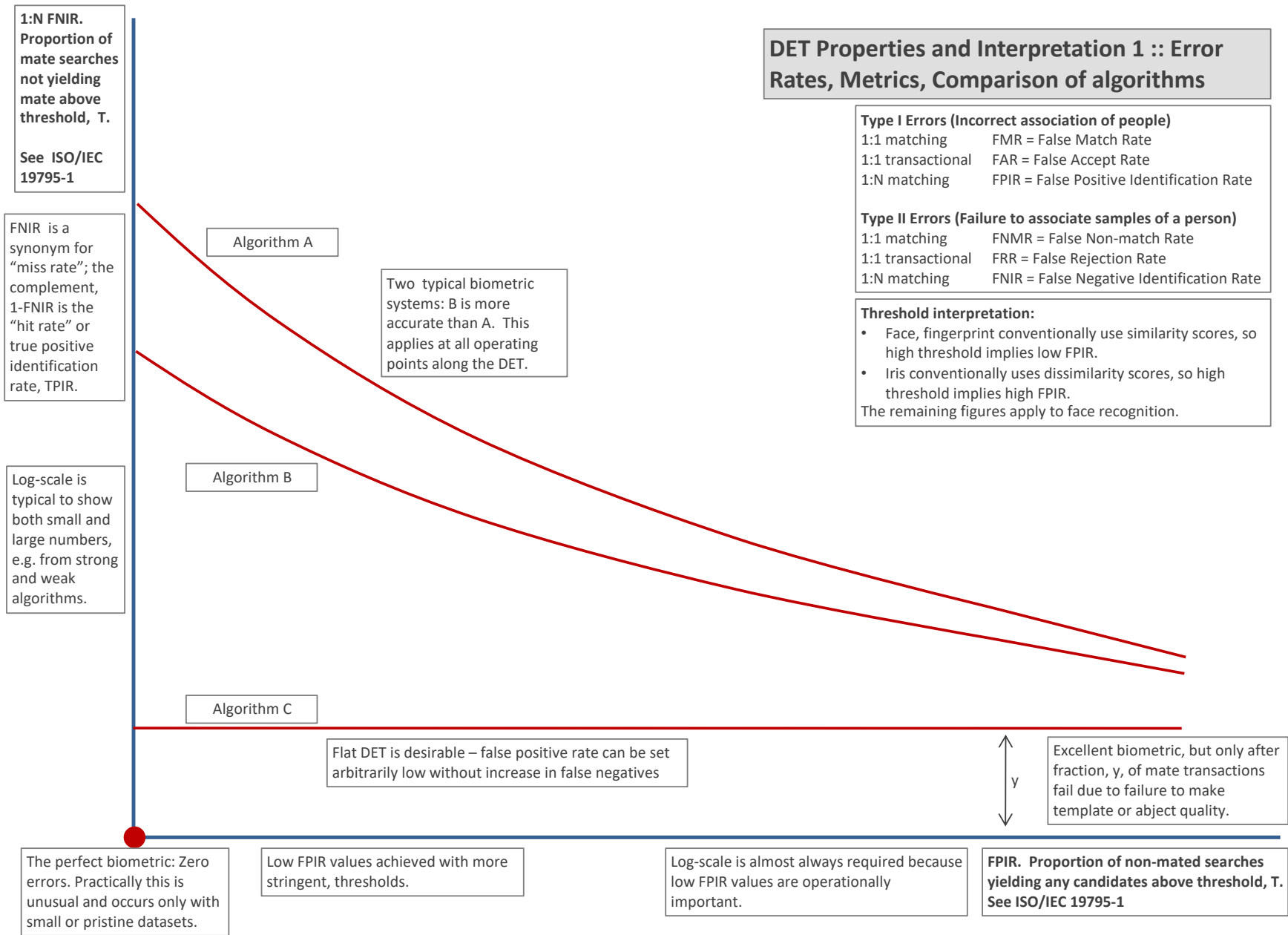


Figure 10: DET as the primary performance reporting mechanism.

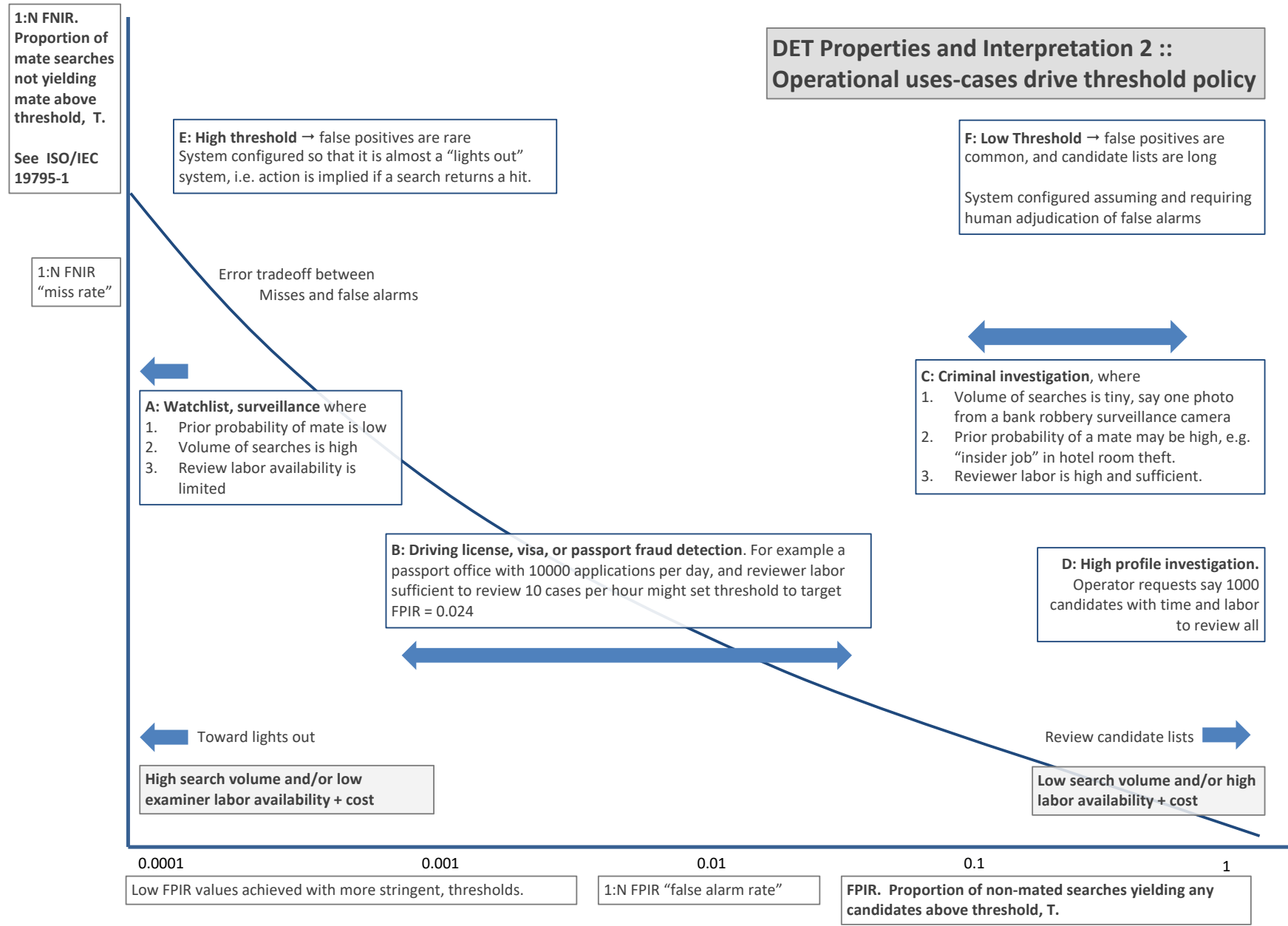
2022/04/28  
22:29:02FNIR(N, R, T) = False neg. identification rate  
FPIR(N, T) = False pos. identification rate  
N = Num. enrolled subjects  
R = Num. candidates examined  
T = ThresholdT = 0 → Investigation  
T > 0 → Identification

Figure 11: DET as the primary performance reporting mechanism.

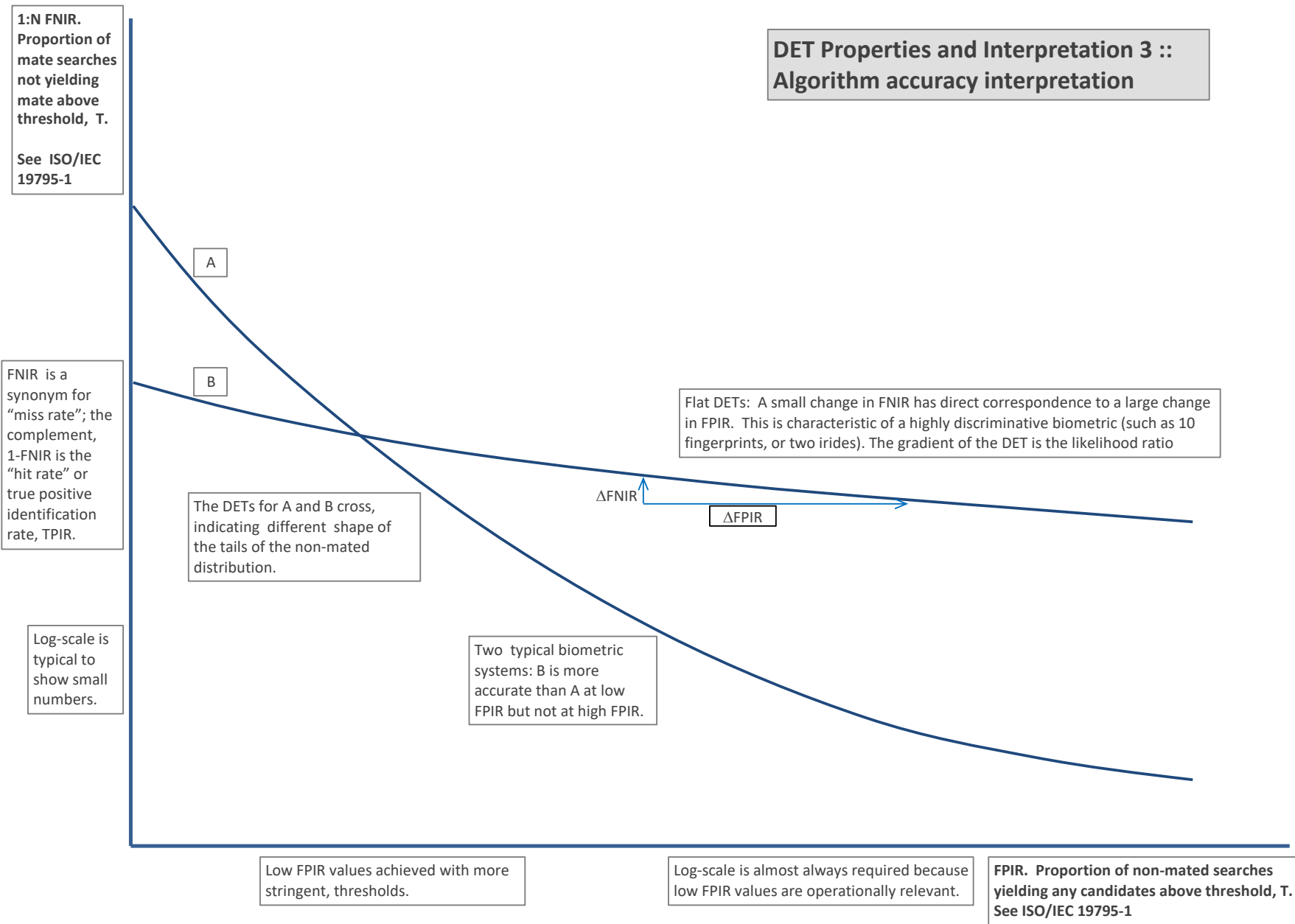
2022/04/28  
22:29:02FNIR(N, R, T) = False neg. identification rate  
FPIR(N, T) = False pos. identification rateN = Num. enrolled subjects  
R = Num. candidates examinedT = Threshold  
T = 0 → Investigation  
T > 0 → Identification

Figure 12: DET as the primary performance reporting mechanism.

2022/04/28  
22:29:02FNIR(N, R, T) = False neg. identification rate  
FPIR(N, T) = False pos. identification rateN = Num. enrolled subjects  
R = Num. candidates examined

T = Threshold

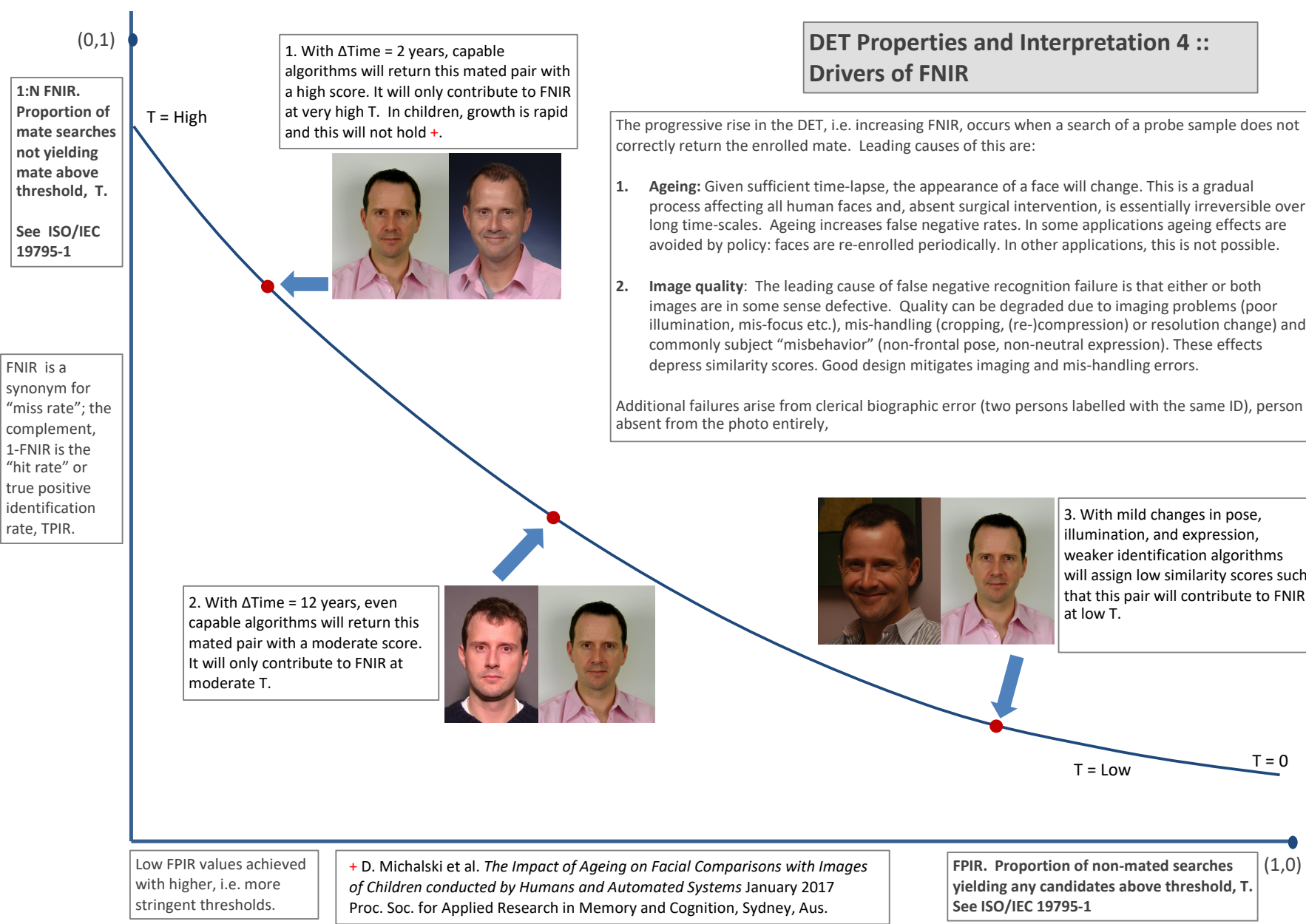
T = 0 → Investigation  
T > 0 → Identification

Figure 13: DET as the primary performance reporting mechanism.

2022/04/28  
22:29:02FNIR(N, R, T) = False neg. identification rate  
FPIR(N, T) = False pos. identification rate

T = Threshold

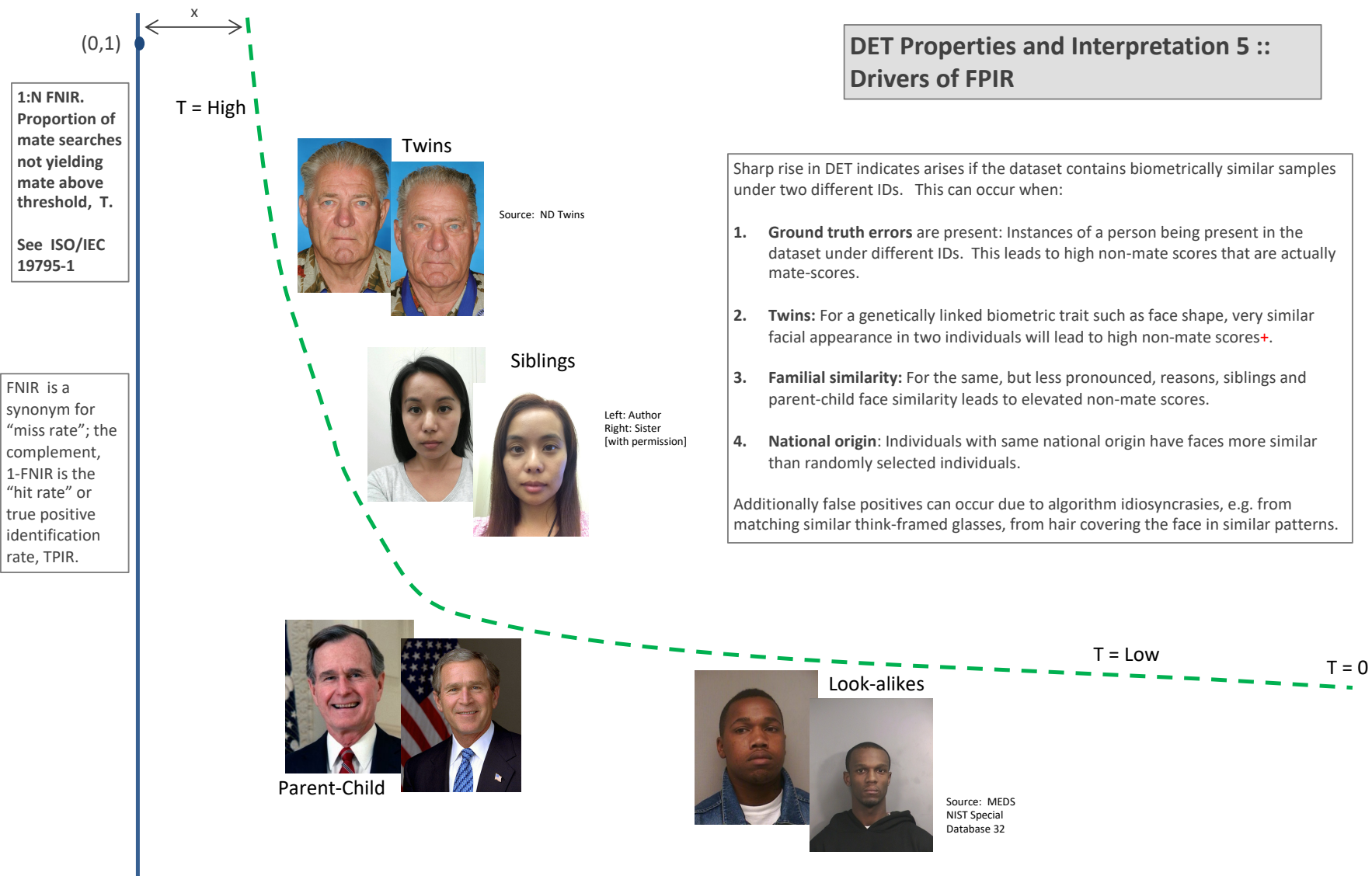
T = 0 → Investigation  
T > 0 → Identification

Figure 14: DET as the primary performance reporting mechanism.

2022/04/28  
22:29:02

$\text{FNIR}(N, R, T) =$  False neg. identification rate  
 $\text{FPIR}(N, T) =$  False pos. identification rate

$N$  = Num. enrolled subjects  
 $R$  = Num. candidates examined

$T$  = Threshold

$T = 0 \rightarrow$  Investigation  
 $T > 0 \rightarrow$  Identification

**1:N FNIR.**  
Proportion of mate searches not yielding mate above threshold,  $T$ .  
See ISO/IEC 19795-1

Algorithm X,  
Condition 1

Algorithm X,  
Condition 2

FNIR is a synonym for "miss rate"; the complement, 1-FNIR is the "hit rate" or true positive identification rate, TPIR.

Log-scale is typical to show small numbers.

If system X is used with images of different properties, say from different imaging systems, or from different populations, generally both FNIR and FPIR will change. The dotted line joins points of the same threshold. Horizontal (vertical) lines indicate change in FPIR (FNIR) only. Two cases concerning population size are shown below (A and B), for the blue curves.

Algorithm Y,  
Condition 1

Algorithm Y,  
Condition 2

If DETs are computed for two categories (men and women) or (cameras A and B) or (indoor vs. outdoor), generally the Type I and Type II errors will differ and the line of constant threshold will be neither horizontal nor vertical.

The ideal situation in most applications is that a fixed threshold yields a fixed FPIR so that system owners see no change in false alarms across populations or conditions.

Low FPIR values achieved with higher, i.e. more stringent, thresholds.

Log-scale is often required because low FPIR values are operationally relevant.

**FPIR.** Proportion of non-mated searches yielding any candidates above threshold,  $T$ . See ISO/IEC 19795-1

Figure 15: DET as the primary performance reporting mechanism.

## DET Properties and Interpretation 6 :: Fixed thresholds, change in image properties or demographics

2022/04/28  
22:29:02FNIR(N, R, T) = False neg. identification rate  
FPIR(N, T) = False pos. identification rateN = Num. enrolled subjects  
R = Num. candidates examined  
T = ThresholdT = 0 → Investigation  
T > 0 → Identification

**1:N FNIR.**  
Proportion of mate searches not yielding mate above threshold, T.  
See ISO/IEC 19795-1

FNIR is a synonym for "miss rate"; the complement, 1-FNIR is the "hit rate" or true positive identification rate, TPIR.

Log-scale is typical to show small numbers.

A: Typical case: In theory, and often in practice, a 1:N search is implemented by executing N 1:1 comparisons independently and then sorting by similarity score:

**Mate scores:** A mate comparison score is independent of the rest of enrollment data, and so independent of N. This implies the horizontal line above  $\text{FNIR}(T, N) = \text{FNMR}(T, 1)$ .

**Non-mate scores:** FPIR increases linearly with N from binomial theory:  $\text{FPIR}(N, T) = 1 - (1 - \text{FMR}(T))^N \rightarrow N \text{ FMR}(T)$  for small FPIR.

Pop. N1



Pop. N2 &gt; N1

B: Special case: An enrollment database is not just a linear data structure, it could be an index, or tree, then search is not simply N 1:1 comparisons and a sort. In that case:

**Mate scores** become dependent on the enrollment data, either its size or actual content, then generally  $\text{FNIR}(T, N) \neq \text{FNIR}(T, 1)$ .

Non-mate scores are normally no longer just the highest 1:1 comparison score. Instead, for example, scores may be normalized as the implementation attempts to make FPIR independent of N will yield the vertical line linking points of equal threshold.

Low FPIR values achieved with higher, i.e. more stringent, thresholds.

Log-scale is often required because low FPIR values are operationally important.

## DET Properties and Interpretation 7 :: Effect of enrolled population size.

**FPIR.** Proportion of non-mated searches yielding any candidates above threshold, T.  
See ISO/IEC 19795-1

Figure 16: DET as the primary performance reporting mechanism.

2022/04/28  
22:29:02FNIR(N, R, T) = False neg. identification rate  
FPIR(N, T) = False pos. identification rateN = Num. enrolled subjects  
R = Num. candidates examined

T = Threshold

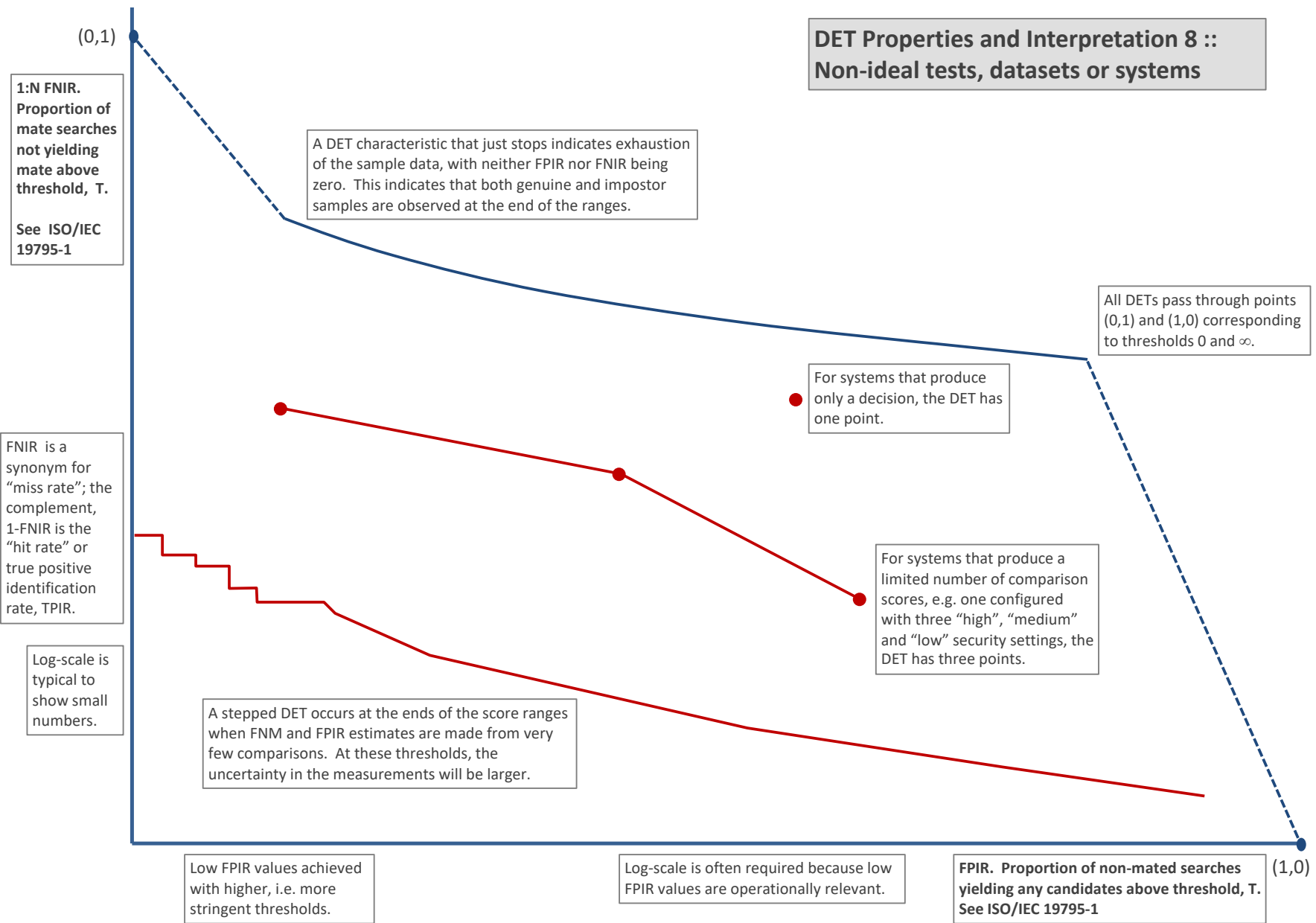
T = 0 → Investigation  
T > 0 → Identification

Figure 17: DET as the primary performance reporting mechanism.

### 3.4 Best practice testing requires execution of searches with and without mates

FRVT embeds 1:N searches of two kinds: Those for which there is an enrolled mate, and those for which there is not. The respective numbers for these types of searches appear in Table 1. However, it is common to conduct only mated searches<sup>10</sup>. The cumulative match characteristic is computed from candidate lists produced in mated searches. Even if the CMC is the only metric of interest, the actual trials executed in a test should nevertheless include searches for which no mate exists. As detailed in Table 1 the FRVT reserved disjoint populations of subjects for executing true non-mate searches.

### 3.5 Failure to extract features

During enrollment some algorithms fail to convert a face image to a template. The proportion of failures is the failure-to-enroll rate, denoted by FTE. Similarly, some search images are not converted to templates. The corresponding proportion is termed failure-to-extract, denoted by FTX.

We do not report FTX because we assume that the same underlying algorithm is used for template generation for enrollment and search.

Failure to extract rates are incorporated into FNIR and FPIR measurements as follows.

- ▷ **Enrollment templates:** Any failed enrollment is regarded as producing a zero length template. Algorithms are required by the API [10] to transparently process zero length templates. The effect of template generation failure on search accuracy depends on whether subsequent searches are mated, or non-mated: Mated searches will fail giving elevated FNIR; non-mated searches will not produce false positives so, to first order, FPIR will be reduced by a factor of  $1 - \text{FTE}$ .
- ▷ **Search templates and 1:N search:** In cases where the algorithm fails to produce a search template from input imagery, the result is taken to be a candidate list whose entries have no hypothesized identities and zero score. The effect of template generation failure on search accuracy depends on whether searches are mated, or non-mated: Mated searches will fail giving elevated FNIR; Non-mated searches will not produce false positives, so FPIR will be reduced. Thus given a measurement of false negative and positive rates made over only those where failures-to-extract did not occur, those rates - call them  $\text{FNIR}^\dagger$  and  $\text{FPIR}^\dagger$  - could be adjusted by an explicit measurement of FTX as follows

$$\text{FNIR} = \text{FTX} + (1 - \text{FTX})\text{FNIR}^\dagger \quad (8)$$

$$\text{FPIR} = (1 - \text{FTX})\text{FPIR}^\dagger \quad (9)$$

This approach is the correct treatment for positive-identification applications such as access control where cooperative users are enrolled and make attempts at recognition. This approach is not appropriate to negative identification applications, such as visa fraud detection, in which hostile individuals may attempt to evade detection by submitting poor quality samples. In those cases, template generation failures should be investigated as though a false alarm had occurred.

<sup>10</sup>For example, the [Megaface benchmark](#). This is bad practice for several reasons: First, if a developer knows, or can reasonably assume, that a mate always exists, then unrealistic gaming of the test is possible. A second reason is that it does not put FPIR on equal footing with FNIR and that matters because in most applications, not all searches have mates - not everyone has been previously enrolled in a driving license issuance or a criminal justice system - so addressing between-class separation becomes necessary.

### 3.6 Fixed length candidate lists, threshold independent workload

Suppose an automated face identification algorithm returns  $L$  candidates, and a human reviewer is retained to examine up to  $R$  candidates, where  $R \leq L$  might be set by policy, preference or labor availability. For now, assume also that the reviewer is not provided with, or ignores, similarity scores, and thresholds are not applied. Given the algorithm typically places mates at low (good) ranks, the number of candidates a reviewer can be expected to review can be derived as follows. Note that the reviewer will:

- ▷ Always inspect the first ranked image Frac. reviewed = 1
- ▷ Then inspect those candidates where mate not confirmed at rank 1 Frac. reviewed = 1-CMC(1)
- ▷ Then inspect those candidates where mate not confirmed at rank 1 or 2 Frac. reviewed = 1-CMC(2)

etc. Thus if the reviewer will stop after a maximum of  $R$  candidates, the expected number of candidate reviews is

$$M(R) = 1 + (1 - CMC(1)) + (1 - CMC(2)) + \dots + (1 - CMC(R - 1)) \quad (10)$$

$$= R - \sum_{r=1}^{R-1} CMC(r) \quad (11)$$

A recognition algorithm that front-loads the cumulative match characteristic will offer reduced workload for the reviewer. This workload is defined only over the searches for which a mate exists. In the cases where there truly is no mate, the reviewer would review all  $R$  candidates. Thus, if the proportion of searches for which a mate does exist is  $\beta$ , which in the law enforcement context would be the recidivism rate [3], the full expression for workload becomes:

$$M(R) = \beta \left( R - \sum_{r=1}^{R-1} CMC(r) \right) + (1 - \beta)R \quad (12)$$

$$= R - \beta \sum_{r=1}^{R-1} CMC(r) \quad (13)$$

### 3.7 Timing measurement

Algorithms were submitted to NIST as implementations of the application programming interface(API) specified by NIST in the Evaluation Plan [10]. The API includes functions for initialization, template generation, finalization, search, gallery insert, and gallery delete. Two template generation functions are required, one for the preparation of an enrollment template, and one for a search template.

In NIST's test harness, all functions were wrapped by calls to the C++ std::chrono::high\_resolution\_clock which on the dedicated timing machine counts 1ns clock ticks. Precision is somewhat worse than that however.

## 3.8 Uncertainty estimation

### 3.8.1 Random error

This study leverages operational datasets for measurement of recognition error rates. This affords several advantages. First, large numbers of searches are conducted (see Table 1) giving precision to the measurements. Moreover, for the two mugshot datasets, these do not involve reuse of individuals so binomial statistics can be expected to apply to recognition error counts. In that case, an observed count of a particular recognition outcome (i.e. a false negative or false positive) in  $M$  trials will sustain 95% confidence that the actual error rate is no larger than some value.

As an example, the minimum number of mugshot searches conducted in this report is  $M = 154\,549$ , and for an observed FNIR around 0.002, the measurement supports a conclusion that the actual FNIR is no higher than 0.00228 at 99% confidence level. On the false positive side, we tabulate FNIR at FPIR values as low as 0.001. Given estimates based on 331 254 non-mate trials, the actual FPIR values will be below 0.00115 at 99% confidence. In conclusion, large scale evaluation, without reuse of subjects, supports tight uncertainty bounds on the measured error rates.

### 3.8.2 Systematic error

The FRVT 2018 dataset includes anomalies discovered as a result of inspecting images involved in recognition failures from the most accurate algorithms. Two kinds of failure occur: False negatives (which, for the purpose here, include failures to make templates) and false positives.

**False negative errors:** We reviewed 600 false negative pairs for which either or both of the leading two algorithms did not put the correct mate in the top 50 candidates. Given 154 549 searches, this number represents 0.39% of the total, resulting in  $\text{FNIR} \sim 0.0039$ . Of the 600 pairs:

- ▷ **A: Poor quality:** About 20% of the pairs included images of very low quality, often greyscale, low resolution, blurred, low contrast, partially cropped, interlaced, or noisy scans of paper images. Additionally, in a few cases, the face is injured or occluded by bandages or heavy cosmetics.
- ▷ **B: Ground truth identity label bugs:** About 15% of the pairs are not actually mated. We only assigned this outcome when a pair is clearly not mated.
- ▷ **C: Profile views:** About 35% included an image of a profile (side) view of the face, or, more rarely, an image that was rotated 90 degrees in-plane (roll).
- ▷ **D: Tattoos:** About 30% included an image of a tattoo that contained a face image. These arise from mis-labelling in the parent dataset metadata.
- ▷ **E: Ageing:** There is considerable time-lapse between the two captures.

All these estimates are approximate. Of these, the tattoo and mislabeled images can never be matched. These constitute an accuracy floor in the sample implying that FNIR cannot be below 0.0018<sup>11</sup>. The profile-views, low-quality images, and images with considerable ageing can, in principle, be successfully matched - indeed some algorithms do so - so are not part of the accuracy floor.

<sup>11</sup>This value is the sum of two partial false negative rates:  $\text{FNIR}_B = 0.15 * 0.0039$  plus  $\text{FNIR}_D = 0.3 * 0.0039$

For the microsoft-4 algorithm the lowest miss rate from (recent entry in Table 23) is  $\text{FNIR}(640\,000, 50, 0) = 0.0018$ . This is close to the value estimated from the inspection of misses. It is below the 0.0039 figure because the algorithm does match some profile and poor quality images, that the yitu-2 algorithm does not.

For many tables (e.g. Table 23), the FNIR values obtained for the FRVT-2018 mugshots could be corrected by reducing them by 0.0018. The best values would then be indistinct from zero. The results in this report *were not* adjusted to account for this systematic error.

**False positive errors:** As shown in Figure 1 and discussed in Figure 14 many of the DET characteristics in this report exhibit a pronounced turn upward at low false positive rates. The shape can be caused by identity labelling errors in the ground truth of a dataset, specifically persons present in the database under two IDs such that some proportion of non-mate pairs are actually mated. To look for such possibilities, we merged the highest 1000 non-mate pairs produced by three different algorithms which resulted in 1839 unique pairs. This constitutes 0.56% of all non-mate searches. We assert that it is *very* difficult for human reviewers to assign the pairs into the following three categories: twins; doppelgangers; or ground-truth errors (instances of the same person under two IDs). Given this difficulty we made no attempt to correct any possible ground truth errors except by removing 57 pairs in the following categories:

- ▷ **A: Profile views:** Thirteen pairs included one or two profile-view images. As described in Figure 133, these can cause false positives.
- ▷ **B: Same-session photographs:** For twelve pairs, the images were identical or trivially altered (e.g. cropped) versions of the same photo. These were present under a different ID likely due to some clerical or procedural mistake.
- ▷ **C: Tattoos of faces:** There were fourteen instances of tattoo photographs that contained faces causing false matches.
- ▷ **D: T-shirt faces:** There were six instances of T-shirt photographs (of Bob Marley and Che Guevara) being detected instead of the face and causing false positives.
- ▷ **E: Background faces:** There were twelve instances of one subject appearing in the background of two otherwise correct portrait photos.

Note we did not remove any images where there was a chance that the pair was actually a different person.

In any case, the results in this report have not been adjusted for this systematic error.

## 4 Results

This section gives extensive results for algorithms submitted to FRVT 2018. Three page “report cards” for each algorithm are contained in a [separate supplement](#). Performance metrics were described in section 3. The main results are summarized in tabular form with more exhaustive data included as DET, CMC and related graphs in appendices as follows:

- ▷ The three tables 2-4 list algorithms alongside full developer names, acceptance date, size of the provided configuration data, template size and generation time, and search duration data.
  - The **template generation duration** is most important to applications that require fast response. For example, an eGate taking more than two seconds to produce a template might be unacceptable. Note that GPUs may be of utility in expediting this operation for some algorithms, though at additional expense. Two additional factors should be considered<sup>1213</sup>.
  - The **search duration** is the time taken for a search of a search template into a gallery of  $N$  enrollment templates. This performance variable, together with the volume of searches, is influential on the amount of hardware needed to sustain an operational deployment. This is measured here with the algorithm running on a single core of a contemporary CPU. Search is most simply implemented as  $N$  computations of a distance metric followed by a sort operation to find the closest enrollments. However, considerable optimization of this process is possible, up to and including fast-search algorithms that, by various means, avoid computation of all  $N$  distances.
  - The **template size** is the size of the extracted feature vector (or vectors) and any needed header information. Large template sizes may be influential on bus or network bandwidth, storage requirements, and on search duration. While the template itself is an opaque data blob, the feature dimensionality might be estimated by assuming a four-bytes-per-float encoding. There is a wide range of encodings. For the more accurate algorithm, sizes range from 256 bytes to about 2KB bytes, indicating essentially no consensus on face modeling and template design.
  - The **template size multiplier** column shows how, given  $k$  input images, the size of the template grows. Most implementations internally extract features from each image and concatenate them, and implement some score-level fusion logic during search. Other implementations, including many of the most accurate algorithms, produce templates whose size does not grow with  $k$ . This could be achieved via selection of the best quality image - but this is not optimal in handling ageing where the oldest image could be the best quality. Another mechanism would be feature-level fusion where information is fused from all  $k$  inputs. In any case, as a black-box test, the fusion scheme is proprietary and unknown.
  - The size of the **configuration data** is the total size of all files resident in a vendor-provided directory that contains arbitrary read-only files such as parameters, recognition models (e.g caffe). Generally a large value for this quantity may prohibit the use of the algorithm on a resource-constrained device.

<sup>12</sup>The FRVT 2018 API prohibited threading, so some gains from parallelism may be available on multiple-cores or multiple processors, if the feature extraction code could be distributed across them.

<sup>13</sup>Note also that factors of two or more may be realizable by exploiting modern vector processing instructions on CPUs. It is not clear in our measurements whether all developers exploited Intel’s AVX2 instructions, for example. Our machine was so equipped, but we insisted that the same compiled library should also run on older machines lacking that instruction. The more sophisticated implementations may have detected AVX2 presence and branched accordingly. The less sophisticated may be defaulted to the reduced instruction set. Readers should see the FRVT 2018 API document for the specific chip details.

▷ Tables 23-24 report core rank-based accuracy for mugshot images. The population size is limited to  $N = 1.6$  million identities because this is the largest gallery size on which all algorithms were executed. Notable observations from these tables are as follows:

- **Accuracy gains since 2018:** NIST Interagency Report 8238 documented massive gains over those reported in the FRVT 2014 report, NIST Interagency Report 8009. Further gains are documented in this report. Comparing the most accurate algorithm in November 2018, NEC-3, the value of  $\text{FNIR}(N, L, T)$  reduced from 0.0031 to 0.0024 for the Sensetime-004 algorithm with  $N = 12$  million recent images. The tables show broader gains: many developers have made advances since 2018 with between two and five-fold reduction in errors.
- **Wide range in accuracy:** The rank-1 miss rates vary from  $\text{FNIR}(N, 1, 0) = 0.0012$  for sensetime-004 up to about 0.5 for the very fast but inaccurate microfocus-x algorithms. Among the developers who are superior to NEC in 2013, the range is from 0.002 to 0.035 for camvi-3. This large accuracy range is consistent with the buyer-beware maxim, and indicates that face recognition software is far from being commoditized.

▷ Tables 27-28 report threshold-based error rates,  $\text{FNIR}(N, L, T)$ , for  $N = 1.6$  million for mugshot-mugshot accuracy on FRVT 2014, FRVT 2018, and also (in pink) mugshot-webcam accuracy using FRVT 2018 enrollments. Notable observations from these tables are as follows:

- **Order of magnitude accuracy gains since 2014:** As with rank-based results, the gains in accuracy are substantial, though somewhat reduced. At  $\text{FPIR} = 0.01$ , the best improvement over NEC in 2014 is a 27 fold reduction in FNIR using the NEC\_2 algorithm. At  $\text{FPIR} = 0.001$ , the largest gain is a six-fold reduction in FNIR via the NEC\_3 algorithm.
- **Broad gains across the industry:** About 19 companies realize accuracy better than the NEC benchmark from 2014. This is somewhat lower than the 28 developers who succeeded on the rank-1 metric. This may be due to the ubiquity of, and emphasis on, the rank-1 metric in many published algorithm development papers.
- **Webcam images:** Searches of webcam images give  $\text{FNIR}(N, T)$  values around 2 to 3 times higher than mugshot searches. Notably the leading developers with mugshots are approximately the same with poorer quality webcams. But some developers e.g. Camvi, Megvii, TongYi, and Neurotechnology do improve their relative rankings on webcams, perhaps indicating their algorithms were tailored to less constrained images.

▷ Tables 17, 20, 21 and show, respectively, high-threshold, rank 1, and rank 50 FNIR values for all algorithms performing searches into five different gallery sizes,  $N = 640\,000$ ,  $N = 1\,600\,000$ ,  $N = 3\,000\,000$ ,  $N = 6\,000\,000$  and  $12\,000\,000$ . The  $\text{FPIR} = 0.001$  table is included to inform high-volume duplicate detection applications. The Rank-1 table is included as a primary accuracy indicator. The Rank-50 table is included to inform agencies who routinely produce 50 candidates for human-review. The notable results are:

- **Slow growth in rank-based miss rates:**  $\text{FNIR}(N, R)$  generally grows as a power law,  $aN^b$ . From the straight lines of many graphs of Figure 20 this is clearly a reasonable model for most, but not all, algorithms. The coefficient  $a$  can be interpreted as FNIR in a gallery of size 1. The more important coefficient  $b$  indicates scalability, and often,  $b \ll 1$ , implies very benign growth in FNIR. The coefficients of the models appear in the Tables 20 and 21.
- **Slow growth in threshold-based miss rates:**  $\text{FNIR}(N, T)$  also generally grows as a power law,  $aN^b$  except at the high threshold values corresponding to low FPIR values. This is visible in the plots of Figure 36 which

show straight lines except for  $FPIR = 0.001$ , which increase more rapidly with  $N$  above 3 000 000. Each trace in those figures shows  $FNIR(N, T)$  at fixed  $FPIR$  with both  $N$  and  $T$  varying. Thus at large  $N$ , it is usually necessary to elevate  $T$  to maintain fixed  $FPIR$ . This causes increased  $FNIR$ . Why that would no-longer obey a power-law is not known. However, if we expect large galleries to contain individuals with familial relations to the non-mate search images - in the most extreme case, twins - then suppression of false positives becomes more difficult. This is discussed in the Figures starting at Fig. 10

▷ Figure ?? shows false positives from twins against their enrolled siblings, broken out by type of twin: fraternal or identical. The Figure is based on the enrollment of 104 single images on one of a pair of twins, and then the search of 2354 second images. Note that the dataset is heavily skewed towards identical twins which is not representative of the true population. There is also a skew towards same sex fraternal twin pairs compared to different sex fraternal twin pairs again not representative of the true population.

The notable results are:

- For all algorithms tested, the 1087 mated searches (Twin A vs. Twin A) produce scores almost always above typical operational thresholds, with (not shown) matches at rank 1. The images are of good quality, so this is the result expected from the rest of this report.
- For the 1066 identical twin searches (AB), almost all produce the twin at rank 1, with a few producing the mate at further down the candidate lists rank and low score.
- For the 169 fraternal searches (AB) from same sex pairs, most algorithms give a large number of very high scores, implying false positives at all thresholds. However, there are long tails containing lower scores that are correctly below threshold. In general, scores that are higher in this distribution are all rank 1 whereas the lower scores have much higher ranks.
- (Not shown) Of the 169, there are 24 fraternal searches (AB) involving different sex twins. Here most algorithms correctly report scores well below the lowest threshold, and usually not on the candidate list at all.

2022/04/28  
22:29:02FNIR(N, R, T) =  
False neg. identification rate  
FPIR(N, T) =  
False pos. identification rateN = Num. enrolled subjects  
R = Num. candidates examined

T = Threshold

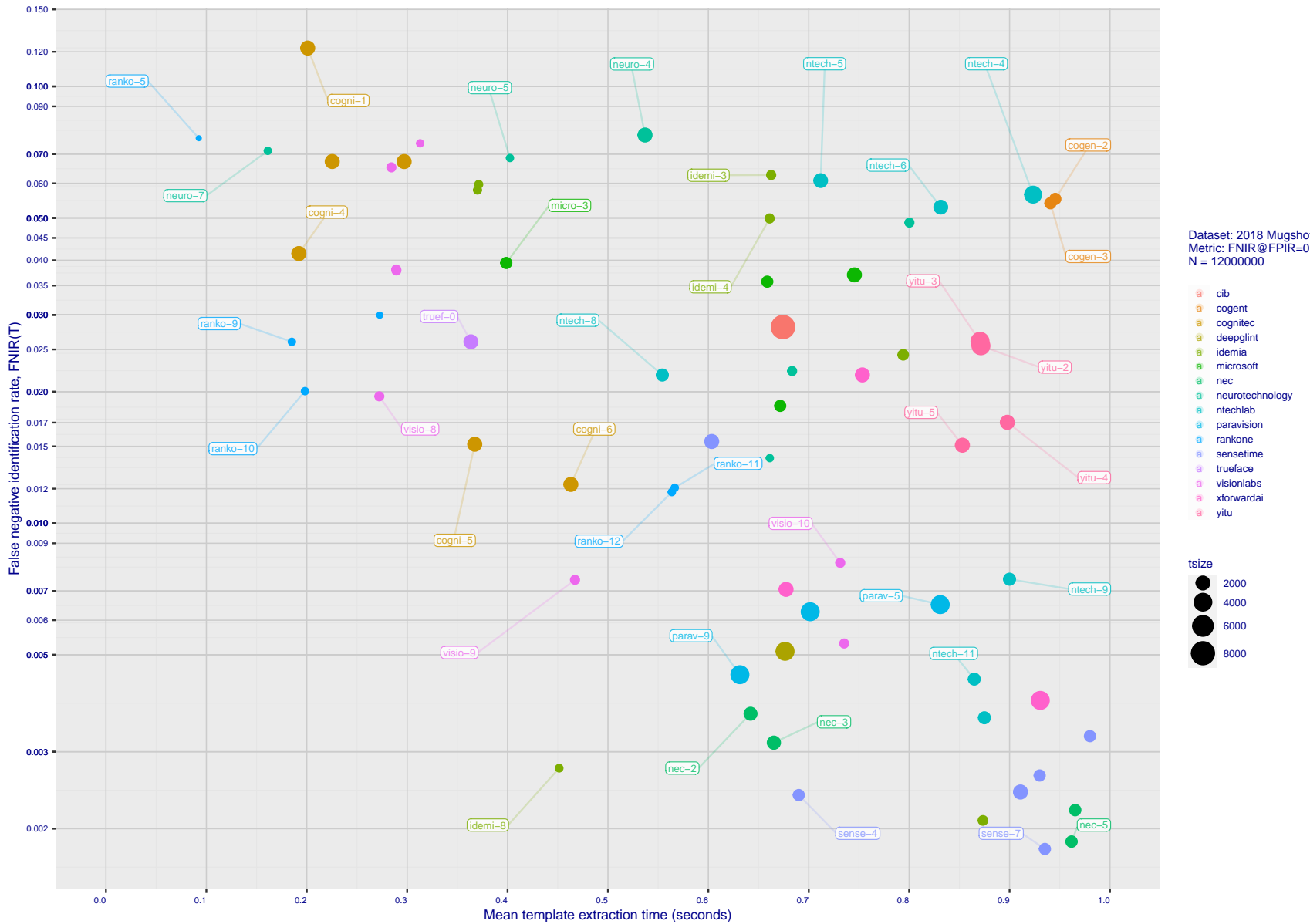
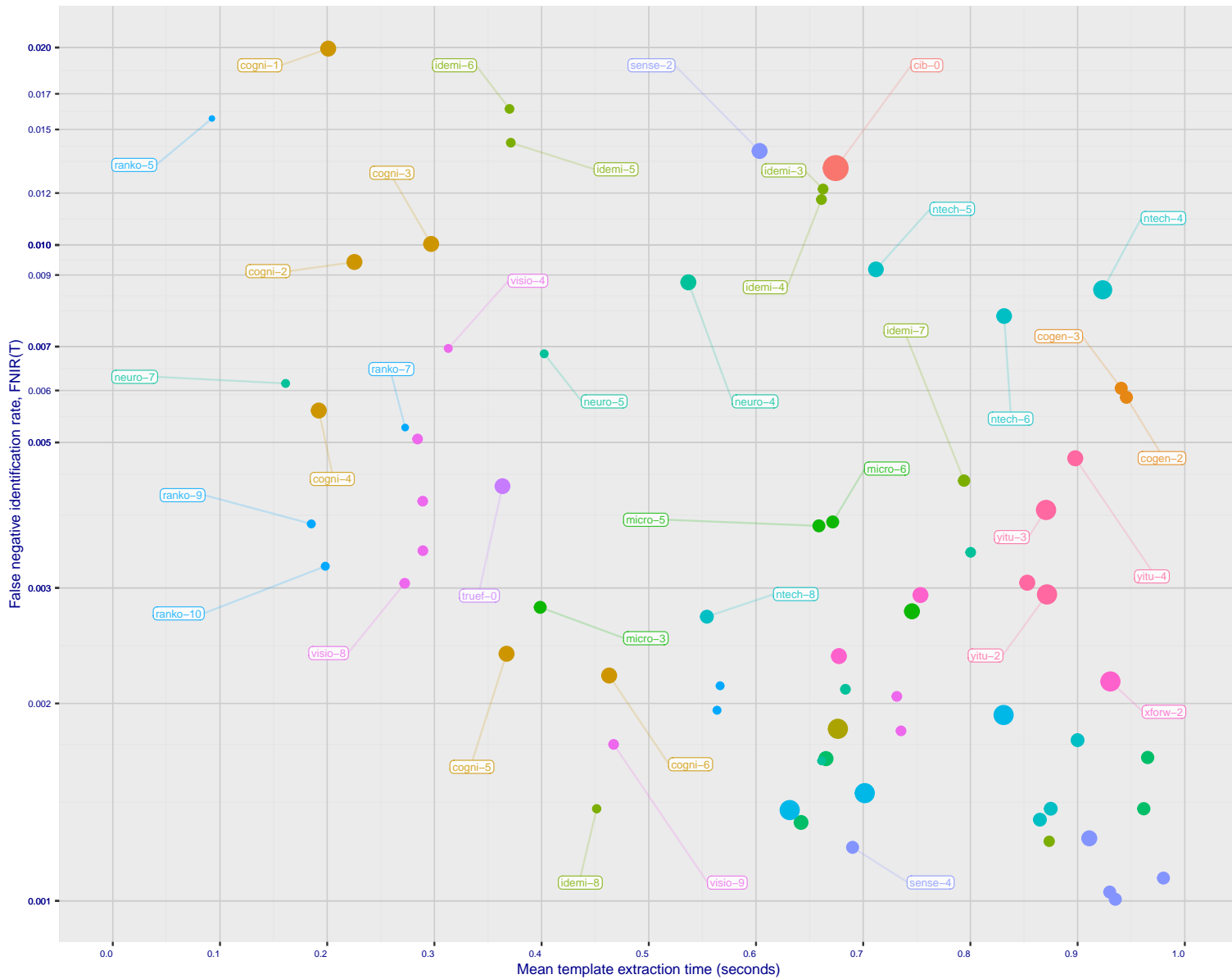
T = 0 → Investigation  
T > 0 → Identification

Figure 18: [Mugshot Dataset] Speed-accuracy tradeoff. For developers of the more accurate algorithms the plot shows the tradeoff of high-threshold recognition miss-rates,  $\text{FNIR}(N, N, T)$  for  $\text{FPIR}(N, T) = 0.003$ , and template generation time. Developers are coded by color. Template size is encoded by the size of the circle. Some labels are quite distant from the respective point, to avoid superposing text. Without any other influences, the assumption would be that taking time to localize the face, and extract features, would lead to better accuracy. The most notable result, for NEC, is that their slower algorithms are much more accurate than the version that extract features in fewer than 90 milliseconds.

2022/04/28  
22:29:02  
  
 $\text{FNIR}(N, R, T) =$   
False neg. identification rate  
 $\text{FPIR}(N, T) =$   
False pos. identification rate  
 $N =$  Num. enrolled subjects  
 $R =$  Num. candidates examined  
 $T =$  Threshold  
 $T = 0 \rightarrow$  Investigation  
 $T > 0 \rightarrow$  Identification



Dataset: 2018 Mugshot  
Metric: FNIR\_at\_RANK=1  
N = 12000000

Legend:  
● cib  
● cognent  
● cognitec  
● deepgplnt  
● idemla  
● microsoft  
● nec  
● neurotechnology  
● ntechlab  
● paravision  
● rankone  
● sensetime  
● trueface  
● visionlabs  
● xforwardai  
● yitu

tsize  
● 2000  
● 4000  
● 6000  
● 8000

Figure 19: [Mugshot Dataset] Speed-accuracy tradeoff. For developers of the more accurate algorithms the plot shows the tradeoff of rank-one recognition miss-rates,  $\text{FNIR}(N, 1, 0)$ , and template generation time. Developers are coded by color. Template size is encoded by the size of the circle. Some labels are quite distant from the respective point, to avoid superposing text. Without any other influences, the assumption would be that taking time to localize the face, and extract features, would lead to better accuracy. This occurs for NEC with their slower algorithm being much accurate than the version that extract features in fewer than 90 milliseconds.

	DEVELOPER	SHORT	SEQ.	VALIDATION	CONFIG <sup>1</sup>	LIB <sup>1</sup>	TEMPLATE GENERATION			FINALIZE <sup>2</sup>	SEARCH DURATION <sup>5</sup> MILLISEC																
							NAME	NUM.	DATE		N=1.6M	N=1.6M	N=1.6M	N=3M	N=6M	N=12M	( $\mu$ s)										
	FULL NAME						N=1.6M	N=1.6M	N=1.6M	N=3M	N=3M	N=6M	N=6M	N=12M													
1	20Face	20face	000	2021-10-01	112	319	123	2048	-	20	236	65	9	(205)	6355	(207)	6341	-	-	-							
2	3Divi	3divi	5	2018-10-26	186	51	203	4096	k	110	638	16	28	(92)	538	(91)	537	(87)	1377	(83)	2614	(79)	5530	141	0.07N <sup>1.1</sup>		
3	3Divi	3divi	6	2018-10-26	187	51	35	528	k	111	640	26	5	(12)	33	(13)	33	-	-	-	-	-	-	-	-		
4	Acer Incorporated	acer	000	2020-08-12	35	67	32	512	-	16	198	16	4	(58)	295	(56)	295	(51)	623	(77)	2302	(71)	4915	172	0.00N <sup>1.3</sup>		
5	Acer Incorporated	acer	001	2021-11-08	42	610	95	2048	-	11	184	62	9	(103)	619	(99)	575	-	-	-	-	-	-	-	-		
6	Akurat Satu Indonesia	ptakuratsatu	000	2020-10-23	0	572	38	538	-	206	905	218	28633	(6)	15	(6)	16	(5)	17	(4)	17	3	6827.74N <sup>0.1</sup>				
7	Alchera Inc	alchera	2	2018-10-30	7	14	109	2048	k	6	114	198	63	(183)	2923	(186)	2929	-	-	-	-	-	-	-	-		
8	Alchera Inc	alchera	3	2018-10-30	251	14	140	2048	k	87	531	199	63	(184)	2955	(187)	2956	(162)	6546	(163)	15013	(163)	35262	167	0.10N <sup>1.2</sup>		
9	Alchera Inc	alchera	004	2021-09-17	476	24	128	2048	-	183	853	187	35	(206)	6657	(213)	6851	-	-	-	-	-	-	-	-		
10	Alivia / Innovation Sys	isystems	3	2018-10-30	350	784	139	2048	1	173	825	137	16	(70)	385	(74)	389	(68)	979	(66)	1822	(105)	9348	173	0.00N <sup>1.3</sup>		
11	AllGoVision	allgogovision	000	2019-07-30	168	150	97	2048	k	52	404	92	12	(187)	3226	(190)	3193	(160)	6129	(160)	12449	(159)	25835	80	1.40N <sup>1.0</sup>		
12	AllGoVision	allgogovision	001	2020-07-14	283	126	100	2048	-	158	777	99	13	(186)	3174	(189)	3183	(159)	6073	(158)	12284	(158)	25701	78	1.42N <sup>1.0</sup>		
13	Anke Investments	anke	0	2018-10-30	779	27	182	2072	k	60	429	135	16	(106)	675	(113)	748	(94)	1483	(92)	2968	(86)	6148	109	0.21N <sup>1.1</sup>		
14	Anke Investments	anke	1	2018-10-30	779	27	183	2072	k	61	430	129	15	(111)	707	(116)	769	-	-	-	-	-	-	-	-		
15	Anke Investments	anke	002	2019-06-27	341	401	171	2056	k	103	623	108	13	(104)	624	(107)	682	(84)	1306	(79)	2403	(76)	5082	70	0.30N <sup>1.0</sup>		
16	Aware	aware	5	2018-10-30	368	27	192	3100	k	165	792	181	34	(16)	95	(21)	98	(20)	203	(18)	371	(15)	252	14	4.13N <sup>0.7</sup>		
17	Aware	aware	6	2018-10-30	368	27	2	124	k	164	789	32	2	(32)	158	(32)	162	-	-	-	-	-	-	-	-		
18	Ayonix	ayonix	1	2018-10-29	74	2	61	1036	k	12	88	89	11	(54)	279	(54)	279	-	-	-	-	-	-	-	-		
19	Ayonix	ayonix	2	2018-10-30	74	2	62	1036	1	11	114	114	11	(53)	279	(53)	276	(40)	535	(40)	1087	(40)	2284	90	0.11N <sup>1.0</sup>		
20	Camvi Technologies	camvitech	4	2018-10-30	233	220	51	1024	1	128	686	179	31	(13)	33	(12)	32	(11)	38	(10)	40	(7)	48	4	8492.66N <sup>0.1</sup>		
21	Camvi Technologies	camvitech	5	2018-10-30	257	220	50	1024	1	150	751	177	31	(11)	31	(10)	30	-	-	-	-	-	-	-	-		
22	Canon Inc	cib	000	2020-10-19	426	127	219	8196	-	122	674	205	113	(188)	3589	(192)	3604	(163)	6738	(161)	13495	(160)	27114	30	2.33N <sup>1.0</sup>		
23	Canon Inc	canon	001	2021-10-27	1139	91	202	4096	-	197	885	156	21	(208)	6804	(211)	6789	(178)	12741	(174)	26560	(171)	51922	52	3.82N <sup>1.0</sup>		
24	Clearview AI Inc	clearviewai	000	2021-11-12	358	316	206	4096	-	155	765	170	30	(117)	802	(104)	657	(79)	1134	(69)	1939	(63)	3889	19	1.59N <sup>0.9</sup>		
25	Cloudwalk - Hengrui AI Technology	hr	000	2021-02-10	501	392	104	2048	-	205	905	122	15	(55)	282	(52)	276	(42)	539	(49)	1268	(57)	3177	145	0.03N <sup>1.1</sup>		
26	Cloudwalk - Moontime Smart Technology	cloudwalk	000	2022-01-31	716	573	108	2048	-	189	869	80	10	(81)	440	(70)	371	(44)	547	(39)	1065	(51)	2902	22	0.53N <sup>0.9</sup>		
27	Cognitec Systems GmbH	cognitec	2	2018-10-30	463	26	159	2052	k	19	225	167	21	(161)	1733	(163)	1763	(144)	3660	(139)	13895	(136)	2729	(136)	13895	75	0.83N <sup>1.0</sup>
28	Cognitec Systems GmbH	cognitec	3	2018-10-30	465	26	163	2052	k	30	297	133	16	(160)	1719	(164)	1791	(143)	3638	(138)	7277	(142)	14904	99	0.66N <sup>1.0</sup>		
29	Cognitec Systems GmbH	cognitec	004	2021-03-08	384	60	158	2052	-	14	192	106	13	(159)	1673	(161)	1727	(130)	2904	(128)	5801	(126)	11707	25	1.15N <sup>1.0</sup>		
30	Cognitec Systems GmbH	cognitec	005	2021-07-30	460	61	156	2052	-	39	367	67	9	(151)	1556	(153)	1551	(132)	2916	(136)	6561	(137)	13958	115	0.38N <sup>1.1</sup>		
31	Cognitec Systems GmbH	cognitec	006	2022-02-10	689	61	153	2052	-	70	463	77	10	(130)	1006	(129)	1002	(108)	2097	(104)	4312	(96)	7624	107	0.30N <sup>1.1</sup>		
32	Cubox	cubox	000	2021-08-24	529	298	102	2048	-	209	917	76	10	(189)	3646	(194)	4076	(165)	7605	(164)	15871	-	108	1.16N <sup>1.1</sup>			
33	Cyberlink Corp	cyberlink	000	2019-06-12	217	93	165	2052	1	115	654	170	30	(108)	696	(109)	701	(88)	1379	(84)	2639	(88)	6214	93	0.28N <sup>1.0</sup>		
34	Cyberlink Corp	cyberlink	001	2019-10-07	459	102	162	2052	1	58	423	170	28	(109)	698	(108)	700	(86)	1350	(126)	5524	(129)	12031	171	0.00N <sup>1.3</sup>		
35	Cyberlink Corp	cyberlink	002	2020-07-31	333	109	212	4140	-	143	724	209	6875	(148)	1353	(191)	3198	(161)	6138	(157)	12205	(134)	13106	17	16.71N <sup>0.8</sup>		
36	Cyberlink Corp	cyberlink	003	2021-01-05	333	100	216	6212	-	131	691	185	35	(84)	488	(110)	723	(91)	1415	(90)	2886	(80)	5643	125	0.12N <sup>1.1</sup>		
37	Cyberlink Corp	cyberlink	004	2021-07-16	371	100	214	6212	-	145	728	160	23	(86)	492	(89)	504	(67)	923	(55)	3350	21	0.73N <sup>0.9</sup>				
38	Cyberlink Corp	cyberlink	005	2022-01-07	371	100	215	6212	-	147	733	170	30	(88)	501	(85)	498	(80)	1193	(85)	2672	(82)	5693	162	0.03N <sup>1.2</sup>		
39	DAON	daon	000	2021-12-23	274	2	179	2069	-	93	583	47	8	(91)	524	(103)	625	(92)	1454	(94)	3097	(93)	6316	163	0.03N <sup>1.2</sup>		
40	Dahua Technology Co Ltd	dahua	0	2018-10-29	276	167	91	2048	k	44	374	158	22	-	(50)	258	-	-	-	-	-	-	-	-			
41	Dahua Technology Co Ltd	dahua	1	2018-10-29	276	167	122	2048	k	40	369	166	28	-	(49)	257	(40)	602	(46)	1202	(54)	3007	152	0.02N <sup>1.2</sup>			
42	Dahua Technology Co Ltd	dahua	002	2019-12-02	607	137	125	2048	k	127	685	151	19	(44)	243	(51)	269	(78)	1189	(91)	2950	(93)	6732	177	0.00N <sup>1.5</sup>		
43	Dahua Technology Co Ltd	dahua	003	2020-11-18	889	154	124	2048	-	142	723	144	18	(56)	283	(46)	249	(37)	468	(37)	935	(35)	1871	32	0.16N <sup>1.0</sup>		
44	Dahua Technology Co Ltd	dahua	004	2021-11-18	812	116	96	2048	-	153	758	82	11	(78)	423	(78)	411	(64)	871	(58)	1568	(56)	3174	82	0.17N <sup>1.0</sup>		
45	Decatul Industries Inc	decatur	000	2022-02-09	411	383	166	2052	-	185	863	69	9	(162)	1761	(170)	2023	(23)	3361	(140)	7283	(140)	14592	55	1.06N <sup>1.0</sup>		
46	Deepglint	deepglint	001	2019-11-15	448	265	197	4096	-	124	676	182	35	(107)	677	(151)	1495	(108)	1724	(87)	2747	(89)	6246	15	25.27N <sup>0.8</sup>		
47	Dermalog	dermalog	5	2018-10-26	0	440	4	128	1	86	528	208	3155	1	0	(1)	0	(1)	0	(1)	0	(1)	0	66.21N <sup>0.2</sup>			
48	Dermalog	dermalog	6	2018-10-26	0	453	11	256	1	81																	

DEVELOPER	SHORT NAME	SEQ. NUM.	VALIDATION DATE	CONFIG <sup>1</sup> DATA (MB)	LIB <sup>1</sup> DATA (MB)	TEMPLATE GENERATION SIZE (B) MULT <sup>3</sup>	FINALIZE <sup>2</sup> TIME (S)	SEARCH DURATION <sup>5</sup> MILLISEC				
								TIME (S)	L=1 N=1.6M	L=50 N=1.6M	L=50 N=3M	L=50 N=6M
53	Fincore Ltd	fincore	000	2021-08-18	250	224	107 2048	-	73 475	87 9	98 562	96 560
54	Fujitsu Research and Development Center	fujitsulab	000	2021-10-12	497	337	53 1032	-	217 945	28 5	158 1668	157 1657
55	Fujitsu Research and Development Center	fujitsulab	001	2022-03-15	675	386	56 1032	-	196 882	98 9	164 1854	165 1817
56	Gorilla Technology	gorilla	2	2018-10-29	91	1252	69 1132	k	34 338	162 24	30 145	30 146
57	Gorilla Technology	gorilla	3	2018-10-26	94	1252	185 2156	k	89 559	213 12020	-	204 2047
58	Gorilla Technology	gorilla	004	2020-01-06	182	1244	18 2192	k	47 388	187 41	57 286	285 799
59	Gorilla Technology	gorilla	005	2021-02-22	306	1420	217 6288	-	77 483	201 78	116 802	117 799
60	Gorilla Technology	gorilla	006	2021-09-30	377	691	220 8336	-	156 767	204 99	154 1626	154 1612
61	Gorilla Technology	gorilla	007	2022-02-16	392	322	218 6290	-	88 526	205 89	114 765	112 745
62	Griaule	griaule	000	2021-11-01	0	584	160 2052	-	57 417	41 8	201 5827	205 6150
63	Guangzhou Pixel Solutions Co Ltd	pixelall	002	2019-07-01	0	165	187 2560	k	13 190	126 15	145 1296	147 1334
64	Guangzhou Pixel Solutions Co Ltd	pixelall	003	2019-11-05	0	690	188 2560	k	136 703	159 22	142 1273	143 1307
65	Guangzhou Pixel Solutions Co Ltd	pixelall	004	2020-07-02	0	538	190 2560	k	62 449	143 17	141 1259	142 1300
66	Guangzhou Pixel Solutions Co Ltd	pixelall	005	2021-03-23	0	717	189 2560	-	179 840	86 11	153 1606	152 1528
67	Hangzhou Allu Network Information Technology	hzuilu	000	2022-03-18	855	97	46 1024	-	113 649	87 11	180 2609	184 2551
68	Hikvision Research Institute	hikvision	5	2018-10-29	593	9	75 1408	1	98 607	132 16	123 883	124 895
69	Hikvision Research Institute	hikvision	6	2018-10-29	593	9	74 1408	1	96 598	134 16	121 871	123 877
70	HyperVerge Inc	hyperverge	001	2021-08-11	1791	212	47 1024	-	181 845	24 5	110 705	106 681
71	HyperVerge Inc	hyperverge	002	2022-04-13	1140	1118	48 1024	-	212 934	61 9	105 661	105 659
72	Idemia	idemia	5	2018-10-29	417	48	22 352	1	43 371	25 5	137 27	138 277
73	Idemia	idemia	6	2018-10-29	417	48	23 352	1	42 370	22 4	127 27	138 287
74	Idemia	idemia	007	2020-01-17	738	113	48 860	1	166 794	112 14	31 151	31 152
75	Idemia	idemia	008	2021-03-15	378	65	21 300	-	64 451	14 3	25 132	25 131
76	Idemia	idemia	009	2022-03-01	735	68	48 636	-	191 873	36 7	40 211	39 205
77	Imagus Technology Pty Ltd	imagus	005	2021-01-15	222	311	106 2048	-	163 786	110 14	43 236	61 313
78	Imagus Technology Pty Ltd	imagus	006	2021-05-27	248	369	99 2048	-	204 904	70 9	62 317	42 234
79	Imagus Technology Pty Ltd	imagus	007	2021-11-16	248	366	105 2048	-	99 609	53 9	42 234	43 238
80	Imperial College London	imperial	000	2019-08-28	461	15	186 2048	1	92 577	98 13	63 360	73 379
81	Incode Technologies Inc	incode	2	2018-10-29	71	31	94 2048	1	27 289	131 15	76 411	75 404
82	Incode Technologies Inc	incode	3	2018-10-29	133	31	135 2048	1	134 697	121 15	70 408	70 412
83	Incode Technologies Inc	incode	004	2019-06-24	254	50	134 2048	1	74 475	91 12	68 365	72 378
84	Incode Technologies Inc	incode	005	2021-07-29	259	21	126 2048	-	79 500	75 10	61 316	83 454
85	Innovatrics	innovatrics	4	2018-10-30	0	400	66 1076	k	48 399	210 10902	8 8	48 398
86	Innovatrics	innovatrics	005	2019-09-30	0	455	46 538	1	175 827	212 11897	8 8	39 398
87	Innovatrics	innovatrics	007	2021-08-16	175	58	39 538	-	159 777	113 14	21 97	22 100
88	Intellivision	intellivision	001	2022-03-08	62	130	172 2056	-	54 406	153 20	71 388	71 377
89	IrexAI	irex	000	2021-02-09	724	46	191 3080	-	189 844	150 19	102 616	100 600
90	Kakao Enterprise	kakao	000	2021-06-23	404	124	164 2052	-	178 835	43 8	41 213	40 215
91	Kedacom International Pte	kedacom	001	2019-09-16	239	36	20 292	1	82 507	5 2	113 764	114 760
92	Kneron	kneron	000	2020-03-03	366	13	119 2048	k	84 523	103 13	179 2535	182 2506
93	Kneron	kneron	001	2021-06-10	270	69	138 2048	-	72 472	89 9	181 2690	185 2642
94	Line Corporation	line	000	2021-06-02	138	397	142 2048	-	76 481	48 8	196 5433	200 5418
95	Line Corporation	line	001	2021-11-21	471	396	143 2048	-	207 907	49 8	165 1872	168 1934
96	Lomonosov Moscow State University	intsyssmu	000	2019-08-19	375	168	114 2048	1	101 614	104 13	70 430	81 431
97	Lookman Electroplost Industries	lookman	3	2018-10-28	203	24	19 292	1	33 336	12 3	112 739	111 745
98	Lookman Electroplost Industries	lookman	4	2018-10-28	184	24	41 548	1	31 320	21 4	127 981	128 998
99	Lookman Electroplost Industries	lookman	005	2019-09-16	239	36	42 548	1	80 506	17 4	129 1005	130 1008
100	Mantra Softech India	mantra	000	2021-10-28	460	61	152 2052	-	56 412	74 10	125 916	125 910
101	Megvii/Face++	megvii	1	2018-10-28	1703	41	205 4096	1	105 631	180 32	94 552	97 561
102	Megvii/Face++	megvii	2	2018-10-28	1735	42	195 4096	1	108 635	178 31	99 553	94 558
103	MicroFocus	microfocus	5	2018-10-29	94	26	14 256	k	24 262	8 2	37 182	36 186
104	MicroFocus	microfocus	6	2018-10-29	94	26	10 256	k	23 262	10 2	38 183	35 186

## Notes

- 1 Configuration size does not capture static data present in libraries. Libraries are included but the size also includes any ancillary libraries for image processing (e.g. openCV) or numerical computation (e.g. blas).
- 2 Finalization is the processing of converting N = 1600000 templates into a searchable data structure an operation which can be a simple copy, or the building of an index or tree, for example. The duration of the operation may be data dependent, and may not be linear in the number of input templates.
- 3 This multiplier expresses the increase in template size when k images are passed to the template generation function.
- 4 All durations are measured on Intel® Xeon® CPU E5-2630 v4 @ 2.20GHz processors. Estimates are made by wrapping the API function call in calls to std::chrono::high\_resolution\_clock which on the machine in (3) counts 1ns clock ticks. Precision is somewhat worse than that however.
- 5 Search durations are measured as in the prior note. The power-law model in the final column mostly fits the empirical results in Figure 134. However in certain cases the model is not correct and should not be used numerically.

Table 3: Summary of algorithms and properties included in this report. The blue superscripts give ranking for the quantity in that column. Missing search durations, denoted by “-”, are absent because those runs were not executed, usually because we did not run on the larger galleries. Caution: The power-law model is sometimes an incorrect model. It is included here only to show broad sublinear behavior, which is flagged in green. The models should not be used for prediction.

2022/04/28

FNIR(N, R, T) = False neg. identification rate

N = Num. enrolled subjects

T = Threshold

T = 0 → Investigation

T ∨ 0 → Identification

	DEVELOPER	SHORT	SEQ.	VALIDATION	CONFIG <sup>1</sup>	LIB <sup>1</sup>	TEMPLATE GENERATION	FINALIZE <sup>2</sup>	SEARCH DURATION <sup>5</sup> MILLISEC						
									TIME (S)	L=1		L=50		L=50	
										N=1.6M	N=1.6M	N=1.6M	N=3M	N=6M	N=12M
105	Microsoft	microsoft	5	2018-10-29	381	155	49 1024 1	116 658	89 11	(152) 1606	(158) 1673	(135) 3076	(132) 6302	(135) 13160	67 0.79 N <sup>1.0</sup>
106	Microsoft	microsoft	6	2018-10-29	478	155	52 1024 1	120 671	125 15	(155) 1642	(156) 1618	(145) 3710	(134) 6401	(133) 12892	85 0.68 N <sup>1.0</sup>
107	N-Tech Lab	ntech	5	2018-10-30	1685	113	87 1940 k	140 711	196 55	(46) 243	(47) 246	(41) 538	(41) 1100	(49) 2867	146 0.02 N <sup>1.1</sup>
108	N-Tech Lab	ntech	6	2018-10-30	1686	117	86 1940 k	177 831	197 63	(45) 243	(46) 246	(43) 546	(42) 1104	(50) 2873	148 0.02 N <sup>1.1</sup>
109	N-Tech Lab	ntechlab	007	2019-06-25	2450	51	193 3348 k	167 795	200 73	(72) 393	(80) 427	(58) 780	(65) 1768	(61) 3499	94 0.16 N <sup>1.0</sup>
110	N-Tech Lab	ntechlab	008	2020-01-06	1111	51	73 1300 k	88 554	187 36	(36) 179	(33) 184	(28) 341	(26) 683	(24) 1395	46 0.11 N <sup>1.0</sup>
111	N-Tech Lab	ntechlab	009	2021-03-01	1208	42	72 1300 -	202 899	184 35	(35) 178	(34) 184	(27) 336	(27) 676	(31) 1704	113 0.05 N <sup>1.1</sup>
112	N-Tech Lab	ntechlab	010	2021-06-24	351	213	71 1280 -	192 874	29 6	(80) 440	(82) 435	(59) 821	(60) 1645	(58) 3337	62 0.22 N <sup>1.0</sup>
113	N-Tech Lab	ntechlab	011	2021-12-07	679	208	70 1280 -	186 864	31 6	(85) 488	(84) 483	(66) 912	(68) 1869	(73) 5003	130 0.07 N <sup>1.1</sup>
114	NEC	nec	2	2018-10-30	705	35	82 1616 k	112 642	147 18	(73) 405	(77) 409	(72) 1072	(63) 1755	(68) 4255	137 0.06 N <sup>1.1</sup>
115	NEC	nec	3	2018-10-30	774	110	83 1712 k	118 665	154 21	(3) 7	(3) 7	(5) 14	(9) 40	(10) 82	156 0.00 N <sup>1.2</sup>
116	NEC	nec	004	2021-07-19	971	63	67 1104 -	220 965	32 7	(65) 349	(66) 351	(53) 662	(51) 1330	(45) 2685	51 0.20 N <sup>1.0</sup>
117	NEC	nec	005	2021-12-13	922	88	68 1104 -	219 961	33 7	(83) 473	(92) 551	(70) 1017	(71) 2091	(66) 4242	59 0.28 N <sup>1.0</sup>
118	Neurotechnology	neurotech	5	2018-10-30	266	53	13 256 k	50 402	9 2	(119) 835	(120) 839	(98) 1690	(96) 3219	(103) 8955	119 0.19 N <sup>1.1</sup>
119	Neurotechnology	neurotech	6	2018-10-30	564	53	8 256 k	144 726	7 2	(120) 839	(121) 842	-	-	-	-
120	Neurotechnology	neurotech	007	2019-10-03	57	51	2 256 k	7 161	6 2	(134) 1118	(134) 1110	(110) 2143	(105) 4397	(104) 9045	66 0.55 N <sup>1.0</sup>
121	Neurotechnology	neurotechnology	008	2021-03-22	355	49	36 514 -	168 800	20 4	(137) 1167	(137) 1149	(112) 2266	(110) 4573	(111) 9586	73 0.55 N <sup>1.0</sup>
122	Neurotechnology	neurotechnology	009	2021-09-01	246	82	35 513 -	126 683	11 3	(132) 1035	(132) 1049	(107) 1977	(103) 4270	(99) 8756	106 0.32 N <sup>1.1</sup>
123	Neurotechnology	neurotechnology	010	2022-01-07	247	83	12 256 -	117 661	2 2	(128) 988	(126) 984	(101) 1897	(97) 3977	(98) 8048	98 0.36 N <sup>1.0</sup>
124	Newland Computer Co Ltd	newland	2	2018-10-30	96	27	120 2048 -	184 855	127 15	(211) 8741	(216) 8854	(183) 17892	(180) 39356	-	132 1.32 N <sup>1.1</sup>
125	Noblis	noblis	1	2018-10-30	114	176	132 2048 1	17 206	125 15	(143) 1273	(141) 1272	-	-	-	-
126	Noblis	noblis	2	2018-10-30	153	176	213 6144 1	83 517	189 43	(178) 2513	(183) 2522	(158) 5649	(159) 12432	(165) 44262	168 0.04 N <sup>1.3</sup>
127	NotionTag Technologies Private Limited	notiontag	000	2022-01-14	265	945	184 2120 -	65 453	78 10	(210) 8619	(215) 8705	(182) 16652	(179) 38794	(176) 90607	136 1.15 N <sup>1.1</sup>
128	Pangiam	pangiam	000	2022-02-22	453	23	147 2048 -	109 636	142 17	(50) 276	(62) 319	(48) 601	(47) 1210	(42) 2443	50 0.18 N <sup>1.0</sup>
129	Paravision (EverAI)	everai	2	2018-10-30	224	304	118 2048 1	38 366	175 30	(52) 278	(56) 283	-	-	-	-
130	Paravision (EverAI)	everai	3	2018-10-30	438	304	129 2048 1	141 717	162 28	(51) 278	(55) 281	(45) 572	(43) 1146	(39) 2278	87 0.12 N <sup>1.0</sup>
131	Paravision (EverAI)	everai-paravision	004	2019-06-19	527	128	194 4096 1	121 672	192 45	(96) 559	(95) 559	(126) 2611	(135) 6445	(139) 14519	176 0.00 N <sup>1.5</sup>
132	Paravision (EverAI)	paravision	005	2019-12-11	543	154	204 4096 1	176 830	194 48	(97) 561	(98) 564	(71) 1056	(75) 2298	(72) 4966	110 0.16 N <sup>1.1</sup>
133	Paravision (EverAI)	paravision	007	2021-02-01	529	235	198 4096 -	135 701	195 48	(99) 569	(93) 558	(73) 1086	(72) 2111	(67) 4254	20 1.11 N <sup>0.9</sup>
134	Paravision	paravision	009	2021-12-14	672	300	207 4100 -	106 631	208 82	(190) 3690	(195) 4230	(166) 8037	(165) 16532	(161) 31422	89 1.62 N <sup>1.0</sup>
135	Qnap Security	qnap	000	2021-07-28	182	15	115 2048 -	66 457	63 9	(139) 1231	(162) 1763	-	-	-	-
136	Qnap Security	qnap	001	2021-12-09	191	13	133 2048 -	100 613	44 8	(157) 1666	(150) 1429	(140) 3472	(141) 7375	(144) 15159	153 0.11 N <sup>1.2</sup>
137	Qnap Security	qnap	002	2022-04-15	338	32	146 2048 -	172 822	140 17	(126) 958	(138) 1179	(114) 2312	(133) 4789	(117) 9791	-
138	Quantasoft	quantasoft	1	2018-10-30	276	452	101 2048 k	46 385	30 6	(212) 15422	(180) 14858	(180) 14717	-	(148) 18323	-
139	Rank One Computing	rankone	4	2018-10-09	0	101	185 k	3 36	34 7	(23) 101	(23) 101	(19) 190	-	-	27 0.07 N <sup>1.0</sup>
140	Rank One Computing	rankone	5	2018-10-24	0	101	5 133 k	4 92	35 7	(28) 140	(28) 144	(24) 266	(23) 525	(22) 1049	24 0.11 N <sup>1.0</sup>
141	Rank One Computing	rankone	006	2019-06-03	0	133	6 165 k	22 245	42 8	-	-	-	-	-	-
142	Rank One Computing	rankone	007	2019-11-12	0	137	7 165 k	26 272	38 7	(24) 116	(24) 115	(21) 215	(21) 439	(19) 877	48 0.07 N <sup>1.0</sup>
143	Rank One Computing	rankone	009	2020-06-26	0	105	15 260 k	12 185	85 11	(17) 95	(20) 96	(16) 181	(16) 362	(17) 727	37 0.06 N <sup>1.0</sup>
144	Rank One Computing	rankone	010	2020-11-05	0	135	16 261 -	15 198	79 10	(18) 95	(16) 95	(14) 178	(14) 357	(15) 714	33 0.06 N <sup>1.0</sup>
145	Rank One Computing	rankone	011	2021-08-27	0	175	17 261 -	91 566	50 8	(20) 96	(17) 95	(17) 183	(17) 370	(14) 714	44 0.06 N <sup>1.0</sup>
146	Rank One Computing	rankone	012	2021-12-27	0	257	18 261 -	90 563	40 8	(19) 95	(18) 95	(15) 179	(15) 361	(16) 718	36 0.06 N <sup>1.0</sup>
147	Realnetworks Inc	realnetworks	2	2018-10-30	105	104	210 4104 k	21 241	167 28	(166) 2008	(172) 2048	(186) 4194	(147) 8642	(143) 15035	60 1.08 N <sup>1.0</sup>
148	Realnetworks Inc	realnetworks	003	2019-06-12	93	102	85 1848 k	10 173	97 13	(136) 1145	(135) 1132	(109) 2142	(120) 5241	(121) 10495	123 0.21 N <sup>1.1</sup>
149	Realnetworks Inc	realnetworks	004	2019-10-17	94	102	84 1848 1	9 171	84 11	(135) 1143	(136) 1137	(111) 2149	(112) 4740	(114) 9693	105 0.36 N <sup>1.0</sup>
150	Realnetworks Inc	realnetworks	005	2021-06-23	168	209	174 2056 -	32 332	56 9	(156) 1654	(155) 1616	(134) 3030	(130) 6068	(130) 12134	41 1.01 N <sup>1.0</sup>
151	Realnetworks Inc	realnetworks	006	2021-12-02	250	56	169 2056 -	36 348	45 8	(93) 543	(90) 531	(69) 996	(70) 1998	(65) 3991	40 0.33 N <sup>1.0</sup>
152	Realnetworks Inc	realnetworks	007	2022-04-11	455	99	176 2056 -	102 634	141 17	(118) 815	(119) 812	(96) 1559	(95) 3159	(91) 6361	-
153	Remark Holdings	remarkai	0	2018-10-30	187	847	131 2048 k	94 593	118 14	(199) 5685	(203) 5723	-	-	-	-
154	Remark Holdings	remarkai	000	2019-06-12	234	1092	93 2048 k	114 650	96 12	(200) 5776	(202) 5703	(172) 11604	(178) 32133	(177) 91436	169 0.05 N <sup>1.3</sup>
155	Remark Holdings	remarkai	1	2018-10-30	187	847	110 2048 k	59 427	120 14	(198) 5680	(204) 5761	(175) 12475	(176) 88726	(174) 59618	158 0.37 N <sup>1.2</sup>
156	Rendip	rendip	000	2021-05-21	0	416	130 2048 -	199 890	66 9	(47) 249	(68) 368	(56) 697	(56) 1452	(52) 2926	116 0.08 N <sup>1.1</sup>

Notes
1 Configuration size does not capture static data present in libraries. Libraries are included but the size also includes any ancillary libraries for image processing (e.g. openCV) or numerical computation (e.g. blas).
2 Finalization is the processing of converting $N = 1600000$ templates into a searchable data structure an operation which can be a simple copy, or the building of an index or tree, for example. The duration of the operation may be data dependent, and may not be linear in the number of input templates.
3 This multiplier expresses the increase in template size when $k$ images are passed to the template generation function.
4 All durations are measured on Intel®Xeon®@CPU E5-2630 v4 @ 2.20GHz processors. Estimates are made by wrapping the API function call in calls to std::chrono::high_resolution_clock which on the machine in (3) counts 1ns clock ticks. Precision is somewhat worse than that however.
5 Search durations are measured as in the prior note. The power-law model in the final column mostly fits the empirical results in Figure 134. However in certain cases the model is not correct and should not be used numerically.

	DEVELOPER	SHORT	SEQ.	VALIDATION	CONFIG <sup>1</sup>	LIB <sup>2</sup>	TEMPLATE GENERATION	FINALIZE <sup>3</sup>	SEARCH DURATION <sup>5</sup> MILLISEC						
									TIME (S)	L=1 N=1.6M	L=50 N=1.6M	L=50 N=3M	L=50 N=6M	L=50 N=12M	
157	Reveal Media Ltd	revealmedia	000	2022-02-02	287	196	154 2052	-	45 383	73 10	(170) 2322	(169) 2019	(147) 3838	(145) 7816	(147) 16559
158	SQLsoft	sqisoft	001	2021-12-20	271	377	170 2056	-	69 462	64 9	(146) 1311	(145) 1319	(118) 2456	(114) 4906	(116) 9755
159	Samsung S1 Corp	s1	000	2021-06-03	257	196	200 4096	-	187 865	152 20	(207) 6715	(212) 6794	(179) 13032	(175) 26372	(173) 55723
160	Samsung S1 Corp	s1	001	2021-11-01	240	198	113 2048	-	170 813	51 8	(172) 2415	(181) 2491	(155) 4718	(153) 9614	(157) 24472
161	Scanovate Ltd	scanovate	000	2020-01-15	250	446	150 2048	-	137 705	118 14	(150) 1419	(149) 1412	(133) 3008	(156) 11616	(128) 12012
162	Scanovate Ltd	scanovate	001	2020-09-10	250	446	144 2048	-	125 675	102 13	(147) 1321	(146) 1320	(121) 2502	(117) 5047	(118) 10163
163	Sensetime Group	sensetime	0	2018-10-30	525	6	208 4104	k	133 693	188 41	(87) 498	(86) 501	(81) 1212	(74) 2281	(74) 5032
164	Sensetime Group	sensetime	1	2018-10-30	525	6	209 4104	k	104 628	193 48	(90) 516	(87) 502	(76) 1146	(76) 2301	(70) 4765
165	Sensetime Group	sensetime	002	2019-06-03	523	6	178 2056	k	97 603	145 18	(66) 359	(69) 370	(103) 1897	(108) 4508	(110) 9543
166	Sensetime Group	sensetime	003	2019-12-02	769	76	173 2056	1	208 910	149 19	(194) 4885	(199) 4989	(174) 12325	(171) 24712	(168) 49445
167	Sensetime Group	sensetime	004	2020-08-10	456	29	54 1032	-	130 690	95 12	(177) 2490	(178) 2477	(153) 4654	(152) 4402	(155) 19651
168	Sensetime Group	sensetime	005	2020-12-17	631	39	57 1032	-	221 980	83 11	(174) 2459	(193) 3939	(164) 7398	(162) 14768	(153) 19016
169	Sensetime Group	sensetime	006	2021-07-26	526	54	59 1032	-	210 929	39 7	(177) 2414	(177) 2422	(151) 4527	(149) 9128	(147) 18640
170	Sensetime Group	sensetime	007	2022-01-15	526	37	58 1032	-	213 935	52 8	(173) 2432	(176) 2406	(150) 4513	(148) 8998	(151) 18796
171	Shaman Software	shaman	6	2018-10-26	0	200	14 2048	k	130 706	117 14	(101) 603	(101) 612	-	-	-
172	Shaman Software	shaman	7	2018-10-26	0	200	149 2048	k	139 707	119 14	(100) 602	(102) 614	(77) 1187	(81) 2448	(77) 5083
173	Shanghai Yitu Technology	yitu	4	2018-10-30	2119	136	181 2070	1	201 897	191 45	(144) 1288	(140) 1203	(117) 2440	(121) 5241	(113) 9671
174	Shanghai Yitu Technology	yitu	5	2018-10-30	2043	136	180 2070	1	182 853	190 44	(140) 1237	(139) 1199	(122) 2513	(116) 5013	(112) 9620
175	Smilart	smilart	4	2018-10-30	65	89	25 512	k	8 167	19 4	(213) 16137	(218) 15633	-	-	-
176	Smilart	smilart	5	2018-10-30	562	89	145 2048	k	63 450	115 14	-	-	-	-	-
177	StaQu Technologies	staqu	000	2021-08-30	1018	690	199 4096	-	178 826	163 24	(195) 4950	(198) 4933	-	-	-
178	Synesis	synesis	003	2019-07-04	143	17	116 2048	k	18 211	92 12	(89) 507	(88) 502	(113) 2297	(109) 4564	(108) 9452
179	Synesis	synesis	3	2018-10-30	237	150	196 4096	k	5 99	171 29	(115) 789	(118) 801	(106) 1941	(100) 3888	(100) 8810
180	Synesis	synesis	005	2020-09-08	494	24	211 4104	-	152 756	161 24	(122) 877	(122) 865	(137) 3182	(111) 4658	(115) 9750
181	Tech5 SA	tech5	001	2019-08-19	1394	116	76 1536	k	198 887	72 10	(69) 383	(115) 766	(128) 2767	(131) 6149	(87) 16178
182	Tech5 SA	tech5	002	2021-04-07	727	112	34 513	-	215 940	15 4	(193) 4682	(210) 6689	(176) 12541	(172) 25145	(170) 50239
183	Tencent Deepsea Lab	deepsea	001	2019-07-29	250	323	127 2048	1	149 737	94 12	(131) 1021	(131) 1020	(129) 2774	(127) 5767	(131) 12341
184	Tevian	tevian	5	2018-10-30	773	15	99 2048	1	53 405	124 15	(74) 405	(76) 408	(61) 854	(64) 1757	(60) 3380
185	Tevian	tevian	006	2021-04-16	769	19	55 1032	-	95 597	71 10	(59) 295	(59) 295	(46) 578	(45) 1187	(48) 2741
186	Tevian	tevian	007	2021-10-12	703	19	60 1032	-	160 777	23 4	(60) 297	(60) 298	(47) 579	(44) 1179	(41) 2418
187	Thales	cogent	2	2018-10-30	681	39	63 1043	k	216 945	165 27	(167) 2017	(174) 2144	(149) 4299	(146) 8472	(146) 16429
188	Thales	cogent	3	2018-10-30	681	39	64 1043	k	214 940	68 9	(138) 1230	(144) 1311	(127) 2687	(122) 5398	(119) 10184
189	Thales	cogent	004	2021-02-10	1376	59	168 2053	-	218 947	109 14	(182) 2908	(166) 1911	(141) 3566	(140) 7498	(145) 16370
190	Thales	cogent	005	2021-09-13	1043	56	65 1062	-	157 769	27 5	(124) 912	(127) 996	(101) 1872	(99) 3845	(95) 7555
191	TigerIT Americas LLC	tiger	2	2018-10-29	416	518	151 2052	k	67 461	128 15	(163) 1816	(167) 1921	(146) 3833	(145) 7526	(141) 14820
192	TigerIT Americas LLC	tiger	3	2018-10-30	416	518	161 2052	k	68 461	220 37431	(39) 191	(37) 189	-	-	-
193	Toshiba	toshiba	0	2018-10-30	961	105	81 1548	k	194 876	90 12	(204) 6153	(206) 6236	(173) 12221	(173) 25355	(169) 49448
194	Toshiba	toshiba	1	2018-10-30	961	105	128 2060	k	193 875	221 4701	(203) 6007	(208) 6355	-	-	-
195	Tripleize	aize	001	2021-08-06	262	150	92 2048	-	49 402	60 9	(180) 3087	(188) 3080	-	-	-
196	Trueface.ai	trueface	000	2021-01-27	247	119	88 2000	-	37 363	100 13	(49) 271	(65) 327	(50) 614	(48) 1239	(44) 2678
197	Veridas Digital Authentication Solutions S.L.	veridas	001	2021-03-05	347	875	89 2048	-	190 872	101 13	(197) 5493	(201) 5469	(170) 10350	(168) 20655	(164) 41264
198	Veridas Digital Authentication Solutions S.L.	veridas	002	2021-07-06	347	870	103 2048	-	195 877	81 302	(63) 322	(63) 325	(55) 685	(53) 1365	(47) 2730
199	Veridas Digital Authentication Solutions S.L.	veridas	003	2021-11-09	346	870	111 2048	-	188 867	54 9	(62) 440	(64) 327	(57) 699	(54) 1401	(64) 3954
200	Viettel Group	vts	000	2021-03-12	250	257	157 2048	-	78 492	207 2295	(2) 4	(2) 4	(2) 6	(4) 11	-
201	Viettel Group	vts	001	2021-07-16	352	600	141 2048	-	200 891	157 21	(175) 2477	(180) 2487	(152) 4644	(150) 9313	(150) 18713
202	Viettel Group	vts	002	2022-02-08	244	600	98 2048	-	203 903	172 29	(176) 2485	(154) 4678	(151) 9370	(152) 18833	(47) 1.49 N <sup>1.0</sup>
203	Vigilant Solutions	vigilant	5	2018-10-30	335	122	79 1544	k	154 762	148 19	-	-	-	-	-
204	Vigilant Solutions	vigilant	6	2018-10-30	337	122	80 1544	k	17 816	155 21	-	(159) 1713	-	-	-
205	Vigilant Solutions	vigilantsolutions	007	2021-01-08	340	51	78 1544	-	102 616	139 16	(149) 1354	(148) 1352	(131) 2911	(129) 5966	(125) 11466
206	Vigilant Solutions	vigilantsolutions	008	2021-07-23	340	51	77 1544	-	51 403	105 13	(133) 1062	(133) 1061	(115) 2330	(125) 5520	(109) 9499
207	Visidon	visidon	1	2018-10-30	166	42	155 2052	k	119 667	130 15	(191) 4370	(197) 4472	(167) 8454	(166) 17262	(162) 34288
208	Visidon	vd	002	2021-05-18	248	42	167 2052	-	128 687	95 9	(168) 2089	(175) 2336	-	-	-

Notes
1 Configuration size does not capture static data present in libraries. Libraries are included but the size also includes any ancillary libraries for image processing (e.g. openCV) or numerical computation (e.g. blas).
2 Finalization is the processing of converting $N = 1600000$ templates into a searchable data structure an operation which can be a simple copy, or the building of an index or tree, for example. The duration of the operation may be data dependent, and may not be linear in the number of input templates.
3 This multiplier expresses the increase in template size when $k$ images are passed to the template generation function.
4 All durations are measured on Intel® Xeon®@CPU E5-2630 v4 @ 2.0GHz processors. Estimates are made by wrapping the API function call in calls to std::chrono::high_resolution_clock which on the machine in (3) counts 1ns clock ticks. Precision is somewhat worse than that however.
5 Search durations are measured as in the prior note. The power-law model in the final column mostly fits the empirical results in Figure 134. However in certain cases the model is not correct and should not be used numerically.

Table 5: Summary of algorithms and properties included in this report. The blue superscripts give ranking for the quantity in that column. Missing search durations, denoted by “-”, are absent because those runs were not executed, usually because we did not run on the larger galleries. Caution: The power-law model is sometimes an incorrect model. It is included here only to show broad sublinear behavior, which is flagged in green. The models should not be used for prediction.

2022/04/28  
22:29:02FNIR(N, R, T) = False neg. identification rate  
FPIR(N, T) = False pos. identification rate

N = Num. enrolled subjects

R = Num. candidates examined

T = Threshold

T = 0 → Investigation  
T √ 0 → Identification

2022/04/28  
22:29:02FNIR(N, R, T) = False neg. identification rate  
FPIR(N, T) = False pos. identification rateN = Num. enrolled subjects  
R = Num. candidates examined

T = Threshold

T = 0 → Investigation  
T > 0 → Identification

	DEVELOPER	SHORT	SEQ.	VALIDATION	CONFIG <sup>1</sup>	LIB <sup>1</sup>	TEMPLATE GENERATION	FINALIZE <sup>2</sup>	SEARCH DURATION <sup>5</sup> MILLISEC						
									SIZE (B)	MULT <sup>3</sup>	TIME (MS) <sup>4</sup>	TIME (S)	L=1	L=50	POWER LAW
	FULL NAME	NAME	NUM.	DATE	DATA (MB)	DATA (MB)			N=1.6M	N=1.6M	N=3M	N=6M	N=12M	(μs)	
209	Visidon	vd	003	2021-10-12	497	43	<sup>157</sup> 2052	-	<sup>132</sup> 692	<sup>46</sup> 8	<sup>(169)</sup> 2095	<sup>(173)</sup> 2082	-	-	-
210	Visiob-Box	visionbox	000	2021-09-17	252	274	<sup>177</sup> 2059	-	<sup>75</sup> 481	<sup>138</sup> 16	<sup>(77)</sup> 422	<sup>(67)</sup> 359	<sup>(62)</sup> 855	<sup>(26)</sup> 631	<sup>(37)</sup> 2096
211	VisionLabs	visionlabs	6	2018-10-30	360	17	<sup>30</sup> 512	1	<sup>29</sup> 289	<sup>217</sup> 20290	<sup>(14)</sup> 36	<sup>(14)</sup> 36	<sup>(12)</sup> 39	<sup>(11)</sup> 44	<sup>(9)</sup> 53
212	VisionLabs	visionlabs	7	2018-10-30	360	17	<sup>24</sup> 512	1	<sup>28</sup> 289	<sup>218</sup> 34666	<sup>(15)</sup> 63	<sup>(15)</sup> 63	<sup>(13)</sup> 72	<sup>(13)</sup> 80	<sup>(11)</sup> 115
213	VisionLabs	visionlabs	008	2019-06-18	348	17	<sup>31</sup> 512	1	<sup>25</sup> 272	<sup>215</sup> 12747	<sup>(9)</sup> 23	<sup>(8)</sup> 24	<sup>(7)</sup> 26	<sup>(6)</sup> 29	<sup>(5)</sup> 33
214	VisionLabs	visionlabs	009	2020-08-04	689	20	<sup>29</sup> 512	-	<sup>71</sup> 467	<sup>210</sup> 13245	<sup>(10)</sup> 23	<sup>(9)</sup> 29	<sup>(9)</sup> 34	<sup>(12)</sup> 61	<sup>(12)</sup> 145
215	VisionLabs	visionlabs	010	2021-02-05	1042	20	<sup>26</sup> 512	-	<sup>146</sup> 731	<sup>211</sup> 11837	<sup>(7)</sup> 21	<sup>(11)</sup> 32	<sup>(10)</sup> 36	<sup>(8)</sup> 39	<sup>(6)</sup> 43
216	VisionLabs	visionlabs	011	2021-10-20	1042	20	<sup>28</sup> 512	-	<sup>148</sup> 735	<sup>214</sup> 12255	<sup>(8)</sup> 21	<sup>(7)</sup> 23	<sup>(8)</sup> 26	<sup>(7)</sup> 34	<sup>(8)</sup> 51
217	Vocord	vocord	5	2018-10-30	1035	185	<sup>44</sup> 768	k	<sup>161</sup> 780	<sup>37</sup> 7	<sup>(33)</sup> 158	<sup>(38)</sup> 204	<sup>(30)</sup> 383	<sup>(31)</sup> 767	<sup>(26)</sup> 1466
218	Vocord	vocord	6	2018-10-30	1035	185	<sup>221</sup> 10240	k	<sup>162</sup> 785	<sup>206</sup> 243	<sup>(34)</sup> 170	<sup>(41)</sup> 216	-	-	-
219	Xforward AI Technology	xforwardai	000	2020-07-24	236	171	<sup>117</sup> 2048	-	<sup>151</sup> 753	<sup>107</sup> 13	<sup>(192)</sup> 4603	<sup>(214)</sup> 7647	<sup>(181)</sup> 15723	<sup>(370)</sup> 23900	<sup>(372)</sup> 53729
220	Xforward AI Technology	xforwardai	001	2021-01-21	332	50	<sup>121</sup> 2048	-	<sup>125</sup> 677	<sup>136</sup> 16	<sup>(202)</sup> 5887	<sup>(196)</sup> 4384	<sup>(168)</sup> 8798	<sup>(167)</sup> 18553	<sup>(15)</sup> 48993
221	Xforward AI Technology	xforwardai	002	2021-05-24	691	50	<sup>201</sup> 4096	-	<sup>211</sup> 930	<sup>146</sup> 18	<sup>(209)</sup> 6957	<sup>(209)</sup> 6400	<sup>(177)</sup> 12659	<sup>(177)</sup> 31077	<sup>(175)</sup> 65158

## Notes

- Configuration size does not capture static data present in libraries. Libraries are included but the size also includes any ancillary libraries for image processing (e.g. openCV) or numerical computation (e.g. blas).
- Finalization is the processing of converting N = 1600000 templates into a searchable data structure an operation which can be a simple copy, or the building of an index or tree, for example. The duration of the operation may be data dependent, and may not be linear in the number of input templates.
- This multiplier expresses the increase in template size when  $k$  images are passed to the template generation function.
- All durations are measured on Intel®Xeon®CPU E5-2630 v4 @ 2.20GHz processors. Estimates are made by wrapping the API function call in calls to std::chrono::high\_resolution\_clock which on the machine in (3) counts 1ns clock ticks. Precision is somewhat worse than that however.
- Search durations are measured as in the prior note. The power-law model in the final column mostly fits the empirical results in Figure 134. However in certain cases the model is not correct and should not be used numerically.

Table 6: Summary of algorithms and properties included in this report. The blue superscripts give ranking for the quantity in that column. Missing search durations, denoted by “-”, are absent because those runs were not executed, usually because we did not run on the larger galleries. Caution: The power-law model is sometimes an incorrect model. It is included here only to show broad sublinear behavior, which is flagged in green. The models should not be used for prediction.

#	ALGORITHM	INVESTIGATION, FNIR(N, R = 1, T = 0)								IDENTIFICATION, FNIR(N, R = L, T ≥ 0) FOR FPIR = 0.001									
		(0, 2]	(2, 4]	(4, 6]	(6, 8]	(8, 10]	(10, 12]	(12, 14]	(14, 18]	(0, 2]	(2, 4]	(4, 6]	(6, 8]	(8, 10]	(10, 12]	(12, 14]	(14, 18]		
1	3DIVI-005	<sup>97</sup> 0.0207	<sup>97</sup> 0.0304	<sup>97</sup> 0.0415	<sup>97</sup> 0.0533	<sup>97</sup> 0.0646	<sup>112</sup> 0.0735	<sup>112</sup> 0.0884	<sup>113</sup> 0.1148	<sup>107</sup> 0.1580	<sup>98</sup> 0.2316	<sup>98</sup> 0.3033	<sup>98</sup> 0.3740	<sup>98</sup> 0.4285	<sup>113</sup> 0.4742	<sup>111</sup> 0.5329	<sup>117</sup> 0.5975		
2	ANKE-000	<sup>95</sup> 0.0162	<sup>95</sup> 0.0245	<sup>95</sup> 0.0333	<sup>95</sup> 0.0428	<sup>95</sup> 0.0515	<sup>106</sup> 0.0615	<sup>109</sup> 0.0780	<sup>109</sup> 0.1028	<sup>96</sup> 0.1132	<sup>96</sup> 0.1761	<sup>96</sup> 0.2402	<sup>96</sup> 0.3057	<sup>95</sup> 0.3640	<sup>110</sup> 0.4200	<sup>110</sup> 0.4928	<sup>110</sup> 0.5680		
3	ANKE-002	<sup>4</sup> 0.0055	<sup>50</sup> 0.0074	<sup>50</sup> 0.0090	<sup>49</sup> 0.0103	<sup>48</sup> 0.0116	<sup>64</sup> 0.0135	<sup>63</sup> 0.0162	<sup>65</sup> 0.0202	<sup>54</sup> 0.0329	<sup>54</sup> 0.0560	<sup>56</sup> 0.0843	<sup>57</sup> 0.1169	<sup>57</sup> 0.1481	<sup>71</sup> 0.1820	<sup>72</sup> 0.2280	<sup>71</sup> 0.2831		
4	AWARE-005	<sup>106</sup> 0.0328	<sup>106</sup> 0.0519	<sup>106</sup> 0.0712	<sup>109</sup> 0.0910	<sup>104</sup> 0.1078	<sup>119</sup> 0.1235	<sup>119</sup> 0.1457	<sup>119</sup> 0.1831	<sup>108</sup> 0.3605	<sup>107</sup> 0.4949	<sup>107</sup> 0.5948	<sup>107</sup> 0.6783	<sup>108</sup> 0.7393	<sup>123</sup> 0.7905	<sup>123</sup> 0.8408	<sup>124</sup> 0.8831		
5	AWARE-006	<sup>110</sup> 0.0702	<sup>111</sup> 0.1110	<sup>111</sup> 0.1502	<sup>118</sup> 0.2253	<sup>126</sup> 0.2614	<sup>125</sup> 0.3045	<sup>125</sup> 0.3659											
6	AYONIX-002	<sup>113</sup> 0.3360	<sup>114</sup> 0.4389	<sup>114</sup> 0.5144	<sup>114</sup> 0.5814	<sup>114</sup> 0.6340	<sup>129</sup> 0.6818	<sup>129</sup> 0.7297	<sup>130</sup> 0.7774	<sup>116</sup> 0.8288	<sup>111</sup> 0.9013	<sup>111</sup> 0.9375	<sup>111</sup> 0.9603	<sup>111</sup> 0.9744	<sup>127</sup> 0.9837	<sup>127</sup> 0.9893	<sup>127</sup> 0.9927		
7	CAMVI-004	<sup>109</sup> 0.0623	<sup>109</sup> 0.0944	<sup>108</sup> 0.1243	<sup>108</sup> 0.1548	<sup>108</sup> 0.1812	<sup>123</sup> 0.2056	<sup>123</sup> 0.2344	<sup>121</sup> 0.2672	<sup>91</sup> 0.0810	<sup>91</sup> 0.1267	<sup>88</sup> 0.2203	<sup>88</sup> 0.2619	<sup>101</sup> 0.3040	<sup>108</sup> 0.3543	<sup>96</sup> 0.4124			
8	CAMVI-005	<sup>111</sup> 0.0849	<sup>111</sup> 0.1255	<sup>111</sup> 0.1631	<sup>111</sup> 0.1989	<sup>117</sup> 0.2298	<sup>125</sup> 0.2585	<sup>124</sup> 0.2915	<sup>124</sup> 0.3246										
9	CANON-001					<sup>25</sup> 0.0052	<sup>22</sup> 0.0057	<sup>17</sup> 0.0042							<sup>27</sup> 0.0491	<sup>27</sup> 0.0606	<sup>28</sup> 0.0826		
10	CIB-000	<sup>14</sup> 0.0022	<sup>14</sup> 0.0030	<sup>15</sup> 0.0037	<sup>15</sup> 0.0044	<sup>17</sup> 0.0049	<sup>27</sup> 0.0057	<sup>27</sup> 0.0069	<sup>25</sup> 0.0139	<sup>26</sup> 0.0240	<sup>27</sup> 0.0373	<sup>28</sup> 0.0525	<sup>28</sup> 0.0689	<sup>37</sup> 0.0859	<sup>38</sup> 0.1109	<sup>38</sup> 0.1454			
11	CLEARVIEWAI-000	<sup>7</sup> 0.0017	<sup>4</sup> 0.0023	<sup>4</sup> 0.0028	<sup>9</sup> 0.0034	<sup>11</sup> 0.0039	<sup>18</sup> 0.0046	<sup>21</sup> 0.0056	<sup>24</sup> 0.0047	<sup>16</sup> 0.0066	<sup>18</sup> 0.0121	<sup>18</sup> 0.0194	<sup>19</sup> 0.0287	<sup>19</sup> 0.0385	<sup>26</sup> 0.0493	<sup>30</sup> 0.0662	<sup>30</sup> 0.0873		
12	CLOUDWALK-HR-000	<sup>8</sup> 0.0019	<sup>7</sup> 0.0024	<sup>8</sup> 0.0029	<sup>6</sup> 0.0032	<sup>5</sup> 0.0036	<sup>5</sup> 0.0041	<sup>3</sup> 0.0020	<sup>1</sup> 0.0029	<sup>1</sup> 0.0041	<sup>1</sup> 0.0054	<sup>1</sup> 0.0064	<sup>2</sup> 0.0073	<sup>4</sup> 0.0085	<sup>4</sup> 0.0102	<sup>4</sup> 0.0112			
13	CLOUDWALK-MT-000							<sup>7</sup> 0.0037	<sup>7</sup> 0.0038	<sup>7</sup> 0.0013					<sup>1</sup> 0.0065	<sup>1</sup> 0.0072	<sup>1</sup> 0.0075		
14	COGENT-000	<sup>97</sup> 0.0128	<sup>98</sup> 0.0184	<sup>98</sup> 0.0250	<sup>93</sup> 0.0327	<sup>93</sup> 0.0407	<sup>108</sup> 0.0488	<sup>106</sup> 0.0611	<sup>104</sup> 0.0794	<sup>77</sup> 0.0559	<sup>79</sup> 0.0923	<sup>78</sup> 0.1342	<sup>78</sup> 0.1812	<sup>78</sup> 0.2243	<sup>89</sup> 0.2675	<sup>88</sup> 0.3240	<sup>93</sup> 0.3992		
15	COGENT-001	<sup>9</sup> 0.0128	<sup>91</sup> 0.0184	<sup>92</sup> 0.0250	<sup>92</sup> 0.0327	<sup>92</sup> 0.0407	<sup>102</sup> 0.0488	<sup>105</sup> 0.0611	<sup>105</sup> 0.0794	<sup>78</sup> 0.0559	<sup>78</sup> 0.0923	<sup>77</sup> 0.1342	<sup>77</sup> 0.1812	<sup>77</sup> 0.2243	<sup>89</sup> 0.2675	<sup>89</sup> 0.3240	<sup>92</sup> 0.3992		
16	COGENT-002	<sup>69</sup> 0.0081	<sup>66</sup> 0.0105	<sup>63</sup> 0.0123	<sup>64</sup> 0.0137	<sup>62</sup> 0.0157	<sup>77</sup> 0.0175	<sup>75</sup> 0.0215	<sup>75</sup> 0.0280	<sup>69</sup> 0.0499	<sup>68</sup> 0.0827	<sup>67</sup> 0.1207	<sup>67</sup> 0.1639	<sup>67</sup> 0.2037	<sup>81</sup> 0.2432	<sup>82</sup> 0.2972	<sup>83</sup> 0.3638		
17	COGENT-003	<sup>71</sup> 0.0082	<sup>67</sup> 0.0108	<sup>65</sup> 0.0128	<sup>67</sup> 0.0145	<sup>66</sup> 0.0168	<sup>83</sup> 0.0191	<sup>84</sup> 0.0239	<sup>81</sup> 0.0312	<sup>80</sup> 0.0582	<sup>80</sup> 0.0971	<sup>80</sup> 0.1417	<sup>80</sup> 0.1918	<sup>80</sup> 0.2380	<sup>98</sup> 0.2836	<sup>99</sup> 0.3440	<sup>99</sup> 0.4207		
18	COGENT-004	<sup>59</sup> 0.0066	<sup>59</sup> 0.0080	<sup>45</sup> 0.0085	<sup>39</sup> 0.0080	<sup>31</sup> 0.0083	<sup>45</sup> 0.0092	<sup>46</sup> 0.0106	<sup>63</sup> 0.0410	<sup>65</sup> 0.0720	<sup>65</sup> 0.1099	<sup>65</sup> 0.1539	<sup>69</sup> 0.1974	<sup>82</sup> 0.2443	<sup>85</sup> 0.3043	<sup>85</sup> 0.3757			
19	COGNITEC-000	<sup>105</sup> 0.0265	<sup>103</sup> 0.0423	<sup>103</sup> 0.0588	<sup>103</sup> 0.0757	<sup>102</sup> 0.0894	<sup>117</sup> 0.1014	<sup>116</sup> 0.1169	<sup>116</sup> 0.1381	<sup>100</sup> 0.1522	<sup>99</sup> 0.2330	<sup>99</sup> 0.3051	<sup>99</sup> 0.3751	<sup>114</sup> 0.4300	<sup>113</sup> 0.5307	<sup>111</sup> 0.5913			
20	COGNITEC-001	<sup>9</sup> 0.0149	<sup>92</sup> 0.0228	<sup>93</sup> 0.0312	<sup>94</sup> 0.0399	<sup>94</sup> 0.0479	<sup>105</sup> 0.0546	<sup>108</sup> 0.0656	<sup>106</sup> 0.0806	<sup>93</sup> 0.0963	<sup>93</sup> 0.1562	<sup>93</sup> 0.2157	<sup>93</sup> 0.2771	<sup>108</sup> 0.3287	<sup>108</sup> 0.3771	<sup>108</sup> 0.4343	<sup>108</sup> 0.4959		
21	COGNITEC-002	<sup>77</sup> 0.0101	<sup>80</sup> 0.0138	<sup>81</sup> 0.0170	<sup>81</sup> 0.0201	<sup>81</sup> 0.0237	<sup>95</sup> 0.0264	<sup>93</sup> 0.0309	<sup>92</sup> 0.0389	<sup>72</sup> 0.0517	<sup>71</sup> 0.0879	<sup>72</sup> 0.1269	<sup>73</sup> 0.1707	<sup>71</sup> 0.2098	<sup>83</sup> 0.2463	<sup>81</sup> 0.2919	<sup>81</sup> 0.3535		
22	COGNITEC-003	<sup>7</sup> 0.0104	<sup>81</sup> 0.0140	<sup>82</sup> 0.0174	<sup>82</sup> 0.0205	<sup>82</sup> 0.0238	<sup>96</sup> 0.0266	<sup>94</sup> 0.0311	<sup>94</sup> 0.0401	<sup>71</sup> 0.0504	<sup>70</sup> 0.0855	<sup>69</sup> 0.1235	<sup>69</sup> 0.1662	<sup>69</sup> 0.2045	<sup>80</sup> 0.2403	<sup>79</sup> 0.2854	<sup>79</sup> 0.3451		
23	COGNITEC-004	<sup>64</sup> 0.0073	<sup>63</sup> 0.0099	<sup>62</sup> 0.0118	<sup>59</sup> 0.0130	<sup>59</sup> 0.0147	<sup>76</sup> 0.0163	<sup>72</sup> 0.0189	<sup>71</sup> 0.0239	<sup>53</sup> 0.0325	<sup>53</sup> 0.0548	<sup>52</sup> 0.0798	<sup>51</sup> 0.1074	<sup>50</sup> 0.1325	<sup>63</sup> 0.1591	<sup>62</sup> 0.1952	<sup>61</sup> 0.2414		
24	COGNITEC-006							<sup>39</sup> 0.0081	<sup>37</sup> 0.0086	<sup>38</sup> 0.0090				<sup>34</sup> 0.0777	<sup>34</sup> 0.0926	<sup>34</sup> 0.1274			
25	CUBOX-000	<sup>7</sup> 0.0019	<sup>5</sup> 0.0024	<sup>5</sup> 0.0028	<sup>4</sup> 0.0031	<sup>4</sup> 0.0032	<sup>6</sup> 0.0037	<sup>7</sup> 0.0044	<sup>6</sup> 0.0052	<sup>6</sup> 0.0039	<sup>6</sup> 0.0059	<sup>7</sup> 0.0083	<sup>8</sup> 0.0111	<sup>8</sup> 0.0141	<sup>13</sup> 0.0185	<sup>13</sup> 0.0252	<sup>13</sup> 0.0339		
26	CYBERLINK-002	<sup>5</sup> 0.0055	<sup>45</sup> 0.0068	<sup>41</sup> 0.0075	<sup>35</sup> 0.0078	<sup>32</sup> 0.0084	<sup>46</sup> 0.0094	<sup>47</sup> 0.0107	<sup>48</sup> 0.0114	<sup>32</sup> 0.0180	<sup>33</sup> 0.0302	<sup>38</sup> 0.0460	<sup>38</sup> 0.0643	<sup>38</sup> 0.0837	<sup>46</sup> 0.1058	<sup>45</sup> 0.1370	<sup>45</sup> 0.1787		
27	CYBERLINK-003	<sup>38</sup> 0.0041	<sup>34</sup> 0.0052	<sup>27</sup> 0.0057	<sup>25</sup> 0.0058	<sup>25</sup> 0.0061	<sup>36</sup> 0.0068	<sup>35</sup> 0.0078	<sup>35</sup> 0.0078	<sup>19</sup> 0.0109	<sup>19</sup> 0.0175	<sup>20</sup> 0.0259	<sup>21</sup> 0.0356	<sup>21</sup> 0.0468	<sup>31</sup> 0.0594	<sup>31</sup> 0.0787	<sup>32</sup> 0.1072		
28	DAHUA-002	<sup>3</sup> 0.0035	<sup>28</sup> 0.0047	<sup>28</sup> 0.0058	<sup>27</sup> 0.0067	<sup>28</sup> 0.0074	<sup>40</sup> 0.0082	<sup>43</sup> 0.0100	<sup>40</sup> 0.0108	<sup>30</sup> 0.0169	<sup>30</sup> 0.0262	<sup>30</sup> 0.0325	<sup>30</sup> 0.0449	<sup>30</sup> 0.0635	<sup>30</sup> 0.0817	<sup>43</sup> 0.1013	<sup>41</sup> 0.1291	<sup>41</sup> 0.1638	
29	DAHUA-003	<sup>19</sup> 0.0026	<sup>19</sup> 0.0036	<sup>19</sup> 0.0043	<sup>20</sup> 0.0050	<sup>29</sup> 0.0062	<sup>29</sup> 0.0080	<sup>31</sup> 0.0073	<sup>29</sup> 0.0160	<sup>30</sup> 0.0280	<sup>29</sup> 0.0432	<sup>29</sup> 0.0615	<sup>29</sup> 0.0794	<sup>41</sup> 0.0987	<sup>41</sup> 0.1270	<sup>39</sup> 0.1587			
30	DEEPLINT-001	<sup>17</sup> 0.0024	<sup>16</sup> 0.0032	<sup>14</sup> 0.0037	<sup>13</sup> 0.0040	<sup>13</sup> 0.0043	<sup>21</sup> 0.0049	<sup>23</sup> 0.0060	<sup>23</sup> 0.0052	<sup>12</sup> 0.0058	<sup>10</sup> 0.0087	<sup>11</sup> 0.0119	<sup>11</sup> 0.0199	<sup>16</sup> 0.0249	<sup>16</sup> 0.0338	<sup>16</sup> 0.0463			
31	DEEPSEA-001	<sup>70</sup> 0.0081	<sup>70</sup> 0.0116	<sup>73</sup> 0.0149	<sup>76</sup> 0.0182	<sup>76</sup> 0.0216	<sup>94</sup> 0.0260	<sup>96</sup> 0.0332	<sup>96</sup> 0.0432	<sup>66</sup> 0.0458	<sup>66</sup> 0.0752	<sup>68</sup> 0.1086	<sup>63</sup> 0.1460	<sup>63</sup> 0.1812	<sup>78</sup> 0.2186	<sup>78</sup> 0.2663	<sup>77</sup> 0.3213		
32	DERMALOG-006	<sup>8</sup> 0.0113	<sup>82</sup> 0.0142	<sup>78</sup> 0.0163	<sup>77</sup> 0.0183	<sup>74</sup> 0.0200	<sup>88</sup> 0.0218	<sup>86</sup> 0.0251	<sup>84</sup> 0.0329	<sup>75</sup> 0.0545	<sup>73</sup> 0.0889	<sup>73</sup> 0.1271	<sup>70</sup> 0.1697	<sup>70</sup> 0.2090	<sup>84</sup> 0.3498	<sup>84</sup> 0.3670			
33	DERMALOG-007	<sup>8</sup> 0.0125	<sup>88</sup> 0.0170	<sup>88</sup> 0.0214	<sup>88</sup> 0.0264	<sup>87</sup> 0.0309	<sup>101</sup> 0.0356	<sup>102</sup> 0.0432	<sup>102</sup> 0.0579	<sup>92</sup> 0.0910	<sup>92</sup> 0.1453	<sup>92</sup> 0.2009	<sup>92</sup> 0.2602	<sup>93</sup> 0.3134	<sup>10</sup> 0.3649	<sup>10</sup> 0.4289	<sup>10</sup> 0.5007		
34	DERMALOG-008	<sup>52</sup> 0.0057	<sup>52</sup> 0.0077	<sup>54</sup> 0.0095	<sup>54</sup> 0.0110	<sup>53</sup> 0.0128	<sup>70</sup> 0.0148	<sup>69</sup> 0.0180	<sup>70</sup> 0.0223	<sup>70</sup> 0.0501	<sup>69</sup> 0.0850	<sup>70</sup> 0.1247	<sup>71</sup> 0.1692	<sup>72</sup> 0.2105	<sup>86</sup> 0.2541	<sup>86</sup> 0.3102	<sup>86</sup> 0.3762		
35	FUJITSULAB-001						<sup>44</sup> 0.0089	<sup>42</sup> 0.0098	<sup>44</sup> 0.0111					<sup>59</sup> 0.1403	<sup>54</sup> 0.1723				
36	GORILLA-001	<sup>100</sup> 0.0213	<sup>100</sup> 0.0359	<sup>101</sup> 0.0528	<sup>102</sup> 0.0716	<sup>103</sup> 0.0895	<sup>118</sup> 0.1088	<sup>118</sup> 0.1367	<sup>118</sup> 0.1765	<sup>103</sup> 0.1828	<sup>104</sup> 0.2787	<sup>104</sup> 0.3654	<sup>104</sup> 0.4485	<sup>104</sup> 0.5168	<sup>117</sup> 0.582				

MISS RATES		INVESTIGATION, FNIR(N, R = 1, T = 0)								IDENTIFICATION, FNIR(N, R = L, T ≥ 0) FOR FPIR = 0.001							
#	ALGORITHM	(0, 2]	(2, 4]	(4, 6]	(6, 8]	(8, 10]	(10, 12]	(12, 14]	(14, 18]	(0, 2]	(2, 4]	(4, 6]	(6, 8]	(8, 10]	(10, 12]	(12, 14]	(14, 18]
45	IDEMIA-009	<sup>38</sup> 0.0039	<sup>37</sup> 0.0052	<sup>31</sup> 0.0061	<sup>29</sup> 0.0067	<sup>30</sup> 0.0077	<sup>45</sup> 0.0088	<sup>44</sup> 0.0103	<sup>45</sup> 0.0109	<sup>39</sup> 0.0212	<sup>39</sup> 0.0357	<sup>40</sup> 0.0539	<sup>40</sup> 0.0755	<sup>38</sup> 0.0967	<sup>51</sup> 0.1183	<sup>50</sup> 0.1485	<sup>48</sup> 0.1893
46	IMAGUS-005	<sup>34</sup> 0.0040	<sup>35</sup> 0.0054	<sup>36</sup> 0.0067	<sup>38</sup> 0.0079	<sup>40</sup> 0.0093	<sup>56</sup> 0.0112	<sup>55</sup> 0.0139	<sup>57</sup> 0.0178	<sup>49</sup> 0.0286	<sup>51</sup> 0.0503	<sup>51</sup> 0.0779	<sup>54</sup> 0.1116	<sup>56</sup> 0.1455	<sup>72</sup> 0.1844	<sup>75</sup> 0.2341	<sup>74</sup> 0.2951
47	IMPERIAL-000	<sup>91</sup> 0.0155	<sup>96</sup> 0.0247	<sup>96</sup> 0.0348	<sup>96</sup> 0.0463	<sup>96</sup> 0.0571	<sup>111</sup> 0.0674	<sup>111</sup> 0.0856	<sup>112</sup> 0.1114	<sup>102</sup> 0.1627	<sup>102</sup> 0.2507	<sup>102</sup> 0.3322	<sup>100</sup> 0.4122	<sup>100</sup> 0.4772	<sup>116</sup> 0.5368	<sup>116</sup> 0.6059	<sup>116</sup> 0.6766
48	INCODE-003	<sup>56</sup> 0.0061	<sup>59</sup> 0.0087	<sup>59</sup> 0.0110	<sup>61</sup> 0.0136	<sup>64</sup> 0.0161	<sup>79</sup> 0.0185	<sup>82</sup> 0.0236	<sup>80</sup> 0.0309	<sup>73</sup> 0.0532	<sup>74</sup> 0.0908	<sup>75</sup> 0.1334	<sup>77</sup> 0.1809	<sup>77</sup> 0.2245	<sup>91</sup> 0.2675	<sup>90</sup> 0.3249	<sup>89</sup> 0.3932
49	INCODE-004	<sup>114</sup> 0.3594	<sup>113</sup> 0.3629	<sup>113</sup> 0.3688	<sup>113</sup> 0.3754	<sup>112</sup> 0.3813	<sup>127</sup> 0.3870	<sup>127</sup> 0.3960	<sup>127</sup> 0.4135	<sup>102</sup> 0.4234	<sup>106</sup> 0.4642	<sup>106</sup> 0.5073	<sup>106</sup> 0.5522	<sup>105</sup> 0.5902	<sup>122</sup> 0.6274	<sup>116</sup> 0.6736	<sup>116</sup> 0.7253
50	INNOVATRICS-004	<sup>41</sup> 0.0046	<sup>41</sup> 0.0063	<sup>42</sup> 0.0078	<sup>45</sup> 0.0092	<sup>45</sup> 0.0106	<sup>58</sup> 0.0124	<sup>58</sup> 0.0149	<sup>58</sup> 0.0178	<sup>35</sup> 0.0343	<sup>56</sup> 0.0590	<sup>58</sup> 0.0886	<sup>58</sup> 0.1222	<sup>59</sup> 0.1544	<sup>73</sup> 0.1881	<sup>74</sup> 0.2321	<sup>72</sup> 0.2874
51	INNOVATRICS-005	<sup>21</sup> 0.0031	<sup>24</sup> 0.0042	<sup>25</sup> 0.0051	<sup>26</sup> 0.0060	<sup>26</sup> 0.0068	<sup>38</sup> 0.0080	<sup>40</sup> 0.0095	<sup>41</sup> 0.0107	<sup>52</sup> 0.0313	<sup>52</sup> 0.0539	<sup>53</sup> 0.0815	<sup>56</sup> 0.1137	<sup>57</sup> 0.1442	<sup>69</sup> 0.1755	<sup>70</sup> 0.2181	<sup>68</sup> 0.2718
52	IREX-000	<sup>76</sup> 0.0101	<sup>79</sup> 0.0135	<sup>80</sup> 0.0169	<sup>79</sup> 0.0197	<sup>80</sup> 0.0228	<sup>92</sup> 0.0256	<sup>92</sup> 0.0304	<sup>93</sup> 0.0398	<sup>90</sup> 0.0779	<sup>98</sup> 0.1258	<sup>91</sup> 0.1759	<sup>90</sup> 0.2299	<sup>90</sup> 0.2758	<sup>104</sup> 0.3204	<sup>104</sup> 0.3763	<sup>102</sup> 0.4401
53	ISYSTEMS-002	<sup>77</sup> 0.0089	<sup>69</sup> 0.0115	<sup>69</sup> 0.0139	<sup>69</sup> 0.0158	<sup>70</sup> 0.0177	<sup>85</sup> 0.0198	<sup>81</sup> 0.0234	<sup>78</sup> 0.0303	<sup>84</sup> 0.0647	<sup>84</sup> 0.1056	<sup>84</sup> 0.1502	<sup>81</sup> 0.1986	<sup>81</sup> 0.2402	<sup>94</sup> 0.2819	<sup>93</sup> 0.3351	<sup>91</sup> 0.3976
54	ISYSTEMS-003	<sup>83</sup> 0.0116	<sup>75</sup> 0.0130	<sup>69</sup> 0.0135	<sup>60</sup> 0.0133	<sup>57</sup> 0.0135	<sup>65</sup> 0.0141	<sup>59</sup> 0.0151	<sup>56</sup> 0.0176	<sup>41</sup> 0.0241	<sup>41</sup> 0.0360	<sup>39</sup> 0.0513	<sup>34</sup> 0.0689	<sup>34</sup> 0.0866	<sup>47</sup> 0.1060	<sup>43</sup> 0.1327	<sup>43</sup> 0.1694
55	KEDACOM-001	<sup>88</sup> 0.0123	<sup>83</sup> 0.0144	<sup>77</sup> 0.0158	<sup>70</sup> 0.0168	<sup>71</sup> 0.0178	<sup>81</sup> 0.0188	<sup>74</sup> 0.0212	<sup>70</sup> 0.0260	<sup>64</sup> 0.0438	<sup>62</sup> 0.0687	<sup>61</sup> 0.0978	<sup>61</sup> 0.1296	<sup>61</sup> 0.1581	<sup>74</sup> 0.1879	<sup>73</sup> 0.2294	<sup>70</sup> 0.2756
56	LOOKMAN-003	<sup>88</sup> 0.0118	<sup>77</sup> 0.0134	<sup>70</sup> 0.0142	<sup>66</sup> 0.0144	<sup>61</sup> 0.0150	<sup>75</sup> 0.0160	<sup>67</sup> 0.0176	<sup>65</sup> 0.0213	<sup>51</sup> 0.0310	<sup>49</sup> 0.0480	<sup>46</sup> 0.0698	<sup>46</sup> 0.0954	<sup>46</sup> 0.1216	<sup>60</sup> 0.1491	<sup>60</sup> 0.1890	<sup>60</sup> 0.2381
57	LOOKMAN-005	<sup>115</sup> 0.4269	<sup>115</sup> 0.5527	<sup>116</sup> 0.6355	<sup>116</sup> 0.7024	<sup>116</sup> 0.7503	<sup>131</sup> 0.7876	<sup>131</sup> 0.8234	<sup>132</sup> 0.8601	<sup>111</sup> 0.8338	<sup>112</sup> 0.9113	<sup>112</sup> 0.9468	<sup>112</sup> 0.9667	<sup>112</sup> 0.9771	<sup>126</sup> 0.9836	<sup>126</sup> 0.9880	<sup>126</sup> 0.9924
58	MICROFOCUS-005	<sup>28</sup> 0.0034	<sup>32</sup> 0.0050	<sup>33</sup> 0.0064	<sup>36</sup> 0.0078	<sup>38</sup> 0.0092	<sup>52</sup> 0.0107	<sup>54</sup> 0.0135	<sup>55</sup> 0.0166	<sup>50</sup> 0.0288	<sup>50</sup> 0.0503	<sup>50</sup> 0.0763	<sup>50</sup> 0.1067	<sup>54</sup> 0.1359	<sup>67</sup> 0.1680	<sup>66</sup> 0.2116	<sup>64</sup> 0.2644
59	MICROSOFT-003	<sup>27</sup> 0.0032	<sup>27</sup> 0.0047	<sup>29</sup> 0.0060	<sup>32</sup> 0.0075	<sup>35</sup> 0.0087	<sup>49</sup> 0.0103	<sup>53</sup> 0.0131	<sup>58</sup> 0.0159	<sup>47</sup> 0.0268	<sup>48</sup> 0.0470	<sup>47</sup> 0.0716	<sup>48</sup> 0.1007	<sup>47</sup> 0.1291	<sup>64</sup> 0.1610	<sup>63</sup> 0.2052	<sup>63</sup> 0.2590
60	MICROSOFT-004	<sup>22</sup> 0.0031	<sup>29</sup> 0.0047	<sup>35</sup> 0.0066	<sup>43</sup> 0.0084	<sup>43</sup> 0.0103	<sup>62</sup> 0.0131	<sup>64</sup> 0.0164	<sup>60</sup> 0.0185	<sup>43</sup> 0.0243	<sup>44</sup> 0.0432	<sup>44</sup> 0.0658	<sup>44</sup> 0.0913	<sup>47</sup> 0.1172	<sup>57</sup> 0.1476	<sup>59</sup> 0.1874	<sup>57</sup> 0.2272
61	MICROSOFT-005	<sup>26</sup> 0.0032	<sup>31</sup> 0.0049	<sup>34</sup> 0.0065	<sup>42</sup> 0.0081	<sup>42</sup> 0.0096	<sup>57</sup> 0.0117	<sup>56</sup> 0.0144	<sup>51</sup> 0.0160	<sup>24</sup> 0.0134	<sup>24</sup> 0.0233	<sup>25</sup> 0.0346	<sup>23</sup> 0.0462	<sup>22</sup> 0.0578	<sup>33</sup> 0.0713	<sup>33</sup> 0.0903	<sup>33</sup> 0.1156
62	MICROSOFT-006	<sup>97</sup> 0.0195	<sup>99</sup> 0.0316	<sup>99</sup> 0.0445	<sup>99</sup> 0.0581	<sup>98</sup> 0.0699	<sup>114</sup> 0.0817	<sup>114</sup> 0.0998	<sup>114</sup> 0.1237	<sup>89</sup> 0.0759	<sup>89</sup> 0.1245	<sup>89</sup> 0.1729	<sup>89</sup> 0.2240	<sup>87</sup> 0.2671	<sup>103</sup> 0.3117	<sup>103</sup> 0.3639	<sup>103</sup> 0.4348
63	NEC-000	<sup>104</sup> 0.0246	<sup>102</sup> 0.0382	<sup>101</sup> 0.0524	<sup>101</sup> 0.0672	<sup>101</sup> 0.0793	<sup>116</sup> 0.0904	<sup>115</sup> 0.1076	<sup>115</sup> 0.1317	<sup>94</sup> 0.1019	<sup>94</sup> 0.1623	<sup>94</sup> 0.2214	<sup>94</sup> 0.2834	<sup>94</sup> 0.3341	<sup>109</sup> 0.3844	<sup>108</sup> 0.4440	<sup>108</sup> 0.5183
64	NEC-001	<sup>104</sup> 0.0246	<sup>102</sup> 0.0382	<sup>101</sup> 0.0524	<sup>101</sup> 0.0672	<sup>101</sup> 0.0793	<sup>116</sup> 0.0904	<sup>115</sup> 0.1076	<sup>115</sup> 0.1317	<sup>94</sup> 0.1019	<sup>94</sup> 0.1623	<sup>94</sup> 0.2214	<sup>94</sup> 0.2834	<sup>94</sup> 0.3341	<sup>109</sup> 0.3844	<sup>108</sup> 0.4440	<sup>108</sup> 0.5183
65	NEC-002	<sup>27</sup> 0.0033	<sup>25</sup> 0.0041	<sup>18</sup> 0.0043	<sup>16</sup> 0.0044	<sup>15</sup> 0.0045	<sup>20</sup> 0.0049	<sup>20</sup> 0.0056	<sup>19</sup> 0.0061	<sup>15</sup> 0.0066	<sup>11</sup> 0.0090	<sup>10</sup> 0.0111	<sup>10</sup> 0.0131	<sup>9</sup> 0.0149	<sup>11</sup> 0.0171	<sup>12</sup> 0.0207	<sup>12</sup> 0.0267
66	NEC-003	<sup>31</sup> 0.0036	<sup>26</sup> 0.0046	<sup>24</sup> 0.0051	<sup>24</sup> 0.0055	<sup>24</sup> 0.0059	<sup>31</sup> 0.0067	<sup>31</sup> 0.0077	<sup>33</sup> 0.0073	<sup>9</sup> 0.0056	<sup>9</sup> 0.0076	<sup>9</sup> 0.0091	<sup>7</sup> 0.0105	<sup>6</sup> 0.0119	<sup>10</sup> 0.0137	<sup>9</sup> 0.0162	<sup>9</sup> 0.0209
67	NEC-004	<sup>37</sup> 0.0039	<sup>25</sup> 0.0045	<sup>22</sup> 0.0047	<sup>18</sup> 0.0046	<sup>14</sup> 0.0044	<sup>19</sup> 0.0046	<sup>18</sup> 0.0052	<sup>17</sup> 0.0036	<sup>7</sup> 0.0046	<sup>5</sup> 0.0057	<sup>4</sup> 0.0063	<sup>4</sup> 0.0069	<sup>2</sup> 0.0076	<sup>2</sup> 0.0090	<sup>2</sup> 0.0105	
68	NEC-005								<sup>8</sup> 0.0037	<sup>4</sup> 0.0041	<sup>4</sup> 0.0020			<sup>3</sup> 0.0080	<sup>3</sup> 0.0091	<sup>3</sup> 0.0107	
69	NEUROTECHNOLOGY-003	<sup>101</sup> 0.0234	<sup>101</sup> 0.0379	<sup>102</sup> 0.0549	<sup>101</sup> 0.0682	<sup>100</sup> 0.0720	<sup>113</sup> 0.0747	<sup>113</sup> 0.0886	<sup>111</sup> 0.1066	<sup>109</sup> 0.6802	<sup>109</sup> 0.8187	<sup>110</sup> 0.8920	<sup>110</sup> 0.9355	<sup>110</sup> 0.9594	<sup>126</sup> 0.9738	<sup>126</sup> 0.9828	<sup>126</sup> 0.9885
70	NEUROTECHNOLOGY-004	<sup>79</sup> 0.0104	<sup>78</sup> 0.0134	<sup>76</sup> 0.0156	<sup>73</sup> 0.0173	<sup>72</sup> 0.0195	<sup>87</sup> 0.0212	<sup>85</sup> 0.0245	<sup>82</sup> 0.0320	<sup>83</sup> 0.0642	<sup>82</sup> 0.1015	<sup>81</sup> 0.1426	<sup>79</sup> 0.1881	<sup>78</sup> 0.2299	<sup>92</sup> 0.2722	<sup>91</sup> 0.3269	<sup>90</sup> 0.3943
71	NEUROTECHNOLOGY-005	<sup>74</sup> 0.0089	<sup>71</sup> 0.0116	<sup>68</sup> 0.0136	<sup>68</sup> 0.0152	<sup>69</sup> 0.0173	<sup>84</sup> 0.0196	<sup>80</sup> 0.0233	<sup>76</sup> 0.0306	<sup>76</sup> 0.0556	<sup>76</sup> 0.0913	<sup>74</sup> 0.1315	<sup>74</sup> 0.1766	<sup>71</sup> 0.2192	<sup>86</sup> 0.2617	<sup>87</sup> 0.3174	<sup>88</sup> 0.3843
72	NEUROTECHNOLOGY-007	<sup>66</sup> 0.0078	<sup>69</sup> 0.0103	<sup>64</sup> 0.0124	<sup>63</sup> 0.0140	<sup>61</sup> 0.0161	<sup>78</sup> 0.0185	<sup>77</sup> 0.0225	<sup>76</sup> 0.0290	<sup>82</sup> 0.0641	<sup>85</sup> 0.1069	<sup>85</sup> 0.1546	<sup>85</sup> 0.2075	<sup>102</sup> 0.3081	<sup>103</sup> 0.3713	<sup>103</sup> 0.4421	
73	NEUROTECHNOLOGY-010								<sup>24</sup> 0.0053	<sup>24</sup> 0.0061	<sup>25</sup> 0.0053			<sup>38</sup> 0.0863	<sup>36</sup> 0.1050	<sup>36</sup> 0.1333	
74	NOBLIS-002	<sup>112</sup> 0.1520	<sup>112</sup> 0.2419	<sup>112</sup> 0.3296	<sup>113</sup> 0.4114	<sup>112</sup> 0.4856	<sup>128</sup> 0.5528	<sup>128</sup> 0.6061	<sup>128</sup> 0.6532	<sup>113</sup> 0.9984	<sup>113</sup> 0.9996	<sup>113</sup> 0.9998	<sup>113</sup> 0.9999	<sup>128</sup> 1.0000	<sup>128</sup> 1.0000	<sup>128</sup> 1.0000	
75	NTechLab-003	<sup>65</sup> 0.0078	<sup>76</sup> 0.0131	<sup>82</sup> 0.0202	<sup>90</sup> 0.0295	<sup>91</sup> 0.0405	<sup>108</sup> 0.0543	<sup>109</sup> 0.0761	<sup>110</sup> 0.1035	<sup>68</sup> 0.0491	<sup>72</sup> 0.0881	<sup>79</sup> 0.1384	<sup>83</sup> 0.1985	<sup>87</sup> 0.2594	<sup>105</sup> 0.3270	<sup>105</sup> 0.4065	<sup>105</sup> 0.4891
76	NTechLab-004	<sup>62</sup> 0.0068	<sup>68</sup> 0.0110	<sup>79</sup> 0.0167	<sup>86</sup> 0.0239	<sup>89</sup> 0.0330	<sup>105</sup> 0.0471	<sup>107</sup> 0.0641	<sup>108</sup> 0.0891	<sup>60</sup> 0.0379	<sup>63</sup> 0.0688	<sup>66</sup> 0.1108	<sup>69</sup> 0.1629	<sup>71</sup> 0.2192	<sup>92</sup> 0.2846	<sup>105</sup> 0.3657	<sup>105</sup> 0.4524
77	NTechLab-006	<sup>51</sup> 0.0056	<sup>62</sup> 0.0095	<sup>72</sup> 0.0148	<sup>83</sup> 0.0218	<sup>85</sup> 0.0301	<sup>103</sup> 0.0413	<sup>104</sup> 0.0591	<sup>107</sup> 0.0814	<sup>56</sup> 0.0349	<sup>60</sup> 0.0636	<sup>63</sup> 0.1023	<sup>64</sup> 0.1506	<sup>66</sup> 0.2024	<sup>87</sup> 0.2617	<sup>94</sup> 0.3374	<sup>98</sup> 0.4185
78	NTechLab-007	<sup>37</sup> 0.0044	<sup>43</sup> 0.0066	<sup>49</sup> 0.0089	<sup>57</sup> 0.0118	<sup>60</sup> 0.0150	<sup>82</sup> 0.0189	<sup>87</sup> 0.0255	<sup>87</sup> 0.0342	<sup>45</sup> 0.0256	<sup>46</sup> 0.0450	<sup>48</sup> 0.0705	<sup>49</sup> 0.1012	<sup>51</sup> 0.1334	<sup>68</sup> 0.1692	<sup>69</sup> 0.2752	

#	ALGORITHM	INVESTIGATION, FNIR(N, R = 1, T = 0)								IDENTIFICATION, FNIR(N, R = L, T ≥ 0) FOR FPIR = 0.001							
		(0, 2]	(2, 4]	(4, 6]	(6, 8]	(8, 10]	(10, 12]	(12, 14]	(14, 18]	(0, 2]	(2, 4]	(4, 6]	(6, 8]	(8, 10]	(10, 12]	(12, 14]	(14, 18]
89	PIXELLALL-002	<sup>72</sup> 0.0085	<sup>78</sup> 0.0119	<sup>71</sup> 0.0147	<sup>72</sup> 0.0172	<sup>73</sup> 0.0198	<sup>89</sup> 0.0225	<sup>88</sup> 0.0270	<sup>89</sup> 0.0349	<sup>97</sup> 0.1193	<sup>97</sup> 0.1900	<sup>97</sup> 0.2601	<sup>97</sup> 0.3322	<sup>97</sup> 0.3955	<sup>112</sup> 0.4565	<sup>112</sup> 0.5268	<sup>111</sup> 0.6030
90	PIXELLALL-003	<sup>46</sup> 0.0050	<sup>42</sup> 0.0063	<sup>39</sup> 0.0072	<sup>34</sup> 0.0077	<sup>33</sup> 0.0085	<sup>47</sup> 0.0095	<sup>48</sup> 0.0113	<sup>46</sup> 0.0119	<sup>44</sup> 0.0248	<sup>43</sup> 0.0418	<sup>43</sup> 0.0622	<sup>43</sup> 0.0861	<sup>43</sup> 0.1104	<sup>53</sup> 0.1364	<sup>53</sup> 0.1723	<sup>53</sup> 0.2167
91	PIXELLALL-004	<sup>45</sup> 0.0049	<sup>40</sup> 0.0063	<sup>40</sup> 0.0072	<sup>37</sup> 0.0079	<sup>36</sup> 0.0089	<sup>51</sup> 0.0103	<sup>51</sup> 0.0127	<sup>51</sup> 0.0146	<sup>38</sup> 0.0211	<sup>40</sup> 0.0360	<sup>42</sup> 0.0553	<sup>42</sup> 0.0792	<sup>39</sup> 0.1045	<sup>36</sup> 0.1317	<sup>52</sup> 0.1700	<sup>56</sup> 0.2246
92	PTAKURATSATU-000	<sup>54</sup> 0.0061	<sup>55</sup> 0.0082	<sup>55</sup> 0.0097	<sup>53</sup> 0.0109	<sup>49</sup> 0.0120	<sup>61</sup> 0.0131	<sup>57</sup> 0.0146	<sup>59</sup> 0.0180	<sup>59</sup> 0.0375	<sup>57</sup> 0.0596	<sup>55</sup> 0.0842	<sup>55</sup> 0.1116	<sup>53</sup> 0.1357	<sup>63</sup> 0.1553	<sup>57</sup> 0.1820	<sup>59</sup> 0.2326
93	RANKONE-002	<sup>99</sup> 0.0212	<sup>98</sup> 0.0313	<sup>98</sup> 0.0431	<sup>98</sup> 0.0562	<sup>99</sup> 0.0712	<sup>111</sup> 0.0881	<sup>116</sup> 0.1130	<sup>117</sup> 0.1543	<sup>95</sup> 0.1111	<sup>95</sup> 0.1707	<sup>95</sup> 0.2305	<sup>95</sup> 0.2968	<sup>96</sup> 0.3646	<sup>111</sup> 0.4345	<sup>111</sup> 0.5172	<sup>111</sup> 0.6110
94	RANKONE-004	<sup>108</sup> 0.0424	<sup>107</sup> 0.0643	<sup>107</sup> 0.0875	<sup>107</sup> 0.1127	<sup>107</sup> 0.1364	<sup>120</sup> 0.1579	<sup>120</sup> 0.1914	<sup>120</sup> 0.2378	<sup>104</sup> 0.1855	<sup>103</sup> 0.2681	<sup>103</sup> 0.3431	<sup>101</sup> 0.4155	<sup>101</sup> 0.4785	<sup>115</sup> 0.5350	<sup>115</sup> 0.5980	<sup>115</sup> 0.6722
95	RANKONE-005	<sup>92</sup> 0.0136	<sup>93</sup> 0.0192	<sup>91</sup> 0.0246	<sup>91</sup> 0.0303	<sup>90</sup> 0.0362	<sup>104</sup> 0.0422	<sup>103</sup> 0.0521	<sup>103</sup> 0.0694	<sup>81</sup> 0.0582	<sup>75</sup> 0.0910	<sup>71</sup> 0.1260	<sup>68</sup> 0.1645	<sup>65</sup> 0.2005	<sup>79</sup> 0.2353	<sup>80</sup> 0.2816	<sup>80</sup> 0.3522
96	RANKONE-007	<sup>67</sup> 0.0078	<sup>69</sup> 0.0099	<sup>61</sup> 0.0113	<sup>58</sup> 0.0123	<sup>58</sup> 0.0139	<sup>74</sup> 0.0156	<sup>73</sup> 0.0191	<sup>72</sup> 0.0242	<sup>42</sup> 0.0242	<sup>42</sup> 0.0376	<sup>41</sup> 0.0542	<sup>38</sup> 0.0737	<sup>37</sup> 0.0935	<sup>49</sup> 0.1130	<sup>47</sup> 0.1416	<sup>47</sup> 0.1811
97	RANKONE-009	<sup>48</sup> 0.0054	<sup>49</sup> 0.0072	<sup>46</sup> 0.0085	<sup>47</sup> 0.0098	<sup>47</sup> 0.0113	<sup>60</sup> 0.0130	<sup>65</sup> 0.0169	<sup>69</sup> 0.0220	<sup>37</sup> 0.0208	<sup>38</sup> 0.0345	<sup>37</sup> 0.0504	<sup>36</sup> 0.0706	<sup>36</sup> 0.0930	<sup>51</sup> 0.1174	<sup>50</sup> 0.2002	<sup>51</sup> 0.3504
98	RANKONE-010	<sup>42</sup> 0.0047	<sup>39</sup> 0.0061	<sup>36</sup> 0.0070	<sup>35</sup> 0.0076	<sup>34</sup> 0.0087	<sup>48</sup> 0.0098	<sup>49</sup> 0.0113	<sup>47</sup> 0.0120	<sup>31</sup> 0.0177	<sup>29</sup> 0.0269	<sup>26</sup> 0.0368	<sup>26</sup> 0.0479	<sup>25</sup> 0.0590	<sup>39</sup> 0.0688	<sup>31</sup> 0.0803	<sup>31</sup> 0.0991
99	RANKONE-011	<sup>23</sup> 0.0031	<sup>23</sup> 0.0041	<sup>23</sup> 0.0047	<sup>23</sup> 0.0053	<sup>22</sup> 0.0058	<sup>34</sup> 0.0067	<sup>30</sup> 0.0077	<sup>32</sup> 0.0073	<sup>23</sup> 0.0127	<sup>20</sup> 0.0194	<sup>21</sup> 0.0265	<sup>20</sup> 0.0345	<sup>21</sup> 0.0422	<sup>29</sup> 0.0499	<sup>28</sup> 0.0611	<sup>26</sup> 0.0756
100	RANKONE-012						<sup>30</sup> 0.0065	<sup>28</sup> 0.0069	<sup>23</sup> 0.0053					<sup>29</sup> 0.0460	<sup>28</sup> 0.0540	<sup>21</sup> 0.0672	
101	REALNETWORKS-002	<sup>107</sup> 0.0381	<sup>108</sup> 0.0687	<sup>108</sup> 0.1062	<sup>108</sup> 0.1495	<sup>109</sup> 0.1963	<sup>124</sup> 0.2513	<sup>126</sup> 0.3206	<sup>126</sup> 0.3927	<sup>105</sup> 0.2153	<sup>108</sup> 0.3323	<sup>108</sup> 0.4444	<sup>105</sup> 0.5485	<sup>106</sup> 0.6355	<sup>121</sup> 0.7132	<sup>122</sup> 0.7855	<sup>123</sup> 0.8437
102	REALNETWORKS-003	<sup>103</sup> 0.0245	<sup>105</sup> 0.0437	<sup>105</sup> 0.0686	<sup>106</sup> 0.0975	<sup>106</sup> 0.1312	<sup>122</sup> 0.1719	<sup>122</sup> 0.2294	<sup>123</sup> 0.2907	<sup>98</sup> 0.1468	<sup>106</sup> 0.2370	<sup>101</sup> 0.3313	<sup>103</sup> 0.4269	<sup>103</sup> 0.5142	<sup>119</sup> 0.5979	<sup>120</sup> 0.6815	<sup>120</sup> 0.7567
103	REALNETWORKS-004	<sup>102</sup> 0.0244	<sup>104</sup> 0.0428	<sup>104</sup> 0.0663	<sup>105</sup> 0.0939	<sup>105</sup> 0.1251	<sup>121</sup> 0.1634	<sup>121</sup> 0.2170	<sup>122</sup> 0.2785	<sup>99</sup> 0.1484	<sup>101</sup> 0.2377	<sup>100</sup> 0.3303	<sup>102</sup> 0.4249	<sup>102</sup> 0.5106	<sup>118</sup> 0.5924	<sup>119</sup> 0.6758	<sup>119</sup> 0.7534
104	REALNETWORKS-006								<sup>37</sup> 0.0069	<sup>32</sup> 0.0077	<sup>36</sup> 0.0080			<sup>44</sup> 0.1022	<sup>46</sup> 0.1253	<sup>40</sup> 0.1622	
105	SCANOVATE-001	<sup>68</sup> 0.0079	<sup>72</sup> 0.0117	<sup>78</sup> 0.0151	<sup>78</sup> 0.0185	<sup>78</sup> 0.0221	<sup>93</sup> 0.0259	<sup>95</sup> 0.0321	<sup>95</sup> 0.0427	<sup>88</sup> 0.0727	<sup>88</sup> 0.1169	<sup>87</sup> 0.1650	<sup>87</sup> 0.2115	<sup>84</sup> 0.2528	<sup>99</sup> 0.2925	<sup>98</sup> 0.3437	<sup>98</sup> 0.4084
106	SENSETIME-002	<sup>95</sup> 0.0186	<sup>92</sup> 0.0191	<sup>84</sup> 0.0183	<sup>73</sup> 0.0179	<sup>68</sup> 0.0173	<sup>63</sup> 0.0133	<sup>39</sup> 0.0089	<sup>26</sup> 0.0059	<sup>40</sup> 0.0220	<sup>25</sup> 0.0236	<sup>19</sup> 0.0237	<sup>18</sup> 0.0240	<sup>12</sup> 0.0245	<sup>18</sup> 0.0219	<sup>11</sup> 0.0195	<sup>10</sup> 0.0222
107	SENSETIME-003	<sup>111</sup> 0.0021	<sup>12</sup> 0.0028	<sup>11</sup> 0.0031	<sup>7</sup> 0.0033	<sup>6</sup> 0.0035	<sup>10</sup> 0.0040	<sup>13</sup> 0.0047	<sup>12</sup> 0.0033	<sup>8</sup> 0.0046	<sup>8</sup> 0.0064	<sup>6</sup> 0.0076	<sup>4</sup> 0.0086	<sup>4</sup> 0.0101	<sup>7</sup> 0.0122	<sup>8</sup> 0.0155	<sup>8</sup> 0.0196
108	SENSETIME-004	<sup>3</sup> 0.0016	<sup>3</sup> 0.0022	<sup>3</sup> 0.0025	<sup>3</sup> 0.0028	<sup>3</sup> 0.0030	<sup>4</sup> 0.0035	<sup>8</sup> 0.0043	<sup>7</sup> 0.0025	<sup>4</sup> 0.0036	<sup>4</sup> 0.0052	<sup>3</sup> 0.0066	<sup>3</sup> 0.0081	<sup>3</sup> 0.0099	<sup>9</sup> 0.0126	<sup>11</sup> 0.0169	<sup>11</sup> 0.0230
109	SENSETIME-005	<sup>2</sup> 0.0015	<sup>2</sup> 0.0020	<sup>2</sup> 0.0024	<sup>2</sup> 0.0026	<sup>2</sup> 0.0029	<sup>3</sup> 0.0035	<sup>3</sup> 0.0043	<sup>10</sup> 0.0028	<sup>5</sup> 0.0036	<sup>5</sup> 0.0059	<sup>8</sup> 0.0089	<sup>8</sup> 0.0128	<sup>10</sup> 0.0177	<sup>12</sup> 0.0240	<sup>12</sup> 0.0345	<sup>12</sup> 0.0493
110	SENSETIME-006	<sup>1</sup> 0.0015	<sup>1</sup> 0.0019	<sup>1</sup> 0.0022	<sup>1</sup> 0.0025	<sup>1</sup> 0.0027	<sup>1</sup> 0.0033	<sup>3</sup> 0.0040	<sup>5</sup> 0.0021	<sup>2</sup> 0.0031	<sup>2</sup> 0.0049	<sup>4</sup> 0.0068	<sup>6</sup> 0.0097	<sup>7</sup> 0.0132	<sup>12</sup> 0.0184	<sup>14</sup> 0.0262	<sup>14</sup> 0.0359
111	SENSETIME-007						<sup>2</sup> 0.0035	<sup>1</sup> 0.0038	<sup>0</sup> 0.0015					<sup>6</sup> 0.0112	<sup>6</sup> 0.0140	<sup>6</sup> 0.0176	
112	SIAT-002	<sup>117</sup> 0.8309	<sup>117</sup> 0.8310	<sup>117</sup> 0.8311	<sup>117</sup> 0.8306	<sup>117</sup> 0.8296	<sup>132</sup> 0.8302	<sup>132</sup> 0.8300	<sup>131</sup> 0.8301	<sup>112</sup> 0.8340	<sup>110</sup> 0.8368	<sup>109</sup> 0.8404	<sup>109</sup> 0.8445	<sup>124</sup> 0.8532	<sup>124</sup> 0.8595	<sup>125</sup> 0.8691	
113	SYNSES-003	<sup>89</sup> 0.0125	<sup>83</sup> 0.0151	<sup>81</sup> 0.0174	<sup>80</sup> 0.0199	<sup>79</sup> 0.0223	<sup>90</sup> 0.0240	<sup>90</sup> 0.0279	<sup>85</sup> 0.0331	<sup>85</sup> 0.0658	<sup>83</sup> 0.1052	<sup>83</sup> 0.1483	<sup>82</sup> 0.1968	<sup>82</sup> 0.2399	<sup>95</sup> 0.2834	<sup>94</sup> 0.3405	<sup>94</sup> 0.4046
114	SYNSES-005	<sup>40</sup> 0.0044	<sup>37</sup> 0.0058	<sup>37</sup> 0.0070	<sup>40</sup> 0.0080	<sup>37</sup> 0.0091	<sup>50</sup> 0.0103	<sup>50</sup> 0.0125	<sup>52</sup> 0.0152	<sup>46</sup> 0.0262	<sup>45</sup> 0.0444	<sup>45</sup> 0.0666	<sup>45</sup> 0.0923	<sup>44</sup> 0.1156	<sup>54</sup> 0.1399	<sup>55</sup> 0.1736	<sup>54</sup> 0.2185
115	TECH-001	<sup>3</sup> 0.0061	<sup>6</sup> 0.0093	<sup>6</sup> 0.0128	<sup>71</sup> 0.0171	<sup>77</sup> 0.0221	<sup>97</sup> 0.0289	<sup>106</sup> 0.0412	<sup>106</sup> 0.0560	<sup>86</sup> 0.0660	<sup>87</sup> 0.1156	<sup>90</sup> 0.1733	<sup>91</sup> 0.2385	<sup>91</sup> 0.2998	<sup>106</sup> 0.3629	<sup>108</sup> 0.4424	<sup>108</sup> 0.5284
116	TOSHIBA-001	<sup>73</sup> 0.0086	<sup>74</sup> 0.0119	<sup>74</sup> 0.0150	<sup>74</sup> 0.0178	<sup>75</sup> 0.0209	<sup>91</sup> 0.0241	<sup>91</sup> 0.0292	<sup>90</sup> 0.0365								
117	TRUEFACE-000	<sup>4</sup> 0.0043	<sup>3</sup> 0.0057	<sup>3</sup> 0.0061	<sup>28</sup> 0.0067	<sup>27</sup> 0.0073	<sup>41</sup> 0.0084	<sup>41</sup> 0.0097	<sup>39</sup> 0.0099	<sup>35</sup> 0.0200	<sup>37</sup> 0.0338	<sup>38</sup> 0.0504	<sup>38</sup> 0.0705	<sup>38</sup> 0.0904	<sup>48</sup> 0.1112	<sup>46</sup> 0.1401	<sup>46</sup> 0.1792
118	VERIDAS-001	<sup>58</sup> 0.0063	<sup>56</sup> 0.0083	<sup>56</sup> 0.0099	<sup>56</sup> 0.0113	<sup>56</sup> 0.0132	<sup>69</sup> 0.0148	<sup>70</sup> 0.0184	<sup>67</sup> 0.0219	<sup>61</sup> 0.0403	<sup>61</sup> 0.0684	<sup>62</sup> 0.1012	<sup>62</sup> 0.1386	<sup>62</sup> 0.1741	<sup>77</sup> 0.2113	<sup>77</sup> 0.2611	<sup>78</sup> 0.3233
119	VISIONLABS-004	<sup>43</sup> 0.0048	<sup>49</sup> 0.0069	<sup>49</sup> 0.0091	<sup>59</sup> 0.0111	<sup>59</sup> 0.0130	<sup>72</sup> 0.0152	<sup>71</sup> 0.0187	<sup>73</sup> 0.0242	<sup>74</sup> 0.0540	<sup>77</sup> 0.0916	<sup>78</sup> 0.1358	<sup>78</sup> 0.1855	<sup>78</sup> 0.2303	<sup>92</sup> 0.2745	<sup>92</sup> 0.3312	<sup>88</sup> 0.3913
120	VISIONLABS-005	<sup>39</sup> 0.0044	<sup>39</sup> 0.0063	<sup>43</sup> 0.0081	<sup>46</sup> 0.0095	<sup>46</sup> 0.0109	<sup>59</sup> 0.0125	<sup>60</sup> 0.0151	<sup>61</sup> 0.0187	<sup>67</sup> 0.0479	<sup>67</sup> 0.0812	<sup>68</sup> 0.1212	<sup>69</sup> 0.1664	<sup>69</sup> 0.2473	<sup>83</sup> 0.2999	<sup>82</sup> 0.3577	
121	VISIONLABS-006	<sup>29</sup> 0.0035	<sup>30</sup> 0.0048	<sup>30</sup> 0.0061	<sup>36</sup> 0.0069	<sup>29</sup> 0.0077	<sup>42</sup> 0.0087	<sup>45</sup> 0.0105	<sup>48</sup> 0.0120	<sup>48</sup> 0.0273	<sup>47</sup> 0.0465	<sup>47</sup> 0.0702	<sup>47</sup> 0.0970	<sup>47</sup> 0.1228	<sup>56</sup> 0.1847	<sup>56</sup> 0.2295	
122	VISIONLABS-008	<sup>21</sup> 0.0028	<sup>20</sup> 0.0037	<sup>21</sup> 0.0047	<sup>22</sup> 0.0053	<sup>23</sup> 0.0058	<sup>32</sup> 0.0067	<sup>36</sup> 0.0081	<sup>37</sup> 0.0085	<sup>27</sup> 0.0143	<sup>27</sup> 0.0241	<sup>28</sup> 0.0373	<sup>27</sup> 0.0519	<sup>28</sup> 0.0677	<sup>30</sup> 0.0850	<sup>30</sup> 0.1104	<sup>30</sup> 0.1444
123	VISIONLABS-009	<sup>10</sup> 0.0020	<sup>11</sup> 0.0026	<sup>10</sup> 0.0030	<sup>10</sup> 0.0034	<sup>16</sup> 0.0044	<sup>17</sup> 0.0052	<sup>19</sup> 0.0064	<sup>14</sup> 0.0065	<sup>15</sup> 0.0105	<sup>15</sup> 0.0156	<sup>15</sup> 0.0217	<sup>16</sup> 0.0289	<sup>23</sup> 0.0368	<sup>22</sup> 0.0499	<sup>22</sup> 0.0681	
124	VISIONLABS-0																

#	ALGORITHM	INVESTIGATION MODE						IDENTIFICATION MODE						FAILURE TO EXTRACT FEATURES						
		RANK ONE MISS RATE, FNIR(N, 0, 1)						HIGH T → FPIR = 0.001, FNIR(N, T, L)												
		N=1.6M						N=1.6M												
GALLERY	MUGSHOT	MUGSHOT	MUGSHOT	VISA	BORDER	BOR <sub>1</sub> 10YR	KIOSK	MUGSHOT	MUGSHOT	MUGSHOT	VISA	BORDER	BOR <sub>1</sub> 10YR	KIOSK	MUGSHOT	MUGSHOT	MUGSHOT	VISA	BORDER	KIOSK
PROBE	MUGSHOT	WEBCAM	PROFILE	BORDER	BOR <sub>1</sub> 10YR	KIOSK		MUGSHOT	WEBCAM	PROFILE	BORDER	BOR <sub>1</sub> 10YR	KIOSK		MUGSHOT	WEBCAM	PROFILE	BORDER	BOR <sub>1</sub> 10YR	KIOSK
1	20FACE-000	<sup>24</sup> 0.055	<sup>23</sup> 0.085	<sup>148</sup> 0.736	<sup>17</sup> 0.056	<sup>99</sup> 0.239	<sup>167</sup> 0.243	<sup>24</sup> 0.348	<sup>240</sup> 0.450	<sup>203</sup> 1.000	<sup>17</sup> 0.424	<sup>9</sup> 0.772	<sup>17</sup> 0.938	0.000	0.000	0.000	0.000	0.000		
2	3DIVI-003	<sup>25</sup> 0.083	<sup>25</sup> 0.206	<sup>185</sup> 0.141	<sup>191</sup> 0.474	<sup>253</sup> 0.400	<sup>253</sup> 0.626	<sup>187</sup> 0.605	<sup>155</sup> 0.821	0.002	0.005									
3	3DIVI-004	<sup>21</sup> 0.018	<sup>22</sup> 0.062	<sup>194</sup> 0.930	<sup>203</sup> 0.821	<sup>172</sup> 0.279	<sup>22</sup> 0.169	<sup>230</sup> 0.343	<sup>166</sup> 0.277	<sup>13</sup> 0.607	0.002	0.005								
4	3DIVI-005	<sup>21</sup> 0.018	<sup>22</sup> 0.062	<sup>194</sup> 0.930	<sup>203</sup> 0.821	<sup>172</sup> 0.279	<sup>22</sup> 0.166	<sup>228</sup> 0.339	<sup>140</sup> 0.996	<sup>192</sup> 0.864	<sup>132</sup> 0.597	0.002	0.005	0.442						
5	3DIVI-006	<sup>22</sup> 0.024	<sup>22</sup> 0.074	<sup>16</sup> 0.047	<sup>180</sup> 0.312	<sup>22</sup> 0.168	<sup>232</sup> 0.342	<sup>16</sup> 0.283	<sup>13</sup> 0.615	0.002	0.005									
6	ACER-000	<sup>194</sup> 0.011	<sup>188</sup> 0.036	<sup>178</sup> 0.827	<sup>15</sup> 0.025	<sup>155</sup> 0.209	<sup>21</sup> 0.146	<sup>207</sup> 0.246	<sup>95</sup> 0.981	<sup>16</sup> 0.201	<sup>120</sup> 0.490	0.000	0.000	0.042						
7	ACER-001	<sup>14</sup> 0.005	<sup>139</sup> 0.020	<sup>94</sup> 0.422	<sup>111</sup> 0.008	<sup>87</sup> 0.050	<sup>65</sup> 0.098	<sup>139</sup> 0.056	<sup>139</sup> 0.109	<sup>175</sup> 0.999	<sup>129</sup> 0.068	<sup>89</sup> 0.406	<sup>11</sup> 0.479	0.001	0.001	0.041	0.000	0.000		
8	AIZE-001	<sup>155</sup> 0.006	<sup>153</sup> 0.022	<sup>138</sup> 0.683	<sup>142</sup> 0.016	<sup>89</sup> 0.050	<sup>139</sup> 0.165	<sup>176</sup> 0.077	<sup>166</sup> 0.143	<sup>120</sup> 0.994	<sup>13</sup> 0.101	<sup>83</sup> 0.364	<sup>101</sup> 0.387	0.001	0.001	0.047				
9	ALCHERA-000	<sup>212</sup> 0.016	<sup>212</sup> 0.047	<sup>182</sup> 0.870	<sup>16</sup> 0.046	<sup>177</sup> 0.292	<sup>211</sup> 0.138	<sup>193</sup> 0.216	<sup>156</sup> 0.999	<sup>156</sup> 0.176	<sup>13</sup> 0.803	0.006	0.014	0.328						
10	ALCHERA-001	<sup>25</sup> 0.987	<sup>29</sup> 1.000	<sup>209</sup> 1.000	<sup>234</sup> 1.000	<sup>289</sup> 0.999	<sup>284</sup> 1.000	<sup>240</sup> 1.000	<sup>193</sup> 1.000	<sup>193</sup> 1.000	<sup>103</sup> 0.006	0.013	0.324							
11	ALCHERA-002	<sup>258</sup> 0.095	<sup>250</sup> 0.166	<sup>207</sup> 0.954	<sup>200</sup> 0.668	<sup>189</sup> 0.446	<sup>260</sup> 0.486	<sup>250</sup> 0.591	<sup>180</sup> 1.000	<sup>19</sup> 0.827	<sup>132</sup> 0.811	0.001	0.002	0.106						
12	ALCHERA-003	<sup>19</sup> 0.010	<sup>186</sup> 0.035	<sup>149</sup> 0.741	<sup>14</sup> 0.016	<sup>153</sup> 0.206	<sup>21</sup> 0.155	<sup>214</sup> 0.239	<sup>115</sup> 0.991	<sup>17</sup> 0.424	<sup>93</sup> 0.708	<sup>129</sup> 0.546	0.001	0.001	0.046	0.000	0.000			
13	ALCHERA-004	<sup>196</sup> 0.011	<sup>191</sup> 0.038	<sup>86</sup> 0.345	<sup>144</sup> 0.017	<sup>95</sup> 0.088	<sup>128</sup> 0.144	<sup>252</sup> 0.394	<sup>246</sup> 0.529	<sup>115</sup> 0.991	<sup>17</sup> 0.424	<sup>93</sup> 0.708	<sup>129</sup> 0.546	0.001	0.001	0.046				
14	ALLGOVISION-000	<sup>19</sup> 0.011	<sup>182</sup> 0.033	<sup>185</sup> 0.894	<sup>14</sup> 0.021	<sup>174</sup> 0.282	<sup>188</sup> 0.088	<sup>182</sup> 0.166	<sup>112</sup> 0.990	<sup>146</sup> 0.117	<sup>12</sup> 0.526	0.002	0.003	0.122						
15	ALLGOVISION-001	<sup>182</sup> 0.009	<sup>197</sup> 0.038	<sup>134</sup> 0.661	<sup>148</sup> 0.021	<sup>165</sup> 0.241	<sup>193</sup> 0.102	<sup>197</sup> 0.221	<sup>102</sup> 0.986	<sup>150</sup> 0.150	<sup>121</sup> 0.491	0.001	0.001	0.042						
16	ANKE-000	<sup>20</sup> 0.013	<sup>192</sup> 0.036	<sup>197</sup> 0.931	<sup>20</sup> 1.000	<sup>253</sup> 1.000	<sup>19</sup> 0.117	<sup>195</sup> 0.220	<sup>121</sup> 0.994	<sup>22</sup> 1.000	<sup>268</sup> 1.000	0.000	0.001	0.080						
17	ANKE-001	<sup>208</sup> 0.018	<sup>193</sup> 0.038	<sup>202</sup> 0.946	<sup>258</sup> 1.000	<sup>218</sup> 1.000	<sup>202</sup> 0.119	<sup>196</sup> 0.220	<sup>126</sup> 0.994	<sup>27</sup> 1.000	<sup>226</sup> 1.000	0.000	0.001	0.080						
18	ANKE-002	<sup>10</sup> 0.003	<sup>115</sup> 0.016	<sup>112</sup> 0.522	<sup>8</sup> 0.005	<sup>103</sup> 0.119	<sup>11</sup> 0.032	<sup>68</sup> 0.948	<sup>80</sup> 0.034	<sup>6</sup> 0.245	0.001	0.001	0.049							
19	AWARE-003	<sup>234</sup> 0.031	<sup>238</sup> 0.090	<sup>219</sup> 0.966	<sup>19</sup> 0.316	<sup>176</sup> 0.290	<sup>206</sup> 0.128	<sup>222</sup> 0.298	<sup>99</sup> 0.984	<sup>178</sup> 0.428	<sup>127</sup> 0.530	0.004	0.003	0.874						
20	AWARE-004	<sup>25</sup> 0.068	<sup>25</sup> 0.176	<sup>227</sup> 0.976	<sup>183</sup> 0.122	<sup>187</sup> 0.414	<sup>25</sup> 0.269	<sup>245</sup> 0.509	<sup>185</sup> 1.000	<sup>173</sup> 0.397	<sup>15</sup> 0.816	0.003	0.003	0.776						
21	AWARE-005	<sup>235</sup> 0.031	<sup>226</sup> 0.067	<sup>228</sup> 0.978	<sup>17</sup> 0.048	<sup>179</sup> 0.308	<sup>24</sup> 0.364	<sup>209</sup> 0.253	<sup>190</sup> 1.000	<sup>165</sup> 0.255	<sup>165</sup> 0.916	0.001	0.002	0.189						
22	AWARE-006	<sup>254</sup> 0.070	<sup>246</sup> 0.128	<sup>230</sup> 0.983	<sup>182</sup> 0.111	<sup>188</sup> 0.421	<sup>238</sup> 0.276	<sup>233</sup> 0.398	<sup>176</sup> 0.999	<sup>17</sup> 0.368	<sup>145</sup> 0.749	0.001	0.002	0.189						
23	AYONIX-000	<sup>27</sup> 0.450	<sup>24</sup> 0.685	<sup>239</sup> 0.996	<sup>19</sup> 0.607	<sup>202</sup> 0.867	<sup>268</sup> 0.811	<sup>268</sup> 0.939	<sup>147</sup> 0.998	<sup>196</sup> 0.954	<sup>178</sup> 0.982	0.010	0.031	0.939						
24	AYONIX-001	<sup>273</sup> 0.341	<sup>267</sup> 0.527	<sup>234</sup> 0.993	<sup>204</sup> 0.994	<sup>200</sup> 0.778	<sup>271</sup> 0.824	<sup>263</sup> 0.920	<sup>174</sup> 0.999	<sup>208</sup> 0.999	<sup>173</sup> 0.969	0.010	0.031	0.939						
25	AYONIX-002	<sup>27</sup> 0.341	<sup>268</sup> 0.527	<sup>235</sup> 0.993	<sup>19</sup> 0.464	<sup>199</sup> 0.778	<sup>27</sup> 0.824	<sup>264</sup> 0.920	<sup>172</sup> 0.999	<sup>197</sup> 0.915	<sup>17</sup> 0.969	0.010	0.031	0.939						
26	CAMVI-003	<sup>247</sup> 0.052	<sup>239</sup> 0.090	<sup>187</sup> 0.911	<sup>178</sup> 0.093	<sup>184</sup> 0.360	<sup>171</sup> 0.071	<sup>158</sup> 0.132	<sup>77</sup> 0.970	<sup>139</sup> 0.114	<sup>104</sup> 0.402	0.006	0.013	0.675						
27	CAMVI-004	<sup>24</sup> 0.047	<sup>233</sup> 0.077	<sup>151</sup> 0.744	<sup>17</sup> 0.072	<sup>178</sup> 0.296	<sup>172</sup> 0.072	<sup>160</sup> 0.136	<sup>169</sup> 0.999	<sup>136</sup> 0.100	<sup>14</sup> 0.787	0.000	0.000	0.000						
28	CAMVI-005	<sup>235</sup> 0.065	<sup>244</sup> 0.103	<sup>153</sup> 0.746	<sup>180</sup> 0.098	<sup>183</sup> 0.341	<sup>192</sup> 0.099	<sup>189</sup> 0.179	<sup>182</sup> 1.000	<sup>151</sup> 0.156	<sup>156</sup> 0.999	0.000	0.000	0.000						
29	CANON-001	<sup>1</sup> 0.001	<sup>26</sup> 0.006	<sup>26</sup> 0.088	<sup>1</sup> 0.001	<sup>13</sup> 0.007	<sup>12</sup> 0.062	<sup>31</sup> 0.005	<sup>23</sup> 0.023	<sup>15</sup> 0.365	<sup>19</sup> 0.008	<sup>23</sup> 0.068	<sup>20</sup> 0.139	0.001	0.000	0.042	0.000	0.000		
30	CIB-000	<sup>42</sup> 0.002	<sup>20</sup> 0.008	<sup>30</sup> 1.000	<sup>26</sup> 0.002	<sup>34</sup> 0.011	<sup>20</sup> 0.069	<sup>35</sup> 0.012	<sup>33</sup> 0.045	<sup>196</sup> 1.000	<sup>49</sup> 0.017	<sup>42</sup> 0.141	<sup>162</sup> 0.894	0.000	0.000	0.000	0.000	0.000		
31	CLEARVIEWAI-000	<sup>1</sup> 0.001	<sup>11</sup> 0.007	<sup>7</sup> 0.062	<sup>12</sup> 0.001	<sup>3</sup> 0.006	<sup>6</sup> 0.056	<sup>30</sup> 0.006	<sup>26</sup> 0.025	<sup>82</sup> 0.974	<sup>20</sup> 0.008	<sup>19</sup> 0.057	<sup>38</sup> 0.268	0.000	0.000	0.037	0.000	0.000		
32	CLOUDWALK-HR-000	<sup>37</sup> 0.001	<sup>37</sup> 0.010	<sup>10</sup> 0.064	<sup>22</sup> 0.002	<sup>12</sup> 0.006	<sup>7</sup> 0.057	<sup>10</sup> 0.002	<sup>10</sup> 0.013	<sup>2</sup> 0.133	<sup>17</sup> 0.005	<sup>7</sup> 0.033	<sup>13</sup> 0.099	0.001	0.000	0.042	0.000	0.000		
33	CLOUDWALK-MT-000	<sup>5</sup> 0.002	<sup>57</sup> 0.011	<sup>3</sup> 0.057	<sup>4</sup> 0.001	<sup>3</sup> 0.004	<sup>2</sup> 0.051	<sup>7</sup> 0.002	<sup>9</sup> 0.013	<sup>1</sup> 0.109	<sup>7</sup> 0.002	<sup>1</sup> 0.018	<sup>1</sup> 0.072	0.001	0.000	0.042	0.000	0.000		
34	COGENT-000	<sup>193</sup> 0.010	<sup>209</sup> 0.046	<sup>217</sup> 0.965						<sup>147</sup> 0.053	<sup>162</sup> 0.140	<sup>133</sup> 0.995								
35	COGENT-001	<sup>19</sup> 0.010	<sup>210</sup> 0.046	<sup>218</sup> 0.965						<sup>146</sup> 0.053	<sup>163</sup> 0.140	<sup>132</sup> 0.995								
36	COGENT-002	<sup>125</sup> 0.004	<sup>141</sup> 0.020	<sup>192</sup> 0.925						<sup>130</sup> 0.044	<sup>129</sup> 0.098	<sup>145</sup> 0.998								
37	COGENT-003	<sup>127</sup> 0.004	<sup>146</sup> 0.021	<sup>201</sup> 0.939						<sup>138</sup> 0.046	<sup>123</sup> 0.095	<sup>146</sup> 0.998								
38	COGENT-004	<sup>76</sup> 0.002	<sup>81</sup> 0.013	<sup>191</sup> 0.922	<sup>73</sup> 0.004	<sup>87</sup> 0.019	<sup>97</sup> 0.113	<sup>118</sup> 0.033	<sup>99</sup> 0.051	<sup>143</sup> 0.997	<sup>60</sup> 0.022	<sup>38</sup> 0.126	<sup>113</sup> 0.456	0.000	0.000	0.000	0.000	0.000		
39	COGENT-005	<sup>51</sup> 0.002	<sup>46</sup> 0.010	<sup>36</sup> 0.126	<sup>27</sup> 0.002	<sup>32</sup> 0.010	<sup>104</sup> 0.120	<sup>40</sup> 0.009	<sup>42</sup> 0.037	<sup>108</sup> 0.989	<sup>39</sup> 0.011	<sup>28</sup> 0.082	<sup>163</sup> 0.905	0.000	0.000	0.000	0.000	0.000		
40	COGNITEC-000	<sup>22</sup> 0.025	<sup>220</sup> 0.059	<sup>215</sup> 0.964						<sup>21</sup> 0.161	<sup>223</sup> 0.303	<sup>116</sup> 0								

#	ALGORITHM	INVESTIGATION MODE						IDENTIFICATION MODE						FAILURE TO EXTRACT FEATURES					
		RANK ONE MISS RATE, FNIR(N, 0, 1)						HIGH T → FPIR = 0.001, FNIR(N, T, L)											
		N=1.6M						N=1.6M											
GALLERY	MUGSHOT	MUGSHOT	MUGSHOT	VISA	BORDER	VISA		MUGSHOT	MUGSHOT	MUGSHOT	VISA	BORDER	VISA	MUGSHOT	MUGSHOT	MUGSHOT	VISA	BORDER	KIOSK
PROBE	MUGSHOT	WEBCAM	PROFILE	BORDER	BOR <sub>i</sub> 10YR	KIOSK		MUGSHOT	WEBCAM	PROFILE	BORDER	BOR <sub>i</sub> 10YR	KIOSK	MUGSHOT	WEBCAM	PROFILE	BORDER	BOR <sub>i</sub> 10YR	KIOSK
47	CUBOX-000	<sup>32</sup> 0.001	<sup>41</sup> 0.010	<sup>4</sup> 0.058	<sup>16</sup> 0.002	<sup>5</sup> 0.004	<sup>1</sup> 0.049	<sup>16</sup> 0.003	<sup>17</sup> 0.019	<sup>4</sup> 0.168	<sup>7</sup> 0.004	<sup>6</sup> 0.028	<sup>2</sup> 0.073	0.001	0.000	0.042	0.000		
48	CYBERLINK-000	<sup>129</sup> 0.004	<sup>138</sup> 0.020	<sup>146</sup> 0.717	<sup>114</sup> 0.007		<sup>120</sup> 0.134	<sup>157</sup> 0.056	<sup>143</sup> 0.116	<sup>133</sup> 0.995	<sup>121</sup> 0.063	<sup>96</sup> 0.339	0.001	0.001	0.063				
49	CYBERLINK-001	<sup>123</sup> 0.004	<sup>126</sup> 0.018	<sup>147</sup> 0.731	<sup>107</sup> 0.007		<sup>119</sup> 0.133	<sup>150</sup> 0.054	<sup>140</sup> 0.109	<sup>130</sup> 0.995	<sup>118</sup> 0.062	<sup>137</sup> 0.652	0.000	0.000	0.040				
50	CYBERLINK-002	<sup>103</sup> 0.003	<sup>69</sup> 0.012	<sup>126</sup> 0.577	<sup>67</sup> 0.004		<sup>85</sup> 0.107	<sup>64</sup> 0.015	<sup>68</sup> 0.053	<sup>107</sup> 0.988	<sup>64</sup> 0.024	<sup>83</sup> 0.288	0.001	0.000	0.042				
51	CYBERLINK-003	<sup>45</sup> 0.002	<sup>27</sup> 0.009	<sup>103</sup> 0.474	<sup>49</sup> 0.003	<sup>35</sup> 0.012	<sup>45</sup> 0.082	<sup>38</sup> 0.008	<sup>39</sup> 0.035	<sup>80</sup> 0.972	<sup>38</sup> 0.012	<sup>23</sup> 1.000	<sup>78</sup> 0.368	0.000	0.000	0.039	0.000		
52	CYBERLINK-004	<sup>58</sup> 0.002	<sup>65</sup> 0.011	<sup>95</sup> 0.423	<sup>46</sup> 0.003	<sup>33</sup> 0.011	<sup>76</sup> 0.104	<sup>25</sup> 0.007	<sup>40</sup> 0.036	<sup>205</sup> 1.000	<sup>39</sup> 0.013	<sup>24</sup> 1.09	<sup>173</sup> 0.954	0.000	0.000	0.011	0.000		
53	CYBERLINK-005	<sup>69</sup> 0.002	<sup>51</sup> 0.011	<sup>54</sup> 0.209	<sup>31</sup> 0.002	<sup>29</sup> 0.010	<sup>66</sup> 0.098	<sup>46</sup> 0.010	<sup>46</sup> 0.041	<sup>186</sup> 1.000	<sup>48</sup> 0.014	<sup>29</sup> 0.089	<sup>169</sup> 0.926	0.000	0.000	0.034			
54	DAHUA-000	<sup>186</sup> 0.009	<sup>171</sup> 0.026					<sup>184</sup> 0.086	<sup>159</sup> 0.135					0.004	0.003				
55	DAHUA-001	<sup>164</sup> 0.007	<sup>163</sup> 0.024	<sup>143</sup> 0.703				<sup>174</sup> 0.073	<sup>151</sup> 0.122	<sup>92</sup> 0.980				0.002	0.002	0.346			
56	DAHUA-002	<sup>64</sup> 0.002	<sup>68</sup> 0.012	<sup>76</sup> 0.304	<sup>42</sup> 0.003		<sup>47</sup> 0.084	<sup>65</sup> 0.015	<sup>35</sup> 0.046	<sup>35</sup> 0.638	<sup>48</sup> 0.017	<sup>41</sup> 0.159	0.001	0.000	0.099				
57	DAHUA-003	<sup>21</sup> 0.001	<sup>12</sup> 0.007	<sup>52</sup> 0.206	<sup>24</sup> 0.002	<sup>27</sup> 0.009	<sup>25</sup> 0.073	<sup>60</sup> 0.014	<sup>48</sup> 0.041	<sup>30</sup> 0.579	<sup>38</sup> 0.013	<sup>27</sup> 0.081	<sup>28</sup> 0.134	0.000	0.000	0.000	0.000	0.000	
58	DAHUA-004	<sup>11</sup> 0.001	<sup>15</sup> 0.008	<sup>40</sup> 0.144	<sup>1</sup> 0.002	<sup>16</sup> 0.007	<sup>18</sup> 0.069	<sup>34</sup> 0.007	<sup>28</sup> 0.026	<sup>24</sup> 0.485	<sup>28</sup> 0.008	<sup>15</sup> 0.051	<sup>22</sup> 0.113	0.000	0.000	0.000	0.000	0.000	
59	DAON-000	<sup>132</sup> 0.004	<sup>120</sup> 0.017	<sup>118</sup> 0.530	<sup>85</sup> 0.005	<sup>59</sup> 0.020	<sup>108</sup> 0.125	<sup>93</sup> 0.023	<sup>81</sup> 0.061	<sup>187</sup> 1.000	<sup>65</sup> 0.025	<sup>59</sup> 0.173	<sup>158</sup> 0.846	0.002	0.002	0.108	0.001		
60	DECATUR-000	<sup>82</sup> 0.002	<sup>67</sup> 0.011	<sup>60</sup> 0.229	<sup>77</sup> 0.004	<sup>56</sup> 0.019	<sup>88</sup> 0.109	<sup>98</sup> 0.023	<sup>87</sup> 0.066	<sup>39</sup> 0.675	<sup>69</sup> 0.027	<sup>38</sup> 0.173	<sup>67</sup> 0.239	0.001	0.000	0.044			
61	DEEPLINT-001	<sup>35</sup> 0.001	<sup>10</sup> 0.007	<sup>50</sup> 0.200	<sup>38</sup> 0.002		<sup>26</sup> 0.073	<sup>20</sup> 0.003	<sup>11</sup> 0.014	<sup>178</sup> 1.000	<sup>15</sup> 0.006	<sup>40</sup> 0.159	0.000	0.000	0.038				
62	DEEPSA-001	<sup>137</sup> 0.004	<sup>110</sup> 0.016	<sup>173</sup> 0.814	<sup>12</sup> 0.010		<sup>126</sup> 0.140	<sup>13</sup> 0.046	<sup>132</sup> 0.101	<sup>100</sup> 0.985	<sup>12</sup> 0.077	<sup>93</sup> 0.326	0.000	0.001	0.047				
63	DERMALOG-003	<sup>262</sup> 0.126	<sup>255</sup> 0.217		<sup>190</sup> 0.296		<sup>194</sup> 0.560	<sup>259</sup> 0.482	<sup>255</sup> 0.655	<sup>190</sup> 0.677	<sup>160</sup> 0.870	0.002	0.002	0.103					
64	DERMALOG-004	<sup>261</sup> 0.125	<sup>254</sup> 0.215	<sup>195</sup> 0.930	<sup>181</sup> 0.135		<sup>190</sup> 0.467	<sup>256</sup> 0.480	<sup>136</sup> 0.657	<sup>186</sup> 0.995	<sup>180</sup> 0.603	<sup>159</sup> 0.856	0.001	0.002	0.107				
65	DERMALOG-005	<sup>211</sup> 0.015	<sup>190</sup> 0.037	<sup>141</sup> 0.701	<sup>189</sup> 0.242		<sup>186</sup> 0.384	<sup>187</sup> 0.088	<sup>173</sup> 0.154	<sup>110</sup> 0.990	<sup>168</sup> 0.300	<sup>135</sup> 0.614	0.001	0.002	0.102				
66	DERMALOG-006	<sup>177</sup> 0.008	<sup>167</sup> 0.024	<sup>132</sup> 0.619	<sup>12</sup> 0.010		<sup>135</sup> 0.155	<sup>145</sup> 0.052	<sup>134</sup> 0.105	<sup>94</sup> 0.981	<sup>118</sup> 0.059	<sup>92</sup> 0.318	0.003	0.006	0.181				
67	DERMALOG-007	<sup>185</sup> 0.009	<sup>172</sup> 0.027	<sup>136</sup> 0.675	<sup>138</sup> 0.014		<sup>141</sup> 0.170	<sup>171</sup> 0.086	<sup>171</sup> 0.152	<sup>111</sup> 0.990	<sup>138</sup> 0.099	<sup>131</sup> 0.557	0.001	0.002	0.102				
68	DERMALOG-008	<sup>111</sup> 0.003	<sup>103</sup> 0.015	<sup>110</sup> 0.516	<sup>104</sup> 0.007	<sup>79</sup> 0.029	<sup>125</sup> 0.139	<sup>135</sup> 0.045	<sup>120</sup> 0.094	<sup>215</sup> 1.000	<sup>113</sup> 0.057	<sup>87</sup> 0.382	<sup>171</sup> 0.940	0.000	0.000	0.002	0.000	0.000	
69	DERMALOG-009	<sup>110</sup> 0.003	<sup>99</sup> 0.014	<sup>46</sup> 0.167	<sup>11</sup> 0.007	<sup>101</sup> 0.999	<sup>79</sup> 0.106	<sup>88</sup> 0.021	<sup>98</sup> 0.066	<sup>198</sup> 1.000	<sup>78</sup> 0.031	<sup>99</sup> 0.999	<sup>157</sup> 0.840	0.001	0.001	0.018	<sup>0.003</sup>		
70	EYEDEA-003	<sup>256</sup> 0.080	<sup>248</sup> 0.148	<sup>213</sup> 0.960	<sup>181</sup> 0.101		<sup>185</sup> 0.379	<sup>249</sup> 0.388	<sup>248</sup> 0.543	<sup>121</sup> 0.994	<sup>184</sup> 0.570	<sup>150</sup> 0.792	0.001	0.003	0.161				
71	F8-001	<sup>204</sup> 0.012		<sup>135</sup> 0.669	<sup>22</sup> 0.100		<sup>273</sup> 1.000		<sup>224</sup> 0.166	<sup>155</sup> 0.998			0.004	1.000	0.158				
72	FINCORE-000	<sup>195</sup> 0.011	<sup>185</sup> 0.034	<sup>159</sup> 0.767	<sup>160</sup> 0.032	<sup>96</sup> 0.117	<sup>150</sup> 0.191	<sup>210</sup> 0.134	<sup>194</sup> 0.217	<sup>191</sup> 1.000	<sup>157</sup> 0.187	<sup>92</sup> 0.598	<sup>114</sup> 0.458	0.000	0.001	0.043	0.000		
73	FUJITSULAB-000	<sup>86</sup> 0.002	<sup>92</sup> 0.014	<sup>98</sup> 0.440	<sup>71</sup> 0.004	<sup>62</sup> 0.023	<sup>67</sup> 0.098	<sup>87</sup> 0.021	<sup>74</sup> 0.056	<sup>65</sup> 0.024	<sup>60</sup> 0.177	<sup>68</sup> 0.240	0.000	0.001	0.016	0.000			
74	FUJITSULAB-001	<sup>68</sup> 0.002	<sup>85</sup> 0.013	<sup>108</sup> 0.455	<sup>74</sup> 0.004	<sup>69</sup> 0.026	<sup>81</sup> 0.106	<sup>77</sup> 0.018	<sup>76</sup> 0.058	<sup>117</sup> 0.992	<sup>63</sup> 0.024	<sup>94</sup> 0.739	<sup>71</sup> 0.247	1.000	1.000	1.000	1.000	1.000	
75	GLORY-000	<sup>266</sup> 0.178	<sup>261</sup> 0.320	<sup>238</sup> 0.994	<sup>188</sup> 0.228		<sup>196</sup> 0.678	<sup>249</sup> 0.547	<sup>129</sup> 0.995	<sup>188</sup> 0.453	<sup>156</sup> 0.839	0.011	0.013	0.985					
76	GLORY-001	<sup>263</sup> 0.127	<sup>258</sup> 0.267	<sup>233</sup> 0.992	<sup>187</sup> 0.178		<sup>195</sup> 0.594	<sup>240</sup> 0.305	<sup>247</sup> 0.537	<sup>118</sup> 0.993	<sup>175</sup> 0.408	<sup>154</sup> 0.819	0.011	0.013	0.988				
77	GORILLA-001	<sup>247</sup> 0.060	<sup>240</sup> 0.095	<sup>195</sup> 0.936	<sup>176</sup> 0.069		<sup>181</sup> 0.329	<sup>259</sup> 0.406	<sup>241</sup> 0.453	<sup>217</sup> 1.000	<sup>181</sup> 0.468	<sup>277</sup> 1.000	0.001	0.001	0.069				
78	GORILLA-002	<sup>223</sup> 0.020	<sup>206</sup> 0.044	<sup>158</sup> 0.753	<sup>154</sup> 0.027		<sup>160</sup> 0.214	<sup>227</sup> 0.188	<sup>216</sup> 0.268	<sup>211</sup> 1.000	<sup>168</sup> 0.250	<sup>190</sup> 1.000	0.001	0.001	0.069				
79	GORILLA-003	<sup>236</sup> 0.036	<sup>228</sup> 0.070	<sup>174</sup> 0.821	<sup>169</sup> 0.048		<sup>169</sup> 0.265	<sup>242</sup> 0.318	<sup>238</sup> 0.434	<sup>280</sup> 1.000	<sup>174</sup> 0.407	<sup>272</sup> 1.000	0.001	0.001	0.069				
80	GORILLA-004	<sup>161</sup> 0.006	<sup>164</sup> 0.024	<sup>146</sup> 0.697	<sup>12</sup> 0.012		<sup>138</sup> 0.162	<sup>190</sup> 0.089	<sup>179</sup> 0.160	<sup>70</sup> 0.959	<sup>145</sup> 0.135	<sup>116</sup> 0.438	0.000	0.001	0.042				
81	GORILLA-005	<sup>117</sup> 0.003	<sup>127</sup> 0.018	<sup>53</sup> 0.209	<sup>97</sup> 0.006		<sup>106</sup> 0.124	<sup>161</sup> 0.058	<sup>165</sup> 0.142	<sup>41</sup> 0.700	<sup>133</sup> 0.088	<sup>96</sup> 0.315	0.000	0.000	0.040				
82	GORILLA-006	<sup>56</sup> 0.002	<sup>71</sup> 0.012	<sup>34</sup> 0.122	<sup>36</sup> 0.003	<sup>52</sup> 0.018	<sup>78</sup> 0.105	<sup>107</sup> 0.027	<sup>114</sup> 0.089	<sup>28</sup> 0.531	<sup>71</sup> 0.028	<sup>25</sup> 0.166	<sup>61</sup> 0.218	0.000	0.001	0.041	0.000	0.000	
83	GORILLA-007	<sup>52</sup> 0.002	<sup>50</sup> 0.011	<sup>32</sup> 0.114	<sup>35</sup> 0.002	<sup>50</sup> 0.016	<sup>52</sup> 0.088	<sup>107</sup> 0.027	<sup>103</sup> 0.077	<sup>29</sup> 0.534	<sup>66</sup> 0.026	<sup>73</sup> 0.264	<sup>49</sup> 0.178	1.000	1.000	1.000	1.000	1.000	
84	GRIAULE-000	<sup>101</sup> 0.002	<sup>86</sup> 0.014	<sup>81</sup> 0.327	<sup>12</sup> 0.011	<sup>82</sup> 0.031	<sup>110</sup> 0.126	<sup>84</sup> 0.020	<sup>84</sup> 0.063	<sup>131</sup> 0.995	<sup>87</sup> 0.033	<sup>64</sup> 0.185	<sup>57</sup> 0.198	0.000	0.002	0.090	0.001	0.001	
85	HIK-003	<sup>201</sup> 0.012	<sup>178</sup> 0.027	<sup>139</sup> 0.689	<sup>130</sup> 0.012		<sup>132</sup> 0.151	<sup>195</sup> 0.103	<sup>175</sup> 0.158	<sup>75</sup> 0.969	<sup>148</sup> 0.142	<sup>112</sup> 0.445	0.000	0.000	0.048	</td			

#	ALGORITHM	INVESTIGATION MODE						IDENTIFICATION MODE						FAILURE TO EXTRACT FEATURES					
		RANK ONE MISS RATE, FNIR(N, 0, 1)						HIGH T → FPIR = 0.001, FNIR(N, T, L)						N=1.6M					
		GALLERY	MUGSHOT	MUGSHOT	MUGSHOT	VISA	BORDER	BOR <sub>L</sub> 10YR	KIOSK	MUGSHOT	MUGSHOT	MUGSHOT	VISA	BORDER	BOR <sub>L</sub> 10YR	KIOSK	MUGSHOT	MUGSHOT	WEBCAM
93	IDEMLA-004	<sup>163</sup> 0.007	<sup>181</sup> 0.032	<sup>203</sup> 0.947	<sup>148</sup> 0.018		<sup>157</sup> 0.210			<sup>126</sup> 0.037	<sup>147</sup> 0.118	<sup>81</sup> 0.973	<sup>141</sup> 0.123		<sup>148</sup> 0.766		0.000	0.000	0.041
94	IDEMLA-005	<sup>178</sup> 0.008	<sup>198</sup> 0.039	<sup>206</sup> 0.954	<sup>151</sup> 0.021		<sup>161</sup> 0.217	<sup>135</sup> 0.044	<sup>170</sup> 0.150	<sup>86</sup> 0.978	<sup>143</sup> 0.130		<sup>161</sup> 0.879		0.000	0.000	0.041		
95	IDEMLA-006	<sup>189</sup> 0.010	<sup>230</sup> 0.072	<sup>221</sup> 0.969	<sup>156</sup> 0.030		<sup>168</sup> 0.253	<sup>129</sup> 0.043	<sup>199</sup> 0.226	<sup>96</sup> 0.982	<sup>149</sup> 0.144		<sup>143</sup> 0.733		0.000	0.000	0.041		
96	IDEMLA-007	<sup>102</sup> 0.003	<sup>160</sup> 0.015	<sup>244</sup> 1.000	<sup>98</sup> 0.006	<sup>83</sup> 0.036	<sup>118</sup> 0.131		<sup>76</sup> 0.018	<sup>71</sup> 0.055	<sup>263</sup> 1.000	<sup>108</sup> 0.052	<sup>62</sup> 0.182	<sup>24</sup> 1.000		0.000	0.000	0.040	
97	IDEMLA-008	<sup>10</sup> 0.001	<sup>6</sup> 0.007	<sup>23</sup> 0.079	<sup>14</sup> 0.001	<sup>17</sup> 0.007	<sup>31</sup> 0.075		<sup>8</sup> 0.002	<sup>8</sup> 0.013	<sup>6</sup> 0.204	<sup>10</sup> 0.005	<sup>11</sup> 0.036	<sup>18</sup> 0.106		0.000	0.000	0.040	
98	IDEMLA-009	<sup>4</sup> 0.001	<sup>5</sup> 0.006	<sup>12</sup> 0.065	<sup>3</sup> 0.001	<sup>8</sup> 0.005	<sup>3</sup> 0.051		<sup>2</sup> 0.002	<sup>2</sup> 0.011	<sup>3</sup> 0.141	<sup>3</sup> 0.003	<sup>5</sup> 0.027	<sup>4</sup> 0.074	1.000	1.000	1.000	1.000	
99	IMAGUS-002	<sup>269</sup> 0.220	<sup>259</sup> 0.301	<sup>232</sup> 0.988						<sup>26</sup> 0.749	<sup>26</sup> 0.816	<sup>207</sup> 1.000					0.004	0.008	0.550
100	IMAGUS-003	<sup>274</sup> 0.356	<sup>265</sup> 0.513	<sup>236</sup> 0.993						<sup>268</sup> 0.807	<sup>262</sup> 0.909	<sup>200</sup> 1.000					0.004	0.008	0.550
101	IMAGUS-005	<sup>75</sup> 0.002	<sup>70</sup> 0.012	<sup>78</sup> 0.319	<sup>96</sup> 0.006	<sup>69</sup> 0.022	<sup>118</sup> 0.132		<sup>80</sup> 0.018	<sup>88</sup> 0.066	<sup>35</sup> 0.838	<sup>72</sup> 0.029	<sup>54</sup> 0.161	<sup>64</sup> 0.231		0.000	0.000	0.000	
102	IMAGUS-006	<sup>78</sup> 0.002	<sup>89</sup> 0.014	<sup>74</sup> 0.293	<sup>79</sup> 0.004	<sup>58</sup> 0.019	<sup>95</sup> 0.112		<sup>82</sup> 0.019	<sup>91</sup> 0.069	<sup>63</sup> 0.897	<sup>71</sup> 0.028	<sup>53</sup> 0.161	<sup>74</sup> 0.260		0.000	0.000	0.000	
103	IMAGUS-007	<sup>77</sup> 0.002	<sup>82</sup> 0.013	<sup>79</sup> 0.321	<sup>68</sup> 0.004	<sup>61</sup> 0.022	<sup>101</sup> 0.117		<sup>95</sup> 0.023	<sup>97</sup> 0.073	<sup>61</sup> 0.893	<sup>79</sup> 0.031	<sup>56</sup> 0.169	<sup>70</sup> 0.265		0.000	0.000	0.000	
104	IMPERIAL-000	<sup>99</sup> 0.002	<sup>104</sup> 0.015	<sup>71</sup> 0.280	<sup>81</sup> 0.004		<sup>63</sup> 0.097		<sup>101</sup> 0.026	<sup>90</sup> 0.068	<sup>159</sup> 0.999	<sup>92</sup> 0.042		<sup>70</sup> 0.245		0.000	0.000	0.000	
105	INCODE-000	<sup>249</sup> 0.049	<sup>242</sup> 0.100	<sup>205</sup> 0.951						<sup>241</sup> 0.310	<sup>239</sup> 0.420	<sup>182</sup> 0.998					0.001	0.004	0.173
106	INCODE-001	<sup>214</sup> 0.017	<sup>211</sup> 0.046	<sup>156</sup> 0.762						<sup>230</sup> 0.212	<sup>219</sup> 0.296	<sup>218</sup> 1.000					0.001	0.004	0.173
107	INCODE-002	<sup>219</sup> 0.018	<sup>213</sup> 0.048	<sup>177</sup> 0.843						<sup>228</sup> 0.184	<sup>217</sup> 0.269	<sup>119</sup> 0.993					0.000	0.001	0.066
108	INCODE-003	<sup>209</sup> 0.013	<sup>200</sup> 0.040	<sup>157</sup> 0.764						<sup>222</sup> 0.167	<sup>213</sup> 0.264	<sup>173</sup> 0.999					0.000	0.001	0.066
109	INCODE-004	<sup>124</sup> 0.004	<sup>124</sup> 0.017	<sup>104</sup> 0.475	<sup>120</sup> 0.008		<sup>122</sup> 0.135		<sup>153</sup> 0.054	<sup>150</sup> 0.120	<sup>128</sup> 0.995	<sup>120</sup> 0.063		<sup>88</sup> 0.313		0.000	0.001	0.066	
110	INCODE-005	<sup>49</sup> 0.002	<sup>63</sup> 0.011	<sup>42</sup> 0.147	<sup>37</sup> 0.002	<sup>40</sup> 0.013	<sup>40</sup> 0.079		<sup>50</sup> 0.011	<sup>51</sup> 0.043	<sup>26</sup> 0.528	<sup>47</sup> 0.017	<sup>45</sup> 0.145	<sup>38</sup> 0.155		0.000	0.000	0.042	
111	INNOVATRICS-002	<sup>244</sup> 0.045	<sup>231</sup> 0.074	<sup>180</sup> 0.853						<sup>238</sup> 0.234	<sup>224</sup> 0.310	<sup>201</sup> 1.000					0.000	0.001	0.046
112	INNOVATRICS-003	<sup>239</sup> 0.026	<sup>216</sup> 0.055	<sup>179</sup> 0.845						<sup>231</sup> 0.221	<sup>229</sup> 0.297	<sup>184</sup> 1.000					0.000	0.001	0.046
113	INNOVATRICS-004	<sup>205</sup> 0.012	<sup>202</sup> 0.040	<sup>210</sup> 0.958						<sup>208</sup> 0.132	<sup>198</sup> 0.222	<sup>91</sup> 0.980					0.000	0.001	0.046
114	INNOVATRICS-005	<sup>108</sup> 0.002	<sup>98</sup> 0.014	<sup>93</sup> 0.407	<sup>83</sup> 0.005		<sup>87</sup> 0.109		<sup>115</sup> 0.034	<sup>118</sup> 0.089	<sup>56</sup> 0.846	<sup>104</sup> 0.047		<sup>72</sup> 0.251		0.000	0.001	0.041	
115	INNOVATRICS-007	<sup>51</sup> 0.002	<sup>62</sup> 0.011	<sup>65</sup> 0.248	<sup>39</sup> 0.002	<sup>42</sup> 0.013	<sup>33</sup> 0.077		<sup>56</sup> 0.013	<sup>61</sup> 0.051	<sup>43</sup> 0.743	<sup>46</sup> 0.017	<sup>31</sup> 0.093	<sup>36</sup> 0.154		0.000	0.001	0.041	
116	INTELLIVISION-001	<sup>239</sup> 0.036	<sup>245</sup> 0.102	<sup>223</sup> 0.972	<sup>173</sup> 0.057	<sup>96</sup> 0.222	<sup>182</sup> 0.333		<sup>238</sup> 0.279	<sup>234</sup> 0.404	<sup>189</sup> 1.000	<sup>169</sup> 0.328	<sup>95</sup> 0.749	<sup>14</sup> 0.685		1.000	1.000	1.000	
117	INTSYSMSU-000	<sup>264</sup> 0.146	<sup>162</sup> 0.023	<sup>125</sup> 0.562	<sup>177</sup> 0.072		<sup>117</sup> 0.132		<sup>278</sup> 0.998	<sup>273</sup> 1.000	<sup>183</sup> 1.000	<sup>199</sup> 0.999		<sup>187</sup> 0.999		0.000	0.000	0.050	
118	IREX-000	<sup>136</sup> 0.004	<sup>31</sup> 0.010	<sup>137</sup> 0.681	<sup>36</sup> 0.002	<sup>36</sup> 0.012	<sup>43</sup> 0.082		<sup>112</sup> 0.028	<sup>89</sup> 0.060	<sup>69</sup> 0.957	<sup>100</sup> 0.044	<sup>78</sup> 0.302	<sup>46</sup> 0.170		0.000	0.000	0.042	
119	ISYSTEMS-002	<sup>162</sup> 0.006	<sup>170</sup> 0.026	<sup>178</sup> 0.844					<sup>178</sup> 0.078	<sup>154</sup> 0.126	<sup>144</sup> 0.998					0.002	0.002	0.142	
120	ISYSTEMS-003	<sup>159</sup> 0.005	<sup>170</sup> 0.023	<sup>162</sup> 0.791					<sup>162</sup> 0.059	<sup>158</sup> 0.107	<sup>188</sup> 1.000					0.002	0.002	0.142	
121	KAKAO-000	<sup>36</sup> 0.001	<sup>49</sup> 0.011	<sup>33</sup> 0.119	<sup>40</sup> 0.002	<sup>39</sup> 0.013	<sup>36</sup> 0.078		<sup>67</sup> 0.015	<sup>73</sup> 0.056	<sup>21</sup> 0.468	<sup>51</sup> 0.019	<sup>41</sup> 0.141	<sup>39</sup> 0.158		0.000	0.000	0.041	
122	KEDACOM-001	<sup>174</sup> 0.008	<sup>187</sup> 0.036	<sup>224</sup> 0.972	<sup>162</sup> 0.034		<sup>165</sup> 0.237		<sup>94</sup> 0.023	<sup>96</sup> 0.072	<sup>103</sup> 0.986	<sup>112</sup> 0.055		<sup>80</sup> 0.305		0.000	0.000	0.000	
123	KNERON-000	<sup>157</sup> 0.006	<sup>174</sup> 0.027	<sup>123</sup> 0.552	<sup>159</sup> 0.028		<sup>151</sup> 0.195									0.000	0.000	0.000	
124	KNERON-001	<sup>239</sup> 0.030	<sup>273</sup> 0.621	<sup>63</sup> 0.237	<sup>186</sup> 0.144	<sup>97</sup> 0.207	<sup>172</sup> 0.280									0.000	0.000	0.000	
125	LINE-000	<sup>87</sup> 0.002	<sup>90</sup> 0.014	<sup>59</sup> 0.223	<sup>89</sup> 0.005	<sup>77</sup> 0.029	<sup>83</sup> 0.107		<sup>118</sup> 0.031	<sup>124</sup> 0.095	<sup>102</sup> 0.046	<sup>78</sup> 0.278	<sup>244</sup> 1.000		0.000	0.000	0.000		
126	LINE-001	<sup>15</sup> 0.001	<sup>14</sup> 0.007	<sup>9</sup> 0.063	<sup>21</sup> 0.002	<sup>24</sup> 0.008	<sup>31</sup> 0.085		<sup>26</sup> 0.005	<sup>28</sup> 0.027	<sup>216</sup> 1.000	<sup>30</sup> 0.009	<sup>21</sup> 0.072	<sup>280</sup> 1.000		0.000	0.000	0.000	
127	LOOKMAN-003	<sup>181</sup> 0.009	<sup>196</sup> 0.038	<sup>168</sup> 0.035			<sup>164</sup> 0.239		<sup>131</sup> 0.044	<sup>142</sup> 0.112	<sup>132</sup> 0.084		<sup>97</sup> 0.355		0.000	0.000	0.000		
128	LOOKMAN-004	<sup>183</sup> 0.009	<sup>199</sup> 0.039	<sup>226</sup> 0.973					<sup>134</sup> 0.045	<sup>136</sup> 0.105	<sup>84</sup> 0.977		0.000	0.000	0.000				
129	LOOKMAN-005	<sup>177</sup> 0.008	<sup>189</sup> 0.036	<sup>225</sup> 0.972	<sup>164</sup> 0.035		<sup>163</sup> 0.237		<sup>118</sup> 0.030	<sup>119</sup> 0.086	<sup>87</sup> 0.978	<sup>119</sup> 0.062		<sup>87</sup> 0.308		0.000	0.000	0.000	
130	MANTRA-000	<sup>55</sup> 0.002	<sup>42</sup> 0.010	<sup>144</sup> 0.709	<sup>108</sup> 0.007	<sup>67</sup> 0.024	<sup>93</sup> 0.112		<sup>47</sup> 0.010	<sup>47</sup> 0.041	<sup>283</sup> 1.000	<sup>75</sup> 0.029	<sup>49</sup> 0.152	<sup>189</sup> 1.000		0.002	0.001	0.591	
131	MEGVII-001	<sup>209</sup> 0.012	<sup>125</sup> 0.017		<sup>270</sup> 1.000				<sup>173</sup> 0.072	<sup>128</sup> 0.097						0.002	0.000		
132	MEGVII-002	<sup>203</sup> 0.012	<sup>125</sup> 0.017	<sup>99</sup> 0.450	<sup>222</sup> 1.000				<sup>177</sup> 0.077	<sup>126</sup> 0.096	<sup>154</sup> 0.998					0.002	0.000	0.033	
133	MICROFOCUS-003	<sup>28</sup> 0.594	<sup>27</sup> 0.781		<sup>20</sup> 0.708				<sup>204</sup> 0.907	<sup>27</sup> 0.931	<sup>198</sup> 0.982		<sup>182</sup> 0.991		0.001	0.005			
134	MICROFOCUS-004	<sup>279</sup> 0.576	<sup>276</sup> 0.758		<sup>20</sup> 0.701				<sup>203</sup> 0.904	<sup>239</sup> 0.999	<sup>207</sup> 0.975		<sup>180</sup> 0.989		0.001	0.005			
135	MICROFOCUS-005	<sup>27</sup> 0.424	<sup>271</sup> 0.601	<sup>197</sup> 0.494			<sup>198</sup> 0.777		<sup>27</sup> 0.835	<sup>26</sup> 0.928	<sup>195</sup> 0.935		<sup>177</sup> 0.985		0.001	0.005			
136	MICROFOCUS-006	<sup>276</sup> 0.427	<sup>270</sup> 0.583	<sup>196</sup> 0.490			<sup>201</sup> 0.782		<sup>276</sup> 0.978	<sup>265</sup> 0.923	<sup>194</sup> 0.923		<sup>176</sup> 0.971		0.001	0.005			
137	MICROSOFT-003	<sup>4</sup> 0.002	<sup>74</sup> 0.012	</															

#	ALGORITHM	INVESTIGATION MODE								IDENTIFICATION MODE								FAILURE TO EXTRACT FEATURES																							
		RANK ONE MISS RATE, FNIR(N, 0, 1)								HIGH T → FPIR = 0.01, FNIR(N, T, L)								N=1.6M																							
		GALLERY		MUGSHOT	MUGSHOT	MUGSHOT	VISA	BORDER	VISA	MUGSHOT	MUGSHOT	MUGSHOT	VISA	BORDER	VISA	MUGSHOT	MUGSHOT	MUGSHOT	VISA	BORDER	KIOSK	MUGSHOT	MUGSHOT	WEBCAM	PROFILE	BORDER	BOR <sub>L</sub> 10YR	KIOSK													
139	MICROSOFT-005	69	0.002	55	0.011	41	0.144	53	0.003	68	0.099	99	0.026	93	0.070	31	0.587	87	0.027	52	0.180	0.000	0.001	0.049																	
140	MICROSOFT-006	75	0.002	66	0.011	41	0.150	63	0.004	70	0.100	81	0.012	41	0.037	16	0.386	88	0.032	48	0.178	0.000	0.001	0.049																	
141	NEC-000	215	0.017	204	0.041	212	0.959	152	0.025	166	0.243	188	0.079	164	0.140	89	0.979	118	0.474	0.001	0.002	0.890																			
142	NEC-001	224	0.021	217	0.056	220	0.967	161	0.033	170	0.277	197	0.106	191	0.197	104	0.986	144	0.133	117	0.468	0.005	0.003	0.934																	
143	NEC-002	9	0.001	25	0.009	89	0.363	58	0.003	100	0.117	14	0.003	20	0.020	170	0.999	22	0.008	139	0.676	0.000	0.001	0.041																	
144	NEC-003	27	0.001	39	0.010	83	0.352	62	0.004	38	0.013	105	0.120	12	0.002	16	0.017	52	0.824	28	0.008	12	0.036	138	0.668	0.000	0.001	0.041	0.001												
145	NEC-004	33	0.001	24	0.009	117	0.538	51	0.003	20	0.007	30	0.075	6	0.002	7	0.013	34	0.622	8	0.004	3	0.019	14	0.100	0.000	0.001	0.041	0.001												
146	NEC-005	19	0.001	16	0.008	21	0.081	19	0.002	7	0.005	27	0.073	3	0.002	3	0.012	38	0.673	7	0.003	2	0.019	11	0.099	0.000	0.001	0.040	0.001												
147	NEUROTECHNOLOGY-003	225	0.022	205	0.042	210	0.961					265	0.636	215	0.266	284	1.000							0.000	0.001	0.131															
148	NEUROTECHNOLOGY-004	152	0.006	137	0.020	222	0.970					167	0.063	144	0.117	124	0.994							0.000	0.001	0.131															
149	NEUROTECHNOLOGY-005	136	0.004	166	0.024	181	0.893					154	0.054	156	0.130	148	0.998							0.000	0.000	0.030															
150	NEUROTECHNOLOGY-006	219	0.018	208	0.045	130	0.606					236	0.249	235	0.418								0.000	0.000																	
151	NEUROTECHNOLOGY-007	128	0.004	145	0.021	167	0.796	12	0.009			147	0.180	166	0.062	185	0.173	194	1.000	170	0.339	219	1.000	0.001	0.001	0.041															
152	NEUROTECHNOLOGY-008	84	0.002	97	0.014	101	0.457	70	0.004	64	0.023	72	0.101	148	0.053	106	0.080	214	1.000	89	0.035	78	0.293	38	0.203	0.000	0.001	0.052	0.001												
153	NEUROTECHNOLOGY-009	34	0.001	53	0.011	47	0.179	30	0.002	41	0.013	39	0.079	65	0.015	65	0.052	32	0.588	30	0.020	50	0.153	43	0.165	0.001	0.000	0.046	0.000												
154	NEUROTECHNOLOGY-010	22	0.001	30	0.009	16	0.070	9	0.001	19	0.007	17	0.068	45	0.010	43	0.037	12	0.277	33	0.010	26	0.075	25	0.126	0.000	0.000	0.041	0.000												
155	NEWLAND-002	235	0.079	245	0.117	198	0.936					256	0.438	242	0.466	163	0.999							0.007	0.012	0.200															
156	NOBLIS-001	271	0.249	266	0.522	237	0.993					281	1.000	283	1.000	206	1.000							0.000	0.000	0.000															
157	NOBLIS-002	267	0.179	263	0.392	229	0.982					277	0.997	274	1.000	219	1.000							0.000	0.000	0.000															
158	NOTIONTAG-000	98	0.002	75	0.012	51	0.204	72	0.004	48	0.016	60	0.095	71	0.017	79	0.059	33	0.611	59	0.021	48	0.150	47	0.176	0.000	0.000	0.000	0.000												
159	NTECHLAB-003	158	0.006	156	0.023	105	0.504					152	0.054	145	0.118	54	0.837							0.000	0.000	0.040															
160	NTECHLAB-004	145	0.005	132	0.019	107	0.506	116	0.008			113	0.129	127	0.041	135	0.105	53	0.833	111	0.053	76	0.263	0.000	0.000	0.040															
161	NTECHLAB-005	143	0.005	128	0.018	90	0.367	118	0.008			102	0.118	128	0.042	133	0.102	46	0.771	126	0.073	84	0.294	0.000	0.000	0.040															
162	NTECHLAB-006	133	0.004	119	0.017	87	0.347	115	0.007			98	0.113	122	0.037	121	0.094	45	0.754	111	0.057	75	0.260	0.000	0.000	0.040															
163	NTECHLAB-007	104	0.003	76	0.012	80	0.326	80	0.004			82	0.107	98	0.026	89	0.067	44	0.750	83	0.032	63	0.223	0.000	0.000	0.042															
164	NTECHLAB-008	54	0.002	32	0.010	41	0.157	30	0.003			48	0.084	61	0.014	54	0.045	21	0.529	87	0.033	33	0.183	0.000	0.000	0.044															
165	NTECHLAB-009	24	0.001	18	0.008	30	0.138	28	0.002	43	0.013	29	0.074	28	0.005	22	0.022	18	0.430	41	0.015	35	0.109	31	0.142	0.000	0.000	0.041	0.001												
166	NTECHLAB-010	14	0.001	21	0.008	25	0.085	20	0.002	23	0.008	8	0.057	13	0.003	14	0.015	11	0.252	16	0.007	20	0.059	10	0.098	0.001	0.001	0.043	0.000												
167	NTECHLAB-011	8	0.001	8	0.007	19	0.072	11	0.001	22	0.007	4	0.051	17	0.003	13	0.015	9	0.228	25	0.074	7	0.091	0.000	0.000	0.040	0.000														
168	PANGAM-000	20	0.001	17	0.008	21	0.074	23	0.002	21	0.007	15	0.065	33	0.006	35	0.030	14	0.318	32	0.009	40	0.136	17	0.105	1.000	1.000	1.000	1.000	1.000	1.000	1.000	1.000	1.000	1.000						
169	PARAVISION-000	220	0.019	195	0.038	110	0.534	194	0.423			193	0.529	189	0.089	183	0.170	168	0.999	187	0.470			168	0.926	0.000	0.000	0.000													
170	PARAVISION-001	126	0.004	142	0.020	87	0.329	193	0.414			192	0.484	141	0.049	135	0.128	158	0.999	179	0.444			144	0.739	0.000	0.000	0.000													
171	PARAVISION-002	131	0.004	149	0.022	84	0.335	144	0.015			143	0.175	142	0.050	148	0.119	97	0.983	128	0.080			122	0.497	0.000	0.000	0.032													
172	PARAVISION-003	116	0.003	134	0.019	60	0.252	141	0.015			140	0.167	120	0.035	125	0.096	125	0.994	115	0.058			125	0.296	0.000	0.000	0.032													
173	PARAVISION-004	47	0.002	45	0.010	31	0.104	94	0.006			94	0.112	49	0.010	44	0.038	204	1.000	49	0.018			164	0.908	0.000	0.000	0.032													
174	PARAVISION-005	40	0.002	35	0.010	22	0.079	108	0.007			80	0.106	23	0.004	24	0.024	90	0.980	34	0.011			26	0.132	0.000	0.000	0.038													
175	PARAVISION-007	17	0.001	19	0.008	17	0.066	90	0.005	30	0.010	71	0.101	2	0.004	25	0.025	21	1.000	29	0.009	36	0.113	247	1.000	0.000	0.000	0.00													

#	ALGORITHM	INVESTIGATION MODE										IDENTIFICATION MODE										FAILURE TO EXTRACT FEATURES									
		RANK ONE MISS RATE, FNIR(N, 0, 1)					N=1.6M					HIGH T → FPIR = 0.001, FNIR(N, T, L)					N=1.6M														
		GALLERY	MUGSHOT	MUGSHOT	MUGSHOT	VISA	BORDER	BOR <sub>i</sub> 10YR	KIOSK	VISA	MUGSHOT	MUGSHOT	MUGSHOT	VISA	BORDER	BOR <sub>i</sub> 10YR	KIOSK	MUGSHOT	MUGSHOT	MUGSHOT	VISA	BORDER	KIOSK	MUGSHOT	MUGSHOT	MUGSHOT	VISA	BORDER	KIOSK		
185	QUANTASOFT-001	268	0.218	275	0.727					260	0.639										0.000	0.000									
186	RANKONE-002	222	0.019	229	0.071					201	0.118	211	0.261								0.000	0.000									
187	RANKONE-003	221	0.019	227	0.068					200	0.118	210	0.255								0.000	0.000									
188	RANKONE-004	243	0.041	247	0.141					228	0.193	237	0.426								0.000	0.000									
189	RANKONE-005	187	0.009	203	0.041	231	0.986			163	0.059	186	0.173	149	0.998						0.000	0.000	0.489								
190	RANKONE-006	148	0.005	167	0.797					125	0.037	122	0.095	73	0.967						0.002	0.002	0.167								
191	RANKONE-007	120	0.003	131	0.019	167	0.796			92	0.022	122	0.095	73	0.967						0.001	0.001	0.102								
192	RANKONE-009	94	0.002	78	0.013	128	0.549	93	0.006	121	0.134	218	0.018	100	0.076	76	0.969	117	0.062	94	0.328	0.000	0.000	0.000							
193	RANKONE-010	88	0.002	36	0.010	91	0.374	86	0.005	70	0.027	111	0.126	59	0.014	77	0.058	50	0.802	109	0.052	69	0.208	73	0.259	0.000	0.000	0.000			
194	RANKONE-011	39	0.002	64	0.011	58	0.223	61	0.004	55	0.019	46	0.082	39	0.009	56	0.048	9	0.037	61	0.182	177	0.977	0.000	0.000	0.000					
195	RANKONE-012	28	0.001	48	0.010	37	0.127	52	0.003	45	0.014	19	0.069	36	0.008	69	0.053	74	0.029	44	0.144	116	0.465	0.000	0.000	0.000					
196	REALNETWORKS-000	241	0.040	226	0.078					23	0.234	227	0.319								0.001	0.000									
197	REALNETWORKS-001	242	0.040	235	0.078					235	0.234	226	0.319								0.001	0.000									
198	REALNETWORKS-002	238	0.039	234	0.078					232	0.231	225	0.315								0.001	0.000									
199	REALNETWORKS-003	228	0.024	223	0.062	168	0.771	159	0.031	154	0.209	218	0.159	214	0.266	153	0.998	153	0.164	123	0.500	0.001	0.000	0.009							
200	REALNETWORKS-004	226	0.024	221	0.059	166	0.797	158	0.031	159	0.213	217	0.158	212	0.263	166	0.999	154	0.170	134	0.613	0.001	0.000	0.009							
201	REALNETWORKS-005	90	0.002	83	0.013	97	0.433	78	0.004	63	0.023	74	0.102	109	0.028	98	0.074	78	0.971	91	0.037	70	0.223	60	0.215	0.000	0.000	0.006	0.000		
202	REALNETWORKS-006	30	0.001	38	0.010	23	0.287	42	0.002	31	0.010	37	0.078	62	0.015	67	0.053	93	0.980	42	0.016	37	0.120	37	0.154	0.000	0.000	0.000			
203	REALNETWORKS-007	25	0.001	29	0.009	69	0.267	18	0.002	25	0.009	24	0.072	43	0.010	52	0.043	88	0.979	30	0.012	90	0.463	30	0.140	1.000	1.000	1.000			
204	REMARKAI-000	180	0.009	180	0.030					205	0.128	192	0.203								0.000	0.001									
205	REMARKAI-000	122	0.003	129	0.018	133	0.660	115	0.008	130	0.148	159	0.055	149	0.120	164	0.999	125	0.069	142	0.717	0.000	0.000	0.000							
206	REMARKAI-002	178	0.008	179	0.029	168	0.802			204	0.124	190	0.196	114	0.991						0.000	0.001	0.017								
207	RENDIP-000	43	0.002	102	0.015	96	0.424	99	0.006	73	0.028	49	0.084	52	0.012	78	0.059	62	0.894	58	0.022	63	0.185	44	0.167	0.000	0.000	0.041			
208	REVEALMEDIA-000	67	0.002	33	0.010	70	0.275	29	0.002	37	0.012	28	0.074	34	0.012	50	0.042	40	0.680	56	0.021	32	0.093	32	0.143	0.000	0.000	0.041			
209	S1-000	36	0.002	117	0.017	67	0.258	92	0.005	68	0.025	54	0.090	111	0.028	109	0.085	221	1.000	10	0.047	202	1.000	235	1.000	0.000	0.000	0.040			
210	S1-001	115	0.003	93	0.014	59	0.215	47	0.003	53	0.018	32	0.077	69	0.016	64	0.052	101	0.985	50	0.019	39	0.136	33	0.148	0.001	0.000	0.035			
211	SCANOVATE-000	147	0.005	207	0.045	124	0.560	163	0.035	158	0.211	170	0.067	206	0.240	60	0.893	162	0.215	103	0.400	0.000	0.001	0.057							
212	SCANOVATE-001	151	0.005	201	0.040	128	0.585	157	0.031	146	0.178	181	0.081	200	0.227	64	0.911	159	0.192	106	0.404	0.000	0.001	0.044							
213	SENSETIME-000	92	0.002	109	0.016	114	0.528			88	0.021	83	0.063	246	1.000						0.004	0.000	0.042								
214	SENSETIME-001	93	0.002	108	0.016					91	0.022	85	0.064								0.004	0.000									
215	SENSETIME-002	209	0.014	135	0.020	92	0.384	124	0.011	75	0.104	63	0.015	33	0.028	123	0.994	81	0.032	125	0.523	0.009	0.000	0.040							
216	SENSETIME-003	6	0.001	7	0.007	43	0.150	48	0.003	56	0.091	70	0.002	4	0.012	22	0.477	2	0.008	27	0.133	0.000	0.000	0.041							
217	SENSETIME-004	5	0.001	9	0.007	20	0.072	34	0.002	50	0.084	4	0.002	6	0.013	10	0.229	14	0.006	21	0.113	0.000	0.000	0.041							
218	SENSETIME-005	5	0.001	3	0.006	8	0.059	38	0.002	18	0.007	42	0.082	11	0.002	12	0.014	5	0.173	17	0.007	16	0.051	16	0.104	0.000	0.000	0.041			
219	SENSETIME-006	2	0.001	2	0.006	2	0.055	2	0.001	2	0.004	14	0.064	5	0.002	5	0.012	151	0.998	100	0.004	9	0.034	8	0.093	0.000	0.000	0.025			
220	SENSETIME-007	1	0.001	1	0.006	1	0.052	1	0.001	1	0.003	11	0.062	1	0.001	1	0.009	171	0.999	2	0.003	4	0.024	5	0.085	0.000	0.000	0.025			
221	SHAMAN-003	259	0.124	251	0.172					25	0.451	251	0.597								0.020	0.011									
222	SHAMAN-004	270	0.222	260	0.319					264	0.615	258	0.754								0.020	0.011									
223	SHAMAN-006	240	0.040	219	0.058	200	0.938			212	0.141	202	0.237	79	0.972						0.020	0.011	0.869								
224	SHAMAN-007	239	0.040	218	0.057					213	0.141	205	0.240								0.020	0.010									
225	SIAT-001	61	0.002	262	0.333	79	0.004			69	0.099	72	0.018	231	0.365						0.000	0.000									
226	SIAT-002	63	0.002	264	0.446	192	0.348			73	0.102	89	0.022	243	0.478	172	0.372				167	0.923	0.000	0.000							
227	SMILART-004	282	0.965	278	0.974					275	0.968	271	0.976								0.011	0.013									
228	SMILART-005																														

#	ALGORITHM	INVESTIGATION MODE										IDENTIFICATION MODE										FAILURE TO EXTRACT FEATURES																
		RANK ONE MISS RATE, FNIR(N, 0, 1)										HIGH T → FPIR = 0.001, FNIR(N, T, L)										N=1.6M																
		GALLERY	MUGSHOT	MUGSHOT	WEBCAM	PROFILE	BORDER	BOR <sub>L</sub> 10YR	KIOSK	MUGSHOT	MUGSHOT	MUGSHOT	VISA	BORDER	VISA	MUGSHOT	MUGSHOT	WEBCAM	PROFILE	BORDER	BOR <sub>L</sub> 10YR	KIOSK	MUGSHOT	MUGSHOT	WEBCAM	PROFILE	BORDER	BOR <sub>L</sub> 10YR	KIOSK									
231	SYNESIS-003	265	0.170	256	0.235					123	0.136	262	0.582	254	0.646								0.006	0.015														
232	SYNESIS-003	213	0.016	160	0.023	176	0.827	152	0.013	168	0.065	152	0.123	71	0.960	127	0.075		89	0.314		0.000	0.001	0.063														
233	SYNESIS-005	179	0.009	79	0.013	157	0.744	35	0.003	57	0.092	97	0.025	94	0.072	98	0.984	81	0.032	59	0.214		0.001	0.000	0.135													
234	TECH5-001	130	0.004	116	0.017	127	0.584	106	0.007	84	0.107	158	0.057	267	0.935	222	1.000	163	0.244	184	0.994		0.000	0.000	0.006													
235	TECH5-002	105	0.003	52	0.011	77	0.312	34	0.003	78	0.029	53	0.089	105	0.027	92	0.070	51	0.805	97	0.039	67	0.205	111	0.440		0.001	0.000	0.041		0.000							
236	TEVIAN-003	210	0.015	214	0.052							199	0.117	187	0.176									0.001	0.002													
237	TEVIAN-004	197	0.011	194	0.038							186	0.087	167	0.144	72	0.962								0.001	0.002	0.116											
238	TEVIAN-005	170	0.007	178	0.28	105	0.467					175	0.074	141	0.112										0.001	0.002												
239	TEVIAN-006	97	0.002	60	0.011	35	0.123	45	0.003	44	0.013	23	0.071	44	0.010	37	0.032	43	0.016	30	0.093	172	0.951		0.001	0.000	0.062		0.000									
240	TEVIAN-007	59	0.002	28	0.009	27	0.093	25	0.002	28	0.009	16	0.067	30	0.005	21	0.022	15	0.301	31	0.009	22	0.065	23	0.122		0.000	0.000	0.062		0.000							
241	TIGER-000	250	0.062	241	0.095						251	0.390	244	0.500										0.000	0.000													
242	TIGER-002	154	0.006	158	0.023	105	0.514					183	0.086	176	0.158	161	0.999								0.000	0.000	0.056											
243	TIGER-003	153	0.006	157	0.023						182	0.086	177	0.158										0.000	0.000													
244	TONGYITRANS-000	165	0.007	155	0.022						169	0.066	131	0.101										0.003	0.001													
245	TONGYITRANS-001	166	0.007	154	0.022						165	0.062	146	0.118	134	0.995								0.000	0.000	0.070												
246	TOSHIBA-000	139	0.004	147	0.022	158	0.766					160	0.058	119	0.092									0.000	0.000													
247	TOSHIBA-001	144	0.005	151	0.022						188	0.018	82	0.062	57	0.882	75	0.030	65	0.194	55	0.188		0.001	0.001	0.047		0.003										
248	TRUEFACE-000	119	0.003	87	0.014	61	0.230	110	0.007	65	0.024	58	0.092	78	0.018	82	0.062	57	0.882	75	0.030	65	0.194	55	0.188		0.001	0.001	0.047		0.003							
249	VD-000	278	0.474	269	0.551						273	0.917	269	0.946											0.011	0.013												
250	VD-001	232	0.028	215	0.053						229	0.201	218	0.281											0.005	0.001												
251	VD-002	188	0.010	176	0.027	183	0.893	135	0.013	88	0.050	144	0.176	179	0.079	169	0.148	137	0.996	134	0.095	84	0.367	99	0.372		0.004	0.003	0.156		0.002							
252	VD-003	171	0.008	148	0.022	161	0.773	117	0.008	80	0.030	124	0.137	136	0.046	130	0.100	162	0.999	107	0.051	72	0.244	91	0.315		0.003	0.003	0.144		0.002							
253	VERIDAS-001	108	0.003	94	0.014	12	0.550	101	0.006	76	0.028	114	0.131	125	0.037	107	0.082	105	0.987	99	0.044	74	0.266	77	0.264		0.000	0.002	0.093		0.001							
254	VERIDAS-002	107	0.003	95	0.014	122	0.550	100	0.006	75	0.028	115	0.131	124	0.037	108	0.082	106	0.987	98	0.044	75	0.266	78	0.264		0.000	0.002	0.093		0.001							
255	VERIDAS-003	62	0.002	59	0.011	77	0.297	69	0.004	49	0.016	86	0.108	70	0.017	72	0.055	141	0.997	54	0.020	47	0.150	50	0.178		0.000	0.002	0.093		0.001							
256	VIGILANTSOLUTIONS-003	253	0.069	249	0.151	217	0.958					255	0.408	257	0.660	157	0.999									0.000	0.001	0.127										
257	VIGILANTSOLUTIONS-004	260	0.125	257	0.244	210	0.965					261	0.549	261	0.817	139	0.996									0.000	0.001	0.127										
258	VIGILANTSOLUTIONS-005	184	0.009	180	0.920						250	0.388			208	1.000									0.000	0.001	0.127											
259	VIGILANTSOLUTIONS-006	190	0.010	197	0.921						245	0.353			207	1.000									0.000	0.001	0.127											
260	VIGILANTSOLUTIONS-007	121	0.003	121	0.017	197	0.925	135	0.013	93	0.068	142	0.175	113	0.028	113	0.088	139	0.996	131	0.081	86	0.371	102	0.391		0.000	0.001	0.127		0.001							
261	VIGILANTSOLUTIONS-008	113	0.003	122	0.017	188	0.913	137	0.014	94	0.072	145	0.178	85	0.021	101	0.077	160	0.999	138	0.104	88	0.398	124	0.511		0.000	0.001	0.127		0.001							
262	VISIONBOX-000	71	0.002	61	0.011	151	0.752	82	0.005	51	0.017	38	0.078	75	0.018	75	0.057	113	0.990	61	0.023	46	0.146	42	0.162		0.000	0.001	0.043		0.001							
263	VISIONLABS-004	106	0.003	136	0.020	85	0.343					143	0.050	168	0.147	58	0.888									0.001	0.001	0.046										
264	VISIONLABS-005	95	0.002	130	0.019	81	0.334					62	0.096	105	0.027	117	0.090	36	0.672								0.001	0.001	0.051									
265	VISIONLABS-006	66	0.002	106	0.015	56	0.211	64	0.004			61	0.095	104	0.027	116	0.090	37	0.672	80	0.031							0.001	0.001	0.051								
266	VISIONLABS-007	58	0.002	105	0.015	5	0.211	60	0.004			41	0.081	57	0.013	63	0.051	23	0.481	44	0.017							0.001	0.000	0.075								
267	VISIONLABS-008	77	0.002	88	0.014	37	0.141	32	0.002			22	0.071	25	0.005	27	0.025	49	0.799	20	0.008							0.000	0.000	0.060								
268	VISIONLABS-009	16	0.001	23	0.008	25	0.091	19	0.001			274	1.000	284	1.000	277	1.000	269	1.000	202	1.000								0.000	0.000	0.060							
269	VISIONLABS-010	31	0.001	47	0.010	17	0.069	7	0.001	10	0.006	21	0.069	29	0.005	32	0.027	21	0.008	18	0.055	19	0.109		0.000	0.000	0.040		0.000									
270</																																						

#	ALGORITHM	INVESTIGATION MODE						IDENTIFICATION MODE						FAILURE TO EXTRACT FEATURES						
		RANK ONE MISS RATE, FNIR(N, 0, 1)						HIGH T → FPIR = 0.001, FNIR(N, T, L)												
		N=1.6M						N=1.6M												
	GALLERY	MUGSHOT	MUGSHOT	MUGSHOT	VISA	BORDER	VISA	MUGSHOT	MUGSHOT	MUGSHOT	VISA	BORDER	VISA	MUGSHOT	MUGSHOT	MUGSHOT	VISA	BORDER	KIOSK	
	PROBE	MUGSHOT	WEBCAM	PROFILE	BORDER	BOR <sub>i</sub> 10YR	KIOSK	MUGSHOT	WEBCAM	PROFILE	BORDER	BOR <sub>i</sub> 10YR	KIOSK	MUGSHOT	WEBCAM	PROFILE	BORDER	BOR <sub>i</sub> 10YR	KIOSK	
277	VTS-002	72.002	80.013	62.0233	139.014	85.038	102.0125	100.026	99.075	179.1.000	101.045	71.0.231	102.0417	0.000	0.000	0.029	0.000	0.000	0.000	
278	XFORWARDAI-000	89.002	91.014	2.089	65.004	46.015	59.094	66.015	70.053	19.0.440	35.0.021	52.0.159	45.0.169	0.000	0.000	0.000	0.000	0.000	0.000	
279	XFORWARDAI-001	81.002	77.013	15.067	50.003	26.009	44.0.082	27.005	34.0.028	20.0.448	24.0.008	21.0.062	24.0.123	0.000	0.000	0.000	0.000	0.000	0.000	
280	XFORWARDAI-002	74.002	75.012	5.059	41.002	15.007	34.0.077	18.003	15.0.016	23.0.525	12.0.005	13.0.041	12.0.099	0.000	0.000	0.000	0.000	0.000	0.000	
281	YISHENG-001	231.027	222.060		174.058		175.0.287	243.0.346	259.0.808		189.0.666		166.0.919		0.002	0.005				
282	YITU-002	65.002	47.010					73.0.018	57.0.049						0.000	0.000				
283	YITU-003	112.003	111.016					81.0.019	66.0.052						0.003	0.001				
284	YITU-004	25.001	27.008	181.0.866				41.0.010	36.0.027	67.0.936					0.000	0.000	0.000	0.000		
285	YITU-005	91.002	100.014					48.0.010	38.0.032						0.003	0.001				

Table 16: **Miss rates by dataset:** At left, rank 1 miss rates relevant to investigations; at right, with threshold set to target FPIR = 0.01 for higher volume, low prior, uses. Yellow indicates most accurate algorithm. Throughout blue superscripts indicate the rank of the algorithm for that column.

2022/04/28  
22:29:02FNIR(N, R, T) = False neg. identification rate  
FPIR(N, T) = False pos. identification rateN = Num. enrolled subjects  
R = Num. candidates examined

T = Threshold

T = 0 → Investigation  
T > 0 → Identification

#	ALGORITHM	MISSES BELOW THRESHOLD, T	ENROL MOST RECENT			
		DATASET: FRVT 2018 MUGSHOTS				
		N=0.64M	N=1.6M	N=3.0M	N=6.0M	N=12.0M
1	3DIVI-005	<sup>22</sup> 0.1358	<sup>22</sup> 0.1664	<sup>19</sup> 0.1915	<sup>18</sup> 0.2370	<sup>17</sup> 0.3054
2	ACER-000	<sup>21</sup> 0.1185	<sup>21</sup> 0.1455	<sup>18</sup> 0.1714	<sup>17</sup> 0.2074	<sup>17</sup> 0.2537
3	ALCHERA-003	<sup>21</sup> 0.1176	<sup>21</sup> 0.1553	<sup>19</sup> 0.1853	<sup>18</sup> 0.2409	<sup>18</sup> 0.3553
4	ALLGOVISION-000	<sup>18</sup> 0.0688	<sup>18</sup> 0.0881	<sup>17</sup> 0.1084	<sup>16</sup> 0.1389	<sup>15</sup> 0.2129
5	ALLGOVISION-001	<sup>19</sup> 0.0785	<sup>19</sup> 0.1017	<sup>17</sup> 0.1218	<sup>17</sup> 0.1584	<sup>15</sup> 0.2273
6	ANKE-000	<sup>20</sup> 0.0942	<sup>19</sup> 0.1169	<sup>18</sup> 0.1404	<sup>17</sup> 0.1776	<sup>17</sup> 0.2559
7	ANKE-002	<sup>17</sup> 0.0229	<sup>17</sup> 0.0318	<sup>11</sup> 0.0406	<sup>11</sup> 0.0605	<sup>9</sup> 0.1466
8	AWARE-003	<sup>21</sup> 0.1098	<sup>20</sup> 0.1283	<sup>18</sup> 0.1447	<sup>17</sup> 0.1768	<sup>16</sup> 0.2364
9	AWARE-005	<sup>24</sup> 0.3389	<sup>24</sup> 0.3643	<sup>20</sup> 0.3993	<sup>19</sup> 0.4526	<sup>16</sup> 0.5251
10	AYONIX-002	<sup>27</sup> 0.7862	<sup>27</sup> 0.8242	<sup>20</sup> 0.8508	<sup>19</sup> 0.8704	<sup>19</sup> 0.8939
11	CAMVI-004	<sup>14</sup> 0.0367	<sup>17</sup> 0.0716	<sup>16</sup> 0.0983	<sup>18</sup> 0.2508	<sup>17</sup> 0.2701
12	CANON-001	<sup>31</sup> 0.0039	<sup>31</sup> 0.0054	<sup>31</sup> 0.0074	<sup>28</sup> 0.0158	<sup>36</sup> 0.0924
13	CIB-000	<sup>3</sup> 0.0086	<sup>5</sup> 0.0125	<sup>5</sup> 0.0160	<sup>8</sup> 0.0303	<sup>7</sup> 0.1251
14	CLEARVIEWAI-000	<sup>32</sup> 0.0040	<sup>32</sup> 0.0058	<sup>32</sup> 0.0078	<sup>29</sup> 0.0159	<sup>39</sup> 0.0971
15	CLOUDWALK-HR-000	<sup>10</sup> 0.0019	<sup>10</sup> 0.0020	<sup>8</sup> 0.0023	<sup>13</sup> 0.0072	<sup>17</sup> 0.0701
16	CLOUDWALK-MT-000	<sup>11</sup> 0.0019	<sup>9</sup> 0.0020	<sup>7</sup> 0.0022	<sup>5</sup> 0.0049	<sup>9</sup> 0.0466
17	COGENT-000	<sup>16</sup> 0.0430	<sup>14</sup> 0.0527	<sup>14</sup> 0.0695	<sup>19</sup> 0.1133	<sup>13</sup> 0.1960
18	COGENT-001	<sup>16</sup> 0.0430	<sup>14</sup> 0.0527	<sup>14</sup> 0.0695	<sup>14</sup> 0.1133	<sup>13</sup> 0.1960
19	COGENT-002	<sup>12</sup> 0.0322	<sup>13</sup> 0.0444	<sup>13</sup> 0.0610	<sup>14</sup> 0.1116	<sup>13</sup> 0.2180
20	COGENT-003	<sup>13</sup> 0.0328	<sup>13</sup> 0.0463	<sup>14</sup> 0.0683	<sup>15</sup> 0.1294	<sup>16</sup> 0.2445
21	COGENT-004	<sup>11</sup> 0.0210	<sup>11</sup> 0.0331	<sup>12</sup> 0.0527	<sup>15</sup> 0.1138	<sup>14</sup> 0.2119
22	COGENT-005	<sup>4</sup> 0.0064	<sup>40</sup> 0.0091	<sup>40</sup> 0.0123	<sup>39</sup> 0.0303	<sup>21</sup> 0.1233
23	COGNITEC-000	<sup>22</sup> 0.1377	<sup>21</sup> 0.1606	<sup>19</sup> 0.1870	<sup>18</sup> 0.2176	<sup>17</sup> 0.2831
24	COGNITEC-001	<sup>19</sup> 0.0807	<sup>19</sup> 0.1017	<sup>17</sup> 0.1214	<sup>16</sup> 0.1513	<sup>15</sup> 0.2238
25	COGNITEC-002	<sup>15</sup> 0.0406	<sup>14</sup> 0.0531	<sup>14</sup> 0.0666	<sup>13</sup> 0.0935	<sup>14</sup> 0.1874
26	COGNITEC-003	<sup>15</sup> 0.0400	<sup>14</sup> 0.0526	<sup>13</sup> 0.0650	<sup>12</sup> 0.0895	<sup>12</sup> 0.1772
27	COGNITEC-004	<sup>11</sup> 0.0222	<sup>11</sup> 0.0313	<sup>11</sup> 0.0388	<sup>10</sup> 0.0540	<sup>8</sup> 0.1103
28	COGNITEC-005	<sup>40</sup> 0.0063	<sup>42</sup> 0.0096	<sup>48</sup> 0.0144	<sup>33</sup> 0.0287	<sup>38</sup> 0.0967
29	COGNITEC-006	<sup>36</sup> 0.0053	<sup>37</sup> 0.0077	<sup>39</sup> 0.0117	<sup>43</sup> 0.0254	<sup>32</sup> 0.0919
30	CYBERLINK-000	<sup>15</sup> 0.0414	<sup>15</sup> 0.0565	<sup>15</sup> 0.0707	<sup>14</sup> 0.1031	<sup>14</sup> 0.2050
31	CYBERLINK-001	<sup>14</sup> 0.0392	<sup>15</sup> 0.0536	<sup>14</sup> 0.0695	<sup>13</sup> 0.0973	<sup>12</sup> 0.1794
32	CYBERLINK-002	<sup>61</sup> 0.0105	<sup>64</sup> 0.0148	<sup>67</sup> 0.0202	<sup>80</sup> 0.0399	<sup>78</sup> 0.1255
33	CYBERLINK-003	<sup>3</sup> 0.0056	<sup>38</sup> 0.0077	<sup>36</sup> 0.0100	<sup>39</sup> 0.0235	<sup>21</sup> 0.1237
34	CYBERLINK-004	<sup>35</sup> 0.0051	<sup>35</sup> 0.0071	<sup>37</sup> 0.0102	<sup>33</sup> 0.0199	<sup>81</sup> 0.1269
35	CYBERLINK-005	<sup>41</sup> 0.0067	<sup>46</sup> 0.0099	<sup>40</sup> 0.0138	<sup>77</sup> 0.0394	<sup>112</sup> 0.1566
36	DAIHUA-001	<sup>17</sup> 0.0569	<sup>17</sup> 0.0727	<sup>16</sup> 0.0878	<sup>15</sup> 0.1148	<sup>13</sup> 0.1867
37	DAIHUA-002	<sup>66</sup> 0.0108	<sup>65</sup> 0.0151	<sup>64</sup> 0.0191	<sup>55</sup> 0.0291	<sup>66</sup> 0.1153
38	DAIHUA-003	<sup>59</sup> 0.0100	<sup>60</sup> 0.0139	<sup>61</sup> 0.0180	<sup>56</sup> 0.0296	<sup>60</sup> 0.1130
39	DAIHUA-004	<sup>34</sup> 0.0048	<sup>34</sup> 0.0069	<sup>34</sup> 0.0090	<sup>31</sup> 0.0164	<sup>25</sup> 0.0853
40	DAON-000	<sup>93</sup> 0.0161	<sup>93</sup> 0.0226	<sup>92</sup> 0.0293	<sup>111</sup> 0.0562	<sup>12</sup> 0.1702
41	DECATUR-000	<sup>95</sup> 0.0173	<sup>96</sup> 0.0229	<sup>96</sup> 0.0305	<sup>96</sup> 0.0464	<sup>95</sup> 0.1433
42	DEEPLINT-001	<sup>20</sup> 0.0027	<sup>20</sup> 0.0033	<sup>19</sup> 0.0043	<sup>22</sup> 0.0121	<sup>35</sup> 0.0922
43	DEEPSEA-001	<sup>139</sup> 0.0347	<sup>137</sup> 0.0462	<sup>132</sup> 0.0586	<sup>127</sup> 0.0802	<sup>123</sup> 0.1708
44	DERMALOG-005	<sup>19</sup> 0.0700	<sup>18</sup> 0.0880	<sup>17</sup> 0.1144	<sup>16</sup> 0.1578	<sup>16</sup> 0.2451
45	DERMALOG-006	<sup>148</sup> 0.0395	<sup>144</sup> 0.0517	<sup>137</sup> 0.0659	<sup>138</sup> 0.0973	<sup>126</sup> 0.1745
46	DERMALOG-007	<sup>18</sup> 0.0691	<sup>18</sup> 0.0863	<sup>17</sup> 0.1107	<sup>16</sup> 0.1504	<sup>16</sup> 0.2299
47	DERMALOG-008	<sup>135</sup> 0.0338	<sup>135</sup> 0.0455	<sup>135</sup> 0.0626	<sup>143</sup> 0.1060	<sup>158</sup> 0.2276
48	DERMALOG-009	<sup>80</sup> 0.0148	<sup>86</sup> 0.0206	<sup>80</sup> 0.0268	<sup>84</sup> 0.0416	<sup>90</sup> 0.1374
49	FUJITSULAB-000	<sup>87</sup> 0.0148	<sup>87</sup> 0.0206	<sup>91</sup> 0.0277	<sup>107</sup> 0.0541	<sup>125</sup> 0.1739
50	FUJITSULAB-001	<sup>7</sup> 0.0126	<sup>77</sup> 0.0182	<sup>8</sup> 0.0251	<sup>115</sup> 0.0646	<sup>14</sup> 0.2079
51	GORILLA-002	<sup>22</sup> 0.1539	<sup>22</sup> 0.1880	<sup>19</sup> 0.2184	<sup>18</sup> 0.2596	<sup>18</sup> 0.3398
52	GORILLA-004	<sup>19</sup> 0.0699	<sup>19</sup> 0.0892	<sup>16</sup> 0.1048	<sup>16</sup> 0.1370	<sup>14</sup> 0.1969
53	GORILLA-005	<sup>166</sup> 0.0453	<sup>161</sup> 0.0583	<sup>151</sup> 0.0704	<sup>140</sup> 0.0974	<sup>99</sup> 0.1474
54	GORILLA-006	<sup>108</sup> 0.0196	<sup>108</sup> 0.0275	<sup>101</sup> 0.0331	<sup>98</sup> 0.0516	<sup>58</sup> 0.1113
55	GORILLA-007	<sup>10</sup> 0.0190	<sup>107</sup> 0.0271	<sup>107</sup> 0.0348	<sup>101</sup> 0.0520	<sup>59</sup> 0.1129
56	GRIAULE-000	<sup>83</sup> 0.0145	<sup>84</sup> 0.0201	<sup>83</sup> 0.0253	<sup>82</sup> 0.0407	<sup>96</sup> 0.1440
57	HIK-003	<sup>19</sup> 0.0828	<sup>19</sup> 0.1028	<sup>17</sup> 0.1202	<sup>16</sup> 0.1525	<sup>16</sup> 0.2480
58	HIK-004	<sup>194</sup> 0.0796	<sup>191</sup> 0.0988	<sup>174</sup> 0.1147	<sup>164</sup> 0.1474	<sup>168</sup> 0.2483
59	HIK-005	<sup>12</sup> 0.0312	<sup>130</sup> 0.0436	<sup>131</sup> 0.0560	<sup>131</sup> 0.0911	<sup>15</sup> 0.2129
60	HYPERVERGE-001	<sup>24</sup> 0.0033	<sup>24</sup> 0.0045	<sup>24</sup> 0.0059	<sup>19</sup> 0.0117	<sup>27</sup> 0.0872
61	HYPERVERGE-002	<sup>21</sup> 0.0028	<sup>21</sup> 0.0037	<sup>21</sup> 0.0046	<sup>10</sup> 0.0064	<sup>1</sup> 0.0064
62	HZAILU-000	<sup>82</sup> 0.0143	<sup>83</sup> 0.0197	<sup>83</sup> 0.0255	<sup>83</sup> 0.0411	<sup>69</sup> 0.1174
63	IDEMIA-003	<sup>13</sup> 0.0346	<sup>140</sup> 0.0471	<sup>161</sup> 0.0892	<sup>191</sup> 0.2789	<sup>18</sup> 0.4311
64	IDEMIA-004	<sup>126</sup> 0.0300	<sup>126</sup> 0.0373	<sup>123</sup> 0.0447	<sup>113</sup> 0.0617	<sup>120</sup> 0.1635
65	IDEMIA-005	<sup>142</sup> 0.0360	<sup>132</sup> 0.0440	<sup>129</sup> 0.0537	<sup>126</sup> 0.0764	<sup>135</sup> 0.1915
66	IDEMIA-006	<sup>140</sup> 0.0351	<sup>129</sup> 0.0433	<sup>127</sup> 0.0525	<sup>123</sup> 0.0734	<sup>15</sup> 0.2201
67	IDEMIA-007	<sup>78</sup> 0.0136	<sup>76</sup> 0.0181	<sup>71</sup> 0.0228	<sup>70</sup> 0.0357	<sup>93</sup> 0.1402
68	IDEMIA-008	<sup>3</sup> 0.0016	<sup>8</sup> 0.0019	<sup>10</sup> 0.0024	<sup>6</sup> 0.0053	<sup>19</sup> 0.0470
69	IDEMIA-009	<sup>2</sup> 0.0013	<sup>2</sup> 0.0016	<sup>2</sup> 0.0018	<sup>9</sup> 0.0061	<sup>13</sup> 0.0550
70	IMAGUS-005	<sup>79</sup> 0.0137	<sup>80</sup> 0.0185	<sup>77</sup> 0.0237	<sup>72</sup> 0.0368	<sup>51</sup> 0.1067
71	IMAGUS-006	<sup>80</sup> 0.0137	<sup>82</sup> 0.0190	<sup>80</sup> 0.0244	<sup>78</sup> 0.0396	<sup>67</sup> 0.1159
72	IMAGUS-007	<sup>9</sup> 0.0160	<sup>95</sup> 0.0228	<sup>99</sup> 0.0284	<sup>87</sup> 0.0444	<sup>20</sup> 0.1179

**Table 17: Identification-mode: Effect of N on FNIR at high threshold.** Values are threshold-based miss rates i.e. FNIR at FPIR = 0.001 for five enrollment population sizes, N. The right six columns apply for enrollment of one image. Missing entries usually apply because another algorithm from the same developer was run instead. Some developers are missing because less accurate algorithms were not run on galleries with  $N \geq 3\ 000\ 000$ . Throughout blue superscripts indicate the rank of the algorithm for that column.

#	ALGORITHM	MISSES BELOW THRESHOLD, T		ENROL MOST RECENT					
		FNIR(N, T > 0, R > L)		DATASET: FRVT 2018 MUGSHOTS					
		N=0.64M	N=1.6M	N=3.0M	N=6.0M	N=12.0M			
73	IMPERIAL-000	<sup>101</sup> 0.0187	<sup>101</sup> 0.0259	<sup>111</sup> 0.0358	<sup>122</sup> 0.0733	<sup>129</sup> 0.1794			
74	INCODE-003	<sup>220</sup> 0.1324	<sup>222</sup> 0.1672	<sup>195</sup> 0.1961	<sup>183</sup> 0.2345	<sup>159</sup> 0.3123			
75	INCODE-004	<sup>152</sup> 0.0403	<sup>153</sup> 0.0538	<sup>146</sup> 0.0662	<sup>133</sup> 0.0917	<sup>117</sup> 0.1619			
76	INCODE-005	<sup>50</sup> 0.0083	<sup>50</sup> 0.0113	<sup>49</sup> 0.0145	<sup>40</sup> 0.0247	<sup>30</sup> 0.0912			
77	INNOVATRICS-007	<sup>56</sup> 0.0093	<sup>56</sup> 0.0125	<sup>54</sup> 0.0159	<sup>45</sup> 0.0259	<sup>52</sup> 0.1092			
78	INTSYSMU-000	<sup>280</sup> 0.9982	<sup>278</sup> 0.9984	<sup>211</sup> 0.9985	<sup>202</sup> 0.9987	<sup>197</sup> 0.9988			
79	IREX-000	<sup>16</sup> 0.0190	<sup>112</sup> 0.0280	<sup>115</sup> 0.0391	<sup>118</sup> 0.0677	<sup>103</sup> 0.1479			
80	ISYSTEMS-002	<sup>178</sup> 0.0584	<sup>178</sup> 0.0783	<sup>168</sup> 0.0973	<sup>162</sup> 0.1373	<sup>159</sup> 0.2295			
81	ISYSTEMS-003	<sup>164</sup> 0.0438	<sup>162</sup> 0.0590	<sup>158</sup> 0.0807	<sup>154</sup> 0.1259	<sup>161</sup> 0.2357			
82	KAKAO-000	<sup>67</sup> 0.0109	<sup>67</sup> 0.0151	<sup>66</sup> 0.0196	<sup>65</sup> 0.0324	<sup>42</sup> 0.1010			
83	KEDACOM-001	<sup>97</sup> 0.0181	<sup>94</sup> 0.0227	<sup>85</sup> 0.0265	<sup>86</sup> 0.0422	<sup>88</sup> 0.1340			
84	LOOKMAN-003	<sup>138</sup> 0.0346	<sup>131</sup> 0.0437	<sup>125</sup> 0.0514	<sup>121</sup> 0.0724	<sup>118</sup> 0.1620			
85	LOOKMAN-005	<sup>118</sup> 0.0240	<sup>114</sup> 0.0301	<sup>110</sup> 0.0356	<sup>97</sup> 0.0512	<sup>87</sup> 0.1334			
86	MANTRA-000	<sup>42</sup> 0.0065	<sup>47</sup> 0.0101	<sup>50</sup> 0.0151	<sup>60</sup> 0.0308	<sup>45</sup> 0.1035			
87	MEGVII-001	<sup>124</sup> 0.0562	<sup>123</sup> 0.0722	<sup>159</sup> 0.0872	<sup>158</sup> 0.1309	<sup>125</sup> 0.2713			
88	MICROFOCUS-005	<sup>27</sup> 0.9732	<sup>272</sup> 0.8354	<sup>208</sup> 0.8555	<sup>200</sup> 0.8755	<sup>194</sup> 0.8954			
89	MICROSOFT-003	<sup>109</sup> 0.0198	<sup>110</sup> 0.0278	<sup>108</sup> 0.0356	<sup>104</sup> 0.0538	<sup>108</sup> 0.1539			
90	MICROSOFT-004	<sup>100</sup> 0.0185	<sup>102</sup> 0.0259	<sup>105</sup> 0.0333	<sup>99</sup> 0.0517	<sup>100</sup> 0.1510			
91	MICROSOFT-005	<sup>98</sup> 0.0181	<sup>99</sup> 0.0256	<sup>99</sup> 0.0320	<sup>96</sup> 0.0512	<sup>104</sup> 0.1491			
92	MICROSOFT-006	<sup>50</sup> 0.0091	<sup>51</sup> 0.0120	<sup>56</sup> 0.0162	<sup>57</sup> 0.0301	<sup>103</sup> 0.1482			
93	NEC-000	<sup>182</sup> 0.0637	<sup>180</sup> 0.0789	<sup>164</sup> 0.0933	<sup>153</sup> 0.1163	<sup>137</sup> 0.1941			
94	NEC-001	<sup>19</sup> 0.0863	<sup>197</sup> 0.1055	<sup>179</sup> 0.1249	<sup>167</sup> 0.1519	<sup>156</sup> 0.2253			
95	NEC-002	<sup>14</sup> 0.0020	<sup>14</sup> 0.0026	<sup>14</sup> 0.0033	<sup>24</sup> 0.0135	<sup>15</sup> 0.0653			
96	NEC-003	<sup>12</sup> 0.0021	<sup>12</sup> 0.0024	<sup>11</sup> 0.0028	<sup>8</sup> 0.0059	<sup>12</sup> 0.0540			
97	NEC-004	<sup>7</sup> 0.0017	<sup>6</sup> 0.0018	<sup>4</sup> 0.0020	<sup>2</sup> 0.0037	<sup>4</sup> 0.0329			
98	NEC-005	<sup>4</sup> 0.0015	<sup>3</sup> 0.0017	<sup>3</sup> 0.0019	<sup>11</sup> 0.0065	<sup>2</sup> 0.0307			
99	NEUROTECHNOLOGY-003	<sup>284</sup> 0.5698	<sup>265</sup> 0.6362	<sup>208</sup> 0.7035	<sup>198</sup> 0.7602	<sup>192</sup> 0.8224			
100	NEUROTECHNOLOGY-004	<sup>168</sup> 0.0466	<sup>167</sup> 0.0629	<sup>153</sup> 0.0779	<sup>150</sup> 0.1135	<sup>148</sup> 0.2102			
101	NEUROTECHNOLOGY-005	<sup>149</sup> 0.0396	<sup>154</sup> 0.0538	<sup>145</sup> 0.0675	<sup>137</sup> 0.0950	<sup>141</sup> 0.1966			
102	NEUROTECHNOLOGY-007	<sup>163</sup> 0.0436	<sup>166</sup> 0.0623	<sup>158</sup> 0.0802	<sup>159</sup> 0.1320	<sup>163</sup> 0.2393			
103	NEUROTECHNOLOGY-008	<sup>139</sup> 0.0339	<sup>148</sup> 0.0530	<sup>162</sup> 0.0893	<sup>174</sup> 0.1769	<sup>181</sup> 0.3288			
104	NEUROTECHNOLOGY-009	<sup>65</sup> 0.0108	<sup>68</sup> 0.0152	<sup>67</sup> 0.0196	<sup>63</sup> 0.0324	<sup>54</sup> 0.1102			
105	NEUROTECHNOLOGY-010	<sup>46</sup> 0.0069	<sup>45</sup> 0.0099	<sup>47</sup> 0.0138	<sup>89</sup> 0.0449	<sup>124</sup> 0.1727			
106	NOTIONTAG-000	<sup>72</sup> 0.0128	<sup>71</sup> 0.0175	<sup>72</sup> 0.0228	<sup>71</sup> 0.0357	<sup>82</sup> 0.1270			
107	NTECHLAB-003	<sup>158</sup> 0.0421	<sup>152</sup> 0.0537	<sup>147</sup> 0.0674	<sup>130</sup> 0.0907	<sup>111</sup> 0.1582			
108	NTECHLAB-004	<sup>128</sup> 0.0312	<sup>127</sup> 0.0405	<sup>120</sup> 0.0519	<sup>120</sup> 0.0722	<sup>105</sup> 0.1503			
109	NTECHLAB-005	<sup>132</sup> 0.0334	<sup>128</sup> 0.0424	<sup>130</sup> 0.0537	<sup>125</sup> 0.0760	<sup>111</sup> 0.1543			
110	NTECHLAB-006	<sup>124</sup> 0.0288	<sup>122</sup> 0.0367	<sup>122</sup> 0.0471	<sup>117</sup> 0.0670	<sup>107</sup> 0.1523			
111	NTECHLAB-007	<sup>102</sup> 0.0188	<sup>98</sup> 0.0256	<sup>97</sup> 0.0317	<sup>95</sup> 0.0495	<sup>86</sup> 0.1306			
112	NTECHLAB-008	<sup>63</sup> 0.0107	<sup>61</sup> 0.0145	<sup>60</sup> 0.0187	<sup>52</sup> 0.0286	<sup>41</sup> 0.0995			
113	NTECHLAB-009	<sup>28</sup> 0.0037	<sup>28</sup> 0.0049	<sup>27</sup> 0.0062	<sup>23</sup> 0.0125	<sup>20</sup> 0.0735			
114	NTECHLAB-010	<sup>12</sup> 0.0020	<sup>13</sup> 0.0025	<sup>12</sup> 0.0030	<sup>15</sup> 0.0077	<sup>13</sup> 0.0710			
115	NTECHLAB-011	<sup>16</sup> 0.0022	<sup>17</sup> 0.0030	<sup>16</sup> 0.0038	<sup>14</sup> 0.0075	<sup>14</sup> 0.0625			
116	PANGIAM-000	<sup>33</sup> 0.0042	<sup>33</sup> 0.0060	<sup>31</sup> 0.0080	<sup>30</sup> 0.0160	<sup>28</sup> 0.0876			
117	PARAVISION-003	<sup>120</sup> 0.0260	<sup>120</sup> 0.0351	<sup>121</sup> 0.0447	<sup>116</sup> 0.0657	<sup>119</sup> 0.1630			
118	PARAVISION-004	<sup>47</sup> 0.0074	<sup>49</sup> 0.0101	<sup>45</sup> 0.0136	<sup>48</sup> 0.0267	<sup>29</sup> 0.1256			
119	PARAVISION-005	<sup>21</sup> 0.0032	<sup>23</sup> 0.0041	<sup>29</sup> 0.0057	<sup>32</sup> 0.0174	<sup>40</sup> 0.1037			
120	PARAVISION-007	<sup>22</sup> 0.0030	<sup>22</sup> 0.0040	<sup>27</sup> 0.0055	<sup>34</sup> 0.0211	<sup>53</sup> 0.1097			
121	PARAVISION-009	<sup>15</sup> 0.0020	<sup>15</sup> 0.0026	<sup>17</sup> 0.0038	<sup>18</sup> 0.0098	<sup>29</sup> 0.0857			
122	PIXELALL-002	<sup>192</sup> 0.0716	<sup>196</sup> 0.1052	<sup>186</sup> 0.1475	<sup>187</sup> 0.2489	<sup>187</sup> 0.3904			
123	PIXELALL-003	<sup>90</sup> 0.0158	<sup>90</sup> 0.0218	<sup>94</sup> 0.0288	<sup>91</sup> 0.0474	<sup>61</sup> 0.1138			
124	PIXELALL-004	<sup>74</sup> 0.0129	<sup>79</sup> 0.0183	<sup>81</sup> 0.0245	<sup>73</sup> 0.0378	<sup>91</sup> 0.1375			
125	PIXELALL-005	<sup>58</sup> 0.0087	<sup>53</sup> 0.0121	<sup>56</sup> 0.0171	<sup>42</sup> 0.0250	<sup>40</sup> 0.1052			
126	PTAKURATSATU-000	<sup>121</sup> 0.0275	<sup>121</sup> 0.0366	<sup>122</sup> 0.0458	<sup>102</sup> 0.0523	<sup>111</sup> 0.0523			
127	QNAP-001	<sup>15</sup> 0.0404	<sup>151</sup> 0.0536	<sup>139</sup> 0.0661	<sup>132</sup> 0.0916	<sup>111</sup> 0.1595			
128	QNAP-002	<sup>110</sup> 0.0200	<sup>103</sup> 0.0265	<sup>108</sup> 0.0327	<sup>93</sup> 0.0490	<sup>89</sup> 0.1341			
129	QUANTASOFT-001	<sup>26</sup> 0.6387	<sup>266</sup> 0.6387	<sup>208</sup> 0.6387	<sup>190</sup> 0.6387	<sup>190</sup> 0.6387			
130	RANKONE-002	<sup>206</sup> 0.0973	<sup>201</sup> 0.1175	<sup>180</sup> 0.1359	<sup>172</sup> 0.1718	<sup>173</sup> 0.2613			
131	RANKONE-003	<sup>205</sup> 0.0973	<sup>200</sup> 0.1175	<sup>181</sup> 0.1359	<sup>171</sup> 0.1718	<sup>172</sup> 0.2613			
132	RANKONE-005	<sup>167</sup> 0.0473	<sup>163</sup> 0.0592	<sup>147</sup> 0.0700	<sup>135</sup> 0.0944	<sup>14</sup> 0.1998			
133	RANKONE-007	<sup>94</sup> 0.0168	<sup>92</sup> 0.0222	<sup>86</sup> 0.0266	<sup>75</sup> 0.0381	<sup>61</sup> 0.1132			
134	RANKONE-009	<sup>70</sup> 0.0132	<sup>74</sup> 0.0177	<sup>71</sup> 0.0230	<sup>67</sup> 0.0344	<sup>31</sup> 0.0921			
135	RANKONE-010	<sup>62</sup> 0.0106	<sup>59</sup> 0.0136	<sup>59</sup> 0.0174	<sup>47</sup> 0.0265	<sup>22</sup> 0.0785			
136	RANKONE-011	<sup>39</sup> 0.0063	<sup>39</sup> 0.0087	<sup>36</sup> 0.0115	<sup>49</sup> 0.0269	<sup>61</sup> 0.1135			
137	RANKONE-012	<sup>38</sup> 0.0058	<sup>36</sup> 0.0077	<sup>36</sup> 0.0100	<sup>35</sup> 0.0220	<sup>37</sup> 0.1111			
138	REALNETWORKS-002	<sup>233</sup> 0.1943	<sup>232</sup> 0.2314	<sup>208</sup> 0.2656	<sup>193</sup> 0.3134	<sup>181</sup> 0.3208			
139	REALNETWORKS-003	<sup>219</sup> 0.1300	<sup>218</sup> 0.1594	<sup>192</sup> 0.1858	<sup>181</sup> 0.2246	<sup>178</sup> 0.3076			
140	REALNETWORKS-004	<sup>218</sup> 0.1279	<sup>217</sup> 0.1581	<sup>191</sup> 0.1857	<sup>182</sup> 0.2329	<sup>180</sup> 0.3179			
141	REALNETWORKS-005	<sup>111</sup> 0.0202	<sup>109</sup> 0.0277	<sup>108</sup> 0.0355	<sup>110</sup> 0.0560	<sup>91</sup> 0.1431			
142	REALNETWORKS-006	<sup>58</sup> 0.0097	<sup>62</sup> 0.0145	<sup>62</sup> 0.0182	<sup>61</sup> 0.0308	<sup>40</sup> 0.0991			
143	REALNETWORKS-007	<sup>40</sup> 0.0068	<sup>43</sup> 0.0097	<sup>41</sup> 0.0125	<sup>37</sup> 0.0233	<sup>31</sup> 0.0917			
144	REMARKAI-000	<sup>155</sup> 0.0406	<sup>155</sup> 0.0552	<sup>144</sup> 0.0676	<sup>141</sup> 0.1028	<sup>144</sup> 0.2003			

**Table 18: Identification-mode: Effect of N on FNIR at high threshold.** Values are threshold-based miss rates i.e. FNIR at FPIR = 0.001 for five enrollment population sizes, N. The right six columns apply for enrollment of one image. Missing entries usually apply because another algorithm from the same developer was run instead. Some developers are missing because less accurate algorithms were not run on galleries with  $N \geq 3\ 000\ 000$ . Throughout blue superscripts indicate the rank of the algorithm for that column.

#	ALGORITHM	MISSES BELOW THRESHOLD, T		ENROL MOST RECENT			
		FNIR(N, T > 0, R > L)		DATASET: FRVT 2018 MUGSHOTS			
		N=0.64M	N=1.6M	N=3.0M	N=6.0M	N=12.0M	
145	RENDIP-000	<sup>51</sup> 0.0085	<sup>52</sup> 0.0121	<sup>52</sup> 0.0156	<sup>51</sup> 0.0277	<sup>71</sup> 0.1182	
146	REVEALMEDIA-000	<sup>54</sup> 0.0090	<sup>54</sup> 0.0122	<sup>50</sup> 0.0158	<sup>50</sup> 0.0277	<sup>43</sup> 0.1019	
147	S1-000	<sup>117</sup> 0.0204	<sup>111</sup> 0.0279	<sup>111</sup> 0.0382	<sup>114</sup> 0.0630	<sup>122</sup> 0.1707	
148	S1-001	<sup>68</sup> 0.0115	<sup>69</sup> 0.0156	<sup>69</sup> 0.0199	<sup>76</sup> 0.0392	<sup>80</sup> 0.1256	
149	SCANOVATE-000	<sup>120</sup> 0.0498	<sup>170</sup> 0.0667	<sup>156</sup> 0.0804	<sup>145</sup> 0.1097	<sup>56</sup> 0.1109	
150	SCANOVATE-001	<sup>181</sup> 0.0630	<sup>181</sup> 0.0815	<sup>167</sup> 0.0993	<sup>135</sup> 0.1292	<sup>140</sup> 0.1960	
151	SENSETIME-000	<sup>89</sup> 0.0158	<sup>88</sup> 0.0208	<sup>89</sup> 0.0270	<sup>79</sup> 0.0398	<sup>72</sup> 0.1232	
152	SENSETIME-001	<sup>92</sup> 0.0161	<sup>91</sup> 0.0219	<sup>92</sup> 0.0277	<sup>85</sup> 0.0420	<sup>84</sup> 0.1304	
153	SENSETIME-002	<sup>84</sup> 0.0146	<sup>63</sup> 0.0148	<sup>51</sup> 0.0153	<sup>38</sup> 0.0234	<sup>16</sup> 0.0657	
154	SENSETIME-003	<sup>70</sup> 0.0016	<sup>70</sup> 0.0018	<sup>70</sup> 0.0021	<sup>70</sup> 0.0054	<sup>70</sup> 0.0451	
155	SENSETIME-004	<sup>7</sup> 0.0015	<sup>4</sup> 0.0018	<sup>7</sup> 0.0021	<sup>3</sup> 0.0040	<sup>7</sup> 0.0354	
156	SENSETIME-005	<sup>7</sup> 0.0016	<sup>11</sup> 0.0022	<sup>13</sup> 0.0031	<sup>17</sup> 0.0089	<sup>8</sup> 0.0454	
157	SENSETIME-006	<sup>3</sup> 0.0014	<sup>5</sup> 0.0018	<sup>7</sup> 0.0023	<sup>4</sup> 0.0047	<sup>6</sup> 0.0372	
158	SENSETIME-007	<sup>1</sup> 0.0012	<sup>1</sup> 0.0014	<sup>1</sup> 0.0016	<sup>1</sup> 0.0036	<sup>3</sup> 0.0316	
159	SHAMAN-007	<sup>27</sup> 0.1212	<sup>213</sup> 0.1413	<sup>187</sup> 0.1587	<sup>176</sup> 0.1879	<sup>166</sup> 0.2460	
160	SIAT-001	<sup>77</sup> 0.0136	<sup>72</sup> 0.0176	<sup>75</sup> 0.0230	<sup>66</sup> 0.0344	<sup>44</sup> 0.1035	
161	SIAT-002	<sup>88</sup> 0.0154	<sup>89</sup> 0.0216	<sup>96</sup> 0.0273	<sup>81</sup> 0.0404	<sup>83</sup> 0.1283	
162	SQISOFT-001	<sup>198</sup> 0.0921	<sup>209</sup> 0.1322	<sup>189</sup> 0.1781	<sup>184</sup> 0.2348	<sup>195</sup> 0.9271	
163	SYNESIS-003	<sup>26</sup> 0.5341	<sup>262</sup> 0.5821	<sup>209</sup> 0.6113	<sup>197</sup> 0.6479	<sup>19</sup> 0.6822	
164	SYNESIS-003	<sup>171</sup> 0.0499	<sup>168</sup> 0.0652	<sup>157</sup> 0.0804	<sup>144</sup> 0.1095	<sup>136</sup> 0.1916	
165	SYNESIS-005	<sup>98</sup> 0.0181	<sup>97</sup> 0.0248	<sup>96</sup> 0.0319	<sup>100</sup> 0.0518	<sup>113</sup> 0.1580	
166	TECH5-001	<sup>157</sup> 0.0420	<sup>158</sup> 0.0574	<sup>163</sup> 0.0911	<sup>179</sup> 0.2106	<sup>186</sup> 0.3725	
167	TECH5-002	<sup>107</sup> 0.0194	<sup>106</sup> 0.0269	<sup>108</sup> 0.0346	<sup>103</sup> 0.0537	<sup>115</sup> 0.1607	
168	TEVIAN-005	<sup>189</sup> 0.0692	<sup>186</sup> 0.0873	<sup>170</sup> 0.1066	<sup>157</sup> 0.1301	<sup>131</sup> 0.1840	
169	TEVIAN-006	<sup>49</sup> 0.0078	<sup>44</sup> 0.0098	<sup>48</sup> 0.0130	<sup>46</sup> 0.0261	<sup>85</sup> 0.1305	
170	TEVIAN-007	<sup>30</sup> 0.0038	<sup>30</sup> 0.0052	<sup>28</sup> 0.0065	<sup>27</sup> 0.0154	<sup>37</sup> 0.0957	
171	TIGER-002	<sup>184</sup> 0.0647	<sup>183</sup> 0.0861	<sup>168</sup> 0.1036	<sup>160</sup> 0.1332	<sup>154</sup> 0.2231	
172	TOSHIBA-000	<sup>167</sup> 0.0460	<sup>165</sup> 0.0620	<sup>159</sup> 0.0780	<sup>147</sup> 0.1117	<sup>14</sup> 0.2082	
173	TRUEFACE-000	<sup>76</sup> 0.0134	<sup>78</sup> 0.0182	<sup>78</sup> 0.0238	<sup>74</sup> 0.0380	<sup>92</sup> 0.1385	
174	VD-001	<sup>229</sup> 0.1642	<sup>229</sup> 0.2015	<sup>199</sup> 0.2351	<sup>190</sup> 0.2736	<sup>183</sup> 0.3293	
175	VERIDAS-001	<sup>122</sup> 0.0278	<sup>125</sup> 0.0373	<sup>124</sup> 0.0491	<sup>124</sup> 0.0753	<sup>109</sup> 0.1541	
176	VERIDAS-002	<sup>12</sup> 0.0278	<sup>124</sup> 0.0373	<sup>117</sup> 0.0373	<sup>94</sup> 0.0491	<sup>21</sup> 0.0753	
177	VERIDAS-003	<sup>69</sup> 0.0117	<sup>70</sup> 0.0166	<sup>70</sup> 0.0219	<sup>88</sup> 0.0446	<sup>110</sup> 0.1543	
178	VIGILANTSOLUTIONS-008	<sup>88</sup> 0.0146	<sup>85</sup> 0.0205	<sup>88</sup> 0.0269	<sup>92</sup> 0.0489	<sup>68</sup> 0.1164	
179	VISIONBOX-000	<sup>70</sup> 0.0122	<sup>75</sup> 0.0177	<sup>70</sup> 0.0239	<sup>196</sup> 0.9538		
180	VISIONLABS-004	<sup>160</sup> 0.0427	<sup>159</sup> 0.0578	<sup>159</sup> 0.0703	<sup>136</sup> 0.0949	<sup>132</sup> 0.1853	
181	VISIONLABS-005	<sup>145</sup> 0.0369	<sup>143</sup> 0.0502	<sup>134</sup> 0.0626	<sup>128</sup> 0.0847	<sup>130</sup> 0.1815	
182	VISIONLABS-006	<sup>103</sup> 0.0188	<sup>105</sup> 0.0267	<sup>108</sup> 0.0336	<sup>108</sup> 0.0542	<sup>100</sup> 0.1478	
183	VISIONLABS-007	<sup>104</sup> 0.0188	<sup>104</sup> 0.0266	<sup>103</sup> 0.0335	<sup>106</sup> 0.0540	<sup>101</sup> 0.1479	
184	VISIONLABS-008	<sup>57</sup> 0.0096	<sup>57</sup> 0.0131	<sup>57</sup> 0.0166	<sup>54</sup> 0.0291	<sup>26</sup> 0.1247	
185	VISIONLABS-009	<sup>26</sup> 0.0034	<sup>25</sup> 0.0046	<sup>25</sup> 0.0060	<sup>25</sup> 0.0140	<sup>29</sup> 0.0881	
186	VISIONLABS-010	<sup>29</sup> 0.0038	<sup>29</sup> 0.0051	<sup>30</sup> 0.0070	<sup>26</sup> 0.0149	<sup>33</sup> 0.0920	
187	VISIONLABS-011	<sup>18</sup> 0.0025	<sup>19</sup> 0.0033	<sup>20</sup> 0.0044	<sup>21</sup> 0.0120	<sup>24</sup> 0.0825	
188	VOCORD-005	<sup>214</sup> 0.1179	<sup>216</sup> 0.1577	<sup>196</sup> 0.2183	<sup>192</sup> 0.3122	<sup>189</sup> 0.4490	
189	VTS-001	<sup>60</sup> 0.0102	<sup>58</sup> 0.0133	<sup>60</sup> 0.0175	<sup>62</sup> 0.0322	<sup>70</sup> 0.1243	
190	VTS-002	<sup>99</sup> 0.0185	<sup>100</sup> 0.0259	<sup>105</sup> 0.0344	<sup>109</sup> 0.0549	<sup>97</sup> 0.1447	
191	XFORWARDAI-000	<sup>64</sup> 0.0107	<sup>66</sup> 0.0151	<sup>65</sup> 0.0195	<sup>64</sup> 0.0324	<sup>40</sup> 0.1057	
192	XFORWARDAI-001	<sup>27</sup> 0.0037	<sup>27</sup> 0.0049	<sup>26</sup> 0.0060	<sup>20</sup> 0.0120	<sup>23</sup> 0.0800	
193	XFORWARDAI-002	<sup>3</sup> 0.0026	<sup>18</sup> 0.0030	<sup>16</sup> 0.0035	<sup>16</sup> 0.0078	<sup>10</sup> 0.0706	
194	YITU-002	<sup>75</sup> 0.0129	<sup>73</sup> 0.0177	<sup>73</sup> 0.0228	<sup>68</sup> 0.0345	<sup>62</sup> 0.1133	
195	YITU-003	<sup>81</sup> 0.0138	<sup>81</sup> 0.0185	<sup>78</sup> 0.0236	<sup>69</sup> 0.0353	<sup>65</sup> 0.1148	
196	YITU-004	<sup>41</sup> 0.0067	<sup>41</sup> 0.0096	<sup>42</sup> 0.0129	<sup>36</sup> 0.0232	<sup>47</sup> 0.1046	
197	YITU-005	<sup>48</sup> 0.0074	<sup>48</sup> 0.0101	<sup>44</sup> 0.0135	<sup>44</sup> 0.0255	<sup>50</sup> 0.1057	

**Table 19: Identification-mode: Effect of N on FNIR at high threshold.** Values are threshold-based miss rates i.e. FNIR at FPIR = 0.001 for five enrollment population sizes, N. The right six columns apply for enrollment of one image. Missing entries usually apply because another algorithm from the same developer was run instead. Some developers are missing because less accurate algorithms were not run on galleries with  $N \geq 3\,000\,000$ . Throughout blue superscripts indicate the rank of the algorithm for that column.

MISSES AT GIVEN RANK		ENROL MOST RECENT														
#	ALGORITHM	RANK 1						$aN^b$	RANK 50						$aN^b$	
		N=0.64M	N=1.6M	N=3.0M	N=6.0M	N=12.0M			N=0.64M	N=1.6M	N=3.0M	N=6.0M	N=12.0M			
1	3DIVI-005	<sup>219</sup> 0.0137	<sup>217</sup> 0.0176	<sup>187</sup> 0.0210	<sup>181</sup> 0.0253	<sup>176</sup> 0.0302	<sup>142</sup> 0.0004 N <sup>0.271</sup> 158	<sup>200</sup> 0.0040	<sup>200</sup> 0.0049	<sup>177</sup> 0.0057	<sup>173</sup> 0.0068	<sup>168</sup> 0.0081	<sup>48</sup> 0.0002 N <sup>0.240</sup> 163			
2	ACER-000	<sup>188</sup> 0.0081	<sup>194</sup> 0.0106	<sup>178</sup> 0.0128	<sup>173</sup> 0.0157	<sup>168</sup> 0.0195	<sup>61</sup> 0.0001 N <sup>0.299</sup> 182	<sup>146</sup> 0.0020	<sup>165</sup> 0.0026	<sup>154</sup> 0.0031	<sup>154</sup> 0.0037	<sup>150</sup> 0.0045	<sup>19</sup> 0.0000 N <sup>0.284</sup> 176			
3	ALCHERA-003	<sup>184</sup> 0.0079	<sup>191</sup> 0.0104	<sup>173</sup> 0.0123	<sup>172</sup> 0.0147	<sup>167</sup> 0.0180	<sup>90</sup> 0.0002 N <sup>0.278</sup> 169	<sup>181</sup> 0.0027	<sup>180</sup> 0.0032	<sup>160</sup> 0.0035	<sup>159</sup> 0.0042	<sup>151</sup> 0.0048	<sup>56</sup> 0.0002 N <sup>0.199</sup> 153			
4	ALLGOVISION-000	<sup>202</sup> 0.0101	<sup>199</sup> 0.0114	<sup>174</sup> 0.0127	<sup>171</sup> 0.0145	<sup>168</sup> 0.0166	<sup>173</sup> 0.0010 N <sup>0.171</sup> 95	<sup>220</sup> 0.0063	<sup>216</sup> 0.0067	<sup>182</sup> 0.0071	<sup>176</sup> 0.0075	<sup>167</sup> 0.0081	<sup>179</sup> 0.0020 N <sup>0.086</sup> 111			
5	ALLGOVISION-001	<sup>176</sup> 0.0069	<sup>188</sup> 0.0096	<sup>168</sup> 0.0107	<sup>168</sup> 0.0128	<sup>163</sup> 0.0157	<sup>76</sup> 0.0002 N <sup>0.277</sup> 167	<sup>168</sup> 0.0023	<sup>169</sup> 0.0027	<sup>150</sup> 0.0031	<sup>146</sup> 0.0036	<sup>141</sup> 0.0043	<sup>41</sup> 0.0001 N <sup>0.211</sup> 158			
6	ANKE-000	<sup>208</sup> 0.0102	<sup>207</sup> 0.0132	<sup>181</sup> 0.0155	<sup>178</sup> 0.0188	<sup>172</sup> 0.0225	<sup>120</sup> 0.0003 N <sup>0.270</sup> 157	<sup>190</sup> 0.0032	<sup>192</sup> 0.0040	<sup>175</sup> 0.0046	<sup>168</sup> 0.0056	<sup>159</sup> 0.0066	<sup>40</sup> 0.0001 N <sup>0.247</sup> 165			
7	ANKE-002	<sup>110</sup> 0.0024	<sup>108</sup> 0.0026	<sup>118</sup> 0.0032	<sup>108</sup> 0.0037	<sup>101</sup> 0.0043	<sup>69</sup> 0.0002 N <sup>0.203</sup> 111	<sup>119</sup> 0.0016	<sup>120</sup> 0.0017	<sup>115</sup> 0.0017	<sup>103</sup> 0.0018	<sup>97</sup> 0.0019	<sup>105</sup> 0.0000 N <sup>0.367</sup> 99			
8	AWARE-003	<sup>236</sup> 0.0238	<sup>234</sup> 0.0306	<sup>198</sup> 0.0361	<sup>190</sup> 0.0431	<sup>189</sup> 0.0506	<sup>169</sup> 0.0008 N <sup>0.258</sup> 152	<sup>214</sup> 0.0055	<sup>222</sup> 0.0075	<sup>192</sup> 0.0092	<sup>189</sup> 0.0113	<sup>186</sup> 0.0143	<sup>30</sup> 0.0001 N <sup>0.323</sup> 186			
9	AWARE-005	<sup>237</sup> 0.0245	<sup>232</sup> 0.0311	<sup>199</sup> 0.0366	<sup>193</sup> 0.0434	<sup>189</sup> 0.0312	<sup>193</sup> 0.0056 N <sup>0.118</sup> 52	<sup>218</sup> 0.0062	<sup>228</sup> 0.0082	<sup>194</sup> 0.0101	<sup>190</sup> 0.0128	<sup>170</sup> 0.0089	<sup>129</sup> 0.0007 N <sup>0.169</sup> 148			
10	AYONIX-002	<sup>222</sup> 0.2935	<sup>227</sup> 0.3414	<sup>209</sup> 0.3736	<sup>201</sup> 0.4101	<sup>199</sup> 0.4465	<sup>198</sup> 0.0440 N <sup>0.143</sup> 68	<sup>271</sup> 0.0950	<sup>273</sup> 0.1274	<sup>209</sup> 0.1524	<sup>208</sup> 0.1828	<sup>194</sup> 0.2150	<sup>181</sup> 0.0023 N <sup>0.279</sup> 174			
11	CAMVI-004	<sup>212</sup> 0.0124	<sup>245</sup> 0.0468	<sup>203</sup> 0.0719	<sup>200</sup> 0.2363	<sup>194</sup> 0.2367	<sup>180</sup> 0.0000 N <sup>0.155</sup> 96	<sup>244</sup> 0.0117	<sup>259</sup> 0.0464	<sup>205</sup> 0.0715	<sup>162</sup> 0.0261	<sup>195</sup> 0.2364	<sup>3</sup> 0.0000 N <sup>0.171</sup> 96			
12	CANON-001	<sup>14</sup> 0.0011	<sup>12</sup> 0.0011	<sup>14</sup> 0.0012	<sup>15</sup> 0.0013	<sup>13</sup> 0.0014	<sup>108</sup> 0.0002 N <sup>0.113</sup> 45	<sup>18</sup> 0.0009	<sup>17</sup> 0.0009	<sup>17</sup> 0.0009	<sup>16</sup> 0.0010	<sup>104</sup> 0.0006 N <sup>0.26</sup> 45				
13	CIB-000	<sup>45</sup> 0.0014	<sup>42</sup> 0.0015	<sup>48</sup> 0.0017	<sup>43</sup> 0.0019	<sup>15</sup> 0.0131	<sup>40</sup> 0.0000 N <sup>0.635</sup> 195	<sup>57</sup> 0.0012	<sup>50</sup> 0.0012	<sup>48</sup> 0.0012	<sup>46</sup> 0.0012	<sup>182</sup> 0.0122	<sup>4</sup> 0.0000 N <sup>0.647</sup> 195			
14	CLEARVIEWAI-000	<sup>11</sup> 0.0010	<sup>13</sup> 0.0011	<sup>13</sup> 0.0012	<sup>16</sup> 0.0013	<sup>17</sup> 0.0015	<sup>81</sup> 0.0002 N <sup>0.129</sup> 61	<sup>20</sup> 0.0009	<sup>16</sup> 0.0009	<sup>16</sup> 0.0009	<sup>16</sup> 0.0009	<sup>14</sup> 0.0010	<sup>119</sup> 0.0007 N <sup>0.199</sup> 35			
15	CLOUDWALK-HR-000	<sup>49</sup> 0.0015	<sup>37</sup> 0.0015	<sup>34</sup> 0.0015	<sup>28</sup> 0.0016	<sup>23</sup> 0.0017	<sup>168</sup> 0.0007 N <sup>0.84</sup> 11	<sup>106</sup> 0.0014	<sup>92</sup> 0.0014	<sup>82</sup> 0.0014	<sup>77</sup> 0.0014	<sup>58</sup> 0.0014	<sup>163</sup> 0.0012 N <sup>0.012</sup> 16			
16	CLOUDWALK-MT-000	<sup>76</sup> 0.0018	<sup>57</sup> 0.0018	<sup>49</sup> 0.0018	<sup>40</sup> 0.0019	<sup>32</sup> 0.0020	<sup>124</sup> 0.0011 N <sup>0.035</sup> 6	<sup>133</sup> 0.0018	<sup>128</sup> 0.0018	<sup>116</sup> 0.0018	<sup>107</sup> 0.0018	<sup>86</sup> 0.0018	<sup>176</sup> 0.0017 N <sup>0.032</sup> 4			
17	COGENT-000	<sup>203</sup> 0.0101	<sup>193</sup> 0.0105	<sup>169</sup> 0.0109	<sup>161</sup> 0.0115	<sup>154</sup> 0.0125	<sup>188</sup> 0.0038 N <sup>0.071</sup> 17	<sup>157</sup> 0.0021	<sup>157</sup> 0.0024	<sup>150</sup> 0.0028	<sup>151</sup> 0.0036	<sup>174</sup> 0.0095	<sup>8</sup> 0.0000 N <sup>0.466</sup> 192			
18	COGENT-001	<sup>204</sup> 0.0101	<sup>192</sup> 0.0105	<sup>170</sup> 0.0109	<sup>162</sup> 0.0115	<sup>159</sup> 0.0125	<sup>180</sup> 0.0038 N <sup>0.071</sup> 18	<sup>156</sup> 0.0021	<sup>158</sup> 0.0024	<sup>149</sup> 0.0028	<sup>158</sup> 0.0036	<sup>173</sup> 0.0095	<sup>7</sup> 0.0000 N <sup>0.466</sup> 191			
19	COGENT-002	<sup>122</sup> 0.0029	<sup>125</sup> 0.0036	<sup>123</sup> 0.0041	<sup>121</sup> 0.0049	<sup>117</sup> 0.0059	<sup>43</sup> 0.0001 N <sup>0.244</sup> 144	<sup>102</sup> 0.0014	<sup>111</sup> 0.0015	<sup>107</sup> 0.0017	<sup>109</sup> 0.0019	<sup>109</sup> 0.0021	<sup>53</sup> 0.0002 N <sup>0.144</sup> 142			
20	COGENT-003	<sup>128</sup> 0.0031	<sup>122</sup> 0.0032	<sup>128</sup> 0.0043	<sup>121</sup> 0.0051	<sup>120</sup> 0.0060	<sup>57</sup> 0.0001 N <sup>0.230</sup> 133	<sup>113</sup> 0.0015	<sup>123</sup> 0.0017	<sup>122</sup> 0.0018	<sup>121</sup> 0.0020	<sup>114</sup> 0.0022	<sup>56</sup> 0.0002 N <sup>0.143</sup> 141			
21	COGENT-004	<sup>77</sup> 0.0018	<sup>76</sup> 0.0020	<sup>74</sup> 0.0022	<sup>72</sup> 0.0025	<sup>64</sup> 0.0028	<sup>96</sup> 0.0002 N <sup>0.159</sup> 84	<sup>94</sup> 0.0013	<sup>90</sup> 0.0014	<sup>87</sup> 0.0014	<sup>80</sup> 0.0015	<sup>70</sup> 0.0015	<sup>112</sup> 0.0007 N <sup>0.050</sup> 79			
22	COGENT-005	<sup>56</sup> 0.0016	<sup>51</sup> 0.0017	<sup>56</sup> 0.0018	<sup>47</sup> 0.0020	<sup>41</sup> 0.0021	<sup>14</sup> 0.0004 N <sup>0.108</sup> 40	<sup>96</sup> 0.0013	<sup>79</sup> 0.0014	<sup>66</sup> 0.0014	<sup>61</sup> 0.0014	<sup>50</sup> 0.0014	<sup>161</sup> 0.0011 N <sup>0.017</sup> 28			
23	COGNITEC-000	<sup>230</sup> 0.0195	<sup>229</sup> 0.0252	<sup>199</sup> 0.0297	<sup>190</sup> 0.0352	<sup>181</sup> 0.0417	<sup>162</sup> 0.0006 N <sup>0.259</sup> 153	<sup>210</sup> 0.0050	<sup>214</sup> 0.0065	<sup>189</sup> 0.0077	<sup>186</sup> 0.0097	<sup>181</sup> 0.0122	<sup>37</sup> 0.0001 N <sup>0.305</sup> 180			
24	COGNITEC-001	<sup>198</sup> 0.0090	<sup>201</sup> 0.0117	<sup>180</sup> 0.0139	<sup>176</sup> 0.0166	<sup>170</sup> 0.0199	<sup>115</sup> 0.0002 N <sup>0.271</sup> 160	<sup>186</sup> 0.0030	<sup>185</sup> 0.0040	<sup>166</sup> 0.0046	<sup>156</sup> 0.0054	<sup>51</sup> 0.0002 N <sup>0.207</sup> 157				
25	COGNITEC-002	<sup>158</sup> 0.0048	<sup>156</sup> 0.0057	<sup>148</sup> 0.0067	<sup>142</sup> 0.0079	<sup>141</sup> 0.0094	<sup>98</sup> 0.0002 N <sup>0.232</sup> 138	<sup>170</sup> 0.0024	<sup>166</sup> 0.0026	<sup>152</sup> 0.0028	<sup>144</sup> 0.0030	<sup>134</sup> 0.0034	<sup>88</sup> 0.0005 N <sup>0.117</sup> 128			
26	COGNITEC-003	<sup>161</sup> 0.0053	<sup>160</sup> 0.0062	<sup>151</sup> 0.0072	<sup>149</sup> 0.0085	<sup>141</sup> 0.0100	<sup>122</sup> 0.0003 N <sup>0.222</sup> 124	<sup>183</sup> 0.0028	<sup>177</sup> 0.0030	<sup>157</sup> 0.0032	<sup>145</sup> 0.0035	<sup>139</sup> 0.0037	<sup>88</sup> 0.0008 N <sup>0.097</sup> 119			
27	COGNITEC-004	<sup>117</sup> 0.0027	<sup>110</sup> 0.0032	<sup>118</sup> 0.0037	<sup>116</sup> 0.0045	<sup>114</sup> 0.0056	<sup>33</sup> 0.0001 N <sup>0.233</sup> 130	<sup>91</sup> 0.0013	<sup>93</sup> 0.0014	<sup>85</sup> 0.0015	<sup>81</sup> 0.0019	<sup>62</sup> 0.0022	<sup>62</sup> 0.0002 N <sup>0.123</sup> 133			
28	COGNITEC-005	<sup>46</sup> 0.0014	<sup>48</sup> 0.0016	<sup>52</sup> 0.0018	<sup>50</sup> 0.0021	<sup>51</sup> 0.0024	<sup>62</sup> 0.0001 N <sup>0.169</sup> 92	<sup>45</sup> 0.0011	<sup>46</sup> 0.0011	<sup>43</sup> 0.0012	<sup>41</sup> 0.0012	<sup>34</sup> 0.0012	<sup>110</sup> 0.0007 N <sup>0.132</sup> 59			
29	COGNITEC-006	<sup>41</sup> 0.0014	<sup>41</sup> 0.0016	<sup>41</sup> 0.0017	<sup>44</sup> 0.0019	<sup>45</sup> 0.0022	<sup>79</sup> 0.0002 N <sup>0.154</sup> 76	<sup>47</sup> 0.0011	<sup>46</sup> 0.0012	<sup>36</sup> 0.0012	<sup>36</sup> 0.0012	<sup>36</sup> 0.0012	<sup>111</sup> 0.0007 N <sup>0.138</sup> 58			
30	CYBERLINK-000	<sup>134</sup> 0.0034	<sup>129</sup> 0.0040	<sup>131</sup> 0.0046	<sup>127</sup> 0.0054	<sup>123</sup> 0.0063	<sup>92</sup> 0.0002 N <sup>0.209</sup> 117	<sup>153</sup> 0.0021	<sup>152</sup> 0.0022	<sup>149</sup> 0.0022	<sup>141</sup> 0.0023	<sup>137</sup> 0.0025	<sup>128</sup> 0.0027	<sup>101</sup> 0.0006 N <sup>0.092</sup> 116		
31	CYBERLINK-001	<sup>125</sup> 0.0030	<sup>122</sup> 0.0035	<sup>125</sup> 0.0042	<sup>123</sup> 0.0050	<sup>120</sup> 0.0060	<sup>44</sup> 0.0001 N <sup>0.243</sup> 143	<sup>124</sup> 0.0016	<sup>124</sup> 0.0017	<sup>121</sup> 0.0018	<sup>118</sup> 0.0020	<sup>112</sup> 0.0022	<sup>76</sup> 0.0004 N <sup>0.109</sup> 123			
32	CYBERLINK-002	<sup>109</sup> 0.0024	<sup>103</sup> 0.0026	<sup>101</sup> 0.0028	<sup>95</sup> 0.0031	<sup>89</sup> 0.0035	<sup>156</sup> 0.0005 N <sup>0.121</sup> 54	<sup>149</sup> 0.0020	<sup>143</sup> 0.0021	<sup>136</sup> 0.0021	<sup>129</sup> 0.0022	<sup>115</sup> 0.0022	<sup>167</sup> 0.0012 N <sup>0.136</sup> 57			
33	CYBERLINK-003	<sup>47</sup> 0.0015	<sup>46</sup> 0.0016	<sup>42</sup> 0.0017	<sup>36</sup> 0.0018	<sup>33</sup> 0.0020	<sup>130</sup> 0.0003 N <sup>0.110</sup> 42	<sup>50</sup> 0.0011	<sup>48</sup> 0.0012	<sup>46</sup> 0.0013	<sup>44</sup> 0.0012	<sup>40</sup> 0.0013	<sup>77</sup> 0.0004 N <sup>0.097</sup> 35			
34	CYBERLINK-004	<sup>60</sup> 0.0016	<sup>57</sup> 0.0017	<sup>59</sup> 0.0018	<sup>56</sup> 0.0021	<sup>52</sup> 0.0021	<sup>49</sup> 0.0004 N <sup>0.099</sup> 37	<sup>108</sup> 0.0014	<sup>96</sup> 0.0014	<sup>93</sup> 0.0015	<sup>89</sup> 0.0015	<sup>86</sup> 0.0015	<sup>149</sup> 0.0009 N <sup>0.132</sup> 54			
35	CYBERLINK-005	<sup>70</sup> 0.0017	<sup>69</sup> 0.0018	<sup>68</sup> 0.0019	<sup>65</sup> 0.0021	<sup>64</sup> 0.0023	<sup>46</sup> 0.0003	<sup>46</sup> 0.0003	<sup>46</sup> 0.0003	<sup>46</sup> 0.0003	<sup>46</sup> 0.0003	<sup>46</sup> 0.0003	<sup>85</sup> 0.0005 N <sup>0.121</sup> 131			
36	DAHUA-001	<sup>163</sup> 0.0053	<sup>164</sup> 0.0067	<sup>159</sup> 0.0079	<sup>153</sup> 0.0093	<sup>148</sup> 0.0112	<sup>78</sup> 0.0002 N <sup>0.236</sup> 151	<sup>180</sup> 0.0027	<sup>172</sup> 0.0029	<sup>166</sup> 0.0031	<sup>157</sup> 0.0034	<sup>142</sup> 0.0038	<sup>95</sup> 0.0005 N <sup>0.121</sup> 131			
37	DAHUA-002	<sup>68</sup> 0.0017	<sup>64</sup> 0.0018	<sup>67</sup> 0.0021	<sup>62</sup> 0.0023	<sup>58</sup> 0.0027	<sup>97</sup> 0.0002 N <sup>0.156</sup> 78	<sup>83</sup> 0.0013	<sup>83</sup> 0.0013							

MISSES AT GIVEN RANK FNIR(N, T= 0, R)		ENROL MOST RECENT											
#	ALGORITHM	RANK 1					RANK 50						
		N=0.64M	N=1.6M	N=3.0M	N=6.0M	N=12.0M	aN <sup>b</sup>	N=0.64M	N=1.6M	N=3.0M	N=6.0M	N=12.0M	aN <sup>b</sup>
73	IMPERIAL-000	102	0.0022	99	0.0024	97	0.0027	94	0.0030	87	0.0035	121	0.0003 N <sup>0.157</sup> 79
74	INCODE-003	201	0.0098	206	0.0129	182	0.0154	179	0.0191	173	0.0233	86	0.0002 N <sup>0.296</sup> 179
75	INCODE-004	123	0.0029	124	0.0035	124	0.0041	122	0.0049	117	0.0061	42	0.0001 N <sup>0.244</sup> 145
76	INCODE-005	52	0.0015	49	0.0017	47	0.0018	48	0.0020	47	0.0023	107	0.0002 N <sup>0.140</sup> 66
77	INNOVATRICS-007	58	0.0016	53	0.0017	51	0.0019	51	0.0021	52	0.0024	104	0.0002 N <sup>0.143</sup> 70
78	INTSYSMSU-000	264	0.1395	264	0.1457	205	0.1498	197	0.1544	191	0.1591	192	0.0768 N <sup>0.145</sup> 8
79	IREX-000	149	0.0043	138	0.0044	122	0.0044	117	0.0046	106	0.0048	184	0.0028 N <sup>0.132</sup> 5
80	ISYSTEMS-002	162	0.0053	162	0.0064	152	0.0072	148	0.0083	142	0.0096	138	0.0003 N <sup>0.204</sup> 113
81	ISYSTEMS-003	152	0.0046	150	0.0052	144	0.0057	136	0.0066	130	0.0076	148	0.0004 N <sup>0.174</sup> 97
82	KAKAO-000	29	0.0013	36	0.0015	38	0.0016	42	0.0019	45	0.0022	37	0.0001 N <sup>0.192</sup> 107
83	KEDACOM-001	182	0.0076	172	0.0077	151	0.0079	149	0.0083	138	0.0087	189	0.0040 N <sup>0.189</sup> 9
84	KNERON-000	157	0.0048	157	0.0059	149	0.0067	144	0.0079	109	0.0093	109	0.0002 N <sup>0.226</sup> 129
85	LOOKMAN-003	190	0.0083	181	0.0088	161	0.0091	159	0.0096	146	0.0104	180	0.0030 N <sup>0.076</sup> 20
86	LOOKMAN-005	183	0.0078	179	0.0080	159	0.0083	149	0.0086	138	0.0092	186	0.0038 N <sup>0.053</sup> 10
87	MANTRA-000	53	0.0015	55	0.0017	51	0.0019	56	0.0022	54	0.0025	65	0.0002 N <sup>0.171</sup> 94
88	MEGVII-001	207	0.0105	202	0.0118	176	0.0128	170	0.0142	164	0.0161	199	0.0015 N <sup>0.143</sup> 69
89	MICROFOCUS-005	275	0.3700	275	0.4242	210	0.4610	205	0.5000	194	0.5391	196	0.0674 N <sup>0.128</sup> 60
90	MICROSOFT-003	26	0.0013	46	0.0016	23	0.0018	39	0.0022	63	0.0028	14	0.0000 N <sup>0.271</sup> 161
91	MICROSOFT-004	25	0.0012	38	0.0015	46	0.0018	51	0.0021	62	0.0028	13	0.0000 N <sup>0.281</sup> 170
92	MICROSOFT-005	51	0.0015	69	0.0019	80	0.0023	91	0.0030	92	0.0037	9	0.0000 N <sup>0.320</sup> 187
93	MICROSOFT-006	55	0.0016	75	0.0020	88	0.0025	92	0.0030	95	0.0038	12	0.0000 N <sup>0.305</sup> 183
94	NEC-000	215	0.0131	215	0.0170	181	0.0203	180	0.0244	172	0.0294	134	0.0003 N <sup>0.276</sup> 166
95	NEC-001	227	0.0180	224	0.0209	191	0.0233	181	0.0266	177	0.0304	181	0.016 N <sup>0.179</sup> 99
96	NEC-002	5	0.0009	9	0.0010	7	0.0011	1	0.0012	7	0.0013	94	0.0002 N <sup>0.113</sup> 47
97	NEC-003	31	0.0013	27	0.0014	27	0.0015	29	0.0016	20	0.0016	150	0.0005 N <sup>0.079</sup> 22
98	NEC-004	38	0.0014	33	0.0014	27	0.0015	24	0.0016	21	0.0017	161	0.0006 N <sup>0.059</sup> 13
99	NEC-005	23	0.0011	19	0.0012	18	0.0012	13	0.0013	10	0.0014	152	0.0005 N <sup>0.086</sup> 15
100	NEUROTECHNOLOGY-003	226	0.0179	225	0.0225	192	0.0263	187	0.0306	182	0.0361	168	0.0007 N <sup>0.239</sup> 141
101	NEUROTECHNOLOGY-004	154	0.0046	152	0.0056	149	0.0064	141	0.0074	136	0.0088	116	0.0002 N <sup>0.220</sup> 123
102	NEUROTECHNOLOGY-005	138	0.0035	136	0.0043	134	0.0049	130	0.0057	127	0.0066	183	0.0002 N <sup>0.223</sup> 126
103	NEUROTECHNOLOGY-007	131	0.0032	128	0.0039	137	0.0044	125	0.0052	122	0.0062	72	0.0002 N <sup>0.222</sup> 125
104	NEUROTECHNOLOGY-008	81	0.0019	84	0.0022	84	0.0025	87	0.0029	83	0.0034	45	0.0001 N <sup>0.205</sup> 115
105	NEUROTECHNOLOGY-009	32	0.0013	34	0.0014	30	0.0016	37	0.0018	36	0.0021	80	0.0003 N <sup>0.162</sup> 86
106	NEUROTECHNOLOGY-010	22	0.0011	22	0.0012	21	0.0013	21	0.0015	19	0.0016	97	0.0002 N <sup>0.125</sup> 58
107	NOTIONTAG-000	107	0.0023	98	0.0024	95	0.0026	86	0.0029	79	0.0032	151	0.0005 N <sup>0.117</sup> 50
108	NTECHLAB-003	155	0.0046	158	0.0062	154	0.0076	159	0.0094	149	0.0114	26	0.0001 N <sup>0.310</sup> 184
109	NTECHLAB-004	141	0.0037	145	0.0048	140	0.0058	139	0.0071	139	0.0085	25	0.0001 N <sup>0.291</sup> 175
110	NTECHLAB-005	135	0.0035	143	0.0047	143	0.0058	139	0.0073	136	0.0092	160	0.0005 N <sup>0.334</sup> 190
111	NTECHLAB-006	124	0.0030	133	0.0041	135	0.0050	132	0.0062	131	0.0078	15	0.0000 N <sup>0.326</sup> 189
112	NTECHLAB-007	98	0.0022	104	0.0027	101	0.0031	108	0.0037	106	0.0044	36	0.0001 N <sup>0.245</sup> 146
113	NTECHLAB-008	44	0.0014	54	0.0017	60	0.0020	68	0.0024	59	0.0027	23	0.0001 N <sup>0.223</sup> 128
114	NTECHLAB-009	24	0.0012	24	0.0013	24	0.0014	25	0.0015	24	0.0018	80	0.0002 N <sup>0.140</sup> 65
115	NTECHLAB-010	15	0.0011	14	0.0011	12	0.0012	12	0.0014	12	0.0014	150	0.0003 N <sup>0.091</sup> 32
116	NTECHLAB-011	10	0.0010	8	0.0010	7	0.0011	8	0.0013	113	0.0002 N <sup>0.103</sup> 38	15	0.0009 N <sup>0.099</sup> 13
117	PANGIAM-000	21	0.0011	20	0.0012	20	0.0013	19	0.0014	18	0.0016	103	0.0002 N <sup>0.118</sup> 33
118	PARAVISION-003	116	0.0026	116	0.0031	112	0.0042	118	0.0048	67	0.0002 N <sup>0.210</sup> 118	126	0.0016
119	PARAVISION-004	54	0.0015	47	0.0016	45	0.0017	41	0.0019	38	0.0021	136	0.0003 N <sup>0.111</sup> 43
120	PARAVISION-005	48	0.0015	49	0.0015	34	0.0018	39	0.0019	45	0.0044 N <sup>0.094</sup> 34		
121	PARAVISION-007	19	0.0011	17	0.0012	17	0.0012	19	0.0013	17	0.0014	80	0.0013 N <sup>0.094</sup> 32
122	PARAVISION-009	9	0.0010	7	0.0010	8	0.0011	8	0.0012	9	0.0014	89	0.0002 N <sup>0.118</sup> 31
123	PIXELALL-002	143	0.0037	140	0.0045	135	0.0052	139	0.0062	128	0.0075	69	0.0002 N <sup>0.228</sup> 139
124	PIXELALL-003	83	0.0019	83	0.0021	82	0.0024	79	0.0028	73	0.0032	102	0.0002 N <sup>0.202</sup> 101
125	PIXELALL-004	69	0.0017	80	0.0020	79	0.0023	76	0.0030	54	0.0001 N <sup>0.192</sup> 105		
126	PIXELALL-005	74	0.0018	70	0.0019	62	0.0020	54	0.0021	50	0.0024	154	0.0005 N <sup>0.098</sup> 36
127	PTAKURATSATU-000	112	0.0025	114	0.0030	117	0.0036	109	0.0040	97	0.0044	116	0.0002 N <sup>0.167</sup> 90
128	QNAP-001	136	0.0035	134	0.0041	132	0.0047	128	0.0054	124	0.0063	114	0.0002 N <sup>0.200</sup> 109
129	QNAP-002	156	0.0047	146	0.0049	136	0.0052	128	0.0054	108	0.0059	205	0.0002 N <sup>0.079</sup> 23
130	QUANTASOFT-001	271	0.2177	268	0.2177	192	0.2177	198	0.2177	190	0.2177	274	0.1116
131	RANKONE-002	222	0.0155	222	0.0194	182	0.0224	182	0.0262	174	0.0304	166	0.0007 N <sup>0.220</sup> 132
132	RANKONE-003	223	0.0155	221	0.0194	188	0.0224	187	0.0262	178	0.0304	167	0.0007 N <sup>0.220</sup> 131
133	RANKONE-005	180	0.0075	187	0.0084	177	0.0110	167	0.0132	166	0.0156	119	0.0003 N <sup>0.251</sup> 149
134	RANKONE-007	121	0.0028	120	0.0034	119	0.0038	119	0.0045	113	0.0053	75	0.0002 N <sup>0.211</sup> 119
135	RANKONE-009	89	0.0020	94	0.0024	97	0.0032	94	0.0038	41	0.0001 N <sup>0.219</sup> 122	93	0.0013
136	RANKONE-010	92	0.0020	92	0.0022	87	0.0025	87	0.0032	101	0.0043	88	0.0013
137	RANKONE-011	37	0.0014	39	0.0015	38	0.0018	40	0.0021	83	0.0002 N <sup>0.150</sup> 74	53	0.0011
138	RANKONE-012	28	0.0013	28	0.0014	31	0.0015	31	0.0017	30	0.0020	84	0.0002 N <sup>0.144</sup> 71
139	REALNETWORKS-002	242	0.0299	238	0.0393	201	0.0470	197	0.0562	190	0.0580	176	0.0013 N <sup>0.236</sup> 138
140	REALNETWORKS-003	228	0.0183	228	0.0242	191	0.0291	180	0.0343	144	0.0004 N <sup>0.287</sup> 174	205	0.0041
141	REALNETWORKS-004	225	0.0175	226	0.0236	193	0.0284	188	0.0347	183	0.0416	199	0.0040 N <sup>0.295</sup> 177
142	REALNETWORKS-005	88	0.0020	90	0.0023	94	0.0026	90	0.0030	89	0.		

MISSES AT GIVEN RANK FNIR(N, T = 0, R)		ENROL MOST RECENT											
#	ALGORITHM	RANK 1					$aN^b$	RANK 50					
		N=0.64M	N=1.6M	N=3.0M	N=6.0M	N=12.0M		N=0.64M	N=1.6M	N=3.0M	N=6.0M	N=12.0M	$aN^b$
145	REMARKAI-000	119	0.0027	122	0.0034	123	0.0040	123	0.0048	118	0.0058	32	0.0001 N <sup>0.260</sup> 155
146	RENDIP-000	43	0.0014	43	0.0015	44	0.0017	45	0.0019	44	0.0022	74	0.0002 N <sup>0.188</sup> 81
147	REVEALMEDIA-000	66	0.0017	67	0.0019	59	0.0020	60	0.0023	53	0.0025	123	0.0003 N <sup>0.134</sup> 62
148	S1-000	93	0.0021	96	0.0024	100	0.0028	98	0.0032	93	0.0037	55	0.0001 N <sup>0.203</sup> 112
149	S1-001	129	0.0031	115	0.0031	113	0.0034	108	0.0036	98	0.0040	170	0.0009 N <sup>0.092</sup> 33
150	SCANOVATE-000	144	0.0038	147	0.0050	145	0.0059	140	0.0073	128	0.0073	77	0.0002 N <sup>0.235</sup> 157
151	SCANOVATE-001	147	0.0041	151	0.0053	146	0.0064	144	0.0079	144	0.0098	27	0.0001 N <sup>0.299</sup> 180
152	SENSETIME-000	99	0.0022	92	0.0023	92	0.0026	81	0.0028	77	0.0032	139	0.0003 N <sup>0.135</sup> 63
153	SENSETIME-001	97	0.0022	95	0.0023	80	0.0025	89	0.0029	90	0.0037	58	0.0002 N <sup>0.177</sup> 98
154	SENSETIME-002	218	0.0136	209	0.0137	179	0.0137	169	0.0138	158	0.0139	193	0.0124 N <sup>0.007</sup> 2
155	SENSETIME-003	7	0.0010	6	0.0010	6	0.0010	6	0.0011	6	0.0012	129	0.0003 N <sup>0.085</sup> 28
156	SENSETIME-004	6	0.0010	5	0.0010	4	0.0010	3	0.0011	4	0.0012	131	0.0003 N <sup>0.173</sup> 24
157	SENSETIME-005	2	0.0008	3	0.0009	3	0.0009	3	0.0010	3	0.0011	128	0.0003 N <sup>0.085</sup> 27
158	SENSETIME-006	3	0.0008	2	0.0009	2	0.0009	1	0.0010	1	0.0010	133	0.0003 N <sup>0.099</sup> 16
159	SENSETIME-007	1	0.0008	1	0.0008	1	0.0009	1	0.0009	1	0.0010	140	0.0004 N <sup>0.061</sup> 14
160	SHAMAN-007	246	0.0371	239	0.0396	206	0.0416	194	0.0443	188	0.0473	192	0.0122 N <sup>0.083</sup> 25
161	SIAT-001	63	0.0017	61	0.0018	64	0.0020	63	0.0023	60	0.0027	68	0.0002 N <sup>0.173</sup> 96
162	SIAT-002	62	0.0016	63	0.0018	68	0.0020	69	0.0023	59	0.0027	71	0.0002 N <sup>0.171</sup> 93
163	SQISOFT-001	120	0.0028	135	0.0042	144	0.0059	147	0.0084	197	0.9207	2	0.0000 N <sup>1.674</sup> 197
164	SYNESIS-003	265	0.1456	285	0.1700	206	0.1876	196	0.2088	192	0.2317	194	0.0177 N <sup>1.98</sup> 82
165	SYNESIS-003	224	0.0161	213	0.0162	184	0.0163	178	0.0165	174	0.0254	183	0.0027 N <sup>0.127</sup> 59
166	SYNESIS-005	193	0.0085	179	0.0085	162	0.0085	150	0.0086	137	0.0088	191	0.0072 N <sup>0.012</sup> 3
167	TECH5-001	130	0.0032	130	0.0040	135	0.0047	129	0.0057	12	0.0071	31	0.0001 N <sup>0.271</sup> 159
168	TECH5-002	91	0.0020	105	0.0027	108	0.0031	104	0.0037	106	0.0047	17	0.0000 N <sup>0.285</sup> 173
169	TEVIAN-005	168	0.0056	170	0.0073	161	0.0084	160	0.0105	156	0.0130	57	0.0001 N <sup>0.283</sup> 172
170	TEVIAN-006	105	0.0023	97	0.0024	95	0.0026	80	0.0028	74	0.0031	159	0.0005 N <sup>0.106</sup> 39
171	TEVIAN-007	71	0.0017	59	0.0018	51	0.0018	49	0.0020	39	0.0021	163	0.0006 N <sup>0.073</sup> 71
172	TIGER-002	150	0.0044	154	0.0044	150	0.0056	150	0.0068	147	0.0105	29	0.0001 N <sup>0.299</sup> 181
173	TOSHIBA-000	137	0.0035	139	0.0045	139	0.0052	131	0.0061	161	0.0154	50	0.0000 N <sup>0.449</sup> 193
174	TRUEFACE-000	122	0.0031	119	0.0033	115	0.0035	108	0.0039	100	0.0043	164	0.0006 N <sup>0.115</sup> 49
175	VD-001	235	0.0230	232	0.0276	196	0.0315	191	0.0363	189	0.0418	178	0.0115 N <sup>0.204</sup> 114
176	VERIDAS-001	106	0.0023	108	0.0028	109	0.0032	107	0.0037	104	0.0045	40	0.0001 N <sup>0.231</sup> 134
177	VERIDAS-002	104	0.0023	107	0.0028	98	0.0032	91	0.0037	124	0.0003 N <sup>0.158</sup> 80		
178	VERIDAS-003	64	0.0017	62	0.0018	58	0.0020	58	0.0022	55	0.0026	99	0.0002 N <sup>0.150</sup> 73
179	VIGILANTSOLUTIONS-008	111	0.0025	113	0.0029	117	0.0034	111	0.0040	108	0.0047	51	0.0001 N <sup>0.224</sup> 127
180	VISIONBOX-000	72	0.0017	71	0.0019	75	0.0022	209	0.0000	198	0.9526	1	0.0000 N <sup>2.570</sup> 198
181	VISIONLABS-004	100	0.0022	106	0.0027	117	0.0032	118	0.0044	122	0.0070	70	0.0000 N <sup>0.387</sup> 191
182	VISIONLABS-005	87	0.0020	95	0.0024	103	0.0029	108	0.0037	112	0.0051	11	0.0000 N <sup>0.222</sup> 188
183	VISIONLABS-006	61	0.0016	66	0.0018	76	0.0022	82	0.0028	99	0.0041	100	0.0000 N <sup>0.314</sup> 186
184	VISIONLABS-007	59	0.0016	58	0.0018	61	0.0020	60	0.0023	54	0.0034	19	0.0001 N <sup>0.248</sup> 147
185	VISIONLABS-008	80	0.0019	77	0.0020	71	0.0021	73	0.0025	72	0.0030	85	0.0002 N <sup>0.169</sup> 91
186	VISIONLABS-009	17	0.0011	16	0.0011	16	0.0012	16	0.0014	24	0.0017	24	0.0015 N <sup>0.204</sup> 112
187	VISIONLABS-010	36	0.0014	31	0.0014	32	0.0015	32	0.0017	34	0.0021	93	0.0002 N <sup>0.137</sup> 64
188	VISIONLABS-011	18	0.0011	18	0.0012	19	0.0013	19	0.0018	46	0.0001 N <sup>0.162</sup> 87		
189	VCORD-005	169	0.0060	168	0.0070	158	0.0082	157	0.0097	151	0.0117	118	0.0003 N <sup>0.232</sup> 136
190	VTS-001	35	0.0014	41	0.0015	46	0.0017	46	0.0019	48	0.0023	48	0.0001 N <sup>0.179</sup> 100
191	VTS-002	65	0.0017	72	0.0019	77	0.0022	72	0.0026	75	0.0032	36	0.0001 N <sup>0.215</sup> 121
192	XFORWARDAI-000	96	0.0021	89	0.0023	84	0.0024	77	0.0027	69	0.0029	153	0.0005 N <sup>0.111</sup> 44
193	XFORWARDAI-001	90	0.0020	81	0.0020	69	0.0021	57	0.0022	49	0.0024	172	0.0009 N <sup>0.035</sup> 12
194	XFORWARDAI-002	85	0.0019	74	0.0020	63	0.0020	53	0.0021	42	0.0022	175	0.0011 N <sup>0.038</sup> 7
195	YITU-002	57	0.0016	65	0.0018	70	0.0021	69	0.0024	69	0.0029	39	0.0001 N <sup>0.213</sup> 120
196	YITU-003	115	0.0026	112	0.0029	107	0.0031	100	0.0035	96	0.0039	143	0.0004 N <sup>0.141</sup> 67
197	YITU-004	20	0.0011	23	0.0013	30	0.0015	31	0.0017	10	0.0047	30	0.0000 N <sup>0.438</sup> 192
198	YITU-005	101	0.0022	91	0.0023	86	0.0025	78	0.0027	73	0.0031	155	0.0005 N <sup>0.113</sup> 46

Table 22: **Investigation-mode: Effect of N on FNIR on recent images** For five enrollment population sizes,  $N$ , with  $T = 0$  and FPIR = 1. The left five columns are rank 1 miss rates The right five columns are rank 50 miss rates Missing entries usually apply because another algorithm from the same developer was run instead. Some developers are missing because less accurate algorithms were not run on galleries with  $N > 1\,600\,000$ . Throughout blue superscripts indicate the rank of the algorithm for that column, and yellow highlighting indicates the most accurate value. Caution: The Power-low models are mostly intended to draw attention to the kind of behavior, not as a model to be used for prediction.

#	ALGORITHM	MISSES OUTSIDE RANK R		RESOURCE USAGE		ENROL MOST RECENT, N = 1.6M					
		FNIR(N, T=0, R)		TEMPLATE		FRVT 2018 MUGSHOTS					
		BYTES	MSEC	R=1	R=5	R=10	R=20	R=50	WORK-10		
1	20FACE-000	169 2048	49 247	248 0.0552	242 0.0269	241 0.0198	238 0.0146	232 0.0099	241 1.275		
2	3DIVI-003	46 512	150 625	257 0.0833	252 0.0444	252 0.0349	248 0.0270	248 0.0191	253 1.447		
3	3DIVI-004	262 4096	151 628	218 0.0175	209 0.0091	207 0.0075	204 0.0061	199 0.0049	213 1.092		
4	3DIVI-005	261 4096	159 653	217 0.0176	210 0.0091	209 0.0074	203 0.0061	200 0.0049	214 1.092		
5	3DIVI-006	63 528	158 653	227 0.0240	234 0.0171	237 0.0160	239 0.0154	244 0.0148	232 1.162		
6	ACER-000	53 512	39 201	194 0.0106	178 0.0051	174 0.0041	172 0.0034	165 0.0026	179 1.053		
7	ACER-001	146 2048	30 184	149 0.0051	151 0.0032	150 0.0028	149 0.0025	148 0.0022	150 1.031		
8	AIZE-001	168 2048	89 403	158 0.0056	155 0.0037	160 0.0033	161 0.0030	168 0.0027	156 1.035		
9	ALCHERA-000	162 2048	53 263	212 0.0161	221 0.0124	226 0.0117	231 0.0111	234 0.0105	220 1.116		
10	ALCHERA-001	178 2048	16 66	285 0.9869	283 0.9782	287 0.9735	283 0.9679	282 0.9590	287 9.811		
11	ALCHERA-002	175 2048	23 115	258 0.0949	257 0.0555	255 0.0443	255 0.0354	250 0.0254	257 1.544		
12	ALCHERA-003	188 2048	134 548	191 0.0104	181 0.0054	181 0.0045	180 0.0038	180 0.0032	187 1.055		
13	ALCHERA-004	131 2048	282 854	196 0.0110	177 0.0049	169 0.0038	164 0.0032	161 0.0025	177 1.051		
14	ALLGOVISION-000	194 2048	99 425	199 0.0114	204 0.0084	210 0.0078	211 0.0073	216 0.0067	204 1.079		
15	ALLGOVISION-001	174 2048	221 792	182 0.0090	175 0.0048	177 0.0040	171 0.0033	169 0.0027	175 1.048		
16	ANKE-000	257 2072	101 431	206 0.0132	195 0.0073	194 0.0060	193 0.0050	192 0.0040	201 1.072		
17	ANKE-001	259 2072	102 433	208 0.0132	196 0.0073	196 0.0061	194 0.0050	193 0.0040	201 1.073		
18	ANKE-002	223 2056	154 641	169 0.0028	110 0.0020	107 0.0018	116 0.0018	120 0.0017	111 1.019		
19	AWARE-003	237 2076	195 716	234 0.0306	231 0.0162	229 0.0127	225 0.0100	222 0.0075	233 1.163		
20	AWARE-004	119 92	192 712	252 0.0679	249 0.0348	246 0.0274	246 0.0208	243 0.0145	249 1.354		
21	AWARE-005	241 3100	228 827	233 0.0311	232 0.0167	230 0.0134	227 0.0107	228 0.0082	234 1.167		
22	AWARE-006	12 124	225 818	254 0.0697	251 0.0369	247 0.0288	247 0.0223	245 0.0158	251 1.371		
23	AYONIX-000	94 1036	10 10	27 0.4505	278 0.3540	277 0.3176	273 0.2834	278 0.2381	274 4.288		
24	AYONIX-001	91 1036	12 12	273 0.3414	272 0.2338	272 0.1977	273 0.1652	272 0.1274	273 3.226		
25	AYONIX-002	93 1036	11 11	273 0.3414	273 0.2338	273 0.1977	272 0.1652	273 0.1274	273 3.226		
26	CAMVI-003	80 1024	188 707	247 0.0520	256 0.0517	257 0.0517	260 0.0517	260 0.0517	258 1.466		
27	CAMVI-004	73 1024	197 718	24 0.0468	246 0.0465	245 0.0465	246 0.0464	249 0.0464	251 1.419		
28	CAMVI-005	81 1024	212 769	251 0.0652	258 0.0648	261 0.0648	262 0.0648	264 0.0647	258 1.584		
29	CANON-001	264 4096	258 893	12 0.0011	19 0.0010	18 0.0010	17 0.0009	17 0.0009	15 1.009		
30	CIB-000	281 8196	167 674	42 0.0015	46 0.0013	45 0.0012	48 0.0012	50 0.0012	46 1.012		
31	CLEARVIEWAI-000	250 4096	209 765	18 0.0011	18 0.0010	19 0.0010	16 0.0009	16 0.0009	13 1.009		
32	CLOUDWALK-HR-000	153 2048	265 908	37 0.0015	65 0.0014	72 0.0014	82 0.0014	92 0.0014	69 1.013		
33	CLOUDWALK-MT-000	171 2048	250 870	37 0.0018	93 0.0018	103 0.0018	113 0.0018	128 0.0018	89 1.016		
34	COGENT-000	59 525	135 551	193 0.0105	214 0.0096	219 0.0095	165 0.0032	157 0.0024	211 1.088		
35	COGENT-001	60 525	136 552	192 0.0105	215 0.0096	220 0.0095	166 0.0032	158 0.0024	210 1.088		
36	COGENT-002	96 1043	283 987	12 0.0036	120 0.0022	118 0.0020	114 0.0018	111 0.0015	121 1.021		
37	COGENT-003	95 1043	280 960	127 0.0038	131 0.0024	127 0.0021	129 0.0019	123 0.0017	129 1.023		
38	COGENT-004	22 2053	277 952	70 0.0020	78 0.0016	80 0.0015	88 0.0015	90 0.0014	77 1.015		
39	COGENT-005	97 1062	215 774	31 0.0017	64 0.0014	65 0.0014	74 0.0014	84 0.0013	63 1.013		
40	COGNITEC-000	208 2052	28 176	228 0.0252	227 0.0136	228 0.0107	224 0.0085	214 0.0065	228 1.136		
41	COGNITEC-001	210 2052	40 202	200 0.0117	188 0.0062	187 0.0051	188 0.0042	185 0.0034	188 1.062		
42	COGNITEC-002	211 2052	45 227	159 0.0057	154 0.0037	156 0.0032	156 0.0029	166 0.0026	157 1.035		
43	COGNITEC-003	219 2052	63 297	160 0.0062	163 0.0040	166 0.0036	170 0.0033	177 0.0030	168 1.039		
44	COGNITEC-004	219 2052	36 192	118 0.0032	113 0.0020	104 0.0018	97 0.0015	93 0.0014	115 1.020		
45	COGNITEC-005	208 2052	77 367	48 0.0016	42 0.0013	41 0.0012	42 0.0012	46 0.0011	45 1.012		
46	COGNITEC-006	215 2052	111 463	44 0.0016	41 0.0013	39 0.0012	41 0.0012	45 0.0011	39 1.012		
47	CUBOX-000	148 2048	269 918	36 0.0014	54 0.0014	66 0.0014	75 0.0014	85 0.0014	51 1.012		
48	CYBERLINK-000	218 2052	182 699	128 0.0040	141 0.0028	145 0.0026	148 0.0024	149 0.0022	140 1.027		
49	CYBERLINK-001	209 2052	103 433	12 0.0035	126 0.0023	125 0.0021	119 0.0018	124 0.0017	124 1.022		
50	CYBERLINK-002	27 4140	205 738	105 0.0026	122 0.0023	131 0.0022	139 0.0021	143 0.0021	119 1.021		
51	CYBERLINK-003	271 6212	181 696	4 0.0016	45 0.0013	47 0.0013	47 0.0012	48 0.0012	48 1.012		
52	CYBERLINK-004	281 6212	204 738	50 0.0017	71 0.0015	78 0.0015	84 0.0014	95 0.0014	67 1.014		
53	CYBERLINK-005	260 6212	206 739	60 0.0018	79 0.0016	85 0.0015	93 0.0015	96 0.0014	74 1.015		
54	DAHUA-000	181 2048	83 378	158 0.0093	191 0.0066	195 0.0061	201 0.0057	205 0.0054	189 1.062		
55	DAHUA-001	157 2048	79 371	164 0.0067	164 0.0040	168 0.0036	168 0.0033	172 0.0029	164 1.040		
56	DAHUA-002	159 2048	183 699	6 0.0018	68 0.0015	75 0.0014	79 0.0014	83 0.0013	68 1.014		
57	DAHUA-003	181 2048	200 725	21 0.0012	13 0.0010	13 0.0009	12 0.0009	12 0.0009	12 1.009		
58	DAHUA-004	180 2048	208 759	11 0.0011	12 0.0010	14 0.0009	14 0.0009	15 0.0009	11 1.009		
59	DAON-000	230 2069	141 584	132 0.0041	156 0.0038	167 0.0037	177 0.0037	188 0.0036	152 1.034		
60	DECATAR-000	217 2052	252 874	80 0.0021	80 0.0016	84 0.0015	81 0.0014	76 0.0013	80 1.015		
61	DEEPLINT-001	269 4096	172 687	35 0.0014	33 0.0014	57 0.0013	64 0.0013	71 0.0013	50 1.012		
62	DEEPSSEA-001	19 2048	218 780	13 0.0043	121 0.0022	107 0.0018	102 0.0016	87 0.0014	125 1.022		
63	DERMALOG-003	14 128	43 211	262 0.1259	261 0.0744	260 0.0603	259 0.0480	258 0.0347	261 1.731		
64	DERMALOG-004	15 128	41 208	26 0.1251	260 0.0739	259 0.0598	258 0.0475	257 0.0343	260 1.727		
65	DERMALOG-005	16 128	128 532	211 0.0149	224 0.0129	227 0.0125	233 0.0123	239 0.0122	221 1.118		
66	DERMALOG-006	25 256	126 514	17 0.0081	194 0.0069	197 0.0066	205 0.0065	213 0.0063	192 1.063		
67	DERMALOG-007	13 128	96 413	18 0.0092	192 0.0066	193 0.0060	200 0.0057	207 0.0054	196 1.062		
68	DERMALOG-008	44 512	78 370	111 0.0029	109 0.0020	106 0.0018	105 0.0017	108 0.0015	110 1.019		
69	DERMALOG-009	45 512	74 347	110 0.0028	129 0.0024	135 0.0023	142 0.0023	150 0.0022	125 1.022		
70	EYEDEA-003	92 1036	85 385	256 0.0800	253 0.0451	253 0.0362	249 0.0289	249 0.0211	254 1.448		
71	F8-001	136 2048	241 851	20 0.0120	216 0.0105	223 0.0102	226 0.0100	231 0.0099	216 1.096		
72	FINCORE-000	170 2048	116 477	195 0.0108	180 0.0052	176 0.0042	174 0.0034	167 0.0026	181 1.054		

Table 23: **Rank-based accuracy for the FRVT 2018 mugshot sets.** In columns 3 and 4 are template size and template generation duration. Thereafter values are rank-based FNIR with  $T = 0$  and FPIR = 1. This is appropriate to investigational uses but not those with higher volumes where candidates from all searches would need review. The next column is a workload statistic, a small value shows an algorithm front-loads mates into the first 10 candidates. Throughout, blue superscripts indicate the rank of the algorithm for that column, and the best value is highlighted in yellow.

MISSES OUTSIDE RANK R		RESOURCE USAGE		ENROL MOST RECENT, N = 1.6M					
#	ALGORITHM	BYTES	MSEC	R=1	R=5	R=10	R=20	R=50	WORK-10
73	FUJITSULAB-000	<sup>89</sup> 1032	<sup>276</sup> 950	<sup>86</sup> 0.0022	<sup>86</sup> 0.0016	<sup>87</sup> 0.0015	<sup>86</sup> 0.0015	<sup>86</sup> 0.0014	<sup>87</sup> 1.015
74	FUJITSULAB-001	<sup>2</sup> 0	<sup>4</sup> 1	<sup>68</sup> 0.0019	<sup>75</sup> 0.0015	<sup>81</sup> 0.0015	<sup>80</sup> 0.0014	<sup>88</sup> 0.0014	<sup>71</sup> 1.014
75	GLORY-000	<sup>41</sup> 418	<sup>24</sup> 160	<sup>260</sup> 0.1781	<sup>268</sup> 0.1391	<sup>268</sup> 0.1266	<sup>268</sup> 0.1154	<sup>268</sup> 0.1007	<sup>267</sup> 2.298
76	GLORY-001	<sup>120</sup> 1726	<sup>91</sup> 405	<sup>263</sup> 0.1268	<sup>263</sup> 0.0967	<sup>263</sup> 0.0869	<sup>264</sup> 0.0778	<sup>265</sup> 0.0673	<sup>267</sup> 1.903
77	GORILLA-001	<sup>240</sup> 2156	<sup>27</sup> 169	<sup>249</sup> 0.0603	<sup>244</sup> 0.0304	<sup>244</sup> 0.0230	<sup>243</sup> 0.0174	<sup>234</sup> 0.0117	<sup>244</sup> 1.309
78	GORILLA-002	<sup>101</sup> 1132	<sup>72</sup> 341	<sup>223</sup> 0.0197	<sup>211</sup> 0.0092	<sup>201</sup> 0.0070	<sup>196</sup> 0.0054	<sup>194</sup> 0.0041	<sup>212</sup> 1.096
79	GORILLA-003	<sup>239</sup> 2156	<sup>139</sup> 563	<sup>236</sup> 0.0361	<sup>229</sup> 0.0146	<sup>223</sup> 0.0106	<sup>218</sup> 0.0078	<sup>206</sup> 0.0054	<sup>231</sup> 1.158
80	GORILLA-004	<sup>241</sup> 2192	<sup>87</sup> 395	<sup>161</sup> 0.0063	<sup>150</sup> 0.0032	<sup>146</sup> 0.0026	<sup>143</sup> 0.0023	<sup>129</sup> 0.0018	<sup>151</sup> 1.033
81	GORILLA-005	<sup>282</sup> 6288	<sup>119</sup> 483	<sup>117</sup> 0.0032	<sup>99</sup> 0.0019	<sup>96</sup> 0.0017	<sup>89</sup> 0.0015	<sup>69</sup> 0.0013	<sup>108</sup> 1.018
82	GORILLA-006	<sup>284</sup> 8336	<sup>211</sup> 768	<sup>36</sup> 0.0017	<sup>40</sup> 0.0013	<sup>36</sup> 0.0012	<sup>39</sup> 0.0012	<sup>40</sup> 0.0011	<sup>47</sup> 1.012
83	GORILLA-007	<sup>9</sup> 0	<sup>9</sup> 6	<sup>52</sup> 0.0017	<sup>36</sup> 0.0012	<sup>36</sup> 0.0012	<sup>33</sup> 0.0011	<sup>32</sup> 0.0011	<sup>37</sup> 1.012
84	GRIAULE-000	<sup>212</sup> 2052	<sup>98</sup> 419	<sup>10</sup> 0.0025	<sup>10</sup> 0.0020	<sup>11</sup> 0.0019	<sup>11</sup> 0.0018	<sup>11</sup> 0.0017	<sup>10</sup> 1.018
85	HIK-003	<sup>107</sup> 1408	<sup>152</sup> 633	<sup>201</sup> 0.0117	<sup>186</sup> 0.0060	<sup>185</sup> 0.0048	<sup>185</sup> 0.0039	<sup>176</sup> 0.0030	<sup>187</sup> 1.061
86	HIK-004	<sup>102</sup> 1152	<sup>124</sup> 510	<sup>198</sup> 0.0113	<sup>185</sup> 0.0059	<sup>180</sup> 0.0047	<sup>178</sup> 0.0037	<sup>173</sup> 0.0030	<sup>186</sup> 1.060
87	HIK-005	<sup>108</sup> 1408	<sup>149</sup> 619	<sup>142</sup> 0.0046	<sup>133</sup> 0.0025	<sup>121</sup> 0.0020	<sup>108</sup> 0.0017	<sup>105</sup> 0.0015	<sup>133</sup> 1.025
88	HIK-006	<sup>109</sup> 1408	<sup>145</sup> 610	<sup>141</sup> 0.0046	<sup>134</sup> 0.0025	<sup>122</sup> 0.0020	<sup>109</sup> 0.0017	<sup>104</sup> 0.0015	<sup>134</sup> 1.025
89	HYPERVERGE-001	<sup>78</sup> 1024	<sup>240</sup> 846	<sup>25</sup> 0.0014	<sup>44</sup> 0.0013	<sup>50</sup> 0.0013	<sup>59</sup> 0.0013	<sup>74</sup> 0.0013	<sup>41</sup> 1.012
90	HYPERVERGE-002	<sup>7</sup> 0	<sup>5</sup> 1	<sup>25</sup> 0.0014	<sup>43</sup> 0.0013	<sup>51</sup> 0.0013	<sup>58</sup> 0.0013	<sup>61</sup> 0.0013	<sup>40</sup> 1.012
91	HZAILU-000	<sup>8</sup> 0	<sup>2</sup> 1	<sup>85</sup> 0.0022	<sup>83</sup> 0.0016	<sup>88</sup> 0.0015	<sup>91</sup> 0.0015	<sup>95</sup> 0.0014	<sup>89</sup> 1.015
92	IDEMIA-003	<sup>62</sup> 528	<sup>173</sup> 689	<sup>167</sup> 0.0069	<sup>171</sup> 0.0045	<sup>171</sup> 0.0039	<sup>173</sup> 0.0034	<sup>170</sup> 0.0027	<sup>168</sup> 1.043
93	IDEMIA-004	<sup>6</sup> 528	<sup>165</sup> 669	<sup>163</sup> 0.0066	<sup>160</sup> 0.0038	<sup>158</sup> 0.0032	<sup>155</sup> 0.0027	<sup>144</sup> 0.0021	<sup>158</sup> 1.038
94	IDEMIA-005	<sup>39</sup> 352	<sup>81</sup> 374	<sup>126</sup> 0.0081	<sup>167</sup> 0.0044	<sup>165</sup> 0.0036	<sup>167</sup> 0.0032	<sup>122</sup> 0.0030	<sup>171</sup> 1.044
95	IDEMIA-006	<sup>4</sup> 352	<sup>80</sup> 373	<sup>18</sup> 0.0096	<sup>179</sup> 0.0052	<sup>177</sup> 0.0042	<sup>183</sup> 0.0039	<sup>188</sup> 0.0037	<sup>178</sup> 1.052
96	IDEMIA-007	<sup>72</sup> 860	<sup>223</sup> 807	<sup>102</sup> 0.0026	<sup>81</sup> 0.0016	<sup>71</sup> 0.0014	<sup>57</sup> 0.0013	<sup>52</sup> 0.0012	<sup>86</sup> 1.015
97	IDEMIA-008	<sup>3</sup> 300	<sup>10</sup> 6451	<sup>10</sup> 0.0011	<sup>8</sup> 0.0009	<sup>12</sup> 0.0009	<sup>15</sup> 0.0009	<sup>14</sup> 0.0009	<sup>3</sup> 1.009
98	IDEMIA-009	<sup>4</sup> 0	<sup>1</sup> 0	<sup>4</sup> 0.0010	<sup>4</sup> 0.0009	<sup>7</sup> 0.0009	<sup>10</sup> 0.0009	<sup>10</sup> 0.0009	<sup>4</sup> 1.008
99	IMAGUS-002	<sup>51</sup> 512	<sup>16</sup> 76	<sup>269</sup> 0.2203	<sup>267</sup> 0.1342	<sup>266</sup> 0.1090	<sup>265</sup> 0.0871	<sup>263</sup> 0.0632	<sup>268</sup> 2.308
100	IMAGUS-003	<sup>49</sup> 512	<sup>14</sup> 57	<sup>274</sup> 0.3559	<sup>274</sup> 0.2491	<sup>277</sup> 0.2132	<sup>274</sup> 0.1791	<sup>274</sup> 0.1397	<sup>273</sup> 3.363
101	IMAGUS-005	<sup>149</sup> 2048	<sup>220</sup> 788	<sup>73</sup> 0.0019	<sup>82</sup> 0.0016	<sup>79</sup> 0.0015	<sup>78</sup> 0.0014	<sup>82</sup> 0.0013	<sup>79</sup> 1.015
102	IMAGUS-006	<sup>139</sup> 2048	<sup>263</sup> 905	<sup>78</sup> 0.0020	<sup>87</sup> 0.0016	<sup>90</sup> 0.0015	<sup>98</sup> 0.0014	<sup>81</sup> 1.015	
103	IMAGUS-007	<sup>127</sup> 2048	<sup>143</sup> 590	<sup>79</sup> 0.0020	<sup>70</sup> 0.0015	<sup>68</sup> 0.0014	<sup>61</sup> 0.0013	<sup>69</sup> 1.014	
104	IMPERIAL-000	<sup>129</sup> 2048	<sup>161</sup> 654	<sup>99</sup> 0.0024	<sup>101</sup> 0.0019	<sup>108</sup> 0.0018	<sup>115</sup> 0.0018	<sup>121</sup> 0.0017	<sup>108</sup> 1.018
105	INCODE-000	<sup>76</sup> 1024	<sup>34</sup> 190	<sup>246</sup> 0.0489	<sup>241</sup> 0.0261	<sup>242</sup> 0.0204	<sup>240</sup> 0.0160	<sup>237</sup> 0.0117	<sup>241</sup> 1.262
106	INCODE-001	<sup>144</sup> 2048	<sup>176</sup> 690	<sup>214</sup> 0.1616	<sup>205</sup> 0.0084	<sup>198</sup> 0.0067	<sup>198</sup> 0.0055	<sup>197</sup> 0.0043	<sup>208</sup> 1.086
107	INCODE-002	<sup>171</sup> 2048	<sup>261</sup> 291	<sup>218</sup> 0.0178	<sup>208</sup> 0.0090	<sup>202</sup> 0.0070	<sup>199</sup> 0.0056	<sup>198</sup> 0.0043	<sup>217</sup> 1.092
108	INCODE-003	<sup>189</sup> 2048	<sup>184</sup> 704	<sup>28</sup> 0.0129	<sup>190</sup> 0.0064	<sup>186</sup> 0.0051	<sup>186</sup> 0.0040	<sup>178</sup> 0.0031	<sup>194</sup> 1.066
109	INCODE-004	<sup>177</sup> 2048	<sup>123</sup> 508	<sup>124</sup> 0.0035	<sup>127</sup> 0.0024	<sup>129</sup> 0.0021	<sup>132</sup> 0.0020	<sup>132</sup> 0.0019	<sup>120</sup> 1.023
110	INCODE-005	<sup>176</sup> 2048	<sup>122</sup> 500	<sup>49</sup> 0.0017	<sup>55</sup> 0.0014	<sup>63</sup> 0.0014	<sup>62</sup> 0.0013	<sup>58</sup> 0.0013	<sup>61</sup> 1.013
111	INNOVATRICS-002	<sup>65</sup> 530	<sup>50</sup> 255	<sup>244</sup> 0.0451	<sup>247</sup> 0.0342	<sup>240</sup> 0.0322	<sup>251</sup> 0.0308	<sup>253</sup> 0.0297	<sup>248</sup> 1.321
112	INNOVATRICS-003	<sup>64</sup> 530	<sup>51</sup> 255	<sup>230</sup> 0.0263	<sup>222</sup> 0.0126	<sup>218</sup> 0.0095	<sup>213</sup> 0.0074	<sup>205</sup> 0.0053	<sup>225</sup> 1.129
113	INNOVATRICS-004	<sup>98</sup> 1076	<sup>93</sup> 406	<sup>205</sup> 0.0123	<sup>189</sup> 0.0063	<sup>186</sup> 0.0050	<sup>187</sup> 0.0040	<sup>181</sup> 0.0032	<sup>197</sup> 1.064
114	INNOVATRICS-005	<sup>67</sup> 538	<sup>238</sup> 842	<sup>100</sup> 0.0024	<sup>95</sup> 0.0018	<sup>97</sup> 0.0017	<sup>101</sup> 0.0016	<sup>92</sup> 0.0014	<sup>95</sup> 1.017
115	INNOVATRICS-007	<sup>69</sup> 538	<sup>219</sup> 785	<sup>38</sup> 0.0017	<sup>59</sup> 0.0014	<sup>56</sup> 0.0013	<sup>54</sup> 0.0013	<sup>66</sup> 0.0012	<sup>58</sup> 1.013
116	INTELLIVISION-001	<sup>5</sup> 0	<sup>7</sup> 2	<sup>237</sup> 0.0365	<sup>239</sup> 0.0199	<sup>235</sup> 0.0160	<sup>234</sup> 0.0126	<sup>230</sup> 0.0095	<sup>237</sup> 1.199
117	INTSYSMSU-000	<sup>135</sup> 2048	<sup>169</sup> 675	<sup>261</sup> 0.1457	<sup>266</sup> 0.1320	<sup>267</sup> 0.1227	<sup>269</sup> 0.1163	<sup>266</sup> 2.203	
118	IREX-000	<sup>248</sup> 3080	<sup>295</sup> 2379	<sup>138</sup> 0.0044	<sup>163</sup> 0.0043	<sup>179</sup> 0.0043	<sup>189</sup> 0.0043	<sup>196</sup> 0.0043	<sup>163</sup> 1.039
119	ISYSTEMS-002	<sup>150</sup> 2048	<sup>68</sup> 316	<sup>162</sup> 0.0064	<sup>166</sup> 0.0043	<sup>171</sup> 0.0039	<sup>176</sup> 0.0037	<sup>186</sup> 0.0034	<sup>167</sup> 1.041
120	ISYSTEMS-003	<sup>167</sup> 2048	<sup>243</sup> 856	<sup>150</sup> 0.0052	<sup>161</sup> 0.0039	<sup>166</sup> 0.0036	<sup>175</sup> 0.0034	<sup>182</sup> 0.0033	<sup>157</sup> 1.037
121	KAKAO-000	<sup>206</sup> 2052	<sup>243</sup> 840	<sup>36</sup> 0.0015	<sup>27</sup> 0.0011	<sup>27</sup> 0.0011	<sup>22</sup> 0.0010	<sup>25</sup> 0.0010	<sup>28</sup> 1.010
122	KEDACOM-001	<sup>37</sup> 292	<sup>130</sup> 537	<sup>172</sup> 0.0077	<sup>197</sup> 0.0074	<sup>203</sup> 0.0073	<sup>210</sup> 0.0072	<sup>218</sup> 0.0072	<sup>195</sup> 1.067
123	KNERON-000	<sup>198</sup> 2048	<sup>127</sup> 530	<sup>15</sup> 0.0059	<sup>184</sup> 0.0059	<sup>19</sup> 0.0059	<sup>202</sup> 0.0059	<sup>205</sup> 0.0059	<sup>180</sup> 1.053
124	KNERON-001	<sup>164</sup> 2048	<sup>115</sup> 468	<sup>233</sup> 0.0295	<sup>243</sup> 0.0295	<sup>248</sup> 0.0295	<sup>250</sup> 0.0295	<sup>252</sup> 0.0295	<sup>242</sup> 1.266
125	LINE-000	<sup>132</sup> 2048	<sup>482</sup> 482	<sup>87</sup> 0.0022	<sup>76</sup> 0.0015	<sup>69</sup> 0.0014	<sup>52</sup> 0.0013	<sup>45</sup> 0.0012	<sup>78</sup> 1.015
126	LINE-001	<sup>138</sup> 2048	<sup>267</sup> 910	<sup>15</sup> 0.0011	<sup>17</sup> 0.0010	<sup>20</sup> 0.0010	<sup>18</sup> 0.0009	<sup>19</sup> 0.0009	<sup>16</sup> 1.009
127	LOOKMAN-003	<sup>36</sup> 292	<sup>73</sup> 342	<sup>181</sup> 0.0088	<sup>201</sup> 0.0078	<sup>209</sup> 0.0076	<sup>215</sup> 0.0075	<sup>221</sup> 0.0074	<sup>198</sup> 1.071
128	LOOKMAN-004	<sup>69</sup> 548	<sup>69</sup> 325	<sup>183</sup> 0.0091	<sup>202</sup> 0.0079	<sup>206</sup> 0.0076	<sup>214</sup> 0.0075	<sup>227</sup> 0.0073	<sup>199</sup> 1.072
129	LOOKMAN-005	<sup>70</sup> 548	<sup>125</sup> 514	<sup>175</sup> 0.0080	<sup>199</sup> 0.0075	<sup>206</sup> 0.0074	<sup>212</sup> 0.0073	<sup>218</sup> 0.0072	<sup>196</sup> 1.068
130	MANTRA-000	<sup>209</sup> 2052	<sup>94</sup> 412	<sup>35</sup> 0.0017	<sup>50</sup> 0.0013	<sup>52</sup> 0.0013	<sup>51</sup> 0.0012	<sup>54</sup> 0.0012	<sup>57</sup> 1.013
131	MEGVII-001	<sup>264</sup> 4096	<sup>157</sup> 652	<sup>202</sup> 0.0118	<sup>212</sup> 0.0093	<sup>212</sup> 0.0087	<sup>222</sup> 0.0084	<sup>227</sup> 0.0080	<sup>207</sup> 1.086
132	MEGVII-002	<sup>260</sup> 4096	<sup>162</sup> 656	<sup>203</sup> 0.0118	<sup>213</sup> 0.0093	<sup>217</sup> 0.0088	<sup>221</sup> 0.0084	<sup>229</sup> 0.0080	<sup>206</sup> 1.087
133	MICROFOCUS-003	<sup>24</sup> 256	<sup>269</sup> 281	<sup>281</sup> 0.5942	<sup>280</sup> 0.4692	<sup>280</sup> 0.4204	<sup>280</sup> 0.3724	<sup>280</sup> 0.3095	<sup>281</sup> 5.361
134	MICROFOCUS-004	<sup>25</sup> 256	<sup>270</sup> 270	<sup>270</sup> 0.5763	<sup>279</sup> 0.4519	<sup>277</sup> 0.4026	<sup>279</sup> 0.3560	<sup>275</sup> 0.2957	<sup>275</sup> 5.199
135	MICROFOCUS-005	<sup>30</sup> 256	<sup>55</sup> 266	<sup>275</sup> 0.4242	<sup>275</sup> 0.3028	<sup>275</sup> 0.2606	<sup>275</sup> 0.2209	<sup>276</sup> 0.1724	<sup>275</sup> 3.861
136	MICROFOCUS-006	<sup>25</sup> 256	<sup>54</sup> 265	<sup>274</sup> 0.4268	<sup>276</sup> 0.3049	<sup>276</sup> 0.2623	<sup>277</sup> 0.2233	<sup>277</sup> 0.1746	<sup>275</sup> 3.880
137	MICROSOFT-003	<sup>82</sup> 1024	<sup>90</sup> 404	<sup>46</sup> 0.0016	<sup>16</sup> 0.0010	<sup>8</sup> 0.0009	<sup>3</sup> 0.0008	<sup>2</sup> 0.0006	<sup>17</sup> 1.009
138	MICROSOFT-004	<sup>158</sup> 2048	<sup>214</sup> 773	<sup>38</sup> 0.0015	<sup>10</sup> 0.				

MISSES OUTSIDE RANK R		RESOURCE USAGE		ENROL MOST RECENT, N = 1.6M					
#	ALGORITHM	BYTES	MSEC	R=1	R=5	R=10	R=20	R=50	WORK-10
145	NEC-004	<sup>100</sup> 1104	<sup>28</sup> 967	<sup>35</sup> 0.0014	<sup>51</sup> 0.0013	<sup>64</sup> 0.0013	<sup>65</sup> 0.0013	<sup>70</sup> 0.0013	<sup>4</sup> 1.012
146	NEC-005	<sup>99</sup> 1104	<sup>28</sup> 964	<sup>19</sup> 0.0012	<sup>28</sup> 0.0011	<sup>30</sup> 0.0011	<sup>34</sup> 0.0011	<sup>39</sup> 0.0011	<sup>27</sup> 1.010
147	NEUROTECHNOLOGY-003	<sup>155</sup> 2048	<sup>133</sup> 547	<sup>225</sup> 0.0225	<sup>223</sup> 0.0126	<sup>22</sup> 0.0100	<sup>219</sup> 0.0078	<sup>208</sup> 0.0057	<sup>224</sup> 1.125
148	NEUROTECHNOLOGY-004	<sup>180</sup> 2048	<sup>132</sup> 543	<sup>152</sup> 0.0056	<sup>153</sup> 0.0036	<sup>159</sup> 0.0032	<sup>160</sup> 0.0029	<sup>159</sup> 0.0025	<sup>154</sup> 1.035
149	NEUROTECHNOLOGY-005	<sup>26</sup> 256	<sup>412</sup> 746	<sup>136</sup> 0.0043	<sup>143</sup> 0.0029	<sup>147</sup> 0.0027	<sup>147</sup> 0.0024	<sup>153</sup> 0.0023	<sup>144</sup> 1.028
150	NEUROTECHNOLOGY-006	<sup>28</sup> 256	<sup>20</sup> 746	<sup>219</sup> 0.0180	<sup>203</sup> 0.0079	<sup>191</sup> 0.0059	<sup>191</sup> 0.0046	<sup>188</sup> 0.0033	<sup>205</sup> 1.083
151	NEUROTECHNOLOGY-007	<sup>31</sup> 256	<sup>26</sup> 169	<sup>128</sup> 0.0039	<sup>138</sup> 0.0027	<sup>143</sup> 0.0025	<sup>144</sup> 0.0023	<sup>144</sup> 0.0022	<sup>156</sup> 1.026
152	NEUROTECHNOLOGY-008	<sup>58</sup> 514	<sup>227</sup> 804	<sup>84</sup> 0.0022	<sup>72</sup> 0.0015	<sup>78</sup> 0.0014	<sup>76</sup> 0.0014	<sup>77</sup> 0.0013	<sup>73</sup> 1.015
153	NEUROTECHNOLOGY-009	<sup>52</sup> 513	<sup>171</sup> 686	<sup>34</sup> 0.0014	<sup>35</sup> 0.0012	<sup>37</sup> 0.0012	<sup>38</sup> 0.0011	<sup>42</sup> 0.0011	<sup>34</sup> 1.011
154	NEUROTECHNOLOGY-010	<sup>23</sup> 256	<sup>164</sup> 663	<sup>22</sup> 0.0012	<sup>21</sup> 0.0011	<sup>24</sup> 0.0010	<sup>23</sup> 0.0010	<sup>36</sup> 0.0010	<sup>21</sup> 1.010
155	NEWLAND-002	<sup>152</sup> 2048	<sup>248</sup> 868	<sup>255</sup> 0.0786	<sup>253</sup> 0.0480	<sup>254</sup> 0.0397	<sup>254</sup> 0.0332	<sup>251</sup> 0.0263	<sup>256</sup> 1.468
156	NOBLIS-001	<sup>152</sup> 2048	<sup>42</sup> 211	<sup>271</sup> 0.2492	<sup>271</sup> 0.1772	<sup>271</sup> 0.1542	<sup>271</sup> 0.1339	<sup>269</sup> 0.1112	<sup>27</sup> 2.679
157	NOBLIS-002	<sup>278</sup> 6144	<sup>129</sup> 535	<sup>267</sup> 0.1794	<sup>264</sup> 0.1108	<sup>264</sup> 0.0903	<sup>263</sup> 0.0722	<sup>262</sup> 0.0535	<sup>264</sup> 2.077
158	NOTIONTAG-000	<sup>238</sup> 2120	<sup>116</sup> 461	<sup>98</sup> 0.0024	<sup>117</sup> 0.0021	<sup>124</sup> 0.0021	<sup>135</sup> 0.0020	<sup>139</sup> 0.0019	<sup>111</sup> 1.019
159	NTECHLAB-003	<sup>252</sup> 3484	<sup>231</sup> 831	<sup>158</sup> 0.0062	<sup>146</sup> 0.0029	<sup>159</sup> 0.0023	<sup>130</sup> 0.0019	<sup>114</sup> 0.0016	<sup>149</sup> 1.030
160	NTECHLAB-004	<sup>234</sup> 3484	<sup>270</sup> 929	<sup>145</sup> 0.0048	<sup>124</sup> 0.0023	<sup>117</sup> 0.0019	<sup>104</sup> 0.0016	<sup>86</sup> 0.0013	<sup>152</sup> 1.024
161	NTECHLAB-005	<sup>123</sup> 1940	<sup>196</sup> 717	<sup>143</sup> 0.0047	<sup>119</sup> 0.0022	<sup>101</sup> 0.0017	<sup>66</sup> 0.0013	<sup>36</sup> 0.0011	<sup>127</sup> 1.023
162	NTECHLAB-006	<sup>124</sup> 1940	<sup>236</sup> 841	<sup>133</sup> 0.0041	<sup>100</sup> 0.0019	<sup>82</sup> 0.0015	<sup>44</sup> 0.0012	<sup>18</sup> 0.0009	<sup>114</sup> 1.019
163	NTECHLAB-007	<sup>250</sup> 3348	<sup>234</sup> 834	<sup>104</sup> 0.0027	<sup>88</sup> 0.0017	<sup>78</sup> 0.0014	<sup>70</sup> 0.0013	<sup>56</sup> 0.0012	<sup>90</sup> 1.016
164	NTECHLAB-008	<sup>106</sup> 1300	<sup>137</sup> 562	<sup>54</sup> 0.0017	<sup>34</sup> 0.0012	<sup>35</sup> 0.0012	<sup>35</sup> 0.0011	<sup>34</sup> 0.0010	<sup>38</sup> 1.012
165	NTECHLAB-009	<sup>105</sup> 1300	<sup>261</sup> 900	<sup>24</sup> 0.0013	<sup>23</sup> 0.0011	<sup>25</sup> 0.0010	<sup>21</sup> 0.0010	<sup>25</sup> 0.0009	<sup>25</sup> 1.010
166	NTECHLAB-010	<sup>103</sup> 1280	<sup>253</sup> 875	<sup>14</sup> 0.0011	<sup>20</sup> 0.0010	<sup>21</sup> 0.0010	<sup>24</sup> 0.0010	<sup>33</sup> 0.0010	<sup>18</sup> 1.009
167	NTECHLAB-011	<sup>104</sup> 1280	<sup>246</sup> 865	<sup>8</sup> 0.0010	<sup>2</sup> 0.0009	<sup>1</sup> 0.0009	<sup>15</sup> 0.0009	<sup>7</sup> 0.0009	<sup>1</sup> 1.008
168	PANGIAM-000	<sup>1</sup> 0	<sup>8</sup> 2	<sup>20</sup> 0.0012	<sup>24</sup> 0.0011	<sup>26</sup> 0.0011	<sup>27</sup> 0.0010	<sup>31</sup> 0.0010	<sup>24</sup> 1.010
169	PARAVISION-000	<sup>128</sup> 2048	<sup>105</sup> 438	<sup>220</sup> 0.1888	<sup>235</sup> 0.0171	<sup>23</sup> 0.0167	<sup>242</sup> 0.0165	<sup>24</sup> 0.0164	<sup>23</sup> 1.156
170	PARAVISION-001	<sup>196</sup> 2048	<sup>142</sup> 590	<sup>126</sup> 0.0038	<sup>130</sup> 0.0024	<sup>130</sup> 0.0022	<sup>136</sup> 0.0020	<sup>131</sup> 0.0019	<sup>130</sup> 1.023
171	PARAVISION-002	<sup>147</sup> 2048	<sup>82</sup> 377	<sup>131</sup> 0.0040	<sup>135</sup> 0.0025	<sup>135</sup> 0.0022	<sup>138</sup> 0.0021	<sup>133</sup> 0.0019	<sup>133</sup> 1.025
172	PARAVISION-003	<sup>192</sup> 2048	<sup>202</sup> 735	<sup>116</sup> 0.0031	<sup>118</sup> 0.0022	<sup>122</sup> 0.0020	<sup>126</sup> 0.0019	<sup>128</sup> 0.0017	<sup>118</sup> 1.021
173	PARAVISION-004	<sup>265</sup> 4096	<sup>199</sup> 720	<sup>47</sup> 0.0016	<sup>58</sup> 0.0014	<sup>62</sup> 0.0013	<sup>68</sup> 0.0013	<sup>75</sup> 0.0013	<sup>57</sup> 1.013
174	PARAVISION-005	<sup>263</sup> 4096	<sup>244</sup> 858	<sup>40</sup> 0.0015	<sup>56</sup> 0.0014	<sup>61</sup> 0.0013	<sup>69</sup> 0.0013	<sup>79</sup> 0.0013	<sup>52</sup> 1.013
175	PARAVISION-007	<sup>256</sup> 4096	<sup>187</sup> 706	<sup>17</sup> 0.0012	<sup>25</sup> 0.0011	<sup>25</sup> 0.0010	<sup>26</sup> 0.0010	<sup>27</sup> 0.0010	<sup>21</sup> 1.010
176	PARAVISION-009	<sup>268</sup> 4100	<sup>153</sup> 638	<sup>7</sup> 0.0010	<sup>11</sup> 0.0010	<sup>13</sup> 0.0010	<sup>20</sup> 0.0009	<sup>26</sup> 0.0009	<sup>11</sup> 1.009
177	PIXELLALL-002	<sup>245</sup> 2560	<sup>37</sup> 198	<sup>140</sup> 0.0045	<sup>144</sup> 0.0029	<sup>144</sup> 0.0025	<sup>141</sup> 0.0022	<sup>138</sup> 0.0019	<sup>145</sup> 1.028
178	PIXELLALL-003	<sup>247</sup> 2560	<sup>199</sup> 719	<sup>83</sup> 0.0021	<sup>84</sup> 0.0016	<sup>88</sup> 0.0015	<sup>85</sup> 0.0014	<sup>94</sup> 0.0014	<sup>81</sup> 1.015
179	PIXELLALL-004	<sup>242</sup> 2560	<sup>105</sup> 453	<sup>80</sup> 0.0020	<sup>74</sup> 0.0015	<sup>77</sup> 0.0015	<sup>83</sup> 0.0014	<sup>81</sup> 0.0013	<sup>73</sup> 1.014
180	PIXELLALL-005	<sup>243</sup> 2560	<sup>239</sup> 845	<sup>70</sup> 0.0019	<sup>90</sup> 0.0017	<sup>92</sup> 0.0016	<sup>103</sup> 0.0016	<sup>113</sup> 0.0016	<sup>92</sup> 1.015
181	PTAKURATSATU-000	<sup>66</sup> 538	<sup>268</sup> 910	<sup>114</sup> 0.0030	<sup>116</sup> 0.0021	<sup>117</sup> 0.0019	<sup>112</sup> 0.0018	<sup>111</sup> 0.0016	<sup>116</sup> 1.020
182	QNAP-000	<sup>190</sup> 2048	<sup>108</sup> 457	<sup>173</sup> 0.0078	<sup>168</sup> 0.0044	<sup>169</sup> 0.0037	<sup>169</sup> 0.0033	<sup>171</sup> 0.0028	<sup>169</sup> 1.043
183	QNAP-001	<sup>156</sup> 2048	<sup>146</sup> 615	<sup>134</sup> 0.0041	<sup>145</sup> 0.0029	<sup>148</sup> 0.0027	<sup>150</sup> 0.0025	<sup>156</sup> 0.0023	<sup>142</sup> 1.028
184	QNAP-002	<sup>6</sup> 0	<sup>5</sup> 2	<sup>146</sup> 0.0049	<sup>169</sup> 0.0044	<sup>180</sup> 0.0043	<sup>190</sup> 0.0043	<sup>195</sup> 0.0042	<sup>165</sup> 1.040
185	QUANTASOFT-001	<sup>145</sup> 2048	<sup>89</sup> 396	<sup>268</sup> 0.2177	<sup>270</sup> 0.1643	<sup>270</sup> 0.1468	<sup>270</sup> 0.1312	<sup>270</sup> 0.1116	<sup>250</sup> 1.539
186	RANKONE-002	<sup>183</sup> 133	<sup>211</sup> 113	<sup>222</sup> 0.0194	<sup>217</sup> 0.0112	<sup>217</sup> 0.0093	<sup>217</sup> 0.0077	<sup>212</sup> 0.0060	<sup>217</sup> 1.111
187	RANKONE-003	<sup>17</sup> 133	<sup>22</sup> 114	<sup>221</sup> 0.0194	<sup>218</sup> 0.0112	<sup>216</sup> 0.0093	<sup>216</sup> 0.0077	<sup>217</sup> 0.0060	<sup>218</sup> 1.111
188	RANKONE-004	<sup>10</sup> 85	<sup>13</sup> 36	<sup>243</sup> 0.0415	<sup>240</sup> 0.0226	<sup>240</sup> 0.0177	<sup>236</sup> 0.0141	<sup>233</sup> 0.0102	<sup>240</sup> 1.225
189	RANKONE-005	<sup>19</sup> 133	<sup>19</sup> 94	<sup>187</sup> 0.0094	<sup>182</sup> 0.0054	<sup>182</sup> 0.0046	<sup>184</sup> 0.0039	<sup>174</sup> 0.0032	<sup>18</sup> 1.054
190	RANKONE-006	<sup>21</sup> 165	<sup>52</sup> 261	<sup>148</sup> 0.0050	<sup>149</sup> 0.0030	<sup>149</sup> 0.0027	<sup>146</sup> 0.0024	<sup>141</sup> 0.0021	<sup>148</sup> 1.030
191	RANKONE-007	<sup>20</sup> 165	<sup>57</sup> 278	<sup>120</sup> 0.0034	<sup>125</sup> 0.0023	<sup>125</sup> 0.0021	<sup>121</sup> 0.0018	<sup>117</sup> 0.0017	<sup>122</sup> 1.022
192	RANKONE-009	<sup>32</sup> 260	<sup>39</sup> 191	<sup>94</sup> 0.0024	<sup>89</sup> 0.0016	<sup>90</sup> 0.0015	<sup>92</sup> 0.0015	<sup>91</sup> 0.0014	<sup>87</sup> 1.015
193	RANKONE-010	<sup>33</sup> 261	<sup>38</sup> 200	<sup>88</sup> 0.0022	<sup>92</sup> 0.0018	<sup>94</sup> 0.0016	<sup>99</sup> 0.0015	<sup>101</sup> 0.0015	<sup>92</sup> 1.016
194	RANKONE-011	<sup>35</sup> 261	<sup>146</sup> 567	<sup>39</sup> 0.0015	<sup>38</sup> 0.0012	<sup>40</sup> 0.0012	<sup>43</sup> 0.0012	<sup>47</sup> 0.0012	<sup>36</sup> 1.011
195	RANKONE-012	<sup>34</sup> 261	<sup>138</sup> 563	<sup>28</sup> 0.0014	<sup>32</sup> 0.0012	<sup>33</sup> 0.0011	<sup>37</sup> 0.0011	<sup>43</sup> 0.0011	<sup>30</sup> 1.011
196	REALNETWORKS-000	<sup>269</sup> 4100	<sup>47</sup> 244	<sup>241</sup> 0.0402	<sup>238</sup> 0.0195	<sup>238</sup> 0.0149	<sup>229</sup> 0.0111	<sup>222</sup> 0.0077	<sup>238</sup> 1.201
197	REALNETWORKS-001	<sup>274</sup> 4104	<sup>46</sup> 243	<sup>242</sup> 0.0402	<sup>237</sup> 0.0195	<sup>234</sup> 0.0149	<sup>230</sup> 0.0111	<sup>225</sup> 0.0077	<sup>239</sup> 1.201
198	REALNETWORKS-002	<sup>27</sup> 4104	<sup>48</sup> 245	<sup>238</sup> 0.0393	<sup>236</sup> 0.0189	<sup>238</sup> 0.0142	<sup>228</sup> 0.0108	<sup>222</sup> 0.0076	<sup>239</sup> 1.195
199	REALNETWORKS-003	<sup>122</sup> 1848	<sup>29</sup> 178	<sup>228</sup> 0.0242	<sup>220</sup> 0.0117	<sup>215</sup> 0.0090	<sup>209</sup> 0.0070	<sup>209</sup> 0.0054	<sup>222</sup> 1.120
200	REALNETWORKS-004	<sup>121</sup> 1848	<sup>31</sup> 185	<sup>226</sup> 0.0236	<sup>219</sup> 0.0112	<sup>213</sup> 0.0087	<sup>207</sup> 0.0068	<sup>201</sup> 0.0050	<sup>219</sup> 1.116
201	REALNETWORKS-005	<sup>222</sup> 2056	<sup>71</sup> 337	<sup>90</sup> 0.0023	<sup>77</sup> 0.0016	<sup>69</sup> 0.0014	<sup>72</sup> 0.0013	<sup>57</sup> 0.0012	<sup>79</sup> 1.015
202	REALNETWORKS-006	<sup>227</sup> 2056	<sup>73</sup> 350	<sup>30</sup> 0.0014	<sup>33</sup> 0.0012	<sup>32</sup> 0.0011	<sup>30</sup> 0.0011	<sup>28</sup> 0.0010	<sup>31</sup> 1.011
203	REALNETWORKS-007	<sup>7</sup> 0	<sup>6</sup> 2	<sup>25</sup> 0.0013	<sup>30</sup> 0.0012	<sup>29</sup> 0.0011	<sup>28</sup> 0.0011	<sup>29</sup> 0.0010	<sup>29</sup> 1.011
204	REMARKAI-000	<sup>133</sup> 2048	<sup>147</sup> 615	<sup>180</sup> 0.0086	<sup>170</sup> 0.0044	<sup>161</sup> 0.0036	<sup>163</sup> 0.0031	<sup>160</sup> 0.0025	<sup>172</sup> 1.045
205	REMARKAI-000	<sup>191</sup> 2048	<sup>177</sup> 691	<sup>122</sup> 0.0034	<sup>115</sup> 0.0021	<sup>116</sup> 0.0019	<sup>106</sup> 0.0017	<sup>112</sup> 0.0015	<sup>114</sup> 1.020
206	REMARKAI-002	<sup>182</sup> 2048	<sup>104</sup> 434	<sup>178</sup> 0.0081	<sup>162</sup> 0.0040	<sup>154</sup> 0.0031	<sup>151</sup> 0.0026	<sup>142</sup> 0.0021	<sup>166</sup> 1.041
207	RENDIP-000	<sup>126</sup> 2048	<sup>259</sup> 894	<sup>43</sup> 0.0015	<sup>47</sup> 0.0013	<sup>48</sup> 0.0012	<sup>46</sup> 0.0012	<sup>50</sup> 0.0012	<sup>41</sup> 1.012
208	REVEALMEDIA-000	<sup>213</sup> 2052	<sup>84</sup> 385	<sup>67</sup> 0.0019	<sup>49</sup> 0.0013	<sup>55</sup> 0.0013	<sup>55</sup> 0.0013	<sup>59</sup> 0.0012	<sup>56</sup> 1.013
209	S1-000	<sup>25</sup> 4096	<sup>247</sup> 865	<sup>96</sup> 0.0024	<sup>91</sup> 0.0018	<sup>96</sup> 0.0017	<sup>100</sup> 0.0016		

MISSES OUTSIDE RANK R		RESOURCE USAGE		ENROL MOST RECENT, N = 1.6M					
#	ALGORITHM	BYTES	MSEC	R=1	R=5	R=10	R=20	R=50	WORK-10
217	SENSETIME-004	84	1032	190	710	3	0.0010	6	0.0009
218	SENSETIME-005	88	1032	284	1007	3	0.0009	2	0.0008
219	SENSETIME-006	87	1032	278	956	3	0.0009	3	0.0008
220	SENSETIME-007	85	1032	279	958	1	0.0008	1	0.0008
221	SHAMAN-003	178	2048	185	704	29	0.1243	28	0.0823
222	SHAMAN-004	193	2048	155	642	27	0.2221	26	0.1473
223	SHAMAN-006	161	2048	186	706	24	0.0398	24	0.0344
224	SHAMAN-007	154	2048	189	709	23	0.0396	24	0.0342
225	SIAT-001	208	2052	237	842	61	0.0018	60	0.0014
226	SIAT-002	201	2052	264	906	67	0.0018	57	0.0014
227	SMILART-004	50	512	25	167	282	0.9648	282	0.9640
228	SMILART-005	140	2048	113	464				
229	SQISOFT-001	225	2056	109	460	135	0.0042	66	0.0014
230	STAQU-000	255	4096	229	827	167	0.0071	187	0.0060
231	SYNESIS-003	259	4096	20	103	265	0.1700	265	0.1172
232	SYNESIS-003	168	2048	44	215	21	0.0162	230	0.0160
233	SYNESIS-005	272	4104	213	772	179	0.0085	206	0.0085
234	TECH5-001	110	1536	260	898	131	0.0040	128	0.0024
235	TECH5-002	56	513	275	941	107	0.0027	63	0.0014
236	TEVIAN-003	163	2048	65	300	210	0.0147	198	0.0074
237	TEVIAN-004	187	2048	64	299	197	0.0113	183	0.0057
238	TEVIAN-005	130	2048	97	416	170	0.0073	159	0.0038
239	TEVIAN-006	86	1032	144	599	97	0.0024	96	0.0018
240	TEVIAN-007	90	1032	217	779	59	0.0018	52	0.0014
241	TIGER-000	220	2052	100	428	25	0.0616	245	0.0310
242	TIGER-002	207	2052	112	464	151	0.0056	147	0.0029
243	TIGER-003	199	2052	114	464	151	0.0056	148	0.0029
244	TONGYITRANS-000	233	2070	33	190	167	0.0069	157	0.0038
245	TONGYITRANS-001	252	2070	32	189	167	0.0069	158	0.0038
246	TOSHIBA-000	117	1548	291	930	137	0.0045	136	0.0026
247	TOSHIBA-001	229	2060	272	931	141	0.0048	140	0.0027
248	TRUEFACE-000	125	2000	76	365	117	0.0033	142	0.0028
249	VD-000	83	1028	70	337	27	0.4737	279	0.3204
250	VD-001	205	2052	179	695	235	0.0276	235	0.0181
251	VD-002	203	2052	174	689	188	0.0095	200	0.0077
252	VD-003	214	2052	178	693	177	0.0076	193	0.0069
253	VERIDAS-001	143	2048	255	885	108	0.0028	104	0.0019
254	VERIDAS-002	142	2048	256	888	107	0.0028	103	0.0019
255	VERIDAS-003	134	2048	254	877	67	0.0018	69	0.0015
256	VIGILANTSOLUTIONS-003	114	1544	232	832	25	0.0694	250	0.0349
257	VIGILANTSOLUTIONS-004	113	1544	230	830	260	0.1249	259	0.0706
258	VIGILANTSOLUTIONS-005	115	1544	216	778	187	0.0092	172	0.0045
259	VIGILANTSOLUTIONS-006	116	1544	233	834	197	0.0099	174	0.0048
260	VIGILANTSOLUTIONS-007	111	1544	148	618	121	0.0034	106	0.0020
261	VIGILANTSOLUTIONS-008	112	1544	92	405	117	0.0029	98	0.0018
262	VISIONBOX-000	228	2059	117	482	71	0.0019	73	0.0015
263	VISIONLABS-004	25	256	67	315	107	0.0027	94	0.0018
264	VISIONLABS-005	42	512	66	300	95	0.0024	89	0.0017
265	VISIONLABS-006	47	512	61	292	67	0.0018	67	0.0015
266	VISIONLABS-007	48	512	62	293	57	0.0018	62	0.0014
267	VISIONLABS-008	43	512	58	277	77	0.0020	97	0.0018
268	VISIONLABS-009	52	512	121	494	17	0.0011	22	0.0011
269	VISIONLABS-010	53	512	201	732	31	0.0014	48	0.0013
270	VISIONLABS-011	51	512	203	736	17	0.0012	26	0.0011
271	VOCORD-003	73	896	193	714	159	0.0062	152	0.0035
272	VOCORD-004	74	896	131	538	171	0.0079	176	0.0049
273	VOCORD-005	71	768	226	822	168	0.0070	173	0.0046
274	VOCORD-006	289	10240	227	825	281	1.0000	285	1.0000
275	VTS-000	168	2048	120	492	280	0.5937	281	0.5936
276	VTS-001	158	2048	237	891	47	0.0015	31	0.0012
277	VTS-002	137	2048	262	903	77	0.0019	61	0.0014
278	XFORWARDAI-000	151	2048	210	768	89	0.0023	112	0.0020
279	XFORWARDAI-001	141	2048	170	681	87	0.0020	105	0.0019
280	XFORWARDAI-002	257	4096	273	935	74	0.0020	102	0.0019
281	YISHENG-001	253	3704	86	387	23	0.0265	225	0.0130
282	YITU-002	276	4138	249	870	65	0.0018	37	0.0012
283	YITU-003	275	4138	251	871	117	0.0029	123	0.0023
284	YITU-004	234	2070	266	910	23	0.0013	9	0.0009
285	YITU-005	231	2070	245	861	91	0.0023	114	0.0021

Table 26: Rank-based accuracy for the FRVT 2018 mugshot sets. In columns 3 and 4 are template size and template generation duration. Thereafter values are rank-based FNIR with  $T = 0$  and FPIR = 1. This is appropriate to investigational uses but not those with higher volumes where candidates from all searches would need review. The next column is a workload statistic, a small value shows an algorithm front-loads mates into the first 10 candidates. Throughout, blue superscripts indicate the rank of the algorithm for that column, and the best value is highlighted in yellow.

MISSES BELOW THRESHOLD, T		ENROL RECENT MUGSHOT, N = 1.6M												ENROL APPLICATION PORTRAIT, N = 1.6M																				
#	ALGORITHM	ENROL: MUGSHOT			ENROL: MUGSHOT			ENROL: WEBCAM			ENROL: PROFILE			ENROL: VISA			ENROL: BORDER			PROBE: BORDER			PROBE: BORDER 10+YR			PROBE: KIOSK								
		FPIR=0.0003	FPIR=0.001	FPIR=0.01	FPIR=0.0003	FPIR=0.001	FPIR=0.01	FPIR=0.0003	FPIR=0.001	FPIR=0.01	FPIR=0.0003	FPIR=0.001	FPIR=0.01	FPIR=0.0001	FPIR=0.001	FPIR=0.01	FPIR=0.0001	FPIR=0.001	FPIR=0.01	FPIR=0.0001	FPIR=0.001	FPIR=0.01	FPIR=0.0001	FPIR=0.001	FPIR=0.01									
1	20FACE-000	238	0.462	244	0.348	251	0.230	246	0.763	240	0.450	239	0.301	192	1.000	203	1.000	218	1.000	176	0.424	178	0.255	97	0.772	98	0.599	170	0.938	182	0.836			
2	3DIVI-003	237	0.482	253	0.400	259	0.282	241	0.685	253	0.626	255	0.497					187	0.605	188	0.445					135	0.821	173	0.717					
3	3DIVI-004	208	0.256	224	0.169	228	0.093	212	0.400	230	0.343	234	0.237					166	0.277	169	0.172					133	0.607	153	0.485					
4	3DIVI-005	207	0.255	221	0.166	222	0.093	211	0.395	223	0.339	233	0.234	138	0.998	140	0.996	152	0.990	192	0.864	193	0.846					132	0.597	153	0.484			
5	3DIVI-006	206	0.253	223	0.168	230	0.096	215	0.403	229	0.342	235	0.238					167	0.283	170	0.174					136	0.615	153	0.490					
6	ACER-000	192	0.208	214	0.146	217	0.074	196	0.300	207	0.246	209	0.157	87	0.987	95	0.981	117	0.955	161	0.201	167	0.114					120	0.490	138	0.363			
7	ACER-001	138	0.109	156	0.056	160	0.026	133	0.136	139	0.109	142	0.069	166	1.000	175	0.999	197	0.998	124	0.068	124	0.036	89	0.406	91	0.250	119	0.479	92	0.206			
8	AIZE-001	149	0.127	176	0.077	174	0.034	162	0.187	166	0.143	165	0.087	111	0.995	120	0.994	148	0.983	137	0.101	139	0.052	83	0.364	81	0.216	101	0.387	122	0.289			
9	ALCHERA-000	199	0.231	211	0.138	212	0.070	188	0.259	193	0.216	203	0.146	148	0.999	156	0.999	180	0.996	156	0.176	163	0.111					151	0.803	148	0.456			
10	ALCHERA-001	280	1.000	280	0.999	286	0.999	277	1.000	281	1.000	285	1.000					240	1.000	248	1.000					193	1.000			228	1.000			
11	ALCHERA-002	259	0.807	260	0.486	260	0.302	240	0.685	250	0.591	250	0.442	182	1.000	180	1.000	202	0.999	191	0.827	191	0.770					152	0.811	168	0.705			
12	ALCHERA-003	231	0.450	215	0.155	213	0.070	197	0.304	203	0.239	208	0.152	176	1.000	167	0.999	185	0.997	155	0.172	157	0.097					115	0.464	137	0.362			
13	ALCHERA-004	242	0.520	252	0.394	250	0.211	237	0.642	246	0.529	244	0.327	112	0.995	115	0.991	81	0.813	177	0.424	178	0.232	93	0.708	96	0.515	129	0.546	146	0.398			
14	ALLGOVISION-000	158	0.138	188	0.088	194	0.045	173	0.202	182	0.166	189	0.106	98	0.993	112	0.990	141	0.982	140	0.117	145	0.066					126	0.526	143	0.396			
15	ALLGOVISION-001	167	0.155	193	0.102	208	0.053	190	0.275	197	0.221	202	0.141	102	0.993	102	0.986	102	0.933	150	0.150	159	0.081					121	0.491	144	0.389			
16	ANKE-000	178	0.184	198	0.117	209	0.063	184	0.256	195	0.220	206	0.151	108	0.995	121	0.994	150	0.990	221	1.000	265	1.000					266	1.000	253	1.000			
17	ANKE-001	176	0.183	202	0.119	210	0.063	185	0.256	196	0.220	207	0.151	113	0.995	126	0.994	16	0.992	270	1.000	219	1.000					126	1.000	211	1.000			
18	ANKE-002	103	0.062	112	0.032	116	0.014	99	0.103	104	0.079	106	0.050	66	0.975	68	0.948	77	0.795	88	0.034	90	0.018					69	0.245	87	0.190			
19	AWARE-003	175	0.174	206	0.128	223	0.082	207	0.351	222	0.298	227	0.204	84	0.987	99	0.984	137	0.977	178	0.428	181	0.378					127	0.530	147	0.443			
20	AWARE-004	223	0.355	237	0.269	246	0.175	233	0.619	245	0.509	248	0.375	181	1.000	185	1.000	206	0.999	173	0.397	177	0.279					153	0.816	164	0.631			
21	AWARE-005	246	0.608	247	0.364	222	0.085	207	0.342	207	0.253	211	0.163	177	1.000	190	1.000	206	0.999	165	0.255	16	0.122					165	0.916	171	0.714			
22	AWARE-006	246	0.475	238	0.276	247	0.175	223	0.466	233	0.398	238	0.283	162	1.000	176	0.999	198	0.999	171	0.368	174	0.254					145	0.749	161	0.623			
23	AYONIX-000	262	0.846	269	0.811	274	0.724	259	0.956	26	0.939	270	0.892	139	0.998	147	0.998	17	0.995	196	0.954	198	0.891					178	0.982	188	0.959			
24	AYONIX-001	263	0.875	271	0.824	272	0.701	254	0.946	263	0.920	266	0.845	173	1.000	174	0.999	182	0.996	200	0.999					175	0.969	188	0.926					
25	AYONIX-002	264	0.876	270	0.824	273	0.702	255	0.946	264	0.920	265	0.845	172	1.000	172	0.999	181	0.996	193	0.915	192	0.821					174	0.969	184	0.926			
26	CAMVI-003	127	0.094	171	0.071	208	0.058	145	0.152	158	0.132	190	0.108	72	0.979	77	0.970	10	0.940	139	0.114	159	0.100					104	0.402	144	0.377			
27	CAMVI-004	136	0.107	172	0.072	203	0.054	180	0.240	160	0.136	179	0.100	163	1.000	169	0.999	188	0.998	136	0.100	151	0.081					149	0.787	158	0.507			
28	CAMVI-005	159	0.139	192	0.099	217	0.076	187	0.451	181	0.179	197	0.132	168	1.000	182	1.000	199	1.000	151	0.156	16	0.112					186	0.999	194	0.983			
29	CANON-001	25	0.012	31	0.005	28	0.002	23	0.031	23	0.023	23	0.015	25	0.633	15	0.365	23	0.217	19	0.008	20	0.004	23	0.068	25	0.034	29	0.139	20	0.092			
30	CIB-000	75	0.044	55	0.012	50	0.005	72	0.077	53	0.045	49	0.025	206	1.000	196	1.000	214	1.000	48	0.017	49	0.008	42	0.141	41	0.068	162	0.894	156	0.521			
31	CLEARVIEWAI-000	227	0.013	32	0.006	28	0.002	31	0.036	26	0.025	26	0.016	151	0.999	82	0.974	11	0.149	20	0.008	15	0.004	19	0.057	19	0.027	80	0.268	12	0.080			
32	CLOUDWALK-HR-000	8	0.004	10	0.002	14	0.002	8	0.015	10	0.013	13	0.012	208	1.000	208	1.000	195	1.000	11	0.005	11	0.003	7	0.033	10	0.018	13	0.099	7	0.075			
33	CLOUDWALK-MT-000	4	0.003	9	0.002	17	0.002	5	0.015	9	0.013	15	0.012	10	0.169	1	0.109	1	0.077	1	0.002	4	0.002	1	0.018	1	0.009	1	0.072	3	0.063			
34	COGENT-000	163	0.143	147	0.053	165	0.029	154	0.175	162	0.140	183	0.100	118	0.996	132	0.995	157	0.991															
35	COGENT-001	162	0.143	146	0.053	166	0.029	153	0.175	163	0.140	183	0.100	118	0.996	132	0.995	143	0.998	145	0.998	16	0.994											
36	COGENT-002	172	0.159	133	0.044	127	0.017	117	0.124	120	0.098	133	0.063	143	0.998	145	0.998	16	0.994</td															

MISSES BELOW THRESHOLD, T		ENROL RECENT MUGSHOT, N = 1.6M												ENROL APPLICATION PORTRAIT, N = 1.6M																					
#	ALGORITHM	ENROL: MUGSHOT			ENROL: MUGSHOT			ENROL: WEBCAM			PROBE: PROFILE			ENROL: VISA			ENROL: BORDER			PROBE: BORDER 10+YR			ENROL: KIOSK												
		FPIR=0.0003	FPIR=0.001	FPIR=0.01	FPIR=0.0003	FPIR=0.001	FPIR=0.01	FPIR=0.0003	FPIR=0.001	FPIR=0.01	FPIR=0.0003	FPIR=0.001	FPIR=0.01	FPIR=0.0001	FPIR=0.001	FPIR=0.01	FPIR=0.0001	FPIR=0.001	FPIR=0.01	FPIR=0.0001	FPIR=0.001	FPIR=0.01	FPIR=0.0001	FPIR=0.001	FPIR=0.01										
47	CUBOX-000	11	0.005	16	0.003	19	0.002	17	0.022	17	0.019	19	0.014	6	0.276	4	0.168	6	0.104	7	0.004	8	0.003	6	0.028	6	0.014	2	0.073	2	0.062				
48	CYBERLINK-000	157	0.137	157	0.056	14	0.023	148	0.162	143	0.116	145	0.070	131	0.997	135	0.995	140	0.981	121	0.063	119	0.032			96	0.339	10	0.232						
49	CYBERLINK-001	128	0.096	150	0.054	145	0.022	136	0.138	140	0.109	138	0.067	129	0.997	130	0.995	143	0.984	118	0.062	115	0.031			137	0.652	10	0.239						
50	CYBERLINK-002	67	0.038	64	0.015	65	0.006	62	0.068	68	0.053	67	0.032	104	0.994	107	0.988	117	0.957	64	0.024	69	0.013			83	0.288	6	0.157						
51	CYBERLINK-003	79	0.045	38	0.008	38	0.004	36	0.045	39	0.035	36	0.021	105	0.995	80	0.972	85	0.845	37	0.012	38	0.007	33	0.100	34	0.051	98	0.368	40	0.120				
52	CYBERLINK-004	186	0.188	35	0.007	30	0.003	31	0.063	40	0.036	40	0.022	214	1.000	205	1.000	207	0.999	39	0.013	37	0.007	34	0.109	36	0.050	173	0.954	125	0.291				
53	CYBERLINK-005	193	0.208	46	0.010	45	0.004	42	0.054	51	0.026	183	1.000	186	1.000	92	0.888	40	0.014	39	0.007	29	0.089	29	0.043	169	0.926	116	0.266						
54	DAHUA-000	151	0.128	184	0.086	19	0.045	19	0.179	19	0.135	163	0.083																						
55	DAHUA-001	135	0.106	174	0.073	178	0.037	142	0.151	151	0.122	154	0.075	86	0.987	92	0.980	105	0.933																
56	DAHUA-002	48	0.26	65	0.015	60	0.006	48	0.060	55	0.046	56	0.029	30	0.681	35	0.638	47	0.522	45	0.017	44	0.008			41	0.159	44	0.125						
57	DAHUA-003	46	0.025	60	0.014	50	0.005	41	0.054	48	0.041	47	0.024	26	0.647	30	0.579	39	0.447	38	0.013	36	0.006	27	0.081	30	0.043	28	0.134	30	0.109				
58	DAHUA-004	29	0.014	34	0.007	34	0.003	26	0.033	28	0.026	27	0.016	17	0.552	24	0.485	32	0.345	26	0.008	23	0.004	15	0.051	17	0.027	22	0.113	23	0.094				
59	DAON-000	155	0.135	93	0.023	91	0.009	76	0.079	81	0.061	83	0.039	183	1.000	187	1.000	194	0.998	65	0.025	69	0.013	59	0.173	58	0.091	158	0.846	79	0.172				
60	DECATUR-000	72	0.043	96	0.023	96	0.010	81	0.085	87	0.066	85	0.040	33	0.757	39	0.675	43	0.509	69	0.027	74	0.014	58	0.173	65	0.098	62	0.239	65	0.156				
61	DEEPLINT-001	20	0.010	20	0.003	20	0.002	11	0.018	11	0.014	8	0.010	191	1.000	178	1.000	42	0.503	15	0.006	29	0.004			40	0.159	29	0.097						
62	DEEPSA-001	115	0.073	137	0.046	143	0.022	125	0.129	132	0.101	125	0.059	90	0.988	100	0.985	130	0.973	128	0.077	130	0.041			93	0.326	111	0.251						
63	DERMALOG-003	244	0.550	259	0.482	26	0.360	244	0.715	255	0.655	259	0.526	123	0.997	136	0.995	160	0.991	186	0.603	188	0.458			159	0.856	170	0.751						
64	DERMALOG-004	246	0.554	258	0.480	262	0.358	243	0.711	256	0.657	257	0.526	123	0.997	136	0.995	160	0.991	186	0.603	188	0.458			135	0.614	149	0.459						
65	DERMALOG-005	187	0.189	187	0.088	188	0.043	167	0.201	17	0.154	176	0.096	120	0.996	116	0.990	117	0.950	168	0.300	170	0.267			92	0.318	105	0.230						
66	DERMALOG-006	130	0.098	144	0.052	159	0.026	135	0.137	134	0.105	137	0.067	91	0.989	94	0.981	104	0.933	116	0.059	117	0.031			131	0.557	128	0.299						
67	DERMALOG-007	184	0.188	185	0.086	186	0.040	167	0.200	17	0.152	173	0.093	121	0.996	111	0.990	117	0.950	135	0.099	136	0.052			131	0.557	128	0.299						
68	DERMALOG-008	211	0.268	135	0.045	126	0.017	178	0.094	117	0.054	209	1.000	215	1.000	113	0.057	106	0.025	87	0.382	83	0.158	171	0.940	167	0.678								
69	DERMALOG-009	71	0.041	86	0.021	88	0.009	82	0.086	88	0.066	88	0.040	188	1.000	198	1.000	212	1.000	78	0.031	81	0.016	99	0.999	108	0.999	157	0.840	101	0.222				
70	EYEDEA-003	241	0.509	249	0.388	255	0.265	235	0.625	248	0.543	249	0.404	124	0.997	127	0.994	149	0.990	184	0.570	183	0.392			150	0.792	166	0.658						
71	F-001	233	0.458	220	0.166	175	0.036					150	0.999	155	0.998	179	0.995																		
72	FINCORE-000	183	0.187	210	0.134	216	0.071	189	0.267	194	0.217	200	0.140	178	1.000	191	1.000	172	0.995	157	0.187	162	0.108	92	0.598	98	0.418	114	0.458	134	0.349				
73	FUJITSULAB-000	203	0.246	87	0.021	84	0.008	65	0.070	74	0.056	77	0.035							62	0.024	69	0.013	60	0.177	63	0.093	68	0.240	66	0.156				
74	FUJITSULAB-001	251	0.655	77	0.018	68	0.007	106	0.112	76	0.058	69	0.033	117	0.996	117	0.992	109	0.940	63	0.024	59	0.011	94	0.739	91	0.310	111	0.247	67	0.146				
75	GLORY-000	230	0.441	248	0.367	259	0.295	231	0.586	249	0.547	253	0.470	107	0.995	129	0.995	164	0.993	180	0.453	182	0.381			156	0.839	180	0.795						
76	GLORY-001	222	0.355	240	0.305	252	0.236	230	0.582	245	0.537	251	0.448	103	0.994	118	0.993	159	0.991	175	0.408	178	0.336			154	0.819	176	0.753						
77	GORILLA-001	257	0.747	254	0.406	253	0.246	232	0.590	241	0.453	242	0.314	208	1.000	217	1.000	229	1.000	181	0.468	178	0.299			227	1.000	170	0.710						
78	GORILLA-002	210	0.266	227	0.188	237	0.106	20	0.342	216	0.268	217	0.170	197	1.000	211	1.000	167	0.993	164	0.250	168	0.137			190	1.000	157	0.466						
79	GORILLA-003	259	0.694	242	0.318	244	0.157	239	0.684	238	0.434	246	0.247	276	1.000	280	1.000	221	1.000	174	0.407	171	0.213			222	1.000	158	0.562						
80	GORILLA-004	154	0.135	190	0.089	187	0.043	170	0.202	179	0.160	184	0.101	62	0.972	70	0.959	94	0.903	145	0.135	148	0.072			110	0.438	131	0.309						
81	GORILLA-005	125	0.086	161	0.058	161	0.026	156	0.179	165	0.142	167	0.088	36	0.770	41	0.700	51	0.553	133	0.088	129	0.040			90	0.315	102	0.223						
82	GORILLA-006	83	0.046	108	0.027	103	0.011	112	0.118	114	0.089	113	0.053	210	0.602	28	0.531	34	0.369	70	0.028	69	0.013	55	0.166	62	0.093	64	0.154						
83	GORILLA-007	80	0.046	107	0.027	101	0.010	96	0.101	103	0.077																								

MISSES BELOW THRESHOLD, T		ENROL RECENT MUGSHOT, N = 1.6M												ENROL APPLICATION PORTRAIT, N = 1.6M															
		ENROL: MUGSHOT				ENROL: MUGSHOT				ENROL: WEBCAM				ENROL: MUGSHOT				ENROL: PROFILE				ENROL: VISA		ENROL: BORDER		ENROL: BORDER 10+YR		ENROL: VISA	
#	ALGORITHM	FPIR=0.0003	FPIR=0.001	FPIR=0.01	FPIR=0.0003	FPIR=0.001	FPIR=0.01	FPIR=0.0003	FPIR=0.001	FPIR=0.01	FPIR=0.0003	FPIR=0.001	FPIR=0.01	FPIR=0.0003	FPIR=0.001	FPIR=0.01	FPIR=0.0001	FPIR=0.01	FPIR=0.001	FPIR=0.01	FPIR=0.0001	FPIR=0.01	FPIR=0.001	FPIR=0.01	FPIR=0.0001	FPIR=0.01			
93	IDEMIA-004	<sup>96</sup> 0.055	<sup>126</sup> 0.037	<sup>137</sup> 0.021	<sup>138</sup> 0.144	<sup>147</sup> 0.118	<sup>157</sup> 0.079	<sup>69</sup> 0.976	<sup>81</sup> 0.973	<sup>122</sup> 0.968	<sup>141</sup> 0.123	<sup>144</sup> 0.061	<sup>148</sup> 0.766	<sup>163</sup> 0.630	<sup>141</sup> 0.123	<sup>144</sup> 0.061	<sup>148</sup> 0.766	<sup>163</sup> 0.630	<sup>141</sup> 0.123	<sup>144</sup> 0.061	<sup>148</sup> 0.766	<sup>163</sup> 0.630	<sup>141</sup> 0.123	<sup>144</sup> 0.061	<sup>148</sup> 0.766	<sup>163</sup> 0.630			
94	IDEMIA-005	<sup>110</sup> 0.066	<sup>132</sup> 0.044	<sup>158</sup> 0.026	<sup>159</sup> 0.181	<sup>170</sup> 0.150	<sup>187</sup> 0.102	<sup>73</sup> 0.979	<sup>86</sup> 0.978	<sup>128</sup> 0.973	<sup>143</sup> 0.130	<sup>147</sup> 0.070	<sup>163</sup> 0.879	<sup>173</sup> 0.743	<sup>143</sup> 0.130	<sup>147</sup> 0.070	<sup>163</sup> 0.879	<sup>173</sup> 0.743	<sup>143</sup> 0.130	<sup>147</sup> 0.070	<sup>163</sup> 0.879	<sup>173</sup> 0.743	<sup>143</sup> 0.130	<sup>147</sup> 0.070	<sup>163</sup> 0.879	<sup>173</sup> 0.743			
95	IDEMIA-006	<sup>108</sup> 0.065	<sup>129</sup> 0.043	<sup>156</sup> 0.025	<sup>188</sup> 0.266	<sup>210</sup> 0.161	<sup>83</sup> 0.984	<sup>96</sup> 0.982	<sup>139</sup> 0.980	<sup>149</sup> 0.144	<sup>150</sup> 0.090	<sup>141</sup> 0.123	<sup>144</sup> 0.061	<sup>148</sup> 0.766	<sup>163</sup> 0.630	<sup>141</sup> 0.123	<sup>144</sup> 0.061	<sup>148</sup> 0.766	<sup>163</sup> 0.630	<sup>141</sup> 0.123	<sup>144</sup> 0.061	<sup>148</sup> 0.766	<sup>163</sup> 0.630	<sup>141</sup> 0.123	<sup>144</sup> 0.061	<sup>148</sup> 0.766	<sup>163</sup> 0.630		
96	IDEMIA-007	<sup>63</sup> 0.035	<sup>76</sup> 0.018	<sup>79</sup> 0.008	<sup>70</sup> 0.073	<sup>71</sup> 0.055	<sup>70</sup> 0.033	<sup>28</sup> 1.000	<sup>263</sup> 1.000	<sup>263</sup> 1.000	<sup>108</sup> 0.052	<sup>103</sup> 0.022	<sup>62</sup> 0.182	<sup>69</sup> 0.109	<sup>245</sup> 1.000	<sup>192</sup> 0.982	<sup>108</sup> 0.052	<sup>103</sup> 0.022	<sup>62</sup> 0.182	<sup>69</sup> 0.109	<sup>245</sup> 1.000	<sup>192</sup> 0.982	<sup>108</sup> 0.052	<sup>103</sup> 0.022	<sup>62</sup> 0.182	<sup>69</sup> 0.109			
97	IDEMIA-008	<sup>6</sup> 0.004	<sup>8</sup> 0.002	<sup>9</sup> 0.001	<sup>10</sup> 0.016	<sup>8</sup> 0.013	<sup>5</sup> 0.009	<sup>7</sup> 0.276	<sup>6</sup> 0.204	<sup>8</sup> 0.136	<sup>10</sup> 0.005	<sup>9</sup> 0.003	<sup>11</sup> 0.036	<sup>12</sup> 0.019	<sup>18</sup> 0.106	<sup>19</sup> 0.092	<sup>10</sup> 0.005	<sup>9</sup> 0.003	<sup>11</sup> 0.036	<sup>12</sup> 0.019	<sup>18</sup> 0.106	<sup>19</sup> 0.092	<sup>10</sup> 0.005	<sup>9</sup> 0.003	<sup>11</sup> 0.036	<sup>12</sup> 0.019	<sup>18</sup> 0.106	<sup>19</sup> 0.092	
98	IDEMIA-009	<sup>5</sup> 0.004	<sup>4</sup> 0.002	<sup>3</sup> 0.001	<sup>2</sup> 0.012	<sup>2</sup> 0.008	<sup>3</sup> 0.202	<sup>3</sup> 0.141	<sup>4</sup> 0.099	<sup>3</sup> 0.003	<sup>5</sup> 0.027	<sup>3</sup> 0.013	<sup>4</sup> 0.074	<sup>4</sup> 0.064	<sup>141</sup> 0.733	<sup>142</sup> 0.630													
99	IMAGUS-002	<sup>267</sup> 0.908	<sup>267</sup> 0.749	<sup>267</sup> 0.564	<sup>259</sup> 0.944	<sup>262</sup> 0.816	<sup>262</sup> 0.645	<sup>193</sup> 1.000	<sup>207</sup> 1.000	<sup>217</sup> 1.000	<sup>141</sup> 0.123	<sup>144</sup> 0.061	<sup>148</sup> 0.766	<sup>163</sup> 0.630	<sup>141</sup> 0.123	<sup>144</sup> 0.061	<sup>148</sup> 0.766	<sup>163</sup> 0.630	<sup>141</sup> 0.123	<sup>144</sup> 0.061	<sup>148</sup> 0.766	<sup>163</sup> 0.630	<sup>141</sup> 0.123	<sup>144</sup> 0.061	<sup>148</sup> 0.766	<sup>163</sup> 0.630			
100	IMAGUS-003	<sup>266</sup> 0.898	<sup>268</sup> 0.807	<sup>271</sup> 0.669	<sup>258</sup> 0.954	<sup>262</sup> 0.909	<sup>264</sup> 0.809	<sup>211</sup> 1.000	<sup>200</sup> 1.000	<sup>216</sup> 1.000	<sup>141</sup> 0.123	<sup>144</sup> 0.061	<sup>148</sup> 0.766	<sup>163</sup> 0.630	<sup>141</sup> 0.123	<sup>144</sup> 0.061	<sup>148</sup> 0.766	<sup>163</sup> 0.630	<sup>141</sup> 0.123	<sup>144</sup> 0.061	<sup>148</sup> 0.766	<sup>163</sup> 0.630	<sup>141</sup> 0.123	<sup>144</sup> 0.061	<sup>148</sup> 0.766	<sup>163</sup> 0.630			
101	IMAGUS-005	<sup>60</sup> 0.034	<sup>80</sup> 0.018	<sup>80</sup> 0.008	<sup>83</sup> 0.088	<sup>86</sup> 0.066	<sup>86</sup> 0.040	<sup>51</sup> 0.926	<sup>55</sup> 0.838	<sup>62</sup> 0.647	<sup>72</sup> 0.029	<sup>82</sup> 0.016	<sup>54</sup> 0.161	<sup>64</sup> 0.094	<sup>64</sup> 0.231	<sup>85</sup> 0.189	<sup>64</sup> 0.094	<sup>64</sup> 0.231	<sup>85</sup> 0.189	<sup>64</sup> 0.094	<sup>64</sup> 0.231	<sup>85</sup> 0.189	<sup>64</sup> 0.094	<sup>64</sup> 0.231	<sup>85</sup> 0.189	<sup>64</sup> 0.094	<sup>64</sup> 0.231		
102	IMAGUS-006	<sup>68</sup> 0.039	<sup>82</sup> 0.019	<sup>81</sup> 0.008	<sup>87</sup> 0.093	<sup>91</sup> 0.069	<sup>94</sup> 0.042	<sup>76</sup> 0.980	<sup>63</sup> 0.897	<sup>56</sup> 0.621	<sup>71</sup> 0.028	<sup>76</sup> 0.015	<sup>53</sup> 0.161	<sup>69</sup> 0.092	<sup>74</sup> 0.260	<sup>81</sup> 0.181	<sup>69</sup> 0.092	<sup>74</sup> 0.260	<sup>81</sup> 0.181	<sup>69</sup> 0.092	<sup>74</sup> 0.260	<sup>81</sup> 0.181	<sup>69</sup> 0.092	<sup>74</sup> 0.260	<sup>81</sup> 0.181	<sup>69</sup> 0.092	<sup>74</sup> 0.260		
103	IMAGUS-007	<sup>73</sup> 0.044	<sup>95</sup> 0.023	<sup>95</sup> 0.010	<sup>95</sup> 0.100	<sup>97</sup> 0.073	<sup>98</sup> 0.045	<sup>64</sup> 0.973	<sup>63</sup> 0.651	<sup>79</sup> 0.031	<sup>79</sup> 0.016	<sup>56</sup> 0.169	<sup>66</sup> 0.098	<sup>79</sup> 0.265	<sup>80</sup> 0.181	<sup>79</sup> 0.265	<sup>80</sup> 0.181	<sup>79</sup> 0.265	<sup>80</sup> 0.181	<sup>79</sup> 0.265	<sup>80</sup> 0.181	<sup>79</sup> 0.265	<sup>80</sup> 0.181	<sup>79</sup> 0.265	<sup>80</sup> 0.181	<sup>79</sup> 0.265	<sup>80</sup> 0.181		
104	IMPERIAL-000	<sup>166</sup> 0.154	<sup>101</sup> 0.026	<sup>92</sup> 0.009	<sup>85</sup> 0.089	<sup>90</sup> 0.068	<sup>91</sup> 0.041	<sup>202</sup> 1.000	<sup>159</sup> 0.999	<sup>17</sup> 0.995	<sup>97</sup> 0.042	<sup>99</sup> 0.020	<sup>170</sup> 0.245	<sup>168</sup> 0.168	<sup>170</sup> 0.245	<sup>168</sup> 0.168	<sup>170</sup> 0.245	<sup>168</sup> 0.168	<sup>170</sup> 0.245	<sup>168</sup> 0.168	<sup>170</sup> 0.245	<sup>168</sup> 0.168	<sup>170</sup> 0.245	<sup>168</sup> 0.168	<sup>170</sup> 0.245	<sup>168</sup> 0.168	<sup>170</sup> 0.245		
105	INCODE-000	<sup>229</sup> 0.423	<sup>241</sup> 0.310	<sup>248</sup> 0.199	<sup>226</sup> 0.486	<sup>236</sup> 0.420	<sup>241</sup> 0.304	<sup>171</sup> 1.000	<sup>152</sup> 0.998	<sup>169</sup> 0.994	<sup>141</sup> 0.123	<sup>144</sup> 0.061	<sup>148</sup> 0.766	<sup>163</sup> 0.630	<sup>141</sup> 0.123	<sup>144</sup> 0.061	<sup>148</sup> 0.766	<sup>163</sup> 0.630	<sup>141</sup> 0.123	<sup>144</sup> 0.061	<sup>148</sup> 0.766	<sup>163</sup> 0.630	<sup>141</sup> 0.123	<sup>144</sup> 0.061	<sup>148</sup> 0.766	<sup>163</sup> 0.630			
106	INCODE-001	<sup>218</sup> 0.319	<sup>230</sup> 0.212	<sup>235</sup> 0.112	<sup>206</sup> 0.348	<sup>219</sup> 0.296	<sup>223</sup> 0.198	<sup>212</sup> 1.000	<sup>218</sup> 1.000	<sup>213</sup> 1.000	<sup>141</sup> 0.123	<sup>144</sup> 0.061	<sup>148</sup> 0.766	<sup>163</sup> 0.630	<sup>141</sup> 0.123	<sup>144</sup> 0.061	<sup>148</sup> 0.766	<sup>163</sup> 0.630	<sup>141</sup> 0.123	<sup>144</sup> 0.061	<sup>148</sup> 0.766	<sup>163</sup> 0.630	<sup>141</sup> 0.123	<sup>144</sup> 0.061	<sup>148</sup> 0.766	<sup>163</sup> 0.630			
107	INCODE-002	<sup>215</sup> 0.285	<sup>226</sup> 0.184	<sup>233</sup> 0.100	<sup>200</sup> 0.333	<sup>217</sup> 0.269	<sup>219</sup> 0.176	<sup>134</sup> 0.998	<sup>119</sup> 0.993	<sup>135</sup> 0.976	<sup>141</sup> 0.123	<sup>144</sup> 0.061	<sup>148</sup> 0.766	<sup>163</sup> 0.630	<sup>141</sup> 0.123	<sup>144</sup> 0.061	<sup>148</sup> 0.766	<sup>163</sup> 0.630	<sup>141</sup> 0.123	<sup>144</sup> 0.061	<sup>148</sup> 0.766	<sup>163</sup> 0.630	<sup>141</sup> 0.123	<sup>144</sup> 0.061	<sup>148</sup> 0.766	<sup>163</sup> 0.630			
108	INCODE-003	<sup>216</sup> 0.286	<sup>222</sup> 0.167	<sup>227</sup> 0.084	<sup>210</sup> 0.372	<sup>213</sup> 0.264	<sup>213</sup> 0.164	<sup>179</sup> 1.000	<sup>173</sup> 0.999	<sup>181</sup> 0.996	<sup>141</sup> 0.123	<sup>144</sup> 0.061	<sup>148</sup> 0.766	<sup>163</sup> 0.630	<sup>141</sup> 0.123	<sup>144</sup> 0.061	<sup>148</sup> 0.766	<sup>163</sup> 0.630	<sup>141</sup> 0.123	<sup>144</sup> 0.061	<sup>148</sup> 0.766	<sup>163</sup> 0.630	<sup>141</sup> 0.123	<sup>144</sup> 0.061	<sup>148</sup> 0.766	<sup>163</sup> 0.630			
109	INCODE-004	<sup>132</sup> 0.099	<sup>153</sup> 0.054	<sup>149</sup> 0.023	<sup>150</sup> 0.167	<sup>150</sup> 0.120	<sup>146</sup> 0.070	<sup>130</sup> 0.995	<sup>128</sup> 0.995	<sup>101</sup> 0.929	<sup>120</sup> 0.063	<sup>120</sup> 0.031	<sup>120</sup> 0.016	<sup>120</sup> 0.006	<sup>120</sup> 0.003	<sup>120</sup> 0.001													
110	INCODE-005	<sup>36</sup> 0.021	<sup>50</sup> 0.011	<sup>49</sup> 0.005	<sup>48</sup> 0.055	<sup>47</sup> 0.031	<sup>47</sup> 0.020	<sup>273</sup> 1.000	<sup>274</sup> 1.000	<sup>178</sup> 1.000	<sup>189</sup> 1.000	<sup>189</sup> 1.000	<sup>189</sup> 1.000	<sup>189</sup> 1.000	<sup>189</sup> 1.000	<sup>189</sup> 1.000	<sup>189</sup> 1.000	<sup>189</sup> 1.000	<sup>189</sup> 1.000	<sup>189</sup> 1.000	<sup>189</sup> 1.000	<sup>189</sup> 1.000	<sup>189</sup> 1.000	<sup>189</sup> 1.000	<sup>189</sup> 1.000	<sup>189</sup> 1.000			
111	INNOVATRICS-002	<sup>227</sup> 0.379	<sup>235</sup> 0.234	<sup>243</sup> 0.139	<sup>214</sup> 0.403	<sup>228</sup> 0.310	<sup>229</sup> 0.209	<sup>189</sup> 1.000	<sup>201</sup> 1.000	<sup>211</sup> 1.000	<sup>141</sup> 0.123	<sup>144</sup> 0.061	<sup>148</sup> 0.766	<sup>163</sup> 0.630	<sup>141</sup> 0.123	<sup>144</sup> 0.061	<sup>148</sup> 0.766	<sup>163</sup> 0.630	<sup>141</sup> 0.123	<sup>144</sup> 0.061	<sup>148</sup> 0.766	<sup>163</sup> 0.630	<sup>141</sup> 0.123	<sup>144</sup> 0.061	<sup>148</sup> 0.766	<sup>163</sup> 0.630			
112	INNOVATRICS-003	<sup>217</sup> 0.297	<sup>231</sup> 0.221	<sup>239</sup> 0.132	<sup>208</sup> 0.351	<sup>228</sup> 0.297	<sup>226</sup> 0.203	<sup>180</sup> 1.000	<sup>184</sup> 1.000	<sup>184</sup> 1.000	<sup>141</sup> 0.123	<sup>144</sup> 0.061	<sup>148</sup> 0.766	<sup>163</sup> 0.630	<sup>141</sup> 0.123	<sup>144</sup> 0.061	<sup>148</sup> 0.766	<sup>163</sup> 0.630	<sup>141</sup> 0.123	<sup>144</sup> 0.061	<sup>148</sup> 0.766	<sup>163</sup> 0.630	<sup>141</sup> 0.123	<sup>144</sup> 0.061	<sup>148</sup> 0.766	<sup>163</sup> 0.630			
113	INNOVATRICS-004	<sup>181</sup> 0.184	<sup>208</sup>																										

MISSES BELOW THRESHOLD, T		ENROL RECENT MUGSHOT, N = 1.6M												ENROL APPLICATION PORTRAIT, N = 1.6M							
#	ALGORITHM	ENROL: MUGSHOT			ENROL: MUGSHOT			ENROL: WEBCAM			PROBE: PROFILE			ENROL: VISA		ENROL: BORDER		ENROL: KIOSK			
		FPIR=0.0003	FPIR=0.001	FPIR=0.01	FPIR=0.0003	FPIR=0.001	FPIR=0.01	FPIR=0.0003	FPIR=0.001	FPIR=0.01	FPIR=0.0003	FPIR=0.001	FPIR=0.01	FPIR=0.001	FPIR=0.01	FPIR=0.001	FPIR=0.01	FPIR=0.001	FPIR=0.01		
139	MICROSOFT-005	<sup>84</sup> 0.047	<sup>99</sup> 0.026	<sup>99</sup> 0.010	<sup>86</sup> 0.090	<sup>93</sup> 0.070	<sup>92</sup> 0.041	<sup>139</sup> 0.999	<sup>31</sup> 0.587	<sup>33</sup> 0.354	<sup>67</sup> 0.027	<sup>68</sup> 0.013						<sup>52</sup> 0.180	<sup>51</sup> 0.134		
140	MICROSOFT-006	<sup>45</sup> 0.025	<sup>51</sup> 0.012	<sup>62</sup> 0.006	<sup>38</sup> 0.048	<sup>41</sup> 0.037	<sup>48</sup> 0.024	<sup>13</sup> 0.452	<sup>16</sup> 0.386	<sup>25</sup> 0.281	<sup>82</sup> 0.032	<sup>77</sup> 0.015						<sup>48</sup> 0.178	<sup>53</sup> 0.138		
141	NEC-000	<sup>141</sup> 0.113	<sup>180</sup> 0.079	<sup>199</sup> 0.047	<sup>151</sup> 0.171	<sup>164</sup> 0.140	<sup>171</sup> 0.093	<sup>79</sup> 0.983	<sup>89</sup> 0.979	<sup>124</sup> 0.969								<sup>118</sup> 0.474	<sup>142</sup> 0.377		
142	NEC-001	<sup>165</sup> 0.148	<sup>192</sup> 0.106	<sup>208</sup> 0.060	<sup>179</sup> 0.238	<sup>191</sup> 0.197	<sup>198</sup> 0.133	<sup>93</sup> 0.991	<sup>104</sup> 0.986	<sup>126</sup> 0.972	<sup>144</sup> 0.133	<sup>153</sup> 0.082						<sup>117</sup> 0.468	<sup>143</sup> 0.378		
143	NEC-002	<sup>32</sup> 0.018	<sup>14</sup> 0.003	<sup>12</sup> 0.002	<sup>22</sup> 0.029	<sup>20</sup> 0.020	<sup>17</sup> 0.013	<sup>165</sup> 1.000	<sup>170</sup> 0.999	<sup>174</sup> 0.995	<sup>22</sup> 0.008	<sup>32</sup> 0.005						<sup>13</sup> 0.676	<sup>126</sup> 0.292		
144	NEC-003	<sup>10</sup> 0.005	<sup>12</sup> 0.002	<sup>16</sup> 0.002	<sup>16</sup> 0.021	<sup>16</sup> 0.017	<sup>16</sup> 0.013	<sup>49</sup> 0.902	<sup>52</sup> 0.824	<sup>59</sup> 0.628	<sup>25</sup> 0.008	<sup>33</sup> 0.006	<sup>12</sup> 0.036	<sup>13</sup> 0.023	<sup>138</sup> 0.668	<sup>114</sup> 0.261					
145	NEC-004	<sup>1</sup> 0.003	<sup>6</sup> 0.002	<sup>11</sup> 0.002	<sup>7</sup> 0.015	<sup>7</sup> 0.013	<sup>10</sup> 0.010	<sup>27</sup> 0.654	<sup>34</sup> 0.622	<sup>53</sup> 0.575	<sup>8</sup> 0.004	<sup>13</sup> 0.004	<sup>3</sup> 0.019	<sup>4</sup> 0.012	<sup>10</sup> 0.100	<sup>16</sup> 0.088					
146	NEC-005	<sup>15</sup> 0.007	<sup>3</sup> 0.002	<sup>8</sup> 0.001	<sup>3</sup> 0.014	<sup>3</sup> 0.012	<sup>6</sup> 0.009	<sup>48</sup> 0.901	<sup>38</sup> 0.673	<sup>18</sup> 0.177	<sup>5</sup> 0.003	<sup>6</sup> 0.002	<sup>2</sup> 0.019	<sup>2</sup> 0.011	<sup>11</sup> 0.099	<sup>15</sup> 0.087					
147	NEUROTECHNOLOGY-003	<sup>27</sup> 0.999	<sup>265</sup> 0.636	<sup>23</sup> 0.099	<sup>24</sup> 0.773	<sup>21</sup> 0.266	<sup>212</sup> 0.164	<sup>281</sup> 1.000	<sup>284</sup> 1.000	<sup>282</sup> 1.000											
148	NEUROTECHNOLOGY-004	<sup>143</sup> 0.120	<sup>167</sup> 0.063	<sup>163</sup> 0.028	<sup>139</sup> 0.146	<sup>144</sup> 0.117	<sup>148</sup> 0.073	<sup>122</sup> 0.996	<sup>124</sup> 0.994	<sup>151</sup> 0.990											
149	NEUROTECHNOLOGY-005	<sup>142</sup> 0.117	<sup>154</sup> 0.054	<sup>144</sup> 0.022	<sup>182</sup> 0.252	<sup>156</sup> 0.130	<sup>151</sup> 0.074	<sup>147</sup> 0.999	<sup>148</sup> 0.998	<sup>148</sup> 0.989											
150	NEUROTECHNOLOGY-006	<sup>275</sup> 0.987	<sup>236</sup> 0.249	<sup>23</sup> 0.121	<sup>24</sup> 1.000	<sup>23</sup> 0.418	<sup>228</sup> 0.206														
151	NEUROTECHNOLOGY-007	<sup>205</sup> 0.252	<sup>166</sup> 0.062	<sup>141</sup> 0.021	<sup>268</sup> 0.996	<sup>185</sup> 0.173	<sup>139</sup> 0.068	<sup>200</sup> 1.000	<sup>194</sup> 1.000	<sup>186</sup> 0.997	<sup>170</sup> 0.339	<sup>123</sup> 0.036						<sup>219</sup> 1.000	<sup>197</sup> 0.989		
152	NEUROTECHNOLOGY-008	<sup>258</sup> 0.797	<sup>148</sup> 0.053	<sup>112</sup> 0.012	<sup>105</sup> 0.110	<sup>108</sup> 0.080	<sup>103</sup> 0.047	<sup>205</sup> 1.000	<sup>214</sup> 1.000	<sup>228</sup> 1.000	<sup>89</sup> 0.035	<sup>87</sup> 0.017	<sup>78</sup> 0.293	<sup>80</sup> 0.149	<sup>58</sup> 0.203	<sup>63</sup> 0.152					
153	NEUROTECHNOLOGY-009	<sup>49</sup> 0.027	<sup>68</sup> 0.015	<sup>61</sup> 0.006	<sup>57</sup> 0.066	<sup>65</sup> 0.052	<sup>64</sup> 0.032	<sup>28</sup> 0.661	<sup>32</sup> 0.588	<sup>38</sup> 0.436	<sup>53</sup> 0.020	<sup>52</sup> 0.010	<sup>50</sup> 0.153	<sup>55</sup> 0.082	<sup>43</sup> 0.165	<sup>48</sup> 0.129					
154	NEUROTECHNOLOGY-010	<sup>220</sup> 0.346	<sup>45</sup> 0.010	<sup>37</sup> 0.003	<sup>47</sup> 0.047	<sup>45</sup> 0.037	<sup>45</sup> 0.023	<sup>12</sup> 0.377	<sup>12</sup> 0.277	<sup>16</sup> 0.170	<sup>33</sup> 0.010	<sup>27</sup> 0.005	<sup>26</sup> 0.075	<sup>28</sup> 0.039	<sup>23</sup> 0.126	<sup>25</sup> 0.097					
155	NEWLAND-002	<sup>243</sup> 0.523	<sup>256</sup> 0.438	<sup>258</sup> 0.294	<sup>22</sup> 0.535	<sup>242</sup> 0.466	<sup>245</sup> 0.335	<sup>155</sup> 0.999	<sup>163</sup> 0.999	<sup>192</sup> 0.998											
156	NOBLIS-001	<sup>281</sup> 1.000	<sup>281</sup> 1.000	<sup>28</sup> 0.991	<sup>280</sup> 1.000	<sup>281</sup> 1.000	<sup>280</sup> 1.000	<sup>195</sup> 1.000	<sup>206</sup> 1.000	<sup>224</sup> 1.000											
157	NOBLIS-002	<sup>279</sup> 1.000	<sup>277</sup> 0.997	<sup>267</sup> 0.488	<sup>283</sup> 1.000	<sup>274</sup> 1.000	<sup>277</sup> 1.000	<sup>210</sup> 1.000	<sup>219</sup> 1.000	<sup>231</sup> 1.000											
158	NOTIONTAG-000	<sup>58</sup> 0.032	<sup>71</sup> 0.017	<sup>76</sup> 0.007	<sup>71</sup> 0.076	<sup>79</sup> 0.059	<sup>80</sup> 0.036	<sup>29</sup> 0.671	<sup>33</sup> 0.611	<sup>46</sup> 0.467	<sup>57</sup> 0.021	<sup>58</sup> 0.011	<sup>48</sup> 0.150	<sup>56</sup> 0.084	<sup>47</sup> 0.176	<sup>55</sup> 0.140					
159	NTECHLAB-003	<sup>119</sup> 0.080	<sup>152</sup> 0.054	<sup>164</sup> 0.028	<sup>140</sup> 0.148	<sup>148</sup> 0.118	<sup>153</sup> 0.075	<sup>45</sup> 0.873	<sup>54</sup> 0.837	<sup>79</sup> 0.752								<sup>26</sup> 0.263	<sup>99</sup> 0.214		
160	NTECHLAB-004	<sup>106</sup> 0.063	<sup>127</sup> 0.041	<sup>139</sup> 0.021	<sup>122</sup> 0.131	<sup>135</sup> 0.105	<sup>136</sup> 0.065	<sup>44</sup> 0.868	<sup>53</sup> 0.833	<sup>73</sup> 0.746	<sup>111</sup> 0.053	<sup>114</sup> 0.030						<sup>84</sup> 0.294	<sup>104</sup> 0.227		
161	NTECHLAB-005	<sup>105</sup> 0.062	<sup>128</sup> 0.042	<sup>140</sup> 0.021	<sup>120</sup> 0.130	<sup>131</sup> 0.102	<sup>135</sup> 0.063	<sup>41</sup> 0.816	<sup>46</sup> 0.771	<sup>63</sup> 0.661	<sup>126</sup> 0.073	<sup>127</sup> 0.039						<sup>75</sup> 0.260	<sup>95</sup> 0.207		
162	NTECHLAB-006	<sup>99</sup> 0.056	<sup>122</sup> 0.037	<sup>129</sup> 0.018	<sup>116</sup> 0.121	<sup>121</sup> 0.094	<sup>123</sup> 0.059	<sup>39</sup> 0.802	<sup>45</sup> 0.754	<sup>60</sup> 0.635	<sup>114</sup> 0.057	<sup>118</sup> 0.032						<sup>63</sup> 0.223	<sup>76</sup> 0.176		
163	NTECHLAB-007	<sup>69</sup> 0.040	<sup>98</sup> 0.026	<sup>109</sup> 0.012	<sup>80</sup> 0.085	<sup>87</sup> 0.067	<sup>80</sup> 0.041	<sup>38</sup> 0.796	<sup>44</sup> 0.750	<sup>61</sup> 0.642	<sup>83</sup> 0.032	<sup>88</sup> 0.017						<sup>53</sup> 0.183	<sup>56</sup> 0.140		
164	NTECHLAB-008	<sup>43</sup> 0.024	<sup>61</sup> 0.014	<sup>69</sup> 0.007	<sup>46</sup> 0.057	<sup>54</sup> 0.045	<sup>57</sup> 0.029	<sup>20</sup> 0.601	<sup>27</sup> 0.529	<sup>37</sup> 0.391	<sup>87</sup> 0.033	<sup>92</sup> 0.018						<sup>40</sup> 0.136	<sup>24</sup> 0.033	<sup>17</sup> 0.105	<sup>14</sup> 0.083
165	NTECHLAB-009	<sup>19</sup> 0.010	<sup>28</sup> 0.005	<sup>31</sup> 0.003	<sup>21</sup> 0.028	<sup>25</sup> 0.022	<sup>21</sup> 0.014	<sup>15</sup> 0.522	<sup>18</sup> 0.430	<sup>27</sup> 0.311	<sup>41</sup> 0.015	<sup>42</sup> 0.008	<sup>35</sup> 0.109	<sup>37</sup> 0.061	<sup>31</sup> 0.142	<sup>31</sup> 0.114					
166	NTECHLAB-010	<sup>12</sup> 0.005	<sup>13</sup> 0.003	<sup>10</sup> 0.002	<sup>13</sup> 0.018	<sup>14</sup> 0.015	<sup>12</sup> 0.011	<sup>11</sup> 0.334	<sup>11</sup> 0.252	<sup>15</sup> 0.169	<sup>16</sup> 0.007	<sup>18</sup> 0.004	<sup>20</sup> 0.059	<sup>22</sup> 0.031	<sup>10</sup> 0.098	<sup>8</sup> 0.077					
167	NTECHLAB-011	<sup>13</sup> 0.006	<sup>17</sup> 0.003	<sup>12</sup> 0.002	<sup>12</sup> 0.018	<sup>13</sup> 0.015	<sup>11</sup> 0.010	<sup>9</sup> 0.291	<sup>9</sup> 0.228	<sup>12</sup> 0.150	<sup>20</sup> 0.009	<sup>25</sup> 0.004	<sup>27</sup> 0.074	<sup>27</sup> 0.038	<sup>7</sup> 0.015	<sup>6</sup> 0.091	<sup>6</sup> 0.075				
168	PANGIAM-000	<sup>28</sup> 0.014	<sup>33</sup> 0.006	<sup>36</sup> 0.003	<sup>34</sup> 0.039	<sup>30</sup> 0.030	<sup>32</sup> 0.018	<sup>65</sup> 0.974	<sup>14</sup> 0.318	<sup>17</sup> 0.175	<sup>32</sup> 0.009	<sup>26</sup> 0.005	<sup>40</sup> 0.136	<sup>24</sup> 0.033	<sup>17</sup> 0.105	<sup>14</sup> 0.083					
169	PARAVISION-000	<sup>214</sup> 0.278	<sup>189</sup> 0.089	<sup>192</sup> 0.045	<sup>228</sup> 0.447	<sup>187</sup> 0.170	<sup>182</sup> 0.100	<sup>204</sup> 1.000	<sup>165</sup> 0.999	<sup>184</sup> 0.997	<sup>182</sup> 0.470	<sup>186</sup> 0.443						<sup>16</sup> 0.926	<sup>178</sup> 0.779		
170	PARAVISION-001	<sup>160</sup> 0.140	<sup>141</sup> 0.049	<sup>136</sup> 0.020	<sup>174</sup> 0.207	<sup>150</sup> 0.128	<sup>150</sup> 0.074	<sup>196</sup> 1.000	<sup>158</sup> 0.999	<sup>168</sup> 0.994	<sup>179</sup> 0.444	<sup>185</sup> 0.428						<sup>144</sup> 0.739	<sup>160</sup> 0.573		
171	PARAVISION-002	<sup>124</sup> 0.085	<sup>142</sup> 0.050	<sup>146</sup> 0.022	<sup>144</sup> 0.152	<sup>148</sup> 0.119	<sup>155</sup> 0.076	<sup>96</sup> 0.992	<sup>97</sup> 0.983	<sup>74</sup> 0.748	<sup>129</sup> 0.080	<sup>133</sup> 0.043						<sup>122</sup> 0.497	<sup>118</sup> 0.268		
172	PARAVISION-003	<sup>107</sup> 0.063	<sup>120</sup> 0.035	<sup>120</sup> 0.016	<sup>121</sup> 0.124	<sup>126</sup> 0.096	<sup>126</sup> 0.060	<sup>128</sup> 0.997	<sup>125</sup> 0.994	<sup>69</sup> 0.733	<sup>115</sup> 0.058	<sup>121</sup> 0.034						<sup>80</sup> 0.296	<sup>106</sup> 0.232		
173	PARAVISION-004	<sup>44</sup> 0.025	<sup>49</sup> 0.010	<sup>47</sup> 0.004	<sup>39</sup> 0.049	<sup>44</sup> 0.038	<sup>46</sup> 0.024	<sup>190</sup> 1.000	<sup>204</sup> 1.000	<sup>27</sup> 0.797	<sup>49</sup> 0.018	<sup>55</sup> 0.011						<sup>164</sup> 0.908	<sup>96</sup> 0.211		
174	PARAVISION-005	<sup>31</sup> 0.014	<sup>23</sup> 0.004	<sup>25</sup> 0.002	<sup>24</sup> 0.024	<sup>28</sup> 0.016	<sup>126</sup> 0.997	<sup>90</sup> 0.980	<sup>18</sup> 0.181	<sup>34</sup> 0.011	<sup>43</sup> 0.008						<sup>29</sup> 0.132	<sup>39</sup> 0.120			
175	PARAVISION-007	<sup>85</sup> 0.048	<sup>22</sup> 0.004	<sup>18</sup> 0.002	<sup>228</sup> 0.560																

MISSSES BELOW THRESHOLD, T		ENROL RECENT MUGSHOT, N = 1.6M												ENROL APPLICATION PORTRAIT, N = 1.6M																					
#	ALGORITHM	ENROL: MUGSHOT			ENROL: MUGSHOT			ENROL: WEBCAM			ENROL: PROFILE			ENROL: VISA			ENROL: BORDER			ENROL: 10+YR			ENROL: KIOSK												
		FPIR=0.0003	FPIR=0.001	FPIR=0.01	FPIR=0.0003	FPIR=0.001	FPIR=0.01	FPIR=0.0003	FPIR=0.001	FPIR=0.01	FPIR=0.0003	FPIR=0.001	FPIR=0.01	FPIR=0.001	FPIR=0.01	FPIR=0.001	FPIR=0.01	FPIR=0.001	FPIR=0.01	FPIR=0.001	FPIR=0.01	FPIR=0.001	FPIR=0.01	FPIR=0.001	FPIR=0.01										
185	QUANTASOFT-001	256	0.713	266	0.639	268	0.493																												
186	RANKONE-002	177	0.184	207	0.118	214	0.071	198	0.308	211	0.261	220	0.190																						
187	RANKONE-003	180	0.184	200	0.118	215	0.071	195	0.300	210	0.255	220	0.187																						
188	RANKONE-004	207	0.250	228	0.193	238	0.124	225	0.482	237	0.426	243	0.324																						
189	RANKONE-005	128	0.096	163	0.059	172	0.033	175	0.212	186	0.173	194	0.119	156	0.999	149	0.998	170	0.994																
190	RANKONE-006	107	0.061	123	0.037	132	0.020					85	0.987	85	0.977	105	0.937																		
191	RANKONE-007	59	0.034	92	0.022	105	0.011	113	0.118	122	0.095	129	0.061	68	0.975	73	0.967	98	0.924																
192	RANKONE-009	55	0.031	74	0.018	83	0.008	91	0.098	100	0.076	97	0.045	77	0.983	76	0.969	87	0.859	117	0.062	113	0.029		94	0.328	94	0.206							
193	RANKONE-010	38	0.023	50	0.014	74	0.007	73	0.077	77	0.058	79	0.036	80	0.905	80	0.802	64	0.652	109	0.052	110	0.027	69	0.208	72	0.119	70	0.259						
194	RANKONE-011	139	0.109	39	0.009	44	0.004	77	0.079	56	0.048	58	0.029					92	0.037	89	0.017	61	0.182	61	0.092	177	0.977	150	0.465						
195	RANKONE-012	38	0.020	36	0.008	41	0.004	69	0.072	69	0.053	59	0.030					74	0.029	73	0.014	43	0.144	43	0.072	116	0.465	47	0.128						
196	REALNETWORKS-000	225	0.374	234	0.234	241	0.138	218	0.433	227	0.319	231	0.209																						
197	REALNETWORKS-001	223	0.374	235	0.234	242	0.138	217	0.433	226	0.319	230	0.209																						
198	REALNETWORKS-002	224	0.370	232	0.231	240	0.137	216	0.416	225	0.315	232	0.209																						
199	REALNETWORKS-003	21	0.273	218	0.159	224	0.090	203	0.342	214	0.266	218	0.172	153	0.999	153	0.998	145	0.987	153	0.164	158	0.103			123	0.500	139	0.364						
200	REALNETWORKS-004	202	0.242	217	0.158	223	0.090	209	0.353	212	0.263	215	0.169	167	1.000	166	0.999	162	0.992	154	0.170	159	0.103			134	0.613	140	0.370						
201	REALNETWORKS-005	92	0.052	107	0.028	111	0.012	89	0.094	98	0.074	102	0.047	81	0.984	78	0.971	93	0.896	91	0.037	85	0.017	70	0.223	75	0.123	66	0.215	70	0.165				
202	REALNETWORKS-006	47	0.025	62	0.015	58	0.006	63	0.068	67	0.053	68	0.032	97	0.993	93	0.980	84	0.838	42	0.016	45	0.008	37	0.120	39	0.063	37	0.154	33	0.116				
203	REALNETWORKS-007	39	0.019	43	0.010	43	0.004	45	0.057	52	0.043	53	0.027	94	0.992	88	0.979	86	0.855	36	0.012	31	0.005	90	0.463	40	0.063	37	0.140	27	0.100				
204	REMARKAI-000	189	0.197	205	0.128	207	0.059	187	0.263	192	0.203	196	0.123																						
205	REMARKAI-000	148	0.125	155	0.055	148	0.023	152	0.173	149	0.120	144	0.070	160	0.999	164	0.999	173	0.995	125	0.069	120	0.033			142	0.717	132	0.315						
206	REMARKAI-002	18	0.188	204	0.124	206	0.059	181	0.248	190	0.196	195	0.122	101	0.993	114	0.991	138	0.980																
207	RENDIP-000	39	0.023	52	0.012	53	0.005	64	0.189	78	0.059	74	0.034	88	0.945	62	0.894	72	0.744	58	0.022	66	0.013	63	0.185	57	0.089	44	0.167	49	0.130				
208	REVEALMEDIA-000	40	0.024	54	0.012	57	0.006	43	0.054	50	0.042	50	0.025	32	0.755	40	0.680	49	0.539	56	0.021	56	0.011	52	0.093	35	0.051	32	0.143	36	0.118				
209	S1-000	156	0.137	111	0.028	104	0.011	124	0.129	109	0.085	104	0.048	215	1.000	221	1.000	54	0.596	105	0.047	93	0.018	202	1.000	74	0.123	255	1.000	165	0.632				
210	S1-001	95	0.054	69	0.016	71	0.007	56	0.066	64	0.052	75	0.033	95	0.992	101	0.985	115	0.952	50	0.019	51	0.010	39	0.136	47	0.075	35	0.148	37	0.119				
211	SCANOVATE-000	134	0.103	170	0.067	168	0.030	194	0.296	206	0.240	205	0.150	53	0.931	60	0.893	80	0.803	162	0.215	166	0.118			103	0.400	128	0.299						
212	SCANOVATE-001	159	0.128	181	0.081	180	0.037	193	0.281	206	0.227	201	0.140	84	0.935	64	0.911	83	0.834	159	0.192	160	0.103			104	0.404	124	0.290						
213	SENSETIME-000	64	0.036	88	0.021	94	0.009	74	0.078	83	0.063	87	0.040	247	1.000	246	1.000	146	0.988																
214	SENSETIME-001	65	0.036	91	0.022	94	0.010	78	0.080	85	0.064	93	0.041																						
215	SENSETIME-002	66	0.037	63	0.015	119	0.014	120	0.124	33	0.028	43	0.023	125	0.997	123	0.994	137	0.979	81	0.032	86	0.017			125	0.523	69	0.160						
216	SENSETIME-003	7	0.004	70	0.002	6	0.001	4	0.014	4	0.012	4	0.009	22	0.607	22	0.477	28	0.311	20	0.008	30	0.005			2	0.133	32	0.115						
217	SENSETIME-004	3	0.003	4	0.002	5	0.001	6	0.015	6	0.013	9	0.010	10	0.301	10	0.229	12	0.149	14	0.006	14	0.004			21	0.113	26	0.100						
218	SENSETIME-005	28	0.011	11	0.002	4	0.001	14	0.018	12	0.014	7	0.010	4	0.259	3	0.173	5	0.103	7	0.007	16	0.004	15	0.023	16	0.104	21	0.093						
219	SENSETIME-006	9	0.005	5	0.002	2	0.001	9	0.016	5	0.012	3	0.009	145	0.999	151	0.998	66	0.680	6	0.004	5	0.002	9	0.034	8	0.016	8	0.093	11	0.079				
220	SENSETIME-007	0	0.003	1	0.001	1	0.001	1	0.012	1	0.009	1	0.007	169	1.000	171	0.999	48	0.538	2	0.003	1	0.001	1	0.024	3	0.011	3	0.085	5	0.074				
221	SHAMAN-003	239	0.506	257	0.451	261	0.347	238	0.650	251	0.597	254	0.472																						
222	SHAMAN-004	239	0.679	264	0.615	266	0.488	249	0.812	258	0.754	263	0.639																						
223	SHAMAN-006	182	0.185	212	0.141	226	0.092	191	0.278	202	0.237	214	0.168	70	0.978	79	0.972	120	0.960																
224	SHAMAN-007	177	0.183	213	0.141	225	0.092	192	0.280	205	0.240	216	0.169																						
225	SIAT-001	15	0.132	70	0.018	70	0.007	236	0.641	231	0.365	246	0.348																						
226	SIAT-002	228	0.417	89	0.022	75	0.007	252	0.942	247	0.478	252	0.460																			167	0.923	73	0.169
227	SMILART-004	272	0.970	275	0.968	263	0.977	27	0.976	273	0.973																								
228	SMILART-005																																		
229	SQLSOFT-001	198	0.226	209	0.132	190	0.044	201	0.340	208	0.252	191	0.111	61	0.956	48	0.797	55	0.608	65	0.040	95	0.019	82	0.317	81	0.150	168	0.420	86	0.189				
230	STAQU-000	219	0.334	164	0.062	142	0.022	250	0.848</																										

Table 31: **Threshold-based accuracy**. Values are FNIR( $N, T, L$ ) with  $N = 1.6$  million with thresholds set to produce FPIR = 0.0003, 0.001, and 0.01 in non-mate searches. Throughout blue superscripts indicate the rank of the algorithm for that column. Caution: The Power-low models are mostly intended to draw attention to the kind of behavior, not as a model to be used for prediction.

2022/04/28  
22:29:02

FNIR(N, R, T) = False neg. identification rate  
FPIR(N, T) = False pos. identification rate

N = Num. enrolled subjects  
 R = Num. candidates examined

= Threshold

$T = 0 \rightarrow$  Investigation  
 $T > 0 \rightarrow$  Identification

MISSES BELOW THRESHOLD, T		ENROL RECENT MUGSHOT, N = 1.6M												ENROL APPLICATION PORTRAIT, N = 1.6M																							
#	ALGORITHM	ENROL: MUGSHOT			ENROL: MUGSHOT			ENROL: MUGSHOT			ENROL: VISA			ENROL: BORDER			ENROL: VISA		ENROL: BORDER		ENROL: KIOSK																
		FPIR=0.0003	FPIR=0.001	FPIR=0.01	FPIR=0.0003	FPIR=0.001	FPIR=0.01	FPIR=0.0003	FPIR=0.001	FPIR=0.01	FPIR=0.001	FPIR=0.01	FPIR=0.001	FPIR=0.01	FPIR=0.001	FPIR=0.01	FPIR=0.001	FPIR=0.01	FPIR=0.001	FPIR=0.01	FPIR=0.001	FPIR=0.01															
231	SYNESIS-003	250	0.648	262	0.582	265	0.443	242	0.708	254	0.646	256	0.524	63	0.973	71	0.960	99	0.911	127	0.075	126	0.039														
232	SYNESIS-003	140	0.111	168	0.065	169	0.032	145	0.155	152	0.123	156	0.078	109	0.995	98	0.984	76	0.795	84	0.032	80	0.016														
233	SYNESIS-005	88	0.050	92	0.025	107	0.011	84	0.088	94	0.072	96	0.043	109	0.995	98	0.984	76	0.795	59	0.214	68	0.158														
234	TECH5-001	260	0.807	158	0.057	128	0.018	267	0.994	120	0.935	284	1.000	222	1.000	217	1.000	163	0.244	112	0.028	18	0.994	181	0.817												
235	TECH5-002	94	0.053	106	0.027	110	0.012	88	0.094	92	0.070	89	0.040	46	0.874	51	0.805	58	0.627	94	0.039	94	0.019	67	0.205	70	0.111	111	0.440	83	0.182						
236	TEVIAN-003	201	0.239	225	0.177	231	0.096	209	0.346	222	0.298	224	0.198																								
237	TEVIAN-004	174	0.170	199	0.117	211	0.063	176	0.216	187	0.176	192	0.115																								
238	TEVIAN-005	152	0.129	186	0.087	192	0.045	156	0.180	167	0.144	168	0.089	88	0.988	72	0.962	78	0.796																		
239	TEVIAN-006	42	0.024	44	0.010	50	0.005	39	0.041	37	0.032	37	0.021	18	0.562	17	0.425	26	0.291	43	0.016	46	0.009	30	0.093	33	0.050	172	0.951	35	0.117						
240	TEVIAN-007	23	0.011	30	0.005	32	0.003	20	0.028	21	0.022	22	0.015	14	0.504	13	0.301	20	0.183	31	0.009	26	0.005	22	0.065	23	0.033	23	0.122	29	0.102						
241	TIGER-000	234	0.462	251	0.390	259	0.261	227	0.565	241	0.500	247	0.366																								
242	TIGER-002	170	0.158	183	0.086	183	0.039	172	0.202	176	0.158	178	0.095	161	0.999	161	0.999	134	0.975																		
243	TIGER-003	171	0.158	182	0.086	185	0.039	171	0.202	177	0.158	174	0.095																								
244	TONGYITRANS-000	137	0.107	175	0.074	181	0.038	137	0.141	141	0.112	143	0.069																								
245	TONGYITRANS-001	147	0.124	169	0.066	176	0.032	122	0.128	131	0.101	132	0.062																								
246	TOSHIBA-000	146	0.123	165	0.062	162	0.027	141	0.150	146	0.118	149	0.074	127	0.997	134	0.995	147	0.988																		
247	TOSHIBA-001	196	0.225	160	0.058	136	0.019	131	0.133	117	0.092	119	0.054																								
248	TRUEFACE-000	81	0.046	78	0.018	82	0.008	75	0.079	82	0.062	84	0.039	114	0.995	57	0.882	41	0.499	75	0.030	83	0.016	65	0.194	71	0.111	55	0.188	59	0.145						
249	VD-000	269	0.950	273	0.917	276	0.827	269	0.968	269	0.946	269	0.871																								
250	VD-001	213	0.278	229	0.201	236	0.116	199	0.331	218	0.281	221	0.188																								
251	VD-002	164	0.144	179	0.079	174	0.036	161	0.188	161	0.148	169	0.092	136	0.998	137	0.996	144	0.987	134	0.095	137	0.048	84	0.367	88	0.220	99	0.372	120	0.280						
252	VD-003	200	0.234	136	0.046	135	0.020	130	0.133	130	0.100	131	0.061	138	0.999	162	0.999	166	0.994	107	0.051	108	0.027	72	0.244	76	0.133	91	0.315	90	0.203						
253	VERIDAS-001	120	0.080	125	0.037	123	0.016	102	0.106	108	0.082	107	0.051	100	0.993	105	0.987	108	0.938	99	0.044	104	0.023	74	0.266	78	0.146	27	0.264	91	0.204						
254	VERIDAS-002	121	0.080	124	0.037	122	0.016	101	0.106	108	0.082	107	0.051	99	0.993	106	0.987	107	0.938	98	0.044	105	0.023	75	0.266	79	0.146	78	0.264	92	0.204						
255	VERIDAS-003	113	0.072	70	0.017	64	0.006	66	0.071	72	0.055	71	0.033	142	0.998	141	0.997	108	0.927	52	0.020	54	0.011	47	0.150	49	0.078	50	0.178	57	0.142						
256	VIGILANTSOLUTIONS-003	238	0.482	235	0.408	259	0.282	241	0.730	257	0.660	238	0.526	134	0.999	137	0.999	175	0.995																		
257	VIGILANTSOLUTIONS-004	249	0.624	261	0.549	263	0.422	251	0.858	261	0.817	263	0.709	140	0.998	139	0.996	158	0.991																		
258	VIGILANTSOLUTIONS-005	268	0.936	250	0.388	187	0.043							194	1.000	208	1.000	222	1.000																		
259	VIGILANTSOLUTIONS-006	271	0.959	245	0.353	188	0.043							199	1.000	209	1.000	222	1.000																		
260	VIGILANTSOLUTIONS-007	117	0.076	113	0.028	108	0.011	107	0.113	113	0.088	114	0.053	133	0.997	138	0.996	159	0.991	131	0.081	135	0.047	86	0.371	90	0.242	102	0.391	127	0.295						
261	VIGILANTSOLUTIONS-008	91	0.051	85	0.021	93	0.010	108	0.105	101	0.077	100	0.046	164	1.000	160	0.999	158	0.991	138	0.104	140	0.054	88	0.398	92	0.259	124	0.511	133	0.316						
262	VISIONBOX-000	114	0.073	75	0.018	72	0.007	67	0.071	73	0.057	78	0.035	106	0.995	113	0.990	132	0.974	61	0.023	62	0.012	46	0.146	51	0.081	42	0.162	45	0.126						
263	VISIONLABS-004	126	0.091	159	0.058	131	0.024	167	0.199	178	0.159	177	0.097	56	0.944	59	0.890	71	0.742																		
264	VISIONLABS-005	122	0.080	143	0.050	130	0.020	167	0.183	166	0.147	166	0.087	57	0.945	58	0.888	70	0.736																		
265	VISIONLABS-006	77	0.044	105	0.027	96	0.010	111	0.117	117	0.090	110	0.051	35	0.764	36	0.672	46	0.511	80	0.031	73	0.014														
266	VISIONLABS-007	76	0.044	104	0.027	97	0.010	110	0.117	116	0.090	109	0.051	34	0.764	37	0.672	45	0.511	80	0.031	73	0.014														
267	VISIONLABS-008	50	0.028	57	0.013	56	0.006	61	0.068	67	0.051	66	0.032	19	0.574	23	0.481	29	0.317	44	0.017	41	0.008														
268	VISIONLABS-009	26	0.012	25	0.005	21	0.002	25	0.032	27	0.025	29	0.017	52	0.930	49	0.799	22	0.196	27	0.008	24	0.004														
269	VISIONLABS-010	30	0.014	29	0.005	27	0.002	28	0.034	34	0.027	33	0.019					14	0.169	21	0.008	17	0.004	18	0.055	18	0.027	19	0.109	18	0.089						
270	VISIONLABS-011	24	0.011	19	0.003	15	0.002	15	0.024	20	0.020	20	0.014					21	0.194	9	0.004	7	0.002	10	0.034	9	0.017	6	0.090	10	0.079						
271	VOCORD-003	221	0.354	203	0.122	196	0.048	166	0.195	175	0.155	172	0.093	146	0.999	150	0.998	150	0.991	152	0.157	161	0.1														

MISSES BELOW THRESHOLD, T		ENROL RECENT MUGSHOT, N = 1.6M												ENROL APPLICATION PORTRAIT, N = 1.6M													
#	ALGORITHM	ENROL: MUGSHOT			ENROL: MUGSHOT			ENROL: WEBCAM			PROBE: PROFILE			ENROL: VISA		ENROL: BORDER		ENROL: BORDER 10+YR		ENROL: VISA		ENROL: BORDER		ENROL: KIOSK			
		FPIR=0.0003	FPIR=0.001	FPIR=0.01	FPIR=0.0003	FPIR=0.001	FPIR=0.01	FPIR=0.0003	FPIR=0.001	FPIR=0.01	FPIR=0.0003	FPIR=0.001	FPIR=0.01	FPIR=0.001	FPIR=0.01	FPIR=0.001	FPIR=0.01	FPIR=0.001	FPIR=0.01	FPIR=0.001	FPIR=0.01	FPIR=0.001	FPIR=0.01	FPIR=0.001	FPIR=0.01		
277	VTS-002	<sup>93</sup> 0.053	<sup>100</sup> 0.026	<sup>100</sup> 0.010	<sup>93</sup> 0.098	<sup>99</sup> 0.075	<sup>101</sup> 0.046	<sup>174</sup> 1.000	<sup>179</sup> 1.000	<sup>116</sup> 0.953	<sup>101</sup> 0.045	<sup>108</sup> 0.026	<sup>71</sup> 0.231	<sup>77</sup> 0.133	<sup>107</sup> 0.417	<sup>80</sup> 0.187											
278	XFORWARDAI-000	<sup>52</sup> 0.029	<sup>66</sup> 0.015	<sup>67</sup> 0.006	<sup>64</sup> 0.070	<sup>70</sup> 0.053	<sup>76</sup> 0.034	<sup>31</sup> 0.698	<sup>19</sup> 0.440	<sup>21</sup> 0.250	<sup>55</sup> 0.021	<sup>51</sup> 0.011	<sup>52</sup> 0.159	<sup>51</sup> 0.082	<sup>45</sup> 0.169	<sup>50</sup> 0.134											
279	XFORWARDAI-001	<sup>21</sup> 0.010	<sup>27</sup> 0.005	<sup>33</sup> 0.003	<sup>30</sup> 0.036	<sup>34</sup> 0.028	<sup>34</sup> 0.020	<sup>43</sup> 0.838	<sup>20</sup> 0.448	<sup>10</sup> 0.143	<sup>24</sup> 0.008	<sup>29</sup> 0.005	<sup>21</sup> 0.062	<sup>21</sup> 0.030	<sup>24</sup> 0.123	<sup>28</sup> 0.102											
280	XFORWARDAI-002	<sup>14</sup> 0.007	<sup>18</sup> 0.003	<sup>24</sup> 0.002	<sup>15</sup> 0.018	<sup>15</sup> 0.016	<sup>18</sup> 0.014	<sup>67</sup> 0.975	<sup>25</sup> 0.525	<sup>7</sup> 0.095	<sup>12</sup> 0.005	<sup>12</sup> 0.003	<sup>13</sup> 0.041	<sup>11</sup> 0.018	<sup>12</sup> 0.099	<sup>17</sup> 0.089											
281	YISHENG-001	<sup>232</sup> 0.452	<sup>243</sup> 0.346	<sup>249</sup> 0.206	<sup>263</sup> 0.983	<sup>259</sup> 0.808	<sup>257</sup> 0.269						<sup>189</sup> 0.666	<sup>184</sup> 0.396									<sup>166</sup> 0.919	<sup>168</sup> 0.695			
282	YITU-002	<sup>56</sup> 0.031	<sup>73</sup> 0.018	<sup>77</sup> 0.008	<sup>50</sup> 0.063	<sup>57</sup> 0.049	<sup>55</sup> 0.028																				
283	YITU-003	<sup>57</sup> 0.032	<sup>81</sup> 0.019	<sup>88</sup> 0.009	<sup>58</sup> 0.067	<sup>66</sup> 0.052	<sup>72</sup> 0.033																				
284	YITU-004	<sup>33</sup> 0.019	<sup>41</sup> 0.010	<sup>46</sup> 0.004	<sup>29</sup> 0.035	<sup>30</sup> 0.027	<sup>30</sup> 0.017	<sup>60</sup> 0.948	<sup>67</sup> 0.936	<sup>96</sup> 0.913																	
285	YITU-005	<sup>37</sup> 0.022	<sup>48</sup> 0.010	<sup>51</sup> 0.005	<sup>35</sup> 0.039	<sup>38</sup> 0.032	<sup>42</sup> 0.023																				

Table 33: **Threshold-based accuracy.** Values are FNIR(N, T, L) with N = 1.6 million with thresholds set to produce FPIR = 0.0003, 0.001, and 0.01 in non-mate searches. Throughout blue superscripts indicate the rank of the algorithm for that column. Caution: The Power-low models are mostly intended to draw attention to the kind of behavior, not as a model to be used for prediction.

2022/04/28  
22:29:02FNIR(N, R, T) = False neg. identification rate  
FPIR(N, T) = False pos. identification rateN = Num. enrolled subjects  
R = Num. candidates examined  
T = ThresholdT = 0 → Investigation  
T > 0 → Identification

# Appendices

## Appendix A Accuracy on large-population FRVT 2018 mugshots

2022/04/28 22:29:02	$\text{FNIR}(N, R, T) =$ $\text{FPTR}(N, T) =$	False neg. identification rate False pos. identification rate	$N =$ Num. enrolled subjects $R =$ Num. candidates examined	$T =$ Threshold $T > 0 \rightarrow$ Identification	$T = 0 \rightarrow$ Investigation
------------------------	---	--	--	---	-----------------------------------

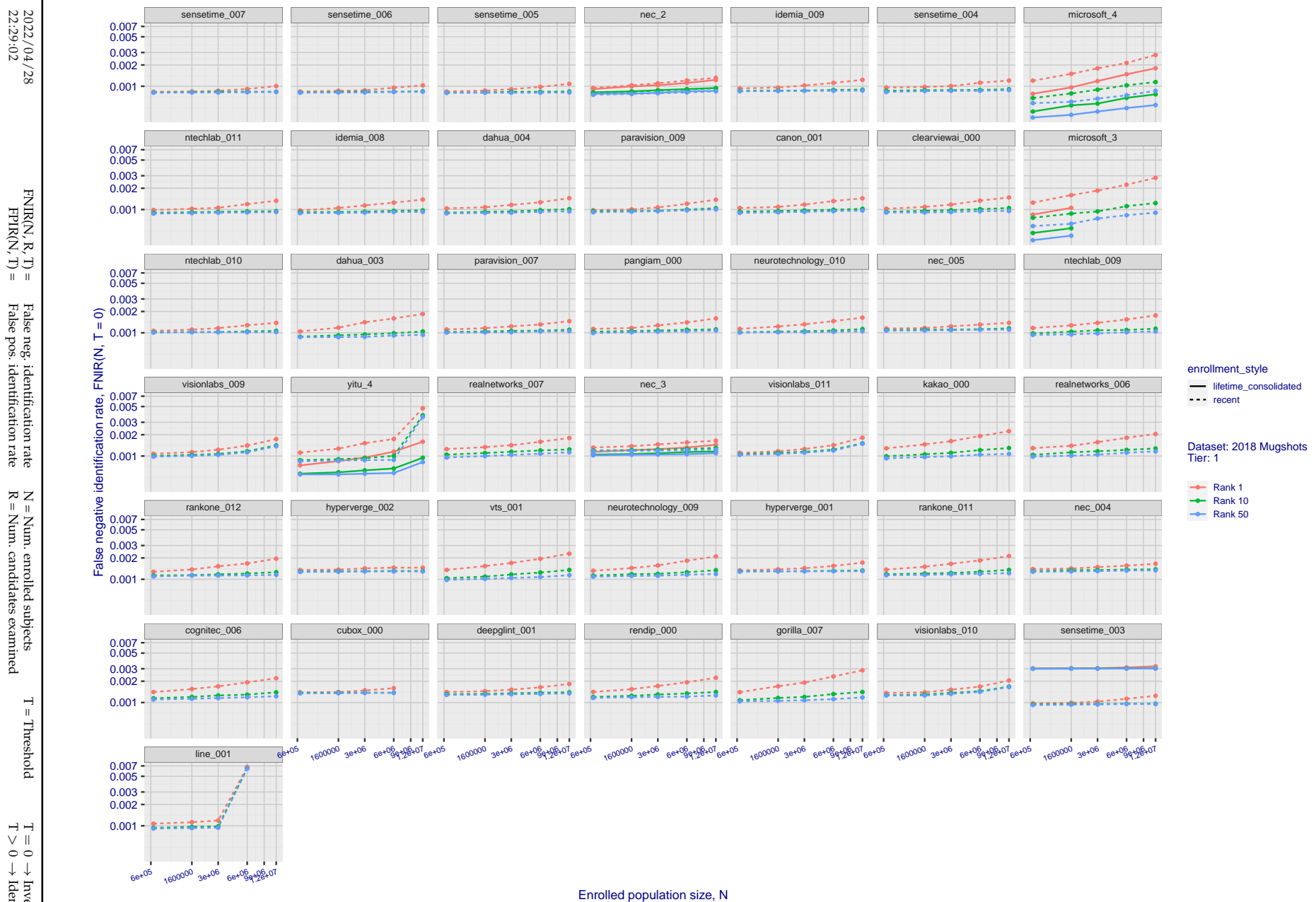


Figure 20: [FRVT-2018 Mugshot Dataset] Rank-based identification miss rates vs. number of enrolled subjects. The figure shows false negative identification rates,  $\text{FNIR}(N, R)$ , across various gallery sizes and ranks 1, 10 and 50. The threshold is set to zero, so this metric rewards even weak scoring rank 1 mates. This also means  $\text{FPIR} = 1$ , so any search without an enrolled mate will return non-mated candidates. For clarity, results are sorted and reported into tiers spanning multiple pages, the tiering criteria being rank 1 hit rate on a gallery size of 640 000.

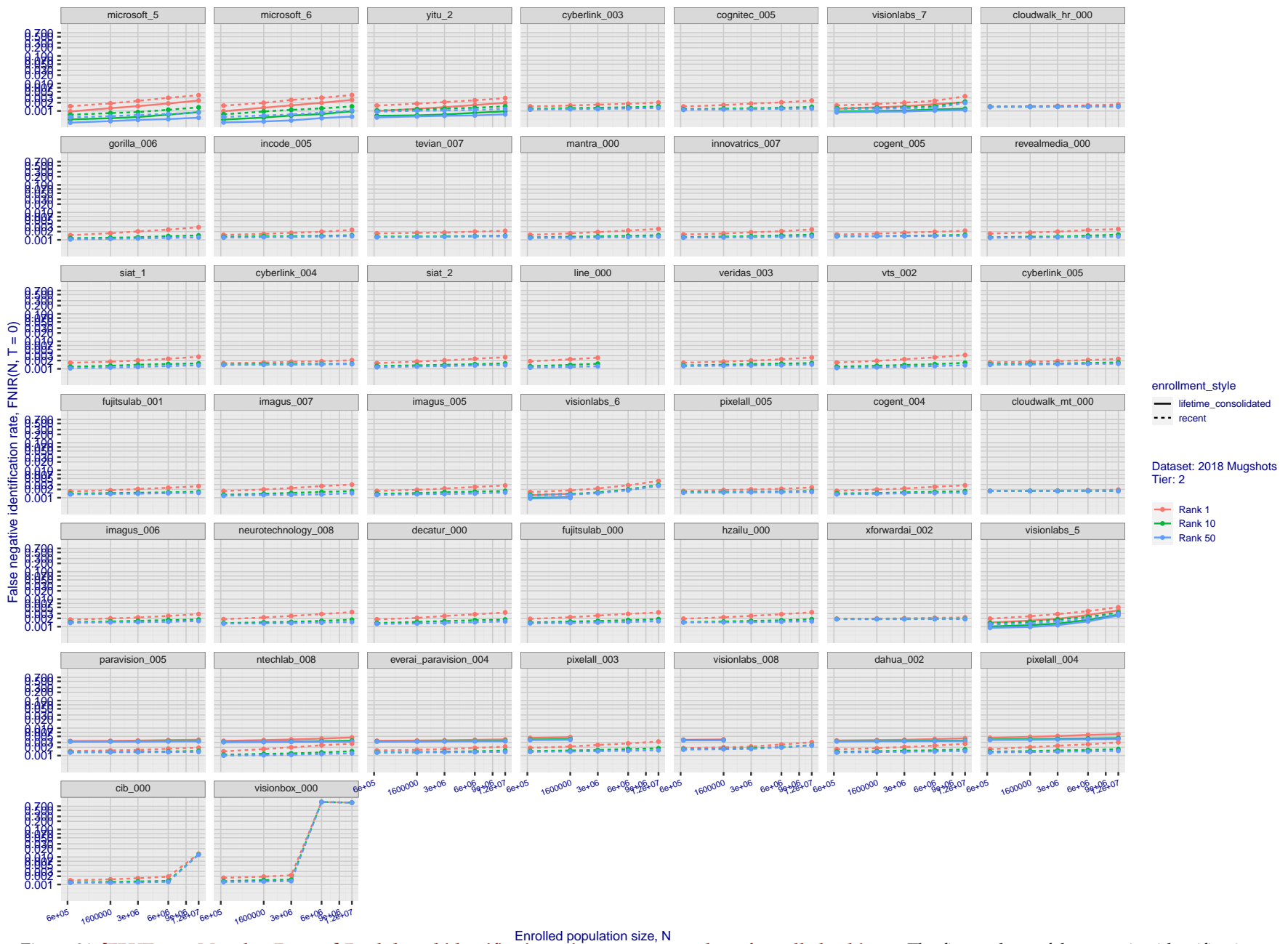


Figure 21: [FRVT-2018 Mugshot Dataset] Rank-based identification miss rates vs. number of enrolled subjects. The figure shows false negative identification rates,  $\text{FNIR}(N, R)$ , across various gallery sizes and ranks 1, 10 and 50. The threshold is set to zero, so this metric rewards even weak scoring rank 1 mates. This also means  $\text{FPIR} = 1$ , so any search without an enrolled mate will return non-mated candidates. For clarity, results are sorted and reported into tiers spanning multiple pages, the tiering criteria being rank 1 hit rate on a gallery size of 640 000.

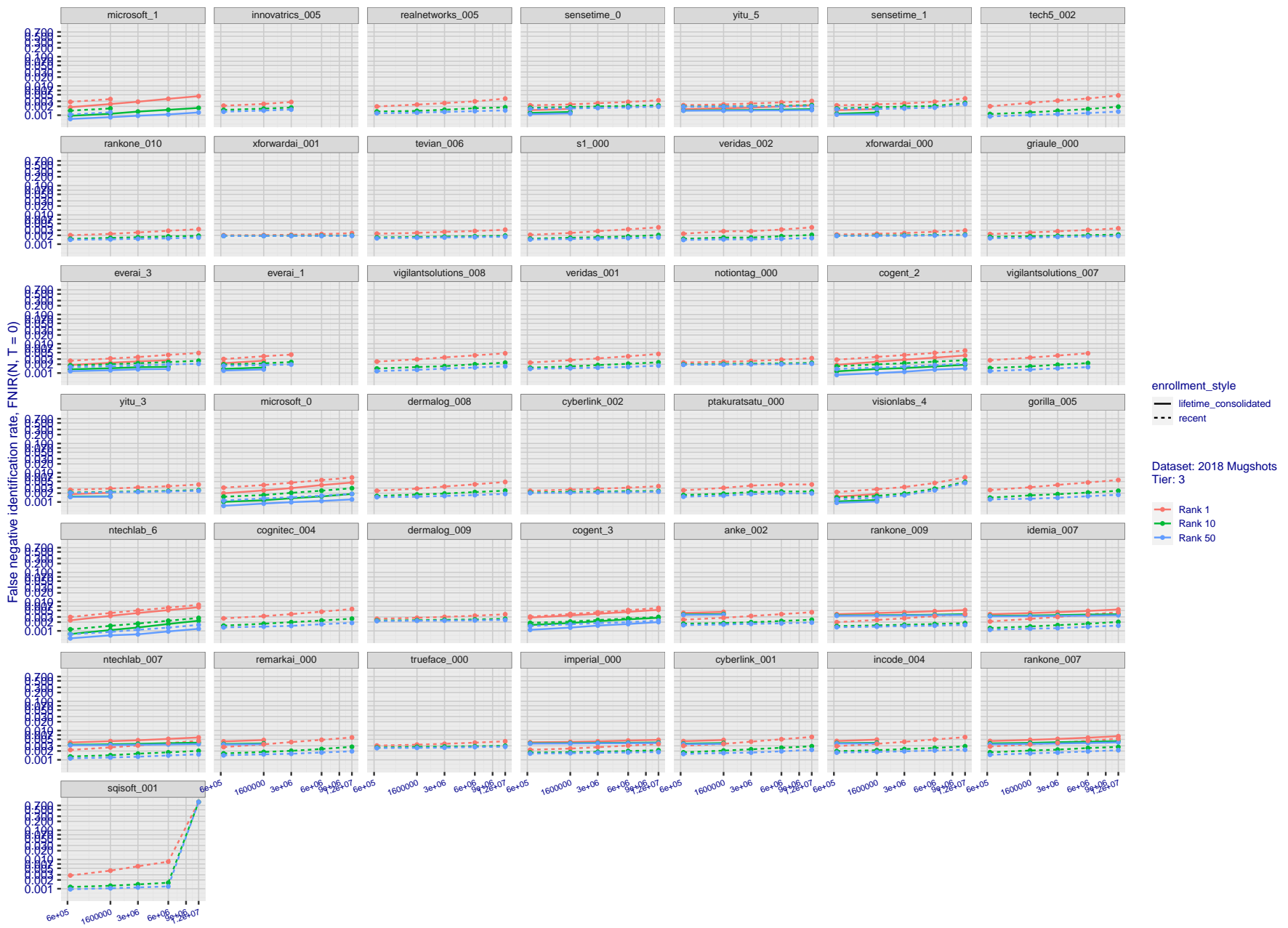
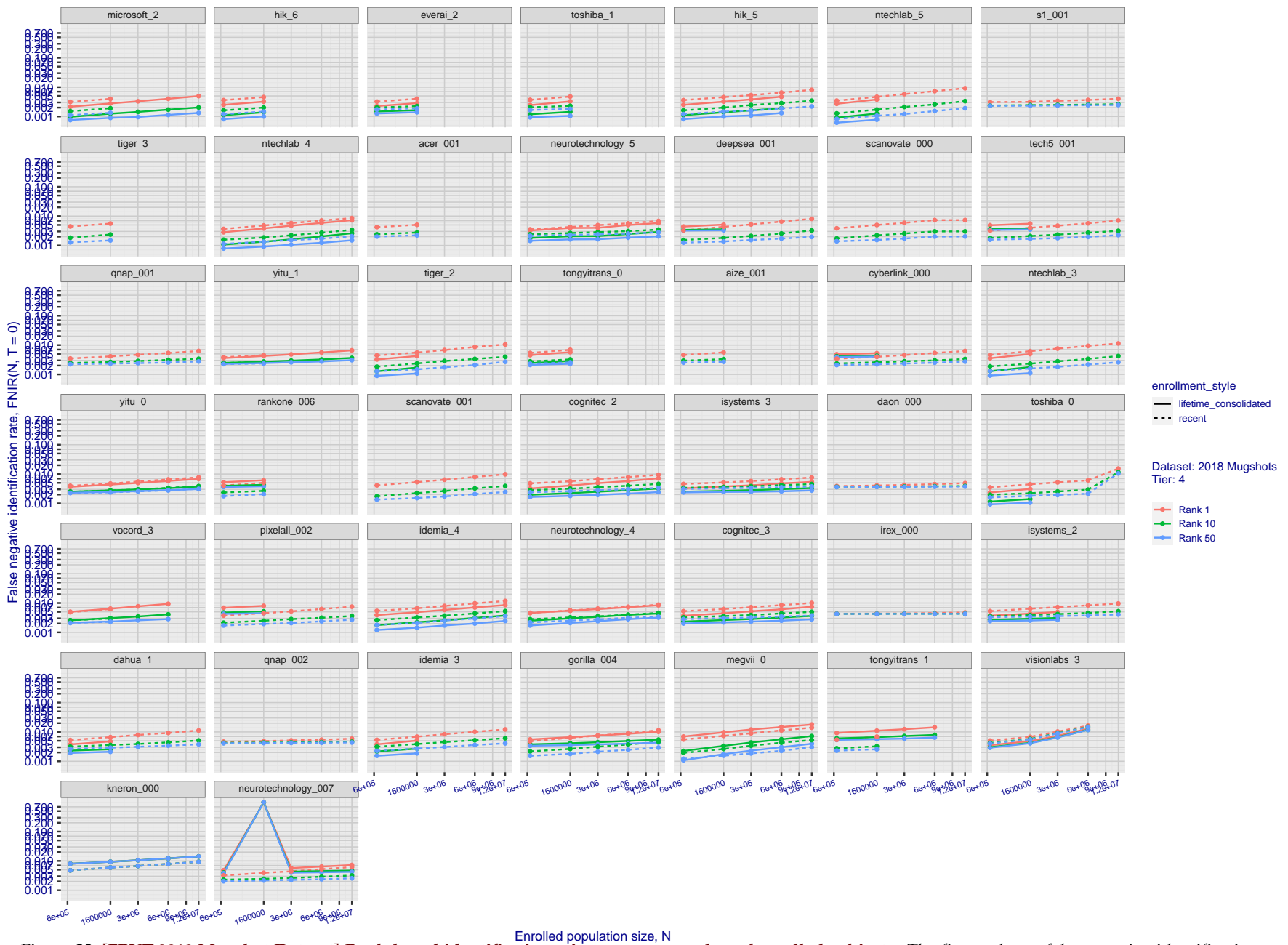


Figure 22: [FRVT-2018 Mugshot Dataset] Rank-based identification miss rates vs. number of enrolled subjects. The figure shows false negative identification rates,  $\text{FNIR}(N, R)$ , across various gallery sizes and ranks 1, 10 and 50. The threshold is set to zero, so this metric rewards even weak scoring rank 1 mates. This also means  $\text{FPIR} = 1$ , so any search without an enrolled mate will return non-mated candidates. For clarity, results are sorted and reported into tiers spanning multiple pages, the tiering criteria being rank 1 hit rate on a gallery size of 640 000.



**Figure 23: [FRVT-2018 Mugshot Dataset] Rank-based identification miss rates vs. number of enrolled subjects.** The figure shows false negative identification rates,  $\text{FNIR}(N, R)$ , across various gallery sizes and ranks 1, 10 and 50. The threshold is set to zero, so this metric rewards even weak scoring rank 1 mates. This also means  $\text{FPIR} = 1$ , so any search without an enrolled mate will return non-mated candidates. For clarity, results are sorted and reported into tiers spanning multiple pages, the tiering criteria being rank 1 hit rate on a gallery size of 640 000.

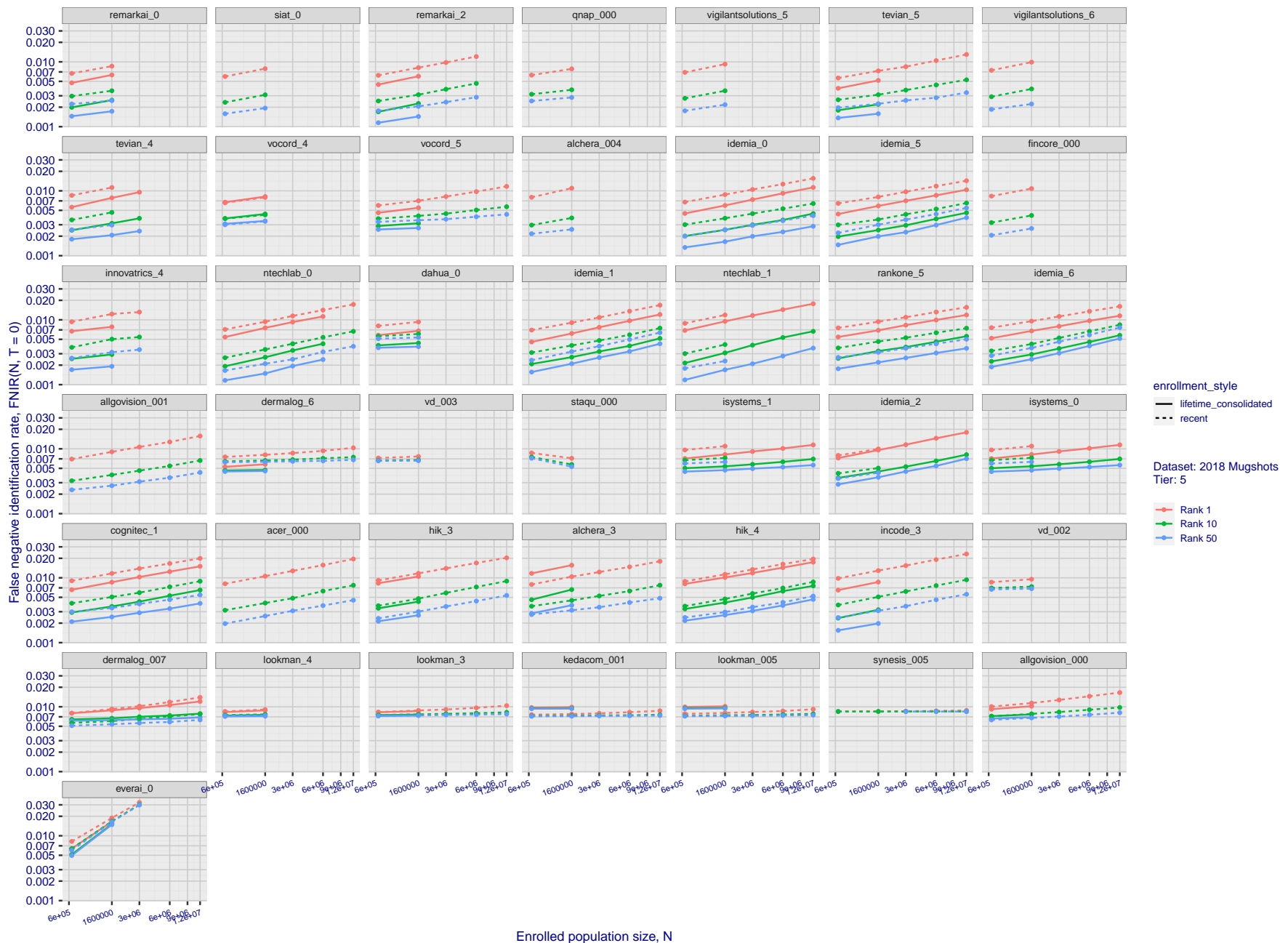
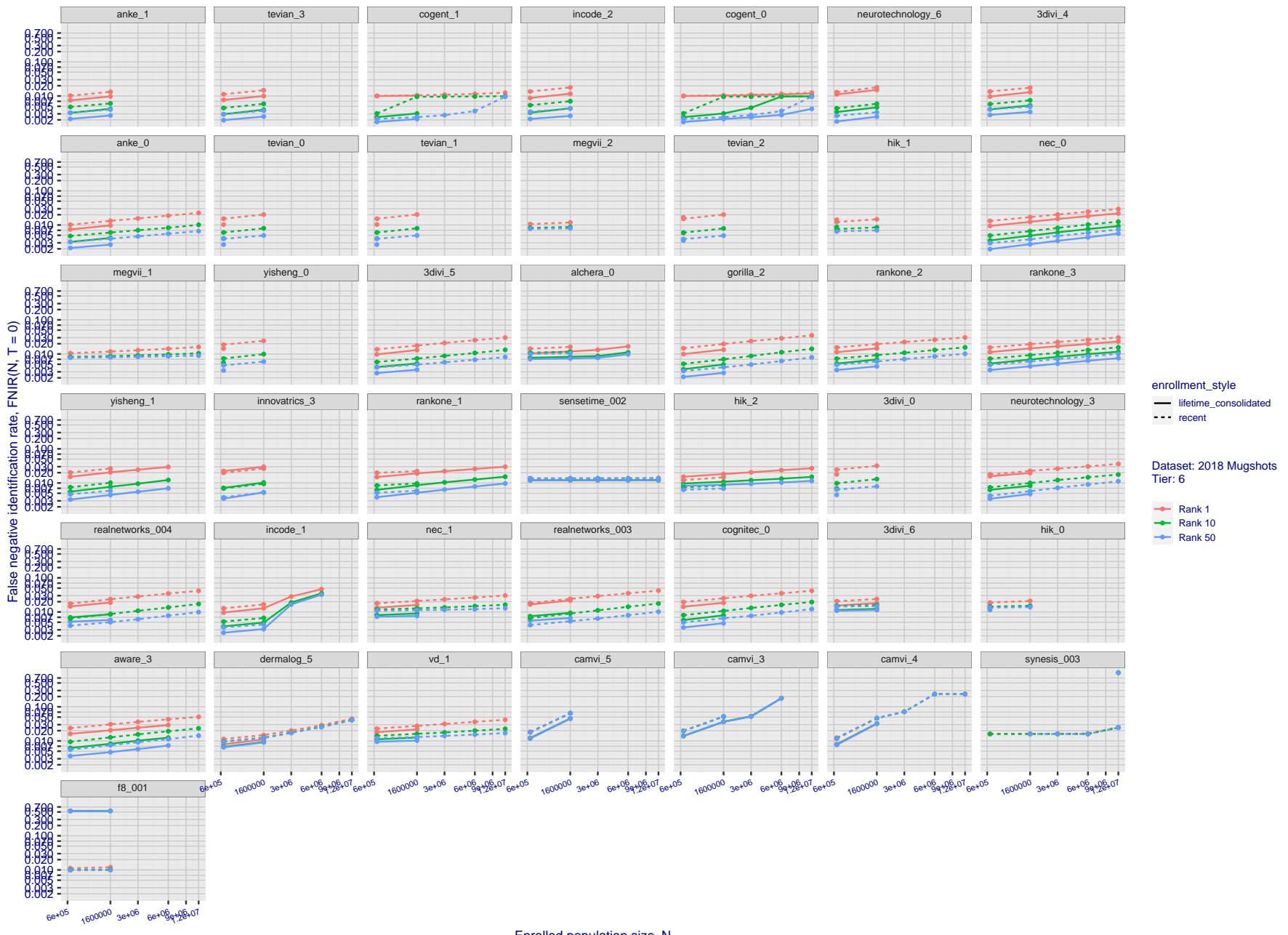


Figure 24: [FRVT-2018 Mugshot Dataset] Rank-based identification miss rates vs. number of enrolled subjects. The figure shows false negative identification rates,  $\text{FNIR}(N, R)$ , across various gallery sizes and ranks 1, 10 and 50. The threshold is set to zero, so this metric rewards even weak scoring rank 1 mates. This also means  $\text{FPIR} = 1$ , so any search without an enrolled mate will return non-mated candidates. For clarity, results are sorted and reported into tiers spanning multiple pages, the tiering criteria being rank 1 hit rate on a gallery size of 640 000.

2022/04/28  
22:29:02FNIR( $N, R, T = 0$ ) = False neg. identification rate  
FPIR( $N, T = 0$ ) = False pos. identification rateN = Num. enrolled subjects  
R = Num. candidates examined

T = Threshold

T = 0 → Investigation  
 $T > 0 \rightarrow$  Identification



**Figure 25: [FRVT-2018 Mugshot Dataset] Rank-based identification miss rates vs. number of enrolled subjects.** The figure shows false negative identification rates,  $\text{FNIR}(N, R)$ , across various gallery sizes and ranks 1, 10 and 50. The threshold is set to zero, so this metric rewards even weak scoring rank 1 mates. This also means  $\text{FPIR} = 1$ , so any search without an enrolled mate will return non-mated candidates. For clarity, results are sorted and reported into tiers spanning multiple pages, the tiering criteria being rank 1 hit rate on a gallery size of 640 000.

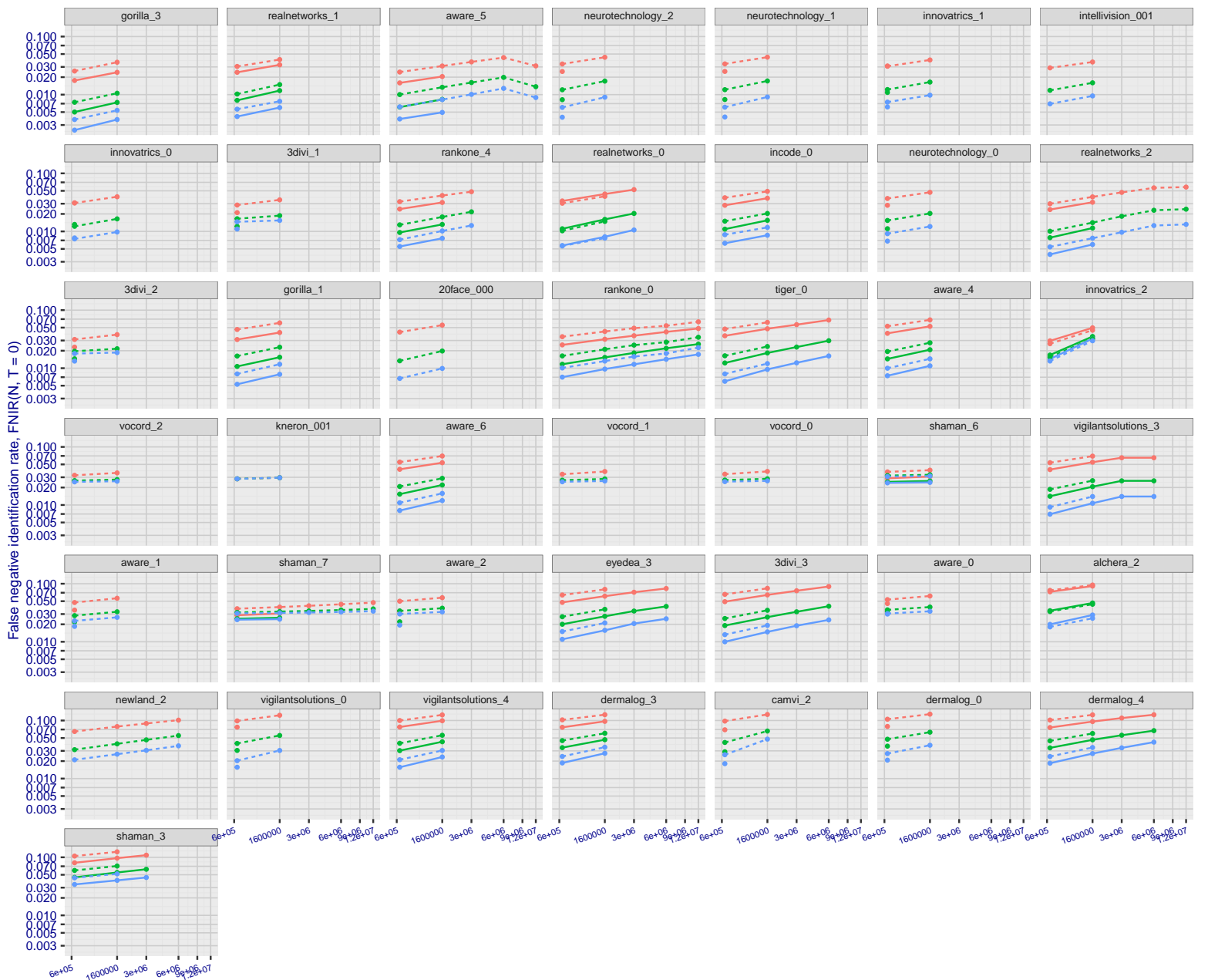


Figure 26: [FRVT-2018 Mugshot Dataset] Rank-based identification miss rates vs. number of enrolled subjects. The figure shows false negative identification rates,  $\text{FNIR}(N, R)$ , across various gallery sizes and ranks 1, 10 and 50. The threshold is set to zero, so this metric rewards even weak scoring rank 1 mates. This also means  $\text{FPIR} = 1$ , so any search without an enrolled mate will return non-mated candidates. For clarity, results are sorted and reported into tiers spanning multiple pages, the tiering criteria being rank 1 hit rate on a gallery size of 640 000.

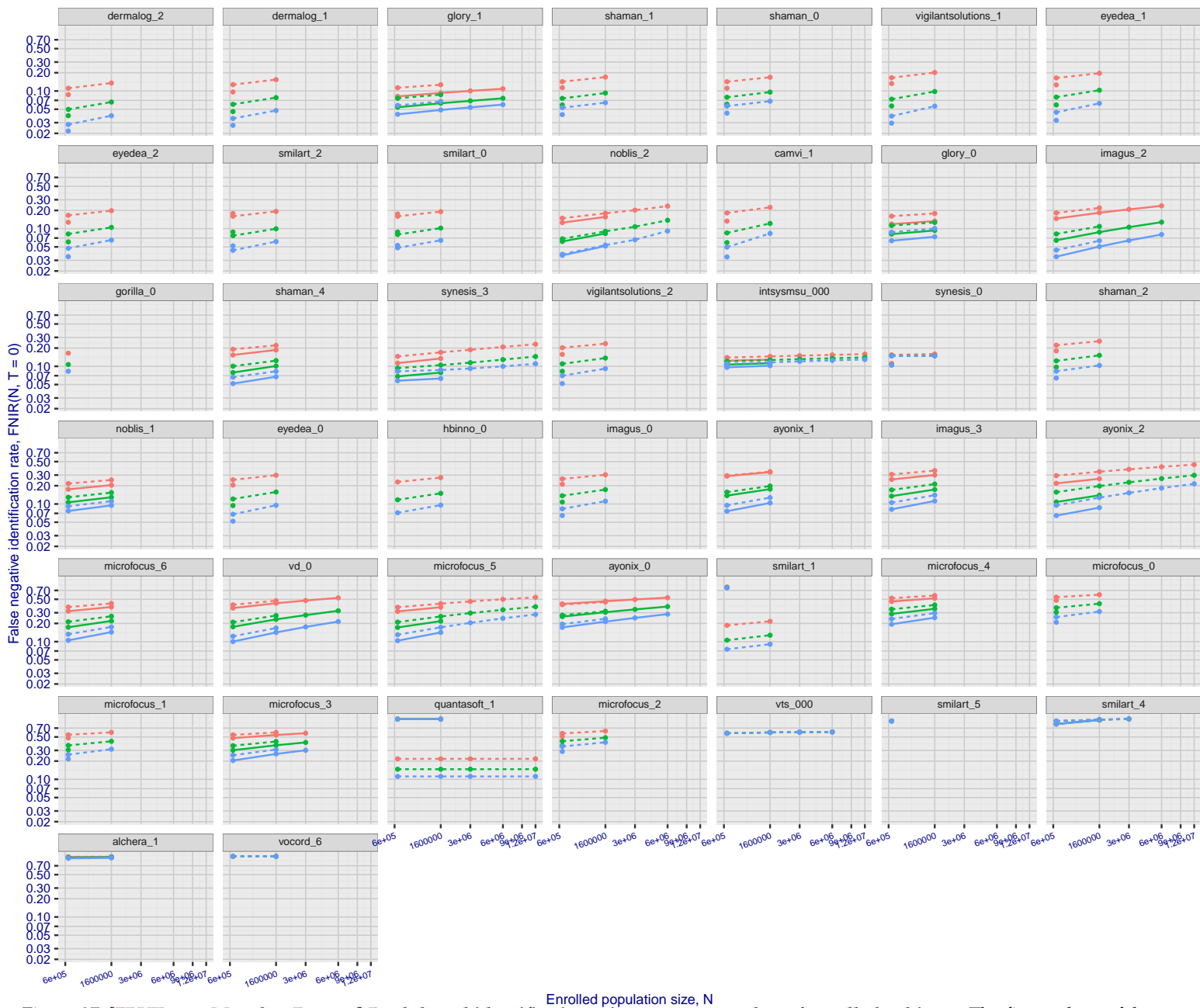
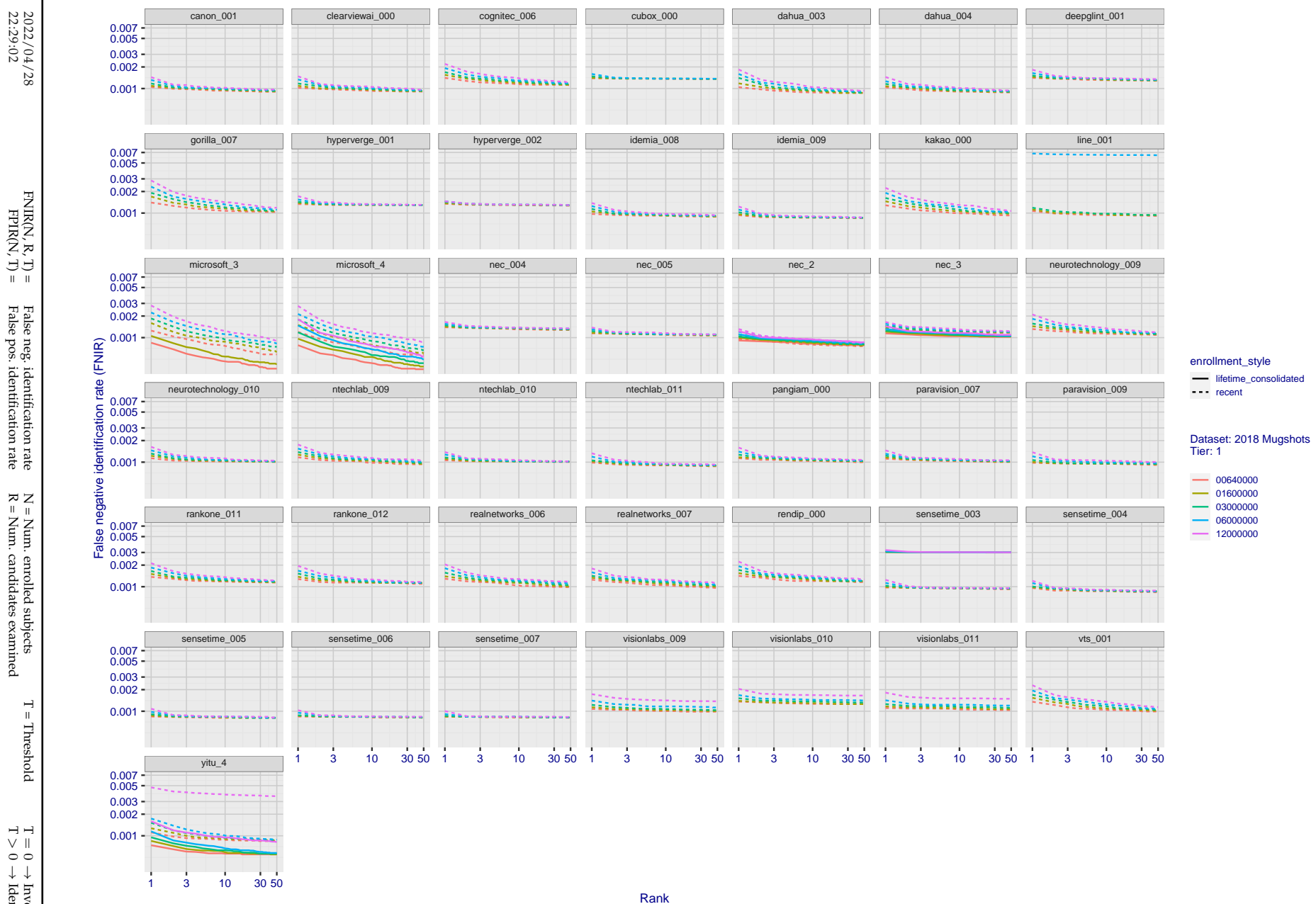
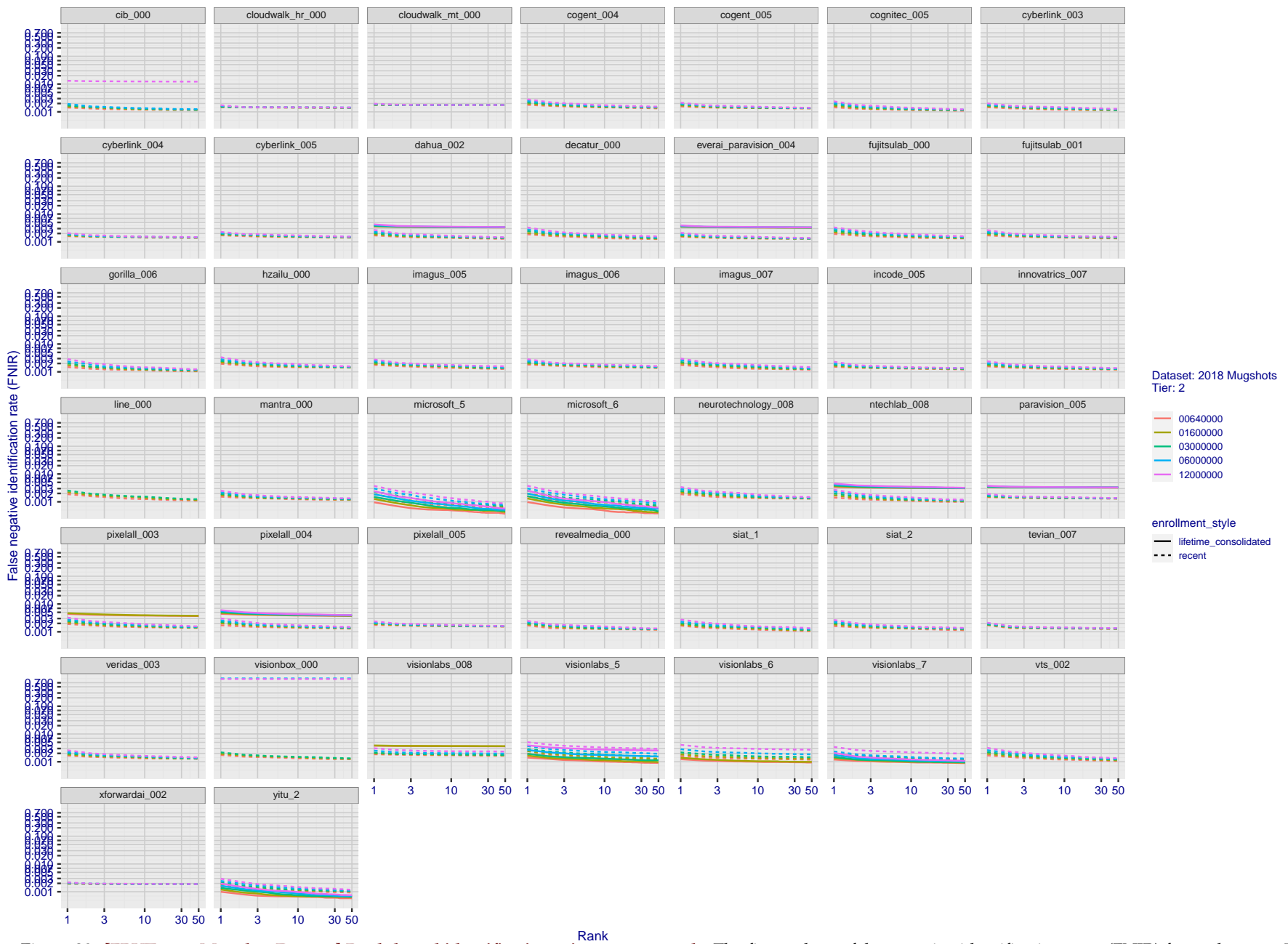


Figure 27: [FRVT-2018 Mugshot Dataset] Rank-based identification miss rates vs. number of enrolled subjects. The figure shows false negative identification rates, FNIR( $N, R$ ), across various gallery sizes and ranks 1, 10 and 50. The threshold is set to zero, so this metric rewards even weak scoring rank 1 mates. This also means FPIR = 1, so any search without an enrolled mate will return non-mated candidates. For clarity, results are sorted and reported into tiers spanning multiple pages, the tiering criteria being rank 1 hit rate on a gallery size of 640 000.

2022/04/28 22:29:02	$\text{FNIR}(N, R, T) =$ $\text{FPTR}(N, T) =$	False neg. identification rate False pos. identification rate	$N =$ Num. enrolled subjects $R =$ Num. candidates examined	$T =$ Threshold $T > 0 \rightarrow$ Identification	$T = 0 \rightarrow$ Investigation
------------------------	---	--	--	---	-----------------------------------



**Figure 28: [FRVT-2018 Mugshot Dataset] Rank-based identification miss rates vs. rank.** The figure shows false negative identification rates (FNIR) for ranks up to 50. This metric is appropriate to investigational applications where human reviewers will adjudicate sorted candidate lists. Note that with threshold set to zero, FPIR = 1, i.e. any search without an enrolled mate will return non-mated candidates. Results are sorted and reported into tiers for clarity, with the tiering criteria being rank 1 hit rate on a gallery size of N = 640 000 subjects.

2022/04/28  
22:29:02FNIR(N, R, T) = False neg. identification rate  
FPIR(N, T) = False pos. identification rateN = Num. enrolled subjects  
R = Num. candidates examined  
T = ThresholdT = 0 → Investigation  
T > 0 → Identification

**Figure 29: [FRVT-2018 Mugshot Dataset] Rank-based identification miss rates vs. rank.** The figure shows false negative identification rates (FNIR) for ranks up to 50. This metric is appropriate to investigational applications where human reviewers will adjudicate sorted candidate lists. Note that with threshold set to zero, FPIR = 1, i.e. any search without an enrolled mate will return non-mated candidates. Results are sorted and reported into tiers for clarity, with the tiering criteria being rank 1 hit rate on a gallery size of N = 640 000 subjects.

2022/04/28  
22:29:02

$\text{FNIR}(N, R, T) =$   
False neg. identification rate  
 $\text{FPIR}(N, T) =$   
False pos. identification rate

$N = \text{Num. enrolled subjects}$   
 $R = \text{Num. candidates examined}$

$T = \text{Threshold}$   
 $T = 0 \rightarrow \text{Investigation}$   
 $T > 0 \rightarrow \text{Identification}$

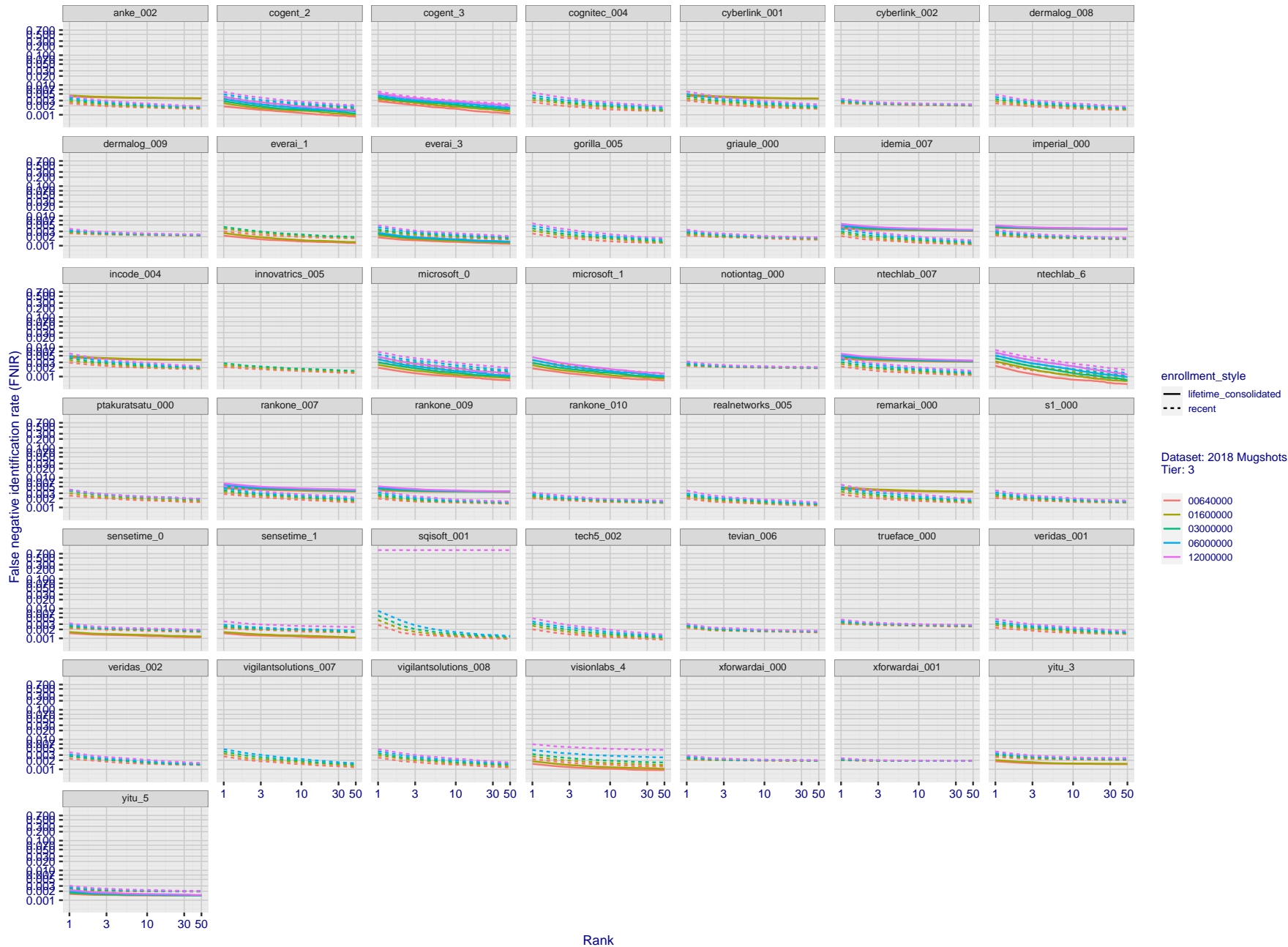


Figure 30: [FRVT-2018 Mugshot Dataset] Rank-based identification miss rates vs. rank. The figure shows false negative identification rates (FNIR) for ranks up to 50. This metric is appropriate to investigational applications where human reviewers will adjudicate sorted candidate lists. Note that with threshold set to zero, FPIR = 1, i.e. any search without an enrolled mate will return non-mated candidates. Results are sorted and reported into tiers for clarity, with the tiering criteria being rank 1 hit rate on a gallery size of  $N = 640\,000$  subjects.

2022/04/28  
22:29:02FNIR(N, R, T) = False neg. identification rate  
FPIR(N, T) = False pos. identification rateN = Num. enrolled subjects  
R = Num. candidates examined

T = Threshold

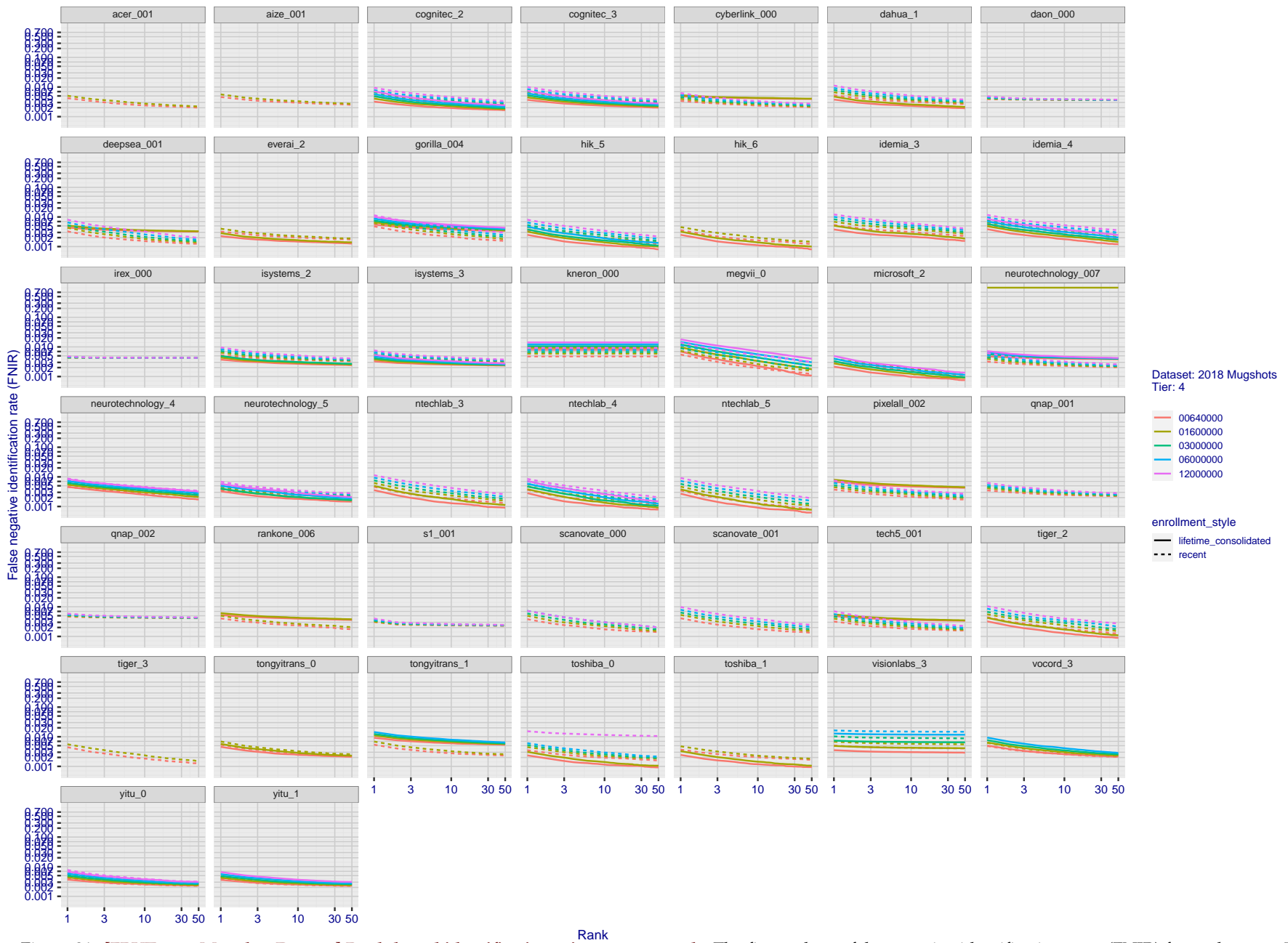
T = 0 → Investigation  
T > 0 → Identification

Figure 31: [FRVT-2018 Mugshot Dataset] Rank-based identification miss rates vs. rank. The figure shows false negative identification rates (FNIR) for ranks up to 50. This metric is appropriate to investigational applications where human reviewers will adjudicate sorted candidate lists. Note that with threshold set to zero, FPIR = 1, i.e. any search without an enrolled mate will return non-mated candidates. Results are sorted and reported into tiers for clarity, with the tiering criteria being rank 1 hit rate on a gallery size of N = 640 000 subjects.

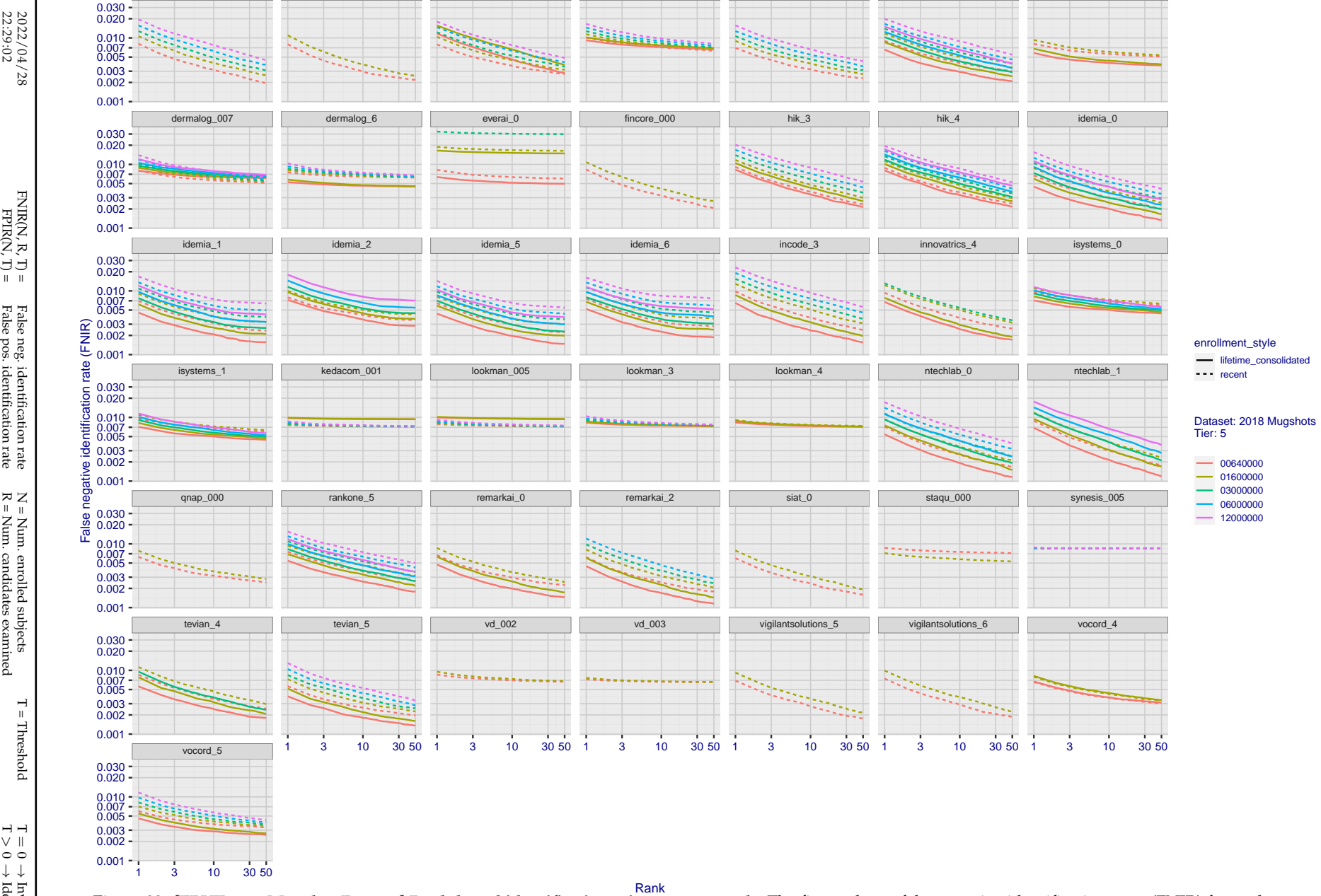


Figure 32: [FRVT-2018 Mugshot Dataset] Rank-based identification miss rates vs. rank. The figure shows false negative identification rates (FNIR) for ranks up to 50. This metric is appropriate to investigational applications where human reviewers will adjudicate sorted candidate lists. Note that with threshold set to zero, FPIR = 1, i.e. any search without an enrolled mate will return non-mated candidates. Results are sorted and reported into tiers for clarity, with the tiering criteria being rank 1 hit rate on a gallery size of N = 640 000 subjects.

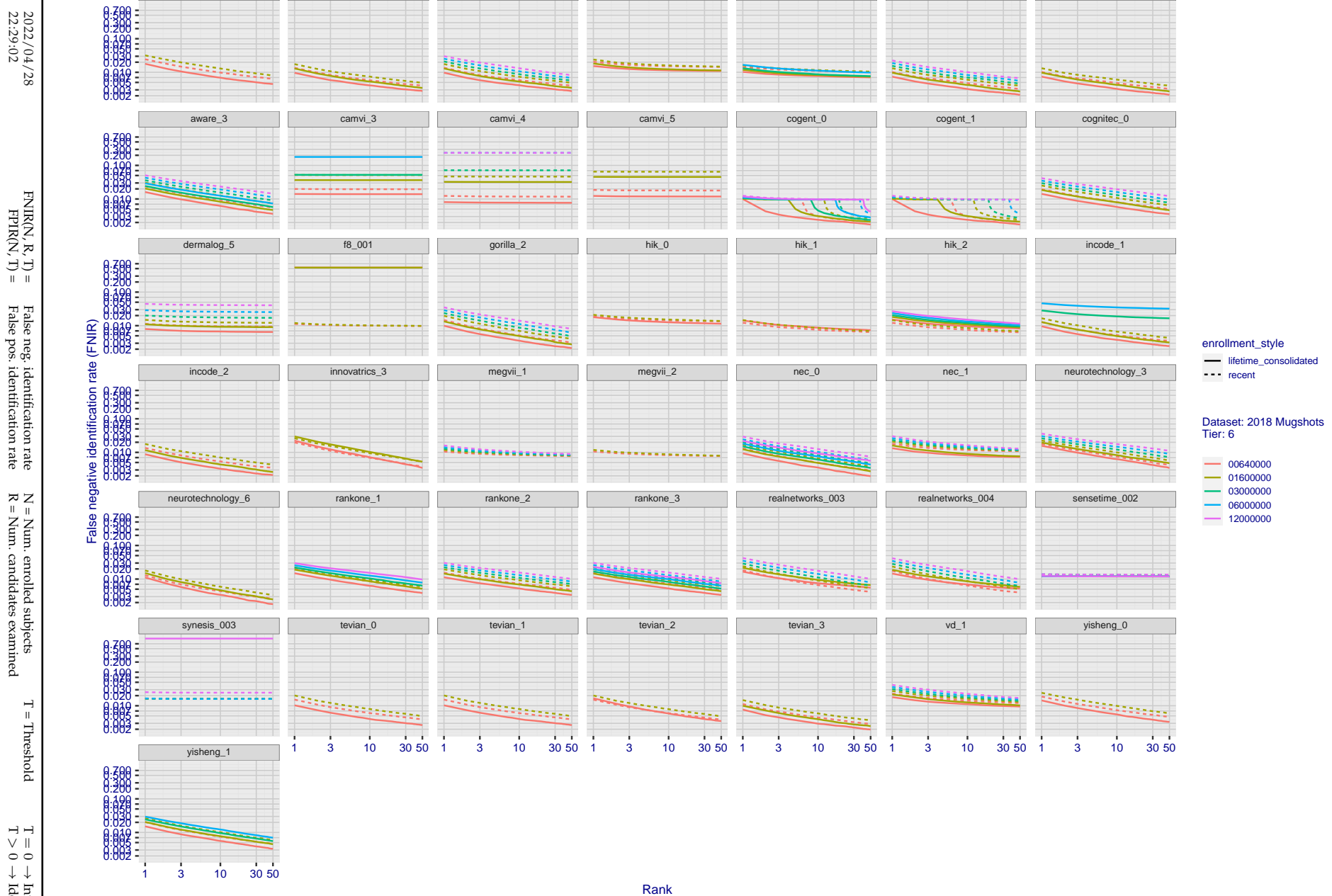


Figure 33: [FRVT-2018 Mugshot Dataset] Rank-based identification miss rates vs. rank. The figure shows false negative identification rates (FNIR) for ranks up to 50. This metric is appropriate to investigational applications where human reviewers will adjudicate sorted candidate lists. Note that with threshold set to zero, FPIR = 1, i.e. any search without an enrolled mate will return non-mated candidates. Results are sorted and reported into tiers for clarity, with the tiering criteria being rank 1 hit rate on a gallery size of N = 640 000 subjects.

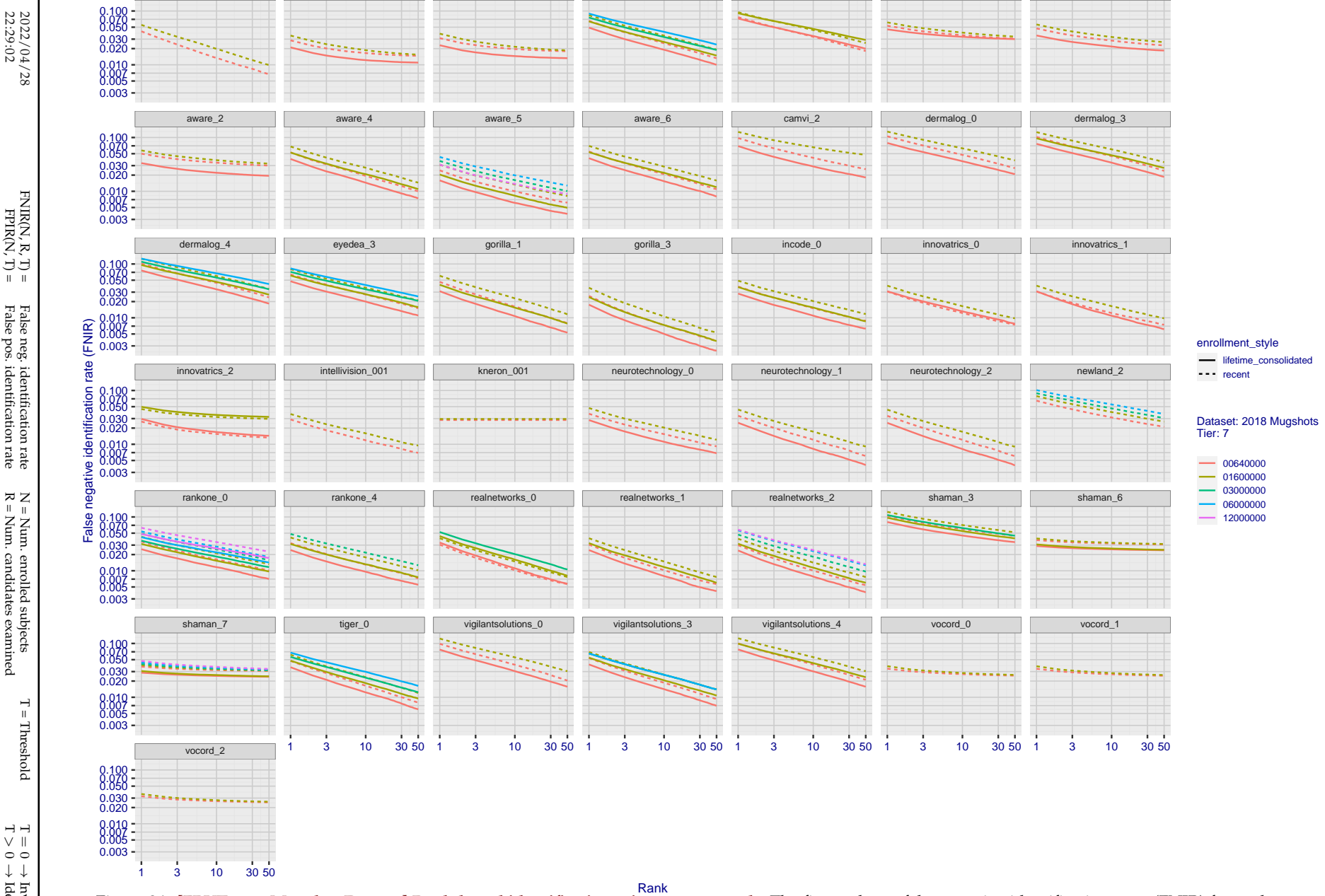
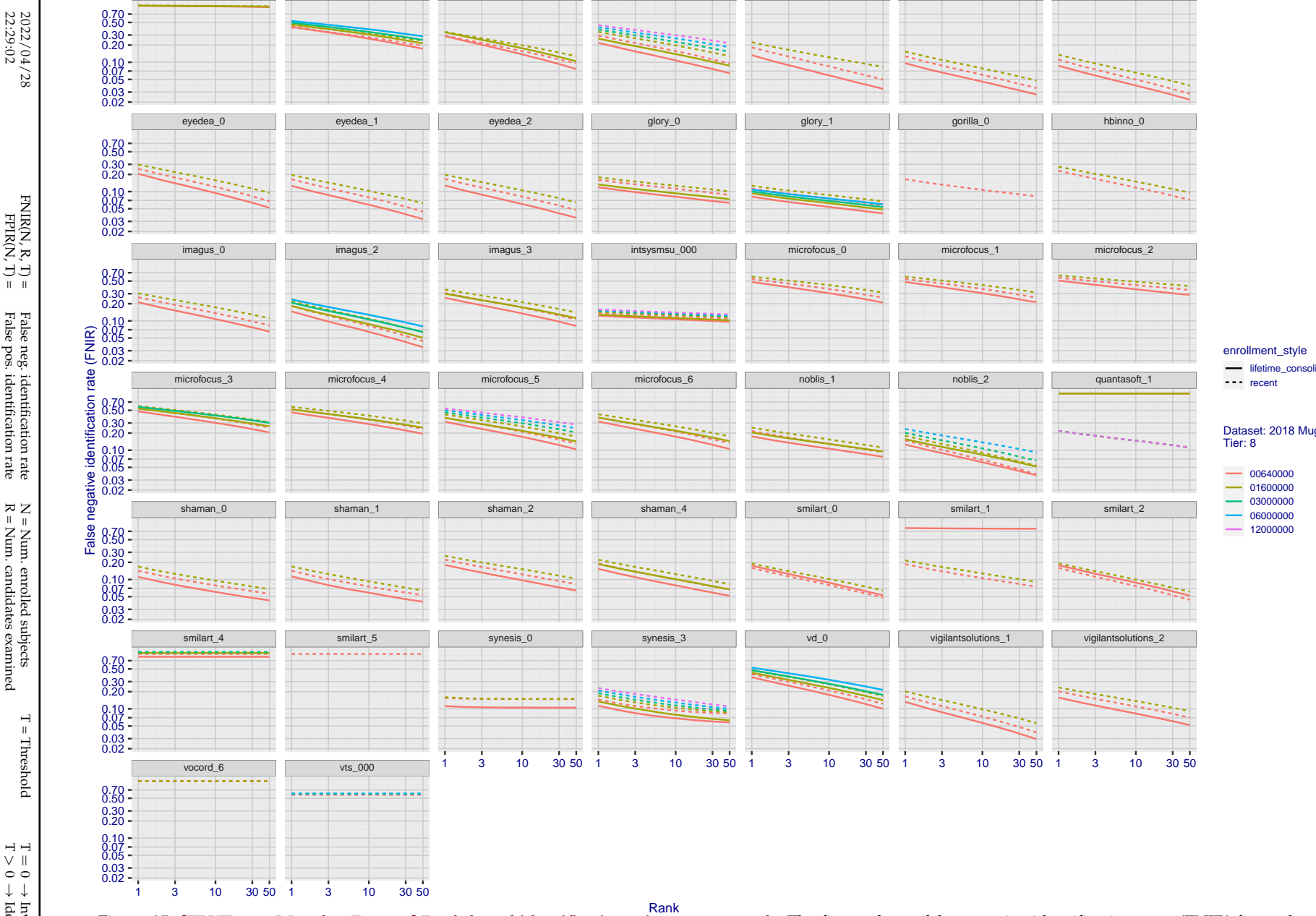


Figure 34: [FRVT-2018 Mugshot Dataset] Rank-based identification miss rates vs. rank. The figure shows false negative identification rates (FNIR) for ranks up to 50. This metric is appropriate to investigational applications where human reviewers will adjudicate sorted candidate lists. Note that with threshold set to zero, FPIR = 1, i.e. any search without an enrolled mate will return non-mated candidates. Results are sorted and reported into tiers for clarity, with the tiering criteria being rank 1 hit rate on a gallery size of N = 640 000 subjects.



**Figure 35: [FRVT-2018 Mugshot Dataset] Rank-based identification miss rates vs. rank.** The figure shows false negative identification rates (FNIR) for ranks up to 50. This metric is appropriate to investigational applications where human reviewers will adjudicate sorted candidate lists. Note that with threshold set to zero, FPIR = 1, i.e. any search without an enrolled mate will return non-mated candidates. Results are sorted and reported into tiers for clarity, with the tiering criteria being rank 1 hit rate on a gallery size of N = 640 000 subjects.

2022/04/28 22:29:02	$\text{FNIR}(N, R, T) =$ $\text{FPTR}(N, T) =$	False neg. identification rate False pos. identification rate	$N =$ Num. enrolled subjects $R =$ Num. candidates examined	$T =$ Threshold $T > 0 \rightarrow$ Identification	$T = 0 \rightarrow$ Investigation
------------------------	---	--	--	---	-----------------------------------

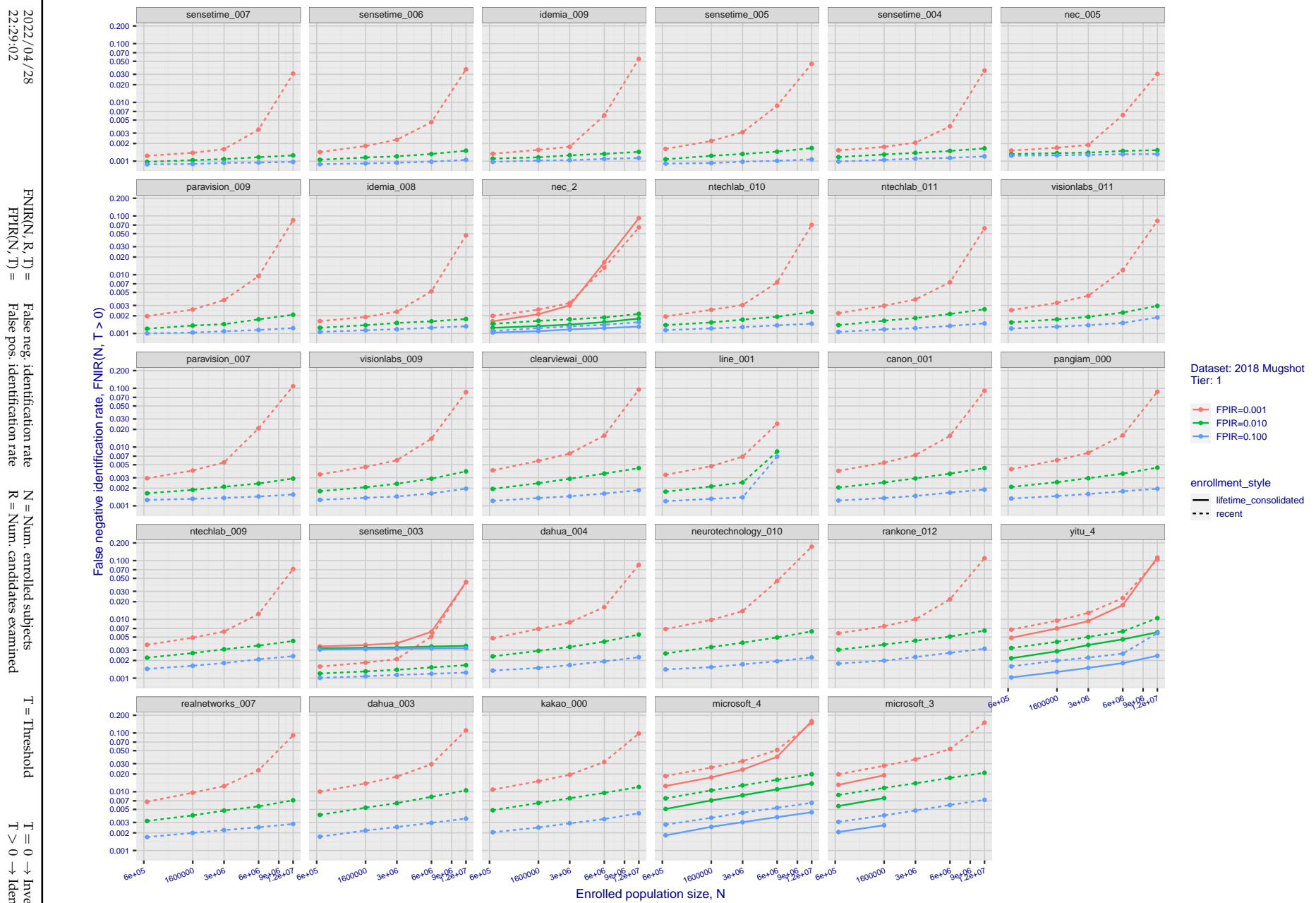
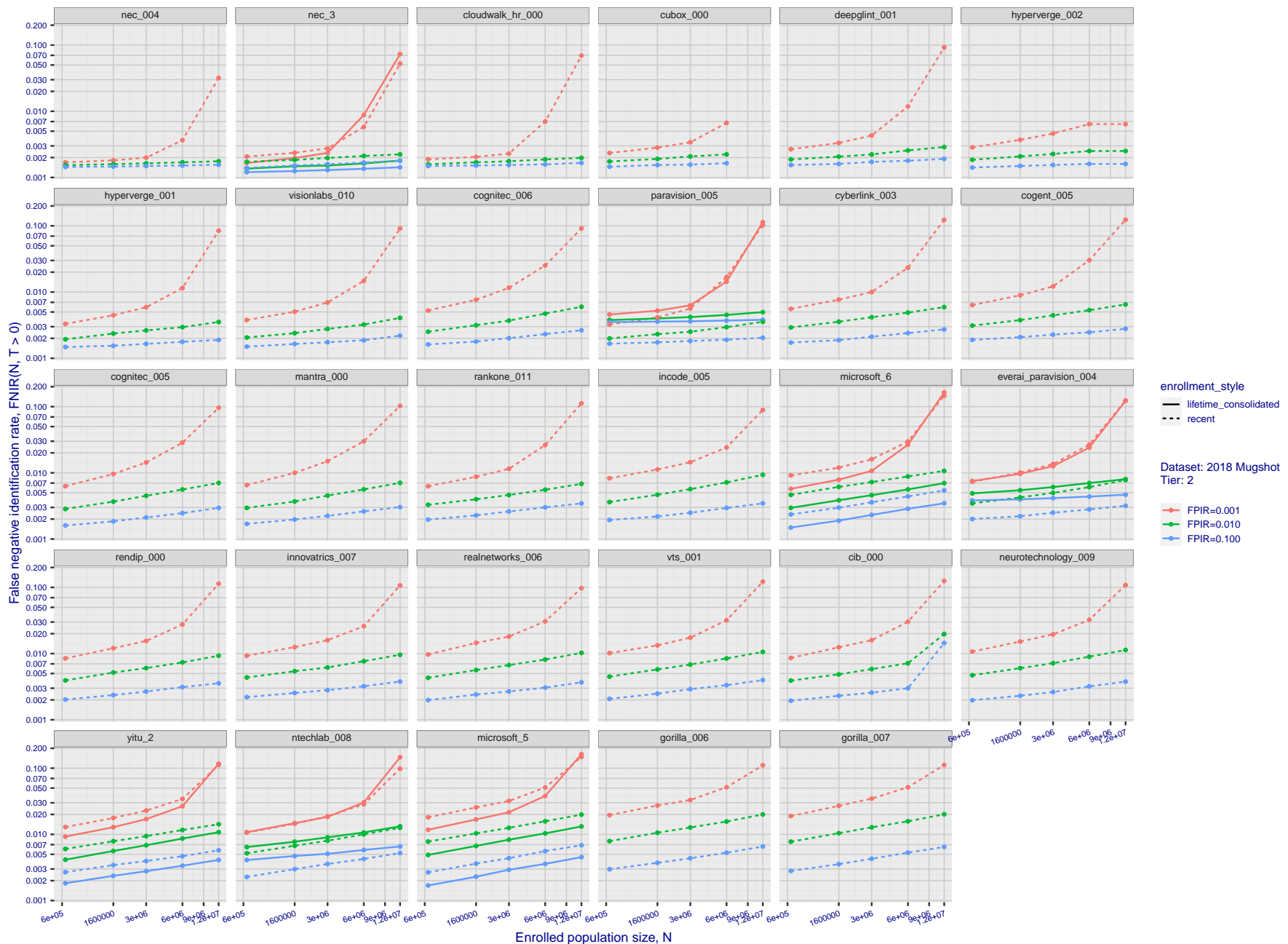


Figure 36: [FRVT-2018 Mugshot Dataset] Threshold-based identification miss rates vs. number of enrolled subjects. The figure shows  $\text{FNIR}(N, T)$  across various gallery sizes when the threshold is set to achieve the given FPIRs. The rank criterion is irrelevant at high thresholds as mates are always at rank 1. The results are computed from the trials listed in rows 1-10 of Table 1. Less accurate algorithms were not run on large  $N$ , so results are missing. For clarity, results are sorted and reported into tiers spanning multiple pages. The tiering criteria is complicated: First paging by  $\text{FNIR}(N_b, 1, 0)$ , then sorting by median  $\text{FNIR}(N_b, T)$ ,  $N_b = 640\,000$ .



**Figure 37: [FRVT-2018 Mugshot Dataset] Threshold-based identification miss rates vs. number of enrolled subjects.** The figure shows  $\text{FNIR}(N, T)$  across various gallery sizes when the threshold is set to achieve the given FPIRs. The rank criterion is irrelevant at high thresholds as mates are always at rank 1. The results are computed from the trials listed in rows 1-10 of Table 1. Less accurate algorithms were not run on large  $N$ , so results are missing. For clarity, results are sorted and reported into tiers spanning multiple pages. The tiering criteria is complicated: First paging by  $\text{FNIR}(N_b, 1, 0)$ , then sorting by median  $\text{FNIR}(N_b, T)$ ,  $N_b = 640\,000$ .

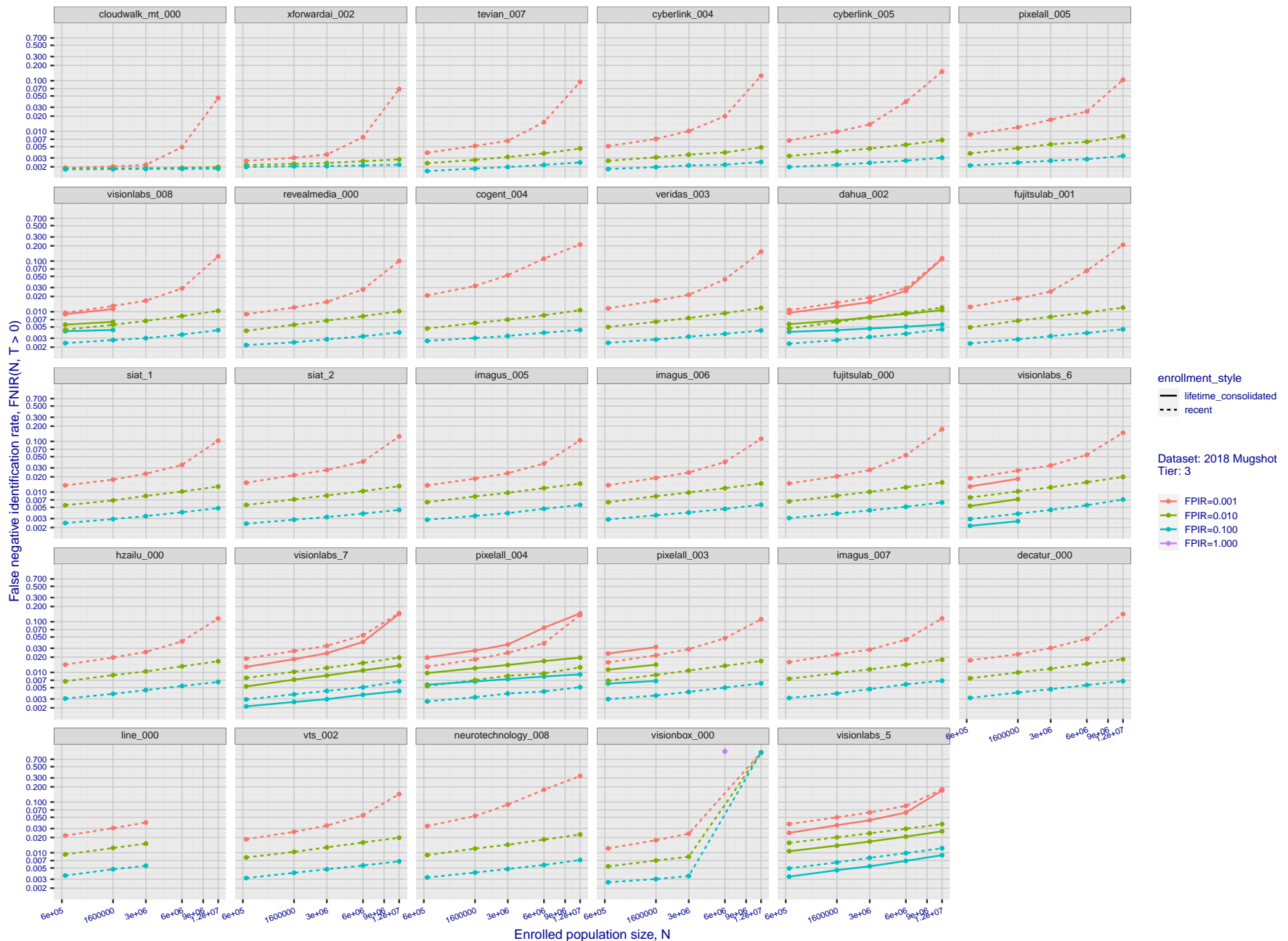
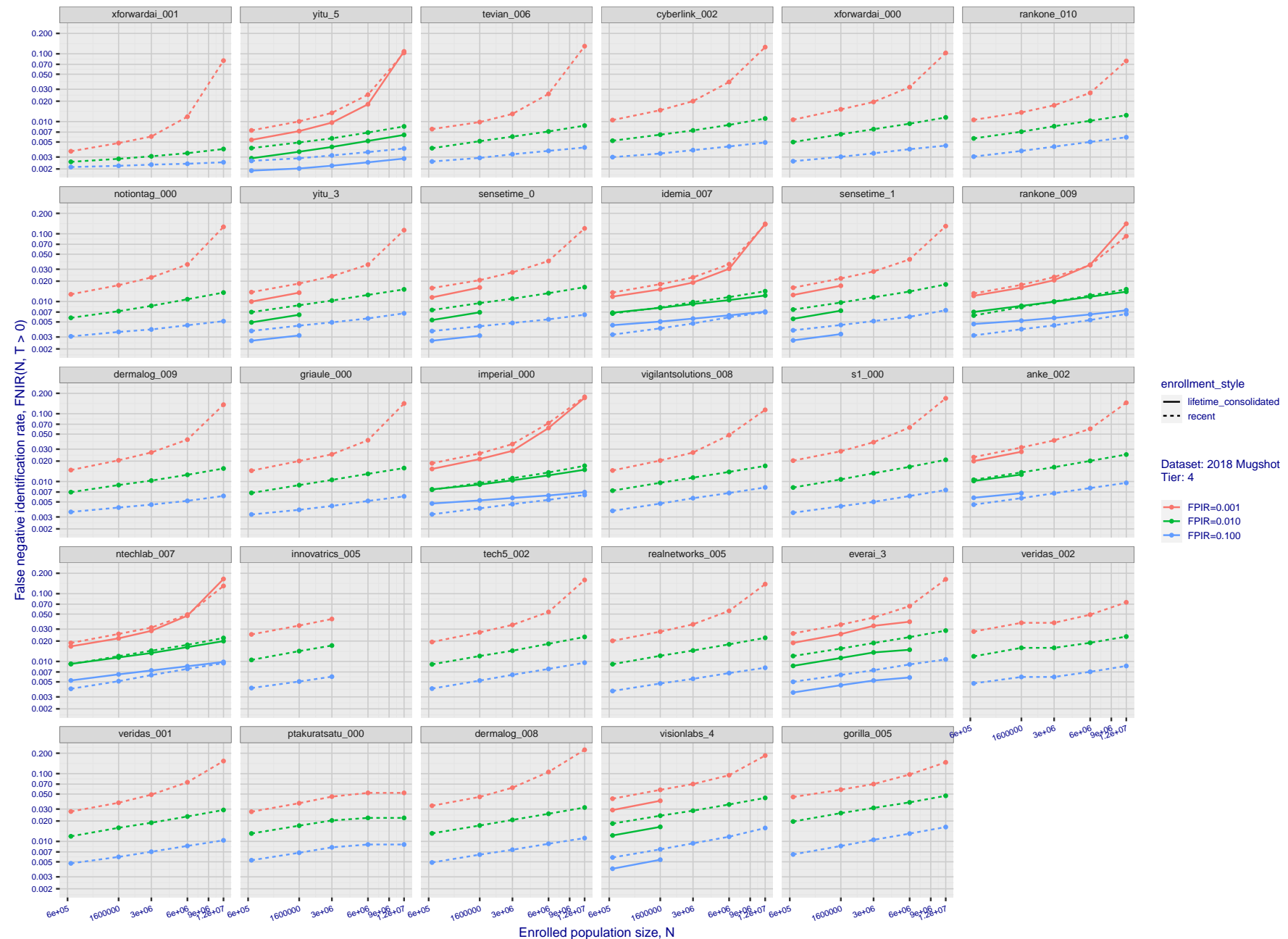
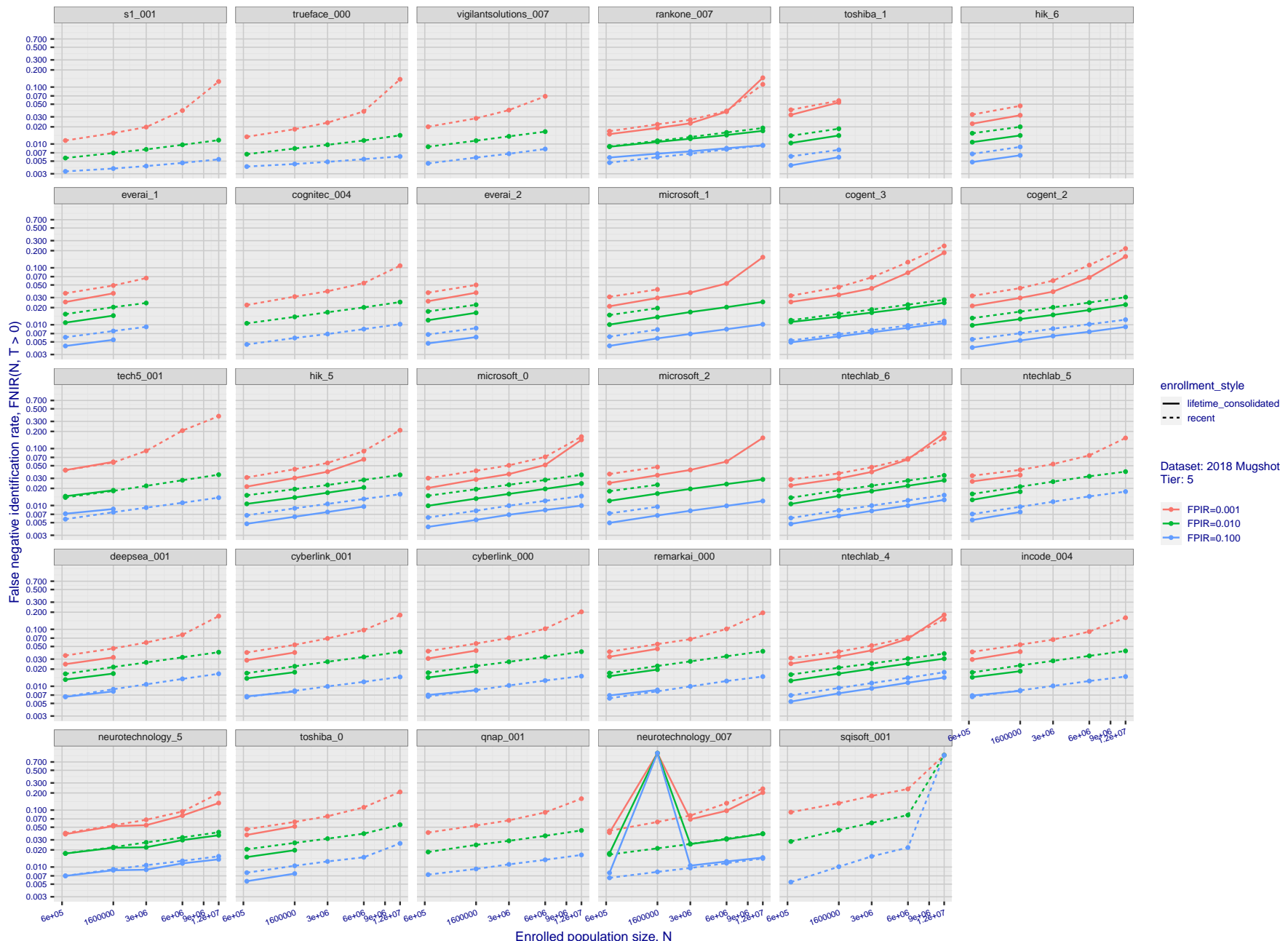


Figure 38: [FRVT-2018 Mugshot Dataset] Threshold-based identification miss rates vs. number of enrolled subjects. The figure shows  $\text{FNIR}(N, T)$  across various gallery sizes when the threshold is set to achieve the given FPIRs. The rank criterion is irrelevant at high thresholds as mates are always at rank 1. The results are computed from the trials listed in rows 1-10 of Table 1. Less accurate algorithms were not run on large  $N$ , so results are missing. For clarity, results are sorted and reported into tiers spanning multiple pages. The tiering criteria is complicated: First paging by  $\text{FNIR}(N_b, 1, 0)$ , then sorting by median  $\text{FNIR}(N_b, T)$ ,  $N_b = 640\,000$ .



**Figure 39: [FRVT-2018 Mugshot Dataset] Threshold-based identification miss rates vs. number of enrolled subjects.** The figure shows FNIR( $N, T$ ) across various gallery sizes when the threshold is set to achieve the given FPIRs. The rank criterion is irrelevant at high thresholds as mates are always at rank 1. The results are computed from the trials listed in rows 1-10 of Table 1. Less accurate algorithms were not run on large  $N$ , so results are missing. For clarity, results are sorted and reported into tiers spanning multiple pages. The tiering criteria is complicated: First paging by  $FNIR(N_b, 1, 0)$ , then sorting by median  $FNIR(N_b, T)$ ,  $N_b = 640\,000$ .



**Figure 40: [FRVT-2018 Mugshot Dataset] Threshold-based identification miss rates vs. number of enrolled subjects.** The figure shows FNIR( $N, T$ ) across various gallery sizes when the threshold is set to achieve the given FPIRs. The rank criterion is irrelevant at high thresholds as mates are always at rank 1. The results are computed from the trials listed in rows 1-10 of Table 1. Less accurate algorithms were not run on large  $N$ , so results are missing. For clarity, results are sorted and reported into tiers spanning multiple pages. The tiering criteria is complicated: First paging by  $\text{FNIR}(N_b, 1, 0)$ , then sorting by median  $\text{FNIR}(N_b, T)$ ,  $N_b = 640\,000$ .

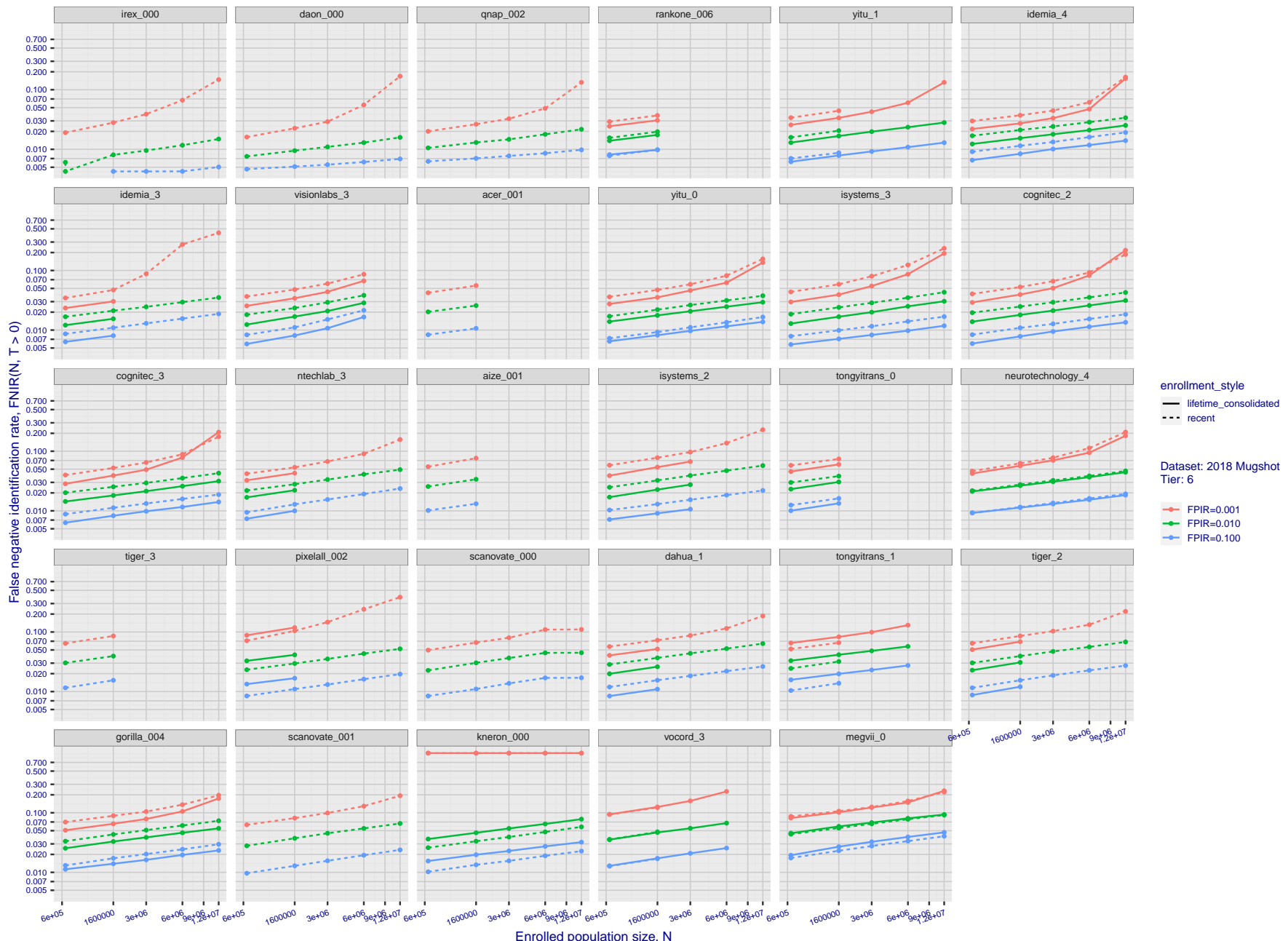


**Figure 41: [FRVT-2018 Mugshot Dataset] Threshold-based identification miss rates vs. number of enrolled subjects.** The figure shows FNIR( $N, T$ ) across various gallery sizes when the threshold is set to achieve the given FPIRs. The rank criterion is irrelevant at high thresholds as mates are always at rank 1. The results are computed from the trials listed in rows 1-10 of Table 1. Less accurate algorithms were not run on large  $N$ , so results are missing. For clarity, results are sorted and reported into tiers spanning multiple pages. The tiering criteria is complicated: First paging by  $\text{FNIR}(N_b, 1, 0)$ , then sorting by median  $\text{FNIR}(N_b, T)$ ,  $N_b = 640\,000$ .

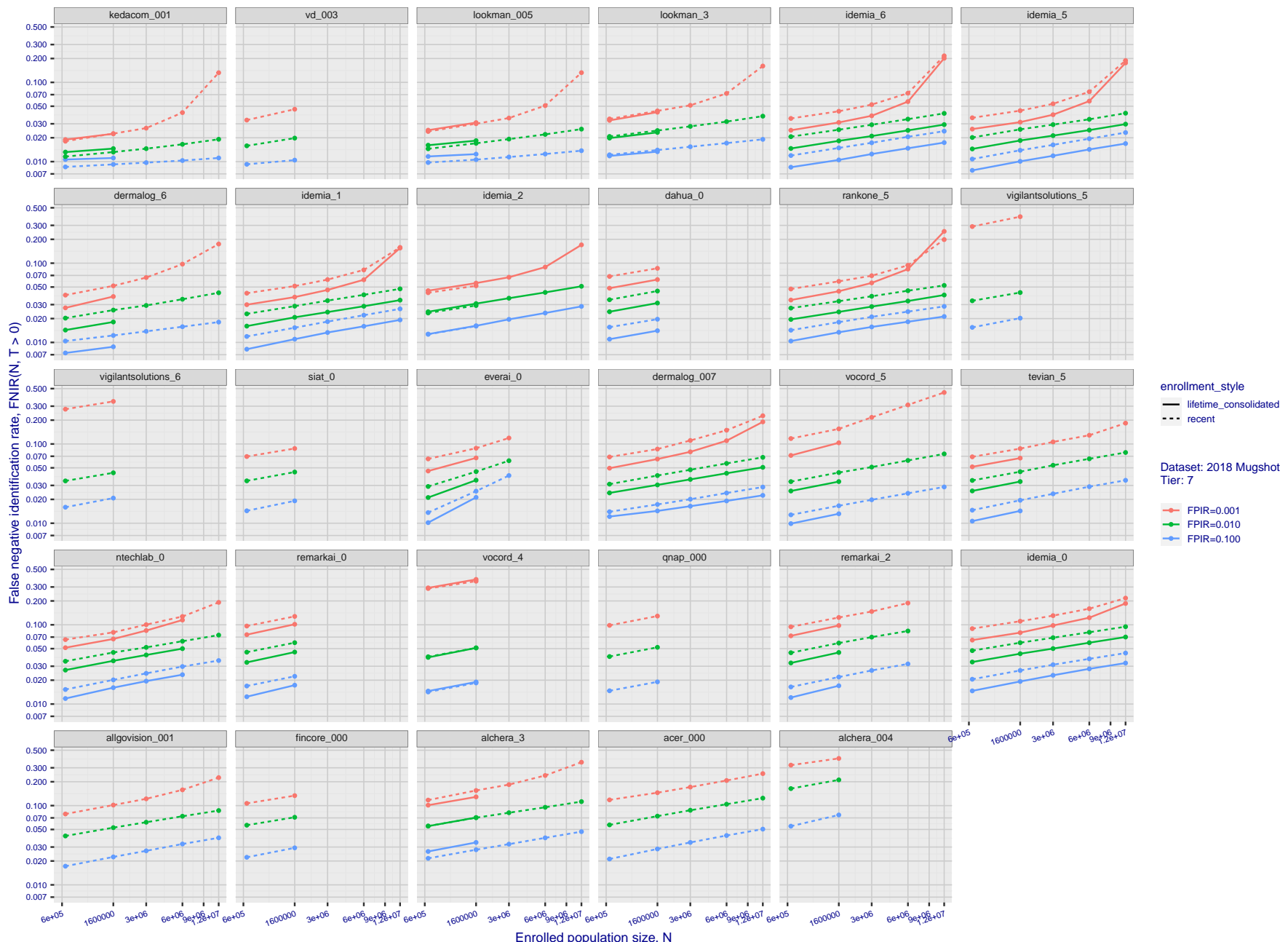
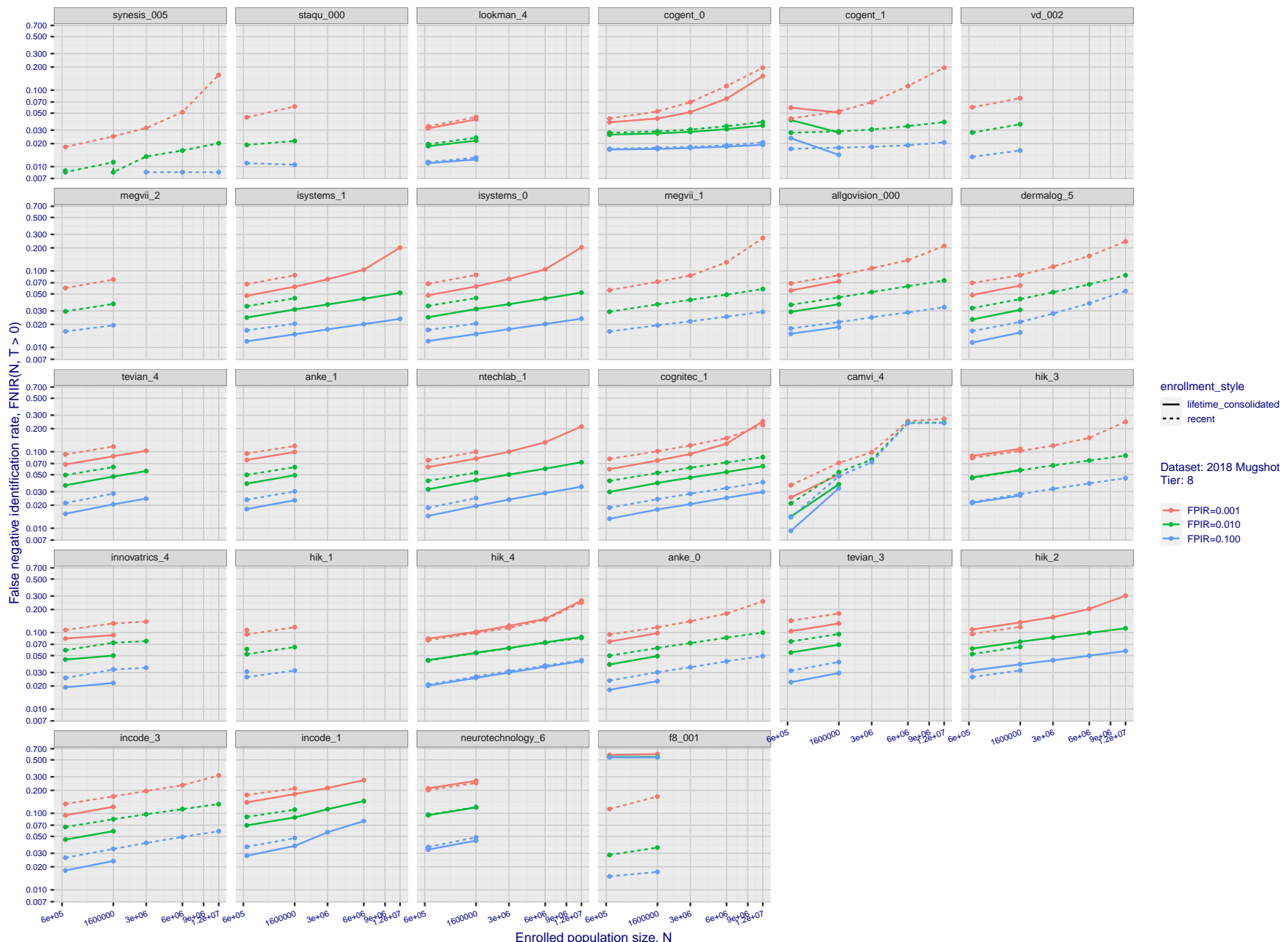
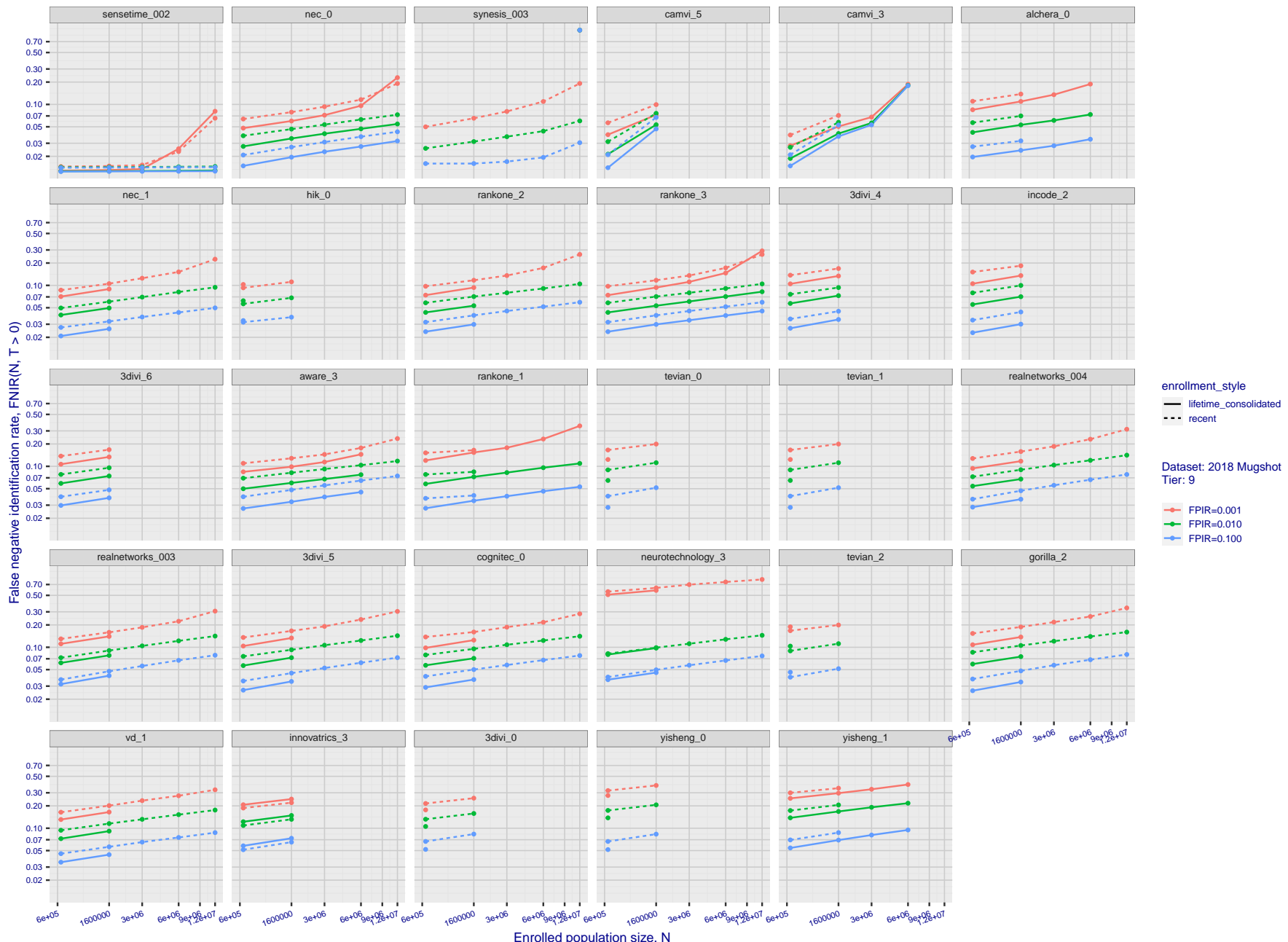


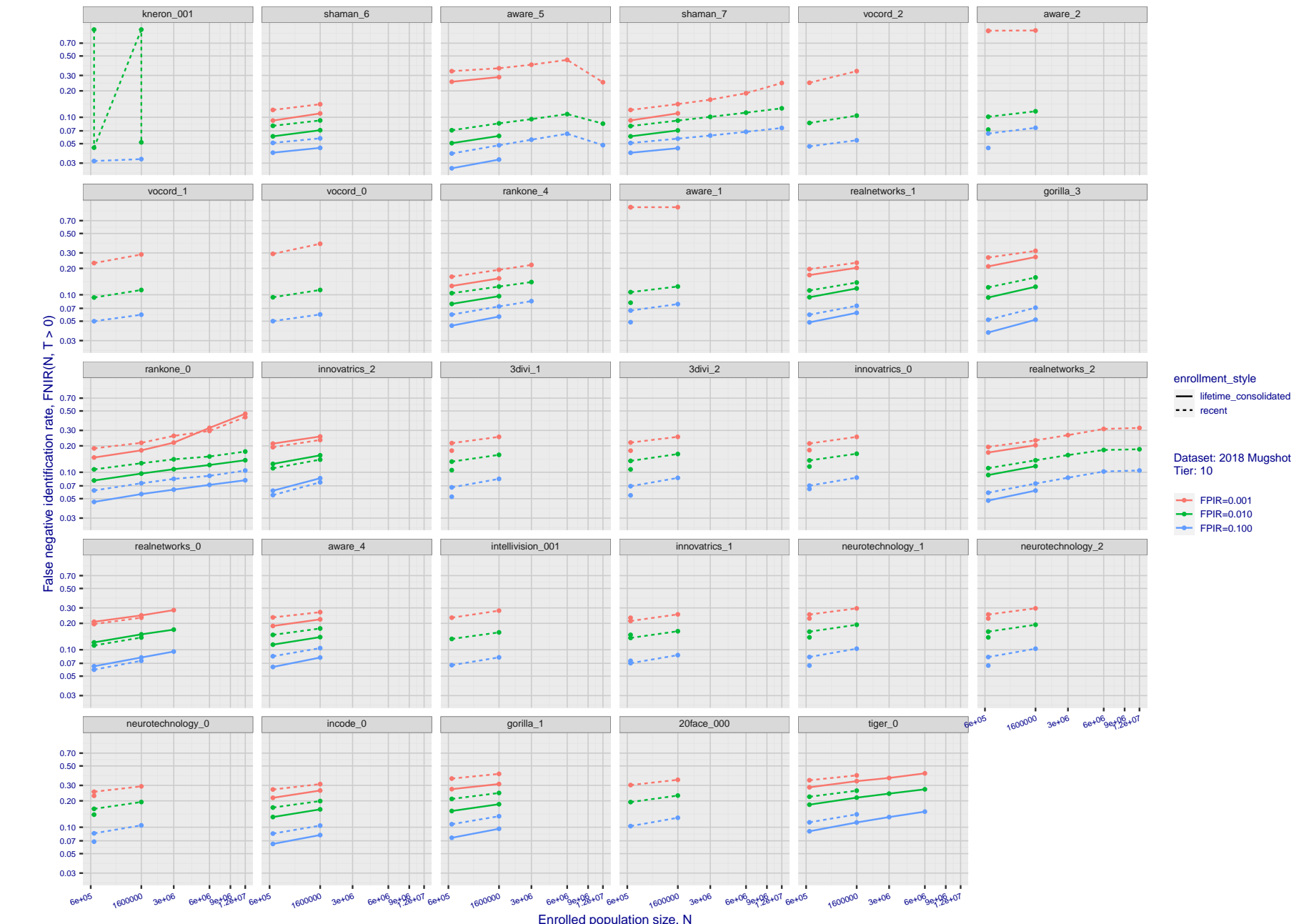
Figure 42: [FRVT-2018 Mugshot Dataset] Threshold-based identification miss rates vs. number of enrolled subjects. The figure shows FNIR( $N, T$ ) across various gallery sizes when the threshold is set to achieve the given FPIRs. The rank criterion is irrelevant at high thresholds as mates are always at rank 1. The results are computed from the trials listed in rows 1-10 of Table 1. Less accurate algorithms were not run on large  $N$ , so results are missing. For clarity, results are sorted and reported into tiers spanning multiple pages. The tiering criteria is complicated: First paging by  $\text{FNIR}(N_b, 1, 0)$ , then sorting by median  $\text{FNIR}(N_b, T)$ ,  $N_b = 640\,000$ .



**Figure 43: [FRVT-2018 Mugshot Dataset] Threshold-based identification miss rates vs. number of enrolled subjects.** The figure shows FNIR( $N, T$ ) across various gallery sizes when the threshold is set to achieve the given FPIRs. The rank criterion is irrelevant at high thresholds as mates are always at rank 1. The results are computed from the trials listed in rows 1-10 of Table 1. Less accurate algorithms were not run on large  $N$ , so results are missing. For clarity, results are sorted and reported into tiers spanning multiple pages. The tiering criteria is complicated: First paging by FNIR( $N_b, 1, 0$ ), then sorting by median FNIR( $N_b, T$ ),  $N_b = 640\,000$ .



**Figure 44: [FRVT-2018 Mugshot Dataset] Threshold-based identification miss rates vs. number of enrolled subjects.** The figure shows FNIR( $N, T$ ) across various gallery sizes when the threshold is set to achieve the given FPIRs. The rank criterion is irrelevant at high thresholds as mates are always at rank 1. The results are computed from the trials listed in rows 1-10 of Table 1. Less accurate algorithms were not run on large  $N$ , so results are missing. For clarity, results are sorted and reported into tiers spanning multiple pages. The tiering criteria is complicated: First paging by  $\text{FNIR}(N_b, 1, 0)$ , then sorting by median  $\text{FNIR}(N_b, T)$ ,  $N_b = 640\,000$ .

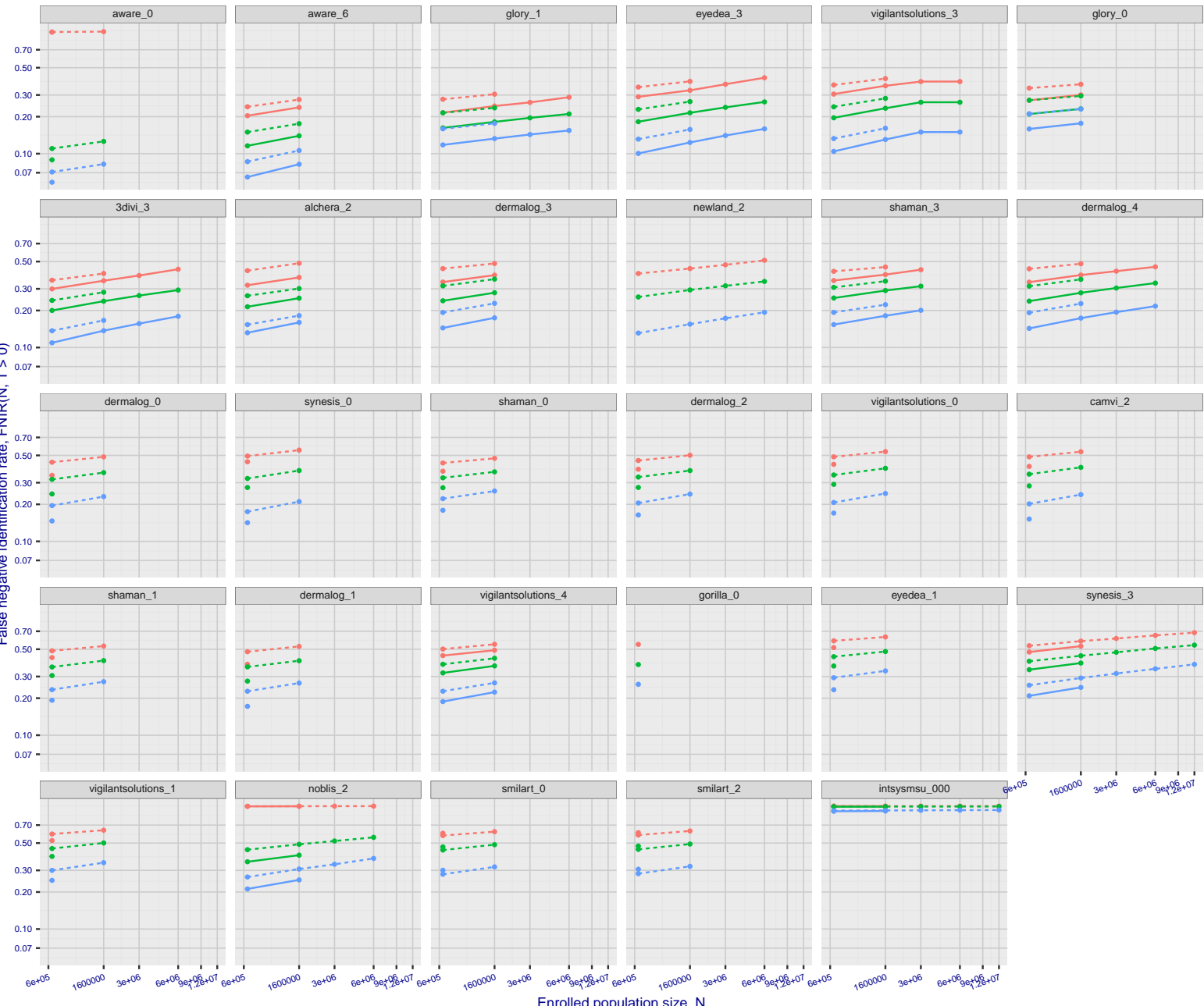


**Figure 45: [FRVT-2018 Mugshot Dataset] Threshold-based identification miss rates vs. number of enrolled subjects.** The figure shows FNIR( $N, T$ ) across various gallery sizes when the threshold is set to achieve the given FPIRs. The rank criterion is irrelevant at high thresholds as mates are always at rank 1. The results are computed from the trials listed in rows 1-10 of Table 1. Less accurate algorithms were not run on large  $N$ , so results are missing. For clarity, results are sorted and reported into tiers spanning multiple pages. The tiering criteria is complicated: First paging by  $\text{FNIR}(N_b, 1, 0)$ , then sorting by median  $\text{FNIR}(N_b, T)$ ,  $N_b = 640\,000$ .

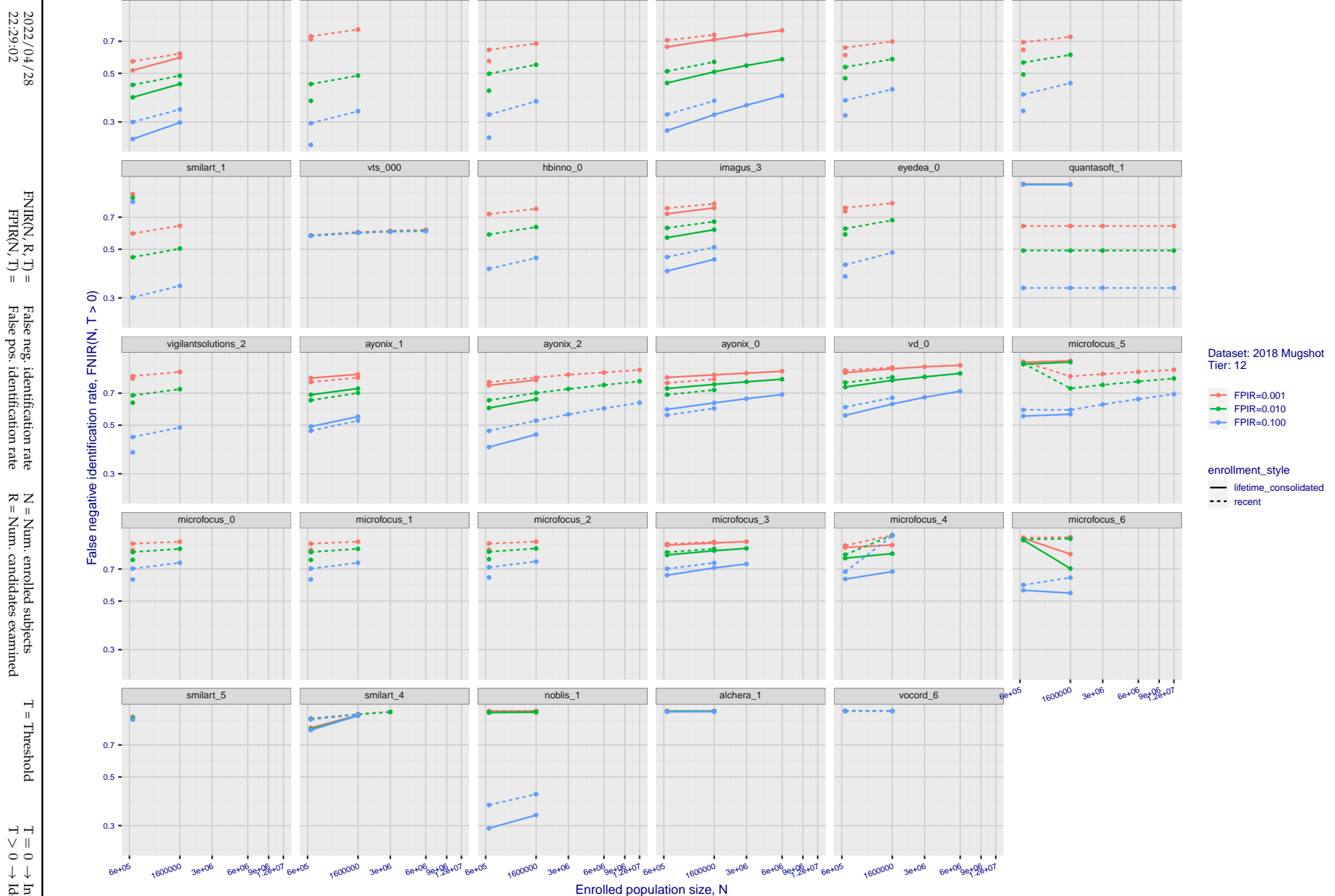
22:29:02

FNIR(N, R, T) = False neg. identification rate  
FPIR(N, T) = False pos. identification rateN = Num. enrolled subjects  
R = Num. candidates examined

T = Threshold

T = 0 → Investigation  
T > 0 → Identification

**Figure 46: [FRVT-2018 Mugshot Dataset] Threshold-based identification miss rates vs. number of enrolled subjects.** The figure shows FNIR(N, T) across various gallery sizes when the threshold is set to achieve the given FPIRs. The rank criterion is irrelevant at high thresholds as mates are always at rank 1. The results are computed from the trials listed in rows 1-10 of Table 1. Less accurate algorithms were not run on large N, so results are missing. For clarity, results are sorted and reported into tiers spanning multiple pages. The tiering criteria is complicated: First paging by FNIR( $N_b$ , 1, 0), then sorting by median FNIR( $N_b$ , T),  $N_b = 640\,000$ .

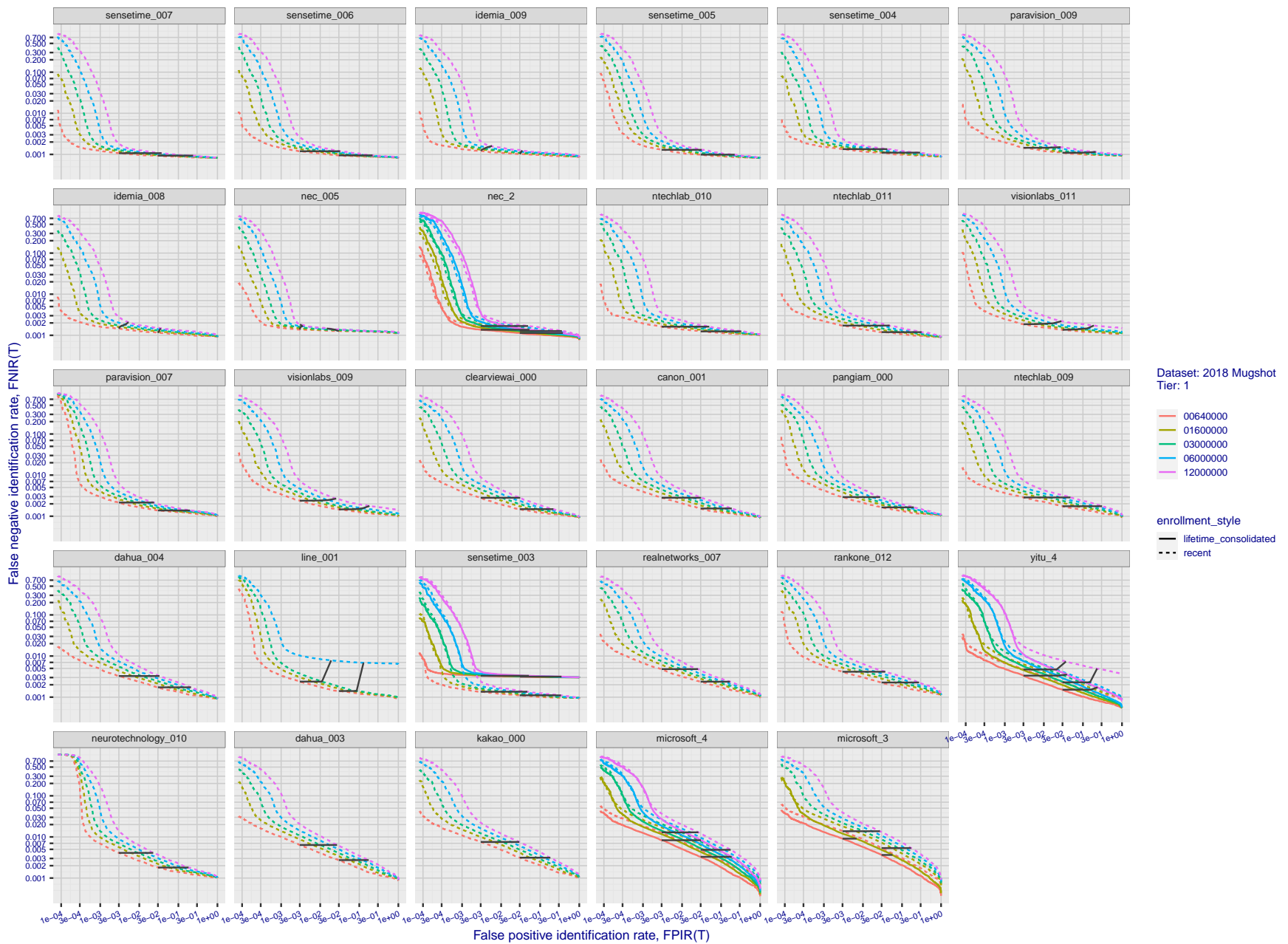


**Figure 47: [FRVT-2018 Mugshot Dataset] Threshold-based identification miss rates vs. number of enrolled subjects.** The figure shows FNIR(N, T) across various gallery sizes when the threshold is set to achieve the given FPIRs. The rank criterion is irrelevant at high thresholds as mates are always at rank 1. The results are computed from the trials listed in rows 1-10 of Table 1. Less accurate algorithms were not run on large N, so results are missing. For clarity, results are sorted and reported into tiers spanning multiple pages. The tiering criteria is complicated: First paging by  $FNIR(N_b, 1, 0)$ , then sorting by median  $FNIR(N_b, T)$ ,  $N_b = 640\,000$ .

2022/04/28 22:29:02	$\text{FNIR}(N, R, T) =$ $\text{FPTR}(N, T) =$	False neg. identification rate False pos. identification rate	$N =$ Num. enrolled subjects $R =$ Num. candidates examined	$T =$ Threshold $T > 0 \rightarrow$ Identification	$T = 0 \rightarrow$ Investigation
------------------------	---	--	--	---	-----------------------------------

2022/04/28  
22:29:02FNIR(N, R, T) = False neg. identification rate  
FPIR(N, T) = False pos. identification rateN = Num. enrolled subjects  
R = Num. candidates examined

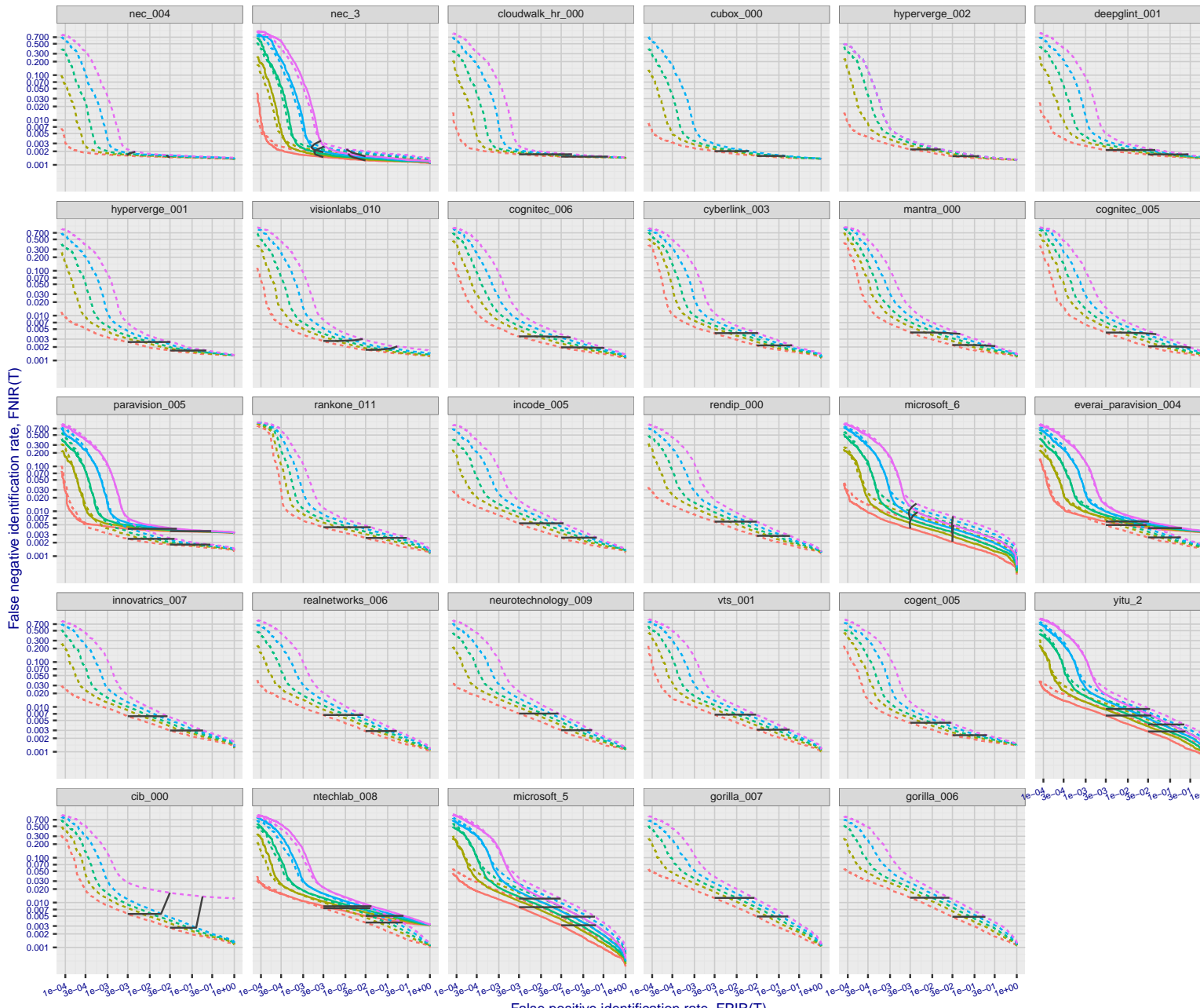
T = Threshold

T = 0 → Investigation  
 $T > 0 \rightarrow$  Identification

**Figure 48: [FRVT-2018 Mugshot Dataset] Identification miss rates vs. false positive rates.** The figure shows miss rates  $\text{FNIR}(N, L, T)$  as a function of  $\text{FPIR}(N, T)$ , with  $N$  ranging from 640 000 to 12 000 000 as noted in rows 1-10 of Table 1. These error tradeoff characteristics are useful for applications where a threshold must be elevated to limit false positives, such as when human reviewer labor is not matched to the volume of searches. Dark lines join points of equal threshold: If horizontal,  $\text{FPIR}(T)$  rises with  $N$ , and mate scores are independent of  $N$ . Other algorithms adjust scores in an attempt to make  $\text{FPIR}$  independent of  $N$ .

2022/04/28  
22:29:02FNIR(N, R, T) = False neg. identification rate  
FPIR(N, T) = False pos. identification rateN = Num. enrolled subjects  
R = Num. candidates examined

T = Threshold

T = 0 → Investigation  
 $T > 0 \rightarrow$  Identification

**Figure 49: [FRVT-2018 Mugshot Dataset] Identification miss rates vs. false positive rates.** The figure shows miss rates  $\text{FNIR}(N, L, T)$  as a function of  $\text{FPIR}(N, T)$ , with  $N$  ranging from 640 000 to 12 000 000 as noted in rows 1-10 of Table 1. These error tradeoff characteristics are useful for applications where a threshold must be elevated to limit false positives, such as when human reviewer labor is not matched to the volume of searches. Dark lines join points of equal  $N$ . If horizontal,  $\text{FPIR}(T)$  rises with  $N$ , and mate scores are independent of  $N$ . Other algorithms adjust scores in an attempt to make  $\text{FPIR}$  independent of  $N$ .

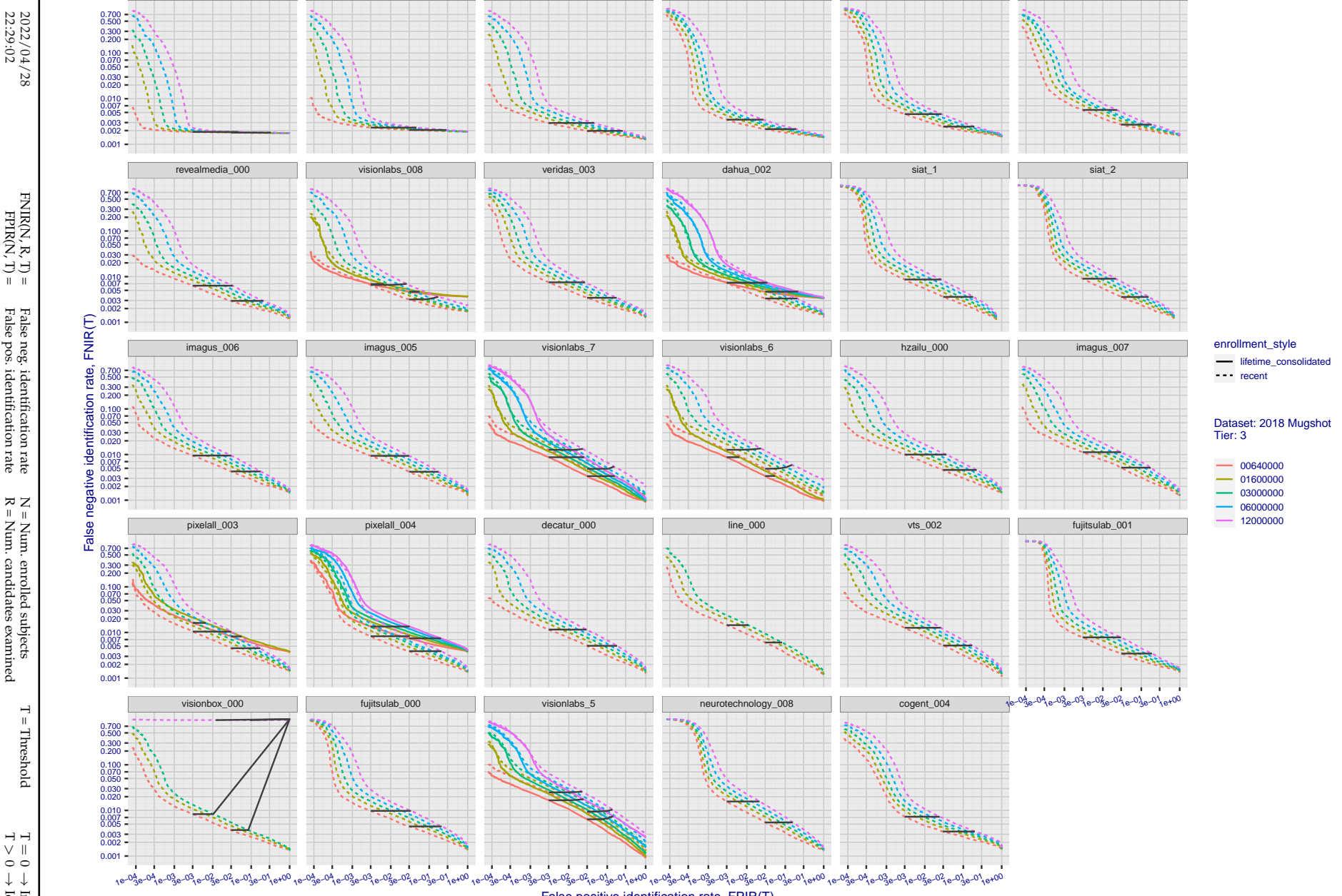


**Figure 50: [FRVT-2018 Mugshot Dataset] Identification miss rates vs. false positive rates.** The figure shows miss rates  $\text{FNIR}(N, L, T)$  as a function of  $\text{FPIR}(N, T)$ , with  $N$  ranging from 640 000 to 12 000 000 as noted in rows 1-10 of Table 1. These error tradeoff characteristics are useful for applications where a threshold must be elevated to limit false positives, such as when human reviewer labor is not matched to the volume of searches. Dark lines join points of equal threshold: If horizontal,  $\text{FPIR}(T)$  rises with  $N$ , and mate scores are independent of  $N$ . Other algorithms adjust scores in an attempt to make  $\text{FPIR}$  independent of  $N$ .

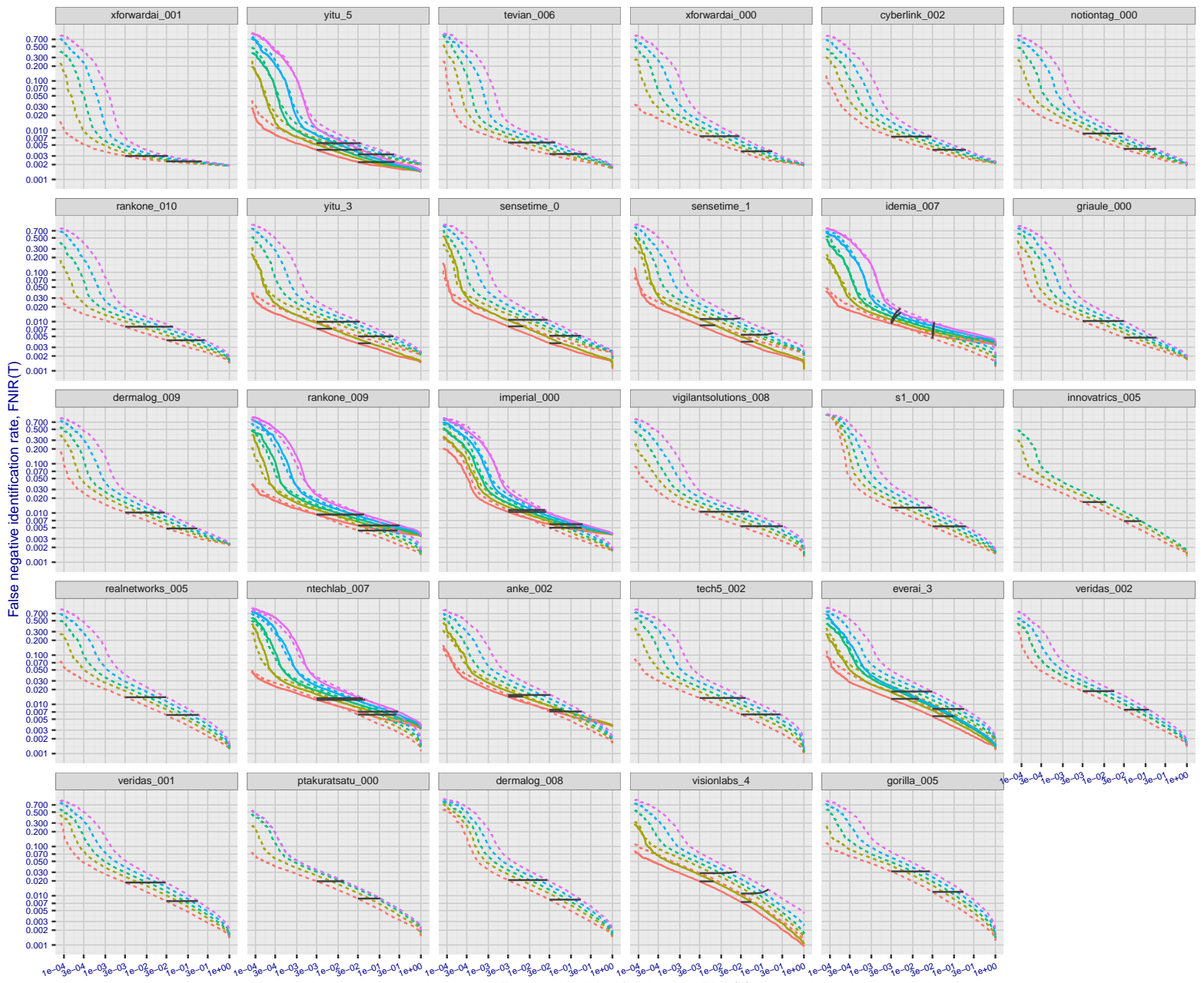


**Figure 51: [FRVT-2018 Mugshot Dataset] Identification miss rates vs. false positive rates.** The figure shows miss rates  $\text{FNIR}(N, L, T)$  as a function of  $\text{FPIR}(N, T)$ , with  $N$  ranging from 640 000 to 12 000 000 as noted in rows 1-10 of Table 1. These error tradeoff characteristics are useful for applications where a threshold must be elevated to limit false positives, such as when human reviewer labor is not matched to the volume of searches. Dark lines join points of equal threshold: If horizontal,  $\text{FPIR}(T)$  rises with  $N$ , and mate scores are independent of  $N$ . Other algorithms adjust scores in an attempt to make  $\text{FPIR}$  independent of  $N$ .

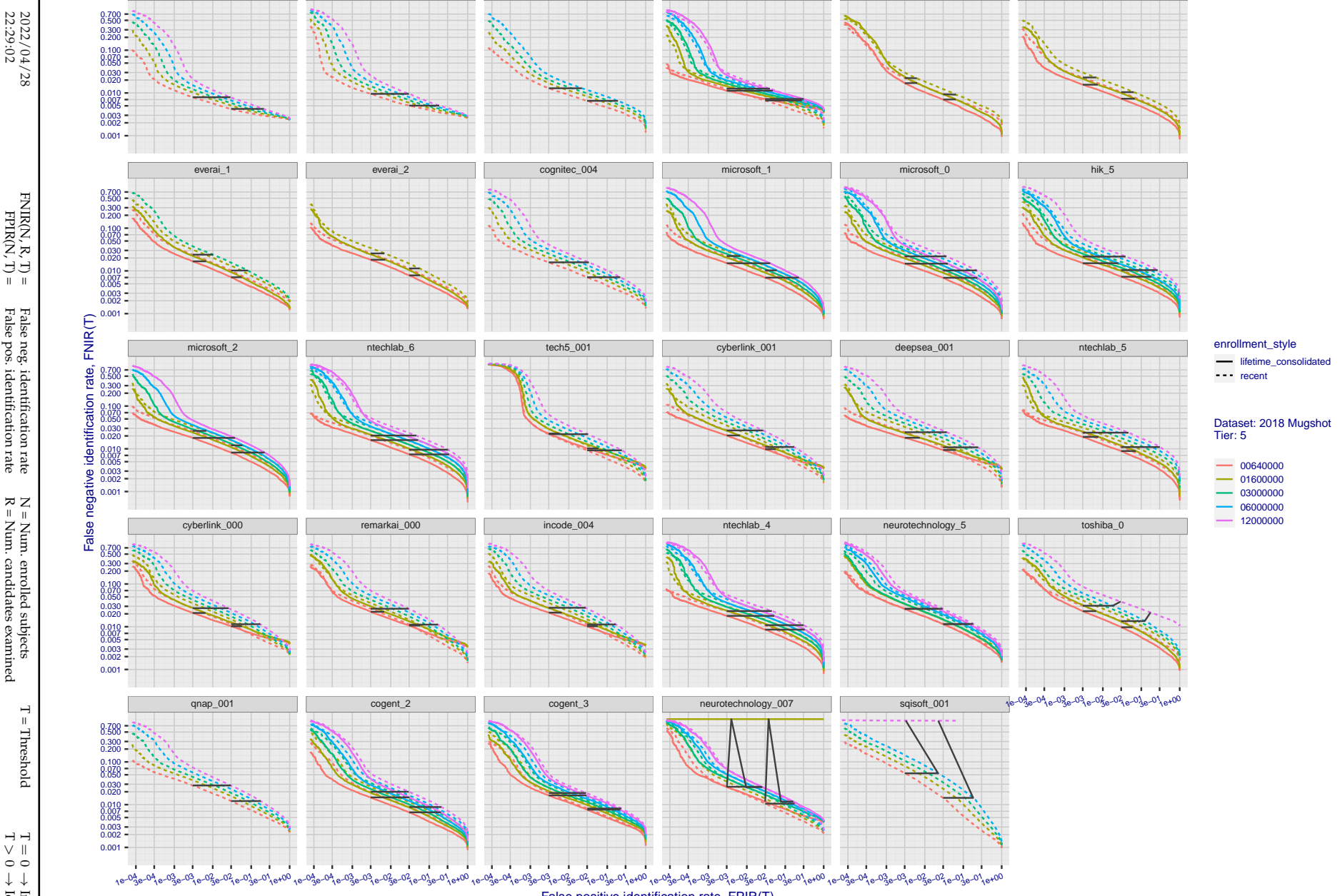


**Figure 52: [FRVT-2018 Mugshot Dataset] Identification miss rates vs. false positive rates.** The figure shows miss rates  $\text{FNIR}(N, L, T)$  as a function of  $\text{FPIR}(N, T)$ , with  $N$  ranging from 640 000 to 12 000 000 as noted in rows 1-10 of Table 1. These error tradeoff characteristics are useful for applications where a threshold must be elevated to limit false positives, such as when human reviewer labor is not matched to the volume of searches. Dark lines join points of equal threshold: If horizontal,  $\text{FPIR}(T)$  rises with  $N$ , and mate scores are independent of  $N$ . Other algorithms adjust scores in an attempt to make  $\text{FPIR}$  independent of  $N$ .

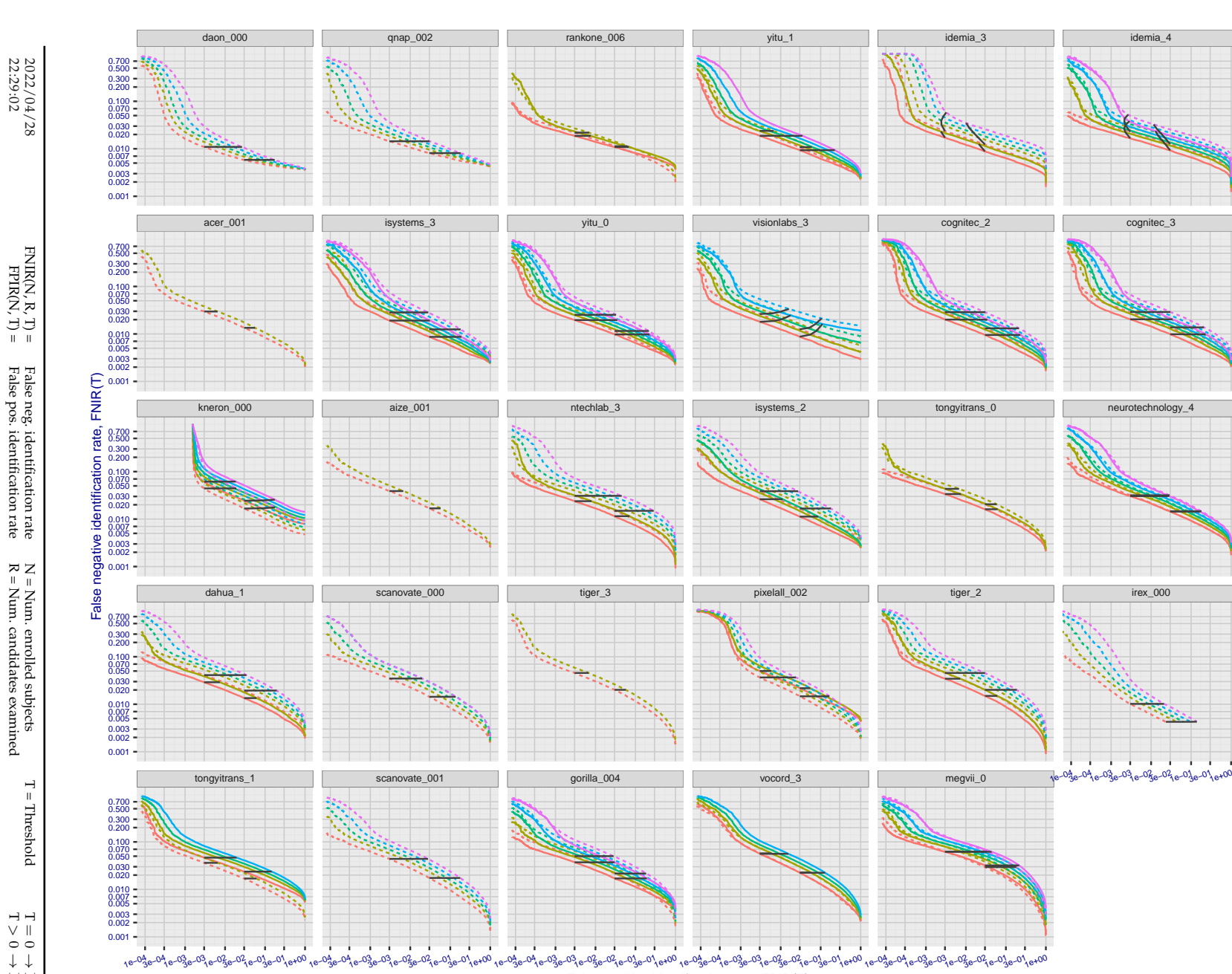
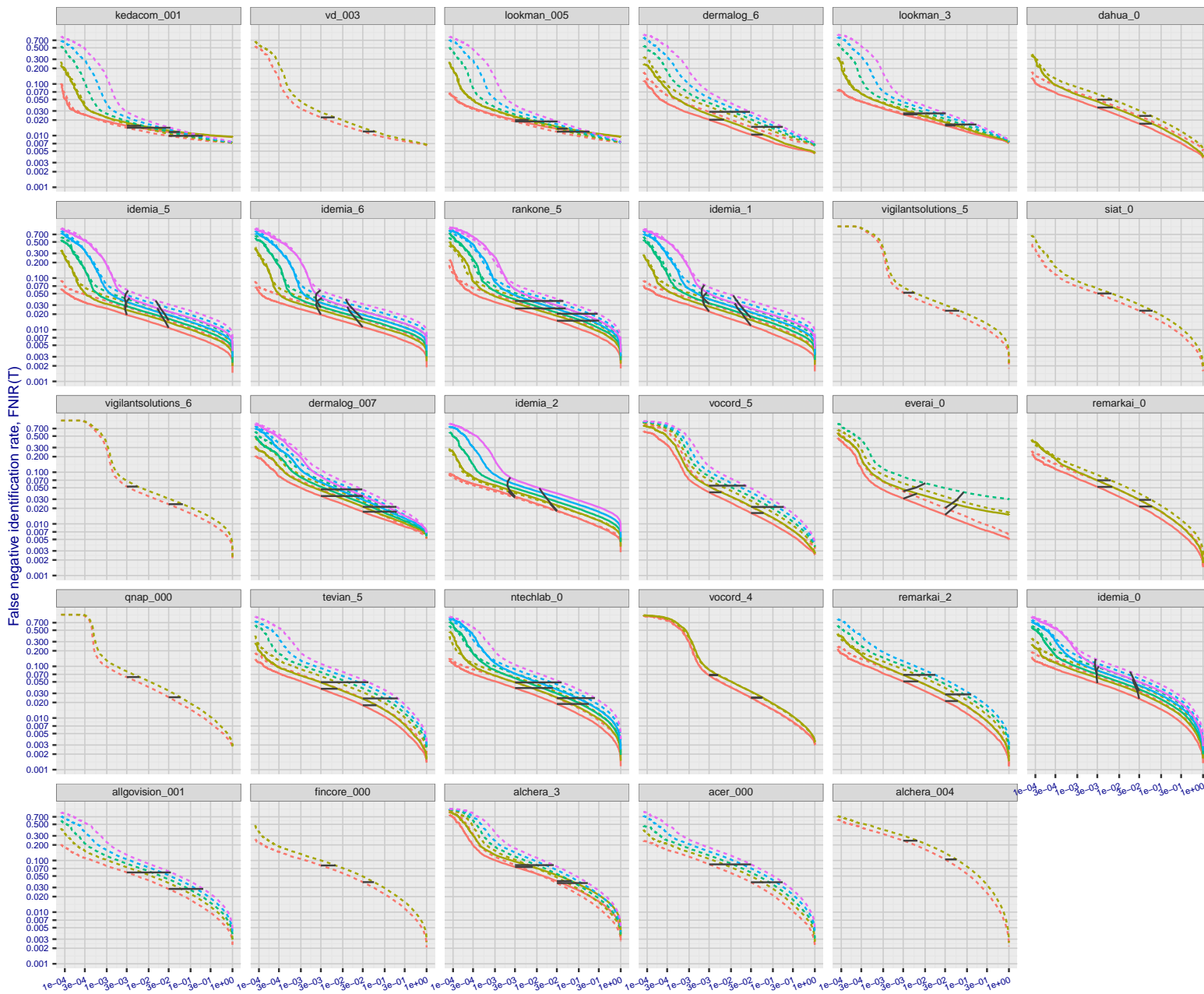
2022/04/28  
22:29:02

Figure 53: [FRVT-2018 Mugshot Dataset] Identification miss rates vs. false positive rates. The figure shows miss rates  $\text{FNIR}(N, L, T)$  as a function of  $\text{FPIR}(N, T)$ , with  $N$  ranging from 640 000 to 12 000 000 as noted in rows 1-10 of Table 1. These error tradeoff characteristics are useful for applications where a threshold must be elevated to limit false positives, such as when human reviewer labor is not matched to the volume of searches. Dark lines join points of equal threshold: If horizontal,  $\text{FPIR}(T)$  rises with  $N$ , and mate scores are independent of  $N$ . Other algorithms adjust scores in an attempt to make  $\text{FPIR}$  independent of  $N$ .

2022/04/28  
22:29:02FNIR(N, R, T) = False neg. identification rate  
FPIR(N, T) = False pos. identification rateN = Num. enrolled subjects  
R = Num. candidates examined

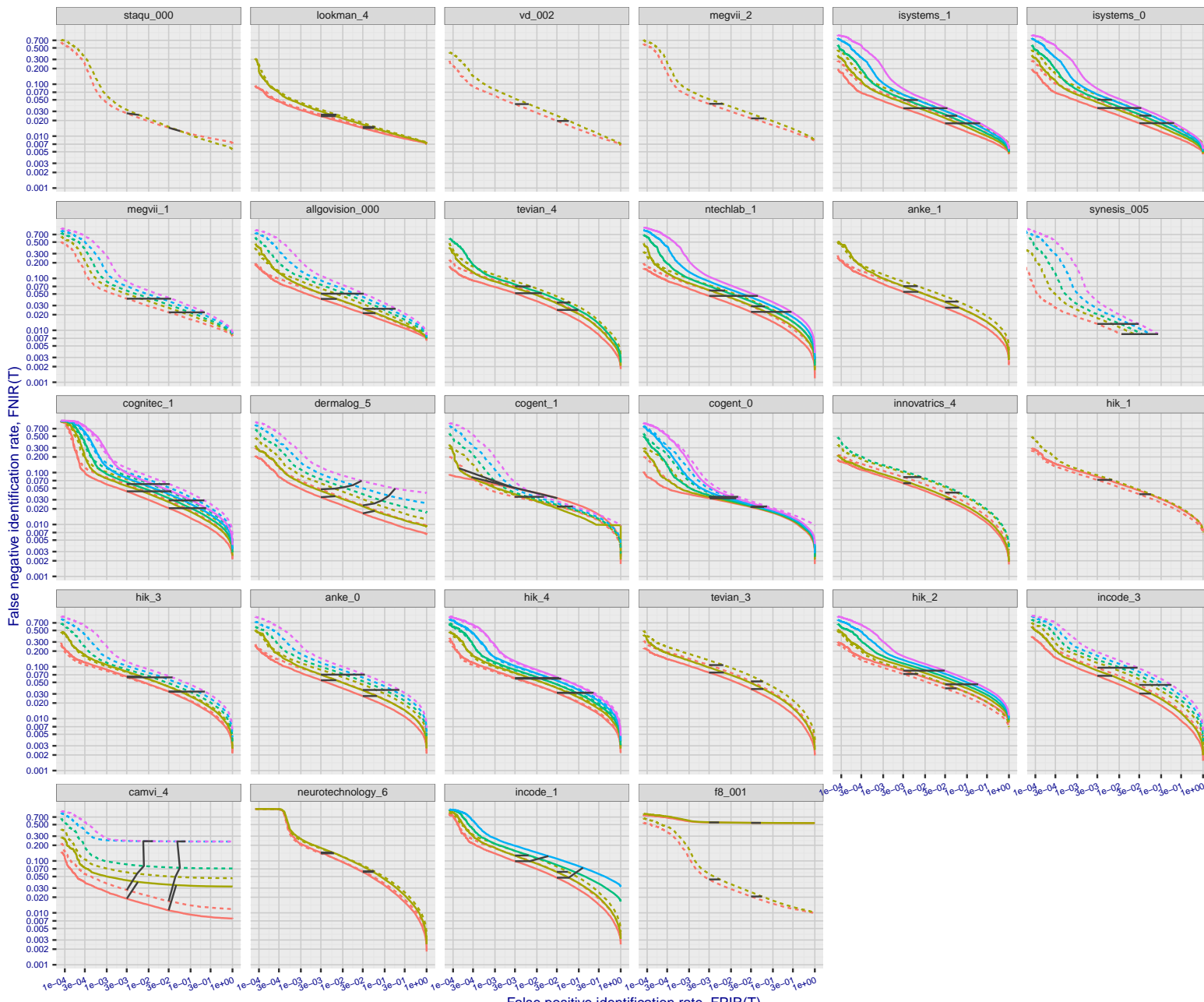
T = Threshold

T = 0 → Investigation  
 $T > 0 \rightarrow$  Identification

**Figure 54: [FRVT-2018 Mugshot Dataset] Identification miss rates vs. false positive rates.** The figure shows miss rates  $\text{FNIR}(N, L, T)$  as a function of  $\text{FPIR}(N, T)$ , with  $N$  ranging from 640 000 to 12 000 000 as noted in rows 1-10 of Table 1. These error tradeoff characteristics are useful for applications where a threshold must be elevated to limit false positives, such as when human reviewer labor is not matched to the volume of searches. Dark lines join points of equal threshold: If horizontal,  $\text{FPIR}(T)$  rises with  $N$ , and mate scores are independent of  $N$ . Other algorithms adjust scores in an attempt to make  $\text{FPIR}$  independent of  $N$ .

2022/04/28  
22:29:02FNIR(N, R, T) = False neg. identification rate  
FPIR(N, T) = False pos. identification rateN = Num. enrolled subjects  
R = Num. candidates examined

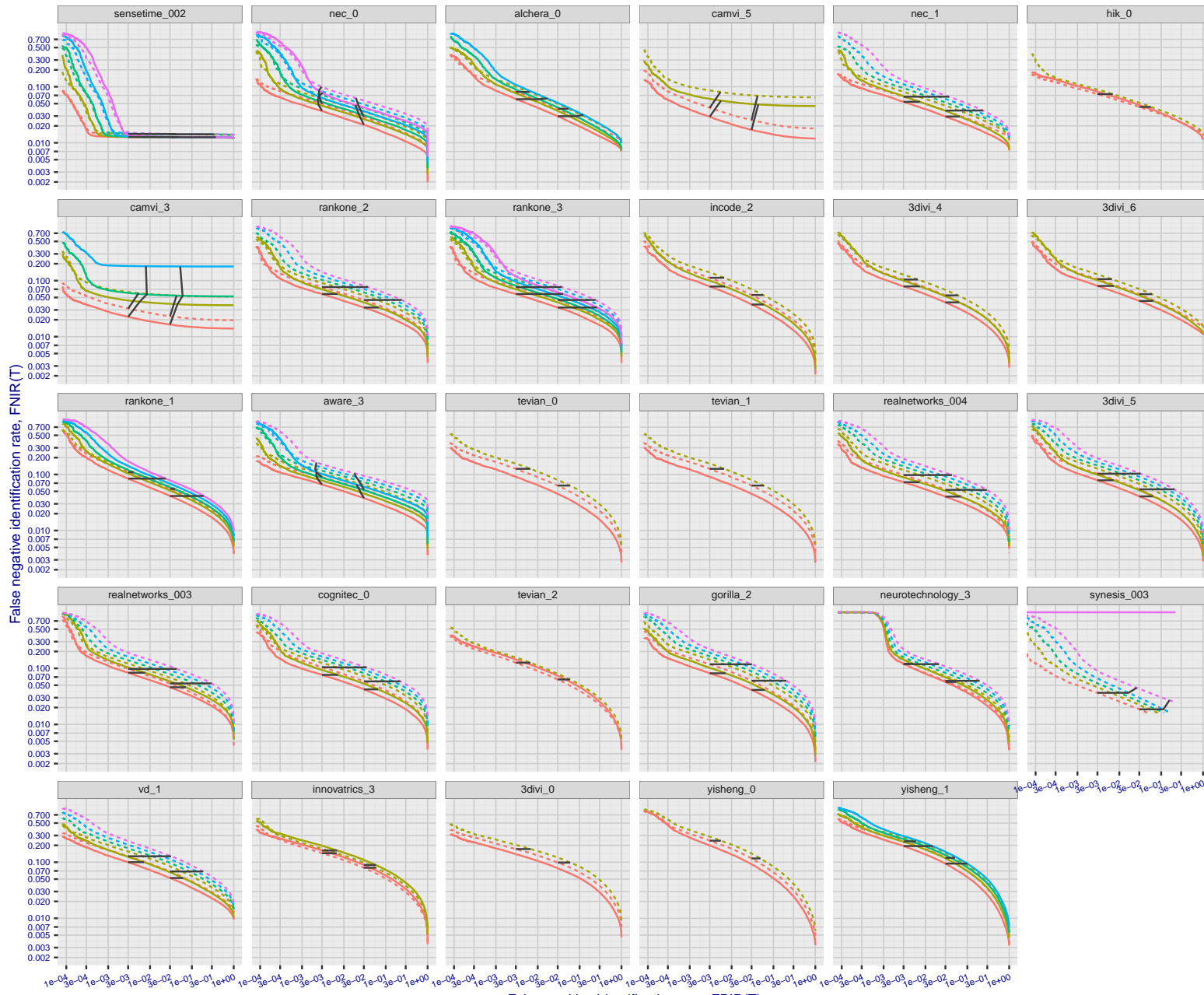
T = Threshold

T = 0 → Investigation  
 $T > 0 \rightarrow$  Identification

**Figure 55: [FRVT-2018 Mugshot Dataset] Identification miss rates vs. false positive rates.** The figure shows miss rates  $\text{FNIR}(N, L, T)$  as a function of  $\text{FPIR}(N, T)$ , with  $N$  ranging from 640 000 to 12 000 000 as noted in rows 1-10 of Table 1. These error tradeoff characteristics are useful for applications where a threshold must be elevated to limit false positives, such as when human reviewer labor is not matched to the volume of searches. Dark lines join points of equal threshold: If horizontal,  $\text{FPIR}(T)$  rises with  $N$ , and mate scores are independent of  $N$ . Other algorithms adjust scores in an attempt to make  $\text{FPIR}$  independent of  $N$ .

2022/04/28  
22:29:02FNIR(N, R, T) = False neg. identification rate  
FPIR(N, T) = False pos. identification rate  
N = Num. enrolled subjects  
R = Num. candidates examined

T = Threshold

T = 0 → Investigation  
 $T > 0 \rightarrow$  Identification

**Figure 56: [FRVT-2018 Mugshot Dataset] Identification miss rates vs. false positive rates.** The figure shows miss rates  $\text{FNIR}(N, L, T)$  as a function of  $\text{FPIR}(N, T)$ , with  $N$  ranging from 640 000 to 12 000 000 as noted in rows 1-10 of Table 1. These error tradeoff characteristics are useful for applications where a threshold must be elevated to limit false positives, such as when human reviewer labor is not matched to the volume of searches. Dark lines join points of equal threshold: If horizontal,  $\text{FPIR}(T)$  rises with  $N$ , and mate scores are independent of  $N$ . Other algorithms adjust scores in an attempt to make  $\text{FPIR}$  independent of  $N$ .

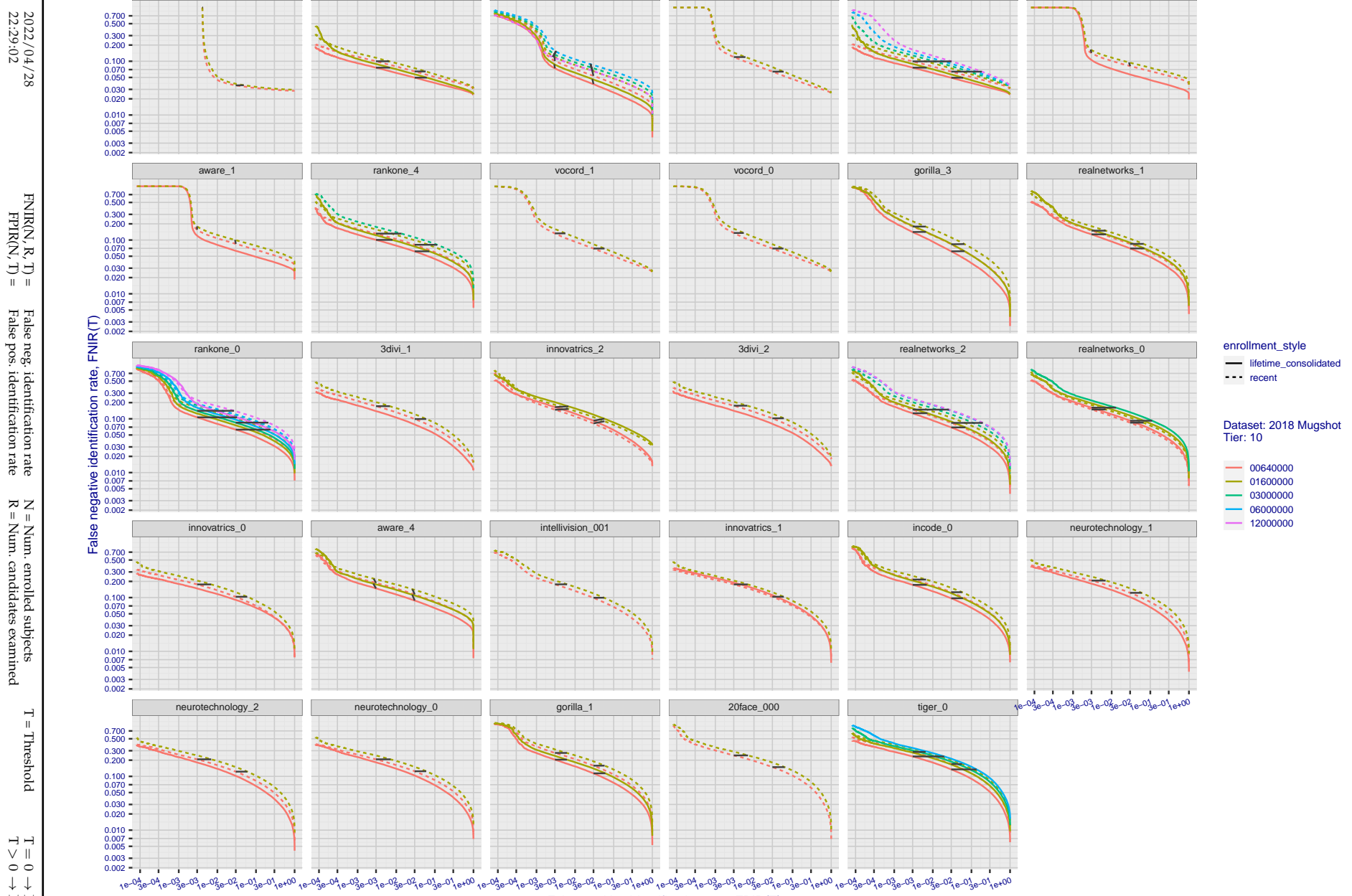


Figure 57: [FRVT-2018 Mugshot Dataset] Identification miss rates vs. false positive rates. The figure shows miss rates  $\text{FNIR}(N, L, T)$  as a function of  $\text{FPIR}(N, T)$ , with  $N$  ranging from 640 000 to 12 000 000 as noted in rows 1-10 of Table 1. These error tradeoff characteristics are useful for applications where a threshold must be elevated to limit false positives, such as when human reviewer labor is not matched to the volume of searches. Dark lines join points of equal threshold: If horizontal,  $\text{FPIR}(T)$  rises with  $N$ , and mate scores are independent of  $N$ . Other algorithms adjust scores in an attempt to make  $\text{FPIR}$  independent of  $N$ .

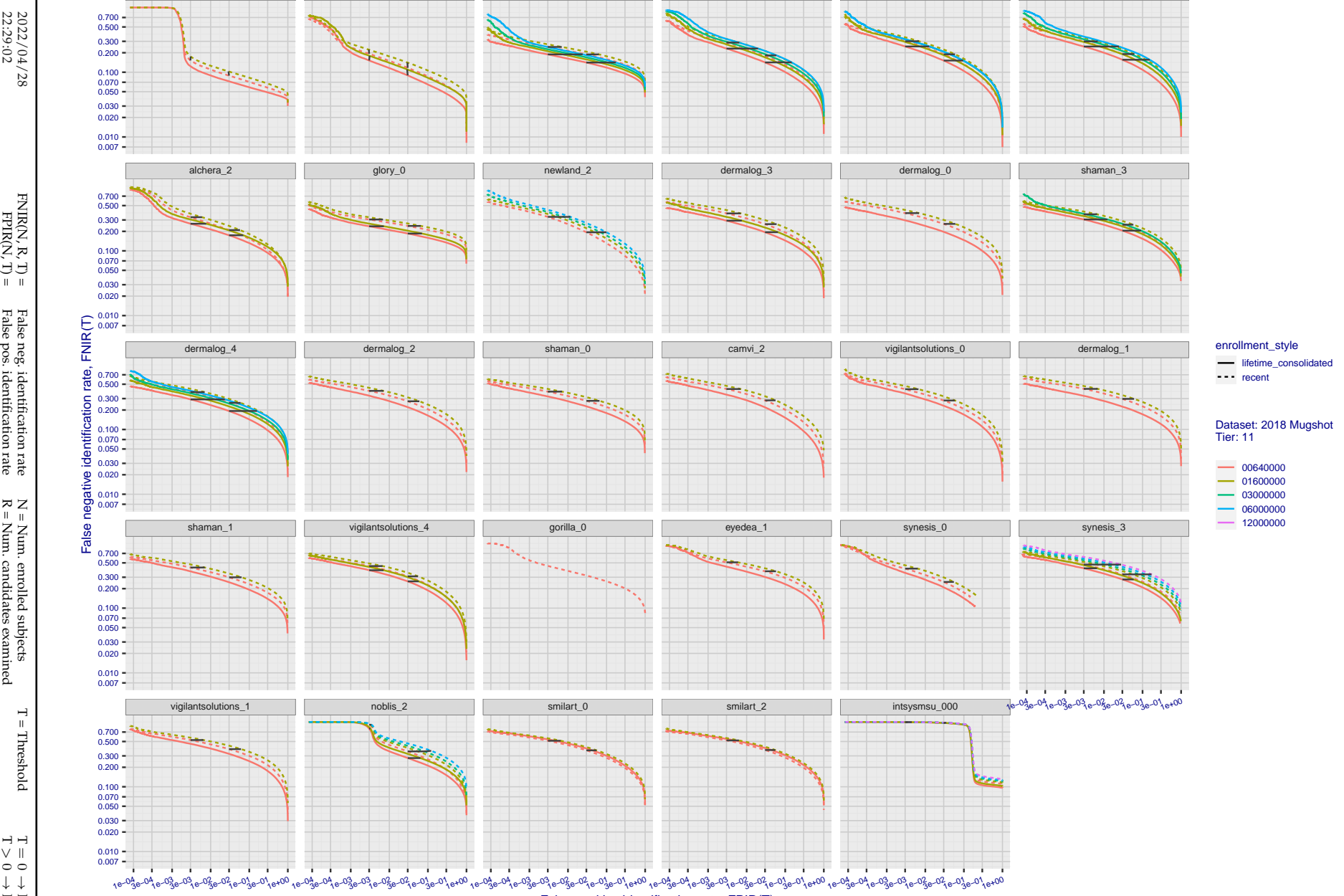
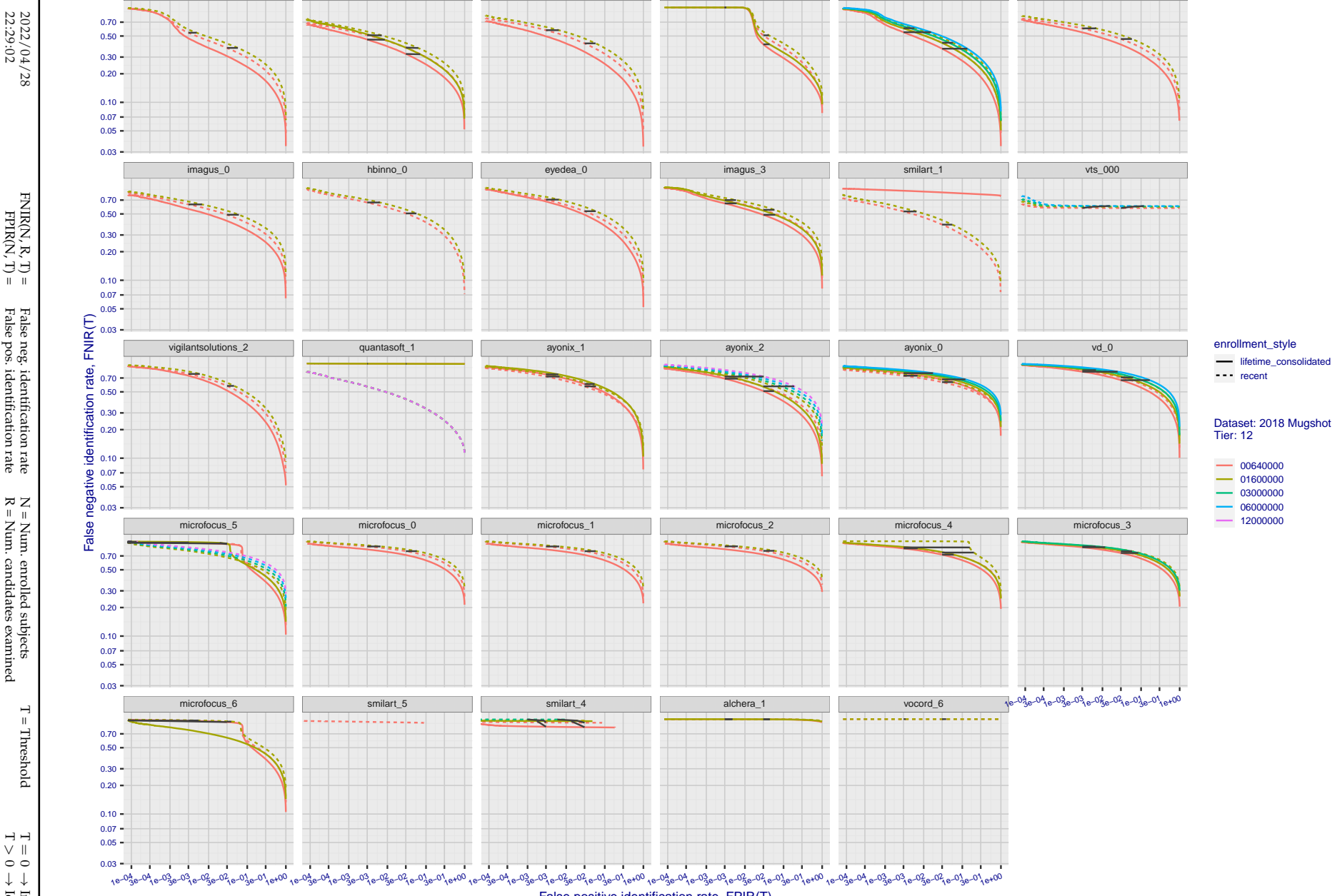


Figure 58: [FRVT-2018 Mugshot Dataset] Identification miss rates vs. false positive rates. The figure shows miss rates  $\text{FNIR}(N, L, T)$  as a function of  $\text{FPIR}(N, T)$ , with  $N$  ranging from 640 000 to 12 000 000 as noted in rows 1-10 of Table 1. These error tradeoff characteristics are useful for applications where a threshold must be elevated to limit false positives, such as when human reviewer labor is not matched to the volume of searches. Dark lines join points of equal threshold: If horizontal,  $\text{FPIR}(T)$  rises with  $N$ , and mate scores are independent of  $N$ . Other algorithms adjust scores in an attempt to make  $\text{FPIR}$  independent of  $N$ .



**Figure 59: [FRVT-2018 Mugshot Dataset] Identification miss rates vs. false positive rates.** The figure shows miss rates  $\text{FNIR}(N, L, T)$  as a function of  $\text{FPIR}(N, T)$ , with  $N$  ranging from 640 000 to 12 000 000 as noted in rows 1-10 of Table 1. These error tradeoff characteristics are useful for applications where a threshold must be elevated to limit false positives, such as when human reviewer labor is not matched to the volume of searches. Dark lines join points of equal threshold: If horizontal,  $\text{FPIR}(T)$  rises with  $N$ , and mate scores are independent of  $N$ . Other algorithms adjust scores in an attempt to make  $\text{FPIR}$  independent of  $N$ .

2022/04/28  
22:29:02FNIR(N, R, T) = False neg. identification rate  
FPIR(N, T) = False pos. identification rateN = Num. enrolled subjects  
R = Num. candidates examined

T = Threshold

T = 0 → Investigation  
 $T > 0 \rightarrow$  Identification

## Appendix B Effect of time-lapse: Accuracy after face ageing

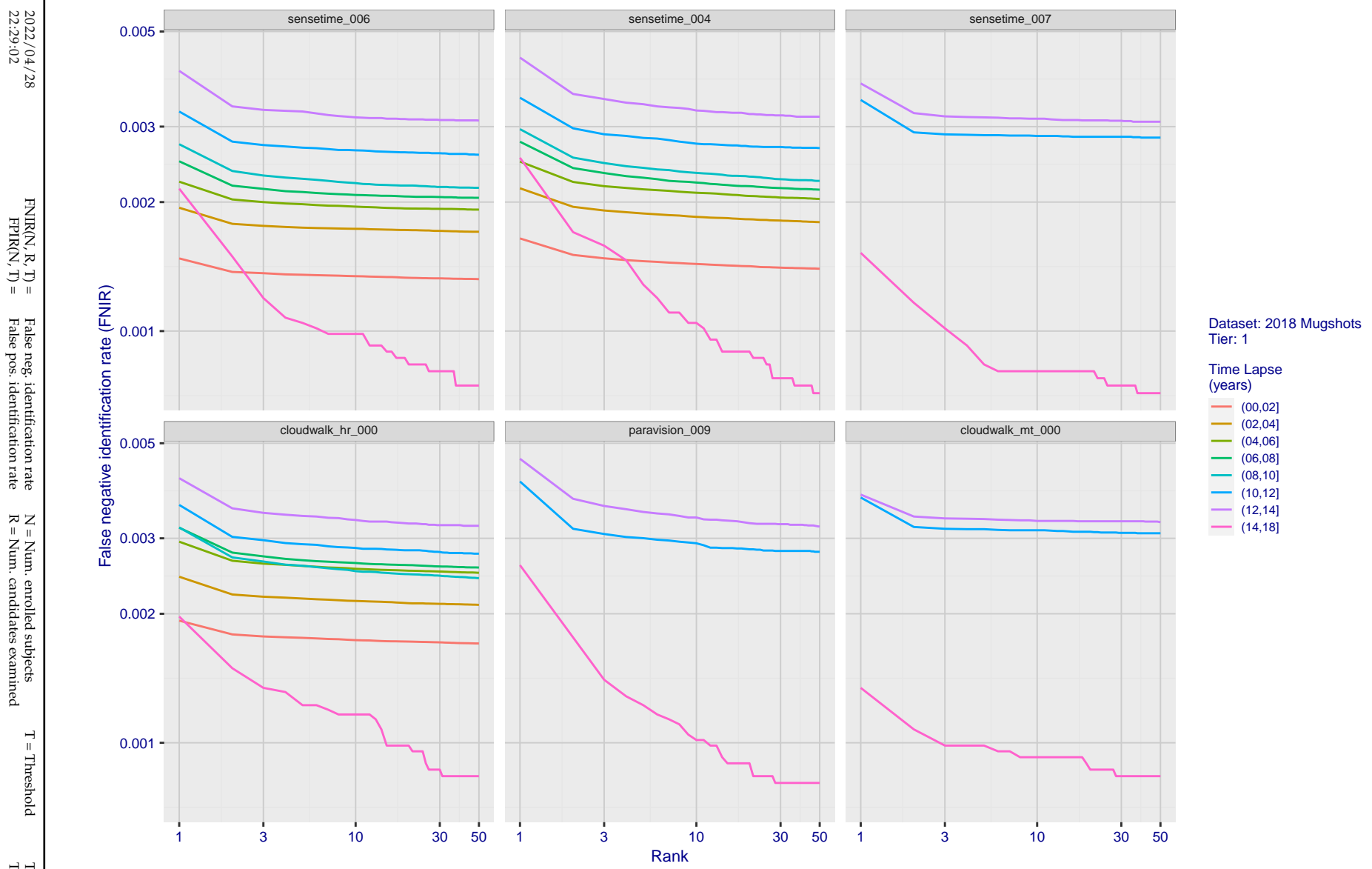


Figure 60: [FRVT-2018 Mugshot Ageing Dataset] Identification miss rates vs. rank by time-elapsed. The oldest image of each individual is enrolled. Thereafter, all more recent images are searched. Miss rates are computed over all searches noted in row 17 of Table 1 and binned by number of years between search and initial enrollment.

2022/04/28  
22:29:02FNIR(N, R, T) = False neg. identification rate  
FPIR(N, T) = False pos. identification rateN = Num. enrolled subjects  
R = Num. candidates examinedT = Threshold  
T = 0 → Investigation

T &gt; 0 → Identification

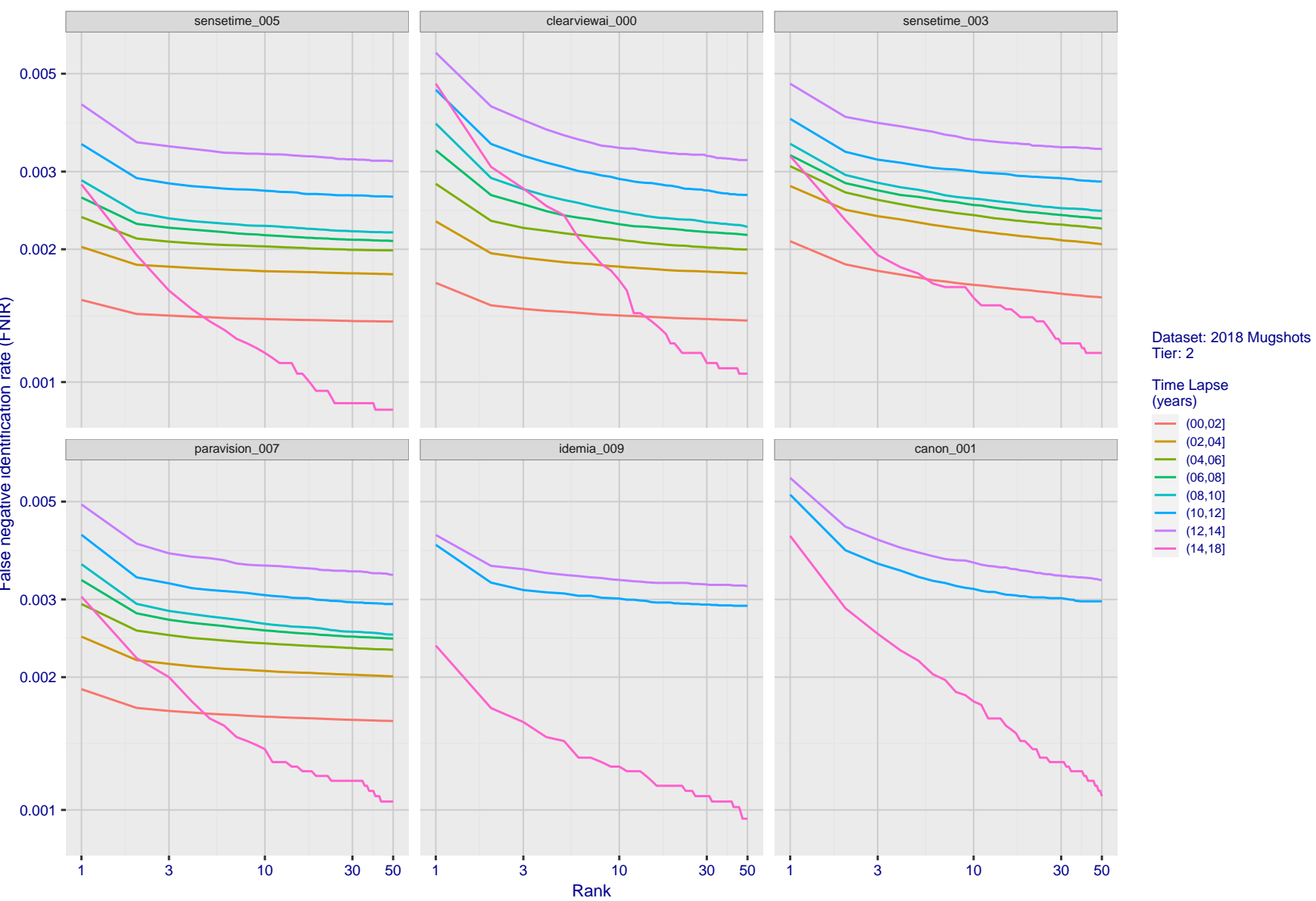


Figure 61: [FRVT-2018 Mugshot Ageing Dataset] Identification miss rates vs. rank by time-elapsed. The oldest image of each individual is enrolled. Thereafter, all more recent images are searched. Miss rates are computed over all searches noted in row 17 of Table 1 and binned by number of years between search and initial enrollment.

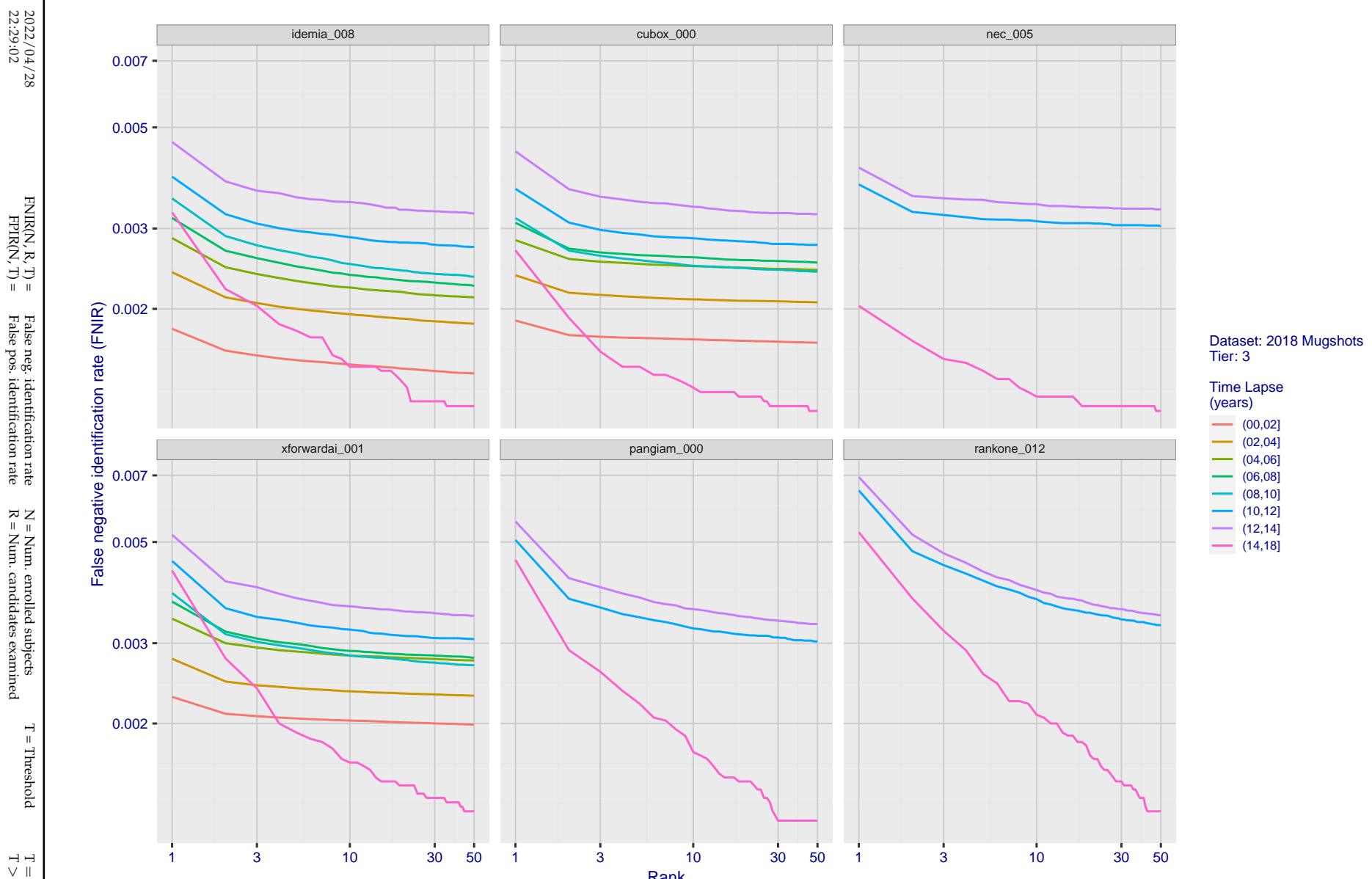


Figure 62: [FRVT-2018 Mugshot Ageing Dataset] Identification miss rates vs. rank by time-elapsed. The oldest image of each individual is enrolled. Thereafter, all more recent images are searched. Miss rates are computed over all searches noted in row 17 of Table 1 and binned by number of years between search and initial enrollment.

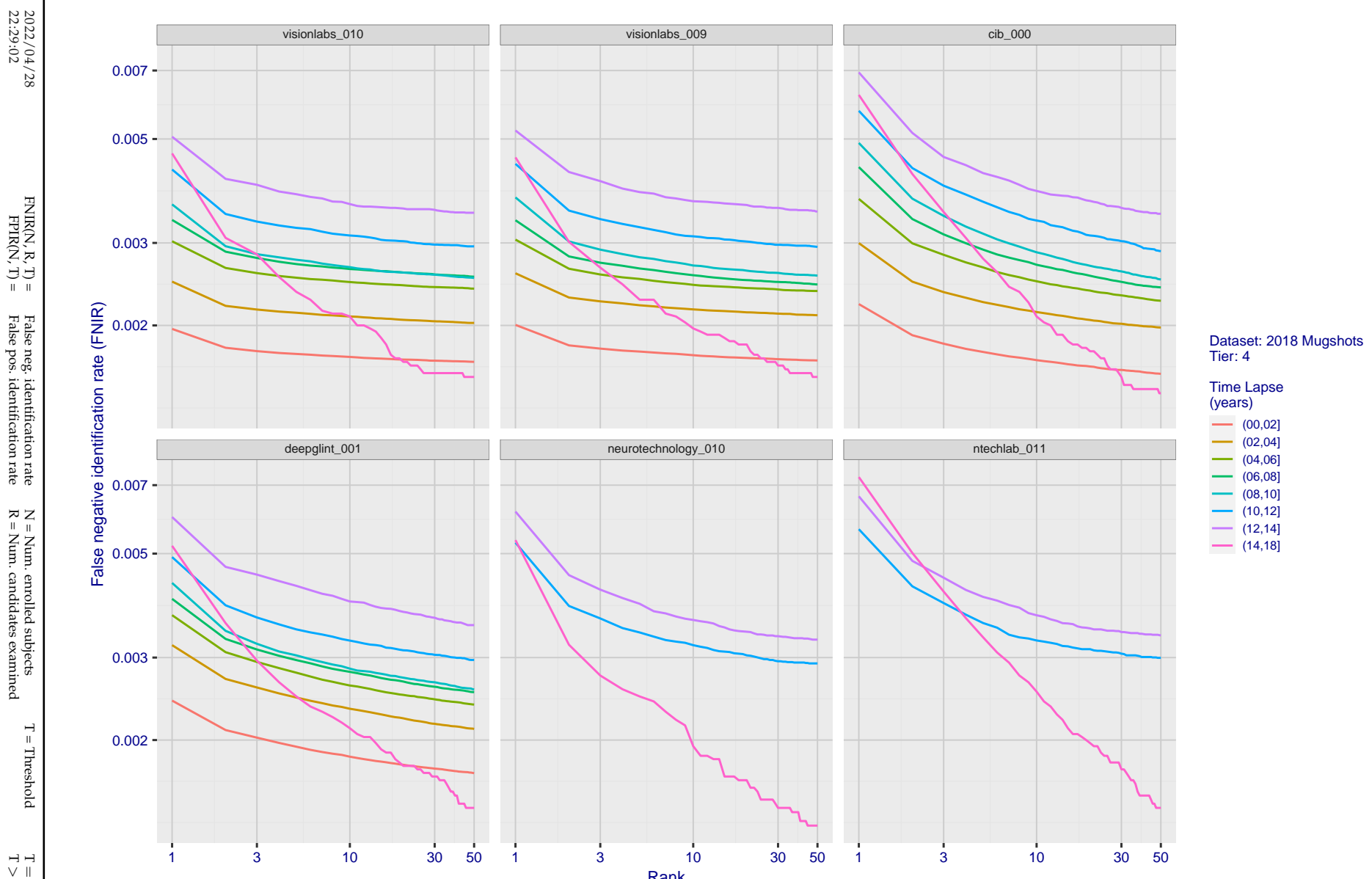


Figure 63: [FRVT-2018 Mugshot Ageing Dataset] Identification miss rates vs. rank by time elapsed. The oldest image of each individual is enrolled. Thereafter, all more recent images are searched. Miss rates are computed over all searches noted in row 17 of Table 1 and binned by number of years between search and initial enrollment.

2022/04/28  
22:29:02FNIR(N, R, T) = False neg. identification rate  
FPIR(N, T) = False pos. identification rateN = Num. enrolled subjects  
R = Num. candidates examinedT = Threshold  
T = 0 → Investigation

T &gt; 0 → Identification

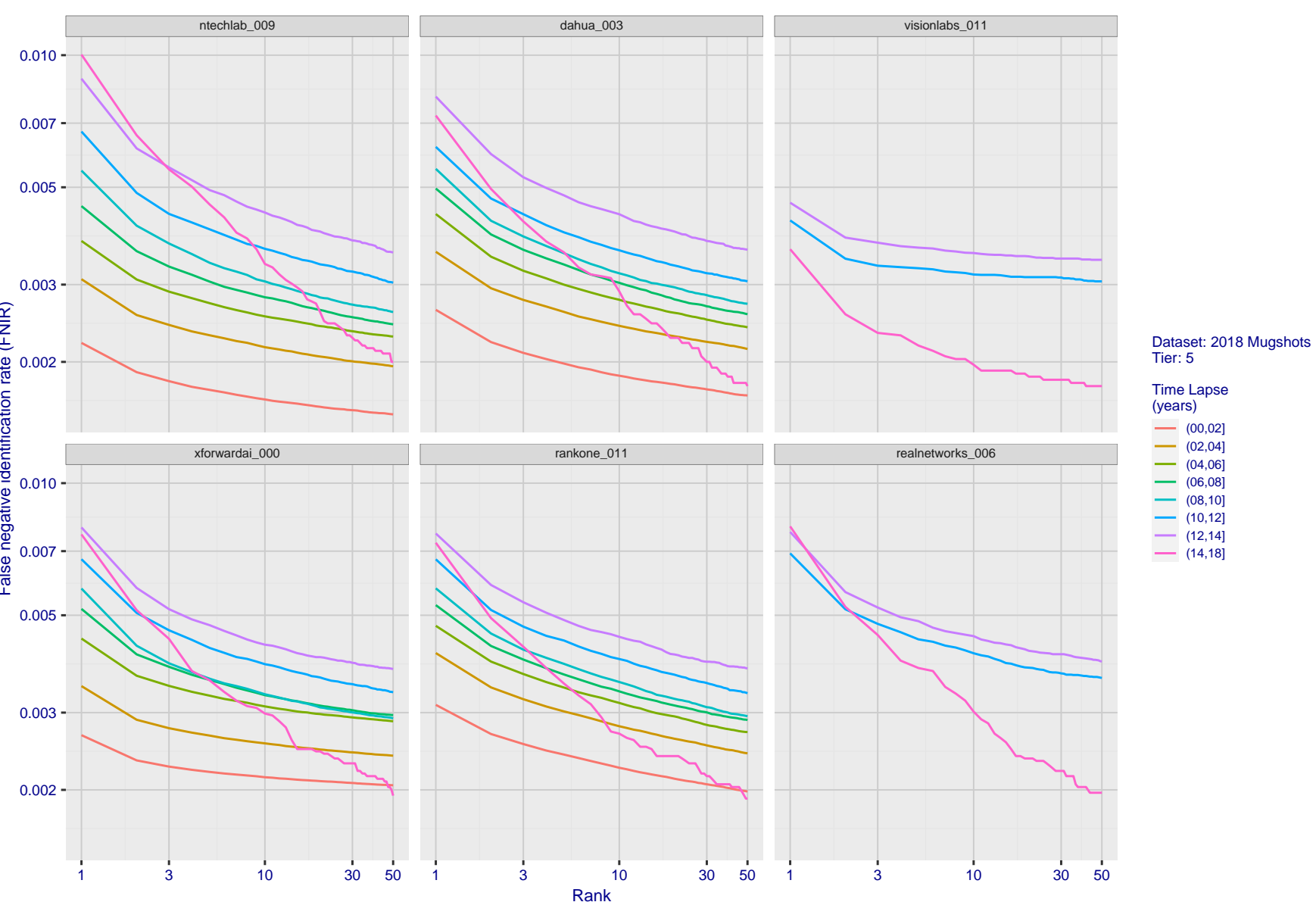


Figure 64: [FRVT-2018 Mugshot Ageing Dataset] Identification miss rates vs. rank by time-elapsed. The oldest image of each individual is enrolled. Thereafter, all more recent images are searched. Miss rates are computed over all searches noted in row 17 of Table 1 and binned by number of years between search and initial enrollment.

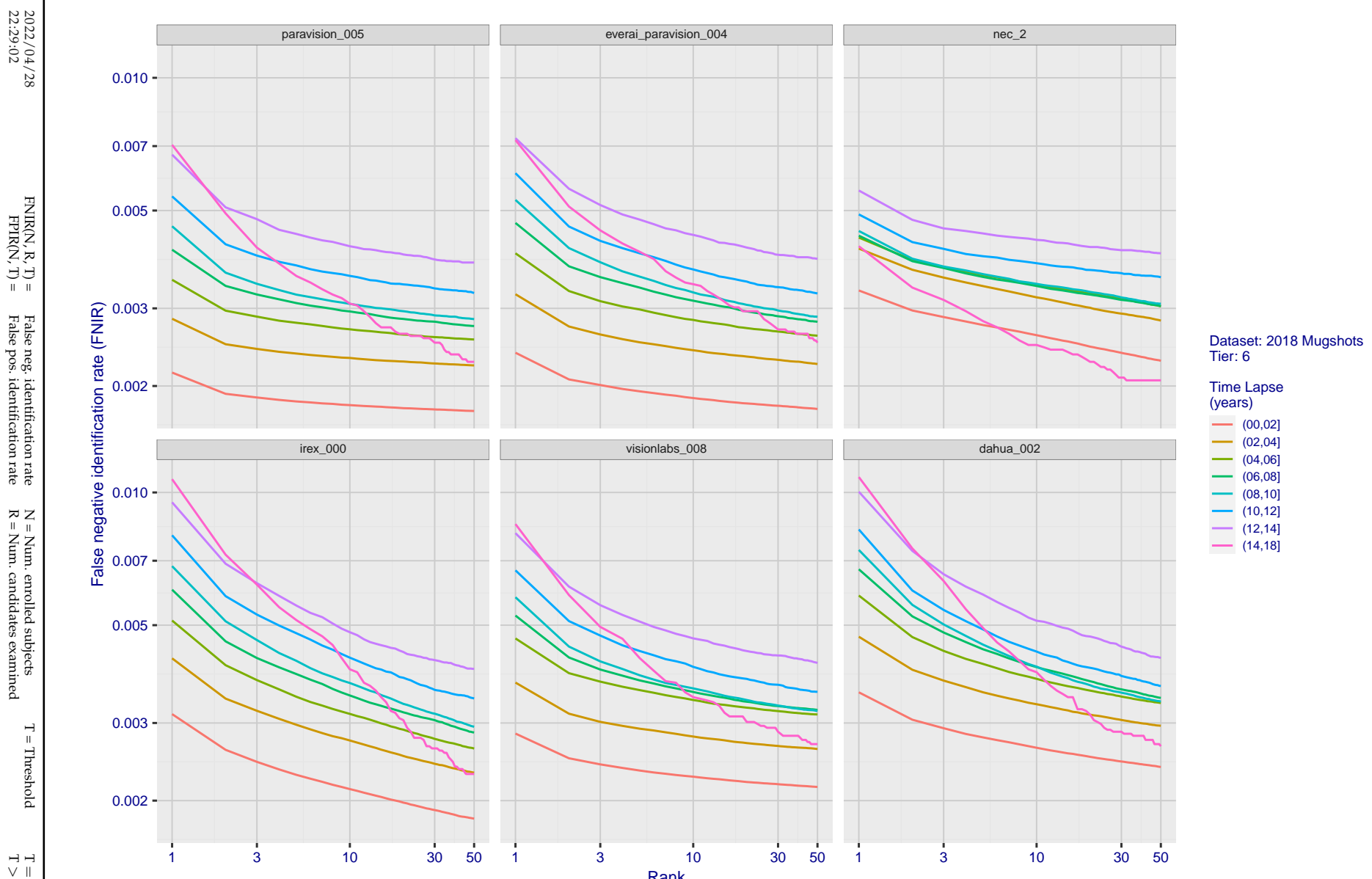


Figure 65: [FRVT-2018 Mugshot Ageing Dataset] Identification miss rates vs. rank by time-elapsed. The oldest image of each individual is enrolled. Thereafter, all more recent images are searched. Miss rates are computed over all searches noted in row 17 of Table 1 and binned by number of years between search and initial enrollment.

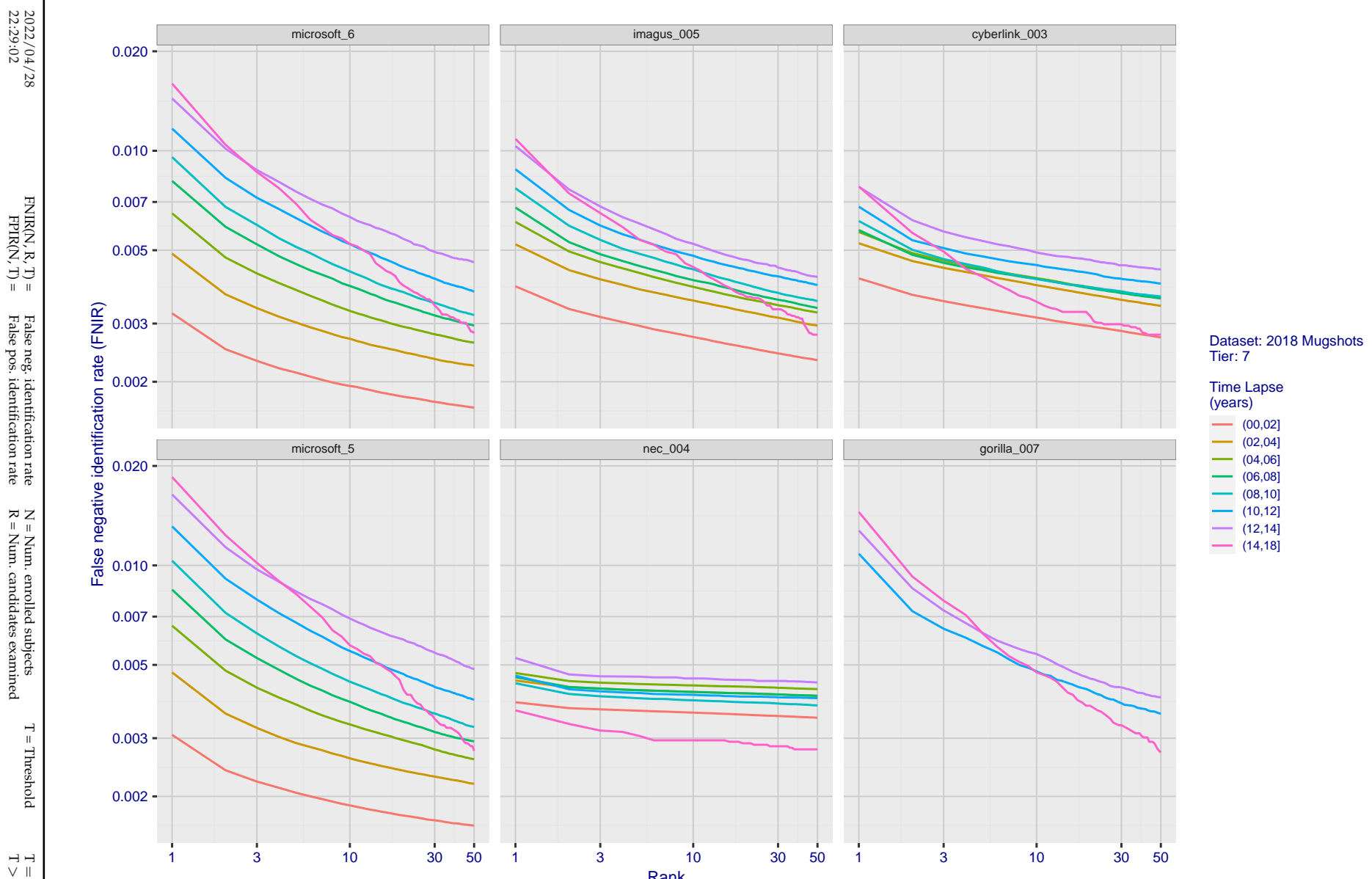
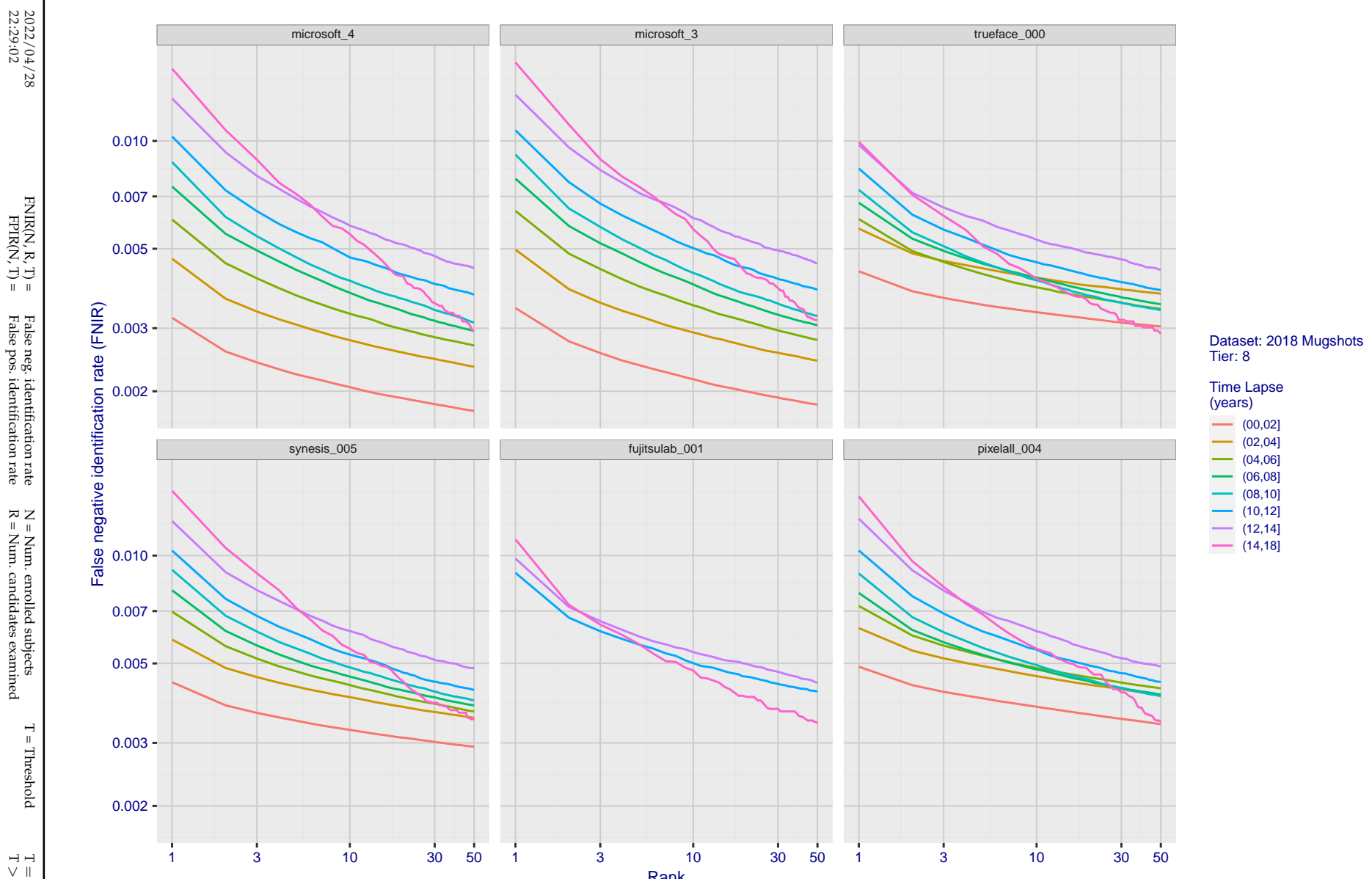


Figure 66: [FRVT-2018 Mugshot Ageing Dataset] Identification miss rates vs. rank by time-elapsed. The oldest image of each individual is enrolled. Thereafter, all more recent images are searched. Miss rates are computed over all searches noted in row 17 of Table 1 and binned by number of years between search and initial enrollment.



**Figure 67: [FRVT-2018 Mugshot Ageing Dataset] Identification miss rates vs. rank by time-elapsed.** The oldest image of each individual is enrolled. Thereafter, all more recent images are searched. Miss rates are computed over all searches noted in row 17 of Table 1 and binned by number of years between search and initial enrollment.

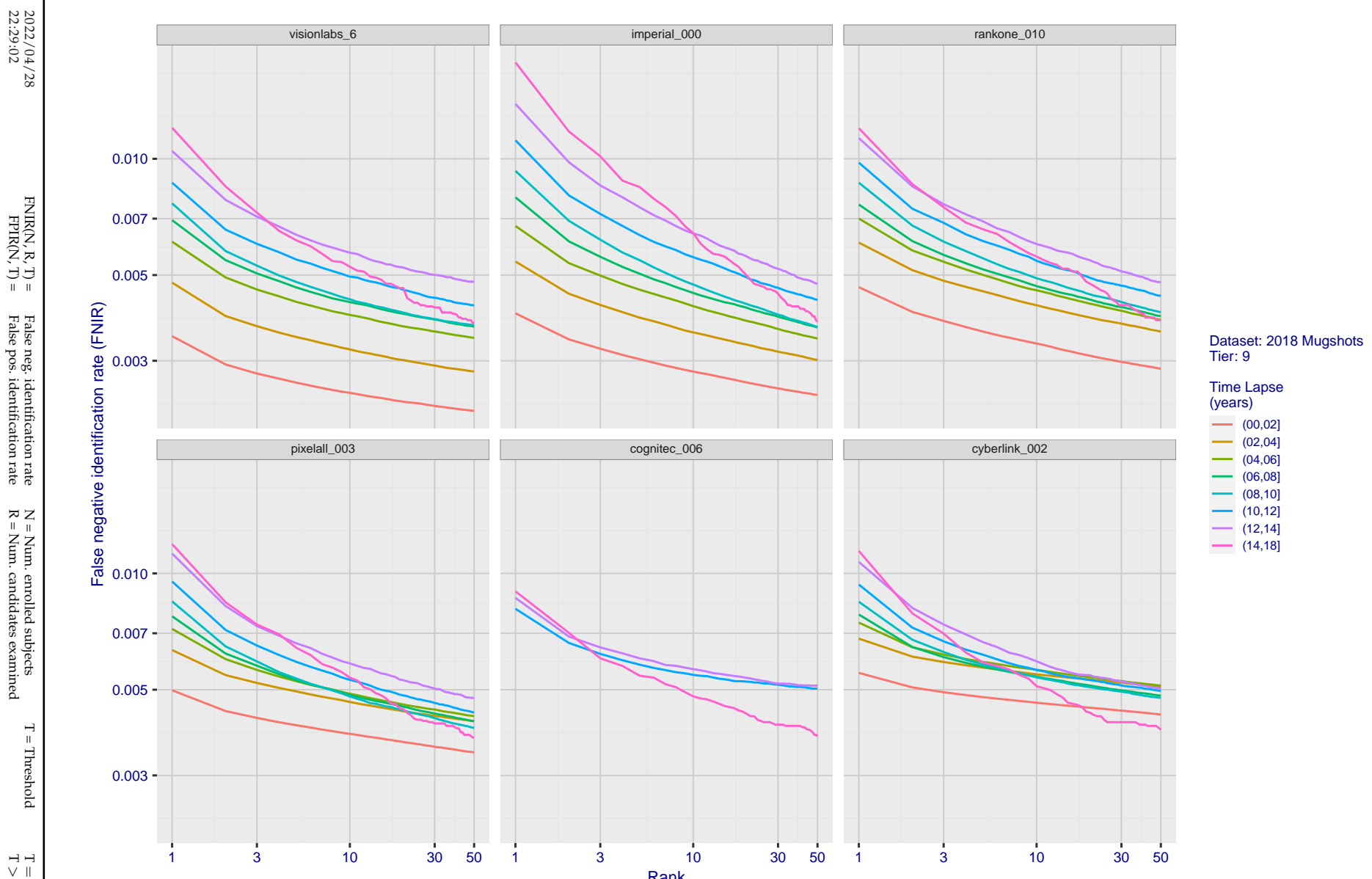


Figure 68: [FRVT-2018 Mugshot Ageing Dataset] Identification miss rates vs. rank by time-elapsed. The oldest image of each individual is enrolled. Thereafter, all more recent images are searched. Miss rates are computed over all searches noted in row 17 of Table 1 and binned by number of years between search and initial enrollment.

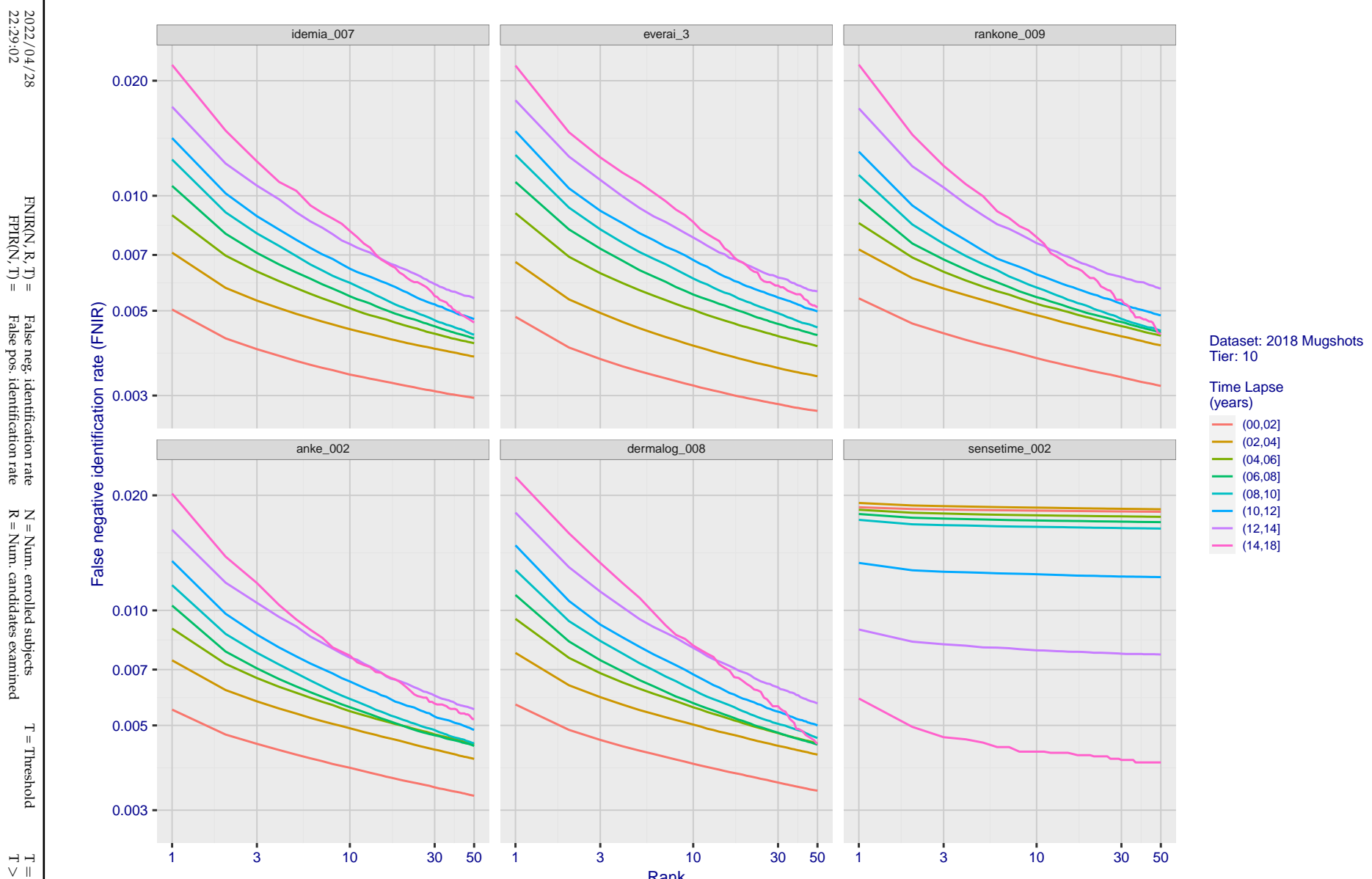


Figure 69: [FRVT-2018 Mugshot Ageing Dataset] Identification miss rates vs. rank by time-elapsed. The oldest image of each individual is enrolled. Thereafter, all more recent images are searched. Miss rates are computed over all searches noted in row 17 of Table 1 and binned by number of years between search and initial enrollment.

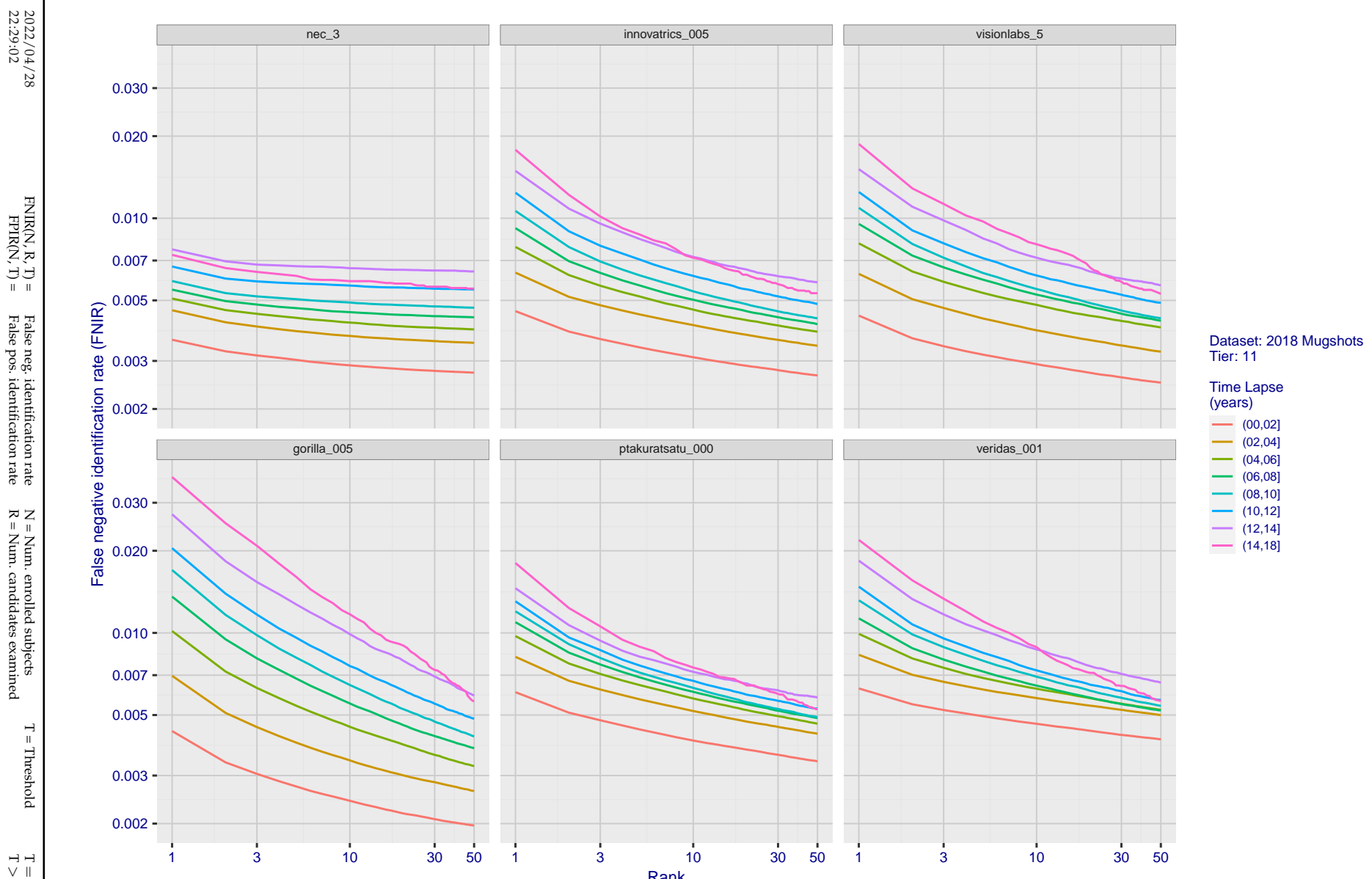


Figure 70: [FRVT-2018 Mugshot Ageing Dataset] Identification miss rates vs. rank by time-elapsed. The oldest image of each individual is enrolled. Thereafter, all more recent images are searched. Miss rates are computed over all searches noted in row 17 of Table 1 and binned by number of years between search and initial enrollment.

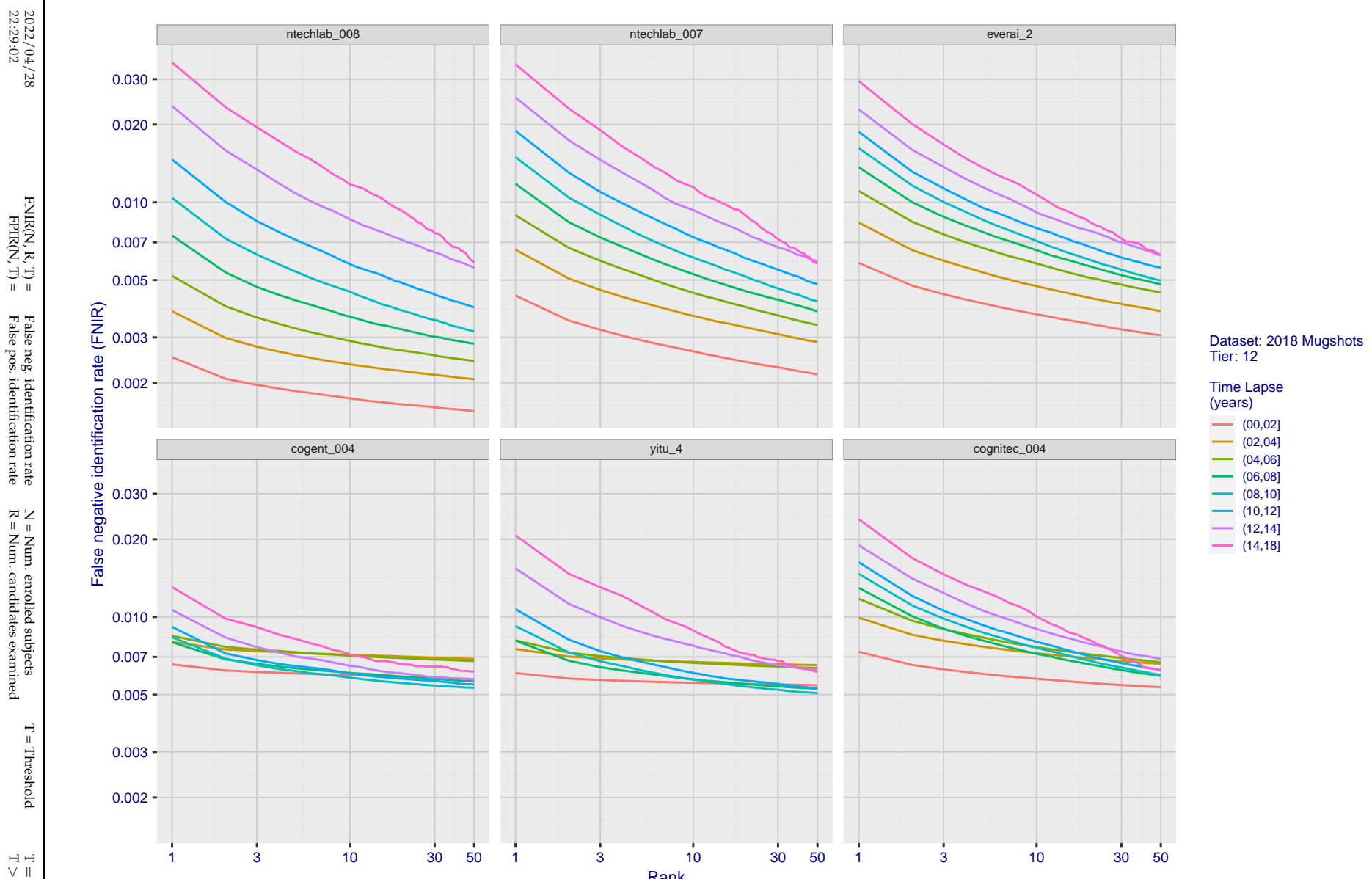


Figure 71: [FRVT-2018 Mugshot Ageing Dataset] Identification miss rates vs. rank by time-elapsed. The oldest image of each individual is enrolled. Thereafter, all more recent images are searched. Miss rates are computed over all searches noted in row 17 of Table 1 and binned by number of years between search and initial enrollment.

2022/04/28  
22:29:02FNIR(N, R, T) = False neg. identification rate  
FPIR(N, T) = False pos. identification rateN = Num. enrolled subjects  
R = Num. candidates examined

T = Threshold

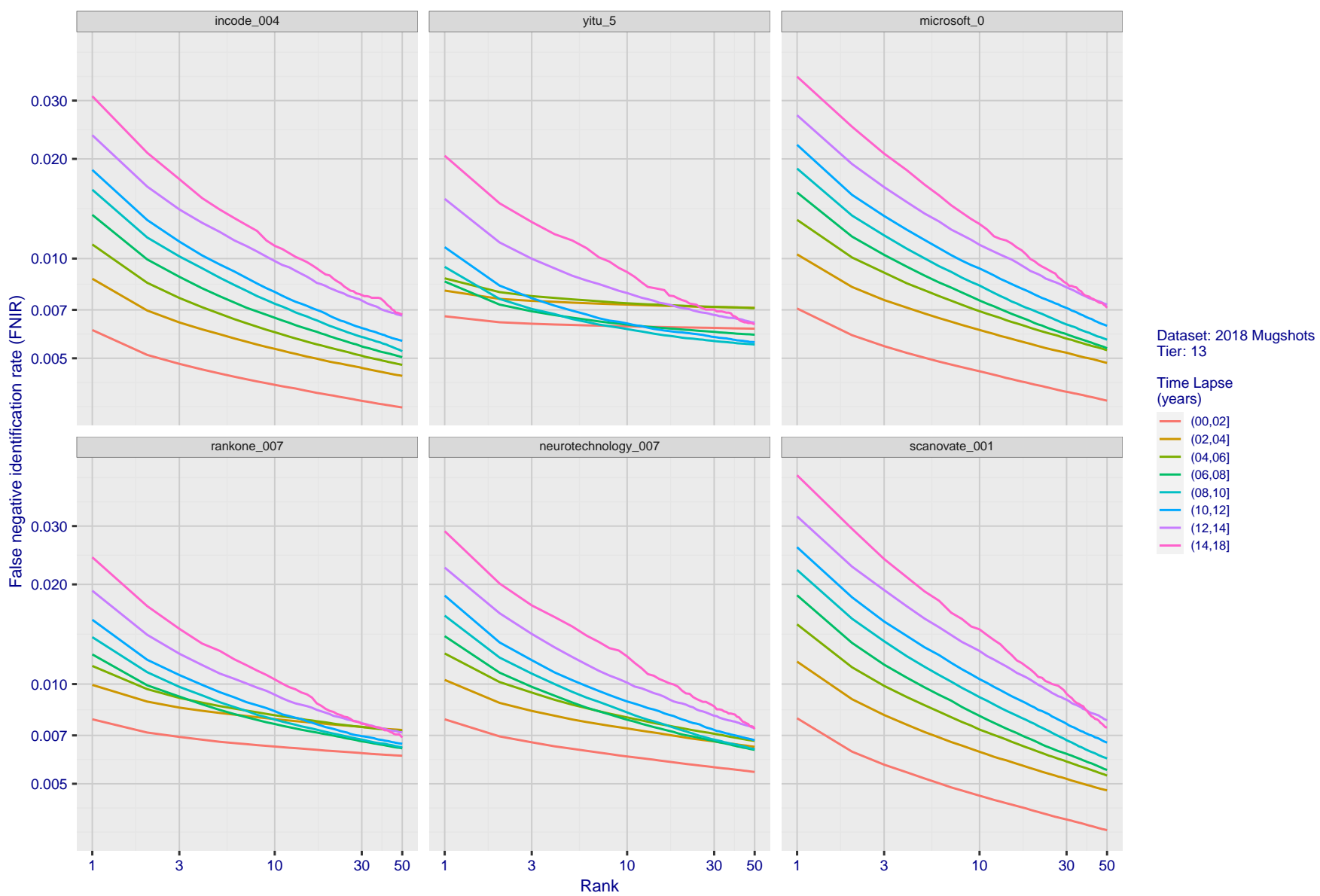
T = 0 → Investigation  
T > 0 → Identification

Figure 72: [FRVT-2018 Mugshot Ageing Dataset] Identification miss rates vs. rank by time-elapsed. The oldest image of each individual is enrolled. Thereafter, all more recent images are searched. Miss rates are computed over all searches noted in row 17 of Table 1 and binned by number of years between search and initial enrollment.

2022/04/28  
22:29:02FNIR(N, R, T) = False neg. identification rate  
FPIR(N, T) = False pos. identification rateN = Num. enrolled subjects  
R = Num. candidates examinedT = Threshold  
T = 0 → Investigation

T &gt; 0 → Identification

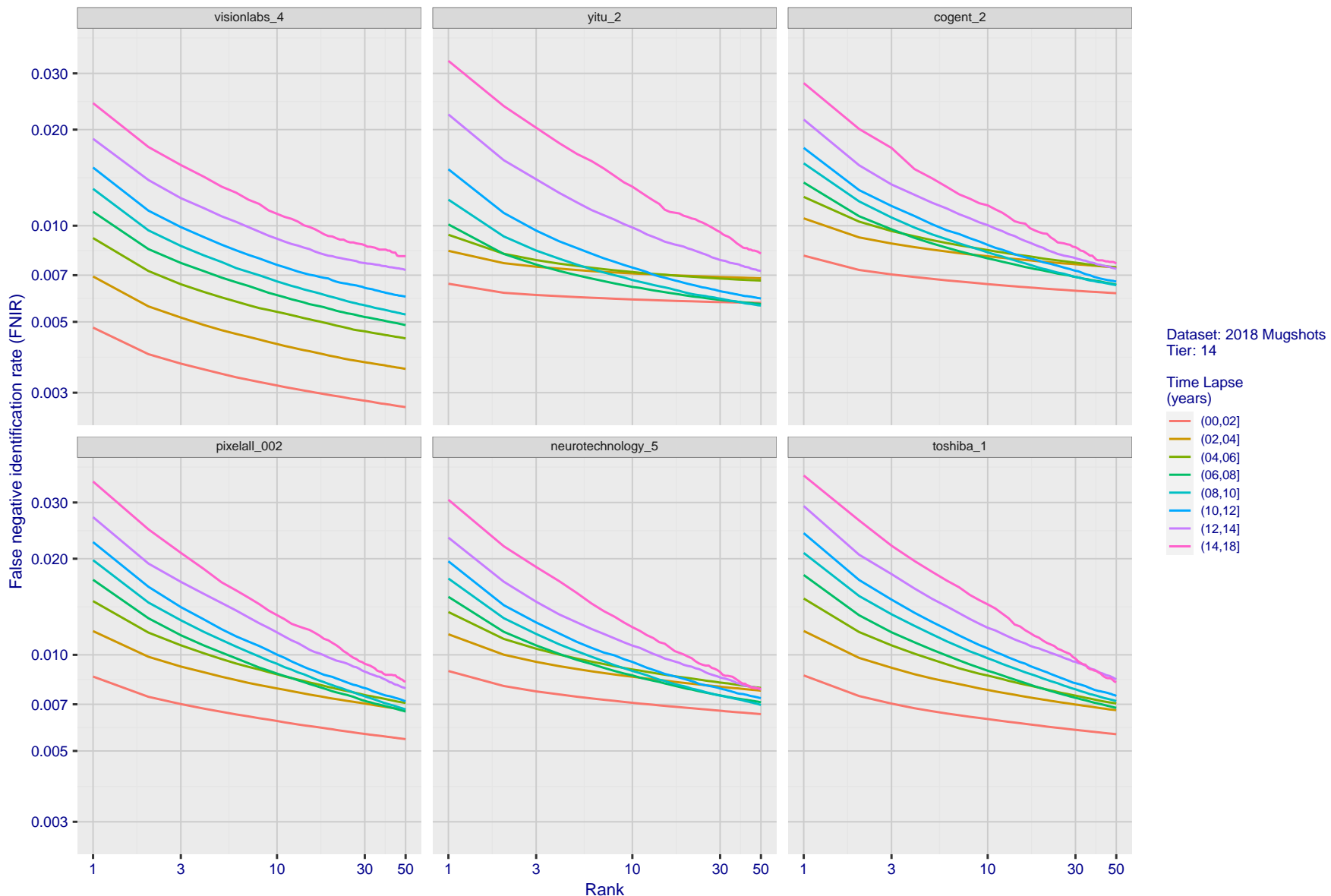


Figure 73: [FRVT-2018 Mugshot Ageing Dataset] Identification miss rates vs. rank by time elapsed. The oldest image of each individual is enrolled. Thereafter, all more recent images are searched. Miss rates are computed over all searches noted in row 17 of Table 1 and binned by number of years between search and initial enrollment.

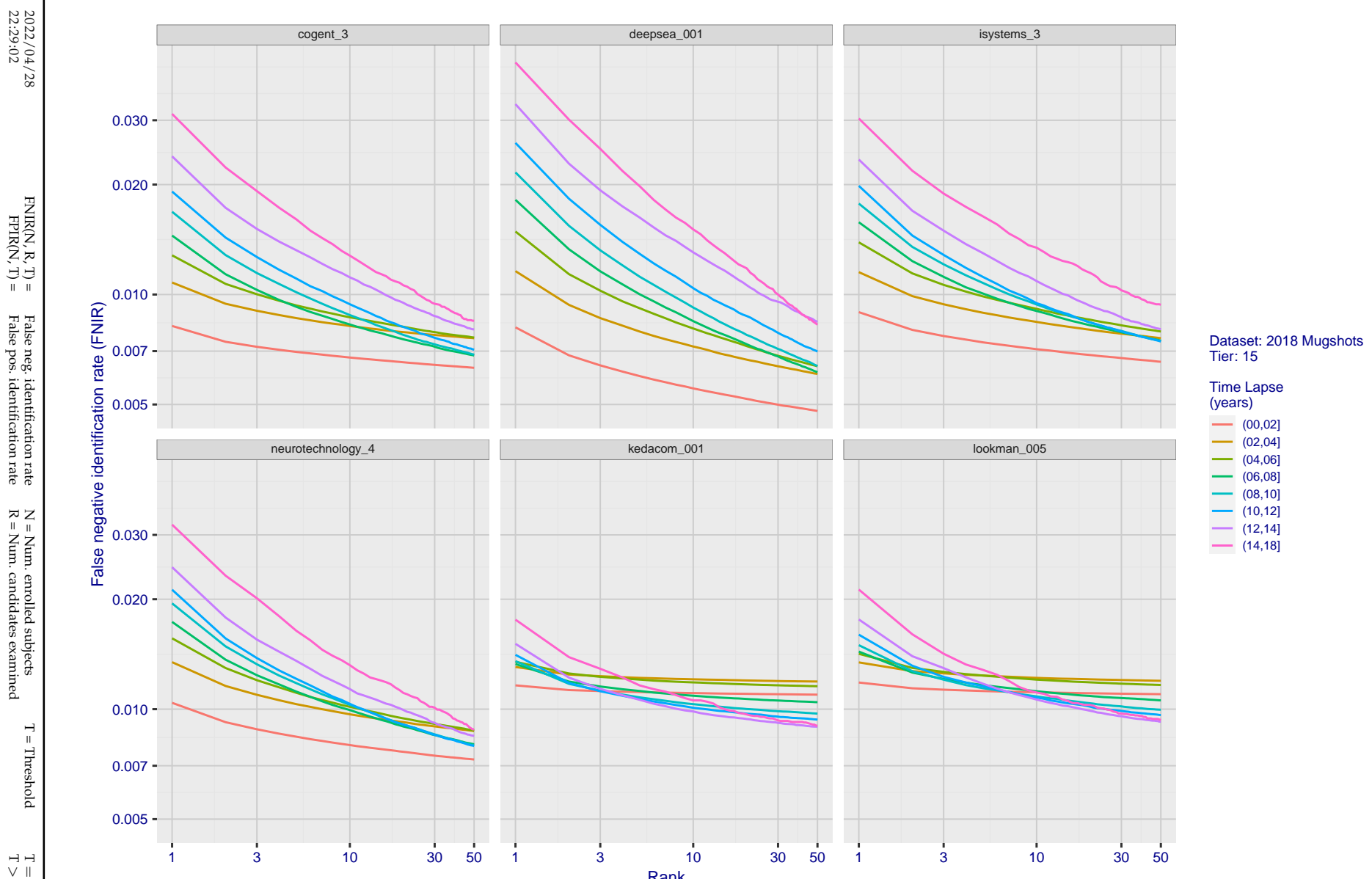
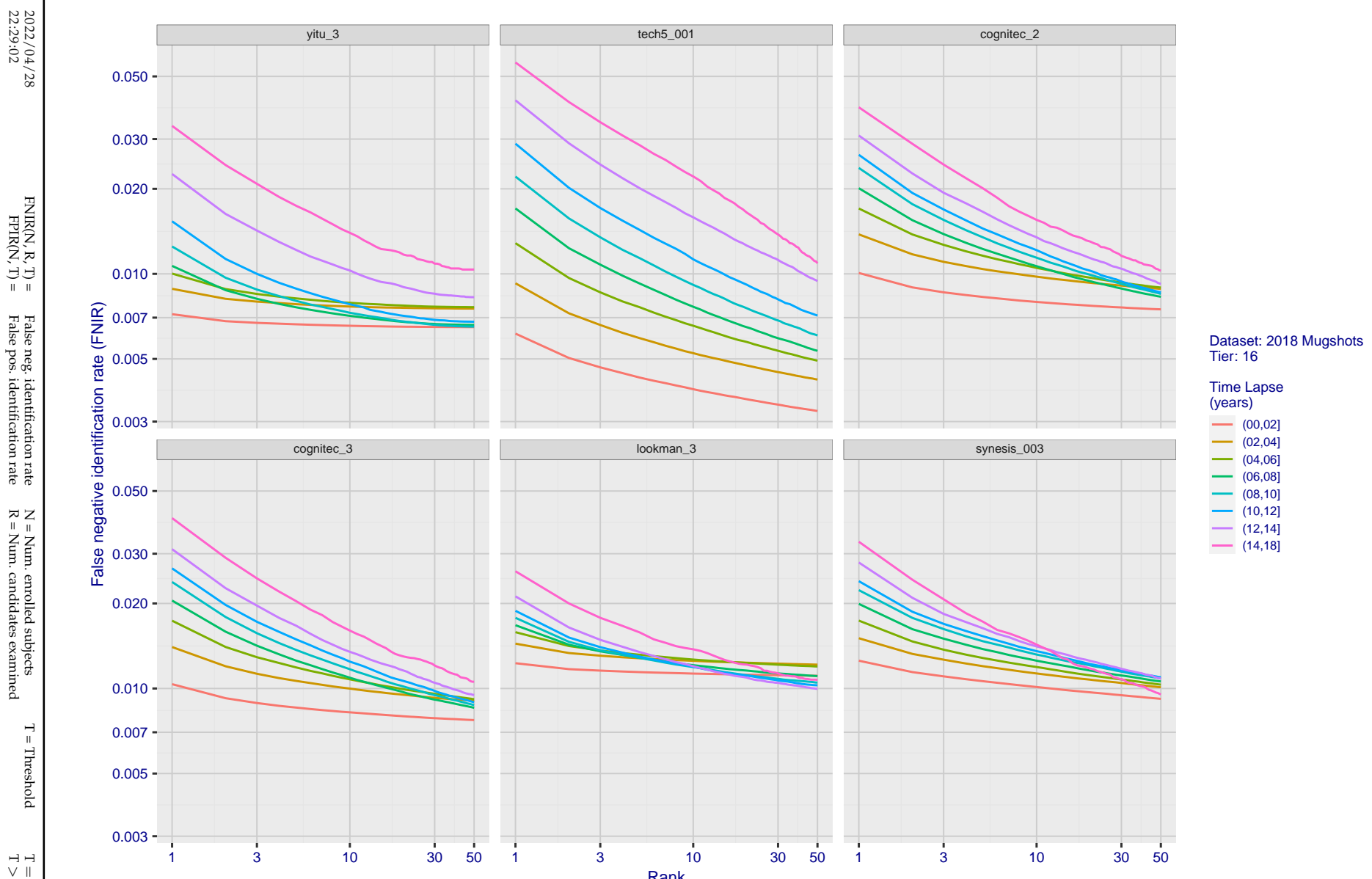


Figure 74: [FRVT-2018 Mugshot Ageing Dataset] Identification miss rates vs. rank by time-elapsed. The oldest image of each individual is enrolled. Thereafter, all more recent images are searched. Miss rates are computed over all searches noted in row 17 of Table 1 and binned by number of years between search and initial enrollment.



**Figure 75: [FRVT-2018 Mugshot Ageing Dataset] Identification miss rates vs. rank by time-elapsed.** The oldest image of each individual is enrolled. Thereafter, all more recent images are searched. Miss rates are computed over all searches noted in row 17 of Table 1 and binned by number of years between search and initial enrollment.

2022/04/28  
22:29:02FNIR(N, R, T) = False neg. identification rate  
FPIR(N, T) = False pos. identification rateN = Num. enrolled subjects  
R = Num. candidates examinedT = Threshold  
T = 0 → Investigation

T &gt; 0 → Identification

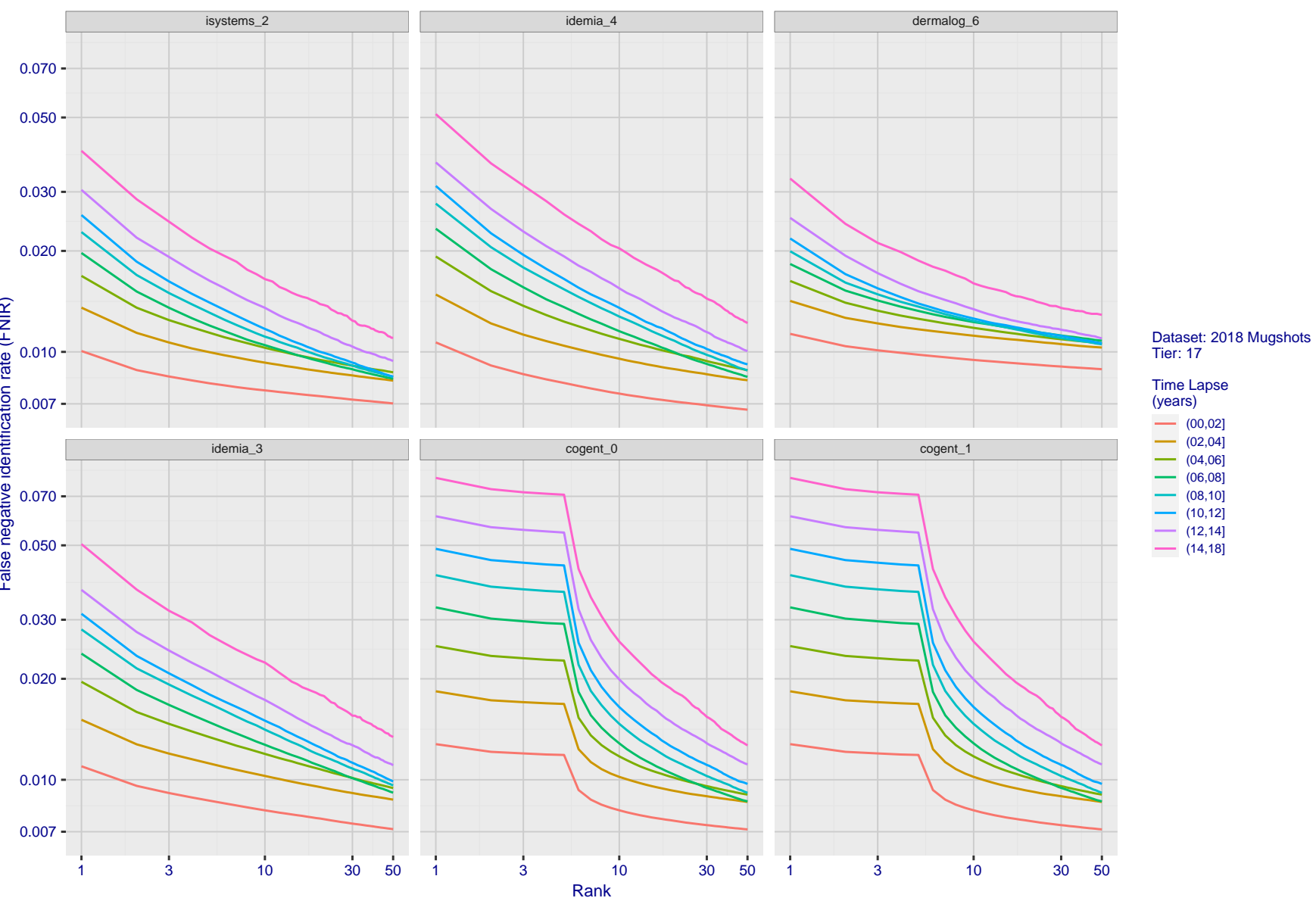


Figure 76: [FRVT-2018 Mugshot Ageing Dataset] Identification miss rates vs. rank by time elapsed. The oldest image of each individual is enrolled. Thereafter, all more recent images are searched. Miss rates are computed over all searches noted in row 17 of Table 1 and binned by number of years between search and initial enrollment.

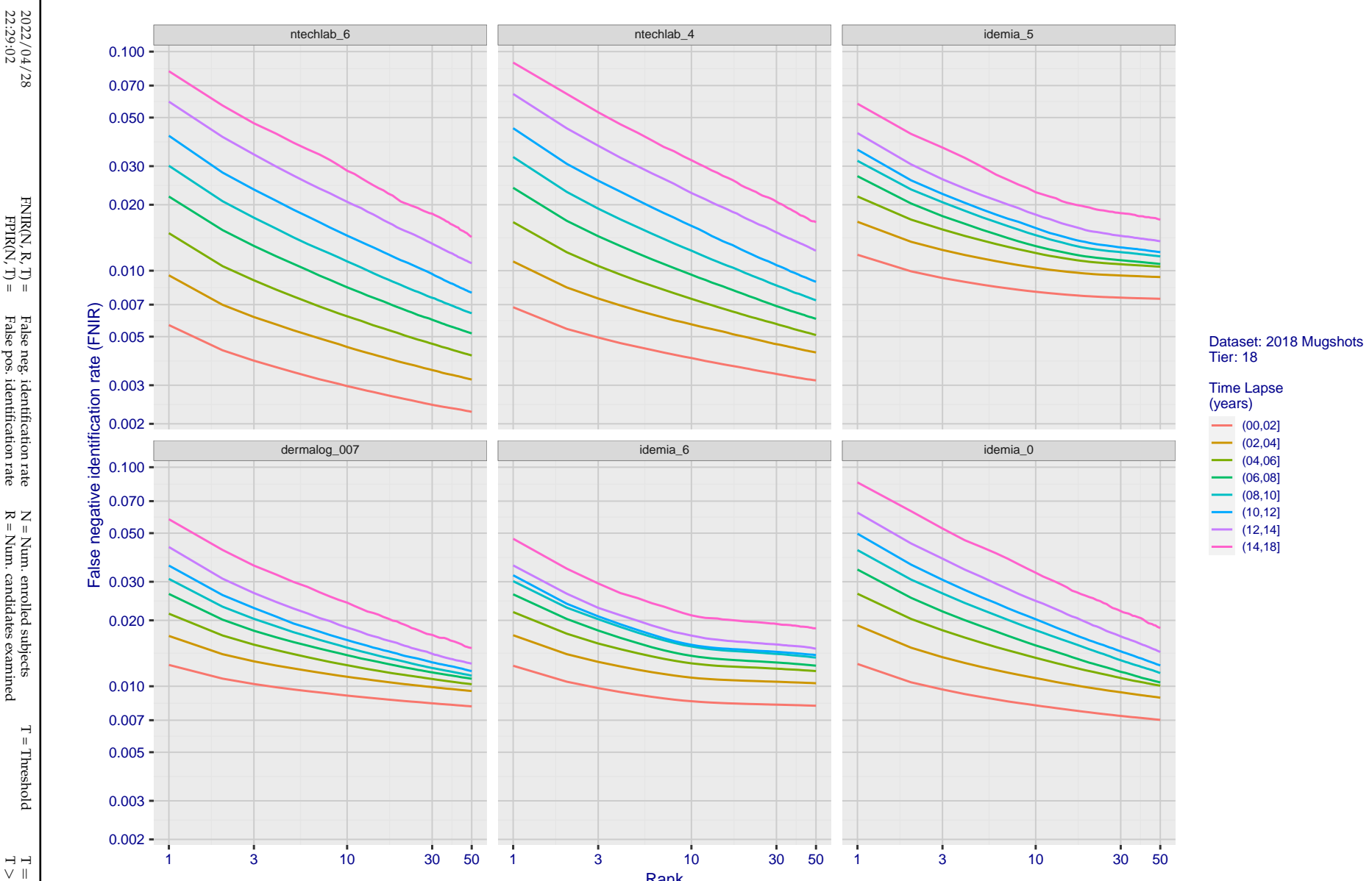


Figure 77: [FRVT-2018 Mugshot Ageing Dataset] Identification miss rates vs. rank by time-elapsed. The oldest image of each individual is enrolled. Thereafter, all more recent images are searched. Miss rates are computed over all searches noted in row 17 of Table 1 and binned by number of years between search and initial enrollment.

2022/04/28  
22:29:02FNIR(N, R, T) = False neg. identification rate  
FPFR(N, T) = False pos. identification rateN = Num. enrolled subjects  
R = Num. candidates examinedT = Threshold  
T = 0 → Investigation

T &gt; 0 → Identification

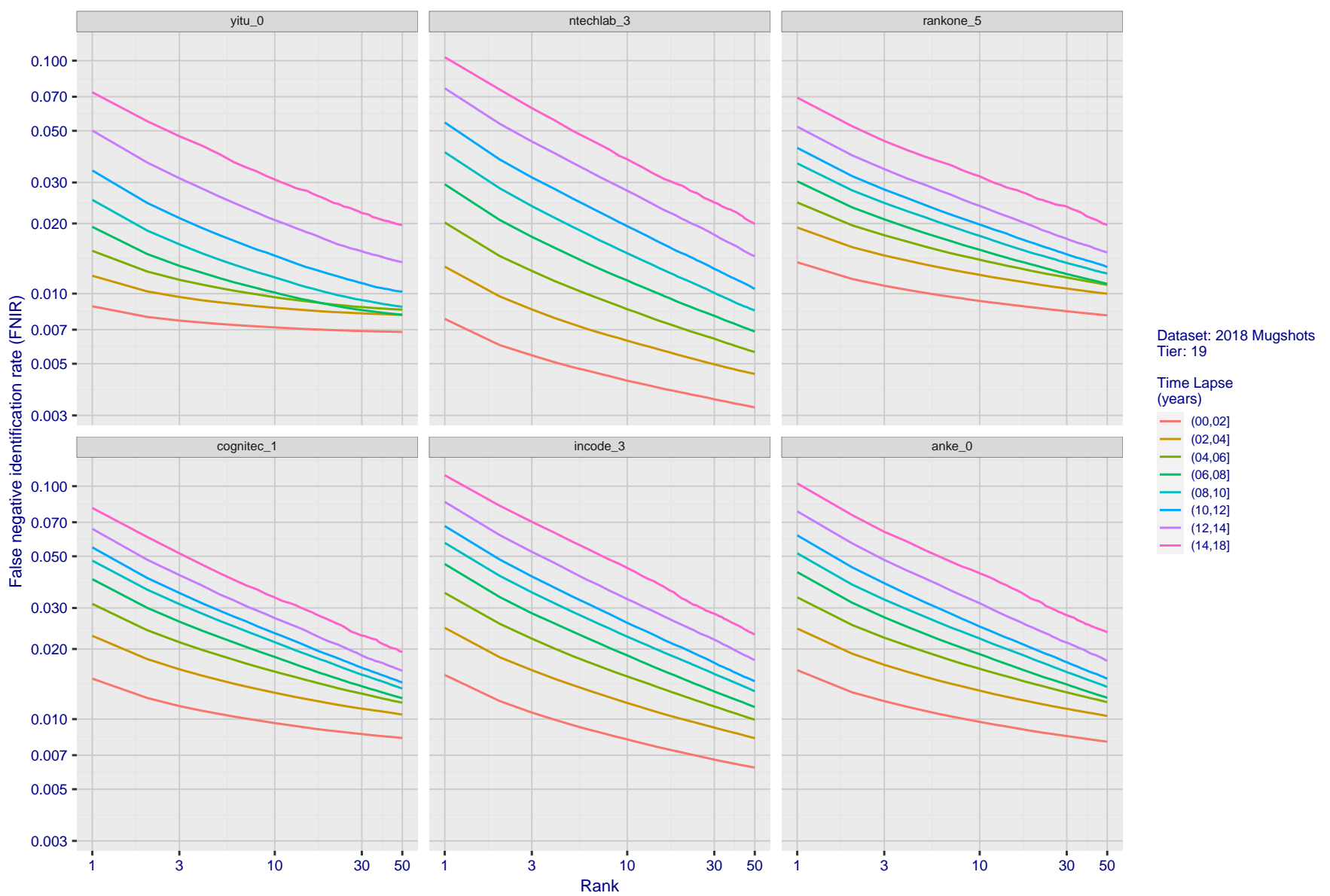


Figure 78: [FRVT-2018 Mugshot Ageing Dataset] Identification miss rates vs. rank by time-elapsed. The oldest image of each individual is enrolled. Thereafter, all more recent images are searched. Miss rates are computed over all searches noted in row 17 of Table 1 and binned by number of years between search and initial enrollment.

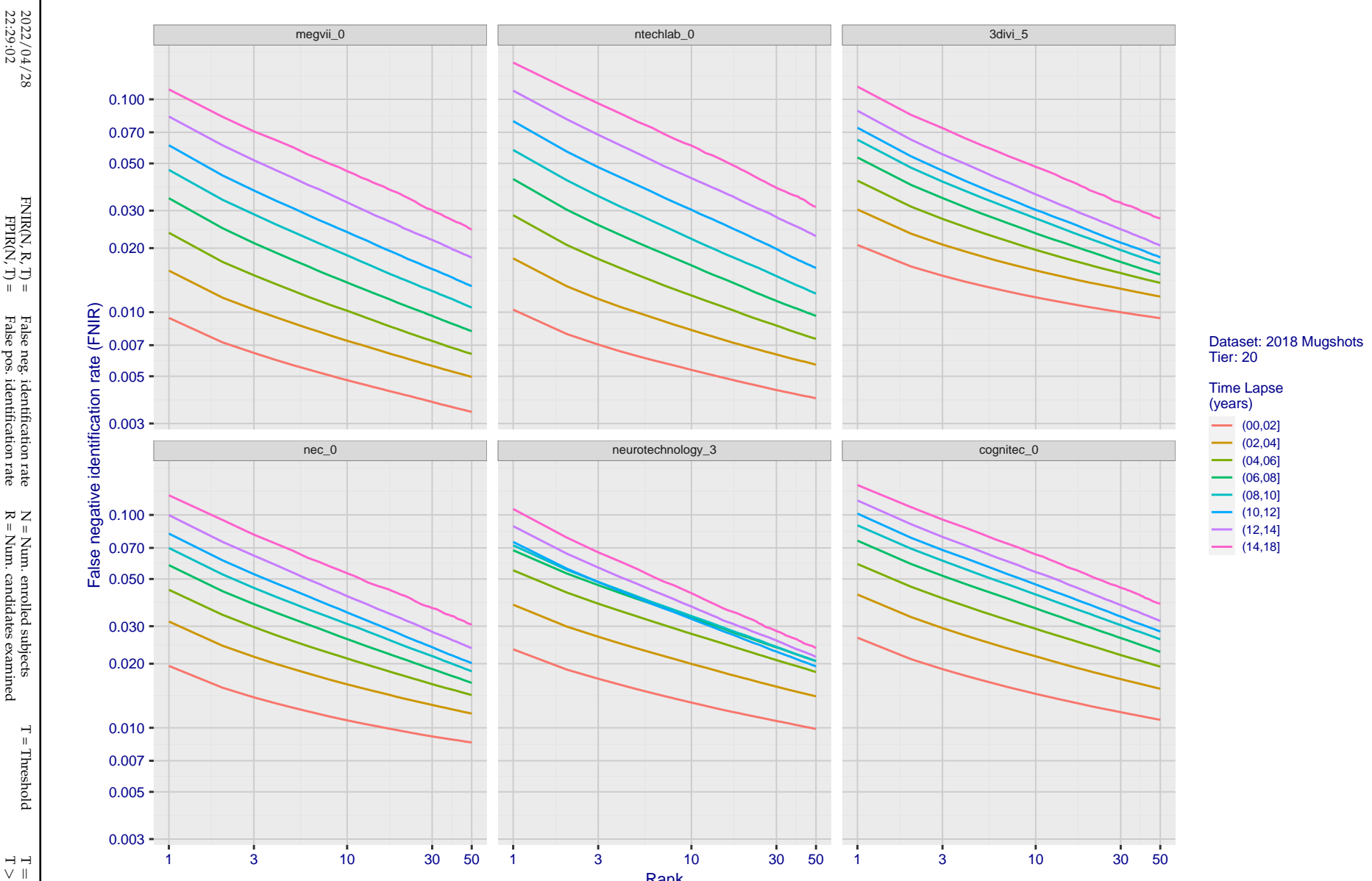


Figure 79: [FRVT-2018 Mugshot Ageing Dataset] Identification miss rates vs. rank by time elapsed. The oldest image of each individual is enrolled. Thereafter, all more recent images are searched. Miss rates are computed over all searches noted in row 17 of Table 1 and binned by number of years between search and initial enrollment.

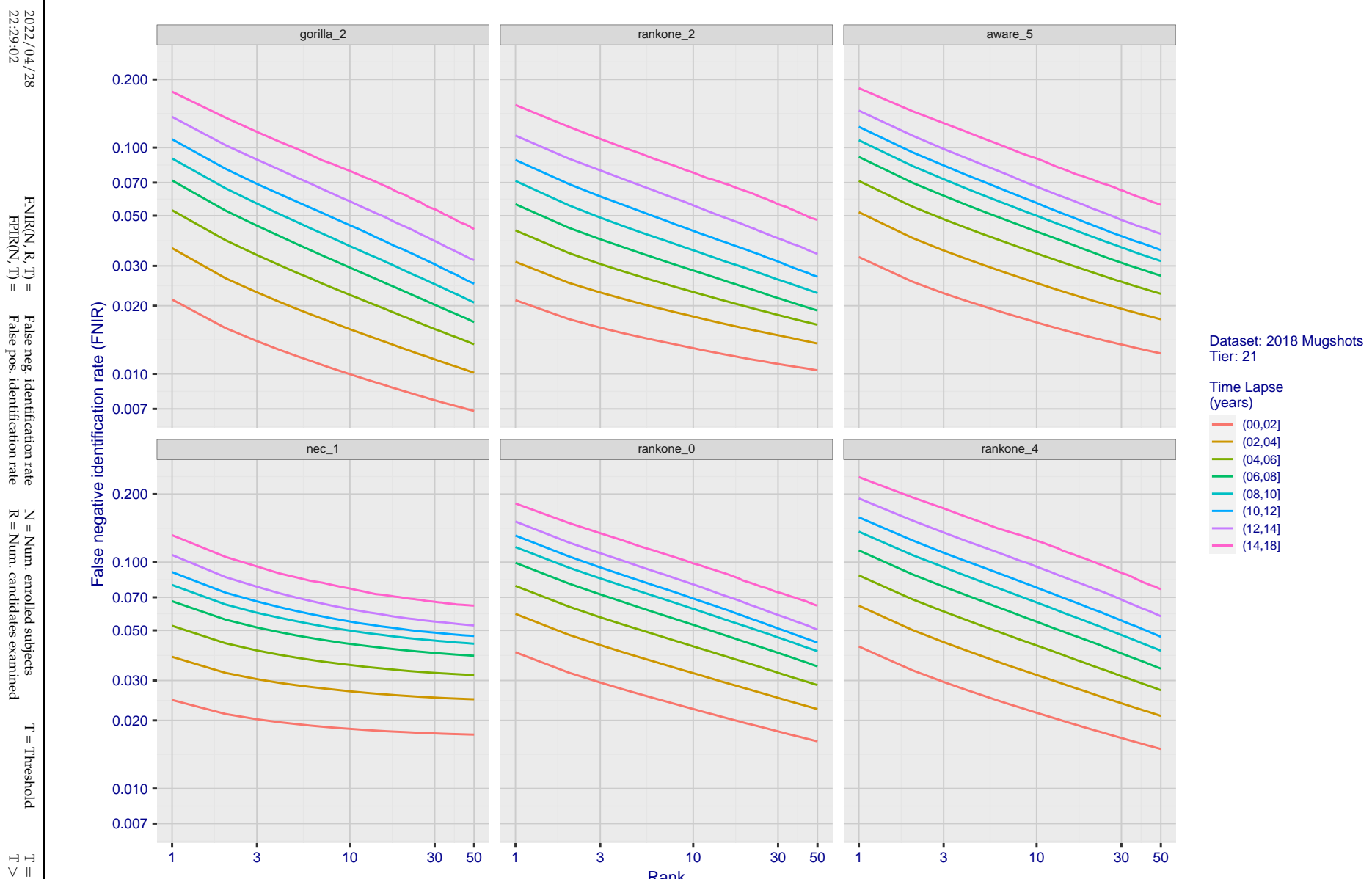


Figure 80: [FRVT-2018 Mugshot Ageing Dataset] Identification miss rates vs. rank by time-elapsed. The oldest image of each individual is enrolled. Thereafter, all more recent images are searched. Miss rates are computed over all searches noted in row 17 of Table 1 and binned by number of years between search and initial enrollment.

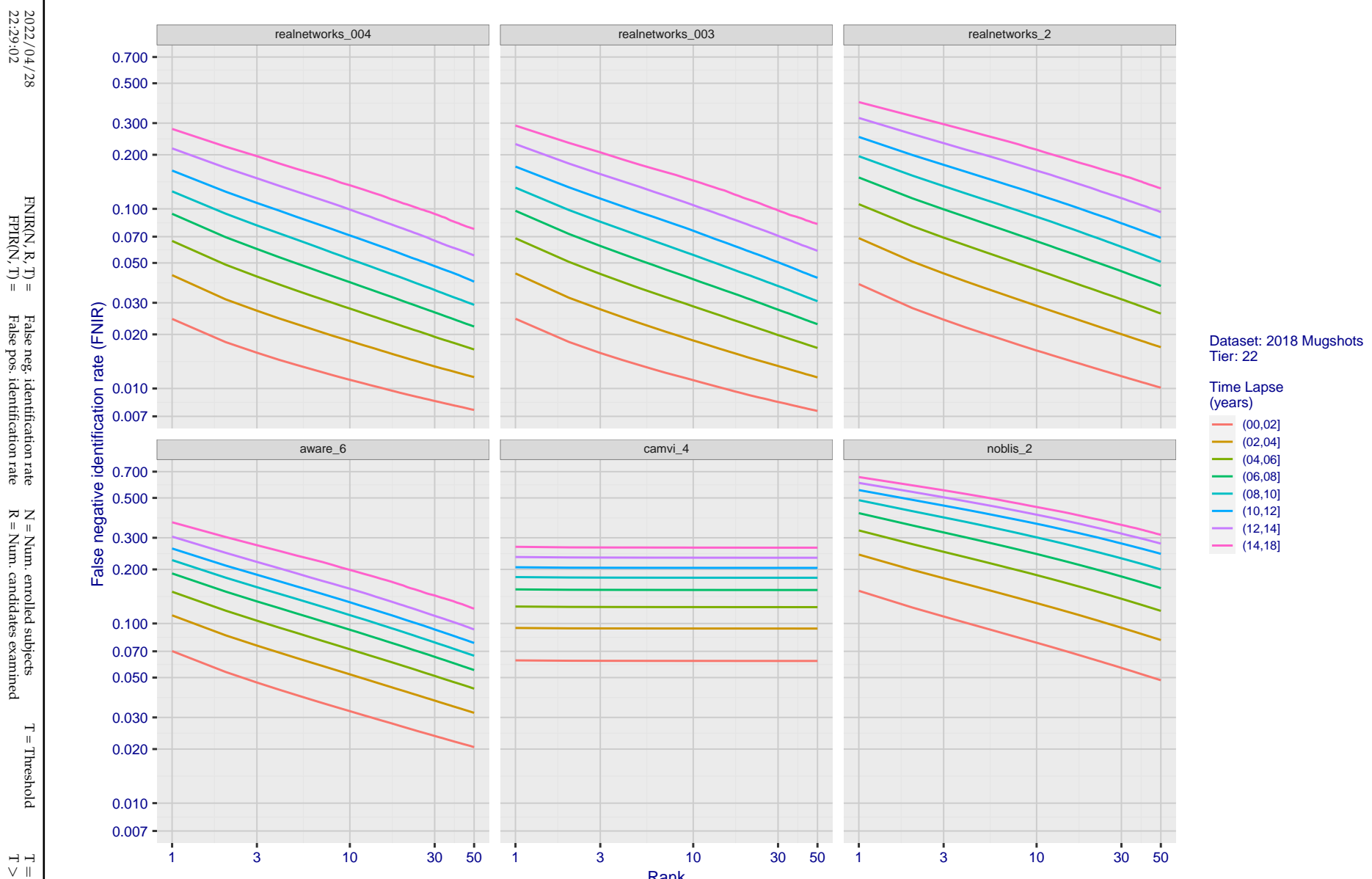


Figure 81: [FRVT-2018 Mugshot Ageing Dataset] Identification miss rates vs. rank by time-elapsed. The oldest image of each individual is enrolled. Thereafter, all more recent images are searched. Miss rates are computed over all searches noted in row 17 of Table 1 and binned by number of years between search and initial enrollment.

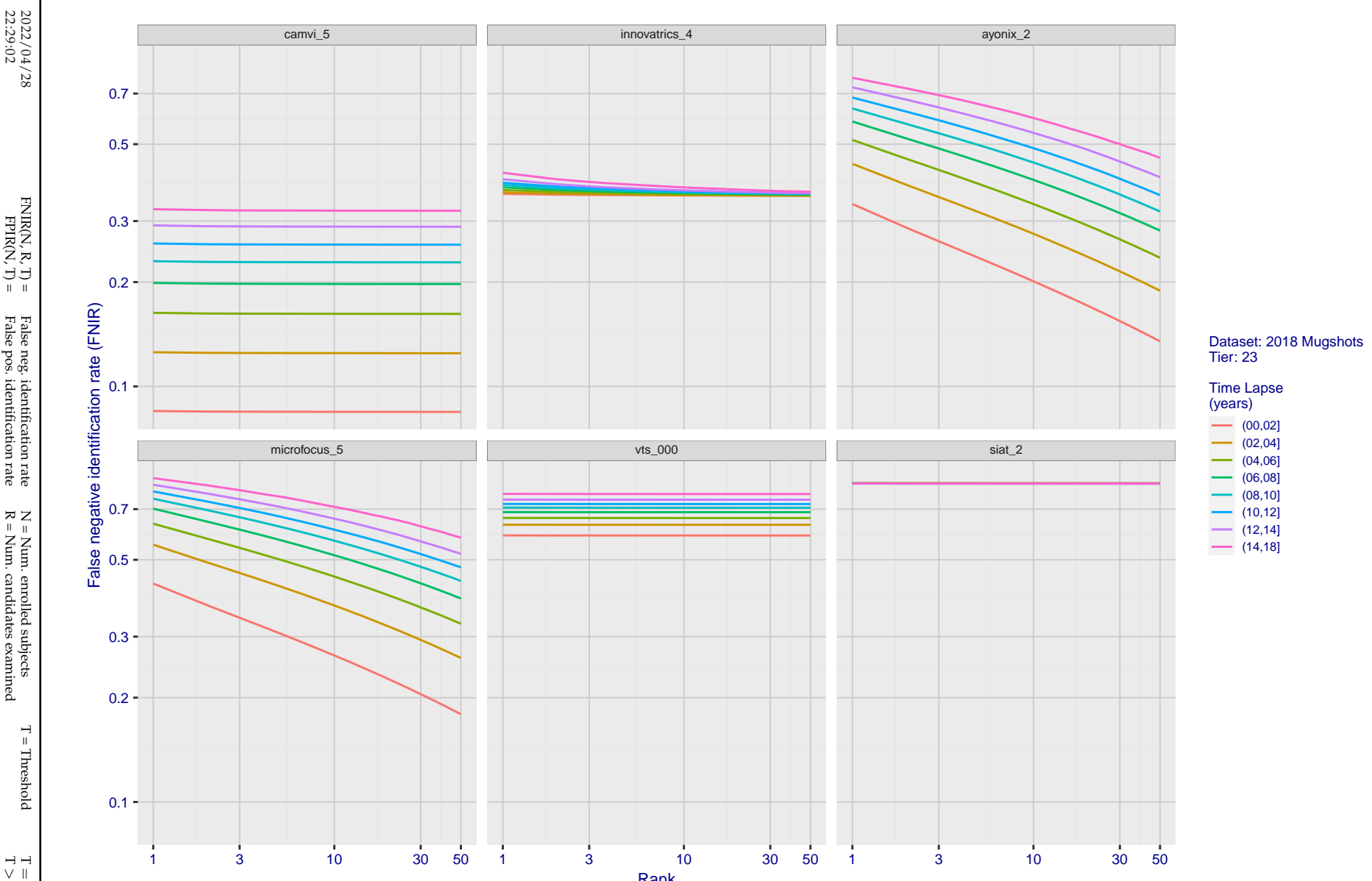


Figure 82: [FRVT-2018 Mugshot Ageing Dataset] Identification miss rates vs. rank by time-elapsed. The oldest image of each individual is enrolled. Thereafter, all more recent images are searched. Miss rates are computed over all searches noted in row 17 of Table 1 and binned by number of years between search and initial enrollment.

2022/04/28 22:29:02	$\text{FNIR}(N, R, T) =$ $\text{FPTR}(N, T) =$	False neg. identification rate False pos. identification rate	$N =$ Num. enrolled subjects $R =$ Num. candidates examined	$T =$ Threshold $T > 0 \rightarrow$ Identification	$T = 0 \rightarrow$ Investigation
------------------------	---	--	--	---	-----------------------------------

2022/04/28  
22:29:02FNIR(N, R, T) = False neg. identification rate  
FPIR(N, T) = False pos. identification rateN = Num. enrolled subjects  
R = Num. candidates examined

T = Threshold

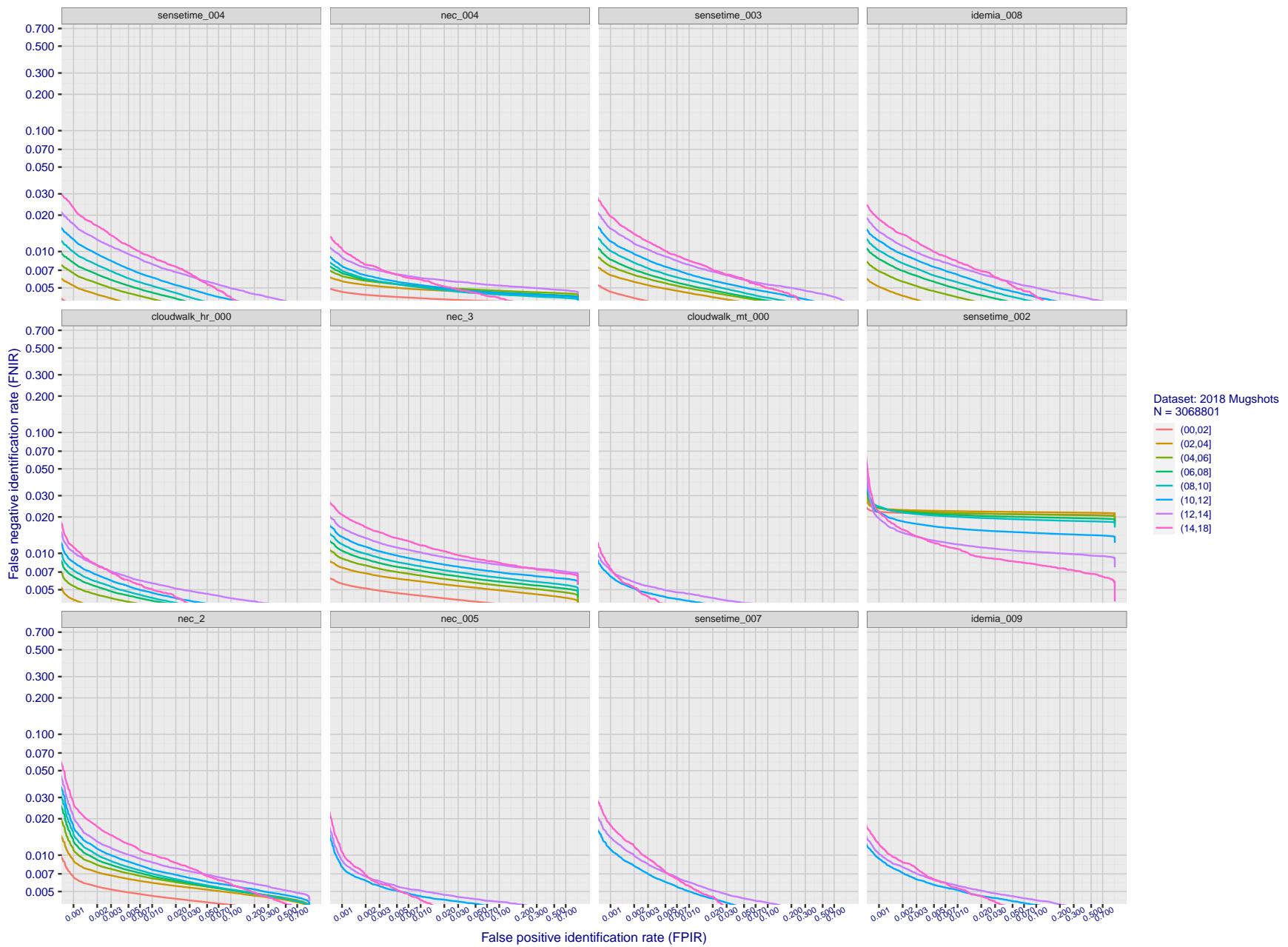
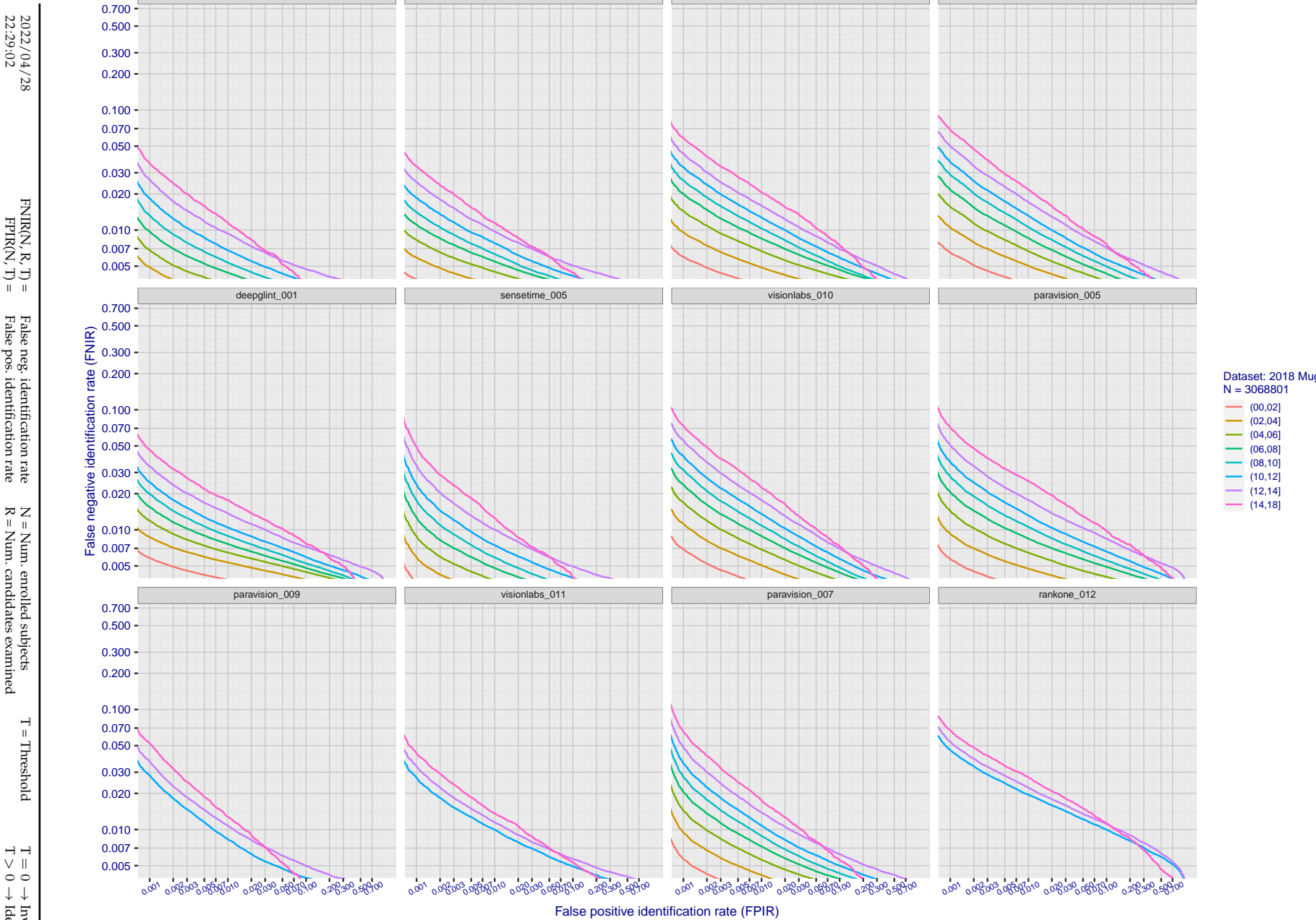
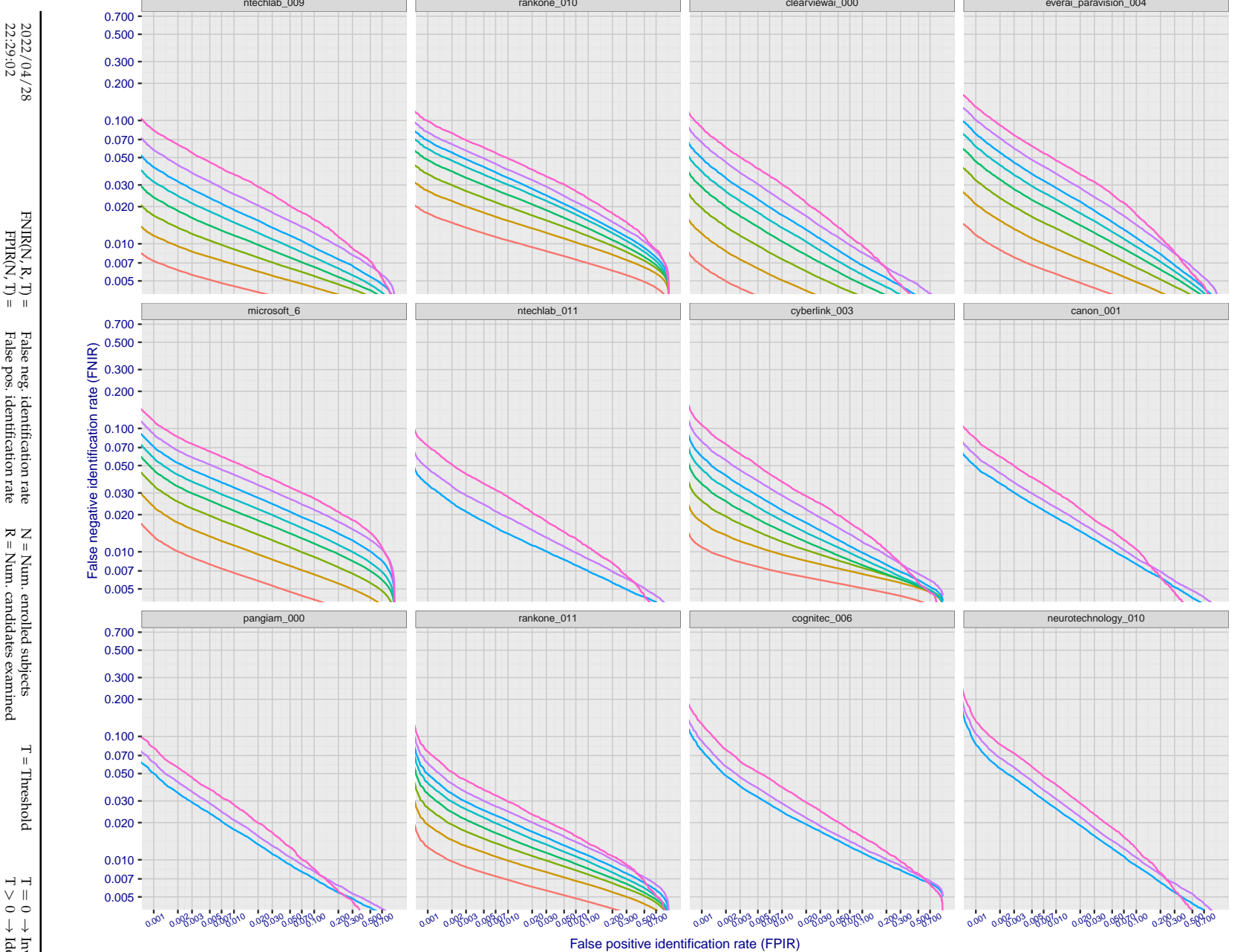
T = 0 → Investigation  
T > 0 → Identification

Figure 83: [FRVT-2018 Mugshot Ageing Dataset] Identification miss rates vs. FPIR by time elapsed. The oldest image of each individual is enrolled. Thereafter, all more recent images are searched. Miss rates are computed over all searches noted in row 17 of Table 1 and binned by number of years between search and initial enrollment. FPIR is computed from the same FRVT 2018 non-mates noted in row 3 of Table 1 with N = 3 000 000.



**Figure 84: [FRVT-2018 Mugshot Ageing Dataset] Identification miss rates vs. FPIR by time-elapsed.** The oldest image of each individual is enrolled. Thereafter, all more recent images are searched. Miss rates are computed over all searches noted in row 17 of Table 1 and binned by number of years between search and initial enrollment. FPIR is computed from the same FRVT 2018 non-mates noted in row 3 of Table 1 with  $N = 3\,000\,000$ .



**Figure 85: [FRVT-2018 Mugshot Ageing Dataset] Identification miss rates vs. FPIR by time-elapsed.** The oldest image of each individual is enrolled. Thereafter, all more recent images are searched. Miss rates are computed over all searches noted in row 17 of Table 1 and binned by number of years between search and initial enrollment. FPIR is computed from the same FRVT 2018 non-mates noted in row 3 of Table 1 with  $N = 3\,000\,000$ .

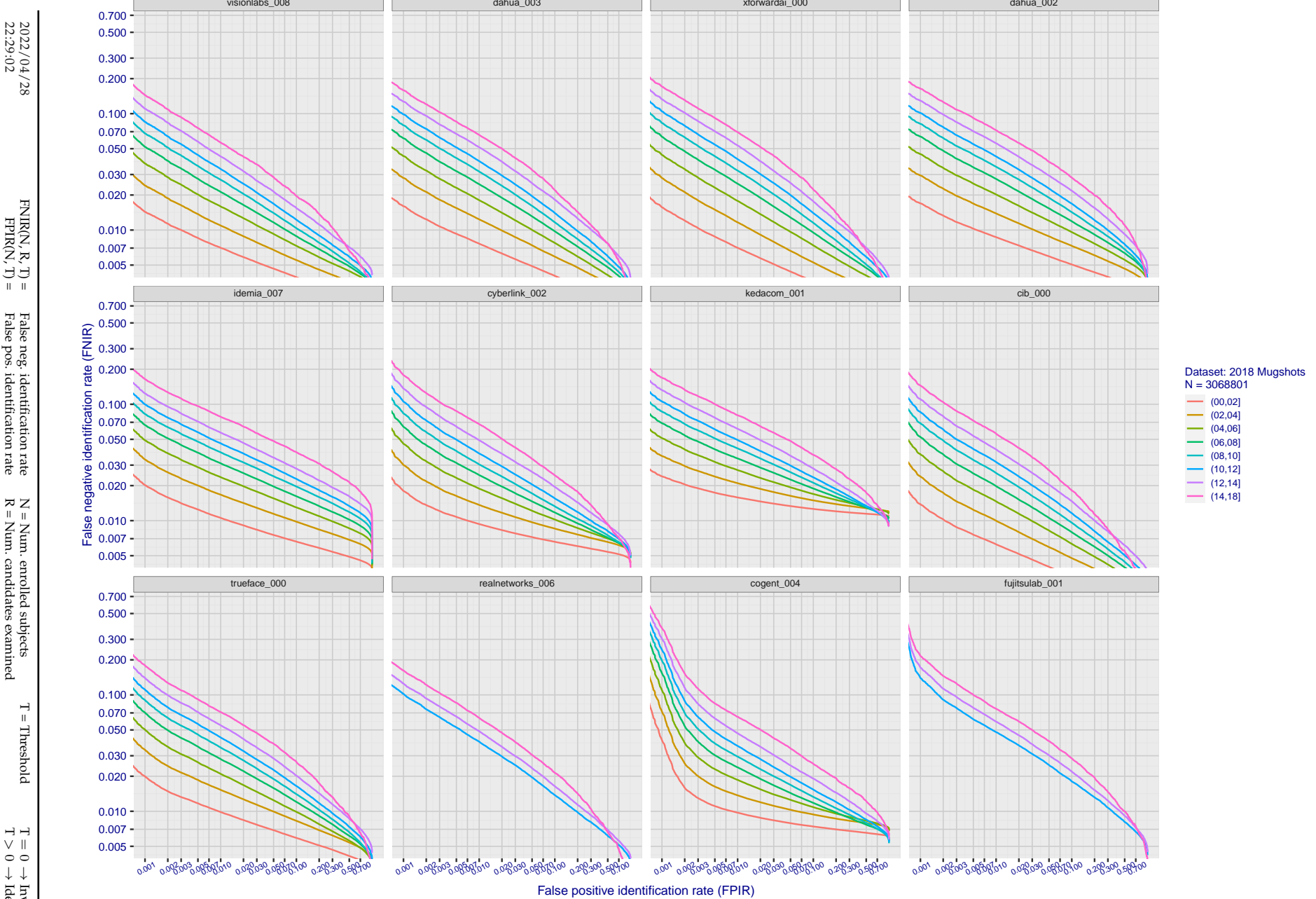


**Figure 86: [FRVT-2018 Mugshot Ageing Dataset] Identification miss rates vs. FPIR by time-elapsed.** The oldest image of each individual is enrolled. Thereafter, all more recent images are searched. Miss rates are computed over all searches noted in row 17 of Table 1 and binned by number of years between search and initial enrollment. FPIR is computed from the same FRVT 2018 non-mates noted in row 3 of Table 1 with  $N = 3\,000\,000$ .

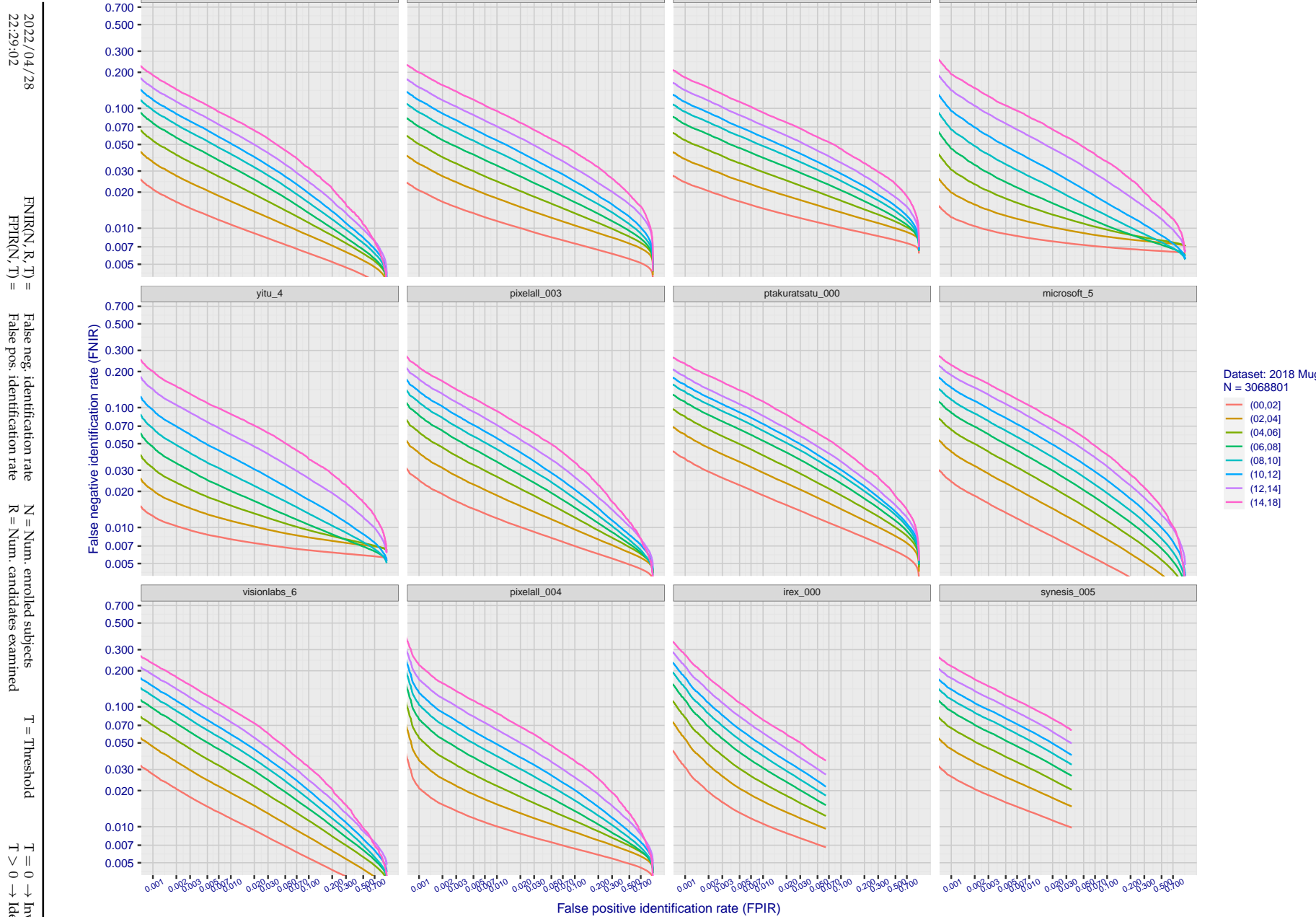


**Figure 87: [FRVT-2018 Mugshot Ageing Dataset] Identification miss rates vs. FPIR by time-elapsed.** The oldest image of each individual is enrolled. Thereafter, all more recent images are searched. Miss rates are computed over all searches noted in row 17 of Table 1 and binned by number of years between search and initial enrollment. FPIR is computed from the same FRVT 2018 non-mates noted in row 3 of Table 1 with  $N = 3\,000\,000$ .

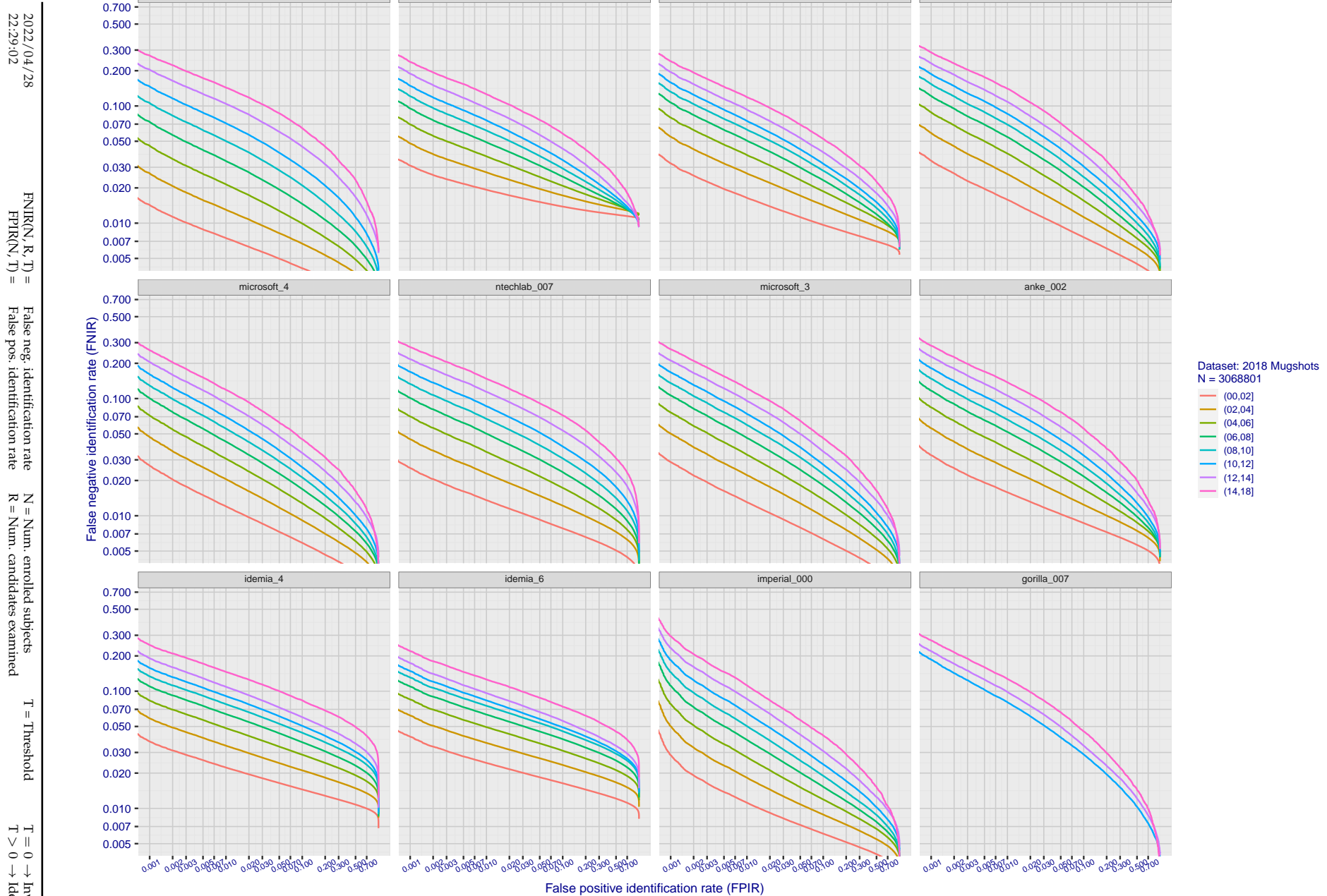


**Figure 88: [FRVT-2018 Mugshot Ageing Dataset] Identification miss rates vs. FPIR by time elapsed.** The oldest image of each individual is enrolled. Thereafter, all more recent images are searched. Miss rates are computed over all searches noted in row 17 of Table 1 and binned by number of years between search and initial enrollment. FPIR is computed from the same FRVT 2018 non-mates noted in row 3 of Table 1 with  $N = 3000000$ .

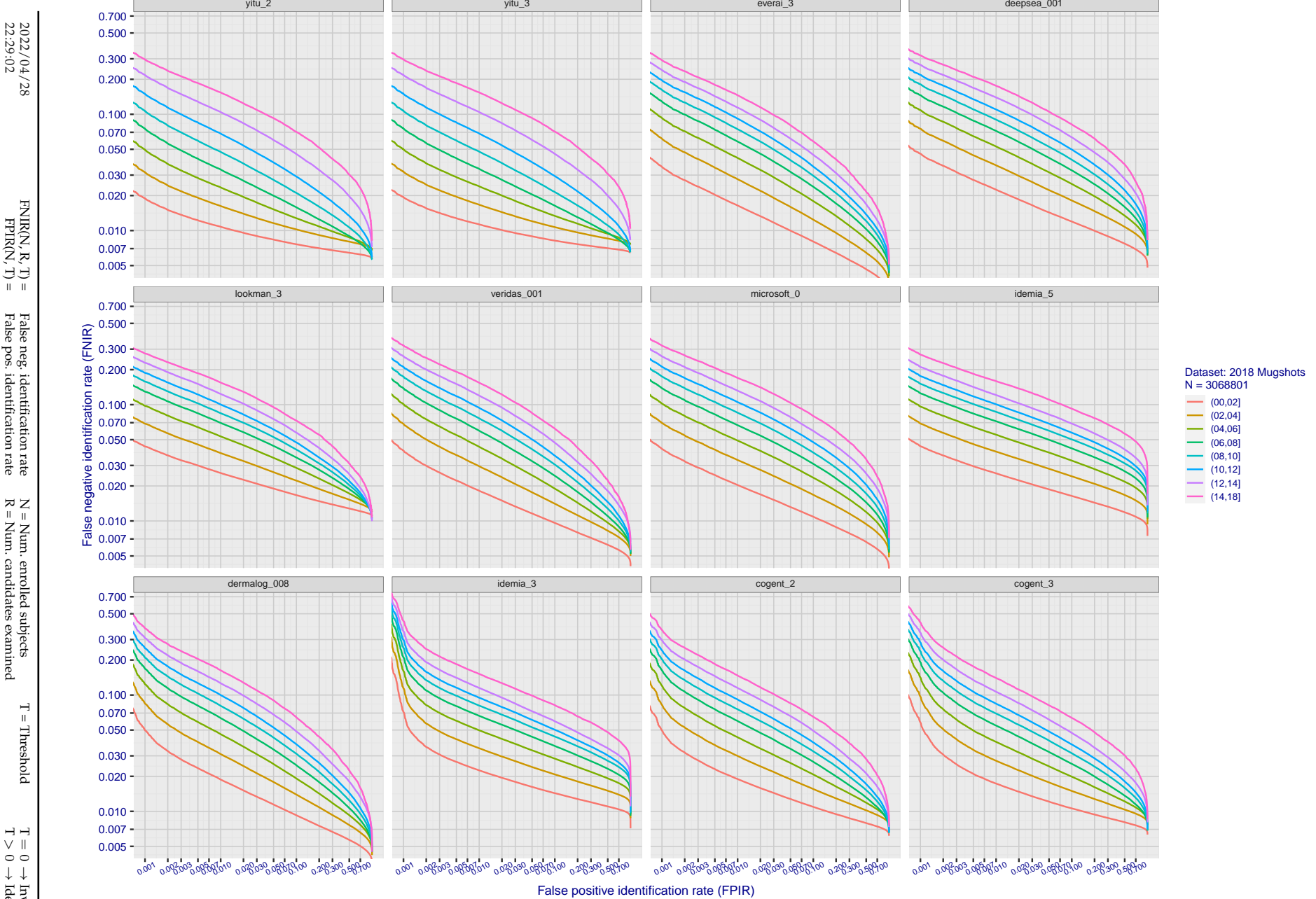


**Figure 89: [FRVT-2018 Mugshot Ageing Dataset] Identification miss rates vs. FPIR by time elapsed.** The oldest image of each individual is enrolled. Thereafter, all more recent images are searched. Miss rates are computed over all searches noted in row 17 of Table 1 and binned by number of years between search and initial enrollment. FPIR is computed from the same FRVT 2018 non-mates noted in row 3 of Table 1 with  $N = 3\,000\,000$ .

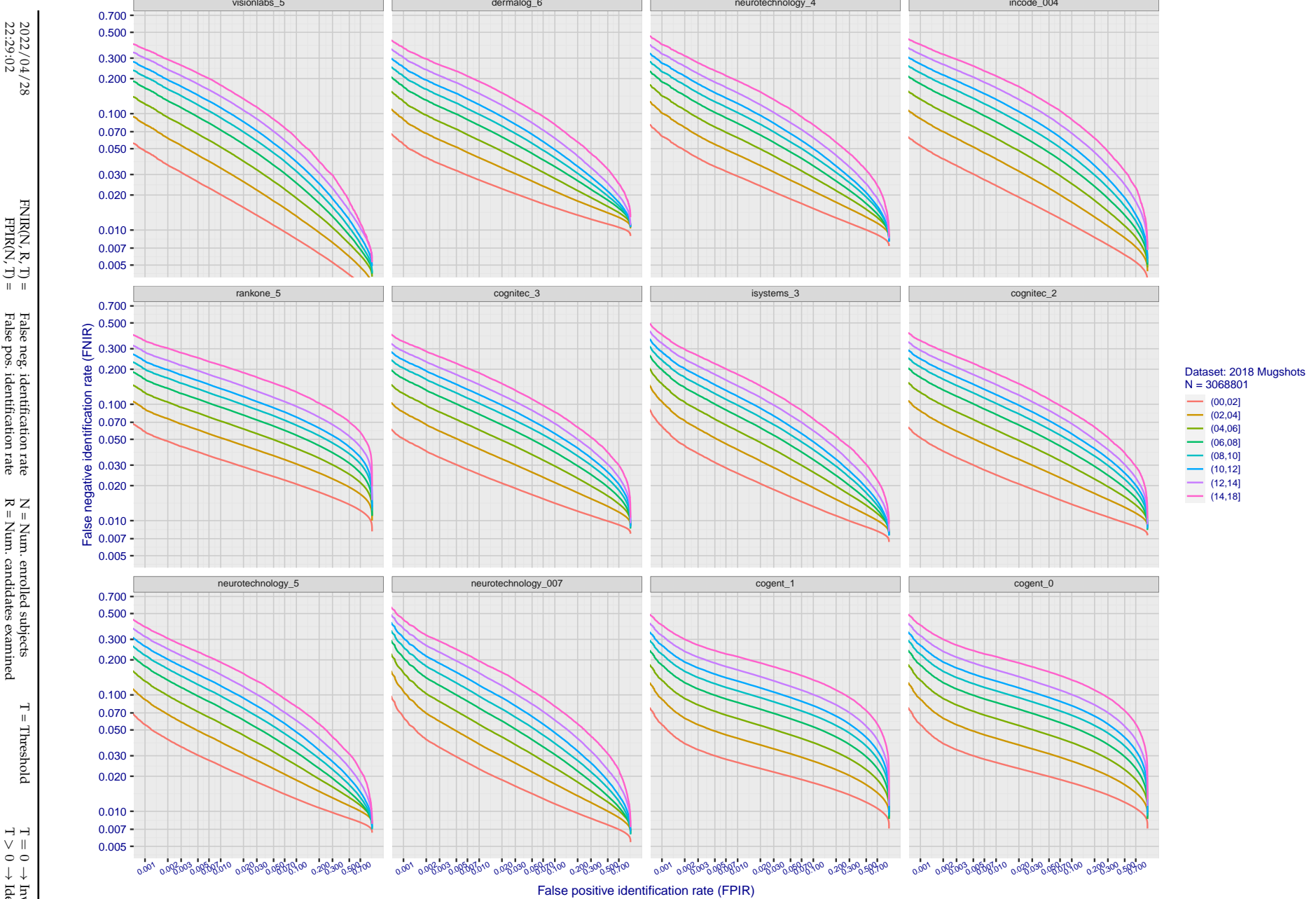


**Figure 90: [FRVT-2018 Mugshot Ageing Dataset] Identification miss rates vs. FPIR by time-elapsed.** The oldest image of each individual is enrolled. Thereafter, all more recent images are searched. Miss rates are computed over all searches noted in row 17 of Table 1 and binned by number of years between search and initial enrollment. FPIR is computed from the same FRVT 2018 non-mates noted in row 3 of Table 1 with  $N = 3000\,000$ .

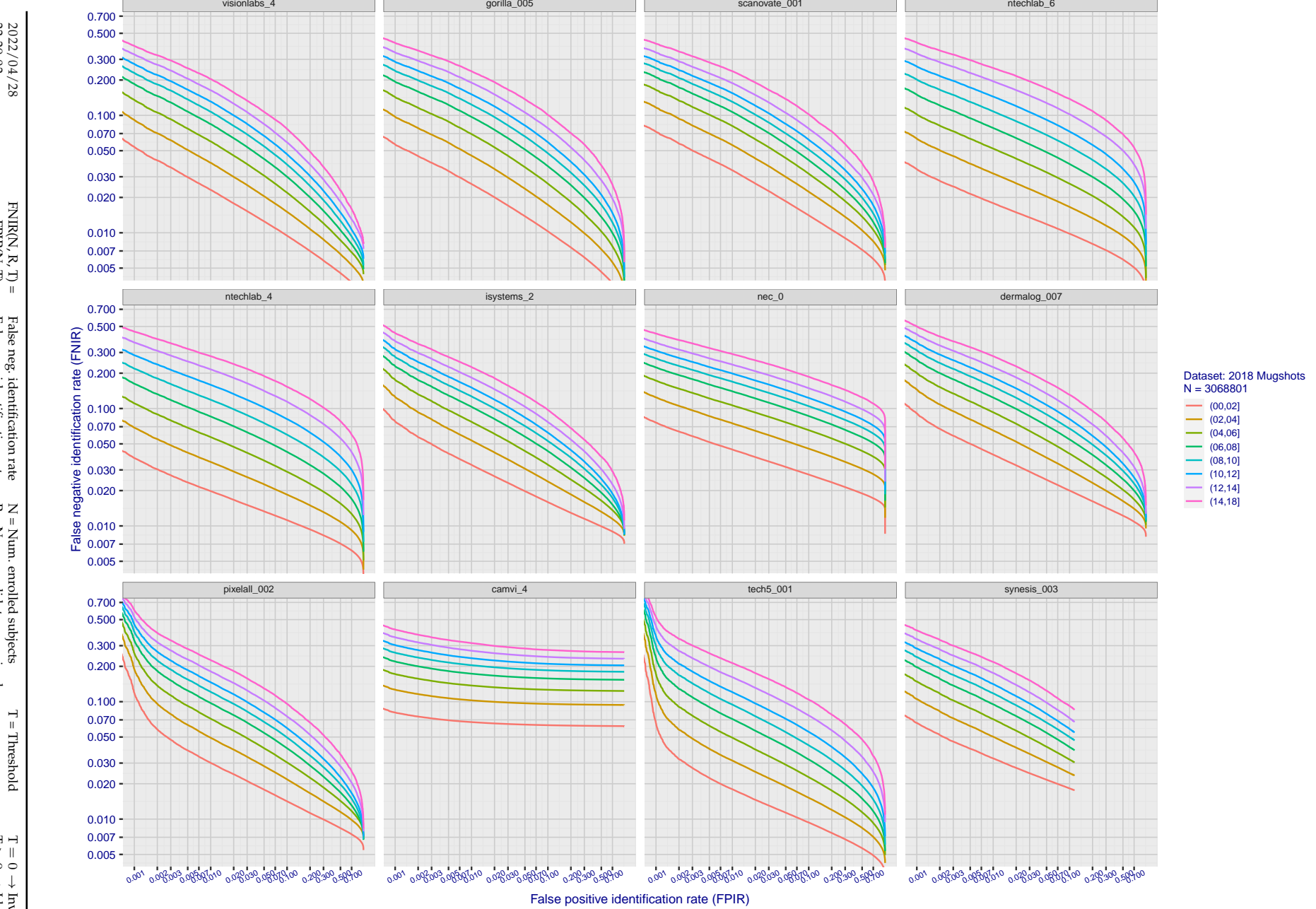


**Figure 91: [FRVT-2018 Mugshot Ageing Dataset] Identification miss rates vs. FPIR by time-elapsed.** The oldest image of each individual is enrolled. Thereafter, all more recent images are searched. Miss rates are computed over all searches noted in row 17 of Table 1 and binned by number of years between search and initial enrollment. FPIR is computed from the same FRVT 2018 non-mates noted in row 3 of Table 1 with  $N = 3\,000\,000$ .

2022/04/28  
22:29:02  
  
 $\text{FNIR}(N, R, T)$  = False neg. identification rate  
 $\text{FPIR}(N, T)$  = False pos. identification rate  
  
 $N$  = Num. enrolled subjects  
 $R$  = Num. candidates examined  
 $T$  = Threshold  
 $T = 0 \rightarrow$  Investigation  
 $T > 0 \rightarrow$  Identification

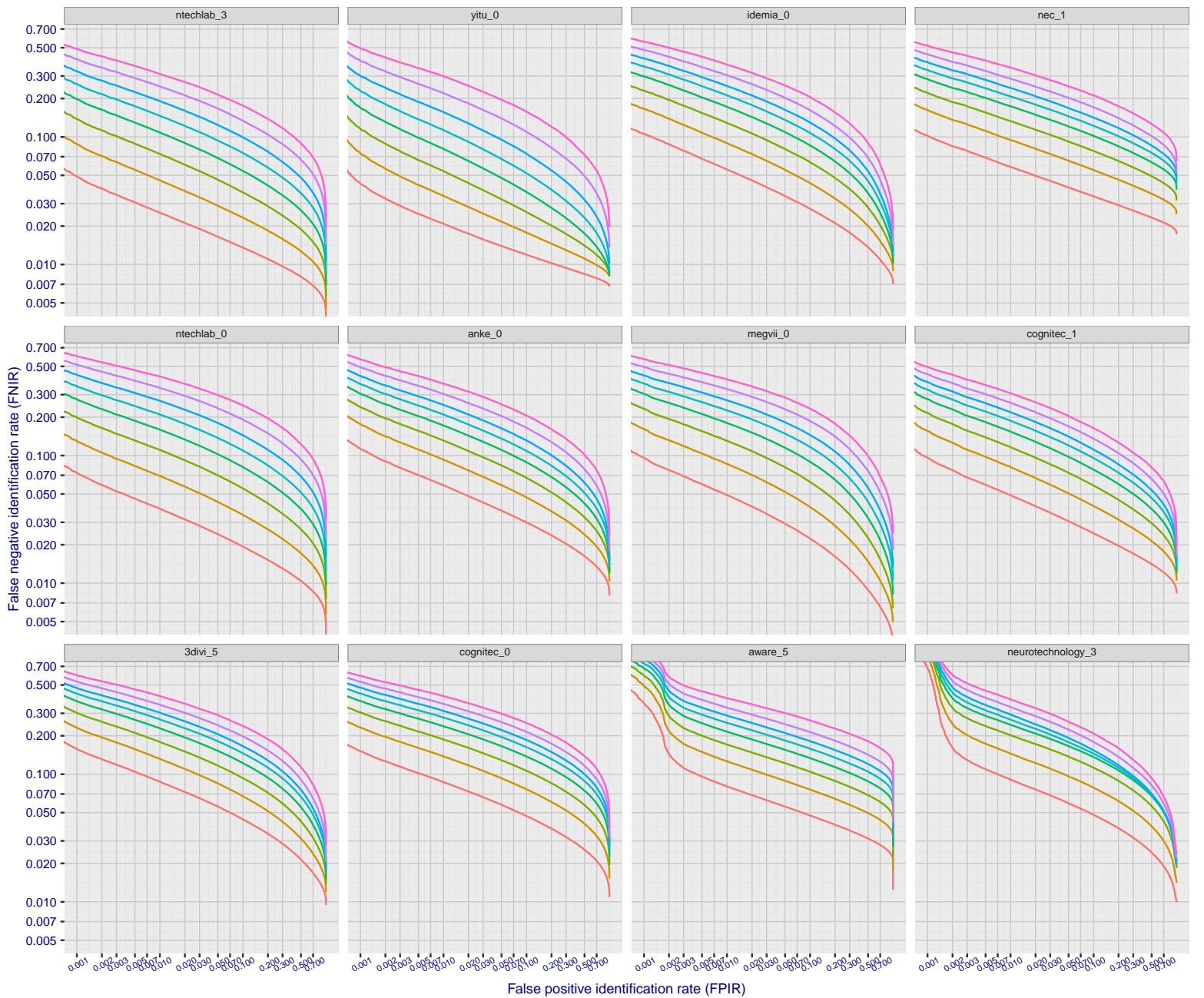


**Figure 92: [FRVT-2018 Mugshot Ageing Dataset] Identification miss rates vs. FPIR by time elapsed.** The oldest image of each individual is enrolled. Thereafter, all more recent images are searched. Miss rates are computed over all searches noted in row 17 of Table 1 and binned by number of years between search and initial enrollment. FPIR is computed from the same FRVT 2018 non-mates noted in row 3 of Table 1 with  $N = 3000\,000$ .

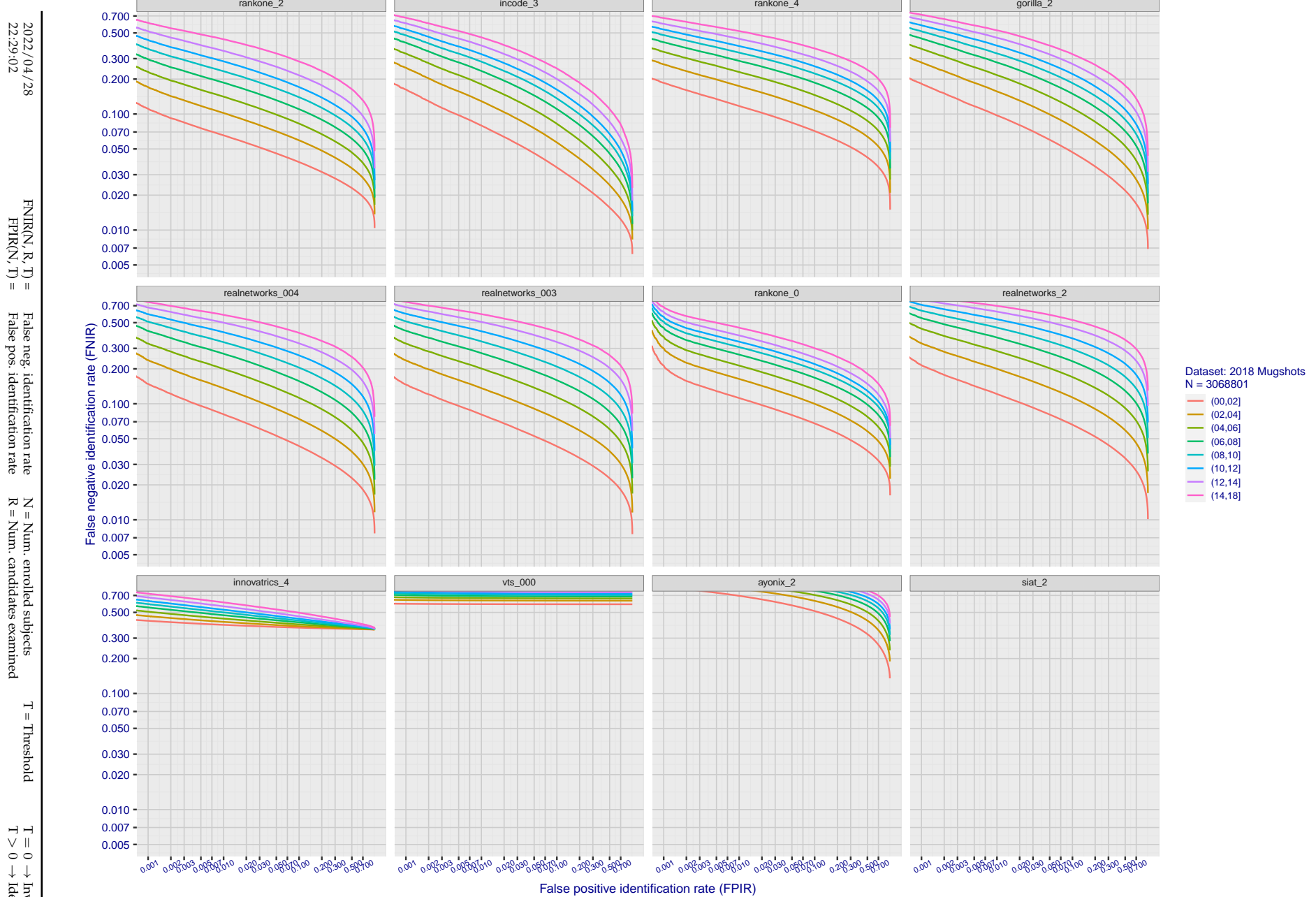


**Figure 93: [FRVT-2018 Mugshot Ageing Dataset] Identification miss rates vs. FPIR by time elapsed.** The oldest image of each individual is enrolled. Thereafter, all more recent images are searched. Miss rates are computed over all searches noted in row 17 of Table 1 and binned by number of years between search and initial enrollment. FPIR is computed from the same FRVT 2018 non-mates noted in row 3 of Table 1 with  $N = 3\,000\,000$ .

2022/04/28  
22:29:02  
  
 $FNIR(N, R, T)$  = False neg. identification rate  
 $FPIR(N, T)$  = False pos. identification rate  
 $N$  = Num. enrolled subjects  
 $R$  = Num. candidates examined  
 $T$  = Threshold  
 $T = 0 \rightarrow$  Investigation  
 $T > 0 \rightarrow$  Identification

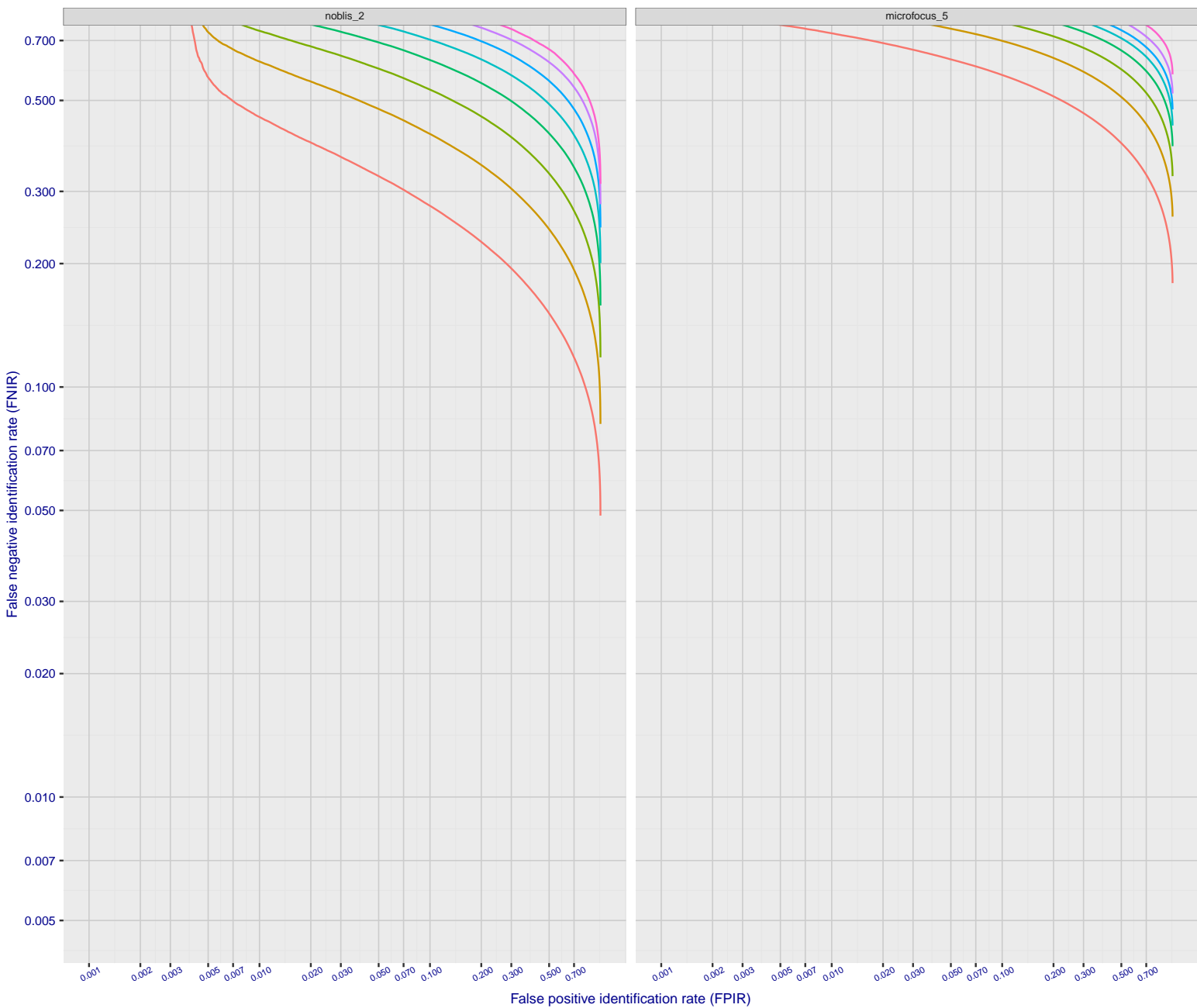


**Figure 94: [FRVT-2018 Mugshot Ageing Dataset] Identification miss rates vs. FPIR by time elapsed.** The oldest image of each individual is enrolled. Thereafter, all more recent images are searched. Miss rates are computed over all searches noted in row 17 of Table 1 and binned by number of years between search and initial enrollment. FPIR is computed from the same FRVT 2018 non-mates noted in row 3 of Table 1 with  $N = 3\,000\,000$ .

---

2022/04/28  
22:29:02      FNIR(N, R, T) = False neg. identification rate  
                  FPIR(N, T) = False pos. identification rate  
N = Num. enrolled subjects  
R = Num. candidates examined  
T = Threshold  
T = 0 → Investigation  
T > 0 → Identification

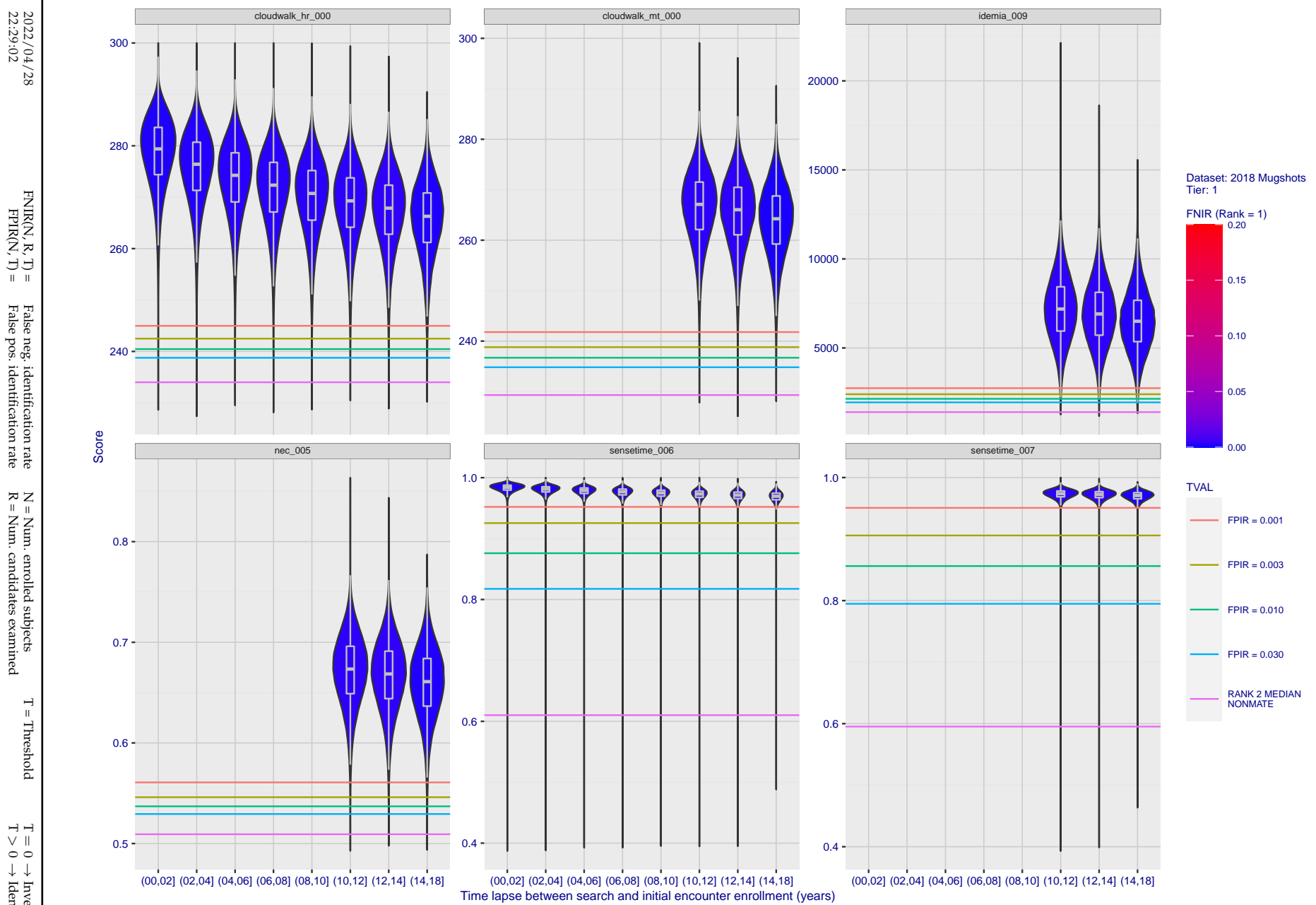


Figure 95: [FRVT-2018 Mugshot Ageing Dataset] Native mate scores vs. time-elapsed. The oldest image of each individual is enrolled. Thereafter, all more recent images are searched. Mated score distributions are computed over all searches noted in row 17 of Table 1 binned by number of years between search and initial enrollment.

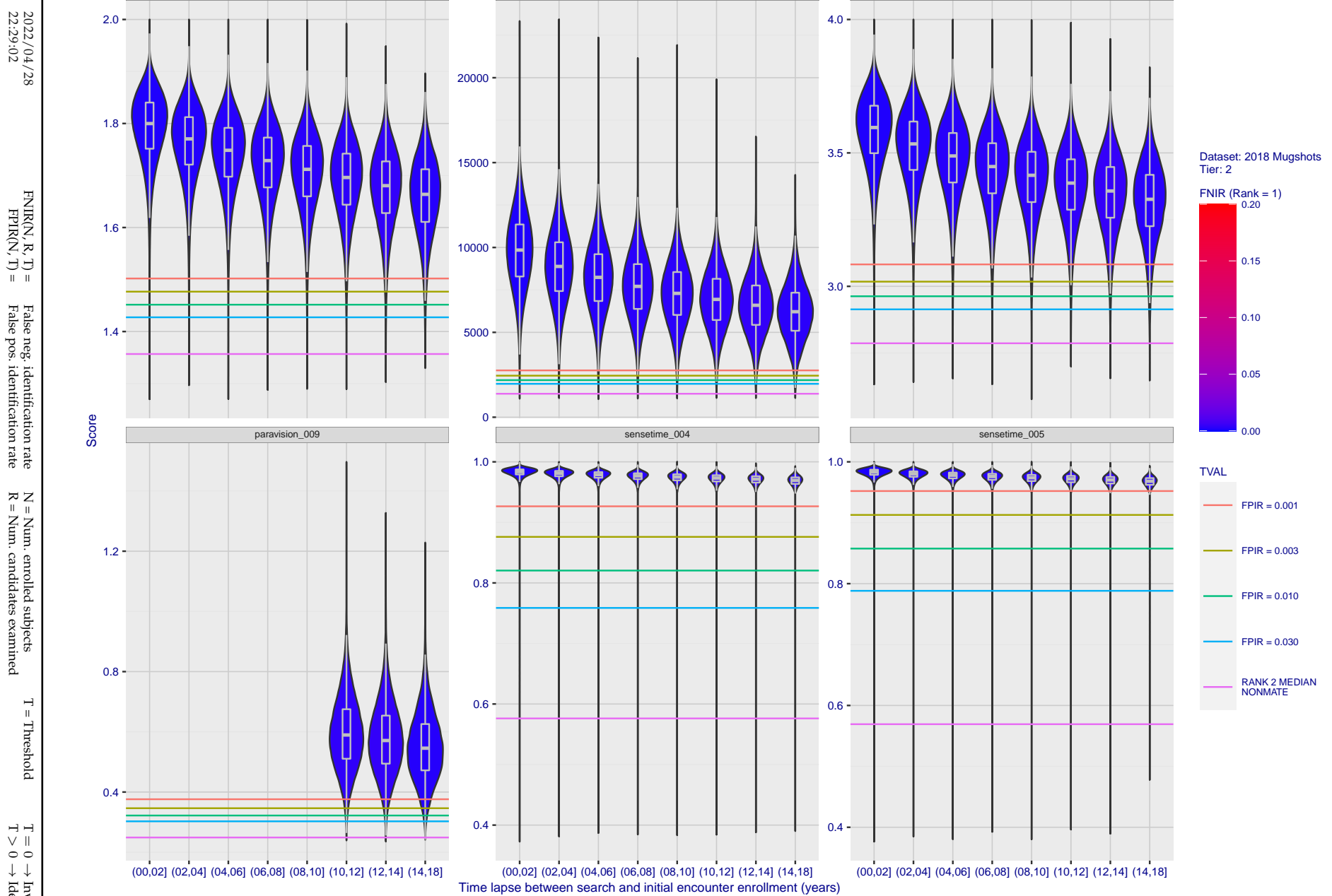


Figure 96: [FRVT-2018 Mugshot Ageing Dataset] Native mate scores vs. time-elapsed. The oldest image of each individual is enrolled. Thereafter, all more recent images are searched. Mated score distributions are computed over all searches noted in row 17 of Table 1 binned by number of years between search and initial enrollment.

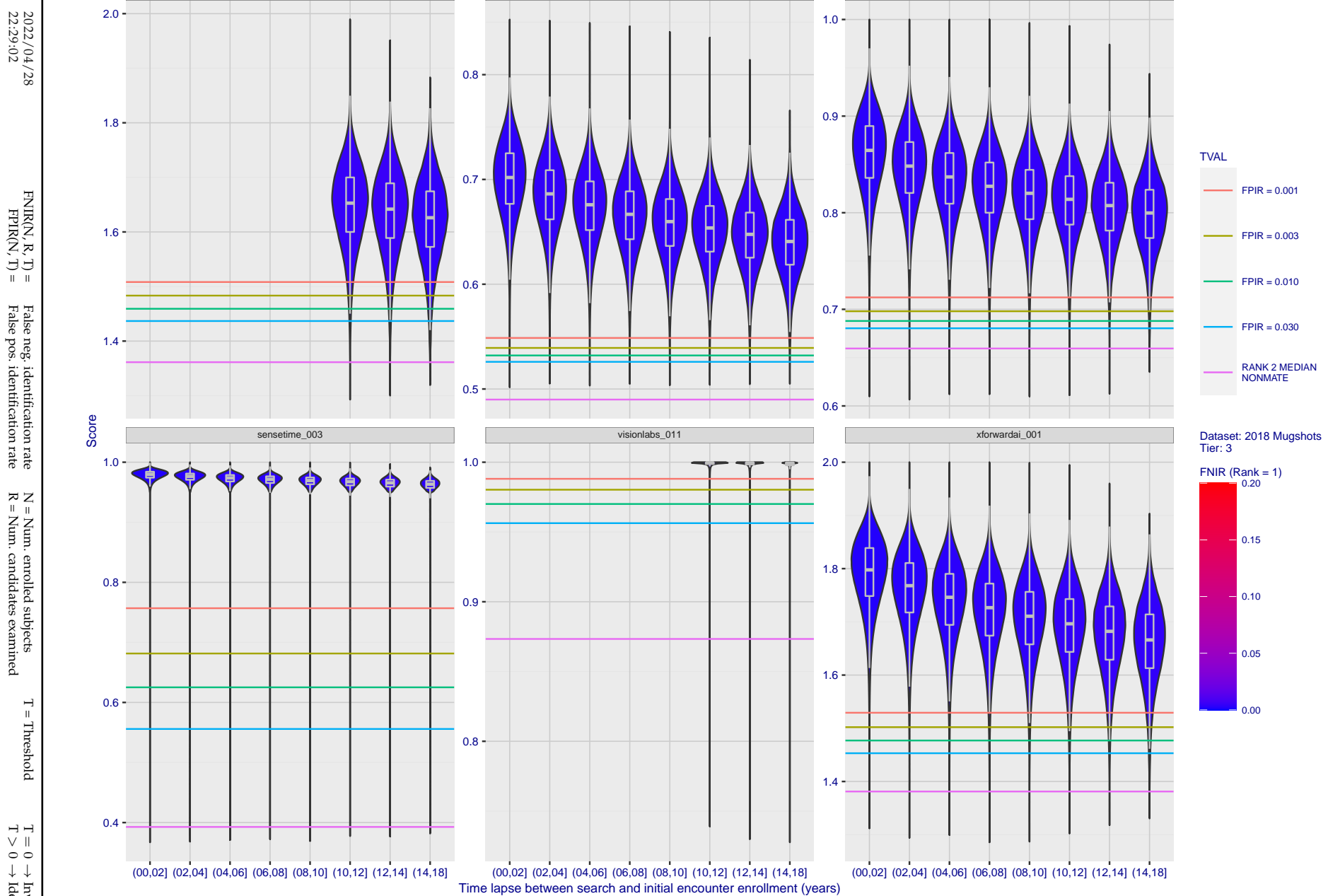


Figure 97: [FRVT-2018 Mugshot Ageing Dataset] Native mate scores vs. time-elapsed. The oldest image of each individual is enrolled. Thereafter, all more recent images are searched. Mated score distributions are computed over all searches noted in row 17 of Table 1 binned by number of years between search and initial enrollment.

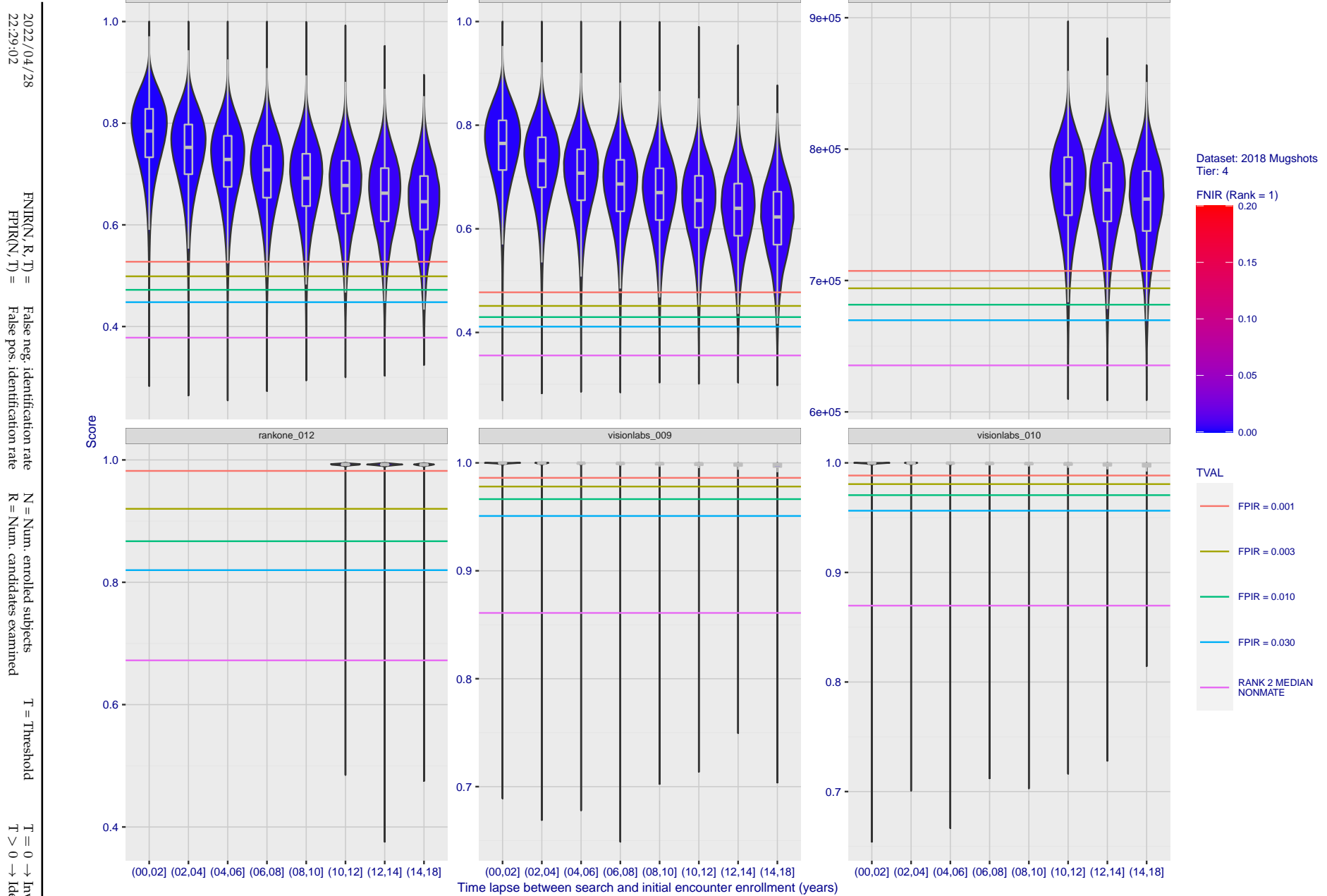


Figure 98: [FRVT-2018 Mugshot Ageing Dataset] Native mate scores vs. time-elapsed. The oldest image of each individual is enrolled. Thereafter, all more recent images are searched. Mated score distributions are computed over all searches noted in row 17 of Table 1 binned by number of years between search and initial enrollment.

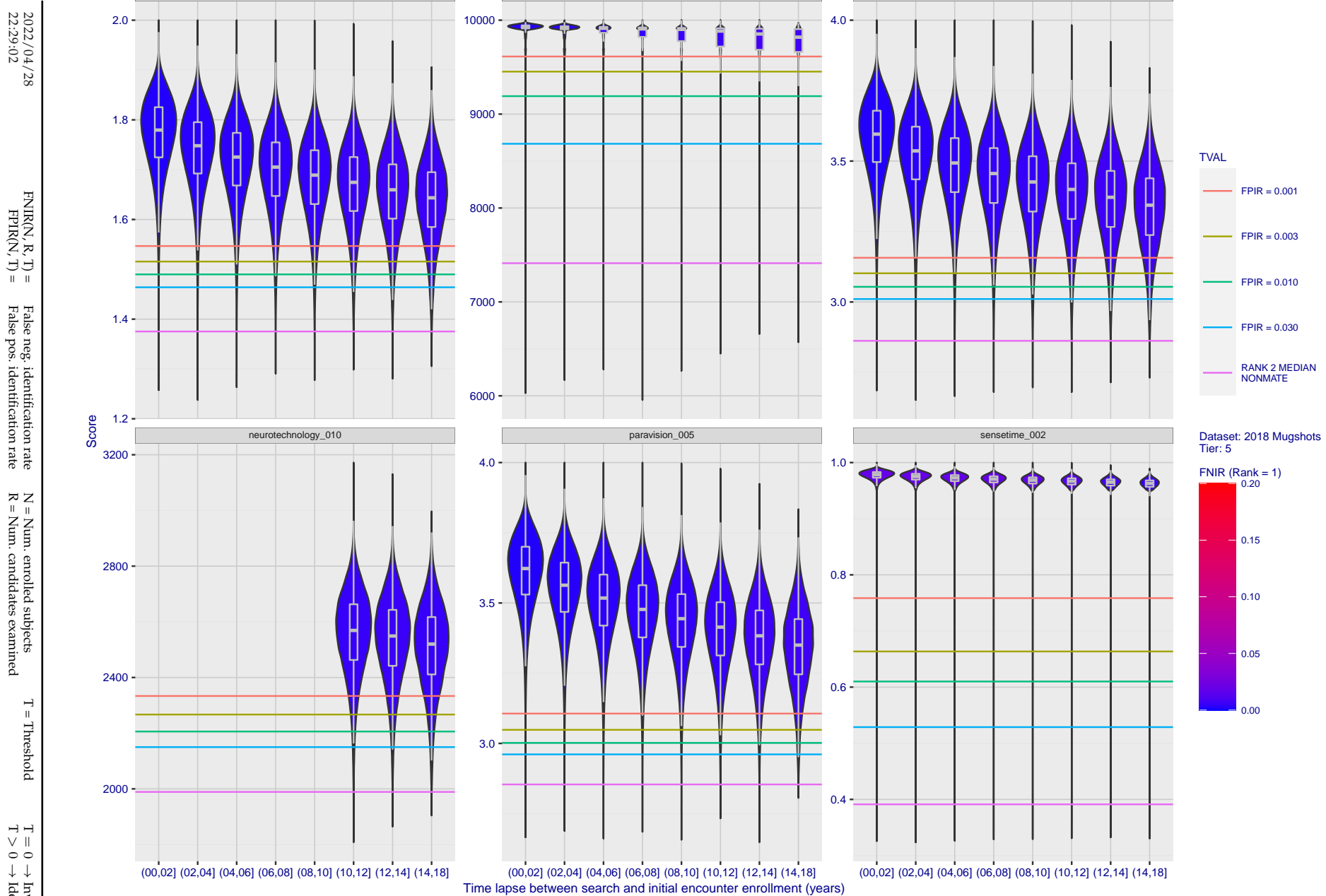


Figure 99: [FRVT-2018 Mugshot Ageing Dataset] Native mate scores vs. time-elapsed. The oldest image of each individual is enrolled. Thereafter, all more recent images are searched. Mated score distributions are computed over all searches noted in row 17 of Table 1 binned by number of years between search and initial enrollment.

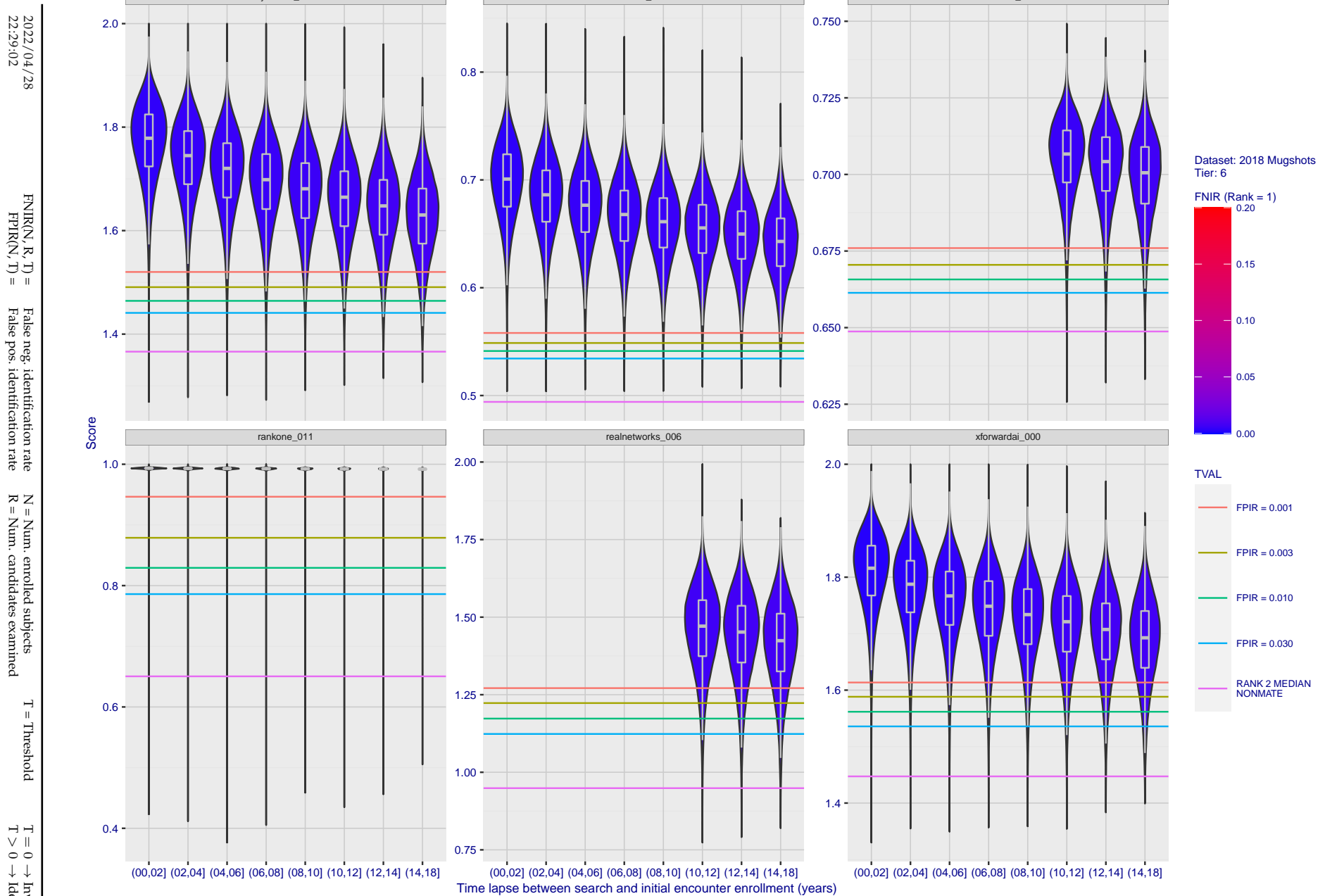


Figure 100: [FRVT-2018 Mugshot Ageing Dataset] Native mate scores vs. time-elapsed. The oldest image of each individual is enrolled. Thereafter, all more recent images are searched. Mated score distributions are computed over all searches noted in row 17 of Table 1 binned by number of years between search and initial enrollment.

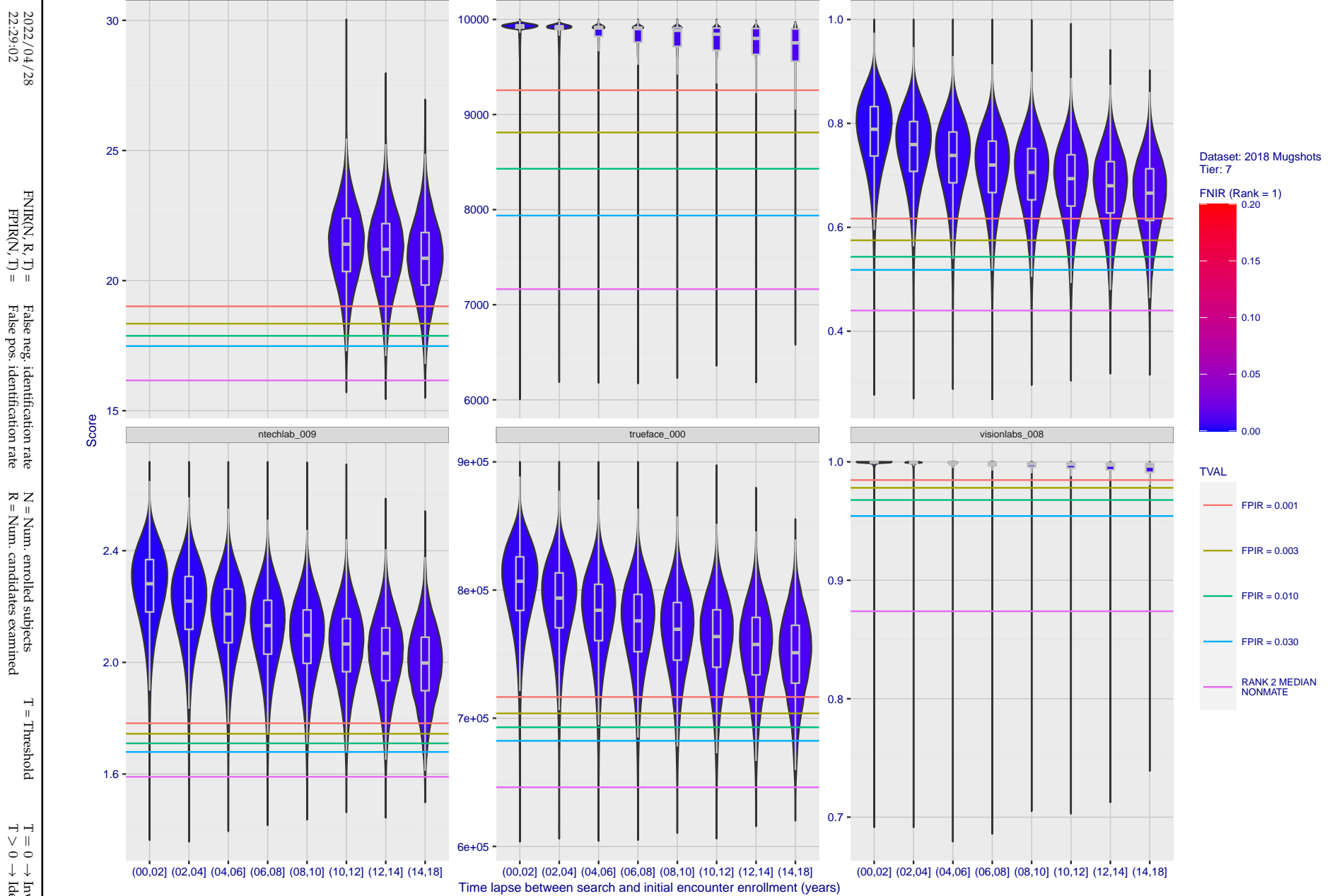


Figure 101: [FRVT-2018 Mugshot Ageing Dataset] Native mate scores vs. time-elapsed. The oldest image of each individual is enrolled. Thereafter, all more recent images are searched. Mated score distributions are computed over all searches noted in row 17 of Table 1 binned by number of years between search and initial enrollment.

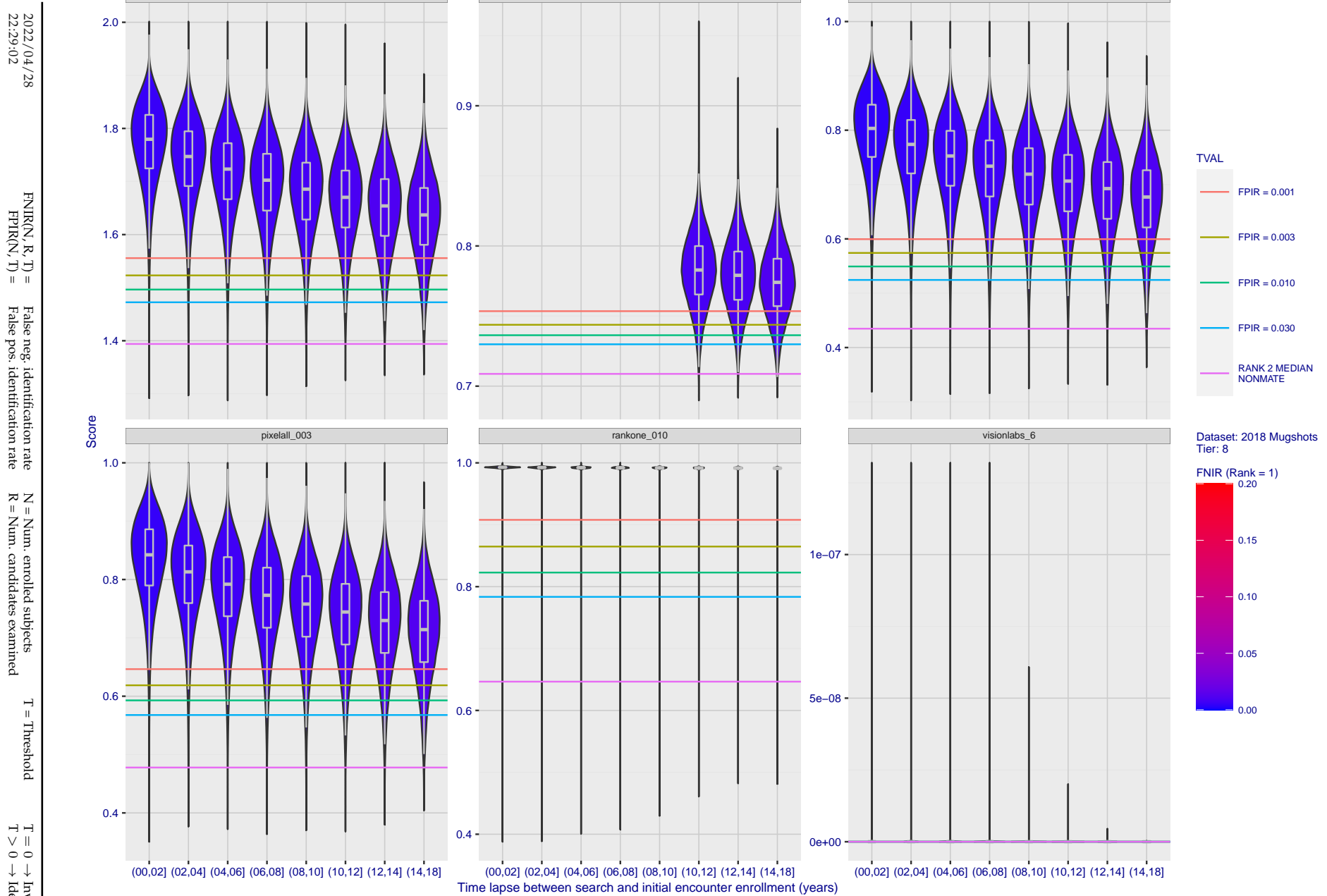
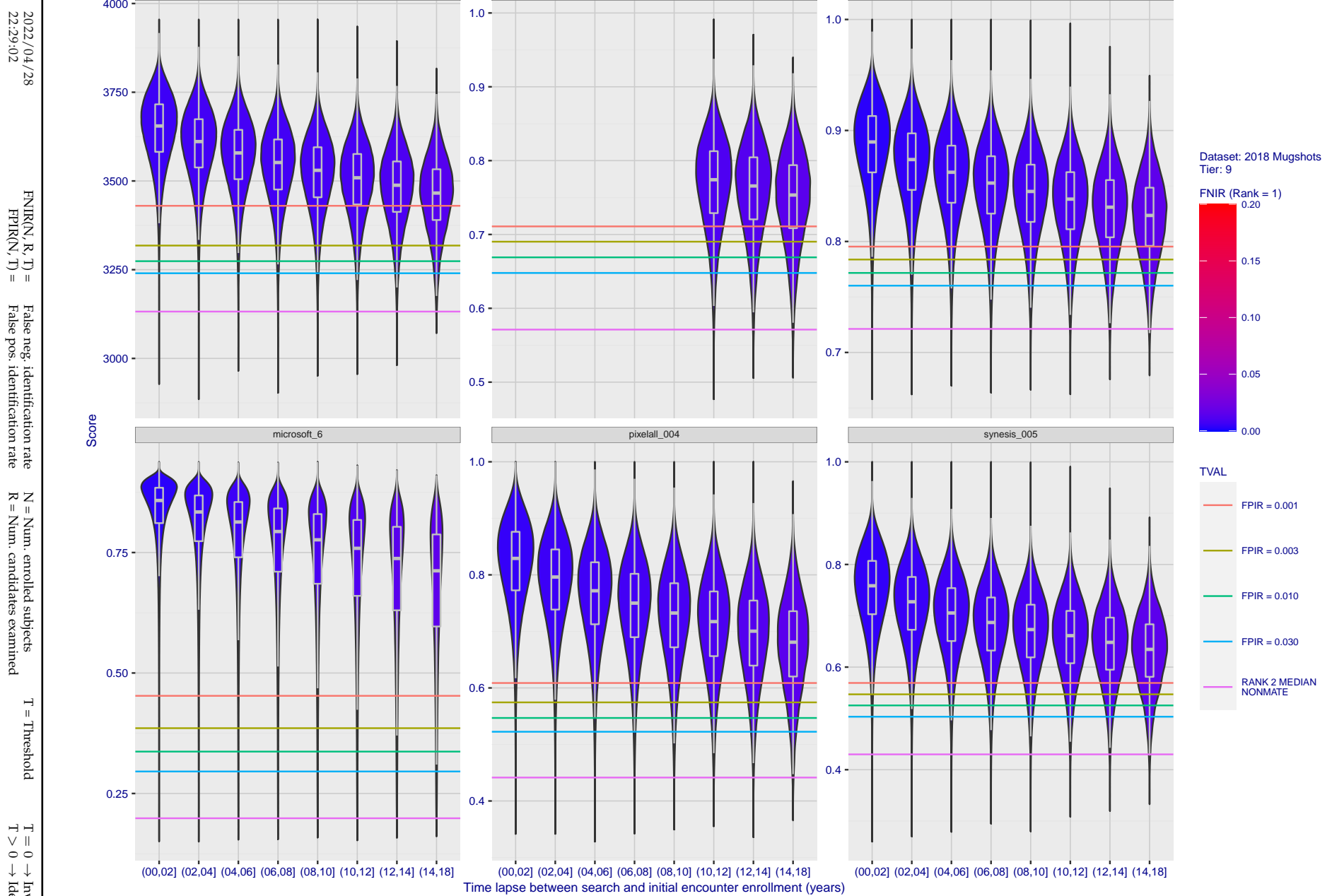


Figure 102: [FRVT-2018 Mugshot Ageing Dataset] Native mate scores vs. time-elapsed. The oldest image of each individual is enrolled. Thereafter, all more recent images are searched. Mated score distributions are computed over all searches noted in row 17 of Table 1 binned by number of years between search and initial enrollment.



**Figure 103: [FRVT-2018 Mugshot Ageing Dataset] Native mate scores vs. time-elapsed.** The oldest image of each individual is enrolled. Thereafter, all more recent images are searched. Mated score distributions are computed over all searches noted in row 17 of Table 1 binned by number of years between search and initial enrollment.

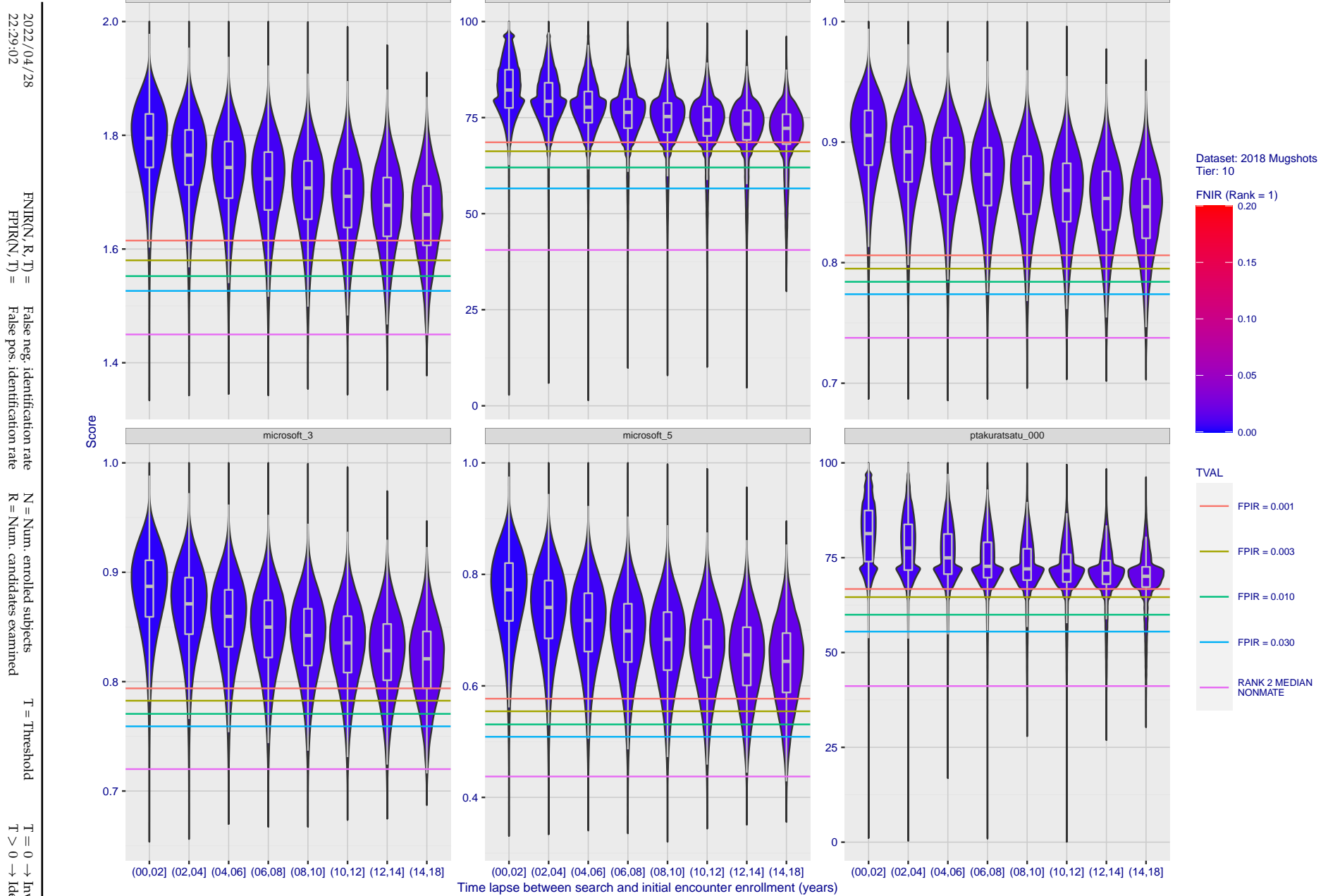


Figure 104: [FRVT-2018 Mugshot Ageing Dataset] Native mate scores vs. time-elapsed. The oldest image of each individual is enrolled. Thereafter, all more recent images are searched. Mated score distributions are computed over all searches noted in row 17 of Table 1 binned by number of years between search and initial enrollment.

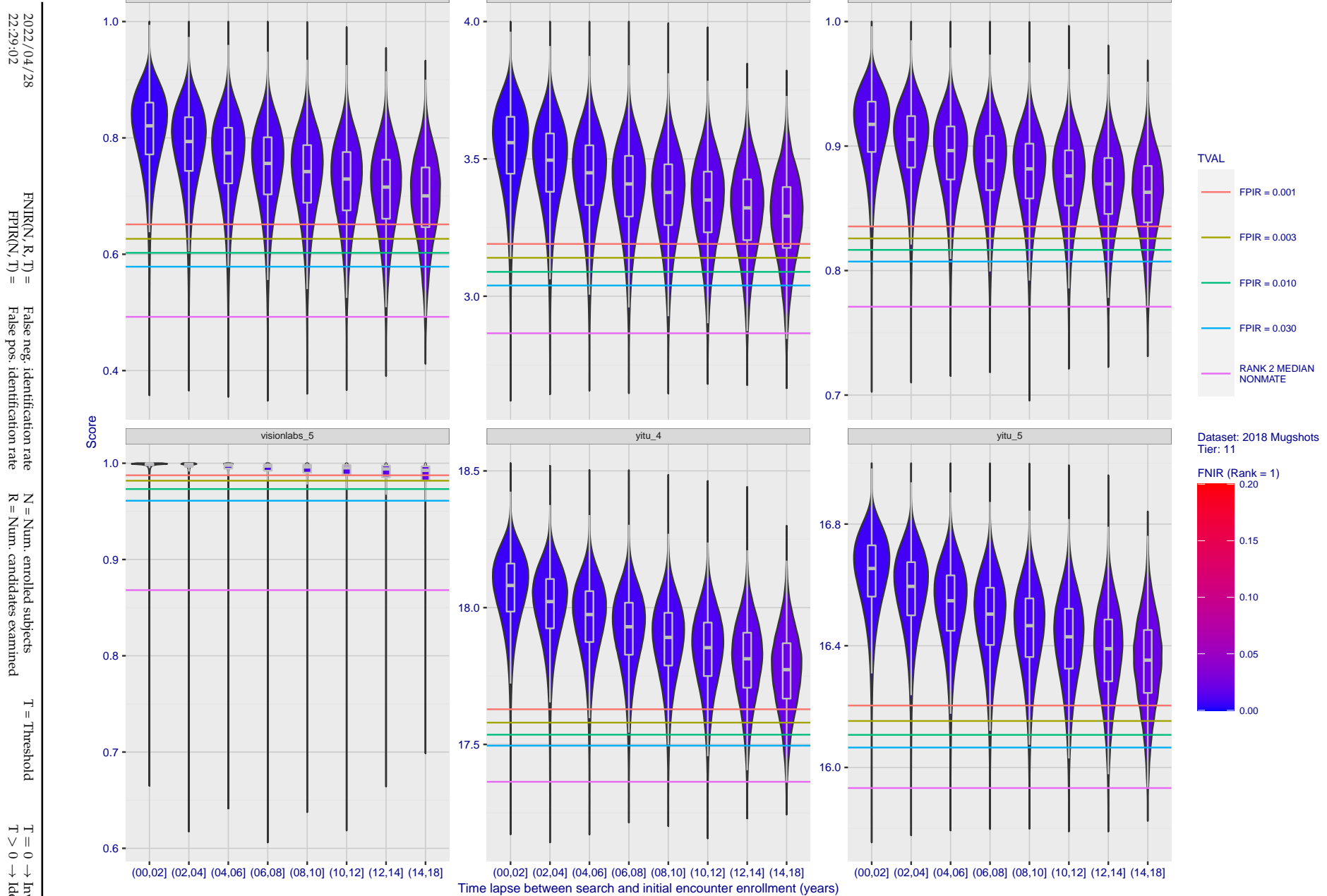
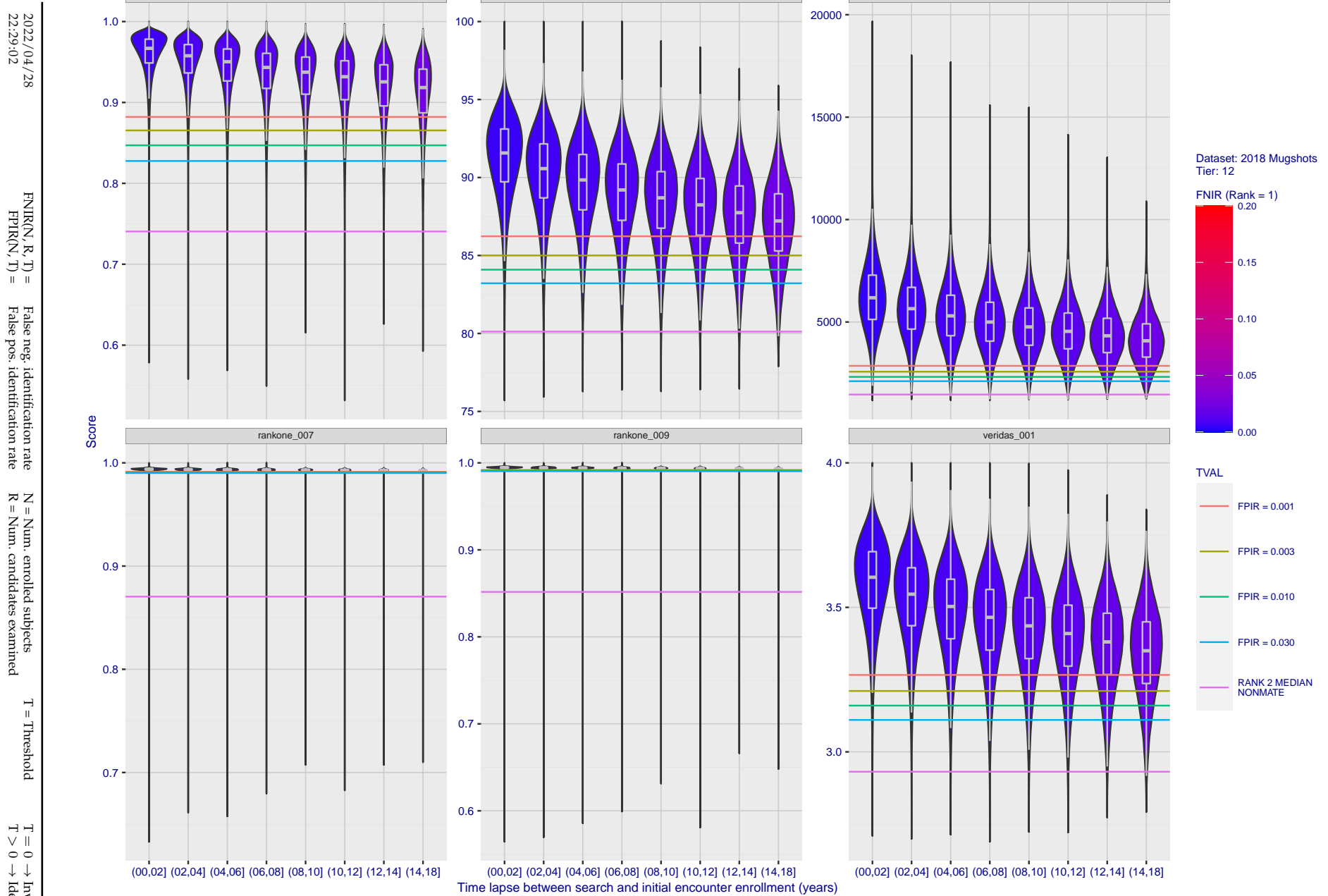


Figure 105: [FRVT-2018 Mugshot Ageing Dataset] Native mate scores vs. time-elapsed. The oldest image of each individual is enrolled. Thereafter, all more recent images are searched. Mated score distributions are computed over all searches noted in row 17 of Table 1 binned by number of years between search and initial enrollment.



**Figure 106: [FRVT-2018 Mugshot Ageing Dataset] Native mate scores vs. time-elapsed.** The oldest image of each individual is enrolled. Thereafter, all more recent images are searched. Mated score distributions are computed over all searches noted in row 17 of Table 1 binned by number of years between search and initial enrollment.

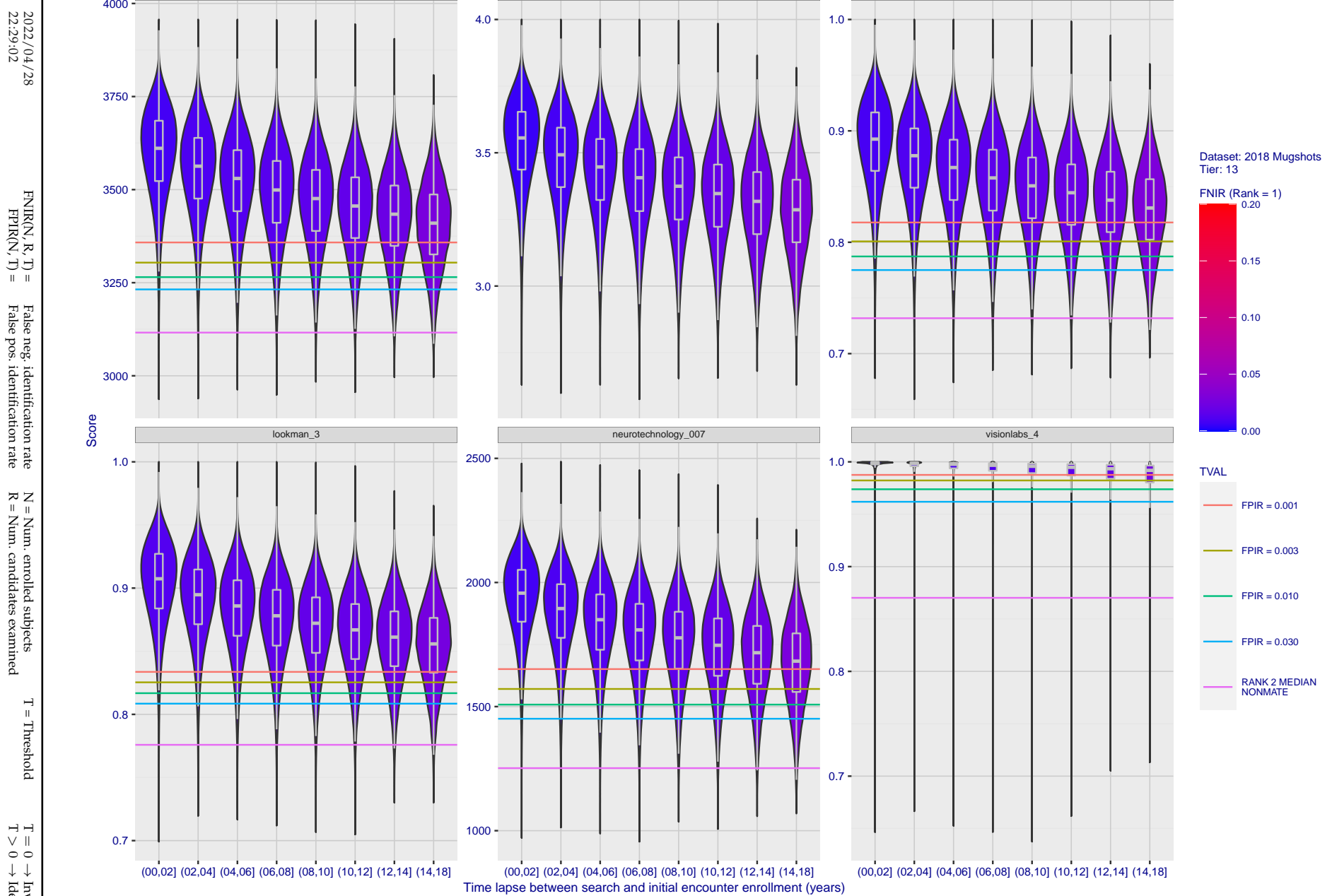


Figure 107: [FRVT-2018 Mugshot Ageing Dataset] Native mate scores vs. time-elapsed. The oldest image of each individual is enrolled. Thereafter, all more recent images are searched. Mated score distributions are computed over all searches noted in row 17 of Table 1 binned by number of years between search and initial enrollment.

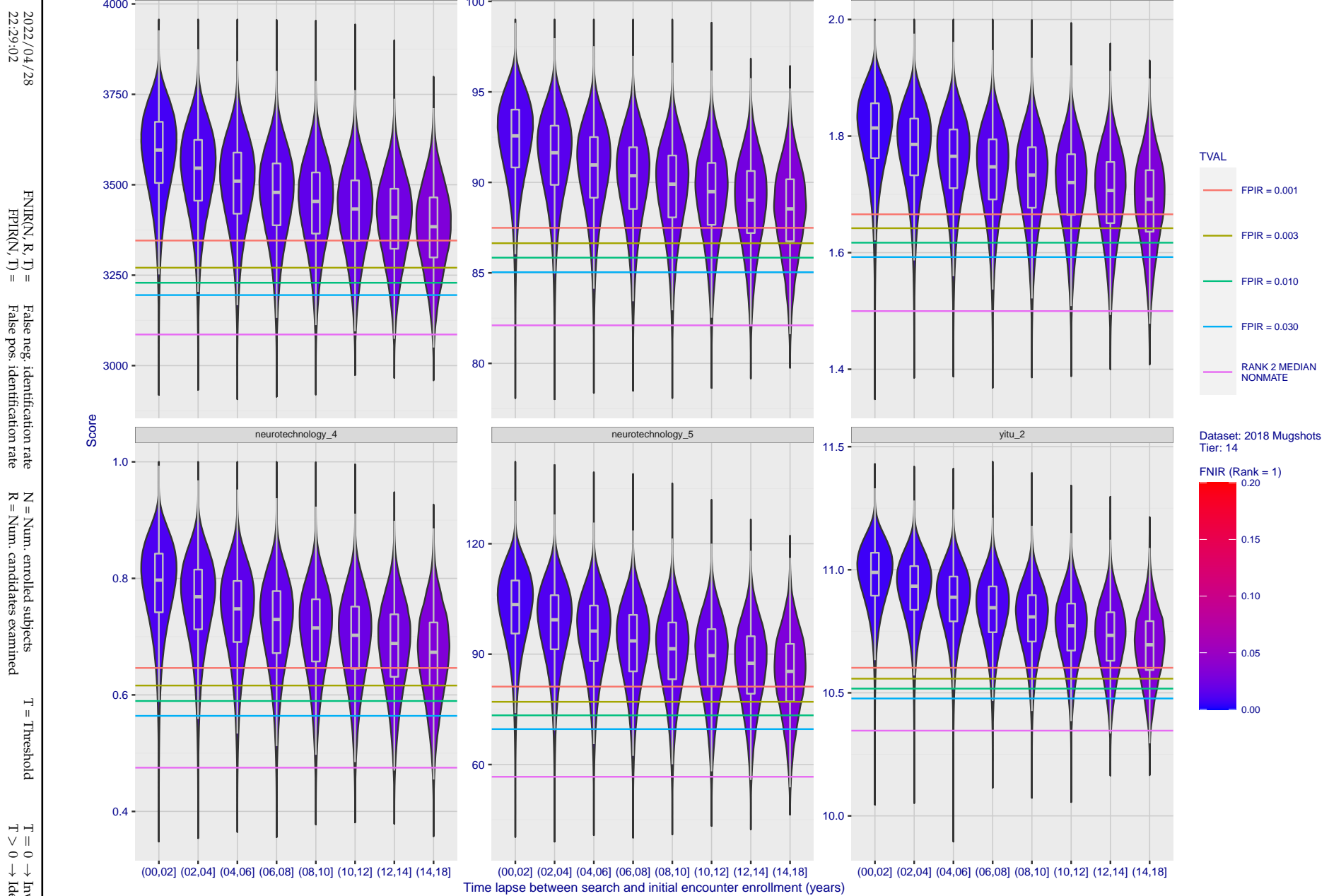


Figure 108: [FRVT-2018 Mugshot Ageing Dataset] Native mate scores vs. time-elapsed. The oldest image of each individual is enrolled. Thereafter, all more recent images are searched. Mated score distributions are computed over all searches noted in row 17 of Table 1 binned by number of years between search and initial enrollment.

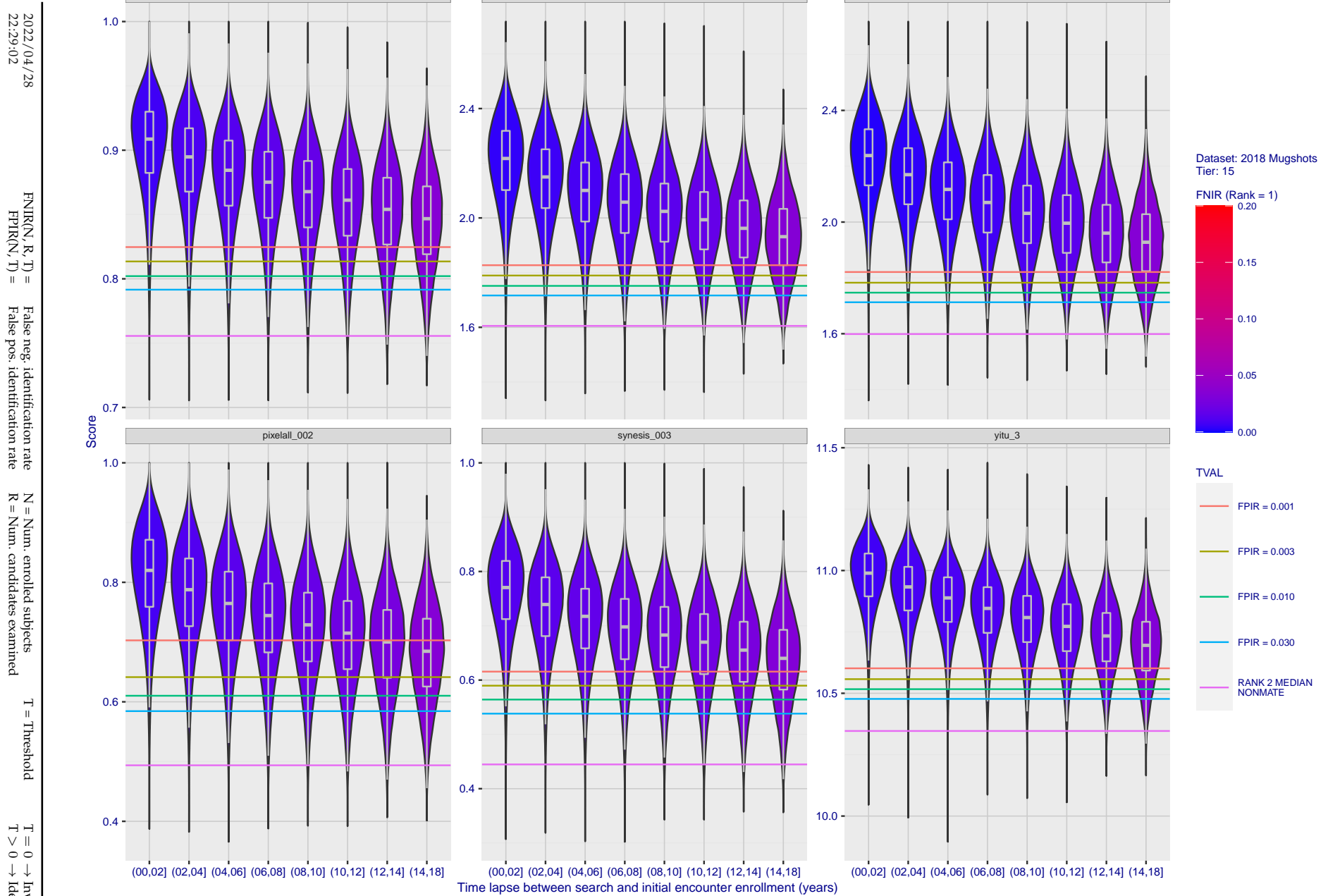
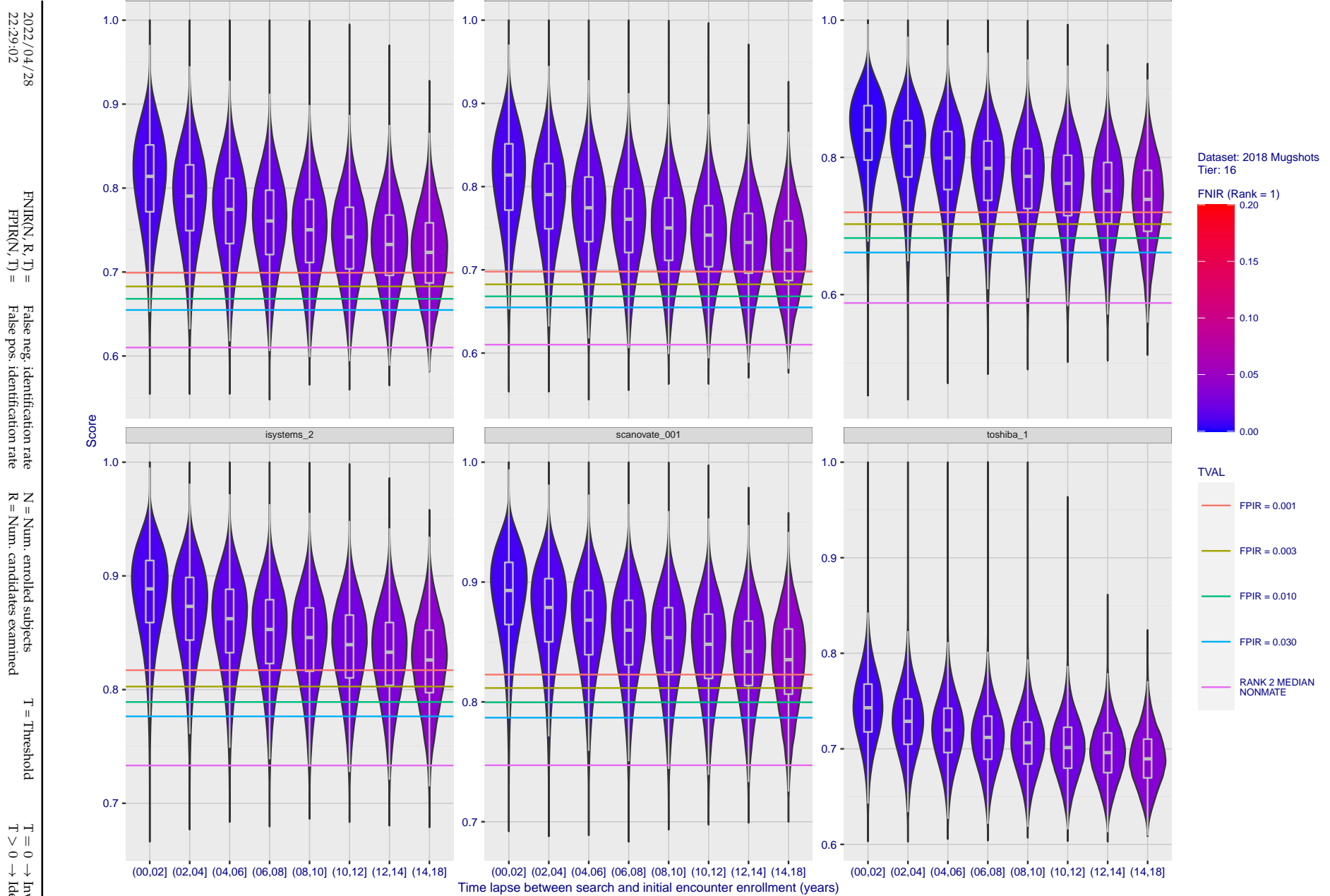
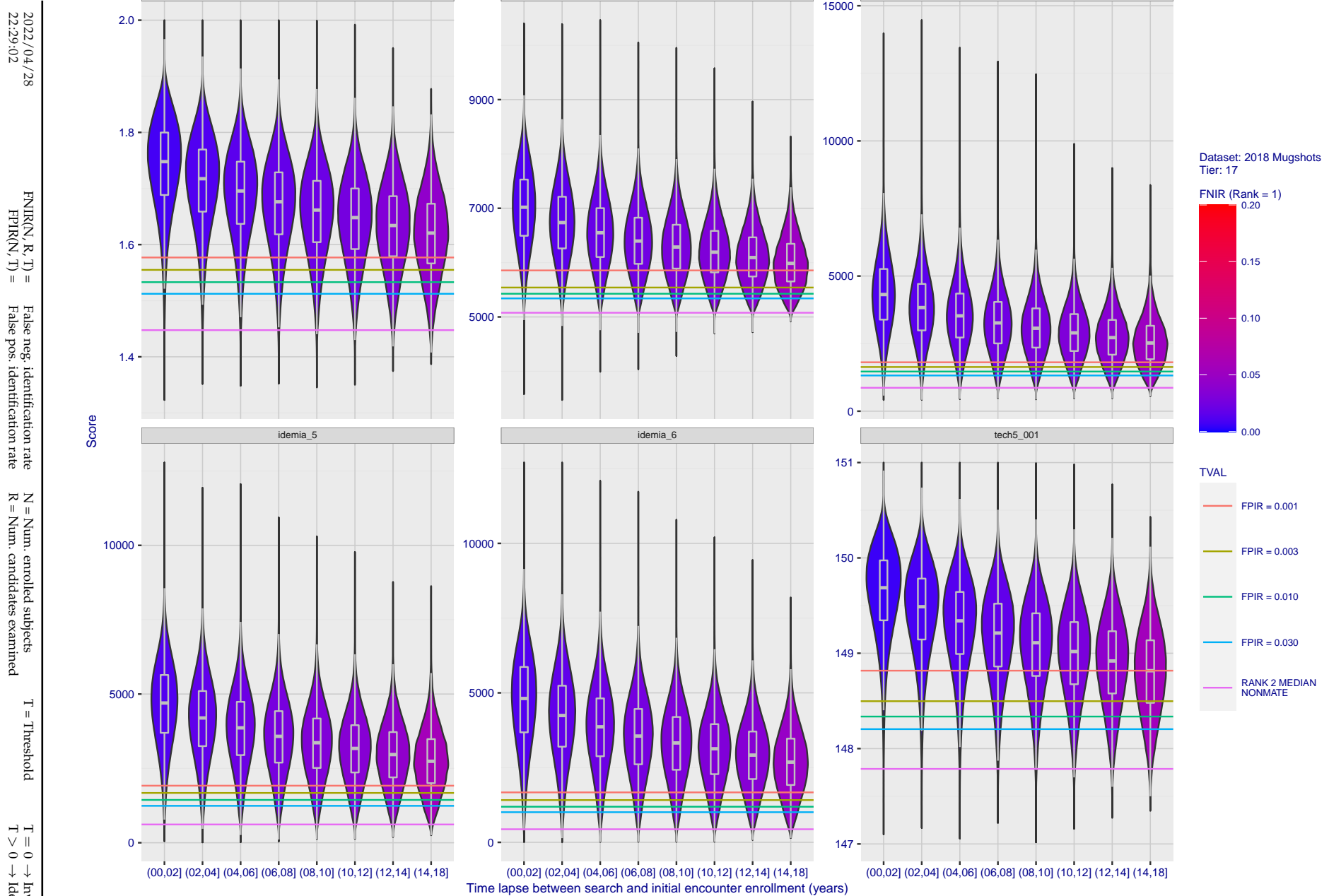


Figure 109: [FRVT-2018 Mugshot Ageing Dataset] Native mate scores vs. time-elapsed. The oldest image of each individual is enrolled. Thereafter, all more recent images are searched. Mated score distributions are computed over all searches noted in row 17 of Table 1 binned by number of years between search and initial enrollment.



**Figure 110: [FRVT-2018 Mugshot Ageing Dataset] Native mate scores vs. time-elapsed.** The oldest image of each individual is enrolled. Thereafter, all more recent images are searched. Mated score distributions are computed over all searches noted in row 17 of Table 1 binned by number of years between search and initial enrollment.



**Figure 111: [FRVT-2018 Mugshot Ageing Dataset] Native mate scores vs. time-elapsed.** The oldest image of each individual is enrolled. Thereafter, all more recent images are searched. Mated score distributions are computed over all searches noted in row 17 of Table 1 binned by number of years between search and initial enrollment.

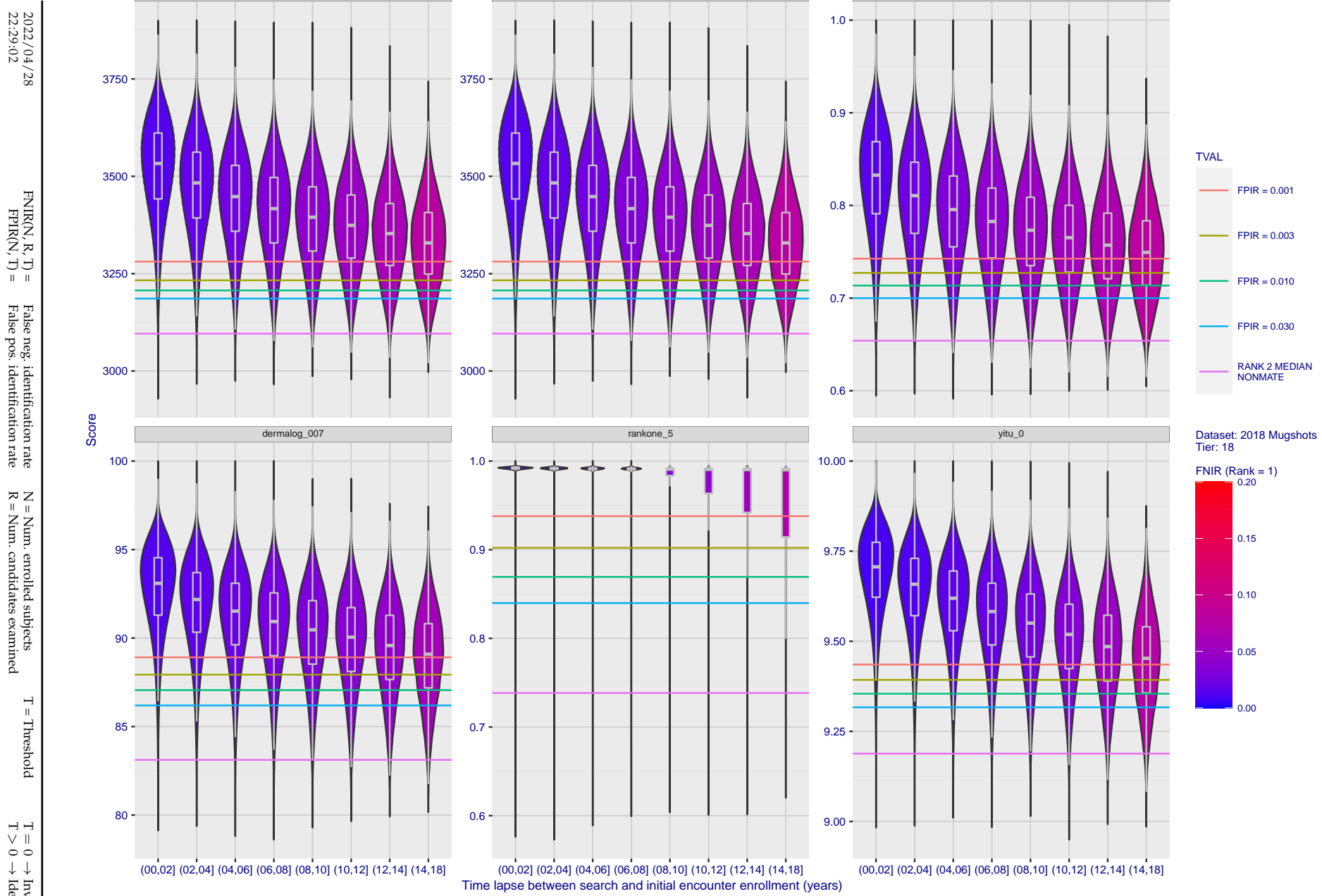
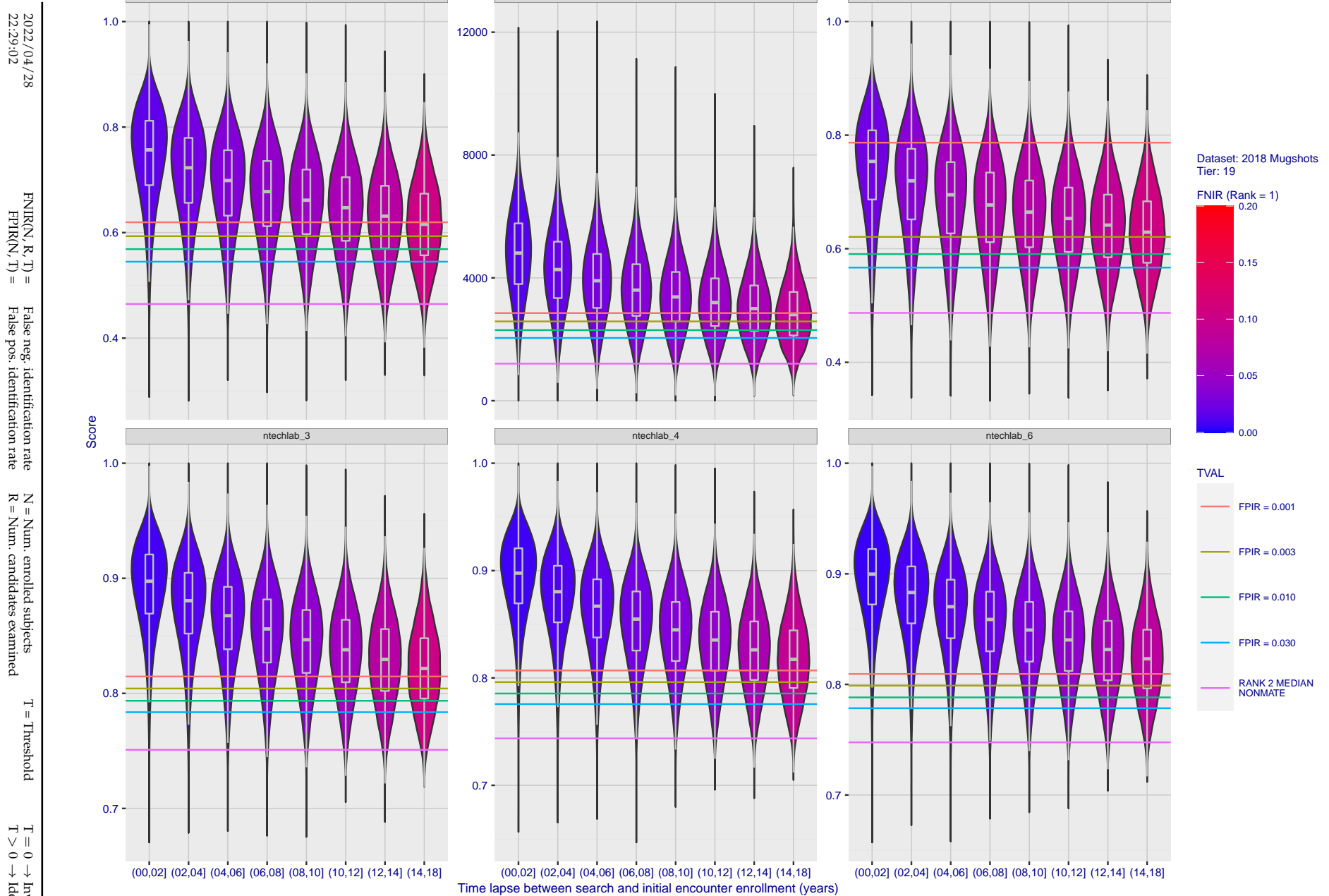


Figure 112: [FRVT-2018 Mugshot Ageing Dataset] Native mate scores vs. time-elapsed. The oldest image of each individual is enrolled. Thereafter, all more recent images are searched. Mated score distributions are computed over all searches noted in row 17 of Table 1 binned by number of years between search and initial enrollment.



**Figure 113: [FRVT-2018 Mugshot Ageing Dataset] Native mate scores vs. time-elapsed.** The oldest image of each individual is enrolled. Thereafter, all more recent images are searched. Mated score distributions are computed over all searches noted in row 17 of Table 1 binned by number of years between search and initial enrollment.

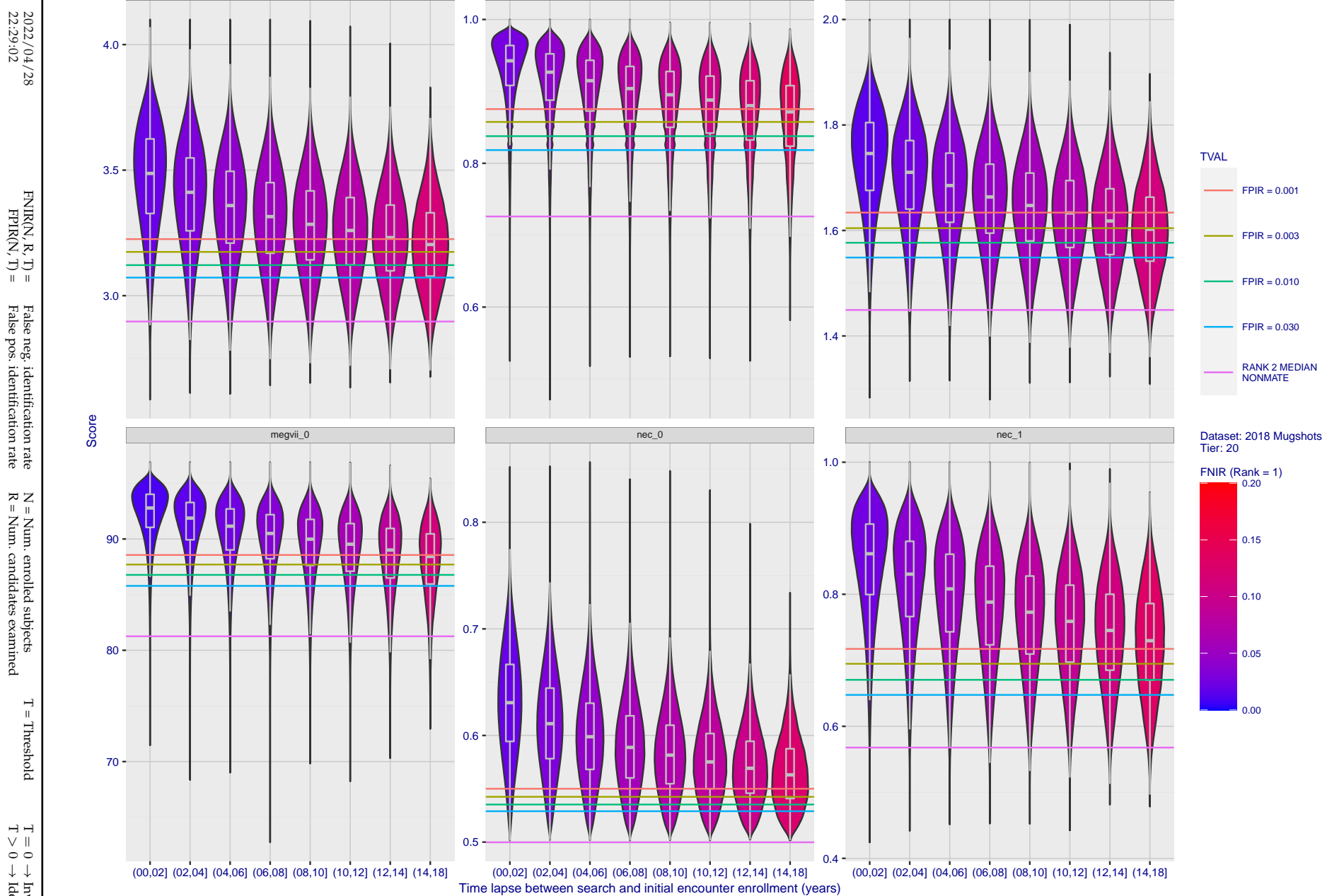


Figure 114: [FRVT-2018 Mugshot Ageing Dataset] Native mate scores vs. time-elapsed. The oldest image of each individual is enrolled. Thereafter, all more recent images are searched. Mated score distributions are computed over all searches noted in row 17 of Table 1 binned by number of years between search and initial enrollment.

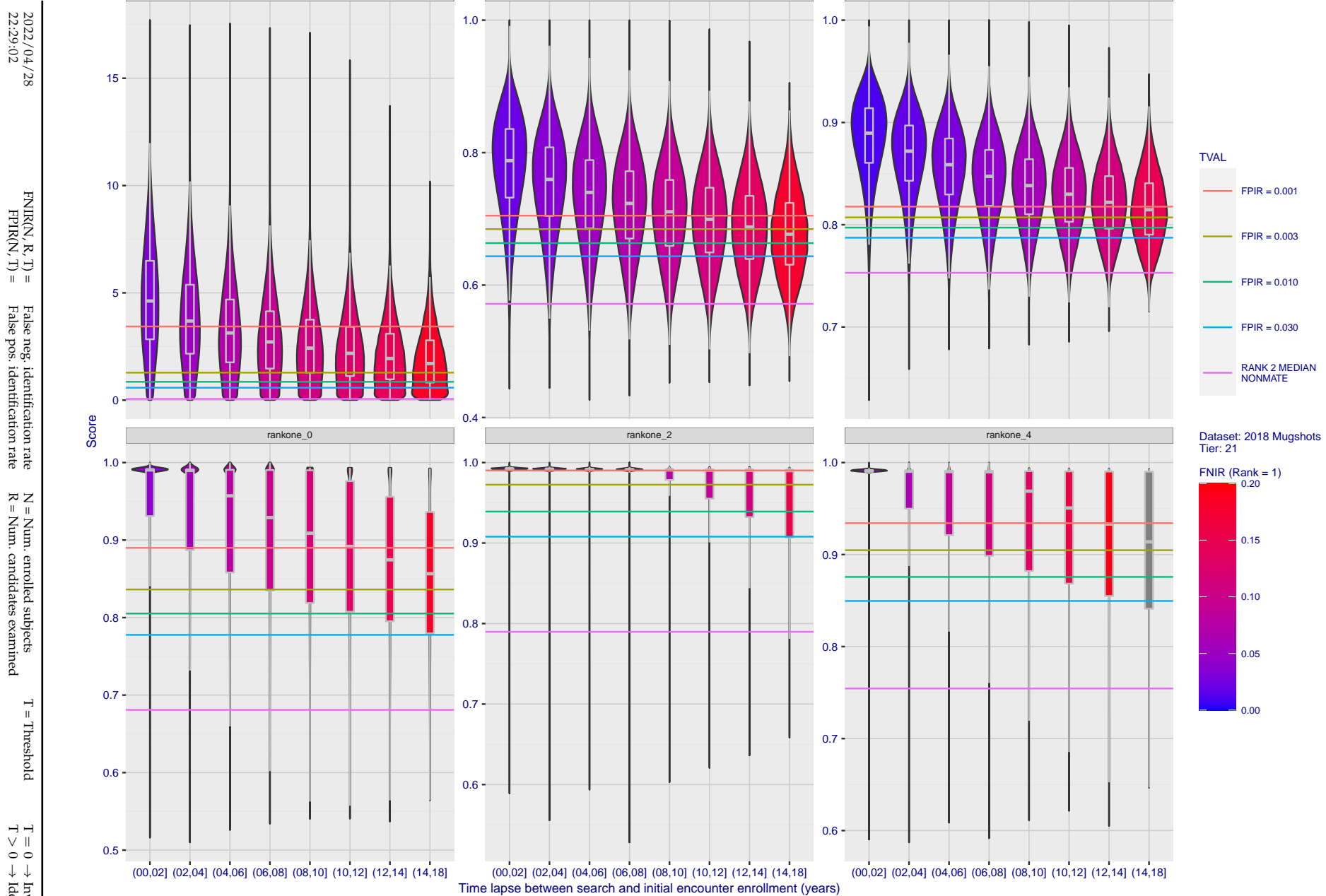


Figure 115: [FRVT-2018 Mugshot Ageing Dataset] Native mate scores vs. time-elapsed. The oldest image of each individual is enrolled. Thereafter, all more recent images are searched. Mated score distributions are computed over all searches noted in row 17 of Table 1 binned by number of years between search and initial enrollment.

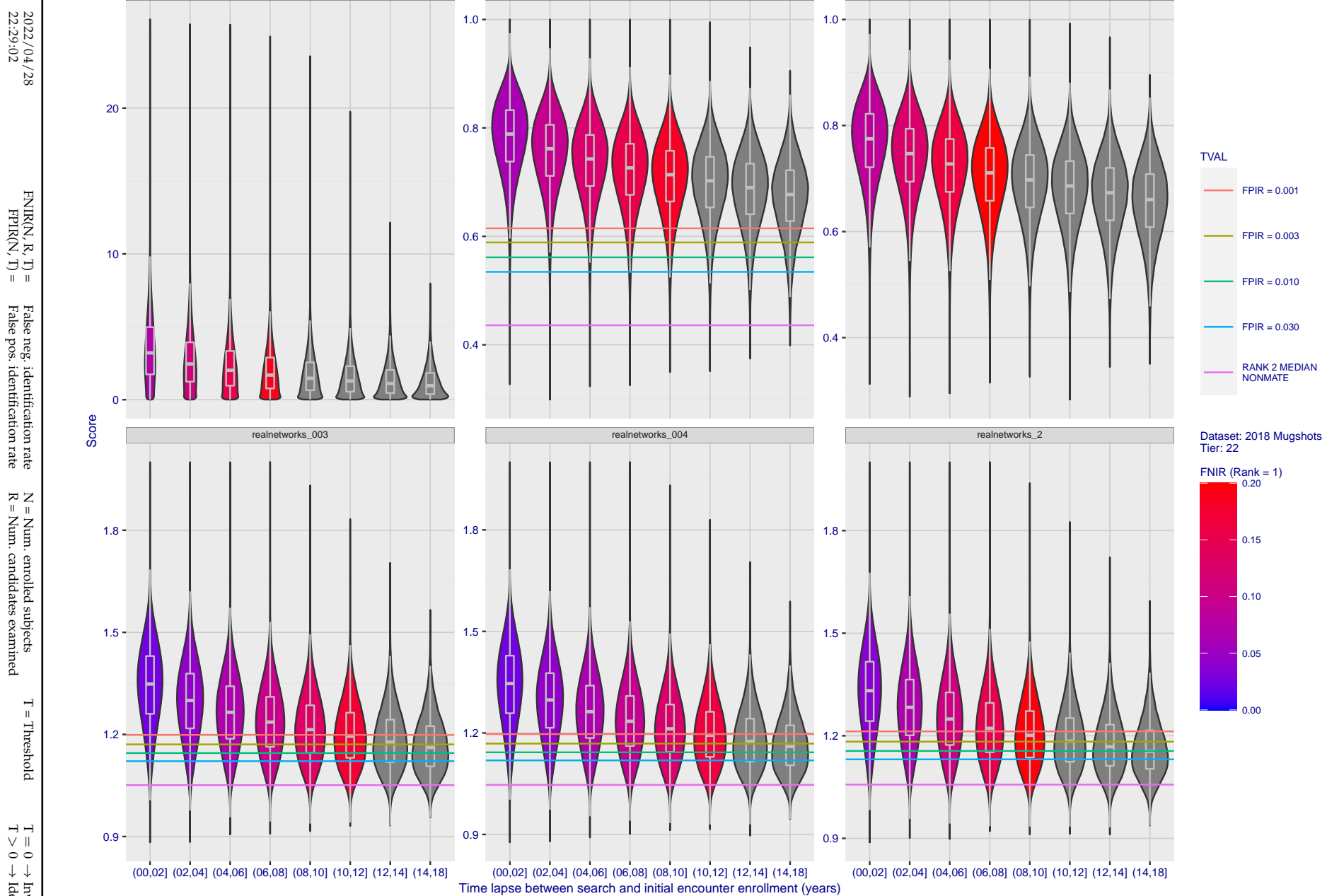
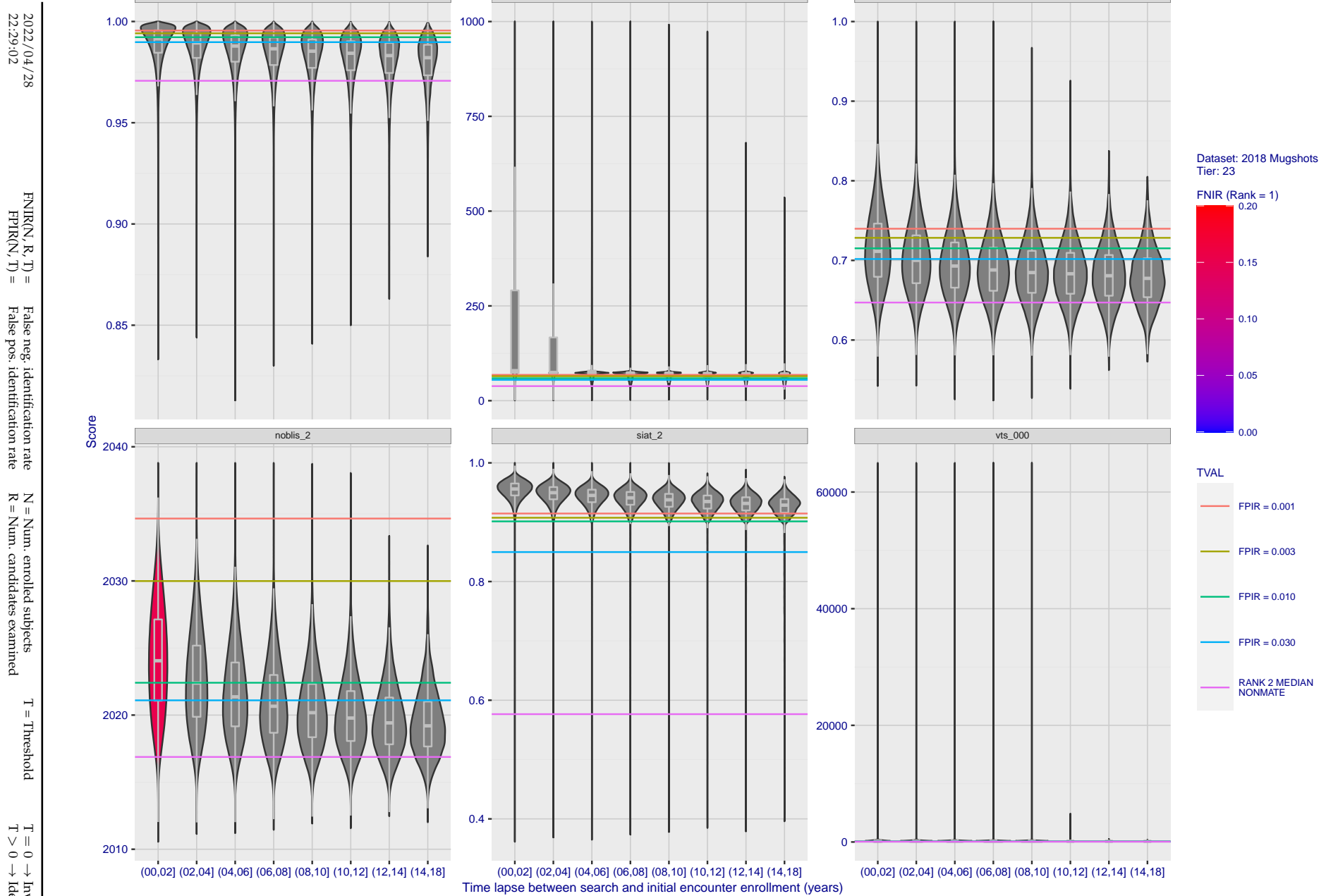


Figure 116: [FRVT-2018 Mugshot Ageing Dataset] Native mate scores vs. time-elapsed. The oldest image of each individual is enrolled. Thereafter, all more recent images are searched. Mated score distributions are computed over all searches noted in row 17 of Table 1 binned by number of years between search and initial enrollment.



**Figure 117: [FRVT-2018 Mugshot Ageing Dataset] Native mate scores vs. time-elapsed.** The oldest image of each individual is enrolled. Thereafter, all more recent images are searched. Mated score distributions are computed over all searches noted in row 17 of Table 1 binned by number of years between search and initial enrollment.

## Appendix C Effect of enrolling multiple images

2022/04/28  
22:29:02FNIR(N, R, T) = False neg. identification rate  
FPIR(N, T) = False pos. identification rateN = Num. enrolled subjects  
R = Num. candidates examined

T = Threshold

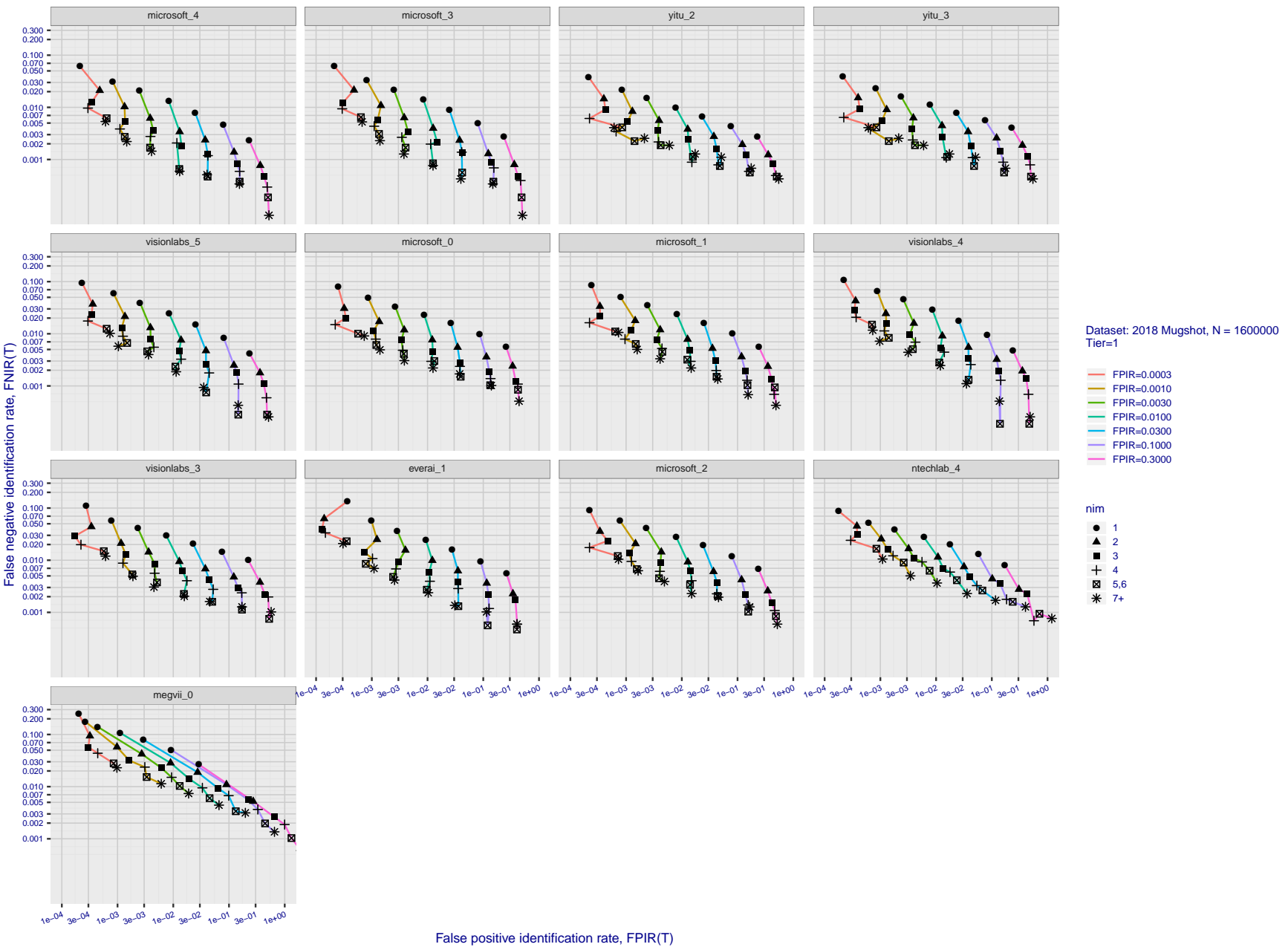
T = 0 → Investigation  
T > 0 → Identification

Figure 118: [FRVT-2018 Mugshot Dataset] Effect of enrolling multiple images for each identity. The plot shows an identification miss rates vs. false positive rates, at seven operating thresholds. The enrolled population size is fixed. The images are enrolled with lifetime-consolidation - see section 2.3.

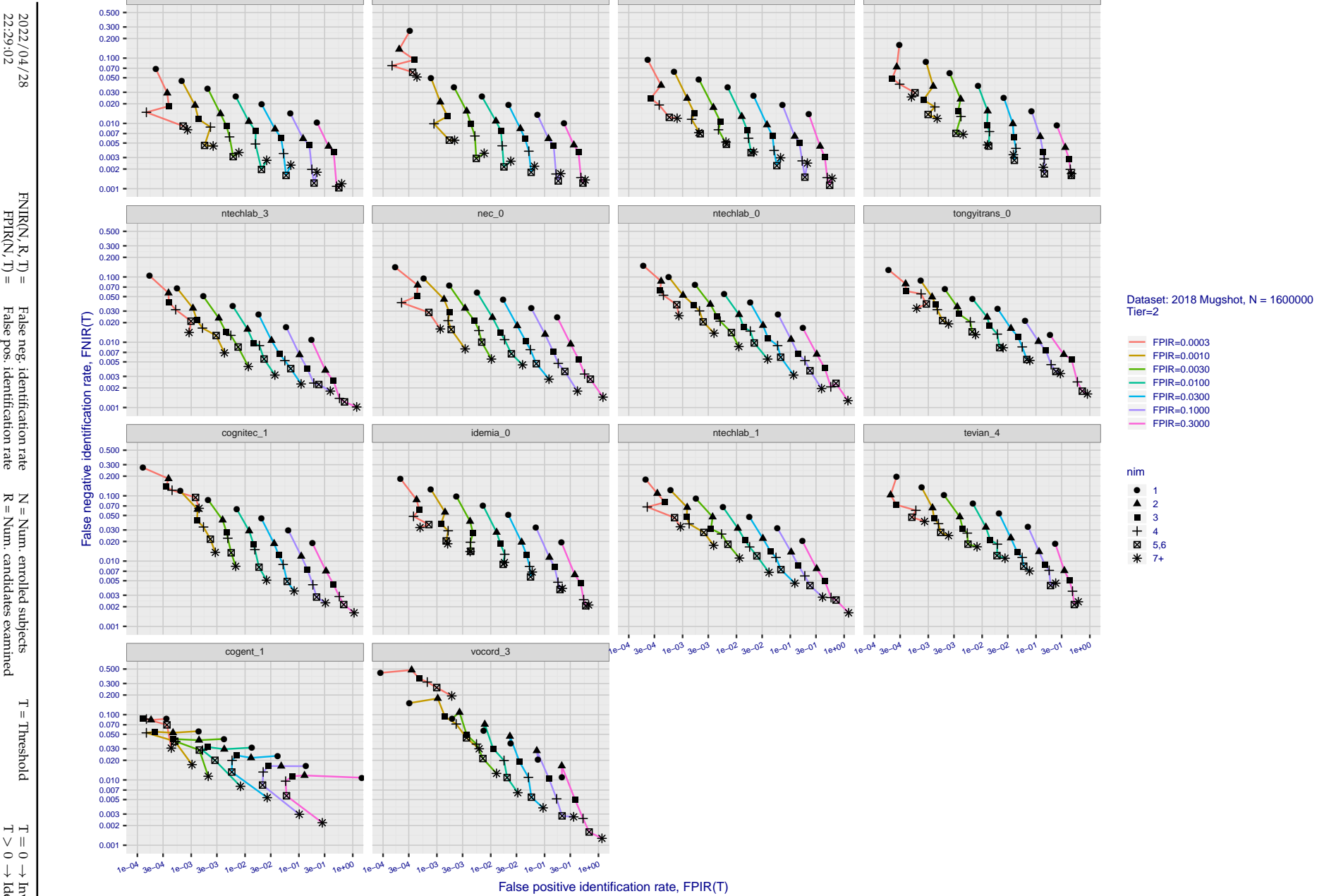


Figure 119: [FRVT-2018 Mugshot Dataset] Effect of enrolling multiple images for each identity. The plot shows an identification miss rates vs. false positive rates, at seven operating thresholds. The enrolled population size is fixed. The images are enrolled with lifetime-consolidation - see section 2.3.

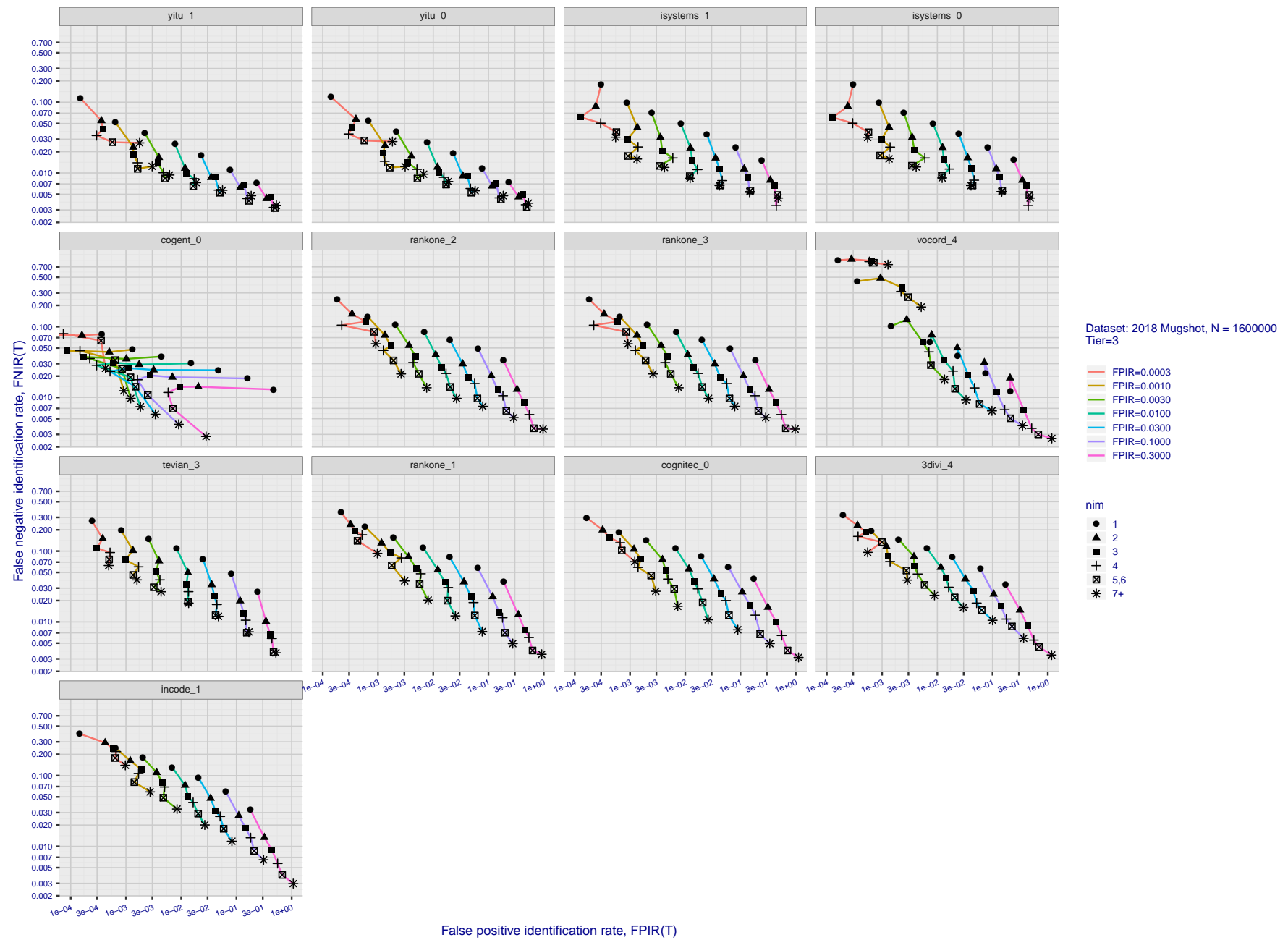


Figure 120: [FRVT-2018 Mugshot Dataset] Effect of enrolling multiple images for each identity. The plot shows an identification miss rates vs. false positive rates, at seven operating thresholds. The enrolled population size is fixed. The images are enrolled with lifetime-consolidation - see section 2.3.

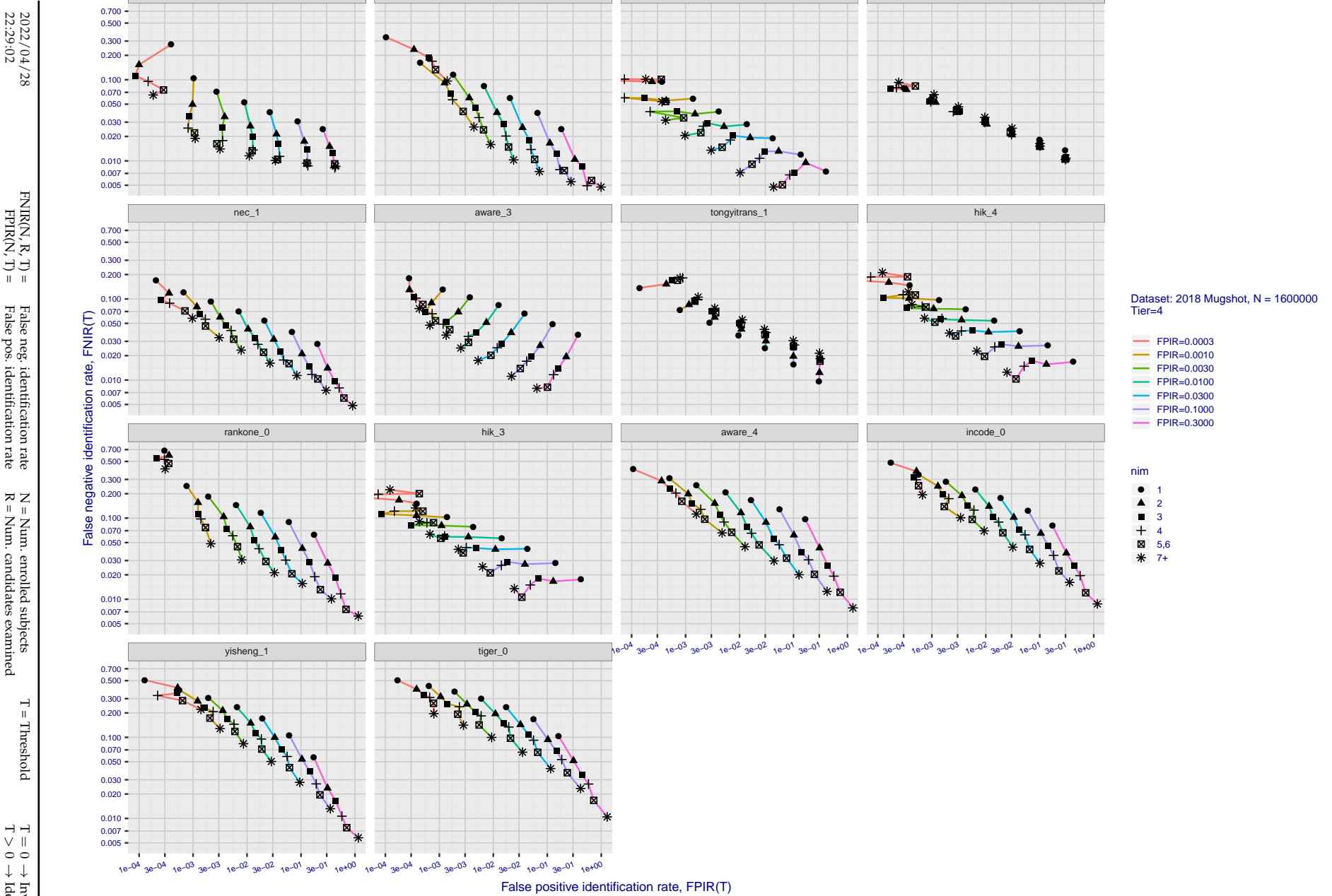


Figure 121: [FRVT-2018 Mugshot Dataset] Effect of enrolling multiple images for each identity. The plot shows an identification miss rates vs. false positive rates, at seven operating thresholds. The enrolled population size is fixed. The images are enrolled with lifetime-consolidation - see section 2.3.

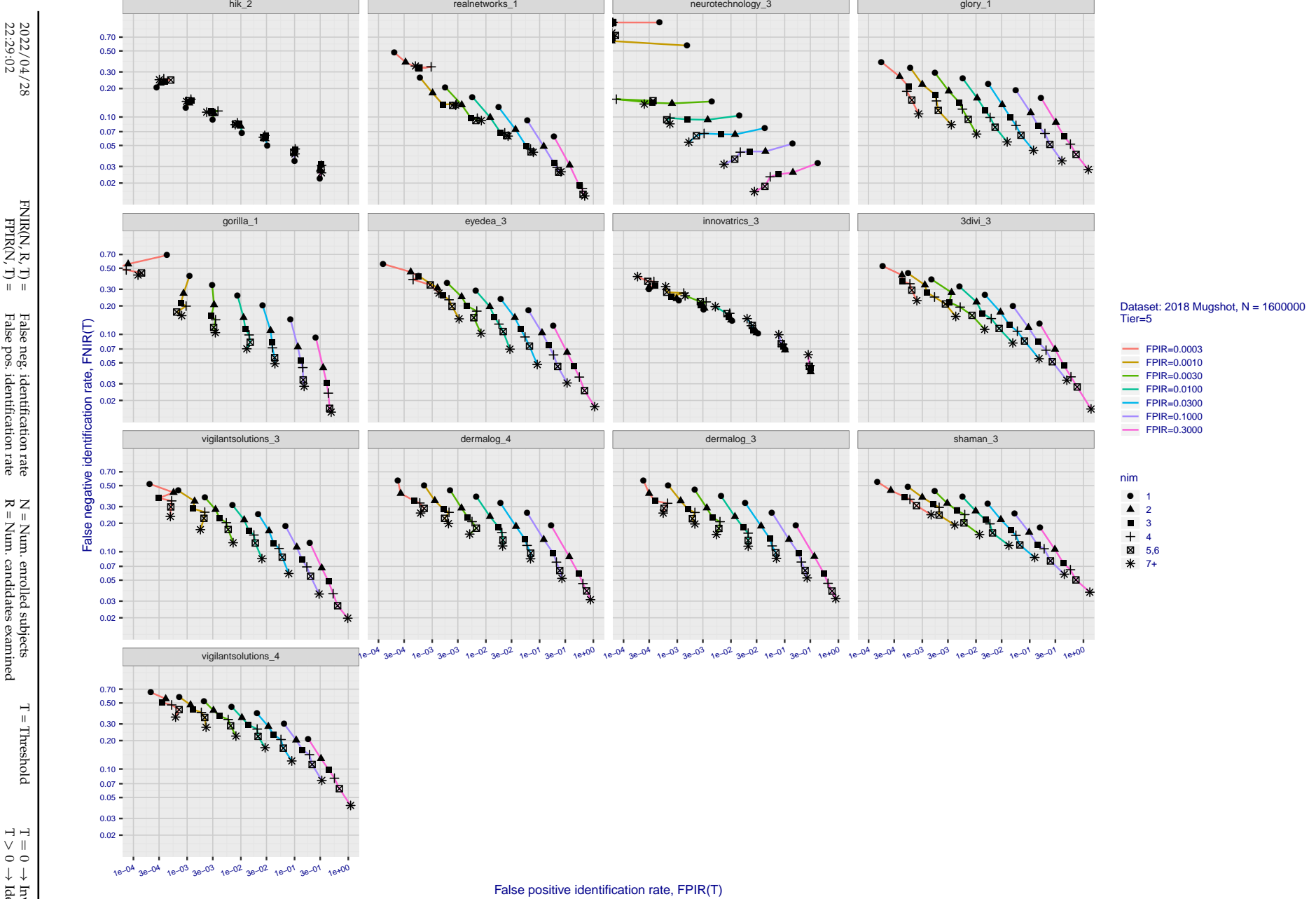


Figure 122: [FRVT-2018 Mugshot Dataset] Effect of enrolling multiple images for each identity. The plot shows an identification miss rates vs. false positive rates, at seven operating thresholds. The enrolled population size is fixed. The images are enrolled with lifetime-consolidation - see section 2.3.

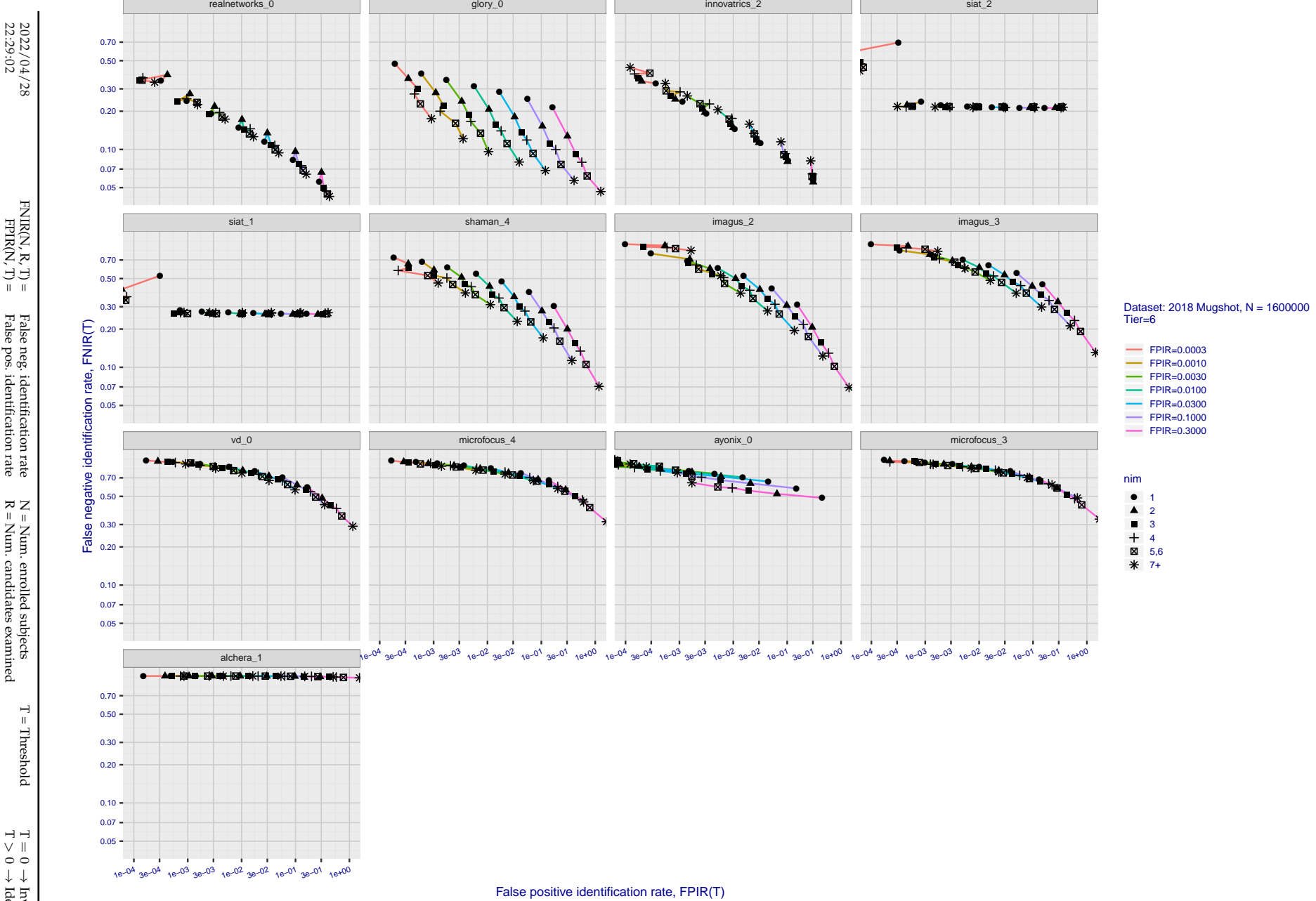


Figure 123: [FRVT-2018 Mugshot Dataset] Effect of enrolling multiple images for each identity. The plot shows an identification miss rates vs. false positive rates, at seven operating thresholds. The enrolled population size is fixed. The images are enrolled with lifetime-consolidation - see section 2.3.

## Appendix D Accuracy with poor quality webcam images

2022/04/28 22:29:02	$\text{FNIR}(N, R, T) =$ $\text{FPTR}(N, T) =$	False neg. identification rate False pos. identification rate	$N =$ Num. enrolled subjects $R =$ Num. candidates examined	$T =$ Threshold $T > 0 \rightarrow$ Identification	$T = 0 \rightarrow$ Investigation
------------------------	---	--	--	---	-----------------------------------

2022/04/28  
22:29:02FNIR(N, R, T) = False neg. identification rate  
FPIR(N, T) = False pos. identification rateN = Num. enrolled subjects  
R = Num. candidates examined

T = Threshold

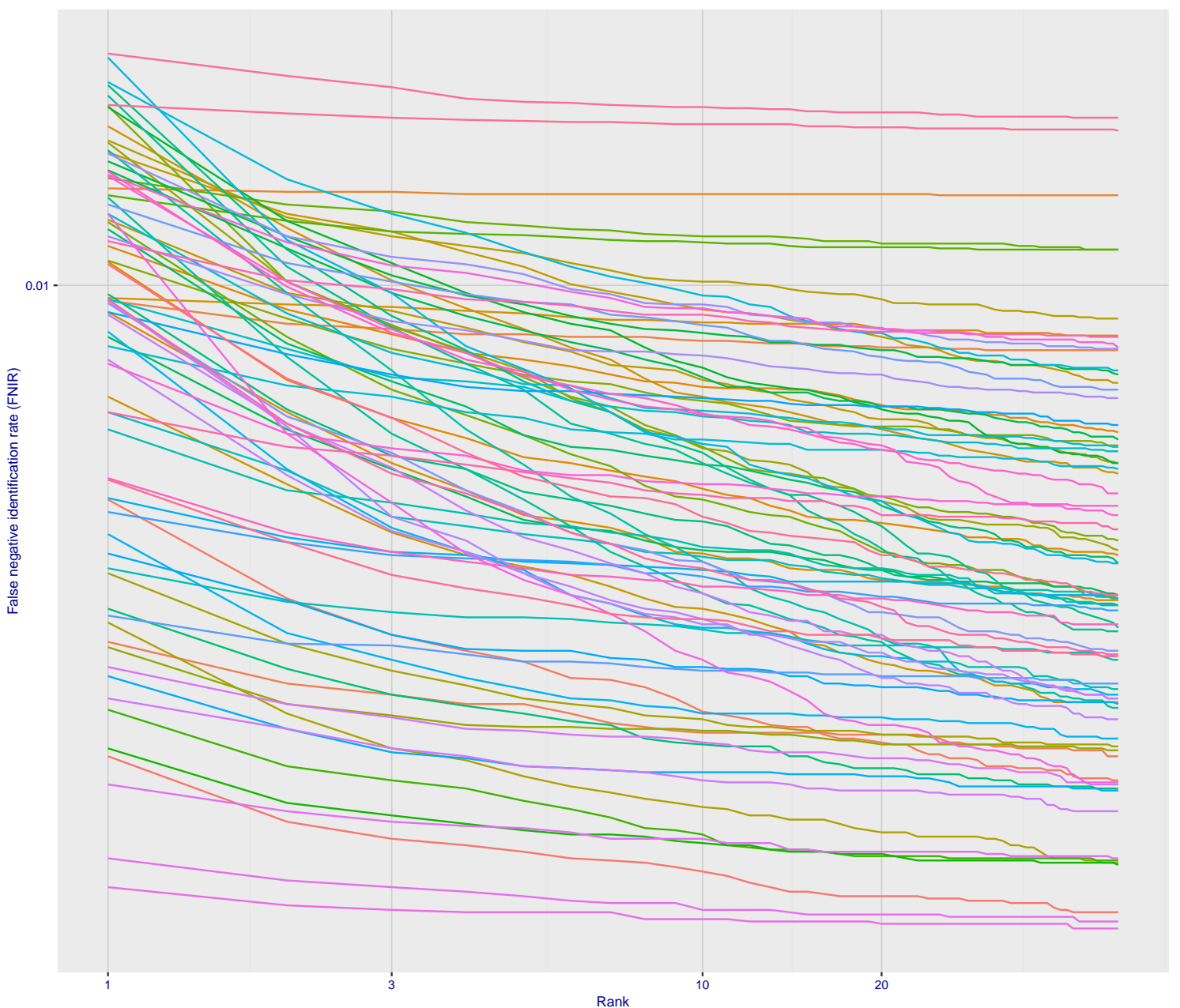
T = 0 → Investigation  
T > 0 → Identification

Figure 124: [Webcam Dataset] Identification miss rates vs. rank. The results apply to cross-domain recognition in which webcams are searched against enrolled mugshots. The FNIR values are higher than those for mugshot-mugshot identification due to low image resolution, lighting and less constrained subject pose in webcam images - see Figure 6.

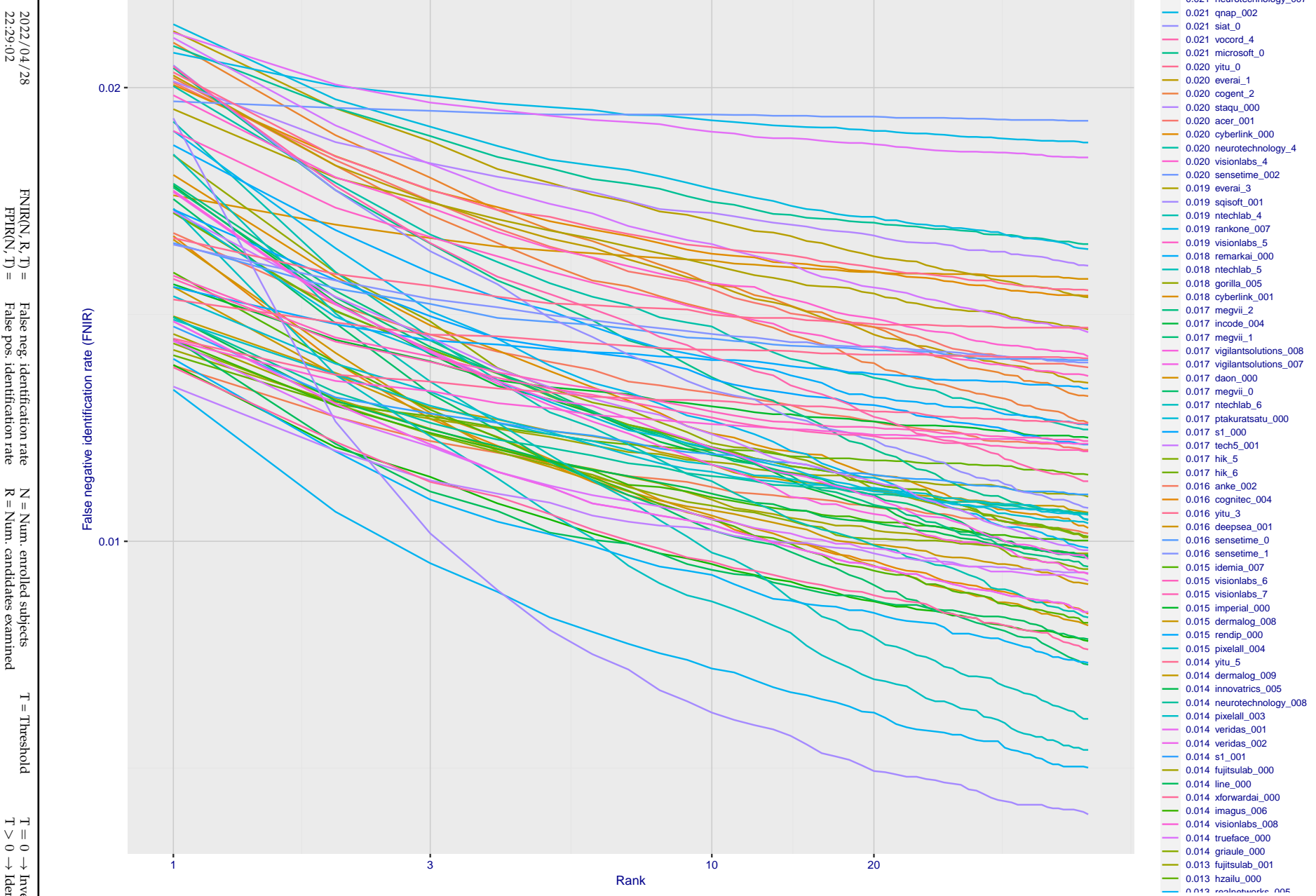


Figure 125: [Webcam Dataset] Identification miss rates vs. rank. The results apply to cross-domain recognition in which webcams are searched against enrolled mugshots. The FNIR values are higher than those for mugshot-mugshot identification due to low image resolution, lighting and less constrained subject pose in webcam images - see Figure 6.

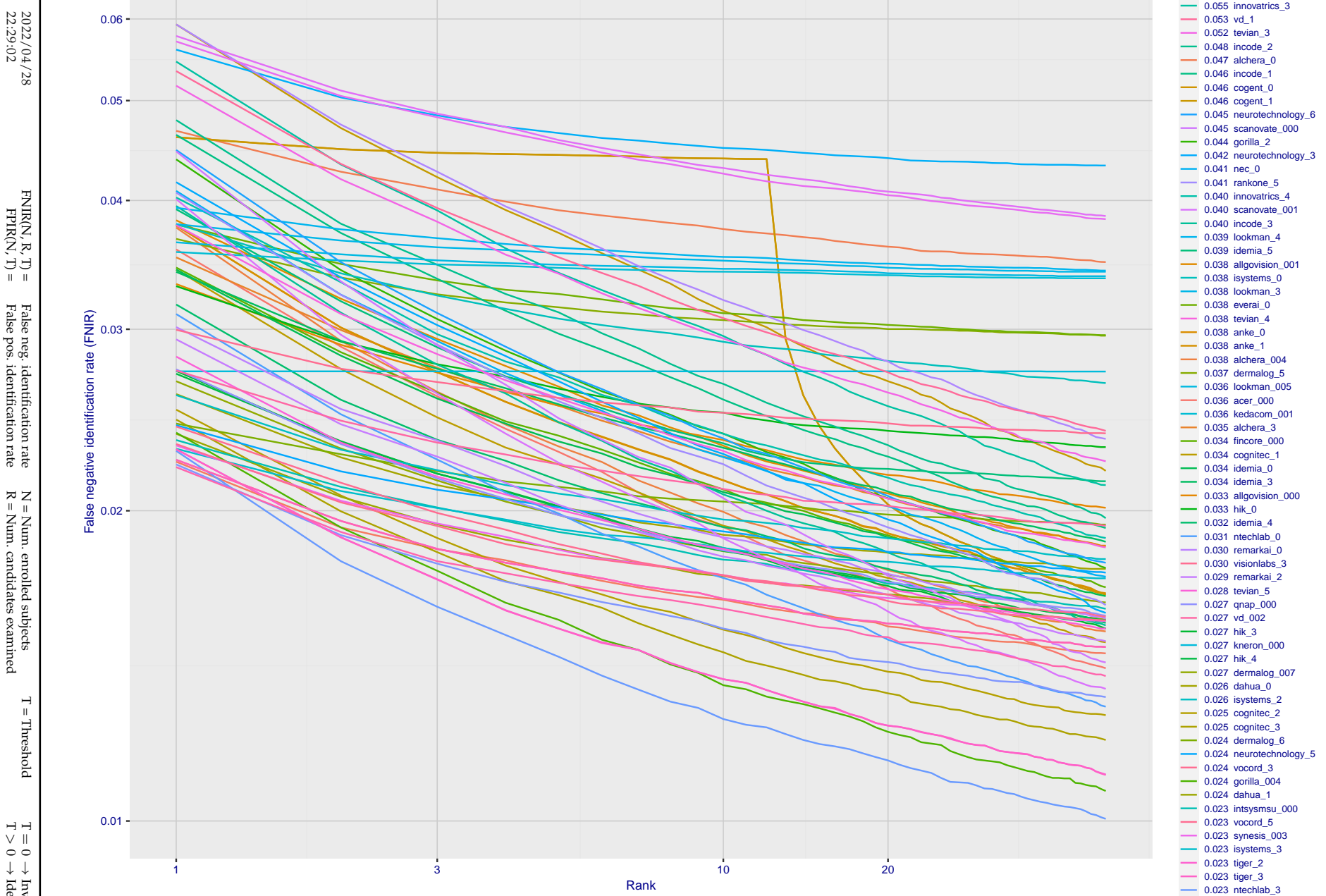


Figure 126: [Webcam Dataset] Identification miss rates vs. rank. The results apply to cross-domain recognition in which webcams are searched against enrolled mugshots. The FNIR values are higher than those for mugshot-mugshot identification due to low image resolution, lighting and less constrained subject pose in webcam images - see Figure 6.

2022/04/28  
22:29:02  
FNIR(N, R, T) = False neg. identification rate  
FPTR(N, T) = False pos. identification rate  
N = Num. enrolled subjects  
R = Num. candidates examined  
T = Threshold  
T = 0 → Investigation  
T > 0 → Identification

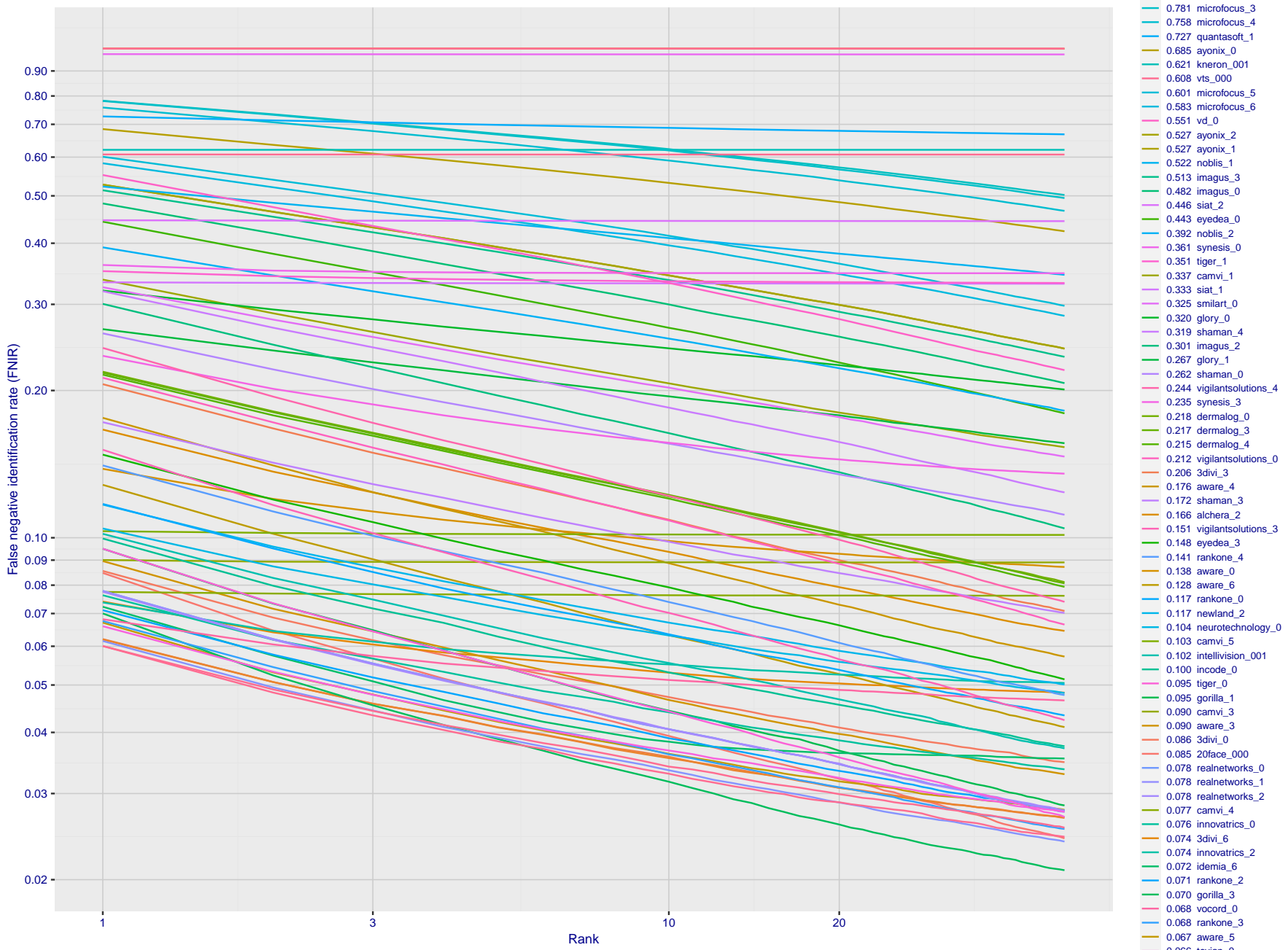
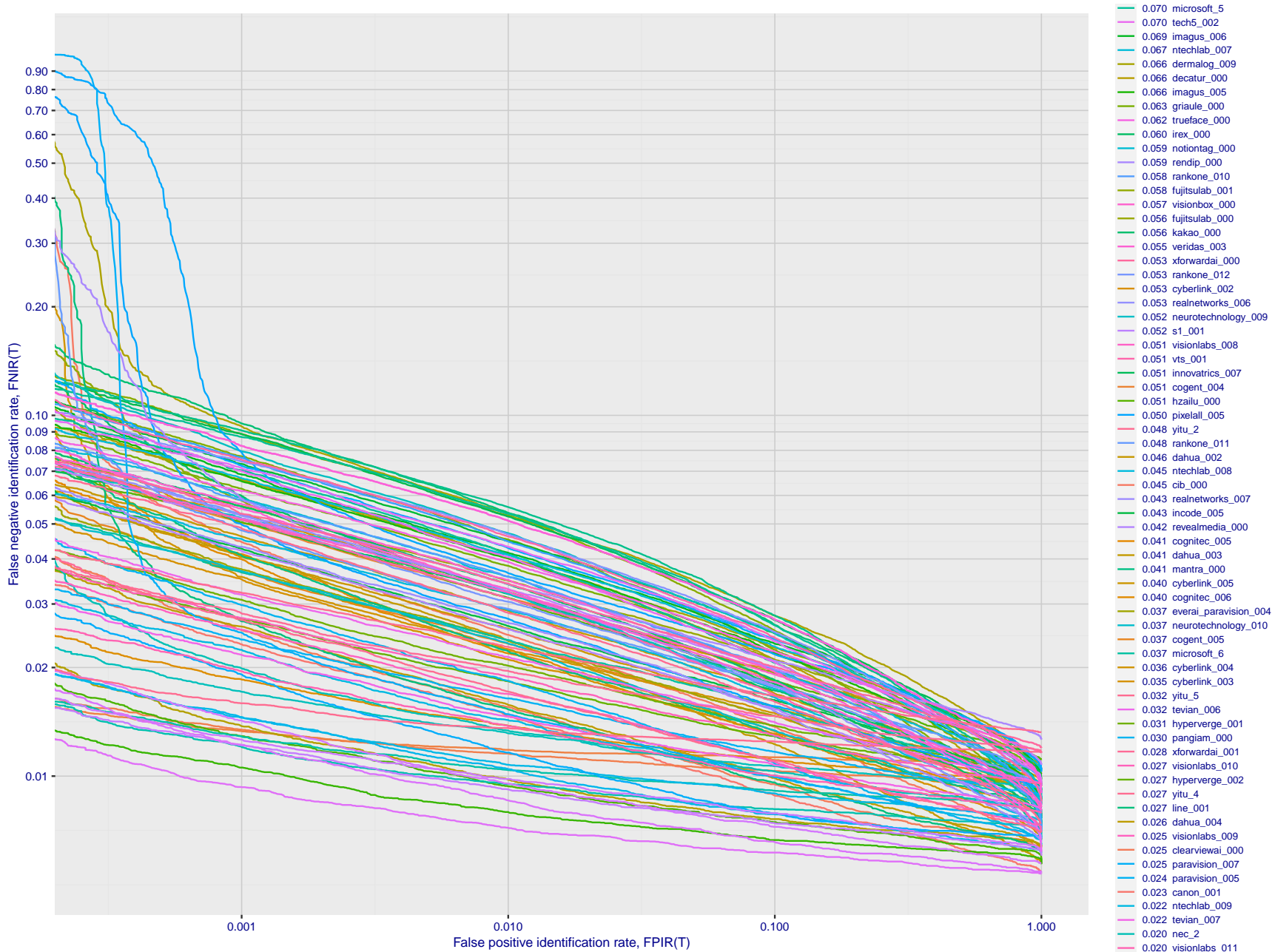


Figure 127: [Webcam Dataset] Identification miss rates vs. rank. The results apply to cross-domain recognition in which webcams are searched against enrolled mugshots. The FNIR values are higher than those for mugshot-mugshot identification due to low image resolution, lighting and less constrained subject pose in webcam images - see Figure 6.

2022/04/28 22:29:02	$\text{FNIR}(N, R, T) =$ $\text{FPTR}(N, T) =$	False neg. identification rate False pos. identification rate	$N =$ Num. enrolled subjects $R =$ Num. candidates examined	$T =$ Threshold $T > 0 \rightarrow$ Identification	$T = 0 \rightarrow$ Investigation
------------------------	---	--	--	---	-----------------------------------

2022/04/28  
22:29:02FNIR(N, R, T) = False neg. identification rate  
FPIR(N, T) = False pos. identification rateN = Num. enrolled subjects  
R = Num. candidates examined

T = Threshold

T = 0 → Investigation  
T > 0 → Identification

**Figure 128: [Webcam Dataset] Identification miss rates vs. false positive rates.** The results apply to cross-domain recognition in which webcams are searched against enrolled mugshots. The FNIR values are higher than those for mugshot-mugshot identification due to low image resolution, lighting and less constrained subject pose in webcam images - see Figure 6.

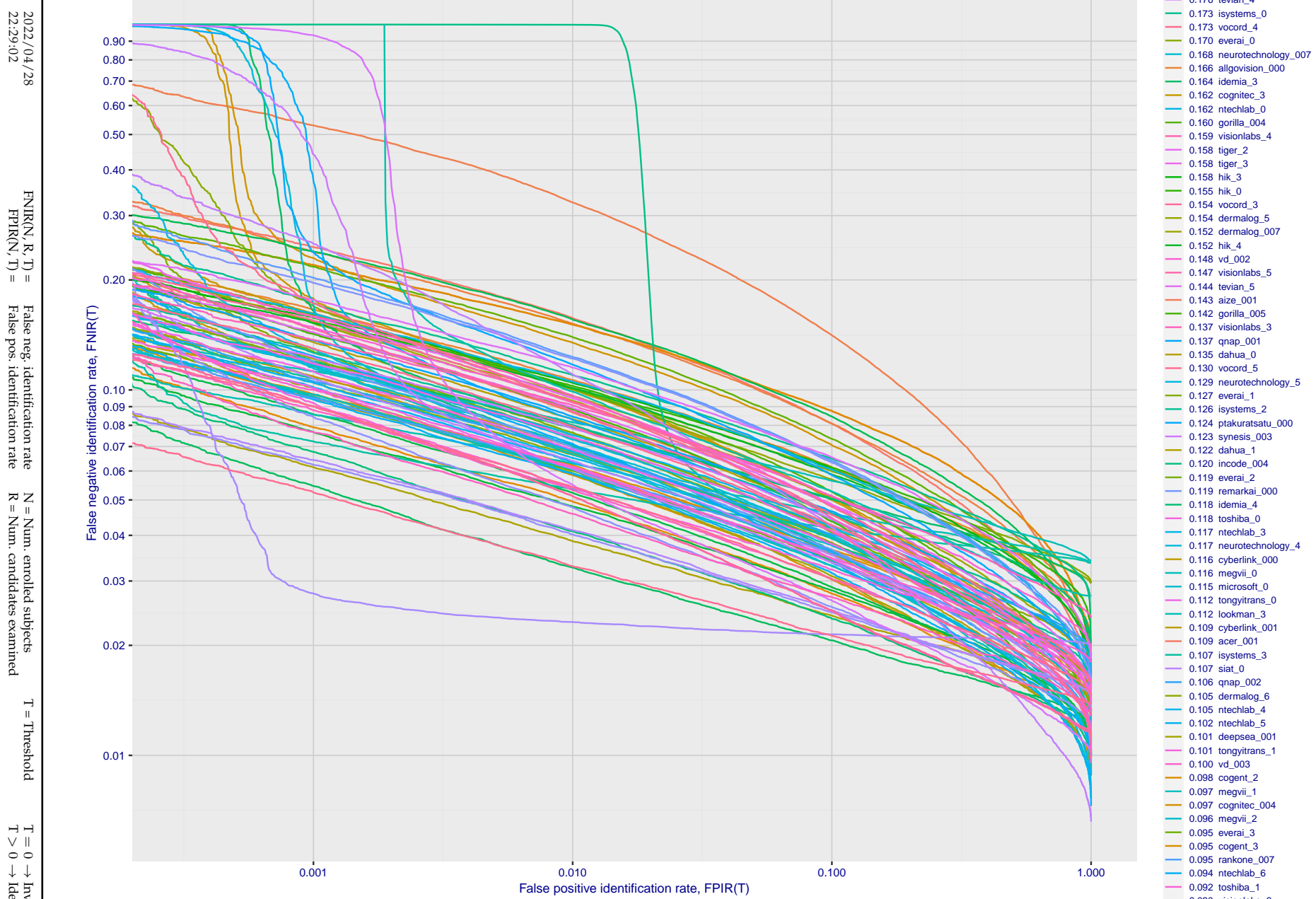
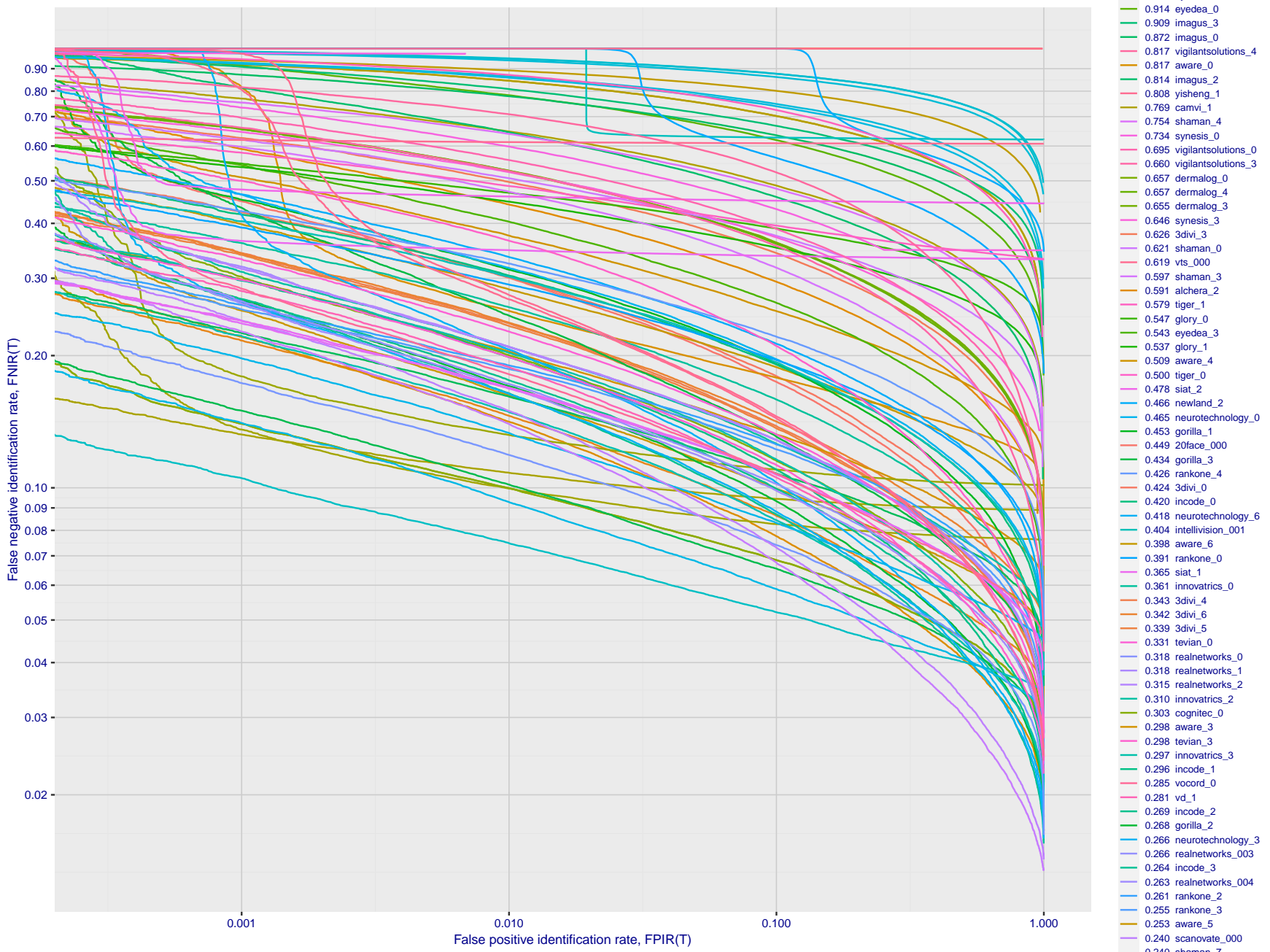


Figure 129: [Webcam Dataset] Identification miss rates vs. false positive rates. The results apply to cross-domain recognition in which webcams are searched against enrolled mugshots. The FNIR values are higher than those for mugshot-mugshot identification due to low image resolution, lighting and less constrained subject pose in webcam images - see Figure 6.

2022/04/28  
22:29:02  
 $\text{FNIR}(N, R, T) =$  False neg. identification rate  
 $\text{FPIR}(N, T) =$  False pos. identification rate  
 $N =$  Num. enrolled subjects  
 $R =$  Num. candidates examined  
 $T =$  Threshold  
 $T = 0 \rightarrow$  Investigation  
 $T > 0 \rightarrow$  Identification



**Figure 130: [Webcam Dataset] Identification miss rates vs. false positive rates.** The results apply to cross-domain recognition in which webcams are searched against enrolled mugshots. The FNIR values are higher than those for mugshot-mugshot identification due to low image resolution, lighting and less constrained subject pose in webcam images - see Figure 6.

## Appendix E Accuracy for profile-view to frontal recognition

Figures 131 - 133 gives accuracy results for searching 100 000 mated and 100 000 non-mated profile-view images against the same FRVT 2018 frontal enrollment dataset,  $N = 1\,600\,000$ , used in the main mugshot trials. This experiment corresponds to row-13 of Table 1. An example of profile-view image is given in Figure 7.

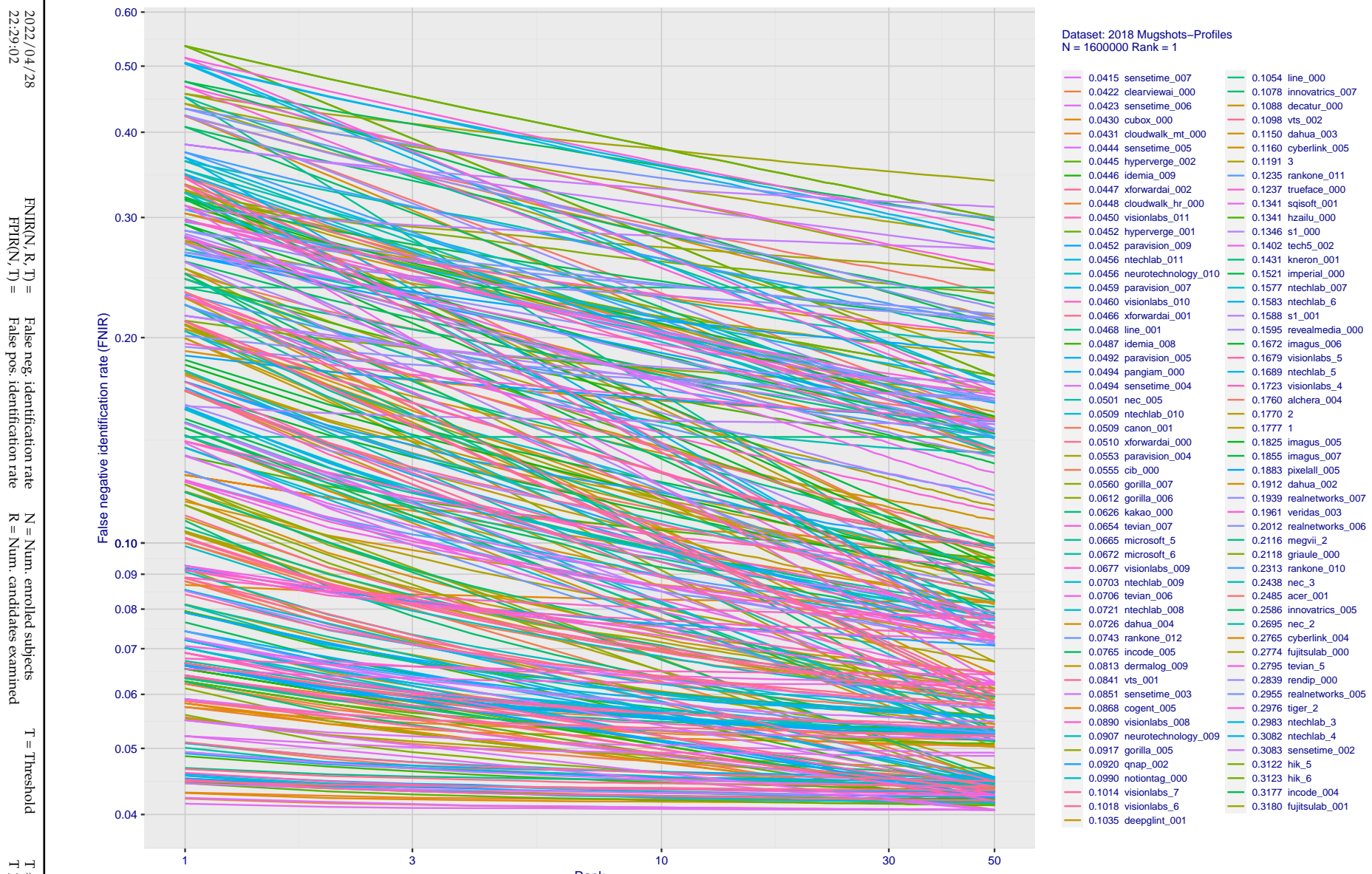


**Figure 131: [Mugshot and profile-view dataset] Rank-based accuracy.** For some of the more accurate Phase 3 algorithms the figure plots error tradeoff characteristics for frontal and profile-view searches into an enrolled set of  $N = 1\,600\,000$  frontal images. Note that some algorithms fail on profile-view images with  $\text{FNIR} \rightarrow 1$  - this evaluation did not ask developers to provide profile-view capability. Some algorithms, on the other hand, give  $\text{FNIR}$  approaching that for frontal-view searches using c. 2010 algorithms. The best result is that 91% of profile-view searches yield the correct mate at rank 1, and better than 94% in the top-50 candidates.

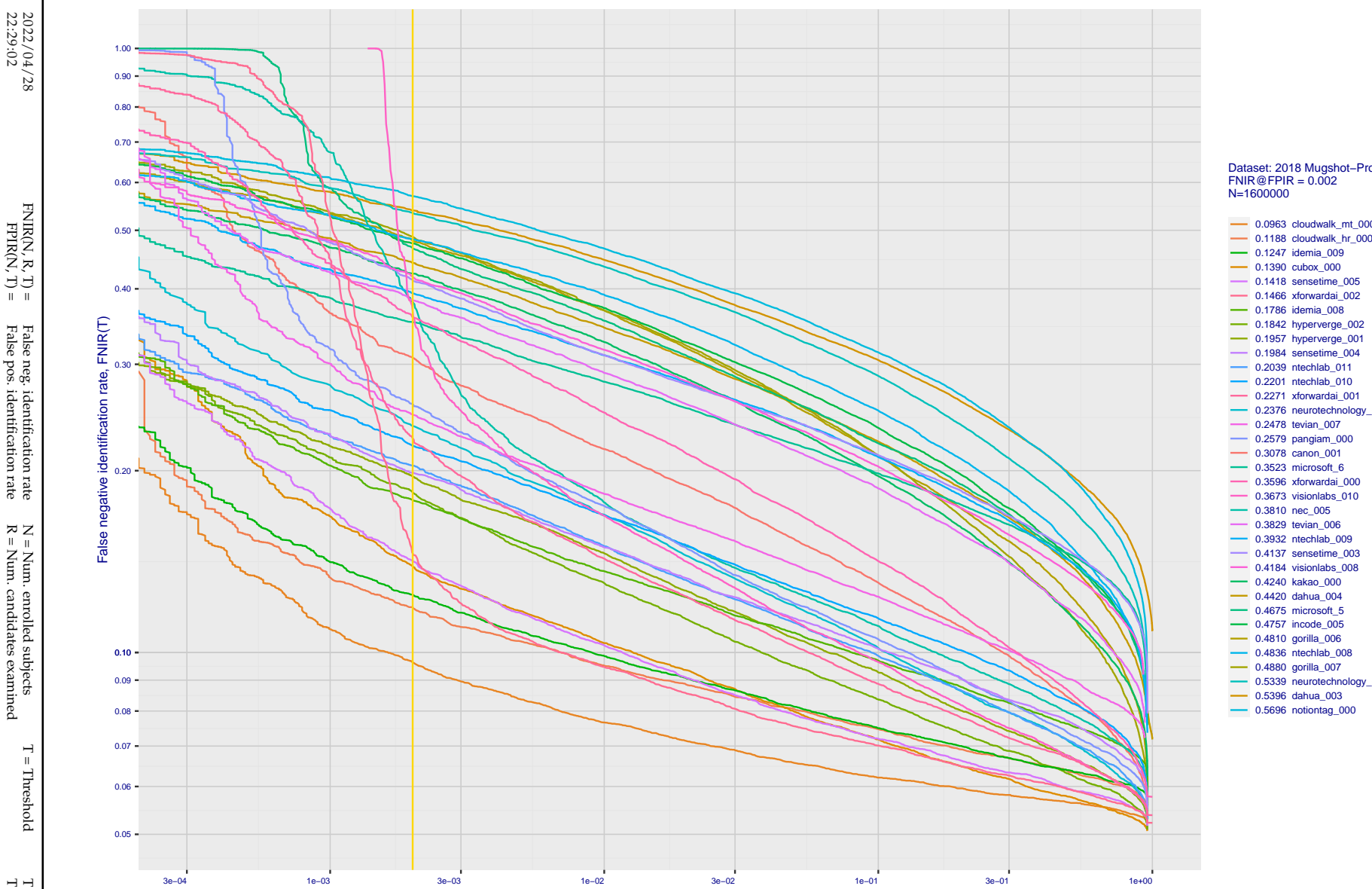


**Figure 132: [Mugshot and profile-view dataset] Threshold-based accuracy.** For some of the more accurate Phase 3 algorithms the figure plots error tradeoff characteristics for frontal and profile-view searches into an enrolled set of  $N = 1\,600\,000$  frontal images. Note that some algorithms fail on profile-view images with  $\text{FNIR} \rightarrow 1$  - this evaluation did not ask developers to provide profile-view capability. Some algorithms, on the other hand, give  $\text{FNIR}$  approaching that for frontal-view searches using c. 2010 algorithms.

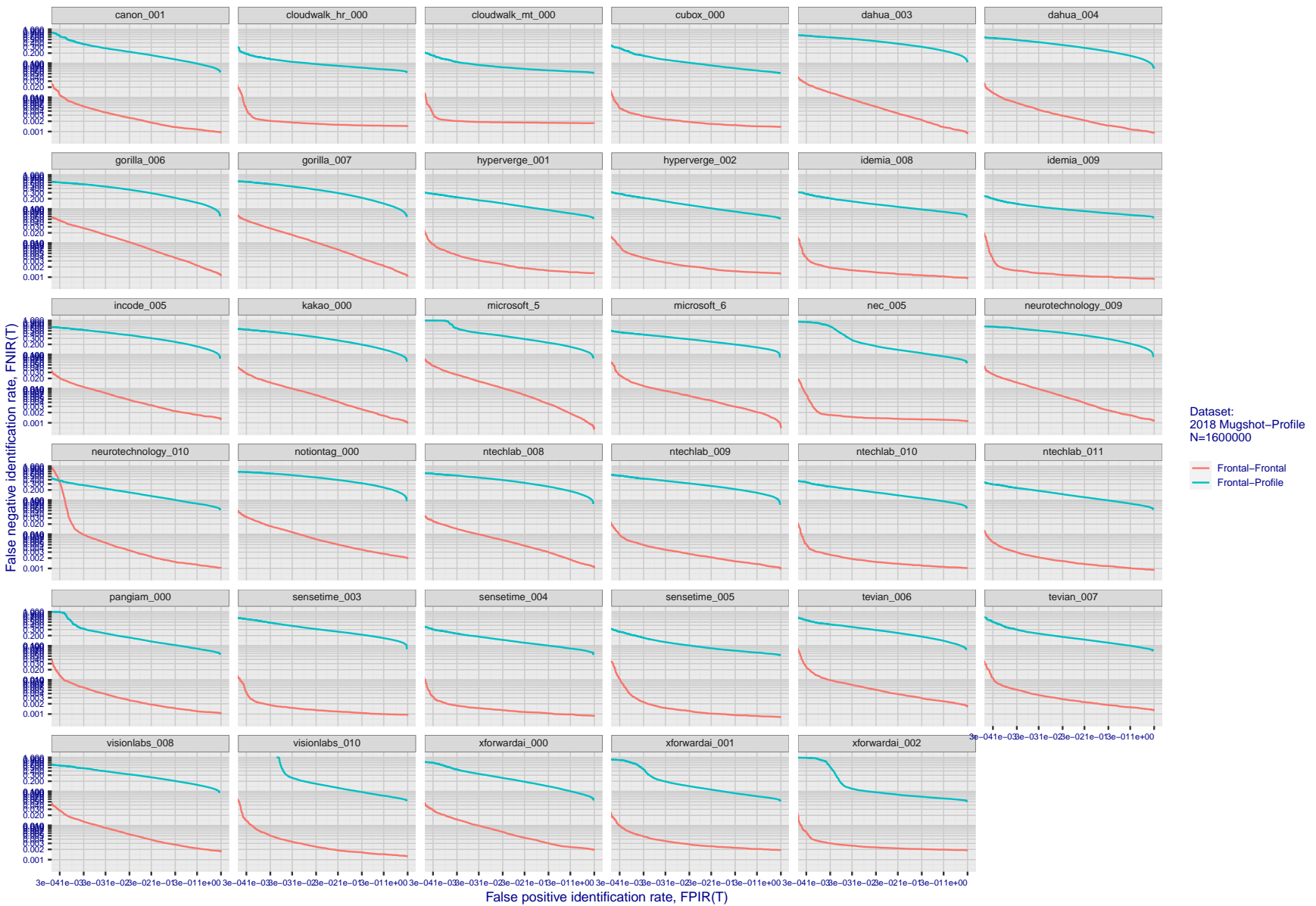


**Figure 133: [Mugshot and profile-view dataset] Speed-accuracy tradeoff.** For some of the more accurate Phase 3 algorithms the figure plots error tradeoff characteristics for frontal and profile-view searches into an enrolled set of  $N = 1\,600\,000$  frontal images. Some algorithms fail on profile-view images with  $\text{FNIR} \rightarrow 1$  - this evaluation did not ask developers to provide profile-view capability. Some algorithms, on the other hand, give  $\text{FNIR}$  approaching that for frontal-view searches using c. 2010 algorithms. Blue lines connect points of equal threshold from which it is evident that some algorithms would give markedly higher false positive outcomes if profile-view images were searched in a system configured for frontal searches. This would be a vulnerability in an access control system.

## Appendix F Search duration

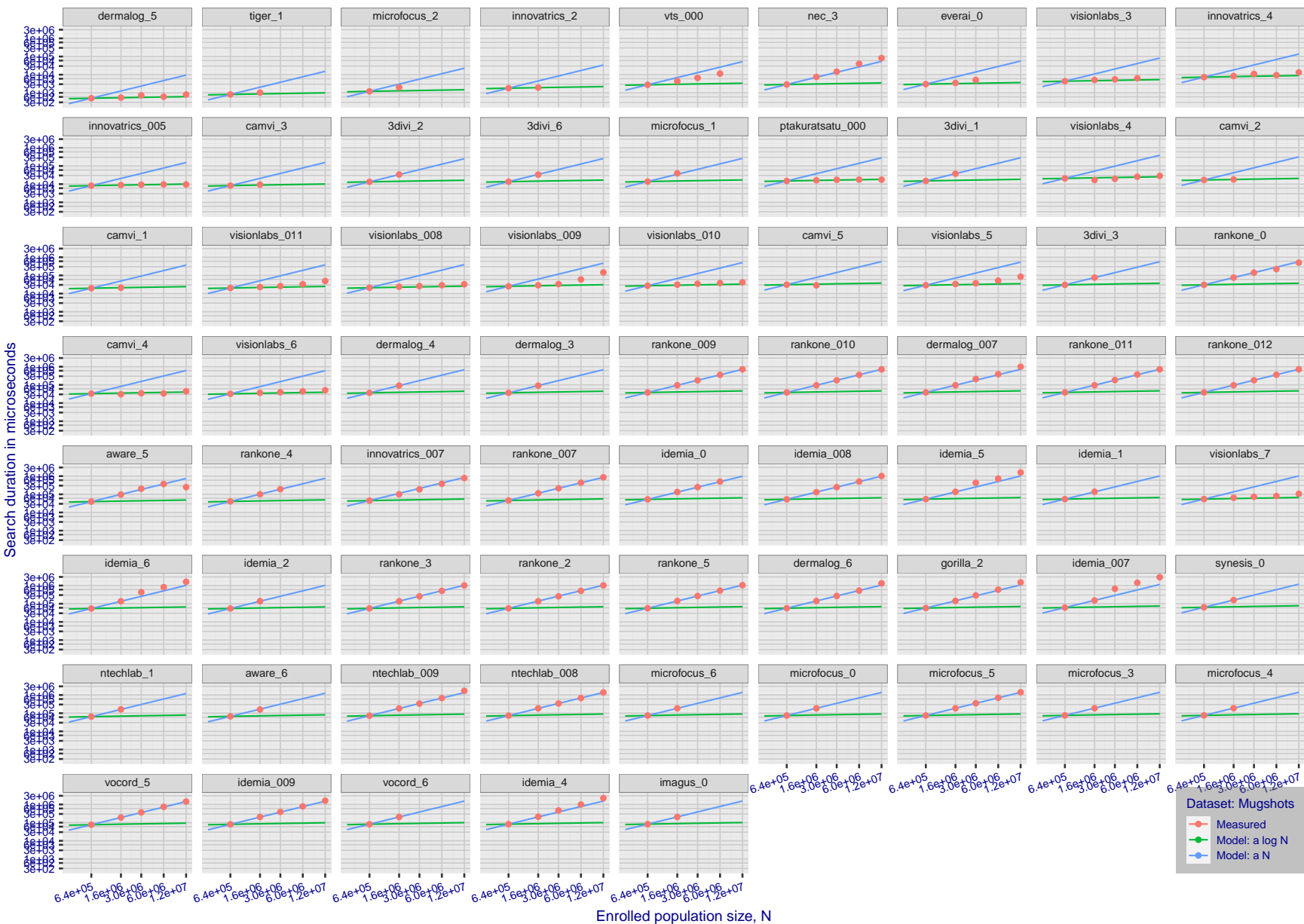
As in and prior tests, this section documents search speeds spanning three orders of magnitude. In applications where search volumes are high enough, this will have implications for hardware requirements especially for large N or when search duration is appreciably larger than the time it takes to prepare a template from the search image(s). Further, given very large (and growing) operational databases, the scalability of algorithms is important. It has been reported previously [8] that search duration can scale sublinearly with enrolled population size N. Further there has been considerable recent research on indexing, exact [13] and approximate nearest neighbor search [1,13] and fast-search [14,16].

Figure 134 charts the search duration measurements presented earlier in Tables 2 - 4.

- ▷ Most algorithms scale linearly. For those in that category, there is a wide range in speed with search durations ranging from 82 milliseconds for a 12 million gallery (for NEC-3) to more than 40 seconds (for Yitu-3, Toshiba-2) and even higher for less accurate algorithms.
- ▷ Some developers (Camvi, Dermalog, EverAI, Innovatrics, and Visionlabs) provide algorithms whose template search durations grow approximately logarithmically i.e.  $T(N) \sim \log N$  with the constant  $a$  varying between implementations. In the figure this model is fit using the point  $T(1) = 0$ , and  $T(640\,000)$ . This very sublinear behaviour affords extremely fast search times in very large galleries. One caveat for the sublinear algorithms is that their fast-search data structures can require considerable computation time - on the order of hours - for N in the millions, and this scales mildly super-linearly, i.e.  $O(N^b)$ ,  $b > 1$ . There are exceptions: the Camvi algorithms take minutes; and Innovatrics' scale sublinearly.

---

2022/04/28  
22:29:02      FNIR(N, R, T) = False neg. identification rate  
                  FPIR(N, T) = False pos. identification rate  
N = Num. enrolled subjects  
R = Num. candidates examined  
T = Threshold  
T = 0 → Investigation  
T > 0 → Identification

2022/04/28  
22:29:02FNIR(N, R, T) = False neg. identification rate  
FPFR(N, T) = False pos. identification rateN = Num. enrolled subjects  
R = Num. candidates examined  
T = ThresholdT = 0 → Investigation  
T > 0 → Identification

**Figure 134: [Mugshot Dataset] Search duration vs. enrolled population size.** In red are the actual point durations measured on a single c. 2016 core. The blue shows linear growth from  $N = 640\,000$ . The green line shows logarithmic growth from that point to  $N = 1\,600\,000$ . Note the sublinear growth from algorithms from Camvi, Dermalog, EverAI, Innovatrics, and Visionlabs. The tiger\_1 algorithm is also sublinear, but inaccurate and inoperable at  $N \geq 3000000$ . This capability sometimes comes at the additional expense of converting a linear gallery data structure into whatever fast-search data structure is used. Note that search times are sometimes dominated by the template generation times shown in Table 23.

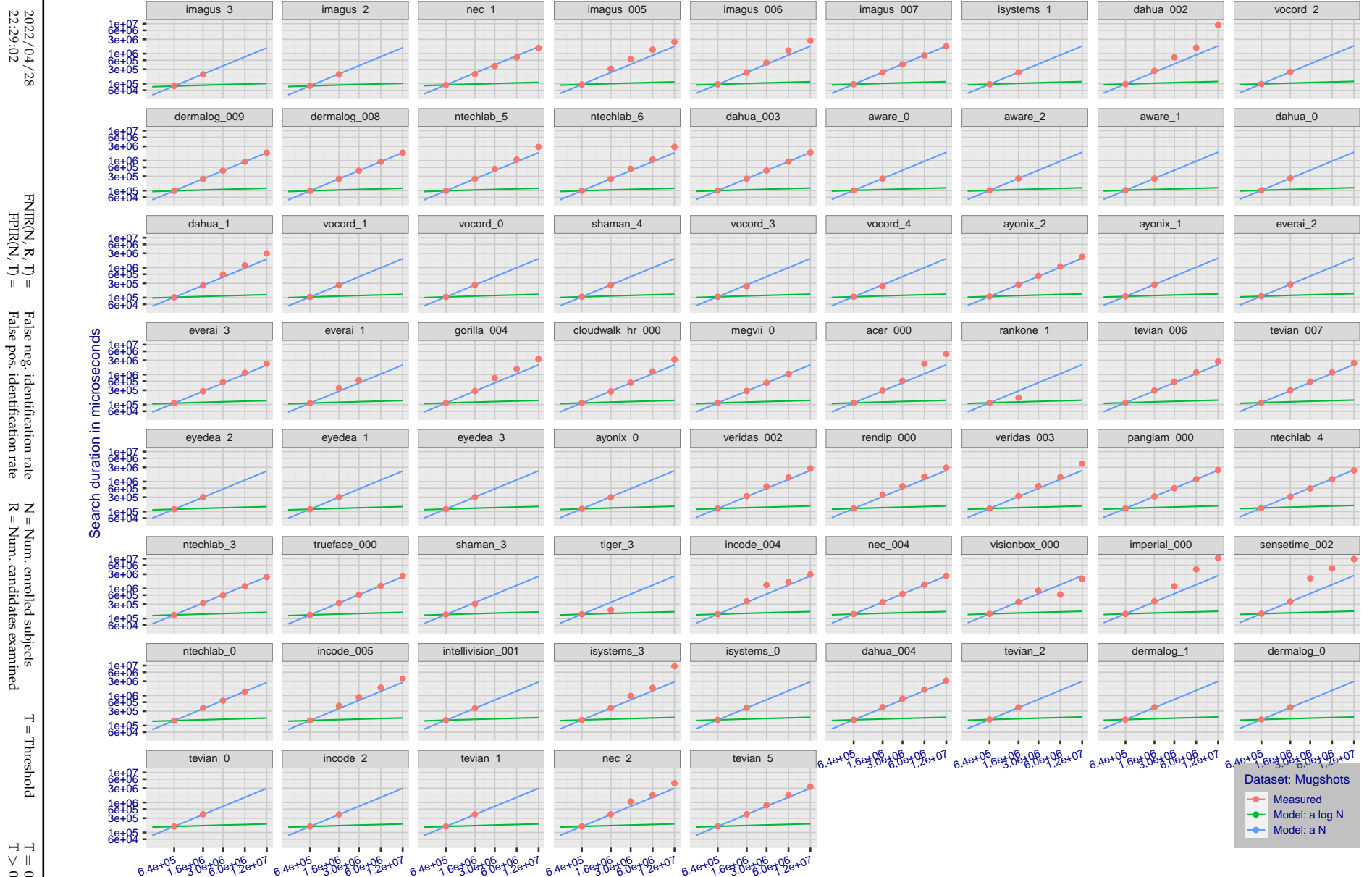


Figure 135: [Mugshot Dataset] Search duration vs. enrolled population size. In red are the actual point durations measured on a single c. 2016 core. The blue shows linear growth from  $N = 640\,000$ . The green line shows logarithmic growth from that point to  $N = 1\,600\,000$ . Note the sublinear growth from algorithms from Camvi, Dermalog, EverAI, Innovatrics, and Visionlabs. The tiger\_1 algorithm is also sublinear, but inaccurate and inoperable at  $N \geq 3000000$ . This capability sometimes comes at the additional expense of converting a linear gallery data structure into whatever fast-search data structure is used. Note that search times are sometimes dominated by the template generation times shown in Table 23.

2022/04/28  
22:29:02FNIR(N, R, T) = False neg. identification rate  
FPTR(N, T) = False pos. identification rateN = Num. enrolled subjects  
R = Num. candidates examined

T = Threshold

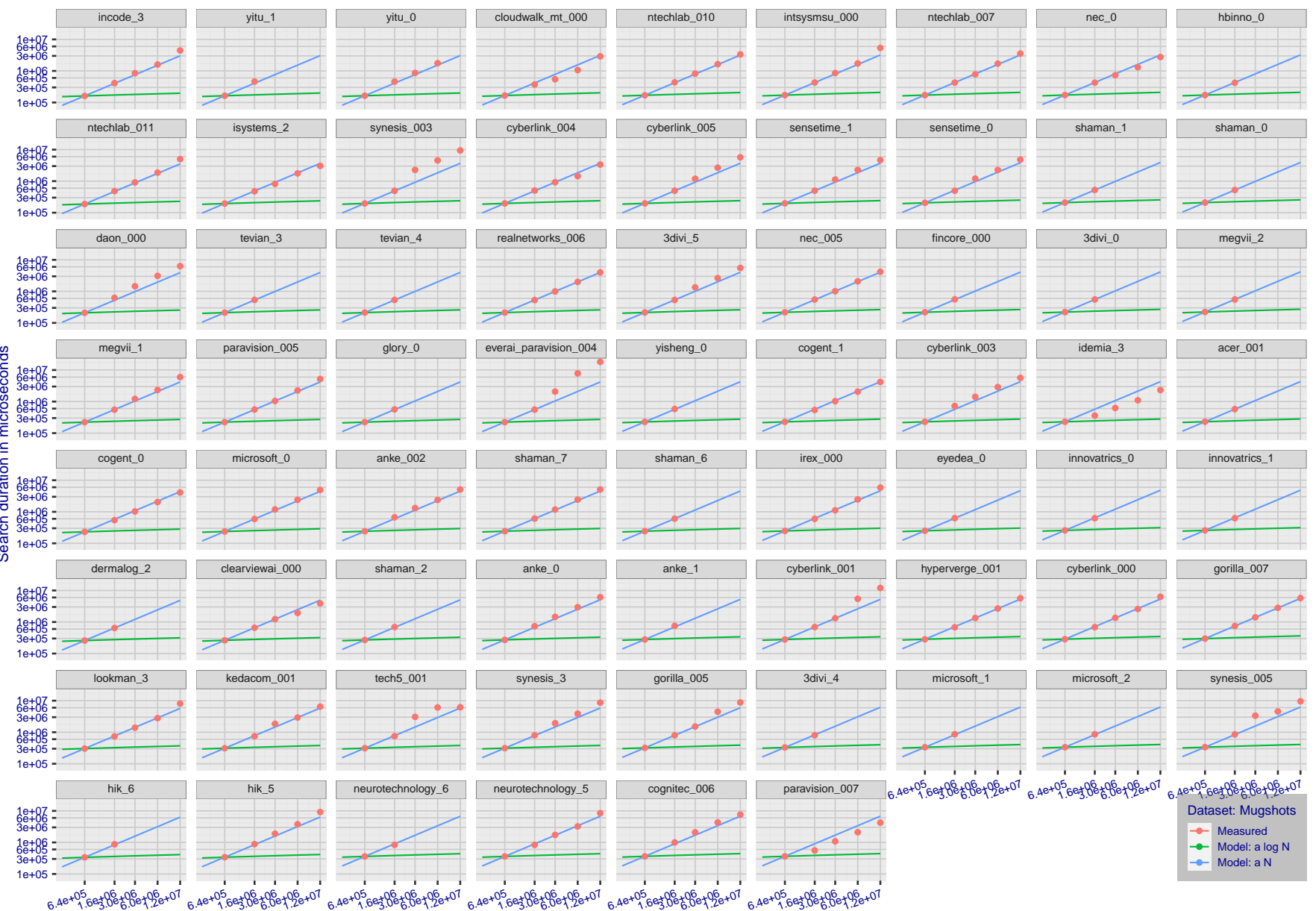
T = 0 → Investigation  
T > 0 → Identification

Figure 136: [Mugshot Dataset] Search duration vs. enrolled population size. In red are the actual point durations measured on a single c. 2016 core. The blue shows linear growth from  $N = 640\,000$ . The green line shows logarithmic growth from that point to  $N = 1\,600\,000$ . Note the sublinear growth from algorithms from Camvi, Dermalog, EverAI, Innovatrics, and Visionlabs. The tiger\_1 algorithm is also sublinear, but inaccurate and inoperable at  $N \geq 3000000$ . This capability sometimes comes at the additional expense of converting a linear gallery data structure into whatever fast-search data structure is used. Note that search times are sometimes dominated by the template generation times shown in Table 23.

2022/04/28  
22:29:02FNIR(N, R, T) = False neg. identification rate  
FPR(N, T) = False pos. identification rateN = Num. enrolled subjects  
R = Num. candidates examined

T = Threshold

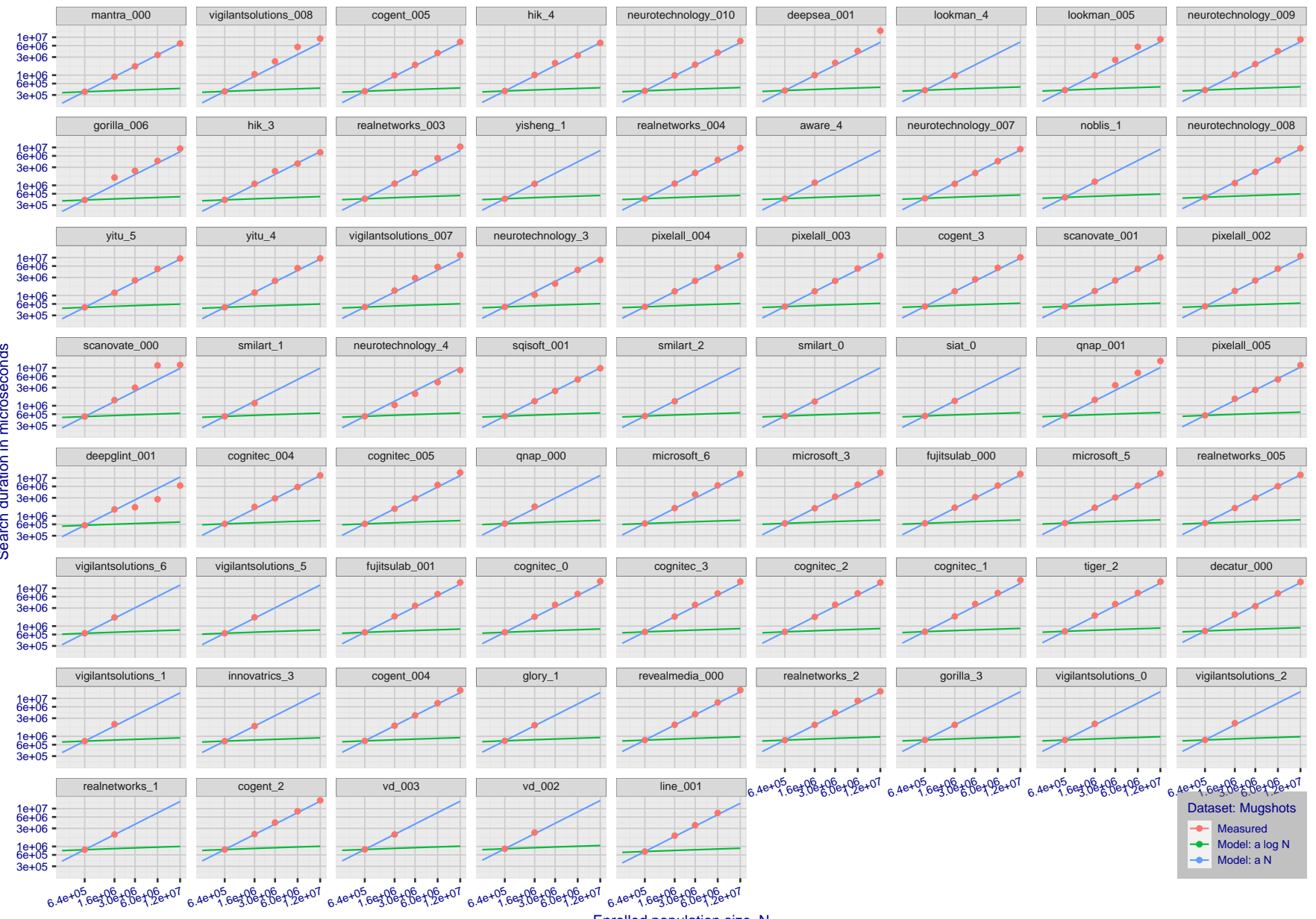
T = 0 → Investigation  
T > 0 → Identification

Figure 137: [Mugshot Dataset] Search duration vs. enrolled population size. In red are the actual point durations measured on a single c. 2016 core. The blue shows linear growth from  $N = 640\,000$ . The green line shows logarithmic growth from that point to  $N = 1\,600\,000$ . Note the sublinear growth from algorithms from Camvi, Dermalog, EverAI, Innovatrics, and Visionlabs. The tiger\_1 algorithm is also sublinear, but inaccurate and inoperable at  $N \geq 3000000$ . This capability sometimes comes at the additional expense of converting a linear gallery data structure into whatever fast-search data structure is used. Note that search times are sometimes dominated by the template generation times shown in Table 23.

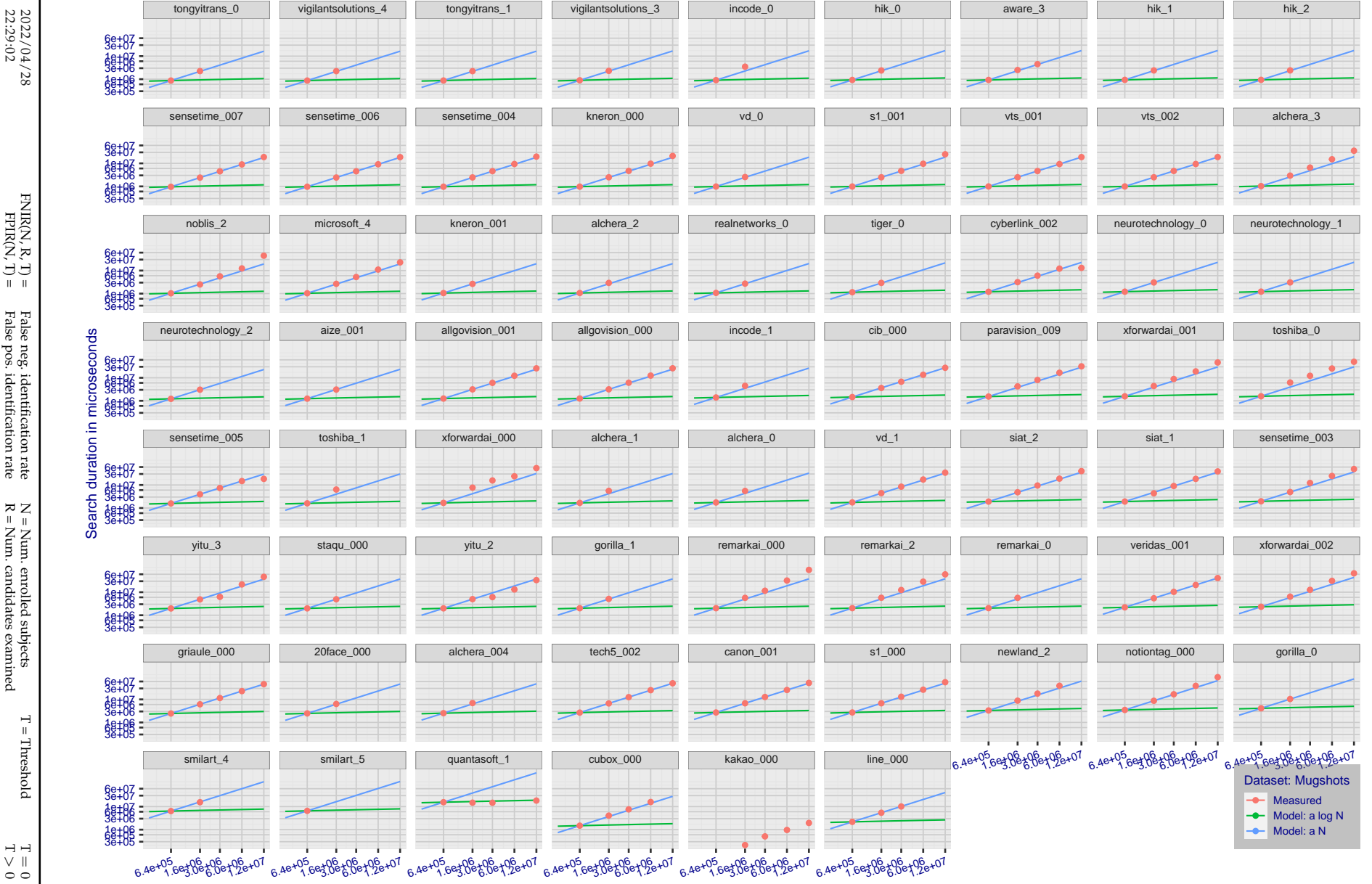


Figure 138: [Mugshot Dataset] Search duration vs. enrolled population size. In red are the actual point durations measured on a single c. 2016 core. The blue shows linear growth from  $N = 640\,000$ . The green line shows logarithmic growth from that point to  $N = 1\,600\,000$ . Note the sublinear growth from algorithms from Camvi, Dermalog, EverAI, Innovatrics, and Visionlabs. The tiger\_1 algorithm is also sublinear, but inaccurate and inoperable at  $N \geq 3000000$ . This capability sometimes comes at the additional expense of converting a linear gallery data structure into whatever fast-search data structure is used. Note that search times are sometimes dominated by the template generation times shown in Table 23.

2022/04/28  
22:29:02FNIR(N, R, T) = False neg. identification rate  
FPFR(N, T) = False pos. identification rateN = Num. enrolled subjects  
R = Num. candidates examined

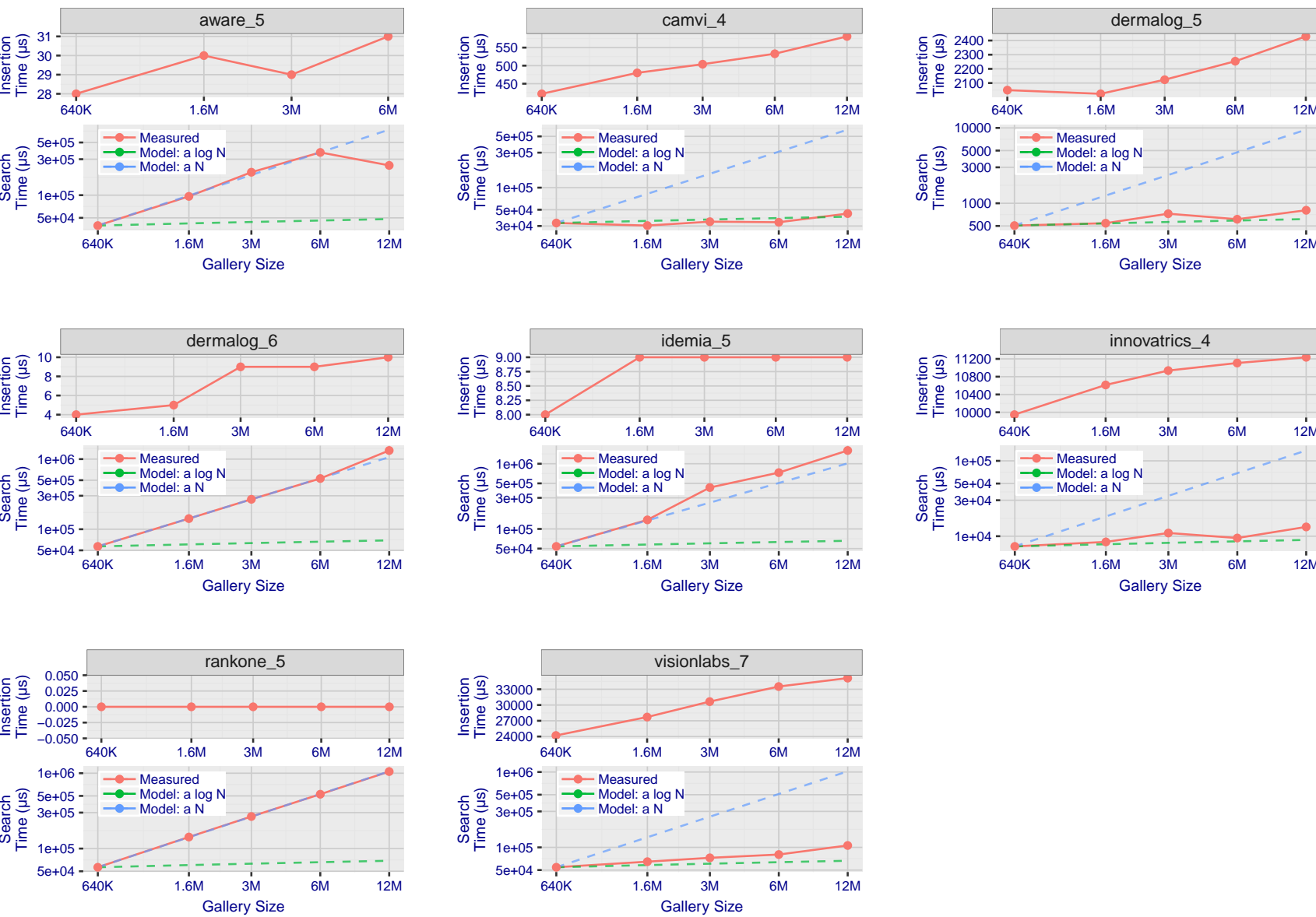
T = Threshold

T = 0 → Investigation  
 $T > 0 \rightarrow$  Identification

## Appendix G Gallery Insertion Timing

2022/04/28  
22:29:02FNIR(N, R, T) = False neg. identification rate  
FPIR(N, T) = False pos. identification rateN = Num. enrolled subjects  
R = Num. candidates examined

T = Threshold

T = 0 → Investigation  
T > 0 → Identification

**Figure 139: [Mugshot Dataset] Gallery insertion duration vs. enrolled population size.** This chart plots the time it takes to insert a single template into a finalized gallery, illustrated over increasing gallery sizes. For reference, search times on finalized galleries of corresponding sizes are plotted right underneath. Gallery insertion time plots were generated on algorithms that 1) successfully implemented gallery insertion with no errors and 2) that were run on galleries with  $N$  up to 12 000 000. Generally, only the more accurate algorithms were run on galleries with  $N$  up to 12 000 000.

2022/04/28  
22:29:02FNIR(N, R, T) = False neg. identification rate  
FPTR(N, T) = False pos. identification rateN = Num. enrolled subjects  
R = Num. candidates examinedT = Threshold  
T = 0 → Investigation

T &gt; 0 → Identification

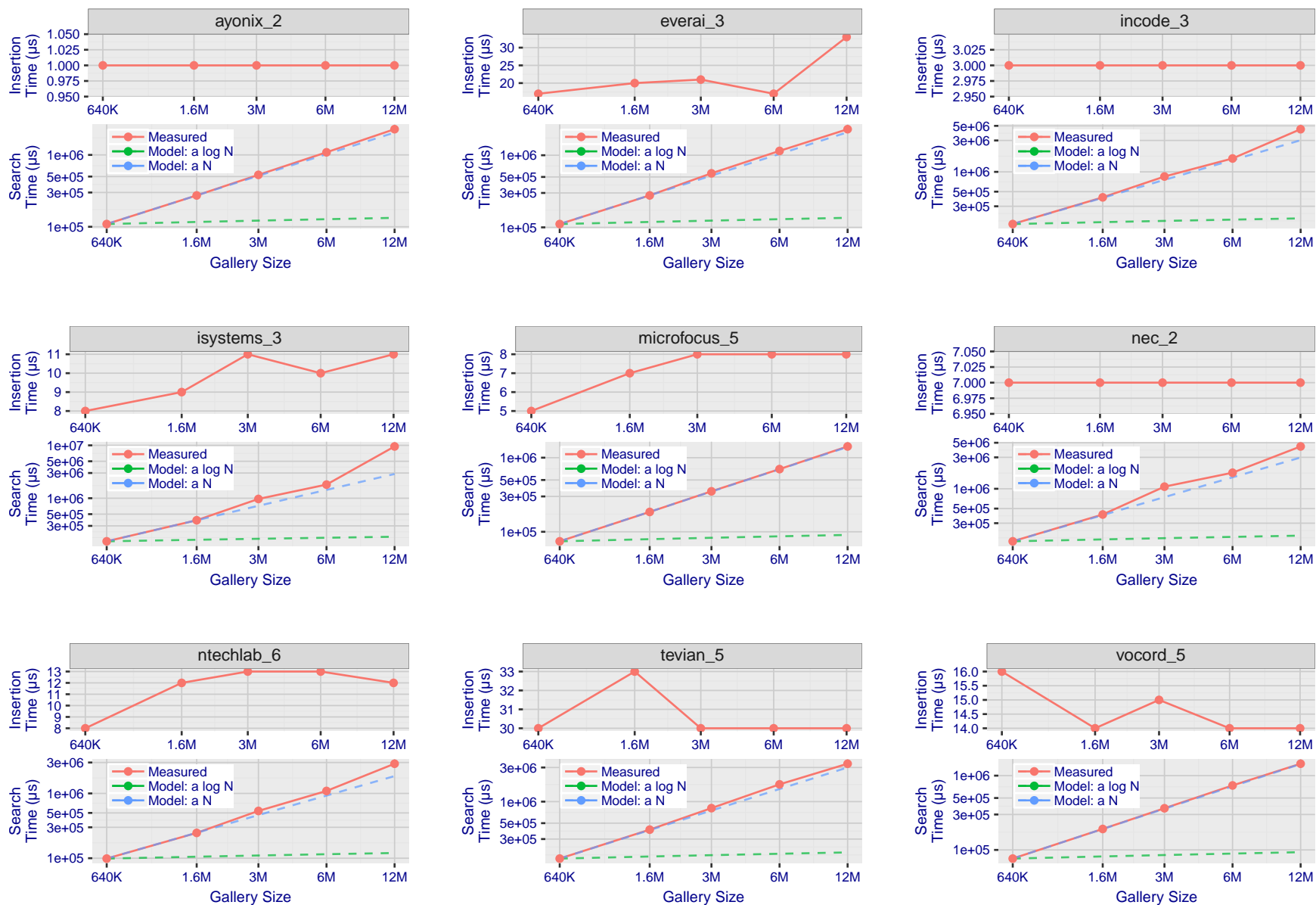


Figure 140: **[Mugshot Dataset] Gallery insertion duration vs. enrolled population size.** This chart plots the time it takes to insert a single template into a finalized gallery, illustrated over increasing gallery sizes. For reference, search times on finalized galleries of corresponding sizes are plotted right underneath. Gallery insertion time plots were generated on algorithms that 1) successfully implemented gallery insertion with no errors and 2) that were run on galleries with  $N$  up to 12 000 000. Generally, only the more accurate algorithms were run on galleries with  $N$  up to 12 000 000.

2022/04/28  
22:29:02FNIR(N, R, T) = False neg. identification rate  
FPIR(N, T) = False pos. identification rateN = Num. enrolled subjects  
R = Num. candidates examined

T = Threshold

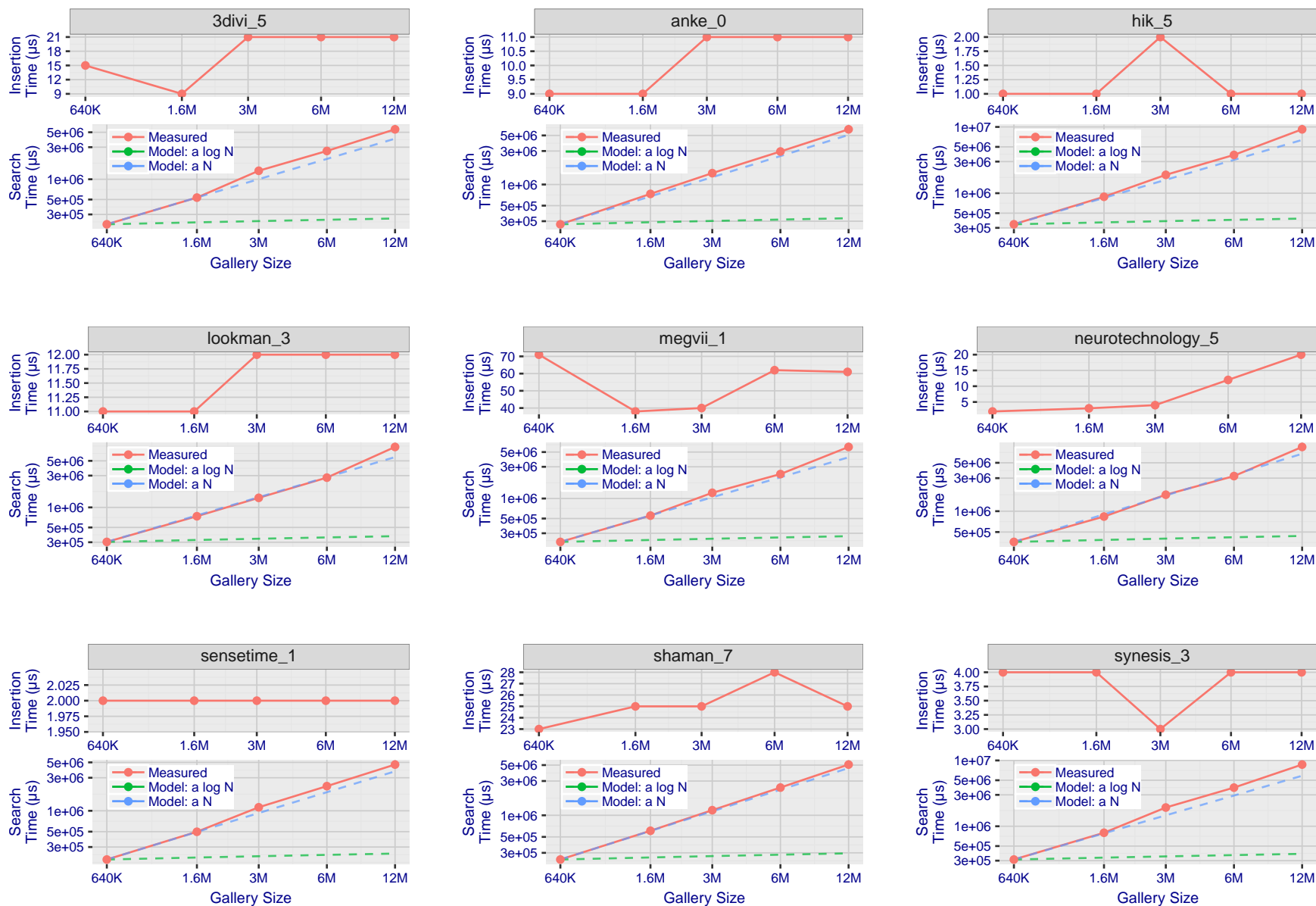
T = 0 → Investigation  
 $T > 0 \rightarrow$  Identification

Figure 141: [Mugshot Dataset] Gallery insertion duration vs. enrolled population size. This chart plots the time it takes to insert a single template into a finalized gallery, illustrated over increasing gallery sizes. For reference, search times on finalized galleries of corresponding sizes are plotted right underneath. Gallery insertion time plots were generated on algorithms that 1) successfully implemented gallery insertion with no errors and 2) that were run on galleries with  $N$  up to 12 000 000. Generally, only the more accurate algorithms were run on galleries with  $N$  up to 12 000 000.

2022/04/28  
22:29:02FNIR(N, R, T) = False neg. identification rate  
FPTR(N, T) = False pos. identification rateN = Num. enrolled subjects  
R = Num. candidates examinedT = Threshold  
T = 0 → Investigation

T &gt; 0 → Identification

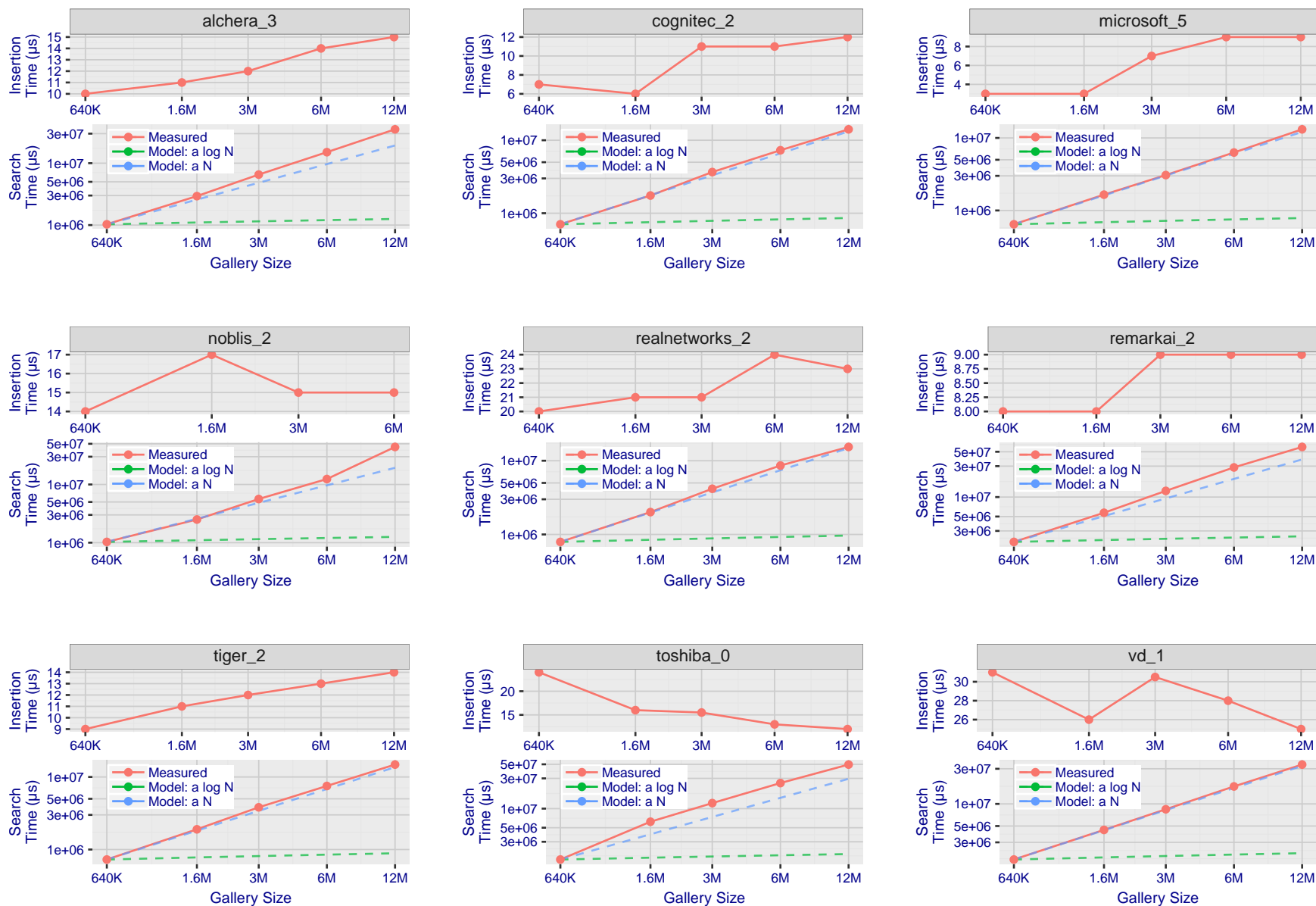


Figure 142: [Mugshot Dataset] Gallery insertion duration vs. enrolled population size. This chart plots the time it takes to insert a single template into a finalized gallery, illustrated over increasing gallery sizes. For reference, search times on finalized galleries of corresponding sizes are plotted right underneath. Gallery insertion time plots were generated on algorithms that 1) successfully implemented gallery insertion with no errors and 2) that were run on galleries with  $N$  up to 12 000 000. Generally, only the more accurate algorithms were run on galleries with  $N$  up to 12 000 000.

## References

- [1] Artem Babenko and Victor Lempitsky. Efficient indexing of billion-scale datasets of deep descriptors. In *The IEEE Conference on Computer Vision and Pattern Recognition (CVPR)*, June 2016.
- [2] L. Best-Rowden and A. K. Jain. Longitudinal study of automatic face recognition. *IEEE Transactions on Pattern Analysis and Machine Intelligence*, 40(1):148–162, Jan 2018.
- [3] Blumstein, Cohen, Roth, and Visher, editors. *Random parameter stochastic models of criminal careers*. National Academy of Sciences Press, 1986.
- [4] Thomas P. Bonczar and Lauren E. Glaze. Probation and parole in the united statesm 2007, statistical tables. Technical report, Bureau of Justice Statistics, December 2008.
- [5] White D., Kemp R. I., Jenkins R., Matheson M, and Burton A. M. Passport officers' errors in face matching. *PLoS ONE*, 9(8), 2014. e103510. doi:10.1371/journal.pone.0103510.
- [6] P. Grother, G. W. Quinn, and P. J. Phillips. Evaluation of 2d still-image face recognition algorithms. NIST Interagency Report 7709, National Institute of Standards and Technology, 8 2010. <http://face.nist.gov/mbe> as MBE2010 FRVT2010.
- [7] P. J. Grother, R. J. Micheals, and P. J. Phillips. Performance metrics for the frvt 2002 evaluation. In *Proceedings of Audio and Video Based Person Authentication Conference (AVBPA)*, June 2003.
- [8] Patrick Grother and Mei Ngan. Interagency report 8009, performance of face identification algorithms. *Face Recognition Vendor Test (FRVT)*, May 2014.
- [9] Patrick Grother, George Quinn, and Mei Ngan. Face in video evaluation (five) face recognition of non-cooperative subjects. Interagency Report 8173, National Institute of Standards and Technology, March 2017. <https://doi.org/10.6028/NIST.IR.8173>.
- [10] Patrick Grother, George W. Quinn, and Mei Ngan. Face recognition vendor test - still face image and video concept, evaluation plan and api. Technical report, National Institute of Standards and Technology, 7 2013. [http://biometrics.nist.gov/cs.links/face/frvt/frvt2012/NIST\\_FRVT2012.api\\_Aug15.pdf](http://biometrics.nist.gov/cs.links/face/frvt/frvt2012/NIST_FRVT2012.api_Aug15.pdf).
- [11] K. He, X. Zhang, S. Ren, and J. Sun. Deep residual learning for image recognition. In *2016 IEEE Conference on Computer Vision and Pattern Recognition (CVPR)*, pages 770–778, June 2016.
- [12] Gary B. Huang, Manu Ramesh, Tamara Berg, and Erik Learned-Miller. Labeled faces in the wild: A database for studying face recognition in unconstrained environments. Technical Report 07-49, University of Massachusetts, Amherst, October 2007.
- [13] Masato Ishii, Hitoshi Imaoka, and Atsushi Sato. Fast k-nearest neighbor search for face identification using bounds of residual score. In *2017 12th IEEE International Conference on Automatic Face & Gesture Recognition (FG 2017)*, pages 194–199, Los Alamitos, CA, USA, May 2017. IEEE Computer Society.
- [14] Jeff Johnson, Matthijs Douze, and Hervé Jégou. Billion-scale similarity search with gpus. *CoRR*, abs/1702.08734, 2017.

- [15] Ira Kemelmacher-Shlizerman, Steven M. Seitz, Daniel Miller, and Evan Brossard. The megaface benchmark: 1 million faces for recognition at scale. *CoRR*, abs/1512.00596, 2015.
- [16] Yury A. Malkov and D. A. Yashunin. Efficient and robust approximate nearest neighbor search using hierarchical navigable small world graphs. *CoRR*, abs/1603.09320, 2016.
- [17] Joyce A. Martin, Brady E. Hamilton, Michelle J.K. Osterman, Anne K. Driscoll, , and Patrick Drake. National vital statistics reports. Technical Report 8, Centers for Disease Control and Prevention, National Center for Health Statistics, National Vital Statistics System, Division of Vital Statistics, November 2018.
- [18] O. M. Parkhi, A. Vedaldi, and A. Zisserman. Deep face recognition. In *British Machine Vision Conference*, 2015.
- [19] P. Jonathon Phillips, Amy N. Yates, Ying Hu, Carina A. Hahn, Eilidh Noyes, Kelsey Jackson, Jacqueline G. Cava-zos, Géraldine Jeckeln, Rajeev Ranjan, Swami Sankaranarayanan, Jun-Cheng Chen, Carlos D. Castillo, Rama Chellappa, David White, and Alice J. O'Toole. Face recognition accuracy of forensic examiners, superrecognitioners, and face recognition algorithms. *Proceedings of the National Academy of Sciences*, 115(24):6171–6176, 2018.
- [20] Florian Schroff, Dmitry Kalenichenko, and James Philbin. Facenet: A unified embedding for face recognition and clustering. *CoRR*, abs/1503.03832, 2015.
- [21] Jeroen Smits and Christiaan Monden. Twinning across the developing world. *PLOS ONE*, 6(9):1–5, 09 2011.
- [22] Yaniv Taigman, Ming Yang, Marc'Aurelio Ranzato, and Lior Wolf. Deepface: Closing the gap to human-level performance in face verification. In *Proceedings of the 2014 IEEE Conference on Computer Vision and Pattern Recognition, CVPR '14*, pages 1701–1708, Washington, DC, USA, 2014. IEEE Computer Society.
- [23] A. Towler, R. I. Kemp, and D White. *Unfamiliar face matching systems in applied settings*. Nova Science, 2017.
- [24] Working Group 3. Ed. M. Werner. *ISO/IEC 19794-5 Information Technology - Biometric Data Interchange Formats - Part 5: Face image data*. JTC1 :: SC37, 2 edition, 2011. <http://webstore.ansi.org>.
- [25] David White, James D. Dunn, Alexandra C. Schmid, and Richard I. Kemp. Error rates in users of automatic face recognition software. *PLoS ONE*, 10:1–14, October 2015.
- [26] Bradford Wing and R. Michael McCabe. Special publication 500-271: American national standard for information systems data format for the interchange of fingerprint, facial, and other biometric information part 1. Technical report, NIST, September 2015. ANSI/NIST ITL 1-2015.
- [27] Andreas Wolf. Portrait quality - (reference facial images for mrtd). Technical report, ICAO, April 2018.
- [28] D. Yadav, N. Kohli, P. Pandey, R. Singh, M. Vatsa, and A. Noore. Effect of illicit drug abuse on face recognition. In *2016 IEEE Winter Conference on Applications of Computer Vision (WACV)*, pages 1–7, Los Alamitos, CA, USA, mar 2016. IEEE Computer Society.